SPACE, DAVID ALEXANDER, Ph.D. Construction of a Homology Model of the Orexin-1 Receptor in its Active and Inactive States and Subsequent Molecular Dynamics Experiments in a Simulated Lipid Bilayer. (2016)
Directed by Dr. Patricia H. Reggio. 315 pp.

The purpose of Phase I of this research was to construct two homology models, one each inactive (R state) and active (R* state), of the orexin-1 receptor (ox1r). The ox1r is a Class A (rhodopsin-like) G protein-coupled receptor (GPCR) that couples to the G_q protein. Homology models were built using an existing crystal structure of a Class A GPCR. The ligands 1-(5-(2-Fluoro-phenyl)-2-methylthiazol-4-yl)-1-((*S*)-2-(5-phenyl-(1,3,4)oxadiazol-2-ylmethyl)-pyrrolidin-1-yl)-methanone (SB-674042), and the orexin-A peptide [pyroglutamate]PLPDCCRQKTCSCRLYELLHGAGNHAAGILTL-NH_2 with residues C6-C12 and C7-C14 disulfide-bonded, were docked in the ox1r R and R* states, respectively.

Another orexin receptor (ox2r) subtype's x-ray crystal structure was published (Yin et al., 2014). The high level of identity between the ox1r and ox2r, and the release of peptide-bound neurotensin crystal structures (Egloff et al., 2014, Krumm et al., 2015), led to the latter being used as a guide to dock orexin-A's C-terminus into the binding pocket. The ligands were docked in ox1r models created by directly mutating ox2r's crystal structure, only using Conformational Memories (CM) (Whitnell et al., 2008) to select an R* TMH6 that kicks out. The new ox1r R* model has orexin-A hold the ox1r's toggle switch residue, Y6.48, in a *trans* $\chi 1$ and has part of orexin-A accept a hydrogen bond from the ox1r R* state's H7.39 as per Darker et al., 2001 and Malherbe et al., 2010. These interactions promote the ox1r R* state. The new ox1r R model has SB-674042

hold the ox1r's Y6.48 in a g^+ $\chi 1$ and accepts a hydrogen bond from the R state's Q3.32, as per Malherbe et al., 2010. These interactions promote the ox1r R state. New IC3 loops and termini were created with Modeller (Sali et al., 1993, University of California San Francisco, San Francisco, CA), and the receptor models were palmitoylated.

The purpose of Phase II was to examine the homology models' behavior in a simulated lipid bilayer environment. To do so, CHARMM force field parameters were created based on SB-674042 and on pyroglutamate using the global minimum structure of each, all calculated at the HF 6-31G* level of theory using Spartan (Wavefunction Inc., Irvine, CA). The result was a list of new parameters that were used in the Molecular Dynamics (MD) simulation, and in turn, the results of the lipid bilayer simulation of each ligand/receptor complex indicated that each complex was stable and retained important GPCR features. Furthermore, each complex was compared with recently released ox1r crystal structures (Yin et al., 2016), and the transmembrane helices match almost perfectly, with an RMSD of 0.5383 for TMH1, 0.2374 for TMH2, 0.3416 for TMH3, 0.3731 for TMH4, 0.3839 for TMH5, 0.2851 for TMH6, 0.3074 for TMH7, and 0.5060 for Helix 8 between the Cαs of the ox1r R model and the ox1r crystal structure 4zjc. The residues in the ox1r R* model's EC2 loop that bind to orexin-A's residues L16, L19, and L20, after running MD on it, match extremely well with the ox1r crystal structures' corresponding EC2 residues, and face the same way as well. SB-674042 in one of those crystal structures accepts no hydrogen bonds, as opposed to the complex. In fact, orexin-B was docked in the ox1r, and the binding interaction energy thereof was calculated as it was for the ox1r ligands, and the results were consistent with experimental data.

CONSTRUCTION OF A HOMOLOGY MODEL OF THE OREXIN-1 RECEPTOR IN ITS ACTIVE AND INACTIVE STATES AND SUBSEQUENT MOLECULAR DYNAMICS EXPERIMENTS IN A SIMULATED LIPID BILAYER

by

David Alexander Space

A Dissertation Submitted to
the Faculty of The Graduate School at
The University of North Carolina at Greensboro
in Partial Fulfillment
of the Requirements for the Degree
Doctor of Philosophy

Greensboro
2016

Approved by

Dr. Patricia H. Reggio
Committee Chair

APPROVAL PAGE

This dissertation, written by David Alexander Space, has been approved by the following committee of the Faculty of The Graduate School at The University of North Carolina at Greensboro.

Committee Chair Patricia H. Reggio

Committee Members Jason J. Reddick

Norman H. L. Chiu

Mitchell P. Croatt

October 26, 2016
Date of Acceptance by Committee

October 26, 2016
Date of Final Oral Examination

TABLE OF CONTENTS

Page

LIST OF TABLES

Page

LIST OF FIGURES

Page

LIST OF EQUATIONS

Page

CHAPTER I

INTRODUCTION

Definition of Orexin-A and Orexin-B, and the Orexin-1 and -2 Receptors

The neuropeptides orexin-A and orexin-B (oxA and oxB), created by cleaving the peptide prepro-orexin,[1] are heavily involved in various activities in the human body by activating the G protein-coupled receptors (GPCRs)[2] ox1r and ox2r (the orexin-1 and -2 receptors),[3,4,5,6] which are in the β-branch of the Class A subfamily.[2,6,7] These neuropeptides are given their name orexin from the Greek word όρεξις (*orexis*), which means appetite.[8,9] A GPCR's general topology can be seen in Figure 1.[2]

Figure 1. Structure of Rhodopsin, a GPCR, as Seen (from Left to Right) with Helix 6 in Front, with Helix 1 in Front, with Helix 4 in Front, and with Helix 5 in Front.[2]

GPCRs are proteins that cross the lipid bilayer, beginning with an N-terminal portion in extracellular (EC) solution.[2] The protein then crosses the membrane seven

times in order, forming the seven transmembrane helices (TMHs), which are grouped together in a closed bundle,[2] ending with a short horizontal helix (HX8) connecting TMH7 to the C-terminus.[2] The helices are connected by extracellular and intracellular (IC) loops, and the GPCR ends with a C-terminal portion in the cytosol.[2]

Binding by the Orexin-1 Receptor to G Protein and to β-arrestin

When ox1r's R (inactive) state binds to the $G_{q/11}$ protein,[10,11] GDP is bound to the α subunit,[12] but the GDP leaves when orexin-A binds to the ox1r to activate it[12] (changing it to the R* state).[10,11,12] GTP can then bind to replace it, causing the G protein to leave the ox1r, as shown in Figure 2.[12]

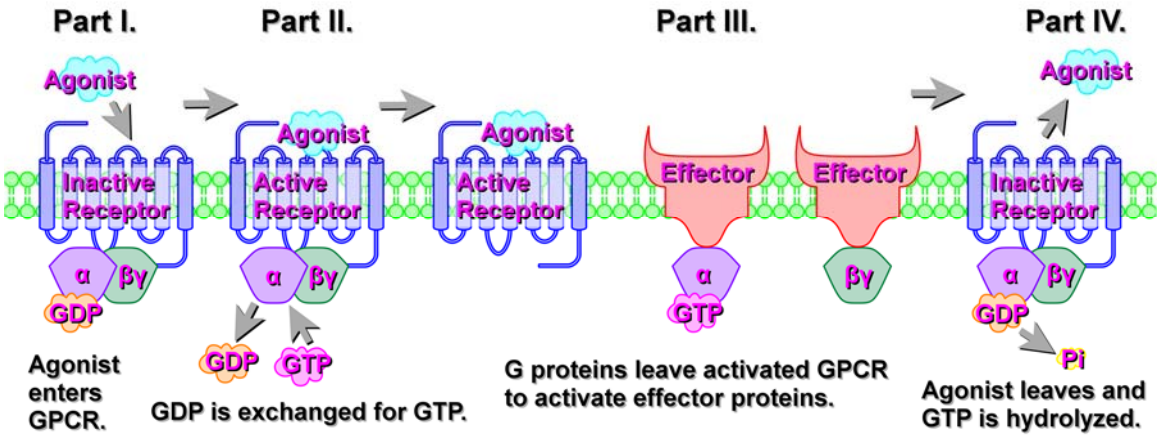

Figure 2. Cycle of G Protein Activation.[12]

While the β and γ subunits increase the activity of GPCR kinases 2 and 3, the α subunit with its bound GTP upregulates phospholipase C, which can produce further messengers that increase protein kinase C activity and intracellular [Ca^{2+}].[12] The ox1r can also activate phospholipase D via PKCδ.[13] When the ox1r is activated, whether via G protein-dependent or -independent means, intracellular [Ca^{2+}] is elevated.[12,14]

Furthermore, PKD1 and PKD3 help modulate $G_{q/11}$ protein-mediated increases in intracellular [Ca^{2+}].[11] The downstream effects of the $G_{q/11}$ protein are shown in Figure 3.[11,12]

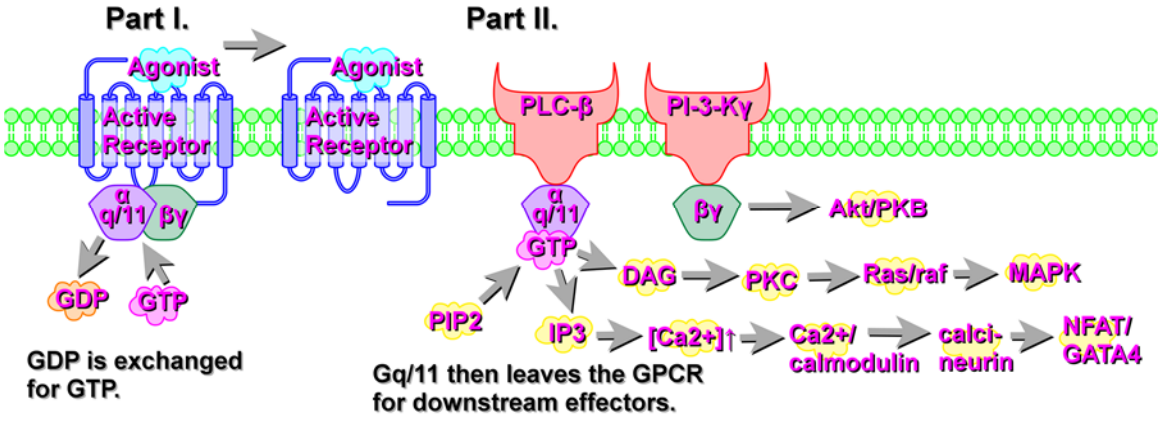

Figure 3. $G_{q/11}$ Protein-mediated Cellular Cascade.[11,12]

A phosphorylated ox1r can also bind a β-arrestin protein for signaling purposes, mainly via a TSVTT cluster at the C-terminus (418-422), of which any 3 of the serines or threonines are necessary,[15] as well as to be internalized into intracellular endosomes if a sufficient signal is delivered, as shown in Figure 4.[16,17]

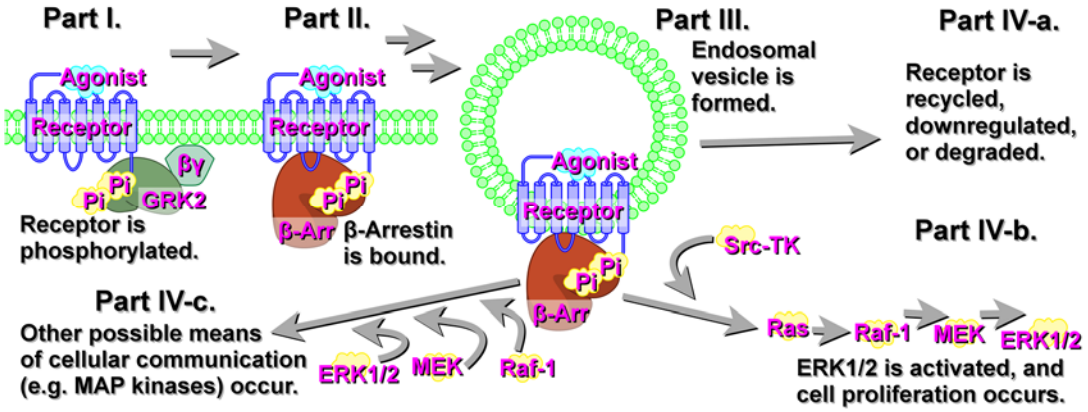

Figure 4. The Process of β-arrestin Signaling.[15,16,17]

The ox1r and ox2r ligand discrimination may depend on the system that uses them, leading to the use of receptor-specific antagonists to determine the receptor responsible for that effect, as well as the fact that ox1r binds orexin-A much more strongly than orexin-B.[3,4,5,6,13,18] The ox1r can homodimerize with itself,[19] or heterodimerize with other receptors, such as the cannabinoid receptor CB1.[20,21] Mutation and/or truncation of orexin-A and -B can actually change their ability to bind ox1r and ox2r,[22,23] with the C-terminus of each as their most vital part.[22] Furthermore, mutation of the ox1r may alter its pharmacological profile.[3,24]

The Orexin-1 Receptor's Role in Energy

The hypothalamus projects orexin throughout the cerebrum, and the ox1r and ox2r are found in differing ratios in the various parts of the hypothalamus, as shown in Figure 5.[25,26]

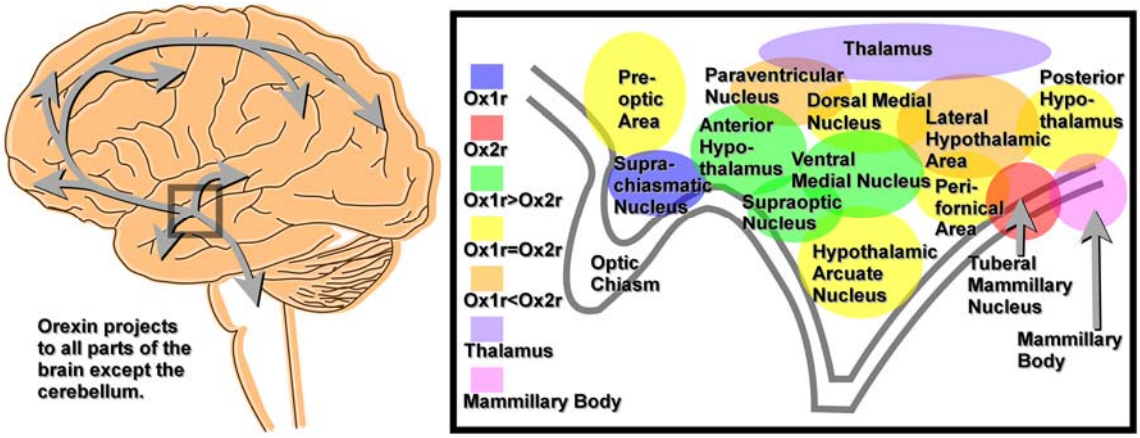

Figure 5. Expression of Ox1r in the Hypothalamus.[25,26]

The ox1r's many functions[10] include, when activated by oxA, increasing feeding and drinking behaviors[27,28,29] as well as causing glucagon release[30] and gastrointestinal

muscular activity.[31] Ox1r can even increase obesity resistance[32] by increasing lung activity[33] and spontaneous physical activity.[34] Additionally, when energy homeostasis is disrupted, when drugs are administered, or when a noxious insult (e.g. arterial occlusion, change of pO_2 or pCO_2, or inflammation) is administered, the expression of prepro-orexin, oxA, and oxB are altered (increased in some cases, decreased in others), and ox1r and ox2r expression tends to increase.[25] Orexin even has a thermoregulating purpose, as heat acclimation can decrease the concentration of orexin, among other molecules.[35] Orexin can even stimulate hypoxia-inducible factor-1 activity, which is important for regulation of hunger and wakefulness, yet can stimulate angiogenesis in hypoxic tumors.[36] Fasting can even increase the levels of orexin and thyrotropin-releasing hormone, as well as decreasing cocaine- and amphetamine-regulated transcript.[37] Orexin receptors, along with histamine receptors, are even necessary to maintain seasonal cycles of energy metabolism.[38] The orexin-1 receptor is also responsible for increased glucose production (via sympathetic means), which is also a side effect of atypical antipsychotic drugs.[39] The ox1r is even responsible for promotion of gastric acid secretion,[40] and cholinergic activity resulting in ileal contractions.[41] Food deprivation may even regulate the expression of orexin receptor mRNA in many parts of the brain.[42] The orexin receptors may even collaborate additionally with ghrelin and gastrin to regulate food intake and energy homeostasis.[43] Orexins can even promote stereotypic behaviors, glucocorticoid release, and metabolic rate, as well as affecting luteinizing hormone production and inhibiting the release of prolactin and growth hormone.[44] Orexin-A's induction of gastric acid secretion is also mediated by the neuropeptide Y system.[45]

The Orexin-1 Receptor's Role in Sleep

The ox1r may even modulate neurons in the retina responsible for the circadian clock.[46] Insomnia affects 20% of the general population[47] and burdens the US economy by $100 billion due to fatal accidents and other problems.[48,49,50,51,52] When the orexin receptors are knocked out, narcolepsy caused by cholinergic activity results,[53,54] as well as a corresponding rise in accidents.[55] The ox1r can also delay the onset of paradoxical sleep, as well as reduce the amount of paradoxical sleep.[56] Furthermore, polymorphisms on prepro-orexin, corresponding to H21A and G22R on orexin-A, were found in many people with early-onset narcolepsy.[22,57] Orexin may even play a role in sleep apnea.[58] One novel treatment involved the use of a bis-amidopiperidine derivative (SB-649868) to antagonize both orexin receptors and treat narcolepsy.[59] Almorexant, a dual orexin receptor antagonist,[3,47,60] can even cause sleep without damaging the capacity of learning and memory acquisition.[61] Other dual orexin receptor antagonists, such as DORA-1, not only promote sleep, but also block drug-related reinforcement and relapse behavior.[62]

The Orexin-1 Receptor's Role in Pleasure and Drug Addiction

Ox1r also reinforces activities of pleasure, such as food, sexual behavior, and drugs,[10] and is responsible for learning and memory functions,[63] drug relapse,[64] and (in conjunction with ox2r) causing wakefulness with exposure to light.[10,65] Furthermore, prenatal exposure to nicotine can greatly increase orexin expression, especially at the dopaminergic system, and significantly alter behaviors of food and drug reward.[66] The ox1r may even be responsible for alcoholic relapse.[67] Additionally, the ox1r can even mediate alcohol preference[68] and cause morphine withdrawal symptoms when it occurs.[69]

Not only that, the ox1r can activate the CB1 receptor by activating diacylglycerol lipase to produce 2-arachidonoyl glycerol,[70] as well as creating an allosteric coactive relationship by heterodimerizing with it,[4,20] to activate it and trigger its effects in the body.[4,20,70] Ox1r activation also supports higher breakpoints for cocaine use.[71,72,73] The ox1r even increases long-term potentiation, a form of synaptic plasticity, in the brain's dentate gyrus.[74] The ox1r also plays a role in amphetamine sensitization and its effects on dopamine activity.[75] The ox1r and ox2r also participate in two opposing means of regulating depression-like behaviors, with ox1r producing a negative emotional state that leads to reward conditioning and response, and ox2r producing an antidepressant-like effect.[76] When the ox1r is repeatedly antagonized, it can cause multiple effects on drug seeking, from attenuation during extinction, to enabling an acute ox1r antagonist dose to reduce cue-induced reinstatement.[77] A low dose of an ox1r antagonist may also increase cue-induced reinstatement, likely from increasing surface ox1r expression due to inhibiting ox1r internalization.[21,77] The ox1r is even responsible for drug tolerance, physical dependence, and physical signs of withdrawal.[78] The ox1r is also responsible for causing the sympathetic responses to stress and moderate doses of methamphetamine use.[79]

The Orexin-1 Receptor's Role in Brain Activity and the Fight/Flight Response

The ox1r is also responsible for benzodiazepine- and caffeine-induced panic behaviors, as well as related anxiety and the panic network in the brain.[80] Orexin is even responsible for many facets of the defense response, such as baroreflex suppression and stress-induced analgesia, leading to the "fight or flight" response.[81] Furthermore, ox1r

activation increases cortical acetylcholine release[82] and catecholamine production,[83] mediating panic responses via the autonomic system, as shown in Figure 6.[84,85]

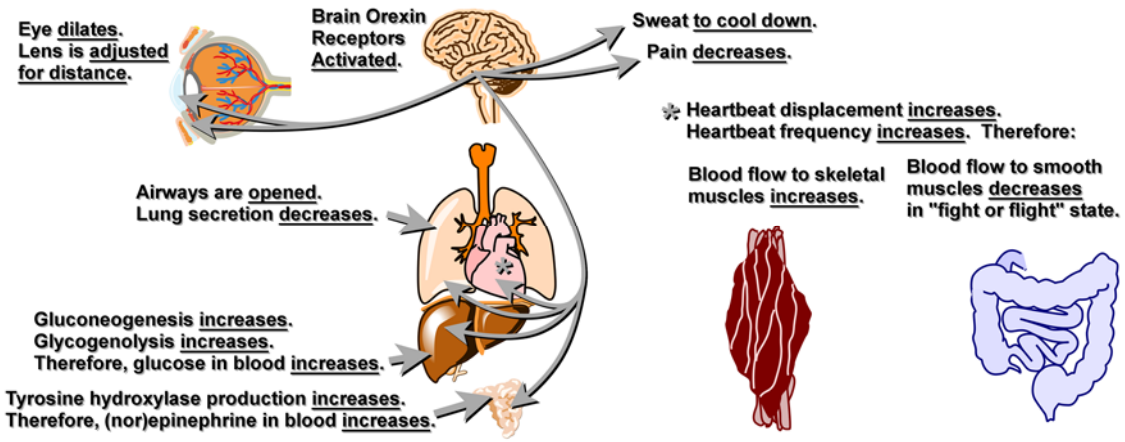

Figure 6. The Autonomic System.[84,85]

Orexin can even assist reproduction in both sexes,[1,86,87] as well as lead to synthesis of steroidal hormones such as testosterone.[88] More specifically, orexin-A can even increase sexual arousal,[89] yet it may lead to anxiety to initiate reproduction.[90] Furthermore, ox1r can even induce the release of arachidonic acid via PLA_2 (phospholipase A_2).[91] Orexin's worth in the body is just as evident when it is absent as it is when present, as orexin loss is part of neurodegenerative diseases such as Parkinson's disease.[92,93] Alteration of orexin-A trafficking is a key part of Parkinson's and Huntington's diseases, dementia, depression, and narcolepsy.[94] Change of ox1r expression may also be responsible for the alteration of brain function that transient ischemia-induced neuronal damage would have.[95] Ischemia causes enhanced ox1r expression in the hippocampus and cortex, and the added ox1r may play a role in the ensuing ischemic insult.[96] Ox1r expression increases in response to traumatic brain

injury, and it may play a role in response.[97] The ox1r may also be responsible for causing the increased anxiety behind intense emotional arousal, such as fear conditioning, drug challenge, or hypercapnia, though antagonism does not lower baseline anxiety.[98] In the cerebellum, the ox1r can assist with learning and timing of motor skills.[99] The ox1r in the CA1 region of the hippocampus has a role in spatial learning/memory acquisition, consolidation, and retrieval,[100] but in the dentate gyrus, the ox1r also has a role in spatial learning/memory acquisition and consolidation, but not retrieval.[101] The ox1r and ox2r can be antagonized systemically without interfering with the hypothalamus-pituitary-adrenal axis, showing that orexin plays a minor, yet important, role at basal orexin levels.[83,102]

The Orexin-1 Receptor's Role in Heart Activity

Furthermore, the ox1r assists the ox2r in directly exciting the neurons responsible for increasing heart rate and arterial pressure.[103] The ox1r can even increase sympathetic outflow and its accompanying effects, including increased heart rate, arterial pressure, and phrenic nerve activity.[104] This is also important, as the orexin system may be downregulated by the cytokine TNF-α.[105] Orexin expression is also regulated by leptin administration.[106] Both orexin receptors, as well as nitric oxide, are also responsible for the increased systolic blood pressure and heart rate that stress-induced hypertension entails.[107] Ox1r and orexin-A expression at the choroid plexus may assist NO or serotonin transmission.[94]

The Orexin-1 Receptor's Role in Ventilation

Among orexin's many roles in triggering locomotion, analgesia, stress, and arousal, it also triggers the central chemoreceptive reflexes through which pCO_2 and pH affect ventilation, in a circadian manner.[108,109] During wakefulness, the ox1r is also responsible for the hyperventilation reflex to high pCO_2.[110]

The Orexin-1 Receptor's Role in Pain

Ox1r can also protect cells from oxidative stress,[111] and relieve pain[112] without decreasing wakefulness.[113] The ox1r is especially responsible for reducing the pain of mechanical allodynia,[114] reducing neuropathic pain[115]—especially pain from diabetic neuropathy,[116] reducing thermal pain via the pontine reticular formation,[113] and can even be responsible for morphine analgesic tolerance.[117] The ox1r can also be responsible for stress-induced antinociception.[118] The ox1r in the ventral tegmental area (VTA) and the nucleus accumbens is responsible for the effects of lateral hypothalamus-stimulated antinociception.[119]

The Orexin-1 Receptor's Role in Possible Side Effects

However, side effects must be taken into account. For instance, care must be taken, when designing a drug to act on the orexin system, to ensure that synergistic effects with other drugs do not occur, and almorexant is a dual orexin receptor antagonist that lacks such synergistic effects with alcohol (though the authors still advise against concurrent use of alcohol).[60] Ox1r-specific antagonists could cause their intended effects without strongly promoting sleep,[120,121] and without interfering with the cerebellar interpositus nucleus.[122]

The Definition of Ballesteros-Weinstein Numbering

The Ballesteros-Weinstein notation takes the most conserved residue in each helix across multiple GPCRs and assigns it the name X#.50, where X is the residue type, and # is the number of the transmembrane helix (1-7), or in the case of the EC2 loop, 45,[39] and residues N- or C-terminal to that conserved residue have lesser or greater numbers in their Ballesteros-Weinstein name, as shown in Figure 7.[123]

	6	6	6	6	6	6	6	6	6	6	6	6	6	6	6	6	6	6	6	6	6
	3	4	4	4	4	4	4	4	4	4	4	5	5	5	5	5	5	5	5	5	5
	9	0	1	2	3	4	5	6	7	8	9	0	1	2	3	4	5	6	7	8	9
Rho	I	M	V	I	A	F	L	I	C	W	V	P	Y	A	S	V	A	F	Y	I	F
Rho	256	257	258	259	260	261	262	263	264	265	266	267	268	269	270	271	272	273	274	275	276
D3	I	V	L	G	A	F	I	V	C	W	L	P	F	F	L	T	H	V	L	N	T
D3	333	334	335	336	337	338	339	340	341	342	343	344	345	346	347	348	349	350	351	352	353
D2L3	I	V	L	G	V	F	I	I	C	W	L	P	F	F	I	T	H	I	L	N	I
D2L3	379	380	381	382	383	384	385	386	387	388	389	390	391	392	393	394	395	396	397	398	399
D2S	I	V	L	G	V	F	I	I	C	W	L	P	F	F	I	T	H	I	L	N	I
D2S	348	349	350	351	352	353	354	355	356	357	358	359	360	361	362	363	364	365	366	367	368
D2L	I	V	L	G	V	F	I	I	C	W	L	P	F	F	I	T	H	I	L	N	I
D2L	377	378	379	380	381	382	383	384	385	386	387	388	389	390	391	392	393	394	395	396	397
D1	V	I	M	G	V	F	V	C	C	W	L	P	F	F	I	L	N	C	I	L	P
D1	276	277	278	279	280	281	282	283	284	285	286	287	288	289	290	291	292	293	294	295	296
S1P1	I	V	L	S	V	F	I	A	C	W	A	P	L	F	I	L	L	L	L	D	V
S1P1	260	261	262	263	264	265	266	267	268	269	270	271	272	273	274	275	276	277	278	279	280
CB1	L	I	L	V	V	L	I	I	C	W	G	P	L	L	A	I	M	V	Y	D	V
CB1	347	348	349	350	351	352	353	354	355	356	357	358	359	360	361	362	363	364	365	366	367
CB2	L	V	L	A	V	L	L	I	C	W	F	P	V	L	A	L	M	A	H	S	L
CB2	249	250	251	252	253	254	255	256	257	258	259	260	261	262	263	264	265	266	267	268	269
Orexin-1	V	V	L	L	V	F	A	L	C	Y	L	P	I	S	V	L	N	V	L	K	R
Orexin-1	302	303	304	305	306	307	308	309	310	311	312	313	314	315	316	317	318	319	320	321	322

Figure 7. Protein Alignment by Ballesteros-Weinstein Notation, Listed Above the Residues of Each Protein, With the Residues and Their Absolute Numbers Beneath.[123]

The Definition of $g^+/g^-/trans$ Conventions

The χ1 dihedral convention used measures the dihedral angle of N-Cα-Cβ-Cγ (or Oγ in the case of serine or threonine, or Sγ in the case of cysteine), by choosing the atom

(with the exception of the Cα atom) with the highest atomic number bound to the Cβ, e.g., threonine would use the atom Oγ1 to define χ1. In case of a tie, such as in isoleucine, the Cγ1 carbon is an ethyl group, whereas Cγ2 is a methyl group, and that breaks the tie. Serine, a residue that uses its hydroxyl oxygen as Oγ, is used as an example, as shown in Figure 8.[124,125,126,127,128,129,130]

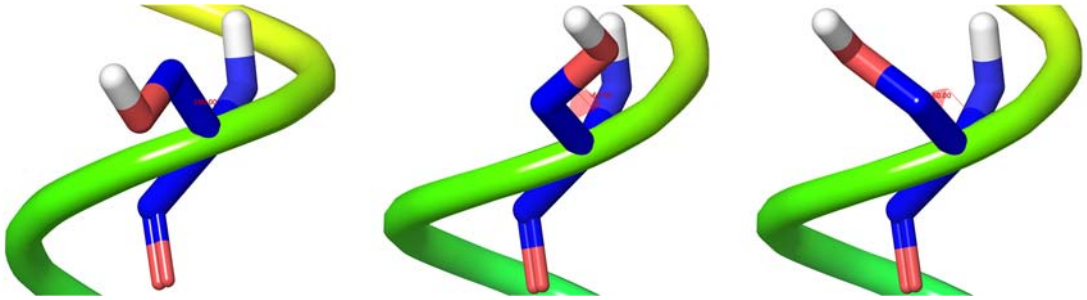

Figure 8. Left, the χ1 Measurement is 180°, Displaying a *Trans* Conformation. Center, the χ1 measurement is –60°, displaying a g^+ conformation. Right, the χ1 measurement is +60°, displaying a g^- conformation.

However, Maestro (Schrödinger 2006) defines its valine χ1 differently, since both Cγ are methyl groups, as shown in Figure 9.

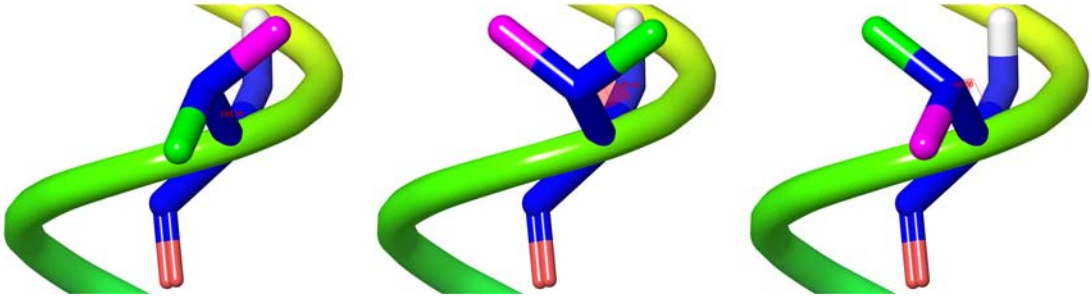

Figure 9. Left, the χ1 Measurement of Valine is 180° Using the Green Cγ, Yet Its g^+ Conformation is Defined by the Magenta Cγ. Center, the χ1 Measurement of Valine is –60° Using the Green Cγ, Yet Its g^- Conformation is Defined by the Magenta Cγ. Right, the χ1 Measurement of Valine is +60° Using the Green Cγ, yet its *trans* Conformation is Defined by the Magenta Cγ.

The Orexin-1 Receptor's Importance and the Reason to Construct These Models

However, for all of the importance of the orexin-1 receptor, no crystal structure exists for it.[3,24] As orexin-1 receptor agonists and antagonists are in their infancy,[10] a model must be built of the ox1r, yet few models have been built, and only recently.[3,24] Previous attempts only involved using a crystal structure as the model's basis by mutating it to the ox1r sequence, docking an antagonist within the R (inactive) structure, and minimizing it.[3,24] Many other ways of receptor modeling have been used, including the use of receptor chimeras.[6,131,132]

The purpose of this experiment is to construct two *in silico* models of the ox1r. First, Conformational Memories[133] is used to create low free energy conformations for the helices, docking the endogenous agonist[4] in the R* (active) model, and improving on previous models' docks.[3,24] This approach also uses Modeller to connect the helices with loops, as well as to add N- and C-termini to the ends,[134,135,136] as well as color-coding each part of the model. Each ligand will be docked according to basic GPCR rules of activation,[124] which hypothesize that orexin-A (an agonist)[3,4,24] will allow Y6.48's $\chi 1$ to be *trans*, and SB-674042 (an antagonist)[3,24,137] will hold Y6.48's $\chi 1$ in g^+[124] using the Ballesteros-Weinstein numbering system.[123]

The reason for Y6.48's importance[124] is that when the "toggle switch" found by Shi et al. in TMH6 has C6.47 in *trans*, W6.48 (Y6.48 in the ox1r) in g^+, and F6.52 (S6.52 in the ox1r) in g^+, i.e. the R state, TMH6 is bent on the IC end toward TMH3.[124,125,126,127,128,129,130] Additionally, Y5.58 is g^+ in the R* state and *trans* in the R state.[138] This bent position is locked in place when R3.50 forms a salt bridge (an "ionic

lock") with E/D6.30.[124,125,126,127,128,129,130] In the case of ox1r, the 6.30 residue is R6.30, so T6.33 is used as a salt bridge acceptor residue, as it is the only residue on TMH6 near R3.50 that can do so, as T6.34 does in the μ-opioid receptor, therefore this interaction is hereafter named an "ionic" lock, as only one of the partners has a charge.[139,140,141] However, the Cα-Cα distance is still measured from R3.50-R6.30, as this measurement is universal in GPCRs regardless of which residue X6.30 may be.[142] Activation to the R* state changes the "toggle switch" so that C6.47 is g^+, W6.48 (Y6.48 in the ox1r) is *trans*, and F6.52 (S6.52 in the ox1r) is *trans*.[124,125,126,127,128,129,130] This straightens the CW/YXP hinge region, straightening TMH6,[125,126,127,128,129,130] pulling its IC end away from R3.50, and breaking the ionic lock.[143]

CHAPTER II

MATERIALS AND METHODS

Ox1r Helices Construction

To begin ox1r model construction, the ox1r sequence was aligned with those of the β_2-adrenergic receptor,[144,145] the ox2r upon its release,[7] the adenosine A_{2A} receptor,[146] and rhodopsin,[2] using the most highly conserved residues for each helix across Class A GPCRs: N1.50, D2.50, R3.50, W4.50, P5.50, P6.50, and P7.50,[2,144,145,146] as well as the conserved cysteine in the EC2 loop involved in a disulfide bond, C45.50.[39] Further care was taken with the motifs TMH3 E/DRY (DRW for ox1r), TMH6 CWXP (CYXP for ox1r), and TMH7 NPXXY[144,145] so that the chosen template would be correctly mutated. The β_2-AR crystal structure[144,145] and the adenosine A_{2A} receptor crystal structure[146] were mutated and renumbered to the ox1r sequence, as raw material for the Monte Carlo/simulated annealing program Conformational Memories (CM).[133,147] This was necessary, as each of the ox1r helices had a helix-deforming residue (e.g., P, G, or T)[148,149] that rendered the template unable to guarantee the proper helical conformation.[3,24]

Ox1r Helices Assembly into Bundle

Helices 1 through 6 of the mutated β_2-AR template,[144,145] as well as a TMH3 made "from scratch" to be used in place of the β_2-AR-based TMH3 CM output,[133,144,145,147] were varied via the Conformational Memories method, which explores each helix's dihedrals and bond angles as follows.[20,133,147,149] The φ dihedrals were set

at–50° to –70°, ψ at –40° to –60°, and ω at 180°, varying φ and ψ ±10°, χ limitlessly, and ω ±20°.[20,133,147] The five-residue-long flexible areas in each helix ending in P (or T1.51 in TMH1[148]) had φ and ψ varied at ±50°.[20,149] The angles were varied ±8°, except for special cases such as methionine's Cγ-Sδ-Cε, lysine's Cε-Nζ-Hζ, and tyrosine's Cζ-Oη-Hη. These special angles were varied ±15°. To acquire the best structures, a region of best probability must be created with an exploratory phase.[133,147] This was done by "heating" the helix to 3000 K, then letting it "cool down" in 18 stages to 310 K, with each stage consisting of 50000 Monte Carlo steps, each with two random dihedral changes and one random bond angle change per Monte Carlo step.[133,147] Every one of these dihedral and bond angle changes use the Metropolis Criterion to ensure that more unfavorable moves would be less likely to be taken, and to give the helix access to more favorable energetic states.[133,147] These "conformational memories" are used in the biased phase, which "heats" the helix to 749.4 K, "cools" it to 310 K in 7 stages, keeping the attempted moves within the "populated conformational space" and producing 105 structures at 310 K.[133,147] For ox1r helices 1-5, the CM output[133,147] was superimposed onto the β_2-AR alignment template using the Cαs on the IC end of each helix, excluding the five-residue-long flexible areas to permit the most variety of helical shape at the other end.[2,20,124,144,145,146,149,150] This must be done this way as the intracellular portions of GPCRs look alike for TMH1 through TMH5.[2,20,133,124,144,145,146,147,150] TMH6 must be superimposed with a different method because it must be free to move, though in the R state, the TMH6 CM output would line up with the template roughly the same way regardless of IC or EC superimposition.[2,20,133,124,144,145,146,147,150] Ox1r's helix 6 used the

EC end's Cαs (6.51-6.61) for alignment, again excluding the five-residue-long flexible areas, as shown in Figure 10.[2,20,124,144,145,146,149,150]

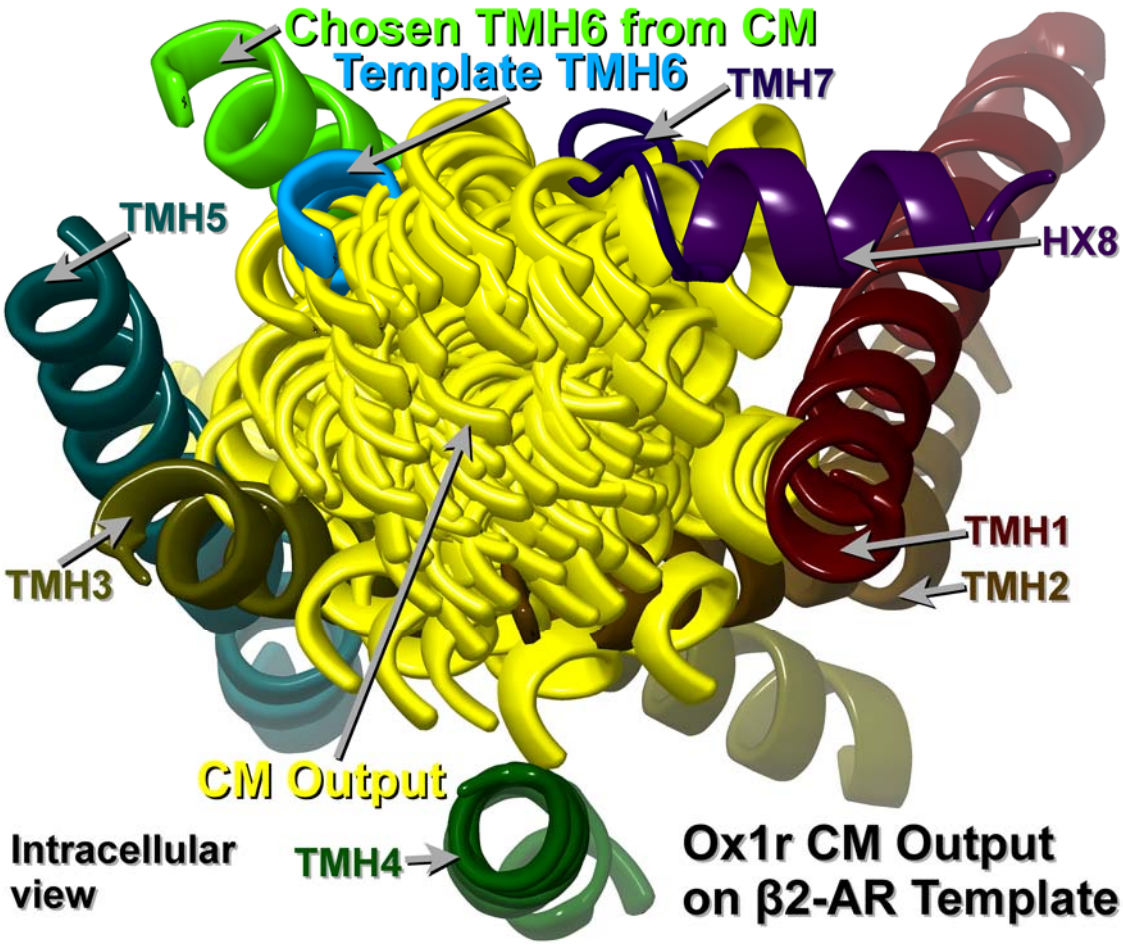

Figure 10. CM Output for TMH6 Superimposed on the β_2-AR.[2,20,124,144,145,146,149,150]

Ox1r's helices 7 and 8 were taken directly from the adenosine A_{2A} receptor since the ox1r and A_{2A} elbow regions that connect helices 7 and 8 have 1 residue more than the β_2-AR's elbow does.[3,144,145,146] The mutated TMH7/HX8 structure was then superimposed directly onto the β_2-AR alignment template using the N, Cα, and C on P7.50.[144,145]

Ox1r Bundle Ligand Docking

Once the seven helices were superimposed, they were pulled apart as shown in Table 1 to ease ligand insertion. The R* structure had orexin-A inserted manually in both the "forward" (C-terminus near TMH3-6) and "reverse" (C-terminus near TMH1, TMH2, and TMH7) directions, with the side chain dihedrals adjusted in both orexin-A and the ox1r R* structure for both docks to optimize interactions, with energy measurements taken, so that Y6.48 can be activated.[3,22]

Table 1

With TMH4 Perpendicular to the Screen, HX8 Parallel to the x-axis and the Bottom of the Screen, and the EC Side Facing out of the Screen, These Were the Distances (in Å) That the Helices Were Moved, with TMH3 Held Stationary

TMH#	***1***	***2***	***4***	***5***	***6***	***7***
x	**+1**	**+1**	**0**	**–1**	**–1**	**0**
y	**0**	**+1**	**+1**	**0**	**–1**	**–1**

The R structure had SB-674042 inserted manually so that Y6.48 can be deactivated.[3,137] Both R and R* structures also had water molecules inserted at similar positions to water molecules in the β_2-AR,[144,145] as long as the ligand did not interfere. These ligands were chosen as orexin-A is the endogenous agonist to ox1r,[3,6] and SB-674042 is an ox1r-specific antagonist.[3,137] The above mentioned "toggle switch" residues, along with Y5.58, in each structure were adjusted to fit the respective state for each receptor,[124,125,126,127,128,129,130,138] with R3.50 adjusted to interact with T6.33 in the R

state and to refrain from doing so in the R* state[141,143] by adjusting these residues' side chain dihedrals.

In order to properly dock each ligand, the SB-674042 dock mutation data had to be consulted to determine the proper ligand orientation within the R structure,[3] and the global minimum structure of SB-674042 (and other local minima) had to be found with several conformational searches (as the aliphatic heterocycle in the middle had two ring pucker conformers) using *ab initio* Hartree-Fock calculations (6-31G*) in the modeling program Spartan (Wavefunction Inc., Irvine, CA).[3] Table 2 reveals the effects of ox1r mutation on SB-674042 antagonism.[3]

Table 2

Effects of Mutation of Ox1r Residues on SB-674042 Antagonism.[3]

SB-674042 K_d(Mutant) / K_d(WT) for Transmembrane Portion of Orexin-1 Receptor								
Q3.32 → A	**A3.33 → T**	**V3.36 → A**	**Y5.38 → A**	**F5.42 → A**	**Y5.47 → A**	**Y6.48 → A**	**H7.39 → A**	**Y7.43 → A**
50.9** $_{*}$	**20.2****	**2.1**	**N.D.B.**	**N.D.B.**	**1.8**	**10.8****	**22.7*****	**9.3*****

Note. $^{*}p < 0.05$, $^{**}p < 0.01$, $^{***}p < 0.001$, N.D.B. means no detectable binding because of high nonspecific binding.[3]

The highest relative K_d in Table 2 was Q3.32's 50.9, so SB-674042 must be docked in a way that gives it a strong energy of interaction.[3] Since mutating the small A3.33 to T creates a large relative K_d, SB-674042 must be close enough to A3.33 for such a mutation to sterically crowd it.[3] Furthermore, the ox2r has T3.33, which can cause TMH3 to bend.[7,24,148,149] Because H7.39A and Y7.43A had high relative K_ds, they must

be able to interact with one of SB-674042's phenyl groups.[3] A strong interaction with Y6.48 is necessary to hold the ox1r in the R state.[3] However, V3.36 and Y5.47 do not have significant relative K_ds, so they should not be involved significantly in SB-674042 binding.[3] For W45.54, Y5.38, and F5.42, the specific binding ability was destroyed by mutation to alanine (which may have caused protein misfolding), so no information of importance or lack thereof could be produced.[3] This means that Q3.32 is the key residue to be used to interact with SB-674042, and since SB-674042 has no hydrogen bond donors, it must accept a key hydrogen bond from Q3.32.[3] Using Spartan (Wavefunction Inc., Irvine, CA), electrostatic maps were created to find the most negative area of potential on SB-674042 and the most positive areas of potential on acetamide (chosen to approximate glutamine's side chain).[3,137] The former was created as Figures 11 and 12.

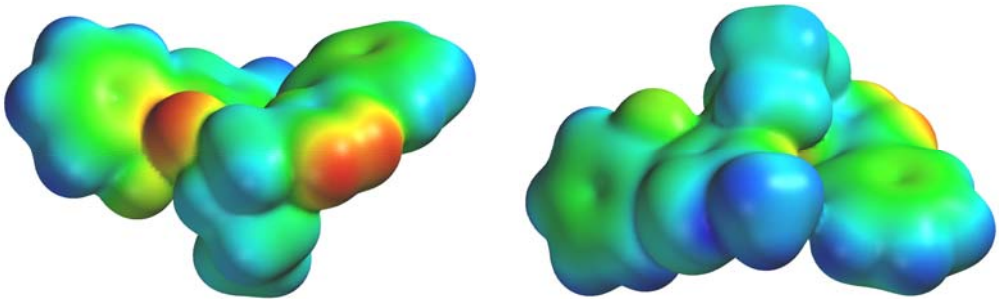

Figure 11. Electrostatic Potential Maps of SB-674042, Where Redder Areas Correspond to the Most Negative Areas of the Molecule and Bluer Areas Correspond to More Positive Parts. These Maps Correspond to the Sides with (Left) the Amide Oxygen and Oxadiazole Ring Nitrogens Facing out from the Page and (Right) the Methyl Pointing out from the Page.[3,137]

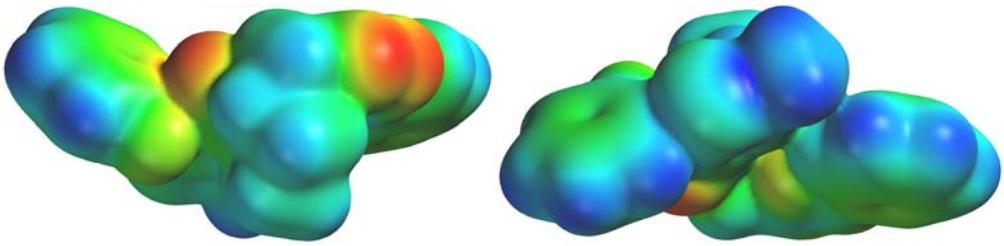

Figure 12. More Electrostatic Potential Maps of SB-674042. These Maps Correspond to the Sides with (Left) the Proline-like Portion Pointing out from the Page and (Right) the Thiazole Ring Facing out from the Page.[3,137]

The acetamide electrostatic potential maps were created as Figure 13.[3] SB-674042 was then docked, and Q3.32's χ1-3 dihedrals adjusted, so that the amide hydrogen on Q3.32 donates a hydrogen bond to SB-674042's amide oxygen.

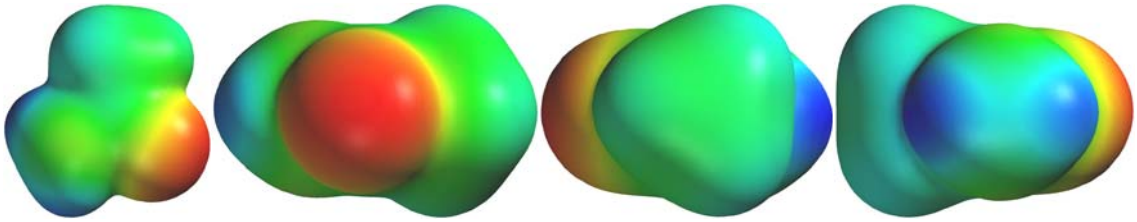

Figure 13. Electrostatic Potential Maps of Acetamide. These Maps Correspond to (Far Left) Acetamide Flat in the Page's Plane, and (Center-left) the Oxygen, (Center-right) the Methyl, and (Far Right) the Nitrogen Pointing out from the Page.

Ox1r Bundle Minimization

For the R* structure, the ligand orexin-A was docked in the "forward" and "reverse" orientations to produce "forward" and "reverse" R* models.[3,22] The R structure and both R* structures were minimized using an OPLS_2005 minimization force field, with no solvent, force field-defined charges, an extended cutoff, and a distance-dependent dielectric constant of 1.0, hereafter referred to as "dry" minimization conditions, to pull the helices together around the ligand to approximate their behavior in a lipid bilayer.

The minimization was done in steps, first constraining the ox1r and orexin-A backbone dihedrals strongly to maintain the helices' shapes, and then successively constraining them less to hold the bundle's shape as a whole. Rough parameters were measured on SB-674042, so that the SB-674042 backbone dihedrals, as well as the $O_{oxadiazole}$-$C_{oxadiazole}$-$C_{tail\ phenyl}$ bond angle were held at 3000 kJ mol^{-1} $Å^{-2}$ to allow SB-674042 to keep its shape. The R structure used the constant restraints at 3000 kJ mol^{-1} $Å^{-2}$ throughout to hold R3.50 in a salt bridge to D3.49 and T6.33,[124,125,126,127,128,129,130,141] hold the three toggle switch residues[124,125,126,127,128,129,130] and Y5.58[138] as they are, and hold K6.58 and R6.59 to keep TMH6 from collapsing on top. The R* structures used the constant restraints at 3000 kJ mol^{-1} $Å^{-2}$ throughout to hold the three toggle switch residues[124,125,126,127,128,129,130] and Y5.58[138] stationary, hold R3.50 straight, and hold R6.30 and R6.31 clear of TMH5 to avoid snagging, so TMH6 can kick out naturally. In all three structures, the R guanidinium systems and the Y χ6 (Cε-Cζ-Oη-Hη) dihedrals were held planar at 3000 kJ mol^{-1} $Å^{-2}$ throughout to keep the π systems undisturbed during minimization. The R structure's "ionic" lock was constrained to 3.1 Å (T6.33 Oγ-closest guanidinium N on R3.50[141]) to keep it far enough apart to allow it to break when activated. These minimized bundles had extracellular (EC1-3) and intracellular (IC1-3) loops added to them using Modeller.[134,135,136] This program adds loops by varying one, two, or three raw loops at once, or even part of one, while keeping the remainder stationary.[134,135,136]

Ox1r Bundle Connection to Loops

First, in order to connect the bundle to the loops to form a single molecule, the N-terminus was built from scratch and attached to TMH1, while the loops and C-terminus were constructed by extending each helix of each bundle, with dihedrals adjusted to attach the loops to the helices. Afterward, the bundle was taken apart and reassembled to ensure that no part of the ox1r is out of order with the rest. Afterward, each bundle's loops and termini were minimized (with all else frozen) for 500 steps in a high dielectric (water), hereafter referred to as "wet" minimization conditions, since the loops and termini are in aqueous conditions that weaken electrostatic interactions. These loops were further prepared by uncapping the termini so that the N- and C-termini have $–NH_3^+$ and $–COO^–$ groups on the backbone, respectively, as the actual ox1r would have. This structure is the finished transmembrane bundle, and to further prepare it, the structure was simplified by removing all hydrogen atoms.

Ox1r Loop Formation and Minimization

Each bundle was run through Modeller,[134,135,136] which works as Fiser et al. described in 2000, by taking the PDB's dihedral template library for each amino acid (with any and all possible conformations on hand), then varying one range (or several ranges) of residues to create the desired loop shape.[134] These loops are given objective function rankings (lower is better) based on hydrophobicity, hydrogen bonding, and absence of steric clashing. Of the 1080 total loop conformation sets for each bundle, the best 250 are given further inspection to see which set best interacts, according to the circumstances, with itself, the ligand, and the transmembrane bundle. Each model had

the three EC loops varied so that the EC2 loop forms a disulfide bridge between C45.50 and C3.25 (on the EC end of the TMH3).[3] This bridge is also common to other GPCRs, such as A_{2A},[146] β_1-AR,[150] β_2-AR,[144,145] CXCR4,[151] and D3.[152] The residues 45.51 to 45.54 in the EC2b loop have the "up-down-up-down" arrangement that points D45.51 and R45.53 up, and E45.52 and W45.54 down.[145] The EC2 loop not only forms the disulfide bridge, its D45.51 and W45.54 also hold the two halves of the EC2 loop out of the way to clear a path for orexin-A.[3,24] Since P45.38 to R45.45 are similar to the β_2-AR's corresponding residues, that part of the EC2a loop is helical, and is kept from blocking the ligand binding cavity by D45.51's interaction with R45.45.[24,145] D45.51A may cause the entry gap to that binding cavity to shrink, but since SB-674042 is far narrower, it is not affected.[3] Another residue is E45.52, which can keep the R state's entry gap closed by interacting with R328 in the EC3 loop, or hold the R* state's entry gap open for orexin-A by interacting with K3.26. W45.54 can interact in an aromatic network that can hold the EC2b loop out of the way of any ligand.[3] To allow sufficient working room to vary each loop, EC1 and EC3 were varied at the same time as EC2 to create rough loops for each structure. EC1 was also refined based on the β_2-AR.[144,145] The IC loops were also varied as well, with IC3 varied so that TMH5 and TMH6 extend their helices into cytoplasm, in a similar manner to rhodopsin[2] and $P2Y_{12}$,[141] and IC1 and IC2 out of the way of IC3. Hydrogens were added, and the loops were reminimized, for 500 steps in "wet" minimization conditions.

Ox1r R* Dock Verification

Both R* structures had their respective docks' energetic interaction measured on a residue-by-residue basis. Table 3 details the effects of mutation of ox1r residues on the relative EC_{50}s were collected[3] and compared to the "reverse" and "forward" energies in "wet" and "dry" environments, especially. These measurements used "wet" (80, constant) and "dry" (3, distance-dependent) dielectric constants to provide the environments for orexin-A to interact with the ox1r. "Wet" refers to the dielectric constant of water, which is high, so that it weakens electrostatic interactions. "Dry" refers to a low dielectric constant, which accentuates electrostatic interactions.

Table 3

Ox1r Residues and Mutation Effects on OxA-induced Ca^{2+} Internalization.[3]

Reverse Energy (kcal/mol)		***Orexin-1 Receptor***	***Forward Energy (kcal/mol)***	
Wet	***Dry***	***EC_{50}(Mutant) / EC_{50}(WT)***	***Wet***	***Dry***
–5.57	**–6.29**	**Q3.32 → A 2.4-fold**	**–3.68**	**–7.94**
–0.29	**–0.36**	**A3.33 → T 1.8-fold**	**–2.35**	**–2.60**
–3.15	**–3.18**	**V3.36 → A 30.6-fold**	**–1.42**	**–1.86**
–3.30	**–3.51**	**Y5.47 → A 84.4-fold**	**n/a (not close enough)**	
–3.18	**–3.31**	**Y6.48 → A 163.9-fold**	**–3.97**	**–6.13**
–5.81	**–5.97**	**H7.39 → A 241.1-fold**	**–6.07**	**–13.52**
–2.05	**–2.30**	**Y7.43 → A 8.7-fold**	**–2.58**	**–2.62**

The data in Table 3 reveal that H7.39 has an important role in binding to orexin-A, since it has a strong interaction energy that is stronger in the "forward" dock.[3] Since it

is stronger in the "forward" dock's "dry" measurement than its "wet" measurement, and the interaction is very far from extracellular solution, this shows that H7.39 interacts via multiple hydrogen bonds. A3.33 has a small role, as A3.33T may not impact the van der Waals interactions.[3] However, despite the small energetic role, V3.36A could lessen hydrophobic surface area, allowing water to enter that part and decrease the favorability of the dock significantly.[3] The high "reverse" energy in both "wet" and "dry" measurements for Q3.32 is inconsistent with its minor role in binding orexin-A.[3] However, its minor role can be donating a single hydrogen bond in the "forward" dock, as the "dry" measurement is more favorable than the "wet" one.[3] The binding role of the vitally important residue of Y6.48[2,127,153,154] is supported by the stronger energy of interaction in the "forward" dock.[3] Y5.47 was close enough to interact with orexin-A in the reverse dock only, but its role is to π-stack with Y6.48.[3] Regardless of the direction of the dock, Y7.43's minor role is consistent with the low interaction energy.[3] Table 4 details how mutating the orexin-A's residues affect the pEC_{50} of that mutant when it binds to the ox1r.[22,155] In Table 4, orexin-A was truncated to residues 15-33 to ease synthesis, and Heifetz et al. rated the mutation effects by arrows (up for significant increase, equal sign for no significant change, and down for significant decrease, and more arrows for more significant change) for easier use.[22,155]

Table 4

Residues of the Peptide, Orexin-A, and Mutation Effects on OxA-induced Ca^{2+} Internalization.[22,155]

Reverse Energy (kcal/mol)		***Orexin-A (15-33)***	***Forward Energy (kcal/mol)***	
Wet	***Dry***	***WT (pEC_{50} 6.45 ± 0.06, =)***	***Wet***	***Dry***
–4.56	**–4.37**	**R15 (→A 6.46 ± 0.03, =)**	**–2.58**	**–7.66**
–3.27	**–3.47**	**L16 (→A 71% of 10 μM oxA, ↓)**	**–4.21**	**–4.70**
+2.01	**–8.29**	**Y17 (→A 6.11 ± 0.03, =)**	**–2.61**	**–3.96**
–3.11	**–3.98**	**E18 (→A 6.71 ± 0.04, =)**	**+3.01**	**–24.28**
–0.73	**–0.77**	**L19 (→A 60% of 10 μM oxA, ↓↓)**	**–7.50**	**–7.42**
n/a (not close enough)		**L20 (→A 37% of 10 μM oxA, ↓↓)**	**–1.64**	**–1.66**
–5.17	**–6.49**	**H21 (→A 5.89 ± 0.02, =)**	**–4.86**	**–5.71**
n/a (not close enough)		**G22 (→A 6.19 ± 0.09, =)**	**–3.97**	**–5.27**
–0.34	**–0.38**	**G24 (→A 6.08 ± 0.03, =)**	**n/a (not close enough)**	
–4.54	**–4.90**	**N25 (→A 6.00 ± 0.09, =)**	**–2.69**	**–4.49**
–12.21	**–13.70**	**H26 (→A 61% of 10 μM oxA, ↓↓)**	**–8.49**	**–15.20**
–2.25	**–2.14**	**G29 (→A 15% of 10 μM oxA, ↓↓↓)**	**–0.97**	**–2.39**
–8.68	**–9.34**	**I30 (→A inactive at 10 μM, ↓↓↓)**	**–8.06**	**–9.16**
–5.83	**–6.28**	**L31 (→A 12% of 10 μM oxA, ↓↓↓)**	**–11.40**	**–12.01**
–2.38	**–2.77**	**T32 (→A 39% of 10 μM oxA, ↓↓↓) (→D-T inactive at 10 μM oxA, n/a)**	**–3.57**	**–5.13**
–10.15	**–10.92**	**L33 (→A 15% of 10 μM oxA, ↓↓↓) (→D-L 18% of 10 μM oxA, n/a)**	**–9.08**	**–10.72**
–1.07	**–2.29**	**Amide34**	**–0.73**	**–1.04**
–119.05	***–175.09***	***Totals (for WT oxA)***	***–132.59***	***–221.86***

Table 4's data show that R15, with "wet" measurements has a less favorable energy of interaction in the "forward" dock than in the "reverse" dock, consistent with its insignificant binding role, since R15 is surrounded with loop residues in water.[22] L16's important role in orexin-A binding is reflected here, however, as its binding energies in the "forward" dock are more favorable than those in the "reverse" dock.[22] Y17 has a minor role, supported by favorable energies in the "forward" dock, yet the "reverse" dock's energies for Y17 are unfavorable (in "wet") or too favorable (in "dry").[22] E18's presence inhibited activity, as shown by unfavorable "wet" energies in the "forward" dock (since it interacts with loop residues), yet the "reverse" dock's energies were favorable.[22] Regardless of the conditions, the favorability of L19's energies in the "forward" dock were ~10× those of the "reverse" dock.[22] L20's importance, though low in energy, may be to keep orexin-A shaped the way it is.[22] H21's "forward" dock energies were more consistent with its minor role than its reverse dock energies are.[22] The roles of G22, G24, and G29 (especially G29) are for flexibility, and N25's forward energies are also consistent with its minor role.[22] H26 has a strong energy in the "forward" dock's "dry" measurements that is consistent with its major role, and since its "dry" energy was more favorable than its "wet" energy, that suggests an electrostatic interaction between the ox1r and H26.[22] I30 and L33 have interactions that are consistent with their major roles regardless of the direction of the dock or the conditions used.[22] L31's stronger energy in the "forward" dock (about ~2× as strong) is also consistent with its major binding role.[22] T32 has a role as a helix stabilizer, which is consistent with a mildly favorable binding energy compared to other major residues.[22] The C-terminal

amide is small, with little role accordingly.[22] The above data suggest strongly that the "forward" dock of the orexin-A peptide in the ox1r is correct mainly due to L19's greater energetic role in orexin-A's "forward" dock than its "reverse" dock, as well as H7.39's more powerful interactions in the "forward" dock, and the "forward" dock's more favorable overall energy. The interaction energies and binding data in Tables 3 and 4 led to the creation of the R* bundle of the ox1r and orexin-A.[3,22]

Ox1r Termini Formation, Palmitoylation, and Minimization

Once the correct direction of ligand docking was chosen, the R structure with docked SB-674042 and the R* structure with orexin-A docked in the "forward" direction both had the N- and C-termini varied 17 residues at a time simultaneously from the bundle to the ends,[134,135,136] all while ensuring the ox1r model's residues are in the correct order at every step, then hydrogens were re-added as before and the termini minimized "wet" for 500 steps. The models had C375 adjusted so that it can point into the lipid bilayer, and a palmitoyl group was added to both models' C375 residue to point into that bilayer.[3,156] Afterward, both models were minimized 500 steps "dry," and the loops and termini 500 steps "wet." Both models were then aligned with the β_2-AR[144,145] from the OPM (Orientations of Proteins in Membranes) database (http://opm.phar.umich.edu/) so that they can be properly used in later experiments.[157] This is because MD simulations use the OPM database's models as a reference.[157]

Ox1r Helices Assembly into Bundle Based on Ox2r Crystal Structure

With the release of the ox2r crystal structure (4s0v), a new pair of ox1r homology models must be built.[7] The ox2r crystal structure was mutated to the ox1r sequence and

renumbered according to the CM output residue numbers.[133,144,145,147] This was necessary for ease of superimposition of the CM output,[133,144,145,147] and the template helices were pulled apart as shown in Table 5 to ease superposition further.

Table 5

With TMH4 Perpendicular to the Screen, HX8 Parallel to the x-axis and the Bottom of the Screen, and the EC Side Facing out of the Screen, These Were the Distances (in Å) That the Helices Were Moved, with TMH3 Held Stationary, and One Template Made for Each Value of z, from 0 to 10 Inclusive. The Structure Chosen for Superposition was z = 4, so That the Helices were Pulled Apart 2.0 Å.

TMH#	***1***	***2***	***4***	***5***	***6***	***7***
x	**+0.5z**	**+0.5z**	**0**	**–0.5z**	**–0.5z**	**0**
y	**0**	**+0.5z**	**+0.5z**	**0**	**–0.5z**	**–0.5z**

As the Conformational Memories method bases its output on favorable moves taken due to the residue sequence of the input,[20,133,147,149] the previous CM output based on Helices 1 through 6 of the mutated β_2-AR template[144,145] was usable here. For ox1r helices 1-5 and the ox1r R structure's helix 6, the CM output[133,144,145,147] was superimposed onto the ox2r alignment template (pulled apart 2.0 Å) using the Cαs on the IC end of each helix, excluding the five-residue-long flexible areas to permit the most variety of helical shape at the other end.[2,7,20,124,149,150] The ox1r R* structure's helix 6 used the EC end's Cαs (6.51-6.61) for alignment, again excluding the five-residue-long flexible areas, as shown in Figure 14.[2,7,20,124,133,147,149,150]

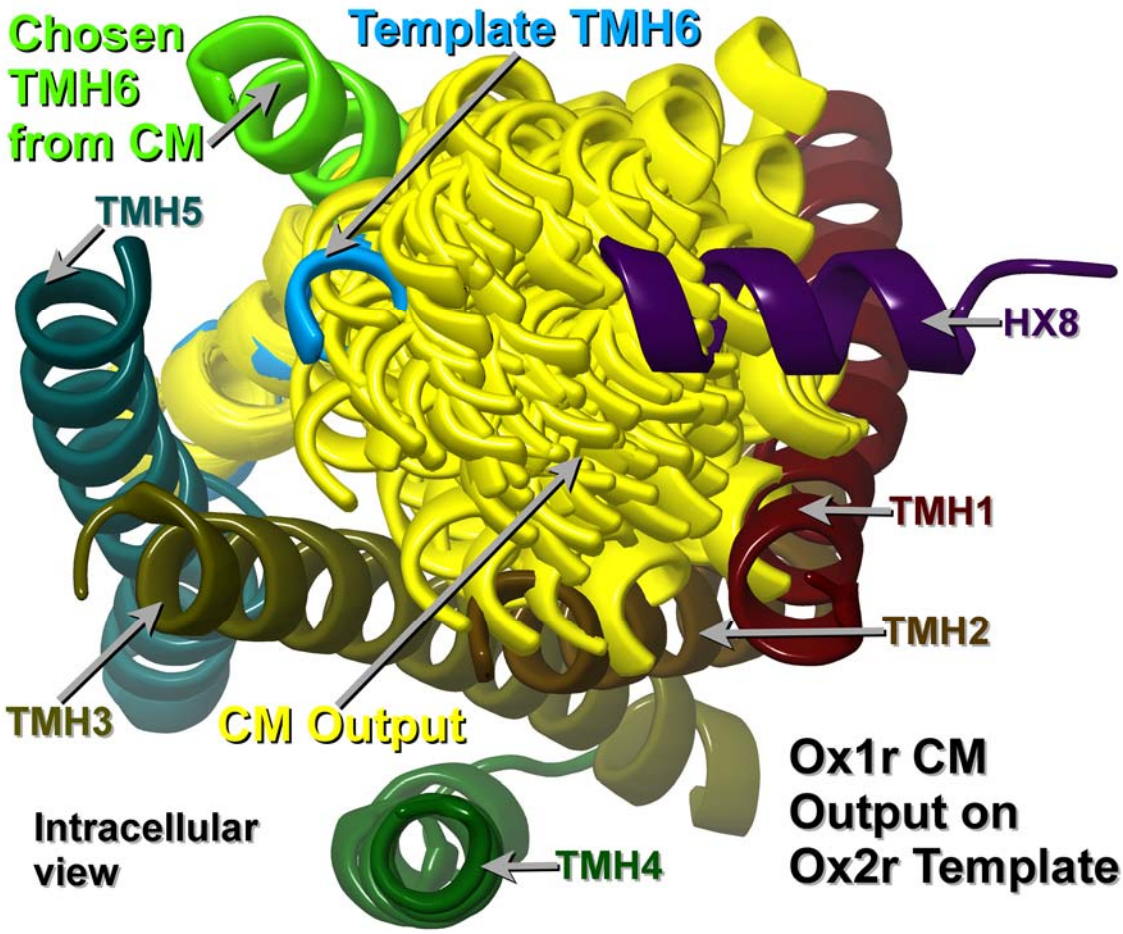

Figure 14. CM Output for TMH6 Superimposed on the Ox2r.[2,7,20,124,133,147,149,150]

This must be done this way as the intracellular portions of GPCRs look alike for TMH1 through TMH5, yet TMH6 must be free to move, though in the R state, the TMH6 CM output would line up with the template roughly the same way regardless of IC or EC superimposition.[2,7,20,124,133,147,149,150] Ox1r's helices 7 and 8 taken directly from the ox2r since the ox1r and ox2r elbow regions that connect helices 7 and 8 have the same number of residues.[3,7] The mutated TMH7/HX8 structure (with C375 attached) was then

superimposed directly onto the ox2r alignment template using the N, Cα, and C on P7.50.[7]

Ox1r Bundle Ligand Docking Based on Ox2r Crystal Structure

Using the ox1r R and R* models based on the β_2-AR[144,145] as examples, the R* structure had orexin-A inserted manually in the "forward" (C-terminus near TMH3-6) direction, and the orexin-A and ox1r side chain dihedrals adjusted to optimize interactions, so that Y6.48 can be activated,[3,22] and the R structure had SB-674042 inserted manually, and Q3.32's side chain dihedrals adjusted to optimize interactions, so that Q3.32 donates a hydrogen bond to SB-674042's amide oxygen, and that Y6.48 can be deactivated.[3] The abovementioned "toggle switch" residues in each structure were adjusted to fit the respective state for each receptor,[124,125,126,127,128,129,130] with R3.50 adjusted to interact with T6.33 in the R state and to refrain from doing so in the R* state,[141,143] by adjusting these residues' side chain dihedrals. Both R and R* structures had water molecules inserted at similar positions to the water molecules in the ox2r,[7] as long as the ligands did not interfere.

Ox1r Bundle Minimization Based on Ox2r Crystal Structure

After docking, the R and R* structures were minimized using "dry" minimization conditions to pull the helices together around the ligand to approximate their behavior in a lipid bilayer. This minimization was done in steps as before, first constraining the ox1r (and orexin-A in the R* structure) backbone dihedrals strongly to maintain the helices' shapes, and successively constraining them less strongly, down to 0 kJ mol^{-1} $Å^{-2}$, to hold the bundle's shape as a whole. As the previous model's attempt to minimize the R model

with SB-674042 docked resulted in SB-674042's dihedrals becoming distorted, a more drastic technique was required, resulting in SB-674042 being frozen in place for the minimization. The R structure used its constant restraints at 3000 kJ mol^{-1} $Å^{-2}$ to hold R3.50 in a salt bridge to D3.49 and T6.33,[124,125,126,127,128,129,130,141] hold the three toggle switch residues[124,125,126,127,128,129,130] and Y5.58[138] as they are, and hold the "ionic" lock at 3.1738 Å (T6.33 Oγ-closest guanidinium N on R3.50[141]) to keep it far enough apart to allow it to break when activated.[124,125,126,127,128,129,130] The R* structure used its constant restraints at 3000 kJ mol^{-1} $Å^{-2}$ to hold the three toggle switch residues[124,125,126,127,128,129,130] and Y5.58[138] as they are, as well as hold R3.50 straight.[124,125,126,127,128,129,130] The restraints of R6.30 and R6.31 in the R* structure and of K6.58 and R6.59 in the R structure as used in the previous model were unnecessary due to the ox2r crystal structure having greater homology than the β_2-AR does with the ox1r.[7,24,144,145] In both structures, the R guanidinium systems and the Y χ6 (Cε-Cζ-Oη-Hη) dihedrals were held planar at 3000 kJ mol^{-1} $Å^{-2}$ throughout to keep the π systems undisturbed during minimization. These minimized bundles had loops added by basing the EC1 loop on the ox2r crystal structure's EC1 loop,[7] and the extracellular (EC2 and EC3) and intracellular (IC1-3) loops added to them using Modeller.[134,135,136]

Ox1r Bundle Based on Ox2r Crystal Structure Connection to Loops

First, in order to connect the bundle to the loops to form a single molecule, the results from the previous model's loops were connected in order to ensure that no part of the ox1r is out of order with the next. During connection, the termini were kept straight as they were so that they would not obstruct loop formation by Modeller,[134,135,136] and the

dihedrals were adjusted so that the EC1 loop resembles that of ox2r,[7] and all loops were attached to their bundle anchors (e.g., EC2 to TMH4 and TMH5) as a rough structure. Afterward, each bundle's loops and termini were minimized (with all else frozen) for 500 steps in "wet" minimization conditions, since the loops and termini are in aqueous conditions that weaken electrostatic interactions. The termini having already been uncapped as before, this structure is the finished transmembrane bundle, further prepared for the next step of adding loops using Modeller[134,135,136] by having all hydrogen atoms removed from it.

Ox1r Based on Ox2r Crystal Structure Loop Formation and Minimization

Each bundle was run through Modeller[134,135,136] to form 1080 loop conformation sets for each bundle, with the best 250 of those 1080 given further inspection to see which set best interacts, according to the circumstances, with itself, the ligand, and the transmembrane bundle. Each model had EC2 and EC3, and all three IC loops, varied so that IC3 would become an extension of TMH5 and TMH6 as before,[2,141] IC1 and IC2 stay out of IC3's way, and that the EC2 loop form a disulfide bridge between C3.25 and C45.50 as before.[3] The "up-down-up-down" arrangement that points D45.51 and R45.53 up, and E45.52 and W45.54 down, is retained.[145] The EC2 loop's D45.51 and W45.54 retained their duties of holding the two halves of the EC2 loop out of the way to clear a path for orexin-A,[3,24] with P45.38-R45.45's helicity from before and the R45.45-D45.51 interaction retained as well to keep the ligand binding cavity open.[24,145] E45.52 was also chosen to interact with R328 in the EC3 loop to keep the R state's entry gap closed, as well as to hold the R* state's entry gap open for orexin-A by interacting with K3.26, just

as before. W45.54's role in an aromatic network to keep the EC2b loop out of the way of any ligand was retained,[3] with EC3 varied at the same time to keep it out of the way of EC2. All five aforementioned loops were varied simultaneously in order to save computational time. The necessary C3.25-C45.50 disulfide bond was formed,[3] hydrogens were added, and the loops were reminimized for 500 steps in "wet" minimization conditions.

Ox1r Based on Ox2r Crystal Structure Termini Formation, Palmitoylation, and Minimization

Afterward, the placeholding termini were replaced with the completed termini from the previous models,[134,135,136] so that the new R model has the previous R model's termini and the new R* model has the previous R* model's termini. This saved computational time, as the termini only needed one anchor for each, as opposed to two anchors for each loop, and were relatively distant from the bundle.[134,135,136] Since C375 for each model was already attached to the bundle and pointed correctly toward the lipid bilayer, no further adjustment was required to allow for proper orientation, and a palmitoyl group was added to both models' C375 residue to point into that bilayer.[3,7,156] Afterward, both models were minimized 500 steps "dry," and the loops and termini 500 steps "wet." Both models were then aligned with the ox2r[7] from the OPM database so that they can be properly used in later experiments.[157]

Parametrization Equation and Necessity

With the completion of the R and R* models, the next step is to equilibrate these models, each with bound ligands, in a molecular dynamics (MD) simulation of a palmitoyl-oleoyl-phosphatidylcholine (POPC) lipid bilayer, aligned based on the OPM

alignment of GPCR crystal structures.[157,158,159,160] This is done using the CHARMM force field, which uses a potential energy function that penalizes deviations from equilibrium values of bond lengths, bond angles, improper dihedral angles, Urey-Bradley distances, dihedral torsion angles, and distances based on Lennard-Jones van der Waals and electrostatic interactions between nonbonded atoms, as shown in Equation 1.[158,159,160]

$$E = \sum_{bond\ lengths} K_b(b - b_0)^2 + \sum_{bond\ angles} K_\theta(\theta - \theta_0)^2 + \sum_{impropers} K_\psi(\psi - \psi_0)^2 + \sum_{Urey-Bradley\ terms} K_{UB}(\alpha - \alpha_0)^2 + \sum_{dihedrals} K_\varphi[1 + \cos(n\varphi - \delta)] + \sum_{nonbonded\ terms} \left\{ \varepsilon_{ij} \left[\left(\frac{R_{min,ij}}{r_{ij}} \right)^{12} - \left(\frac{R_{min,ij}}{r_{ij}} \right)^{6} \right] + \frac{q_i q_j}{\varepsilon_1 r_{ij}} \right\}$$

Equation 1. The CHARMM Potential Energy Function, Where the Potential Energy (E) is a Sum of Deviations from Equilibrium Values for all Bond Lengths, All Bond Angles, All Urey-Bradley Terms, All Dihedral Angles, and All Improper Dihedrals, Each with Its Own Force Constant, and All Nonbonded Terms (a Sum of Lennard-Jones van der Waals and Electrostatic Interactions).

However, such simulation cannot be performed without determining proper force field parameters for SB-674042 (in the R structure) and the pyroglutamic acid residue that begins orexin-A (in the R* structure).[3,4,137] Therefore, such parameters must be constructed and validated as follows, by using QM data (Hartree-Fock 6-31G*) as a basis for developing these new parameters.[159,160] The first step is to use the modeling program Spartan (Wavefunction Inc., Irvine, CA) and run a conformational search to determine a true global minimum for each molecule to be entered into the CHARMM General Force Field (CGenFF, https://cgenff.paramchem.org/) as a starting point in the search for new

parameters, as CGenFF includes organic compounds that the CHARMM topology and parameter files lack.[161,162,163,164] Doing so was necessary to find (and make new Lennard-Jones van der Waals parameters for) new atom types, retrieve the whole molecules' bond length, bond angle, dihedral angle, and improper torsion parameters, produce the CHARMM topology for each molecule, and determine each molecule's charges.[161,162,163,164]

Construction of Model Compounds

Each molecule that needed new parameters (both SB-674042 and pyroglutamate, the latter NMA-capped on the C-terminus) was broken into several model compounds for determining charges (the charge model compounds), as well as bonds, angles, and torsions (the **b**ond length-bond **a**ngle-dihedral **t**orsion (BAT) model compounds) for SB-674042 and its model compounds, with each model compound categorized by their corresponding number, with Charge Model Compounds 1-6 and BAT Model Compounds 1-4 used for SB-674042, and Charge Model Compounds 1, 2, 4, and 7 used for BAT Model Compound 5, which was used solely to repair the CO1-C51-C51-C61 dihedral torsion parameter absent from BAT Model Compounds 1-4.[137,159,160,161,162,163,164] SB-674042 and the charge model compounds are shown in Figures 15 and 16.[137,159,160,161,162,163,164] SB-674042's BAT compounds are shown in Figures 17 and 18.[137,159,160,161,162,163,164]

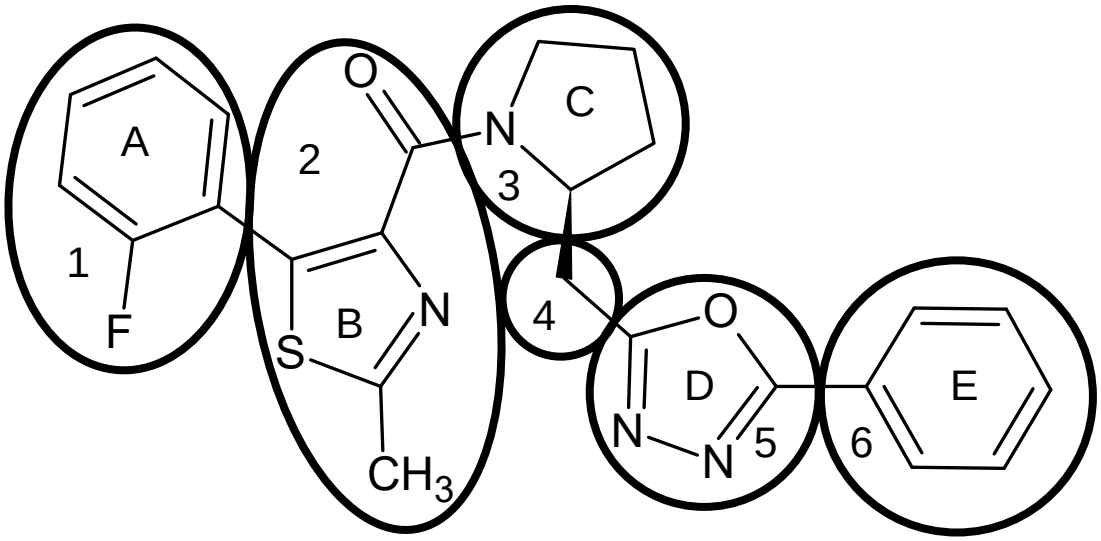

Figure 15. Whole Molecule of SB-674042, With Rings Identified With Letters, and Parts Numbered and Circled.[137,159,160,161,162,163,164]

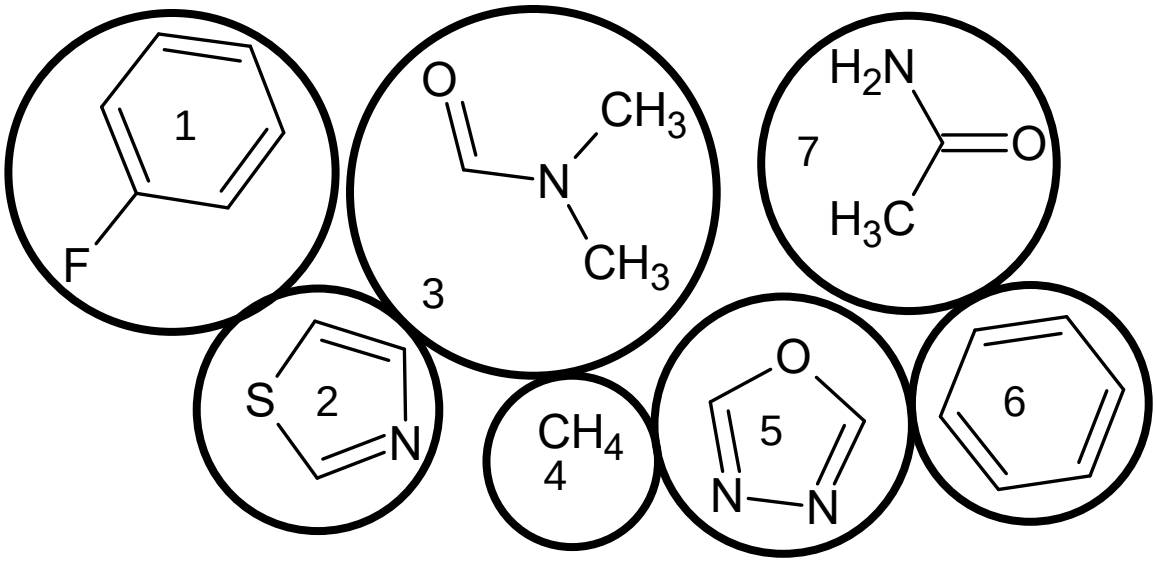

Figure 16. Charge Model Compounds of SB-674042, Labeled by Number.[137,159,160,161,162,163,164]

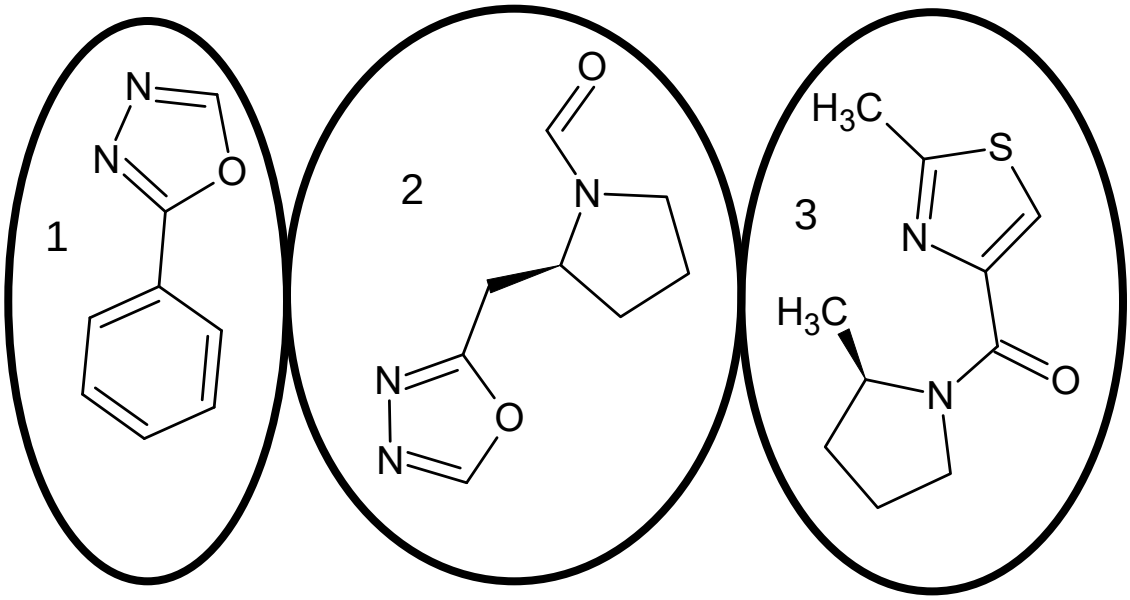

Figure 17. BAT Model Compounds 1-3 of SB-674042.[137,159,160,161,162,163,164]

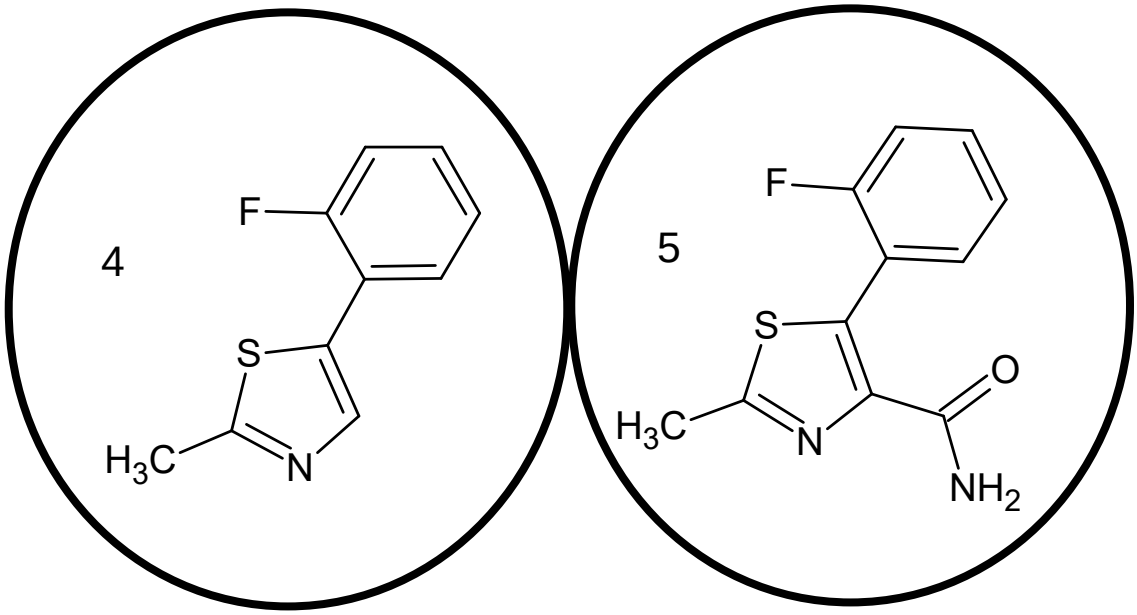

Figure 18. BAT Model Compounds 4-5 of SB-674042.[137,159,160,161,162,163,164]

As pyroglutamate-NMA was already a small molecule, it served as its own BAT model compound, as shown in Figure 19.[4,159,160,161,162,163,164]

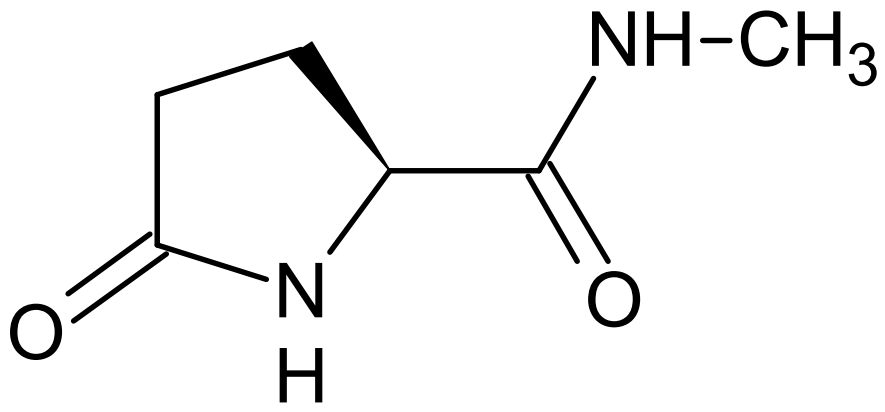

Figure 19. Whole Molecule of Pyroglutamate-NMA.[4,159,160,161,162,163,164]

The charge model compounds were based on the lactam model compound and on the backbone carbonyl groups and NMA C-terminus cap in the CHARMM topology file, as shown in Figure 20.[4,159,160,161,162,163,164]

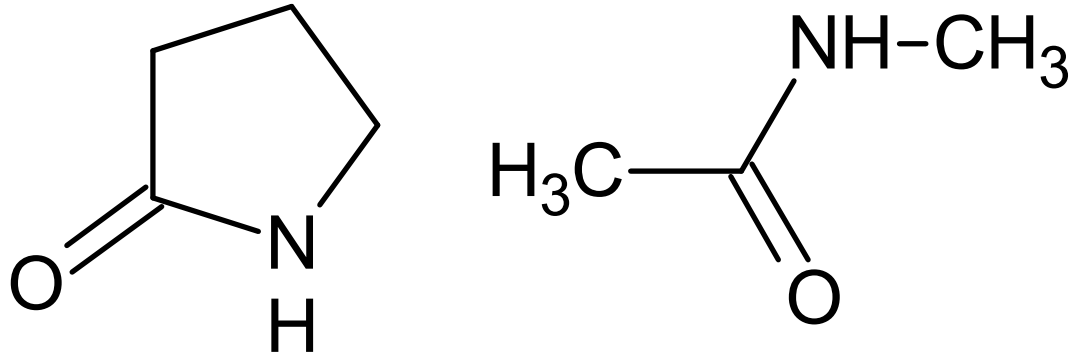

Figure 20. Charge Model Compounds of Pyroglutamate-NMA. The One on the Right was Not Needed, as the Backbone Carbonyl Charges and NMA C-terminus Cap Charges from the CHARMM Topology Files are Used Instead.[4,159,160,161,162,163,164]

Each model compound had a conformational search performed on it as before, and was entered into CGenFF[161,162,163,164] to find (and make new Lennard-Jones van der Waals parameters for) new atom types, retrieve the model compound's bond length, bond angle,

dihedral angle, and improper torsion parameters, produce the CHARMM topology for each molecule, and determine each molecule's charges. New atom types were assigned based on CHARMM's four-character equivalents to the CGenFF six-character atom types, with new types introduced so that repetition of atom types for differently placed atoms, bond lengths, bond angles, and dihedral angles would not happen.[159,160,161,162,163,164] This involves reproducing the masses and Lennard-Jones van der Waals parameters of these atom types from the CGenFF topology and parameter files to use in the four-character CHARMM topology and parameter files.[159,160,161,162,163,164] If the penalty for the charges did not exceed 10, the charges were usable.[161,162,163,164] If the penalty exceeded 10, but was less than 50, the charges could be improved by validation.[161,162,163,164] If the penalty exceeded 50, the charges had to be validated as follows.[161,162,163,164] The only model compound that failed such a charge test was 1,3,4-oxadiazole, whose charges were validated as follows.

Charge Validation

Using Jaguar, energy calculations at the Hartree-Fock 6-31G* level were performed on water and 1,3,4-oxadiazole separately, and on a complex of water and 1,3,4-oxadiazole in which they interact by pointing a hydrogen atom on 1,3,4-oxadiazole toward the oxygen atom on water, or by pointing a hydrogen atom on water toward an oxygen atom or nitrogen atom on 1,3,4-oxadiazole, with the difference (and the hydrogen-oxygen/nitrogen distance) being calculated as the QM interaction energy and distance for each complex of water and 1,3,4-oxadiazole, used as the basis for the MM calculations, as shown in Figure 21.[158]

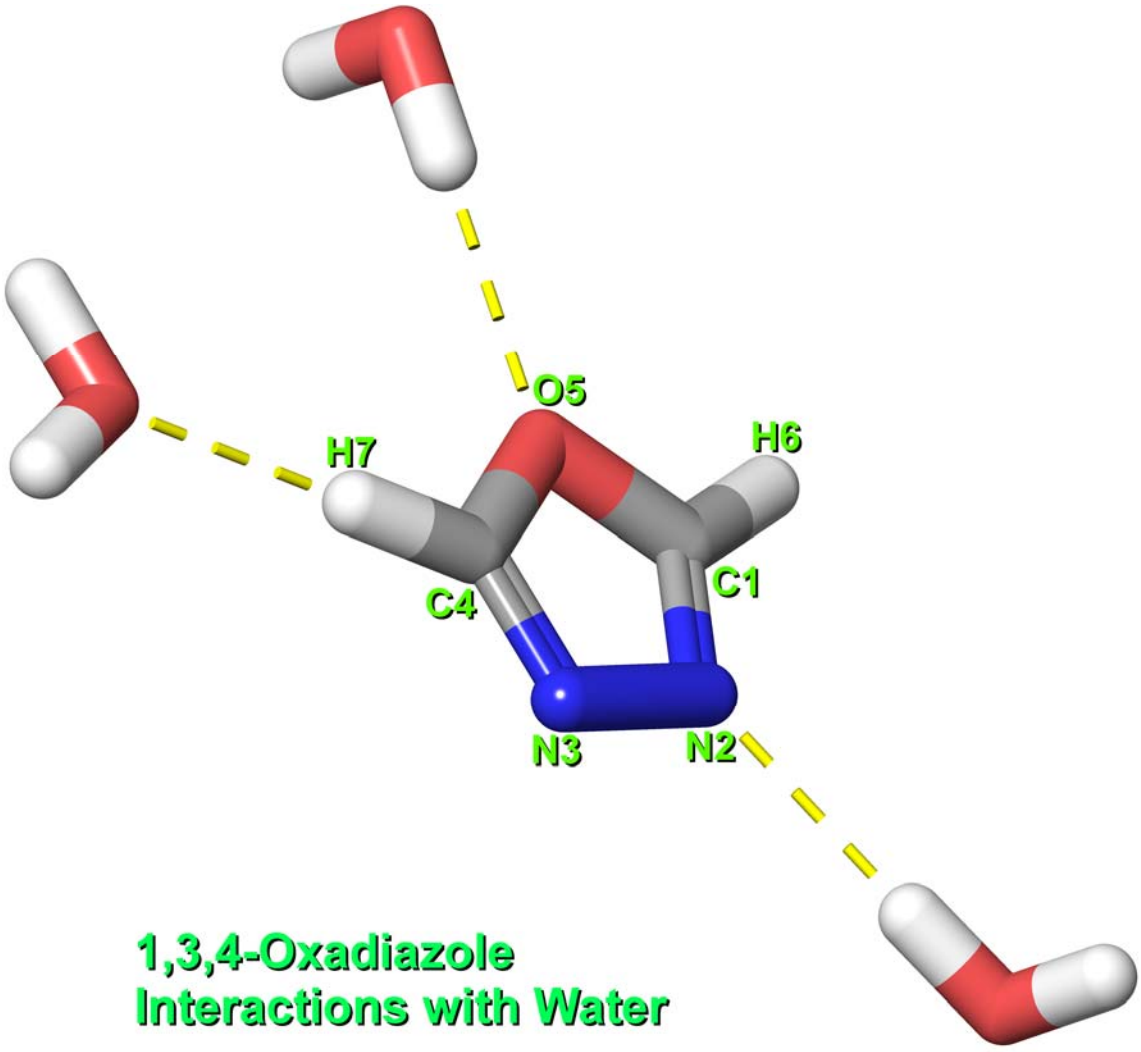

Figure 21. Interactions Between 1,3,4-oxadiazole and Water.[158]

These data were entered into a spreadsheet that calculated the QM interaction energies (in kcal/mol) based on the energy results of the Jaguar energy calculations.[158] Additionally, this spreadsheet also had an inventory of 1,3,4-oxadiazole's charges for each MM calculation, complete with the sums of these charges.[158] A verification formula was added that divides 1 by the sum of the charges, such that a #DIV/0! error message is

returned if the charges are (correctly) neutral, and a non-error-message number returned if the charges are not neutral, as shown in Figure 22.

Atom Name	Positive	Neutral
C1	0.630	0.630
N2	-0.490	-0.490
N3	-0.490	-0.490
C4	0.630	0.630
O5	0.560	-0.440
H6	0.080	0.080
H7	0.080	0.080
Sum	1.000	0.000
Check	1.000000	#DIV/0!

Figure 22. Effect of the Charges of 1,3,4-oxadiazole on the Verification Formula Beneath, With the Left Set of Numbers Showing the Effects of a +1 Charge (Supplied by O5's Charge Changed from –0.44 to +0.56), and the Right Showing the Effects of a Neutral Charge.

For the MM calculations, a similar complex is generated for each QM 1,3,4-oxadiazole and water complex and the charges in the topology of 1,3,4-oxadiazole are adjusted as follows.[158] The charges of the ring oxygen, the ring nitrogen, and the

hydrogen used in these interactions were adjusted, while keeping the charges symmetrical and neutral across the molecule as shown in Figure 23.[158]

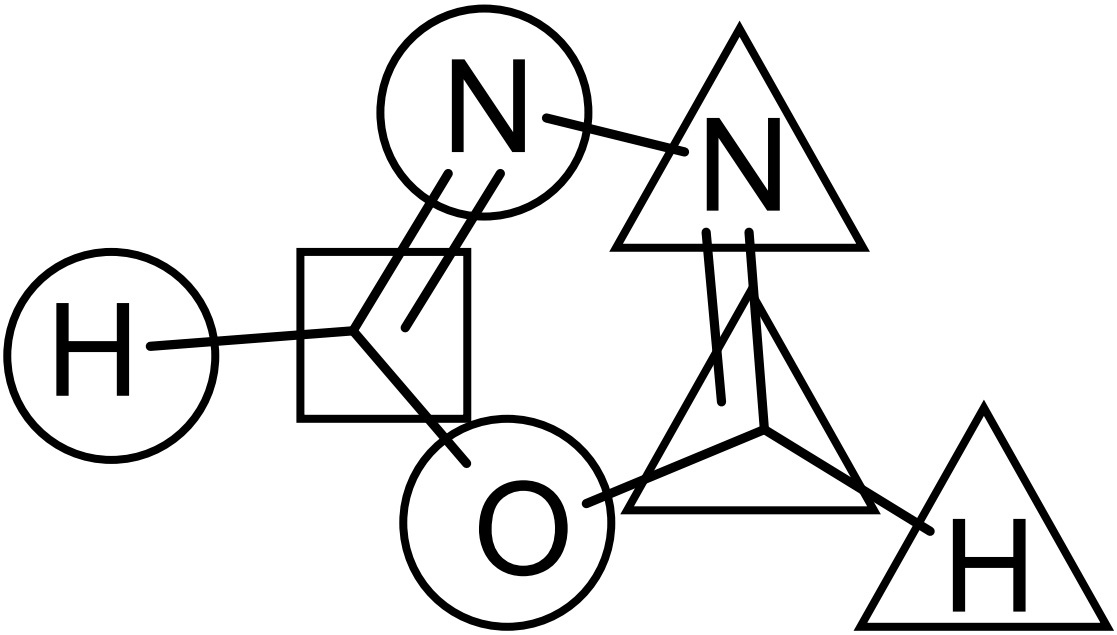

Figure 23. Charge Adjustments in 1,3,4-oxadiazole, in Which the Main Charges to Be Changed are Circled, the Boxed Carbon is Adjusted to Maintain Neutrality, and the Triangled Atoms are Kept Equal to Their Counterparts at All Times.

These adjustments continued until the CHARMM interaction energy was as close to within 0.25 kcal/mol of the QM interaction energy, and the CHARMM interaction distance as close to within 0.1 Å of the QM interaction distance, as possible.[158]

Bond Length, Bond Angle, and Dihedral Angle Measurement of Model Compounds

With the charges for each charge model compound calculated, the BAT model compounds were formed by removing the charges of the extra hydrogen atoms from each heavy atom, adding the charges from these hydrogen atoms to their adjacent heavy atoms, and then connecting these heavy atoms to form the charges for the BAT model

compounds so the bond lengths, bond angles, and dihedral angles can be optimized for each.[165,166,167] This is shown in Figure 24.[165,166,167]

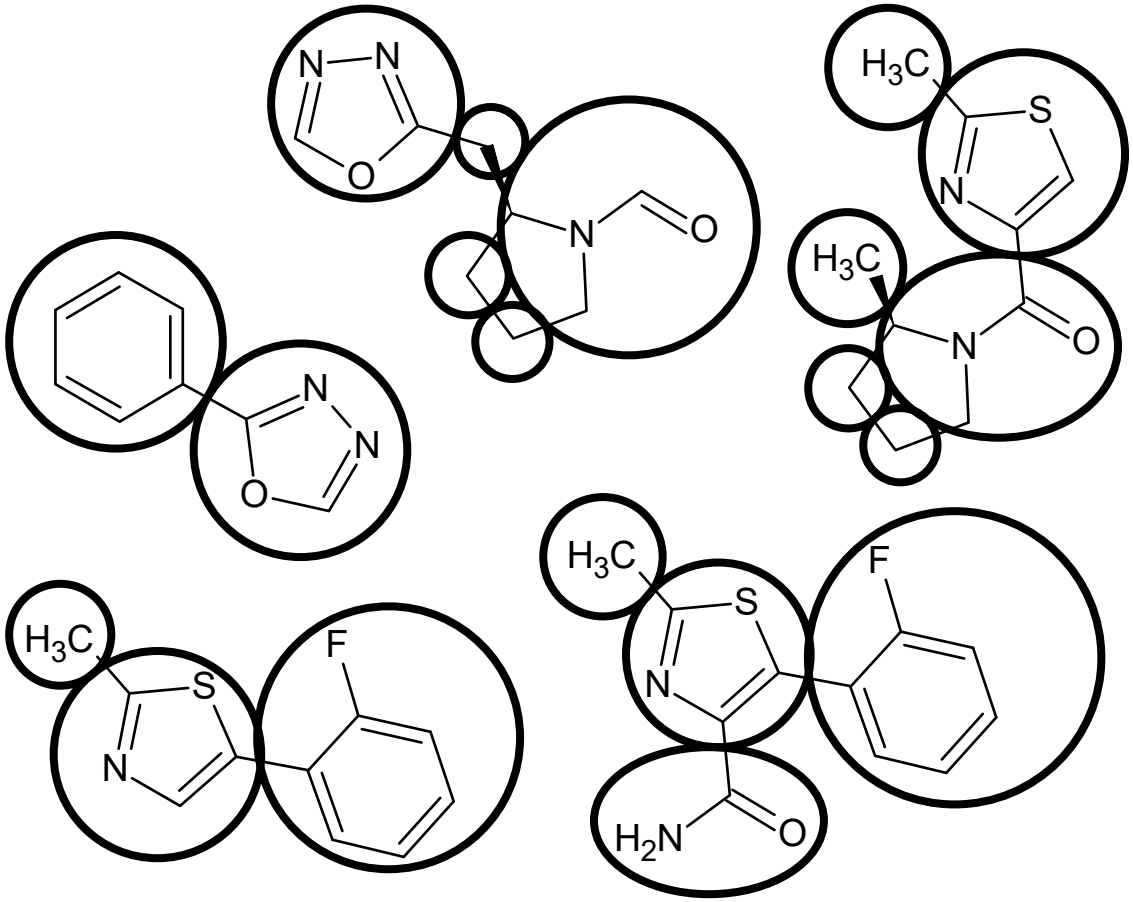

Figure 24. BAT Model Compounds for SB-674042, with the Charge Model Compounds for Each Circled.

The QM structures for these model compounds each had all of its bond lengths, bond angles, and dihedral angles measured and listed in a spreadsheet that also compared its bond lengths, bond angles, and dihedral torsions to the MM measurements, with the difference sent to a pass/fail test that works as follows. A script was created that measured the MM bond lengths, bond angles, and dihedral torsions to be listed in this

spreadsheet for each of those QM measurements, and simultaneously produced the MM-minimized conformation for comparison to the QM global minimum for that compound. The QM-MM difference is listed and the absolute value thereof taken. The bottom of each list also contains the maximum and root-mean-square of these absolute values for that list for ease of quick verification of that compound. Each value in that list, as well as the maximum, is run through a verification formula that determines whether or not the MM is within 0.03 Å of length,[165,166,167] 3° of bond angle,[158] or 8° of dihedral angle[158] of the QM compound, as shown in Equation 2.

$$Check = \frac{1}{Max(x,y) - y} + 100000$$

Equation 2. Verification Formula to Determine if the MM Measurement is Within the Margin of Error of QM, Where x is the Absolute Difference Between a Measurement in QM and the Same in MM, y is 0.03 Å in Length, 3° of Bond Angle, or 8° of Dihedral Angle, and 100000 is Added for Ease of Verification.

An error message #DIV/0! is returned if the measurement falls within the margin of error, but a large number (~100000) is returned if it does not, and the cell is set to five decimal places for the sole reason of increasing the visibility of any failing bond length, bond angle, or dihedral angle immensely to the point of easy distinction, as the error message is significantly shorter than the large number.

A generator script is used to produce a table of internal coordinates to be modified according to the model compound's QM measurements of bonds, angles, and dihedrals, and these modified internal coordinates are added to the topology file for that model compound. This is crucial for the following steps.

For every bond length, bond angle, and dihedral angle that falls outside of the margin of error, energy surfaces had to be produced by varying the problem bond length, bond angle, or dihedral angle in Spartan (Wavefunction Inc., Irvine, CA) using a Hartree-Fock 6-31G* basis set over a certain range of bond length, bond angle, or dihedral angle and at equal intervals to produce 37 separate conformers of the compound.[168] For example, a freely-rotating dihedral would be varied over a 360° range at 10° increments to produce 37 conformers (36 different conformers with the first and last identical).[168] Each of those conformers had an MP2/HF-6-31G* energy calculation performed on it, then each energy measurement was converted to kcal/mol and entered into a QM-MM potential energy surface comparison spreadsheet to produce the QM energy profile reference graph.[158]

Bond Length and Bond Angle Optimization of Model Compounds

The procedure is to repair the bond lengths and bond angles together, then to repair the dihedrals.[165,166,167,168] To create the corresponding MM potential energy surface, the problem bond length or bond angle is frozen in place using the internal coordinate file at the values corresponding to the 37 conformers produced by the corresponding QM energy surface experiment, with the rest of that conformer minimized and an energy measured for that conformer.[165,166,167,168] Using this MM potential energy surface script, lists of measurements and energies were produced in a spreadsheet-friendly format and entered into the QM-MM potential energy surface comparison spreadsheet, which produced energy profile graphs that visualize the difference between the QM and MM energy surfaces.[165,166,167,168] The bond length and bond angle force

constants (K_b and K_θ values) and idealized bond lengths and bond angles (b_0 and θ_0 values) were varied manually until the MM energy surfaces closely matched the QM energy surfaces for all problem bond length and bond angle parameters, and that all bond length and bond angle measurements fall within the margin of error.[158,165,166,167]

Dihedral Angle Optimization of Model Compounds

With the bond lengths and bond angles repaired, the dihedrals followed.[165,166,167,168] A similar script to (and the basis of) the bond length/bond angle potential energy surface script was used to create the CHARMM potential energies.[165,166,167,168] It did not modify the internal coordinate file, but it instead constrained the problem dihedral with an immobilizing non-sinusoidal force restraint to the values corresponding to the 37 conformers produced by the corresponding QM energy surface experiment, with the conformer minimized and an energy measured for that conformer.[165,166,167,168] Like the previous script, this script also produces spreadsheet-friendly lists of measurements to be entered into yet another QM-MM potential energy surface comparison spreadsheet.[165,166,167,168] The torsional force constants (K_φ, listed as K_χ in the parameter file), periodicity values (n), and offset values (δ) were varied manually, with multiple dihedral parameters layered in as necessary in such a way as to not repeat periodicity values, have periodicity values of anything other than 1-4 or 6, or have the offset value be anything other than 0° or 180°, until the MM energy surfaces closely matched the QM energy surfaces for all problem dihedral parameters, and that all dihedral angle measurements fall within the margin of error.[158,165,166,167] In some difficult cases, all force constants for the problem dihedral

would be zeroed, the MM potential energy surface taken and entered into a spreadsheet, and simulated dihedral parameters added to the graph to precisely and accurately choose new dihedral parameters immediately. With the dihedrals repaired, the bond lengths and angles are to be verified to be within the margin of error, and the previous two steps (bond lengths/bond angles and dihedral torsions) repeated iteratively on all BAT model compounds until all bond lengths, bond angles, and dihedral angles fall within the margin of error for all BAT model compounds using the same topology and parameter files for each BAT model compound.[158,165,166,167]

Construction of SB-674042 and Pyroglutamate, and Their Intermodel Connections

In order to parametrize the entire molecule, the charges and atom types were assembled for the complete SB-674042 compound just as the charges for the BAT model compounds were calculated, and an internal coordinate file was created just as those for each BAT model compound was created.[158,159,160,161,162,163,164,165,166,167] The measurement script for SB-674042 was created just as those for the BAT model compounds were, with measurements taken with the old parameters and with the new BAT-based parameters.[158,165,166,167] If any measurements fell outside the margin of error, new QM energy surfaces were created just as they had been for problem bond lengths, bond angles, and dihedral angles for (and using, in the first two cases) the BAT model compounds, with MM energy surface scripts created to match, so that the MM energy surface for the problem parameter can be made to match the QM energy surface by parameter modification in similar fashion to those of the BAT model compounds.[158,165,166,167,168] This is repeated until all bond length, bond angle, and

dihedral angle measurements fall within the margin of error.[158,165,166,167,168] Furthermore, the QM structures for the global minimum and two local minima were minimized using the old and new MM parameters to display the difference between the old and new parameters.[158,165,166,167,168] This produced MM models that resembled the QM output more than the old parameters' MM models did.[158,165,166,167,168]

For pyroglutamate, the remaining steps involve generation of pyroglutamate-proline-NH_2 (PyroEP) to ensure the proper way of connecting pyroglutamate as an N-terminal protein residue and a primary amide cap as a C-terminal residue patch in CHARMM.[161,162,163,164,165,166,167,168] This was followed up with minimization with the CHARMM parameters, then determining if there are any missing parameters and missing internal coordinates pertaining to amino acid connection that needed to be present.[161,162,163,164,165,166,167,168] If there are any, then similar parameters to those connecting one amino acid to another were substituted in with atom names changed to match, so that pyroglutamate can be used as an N-terminal amino acid cap regardless of whether the next residue is a proline or not.[161,162,163,164,165,166,167,168]

Construction of the Simulated Lipid Bilayer Cell to House the Ox1r R and R* Models

The ox1r model, in the inactive state and docked with the antagonist SB-674042 as described above,[3,7,24,137] was truncated at Y41 (N-terminus) and acetylated there. In addition, the receptor was capped at C375 with methylamide. The complex was aligned with the $S1P_1$ structure[169] from the OPM database.[157] In order to ensure that the hydrophobic residues on the amphipathic helix 8 protrude into the hydrophobic region of the initial POPC(1-palmitoyl-2-oleoyl-phosphatidylcholine) lipid bilayer, this structure

was shifted 3 Å along the membrane normal in the +z direction (away from cytoplasm). This results in the transmembrane region of orexin being approximately centered at the middle of the lipid bilayer with Hx8 orientated parallel to the plane of the membrane at the lipid/water interface. The model membrane simulation cell was constructed using the method described in Grossfield et. al[170] with the addition of constraints on the cis-double bond of POPC (force constant = 250 kcal mol^{-1} $radian^{-2}$). This resulted in a simulation cell of initial size 86.14 Å x 86.14 Å x 136.0 Å with 176 molecules of POPC and 22188 molecules of H_2O. Periodic boundary conditions were employed in the molecular dynamics, thus a buffer of at least 12 Å was provided in each dimension to avoid having ox1r interact with its images. The CHARMM 22 protein force field[156] and the CHARMM 36 lipid force field[171] were used in this study. Moreover, C375 was palmitoylated using parameters from earlier CB2 simulation experiments,[172] and missing parameters for SB-674042[137] and for orexin-A's pyroglutamate residue[4] were developed and discussed above. Charge neutrality was enforced with addition of chloride counter ions, and an overall ionic strength of 0.15M was obtained by adding NaCl. The final system contained 95754 atoms.

The simulation cell for the active orexin receptor docked with the orexin-A peptide[3,4,7,22,24] was constructed in a similar fashion as that described above for the inactive state. Similar to the inactive state, the receptor was truncated, capped with methylamide, and palmitoylated at C375. However, the N-terminus was acetylated at L32 rather than Y41, as several of these residues contact the bound peptide agonist, such as L32, L35, W36, L40, Y41, and P42.[3,4,7,22,24] The active receptor has a slightly

different shape than the R state and this leads to a slightly modified initial cell of dimension 91.11 Å x 91.11 Å x 128.0 Å. In addition to the protein and ions, the final system contained 206 POPC molecules and 23385 water molecules, for a total of 104034 atoms.

The simulation cell construction procedure was repeated for a total of 4 independent simulations for the inactive ox1r-SB-674042 complex[3,7,24,137] and 6 independent simulations for the activated ox1r-orexin-A complex.[3,4,7,22,24] Once constructed, minimization and molecular dynamics were performed for each independent system as described below.

Initial Minimization of the Ox1r R and R* Models in a Simulated Lipid Bilayer

As described in Grossfield et al.[170] to relieve poor initial contacts, 2000 steps of steepest descent minimization were performed using CHARMM,[173] with all heavy atoms of the protein, ligands, and internal waters fixed. This was followed by a series of warming/minimization steps using NAMD.[174] Each step included 500 steps of conjugate gradient minimization followed by 500 steps of MD at a 5 K higher temperature. Throughout this phase restraints were applied to the protein/ligand and internal water molecules (force constant = 5 kcal mol^{-1} $Å^{-2}$). This was performed until the target temperature of 310 K was reached. Finally, these restraints were released in a series of minimizations wherein the force constant was gradually reduced from 5.0 to 2.5, then to 1.0, to 0.5, to 0.25, to 0.1, and lastly to 0.05 kcal mol^{-1} $Å^{-2}$, with 500 steps of minimization at each step. Finally, 2000 steps of restraint free minimization were executed. MD simulations were then performed on the fully minimized systems.

Details of Molecular Dynamics Simulations of the Ox1r R and R* Models

Prior to unrestrained molecular dynamics on these systems, 2 ns of position restrained (force constant = 5.0 kcal mol^{-1} $Å^{-2}$) molecular dynamics was performed using the AMBER12 package.[175,176,177] For all production runs the GPU accelerated PME (Particle Mesh Ewald) pmemd.cuda was utilized. Long range electrostatics were included using PME with the recommended 8 Å cutoff[175,176] and default values for the charge grid spacing, which were chosen to be approximately 1 Å and B-spline (cubic). The NPT ensemble was used to maintain temperature (T = 310 K, Langevin dynamics with a collision frequency of 5 ps^{-1}) and pressure (P = 1.0 bar, using the weak coupling Berendsen pressure control with pressure relaxation time of 8 ps).[178] High frequency bonds to hydrogen were restrained using the shake method allowing the use of a 2 fs integration time step. The 2 ns of restrained MD allows the simulation cell to adjust and produce a reasonable density, without perturbing the receptor docked structure.[3,4,7,22,24,137] This was followed by 50 ns of unrestrained MD.

Once the MD runs were finished, the finished MD trajectories and structure files were loaded into the program VMD[179] and monitored to determine the quality of the bundle. This is done so that if the bundle successfully maintained fundamental interactions such as ligand-receptor interaction site distances,[3,4,22] and qualities such as Y6.48 χ1 dihedrals and R3.50-R6.30 distances,[124,125,126,127,128,129,130,141,142,143] as hypothesized, it would be declared successful. If it did not, then the problems would be diagnosed and corrected, and MD experiments repeated, until the MD experiment would be declared successful.[175,176]

Repair of Ox1r R and R* Models Based on Molecular Dynamics Experiments

After performing preliminary MD runs, the R and R* structures' IC1 loops were replaced with an IC1 loop structurally based on that from the ox2r crystal structure so that M77 in both the R and R* structures tucks into a hydrophobic pocket and away from cytoplasm.[7,175,176] Further changes ensued for each bundle. When minimizing, the more modern OPLS3 force field was used in place of OPLS_2005 when available.

The R model had SB-674042 redocked so that it can interact with H7.39[3] (via hydrogen bond to the amide oxygen and π-stack with the fluorophenyl group) and with N6.55[7] (via hydrogen bond to the 1,3,4-oxadiazole nitrogen) as well as with Q3.32.[3] The R structure also had its R3.50-T6.33 "ionic" lock reconfigured as is present in the ox2r crystal structure[7] so that the "ionic" lock would be less likely to break as long as the receptor remains in the R state.[124,125,126,127,128,129,130,141] Furthermore, the R structure had its EC2b and EC3 loops replaced with EC2b and EC3 loops that are structurally based on those from the ox2r crystal structure, with the top end of TMH6 replaced with that from ox2r to allow K6.58 and R6.59 to donate hydrogen bonds to D45.51, for H5.39 to donate a hydrogen bond to E45.52, and for the EC3 loop to be out of the way of these interactions.[7] This was repeated until a successful R bundle was made, which had SB-674042 move to one place, while maintaining its interaction with Q3.32,[3] and had it remain there for the remainder of the simulation.[3,7,24,137,175,176]

The R* structure had small adjustments to improve stability, and as the R* structure has no hydrogen bond partner for R6.59, it would be allowed to interact with phospholipid groups. It was further repaired by repositioning the orexin-A ligand to keep

its N-terminus high enough to clear TMH1, while maintaining its interaction with H7.39.[3,22] The conformational space of the C-terminus (residues 15-33) of orexin-A[22] was then explored, as shown in Figure 25.[133,147]

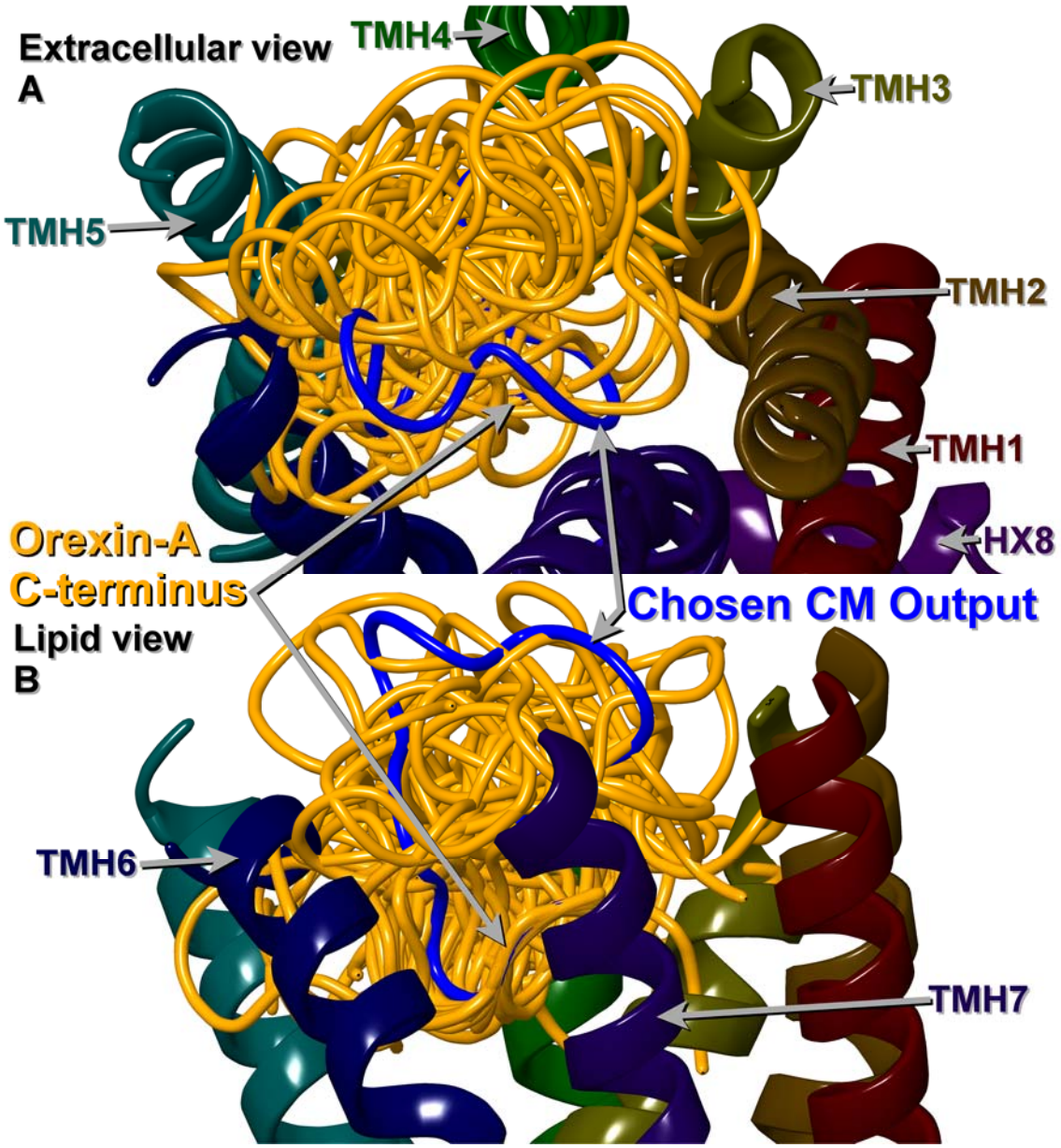

Figure 25. CM Output of Orexin-A (15-33), Superimposed on the Cαs of L31, T32, and L33, With the Chosen C-terminus Displayed in Blue, as the C-terminal End of It Fits Into the Ox1r Binding Pocket Better Than the Other C-termini Do.[4,22,133,147]

The conformational space of the C-terminus of orexin-A had to be explored because it became apparent that the entire ligand was not meant to fit within the ox1r, similar to other peptide-bound crystal structures,[146,180,181,182,183,184,185,186,187] which meant that only a small part of orexin-A would be needed to activate the ox1r.[3,4] It was done by running CM on a protein sequence that matches those residues, using full ±180° ranges for the φ and ψ dihedrals, running 150000 Monte Carlo steps per temperature stage, and producing 112 output peptides in order to be extra thorough.[4,22,133,147] The EC3 loop and top turn of TMH6 was replaced with that from the ox2r crystal structure, and the ox2r-template-based[7] ox1r bundle after the CM helices were superimposed,[133,144,145,147] after crystallographic waters were added,[7] but before orexin-A was docked,[3,4,22] was minimized together so that the bundle would be stable prior to orexin-A docking. The remaining loops and termini from the previous R* structure were reused to save computational time.[134,135,136]

The CM output of orexin-A (15-33)[4,22,133,147] was docked so that its C-terminus could reach into the binding pocket as a random coil, consistent with peptide-bound crystal structures,[146,180,181,182,183,184,185,186,187] as opposed to conventional means of modeling that preserved the α-helical structure for the orexin-A C-terminus.[9,155,188] This produced a dock that permitted H7.39 to accept a hydrogen bond from the amide cap of orexin-A[3,161,162,163,164] and permitted D45.51 to accept a hydrogen bond from orexin-A's H26,[3,22] the latter interaction not simultaneously possible with the former by docking the whole orexin-A molecule,[9,155,188] and produce numerous hydrophobic contacts within.[3,9,22,155,188] Modeller[134,135,136] was used to create the N-terminus, but as no

conformation produced was able to assemble both disulfide bonds while retaining the helical conformation in the orexin-A N-terminus,[134,135,136] the residues 1-14 were taken directly from the orexin-A NMR structure and the backbone dihedrals adjusted to allow it to keep clear of the extracellular loops.[4] This structure had MD experiments performed on it, and they revealed that more repairs would be necessary.[3,4,7,22,24,175,176]

Ox1r Based on Direct Mutation of Ox2r Crystal Structure Termini Formation, Palmitoylation, and Minimization

This experiment showed the shortcomings of pull-apart-and-minimize homology modeling as higher-identity crystal structures became available.[7,188] Therefore, new R and R* structures were made by direct mutation and renumbering using Maestro (Schrödinger 2006), such that the only residues that need to be added are the ic3 loop and termini, which can be reused from other models to save computational time,[134,135,136] and that Conformational Memories need only be used for helices with differing proline locations and for TMH6 of active GPCR models.[124,125,126,127,128,129,130,133,143,144,145,147,148,149]

First, the R structure was created by adding hydrogen atoms to the ox2r crystal structure,[7] removing the *Pyrococcus abysii* glycogen synthase and anything else that is neither ox2r crystal structure nor crystallographic water molecules from it,[7] directly mutating it to the ox1r sequence and numbering,[3] and filling in the short gaps in the sequence, all using Maestro's (Schrödinger 2006) homology modeling program, with minor side chain dihedral changes following afterward, especially those of C, S, and T. Any histidine whose interactions would be more consistent as a histidine with its hydrogen on Nε2, but not on Nδ1, was then mutated accordingly (H75, H76, and H5.39). Minimization of all nonpolar hydrogen atoms and changed side chains within the

structure “dry,” then those in the loop regions “wet,” to ease contacts within the structure followed.

The ligand SB-674042 was docked within the new R structure using the same pose as the final pose from the successful R bundle’s MD experiment, with Q3.32’s side chain oriented to donate a hydrogen bond to SB-674042’s amide oxygen,[3] and the ligand and Q3.32’s side chain were minimized “dry,” then “wet,” within to allow the ligand to relax within the binding pocket, to retain its interaction with Q3.32, and to relieve contacts between SB-674042 and the ox1r structure.[3,7,24,137,175,176] The IC3 loop from the previous R bundle was retained, while reusing the remaining part of the crystal structure that would connect to the IC3 loop in order to maintain fidelity with the crystal structure, and the N- and C-termini were also reused in a similar manner, with the new IC3 loop minimized “wet,” as shown in Figure 26.[7,134,135,136]

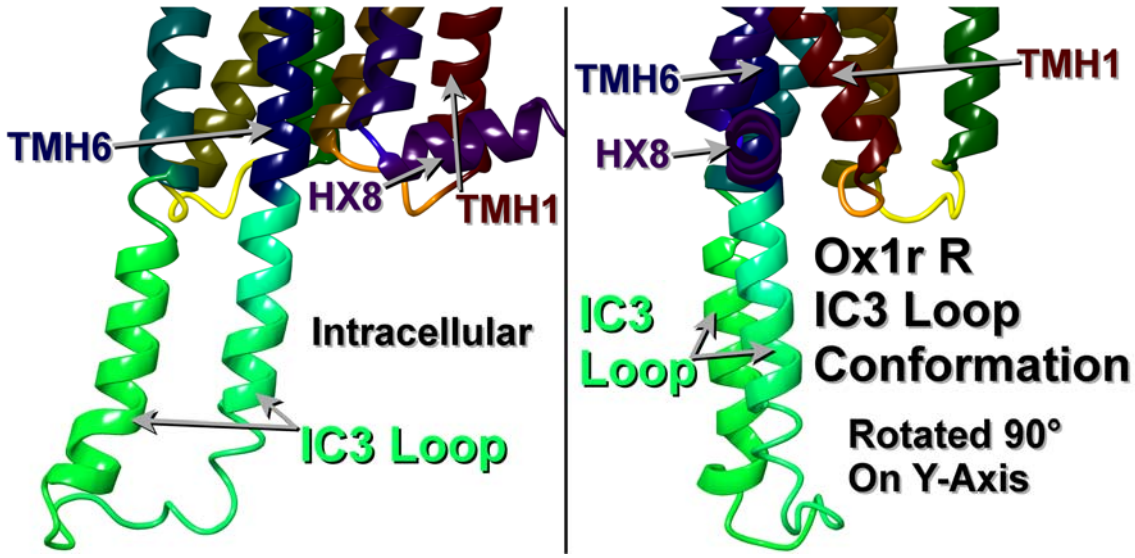

Figure 26. The New IC3 Loop for the R State.[7,134,135,136]

The new R* structure was made by using the newest R structure and aligning the best CM-produced TMH6 that kicked out[124,125,126,127,128,129,130,143] along the Cαs of residues 6.51-6.56 (as opposed to 6.51-6.61),[7,133,144,145,147] as shown in Figure 27. That TMH6 was aligned along the Cαs of residues 6.51-6.56, and not those of 6.51-6.61, for the same reason the top turn of TMH6 was replaced: the ox2r crystal structure's top turn was not wound as tightly as that of the CM helix used.[7,133,144,145,147] This is shown in Figure 28.[7,133,144,145,147]

This meant that removing residues 6.57-6.61 from the superimposition was necessary to improve how the helix superimposed onto the crystal structure's TMH6.[7,133,144,145,147] The residues on TMH6 and its intracellular extension were replaced below I6.51 (so that the C-terminus of the replaced part was P6.50) with the CM output, R3.50 was straightened out, and both R3.50[124,125,126,127,128,129,130,143] and the CM-based half of TMH6[7,133,144,145,147] were minimized "dry" so that no gaps occurred between TMH6 and the rest of the crystal structure, that Y6.48 would be in *trans*[124,125,126,127,128,129,130] and donating a hydrogen bond to T5.46, and that the R3.50-R6.30 distance would be ~17 Å.[124,125,126,127,128,129,130,142,143] Y5.58 was already in g^+ in the ox2r crystal structure,[7,138] so no changes were necessary. The IC3 loop from the previous R* bundle was reused, and the crystal structure residues 5.67-5.68 retained to maintain fidelity with the crystal structure at TMH5, then the new IC3 loop was minimized "wet," as shown in Figure 29.[7,134,135,136]

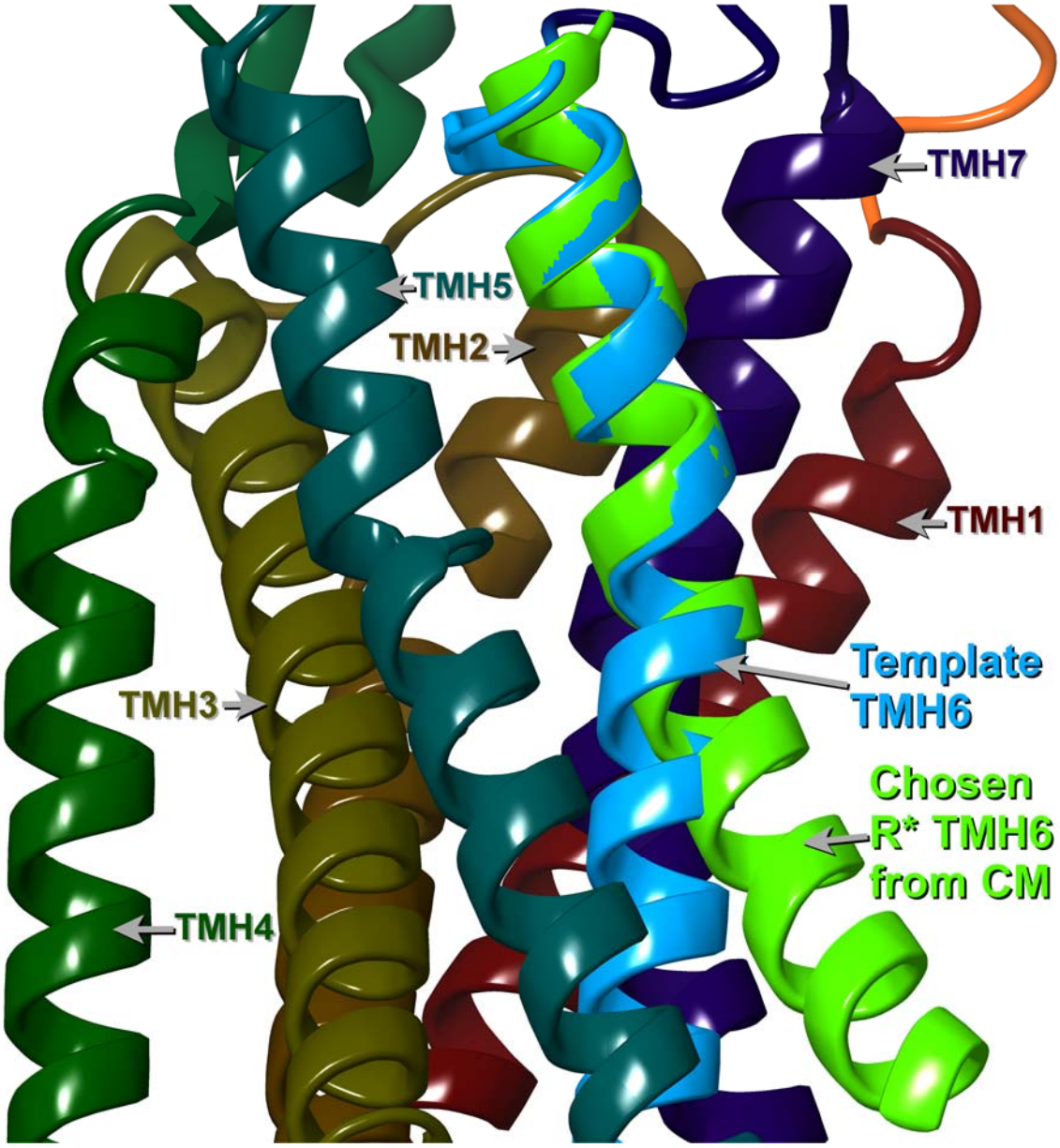

Figure 27. Best CM Helix for TMH6 (in Light Green) Superimposed on the Newest Ox1r R Structure Based on Direct Mutation of the Ox2r in Such a Way as to Permit the New TMH6 to Kick Out with Respect to the Template TMH6 (in Light Blue) and Have a Closer RMSD Match and Better Interhelical Contacts Than It Had in Figure 14.[7,133,144,145,147]

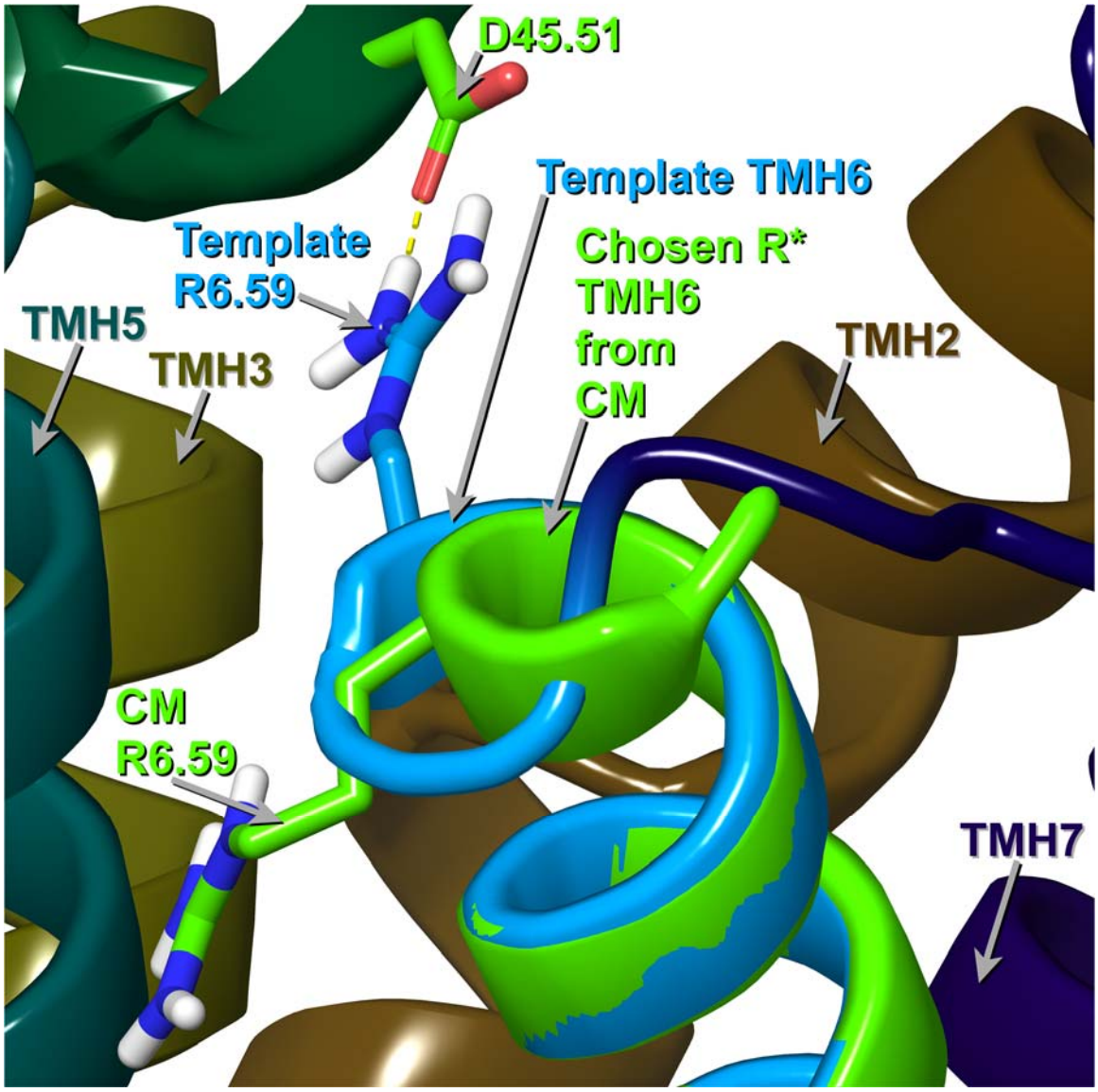

Figure 28. The Best CM Helix for TMH6 Superimposed is Wound Tighter on the EC Side Than the Newest Ox1r R Structure Based on Direct Mutation of the Ox2r.[7,133,144,145,147]

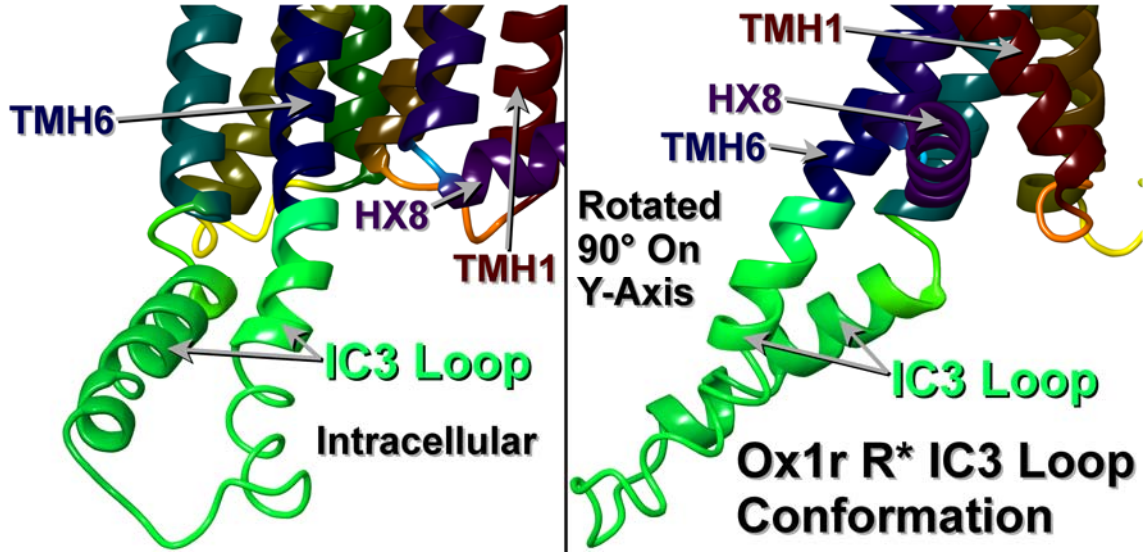

Figure 29. The New IC3 Loop for the R* State.[7,134,135,136]

Orexin-A (15-33)'s CM output[4,22,133,147] was then docked so the C-terminus can reach into the pocket as a random coil as before.[146,180,181,182,183,184,185,186,187] Due to increased knowledge about technique and structure, it was docked so that H7.39's hydrogen bond donor counterpart was instead T32's hydroxyl side chain, as it has a larger positive charge than the amide cap's polar hydrogens, and H7.39 can accept a hydrogen bond from T32 via its Nε2 while its Nδ1 hydrogen donates a hydrogen bond to D2.65.[3,7,22,161,162,163,164] This is similar to Karhu et al. which has T32 interact with H7.39 via its Nδ1.[9] However, unlike Karhu et al.,[9] H26 remained a hydrogen bond donor to D45.51.[3,22] Furthermore, I30, L31, and L33 all had important hydrophobic roles,[22] including L33's van der Waals contacts with F5.42[9] and Y6.48,[3,22] with N6.55 moved to *trans*, letting it donate a hydrogen bond to H5.39's side chain, to permit orexin-A the room to interact with the ox1r. Orexin-A's NMR structure[4] was then placed on the EC2a β-sheet structure with L16, L19, and L20 set up to create van der Waals contacts with that

EC2a loop structure.[7,22] This structure is common to peptide-binding receptors and may permit the peptide ligand to "discharge" itself into the binding pocket.[3,4,7,22,24,140,146,180,181,182,183,184,185,186,187]

The first 24 residues of the NMR structure of orexin-A[4] were then attached to residues 25-33 of the CM output of orexin-A (15-33)[4,22,133,147] and that connection, then the entire orexin-A structure, was minimized "wet" to permit orexin-A to settle in and pursue these good interactions.[3,4,7,22,24] It was then further optimized using the program Schrödinger Prime, holding the transmembrane Cαs at 5000 kJ/mol, to improve these interactions even more.[3,4,7,22,24]

When tested in MD experiments,[157,158,159,160] further repairs for both the R and R* models' ligand docking became necessary.[3,4,7,22,24]

The Procedure of Glide Ligand Docking

The ligand docking program Glide works by simulating the ligand binding site of the receptor with different energetic fields, and also by analyzing the ligand orientation and conformation.[189,190,191] All of the available ligand conformations are tested to fit the receptor grid created by those fields so that only the good poses are tested, then the ligand is minimized in the receptor grid with the OPLS-AA force field to lower the energy of poses that fit the grid, then the docks are scored.[189,190,191] There are two ways to score Glide ligand docks, SP and XP.[189,190,191] The initial parts of Glide ligand docks use the SP function, which totals the free energy changes from bond rotation, Coulombic and van der Waals energies, and polar and nonpolar mismatches.[189,190,191] The XP function goes even further by additionally rewarding water displacement into bulk solution and

rewarding more attractive polar/ionic interactions, as it also punishes restriction of motion.[189,190,191]

Ox1r Based on Direct Mutation of Ox2r Crystal Structure Ligand Dock Repair

The R bundle had SB-674042 docked using the Glide docking program as follows.[3,7,24,189,190,191] First, the R bundle was used as a Glide grid, with Q3.32 and N6.55 listed as hydrogen bond donors, then SB-674042 was docked using the Glide XP (Extra Precision, the most robust Glide docking technique at hand) ligand docking program.[3,7,24,189,190,191] The new dock replaced the hydrogen bond from Q3.32's amide hydrogens to SB-674042's amide oxygen (namely O13) with another hydrogen bond from Q3.32's amide hydrogens to the slightly less negatively charged, but far easier to access, oxadiazole ring nitrogens (namely N40), and allowed for three new π-π interactions to form.[3,7,24,189,190,191]

The R* bundle had the N-terminus reconfigured to add additional contacts between orexin-A's N-terminus and the ox1r's extracellular TMH1-2-7 area and displace additional waters from in between those areas.[3,4,7,22,24] Furthermore, the residues connecting orexin-A's central helix[4,22] to its hydrophobic C-terminus[4,22,133,147] were refined with Modeller,[134,135,136] which cleaned up the conformation so that it would be far more stable, and allowed H26 to donate a hydrogen bond to D45.51 and accept two from R45.53.[3,4,7,22,24]

Further repairs for the ox1r R* structure were necessary, so the last 4 residues of orexin-A were capped N-terminally with an acetyl group and docked with Glide XP, with the R* bundle used as a Glide grid and its H7.39 Nε2 listed as a hydrogen bond

acceptor.[3,4,7,22,24,189,190,191] Afterward, the residues connecting orexin-A's central helix[4,22] to its hydrophobic C-terminus[4,22,133,147] were refined with Modeller,[134,135,136] such that I30 in orexin-A would be remodeled with Modeller after L31 is placed with Glide XP in I30's presence,[4,22,134,135,136,189,190,191] allowing H26 and the orexin-A backbone to donate hydrogen bonds to D45.51, while R45.53 and K6.58 donate several hydrogen bonds to the orexin-A backbone.[3,4,7,22,24]

Still further repairs were needed, as the orexin-A N-terminus bound too well to the ox1r's extracellular TMH1-2-7 area, so the orexin-A N-terminus was reconfigured to bind instead to the ox1r EC2 loop.[3,4,7,22,24] As the previous round of minimizations of ox1r with orexin-A bound had completely optimized the orexin-A C-terminal dock, but since the round of minimizations that reoptimized the N-terminus and middle Helix 1 of orexin-A moved the other end of that connector,[3,4,7,22,24,133,134,135,136,147,189,190,191] the residues connecting orexin-A's central helix[4,22] to its hydrophobic C-terminus[4,22,133,134,135,136,147] were again refined with Modeller,[134,135,136] allowing H26 and the orexin-A backbone to donate hydrogen bonds to D45.51, while R45.53 and K6.58 donate several hydrogen bonds to the orexin-A backbone.[3,4,7,22,24]

The results of that R* structure's MD run, as it had all of the hallmarks of a good R* bundle with the exception of involving H7.39 in an interaction with orexin-A,[3,4,7,22,24,124,125,126,127,128,129,130,139,141,143,175,176] were used for the newest R* structure, but H7.39 was mutated so that its polar hydrogen was on Nε2 so it could donate a hydrogen bond to the orexin-A backbone and T32's hydrogen bond to the side chain of E45.52 was

retained, along with H26's side chain donating a hydrogen bond to D45.51's side chain.[3,4,7,22,24]

After this point, both the R and R* structures were finished[3,4,7,22,24] and, once converted to CHARMM, they were ready to use in MD experiments again.[157,158,159,160,175,176]

Summary of the Number of Programs Required to Dock Orexin-A in the Ox1r

In all, six programs were used to dock orexin-A in the ox1r[3,4,7,22,24]: Conformational Memories to create the rough orexin-A C-terminus,[4,22,133,147] Maestro (Schrödinger 2006) to hand-dock the orexin-A NMR structure and the Conformational Memories output and assemble them together as a complete molecule of orexin-A, while repairing orexin-A's N-terminus,[3,4,7,22,24,133,140,147,146,180,181,182,183,184,185,186,187] Schrödinger Prime to optimize that dock,[3,4,7,22,24] Glide to refine the dock of orexin-A's last four residues,[3,4,7,22,24,189,190,191] Modeller to connect the last three residues of orexin-A (as I30 would have to be refined again) to the central helix optimized by Schrödinger Prime in a low-free-energy fashion,[3,4,7,22,24,134,135,136] and lastly, MD to optimize the orexin-A dock once more.[3,4,7,22,24,175,176]

Calculations of Energies of Interaction and MD Trajectory Data Graphs

With the R and R* structures' successful MD experiments, two further experiments were carried out.[3,4,7,22,24,175,176] The ox1r R and R* models were extracted along with their ligands from the first and last frames of their respective trajectories using VMD[179] and the energies of interaction were calculated for each ligand before and after the MD experiment was allowed to run.[3,4,7,22,24,157,158,159,160,175,176] Furthermore, VMD[179]

was used to create graphs of the backbone and transmembrane Cα RMSD, Y6.48 χ1 dihedral measurements, and various distance measurements.[3,4,7,22,24,157,158,159,160,175,176]

Ox1r Based on Direct Mutation of Ox2r Crystal Structure Comparisons with Orexin-B Docks and with New Ox1r Crystal Structures

Two further experiments were carried out in addition to calculations of interaction energies and VMD graphing.[179] One was comparing the ox1r R* structure with orexin-A docked within it as extracted from the final frame of its MD experiment with a dock of orexin-B into the vacant ox1r R* structure that was extracted from that same frame.[3,4,7,22,24,131,132,157,158,159,160,175,176] Another was comparing the recently released orexin-1 receptor crystal structures (4zj8 and 4zjc)[192] with the orexin-1 receptor models before and after the MD simulations[3,4,7,22,24,157,158,159,160] to see the various structural similarities and differences between them.[3,4,7,22,24,192]

CHAPTER III

RESULTS

Primary Sequence of the Orexin-1 Receptor and Comparisons with Other GPCR Sequences

The orexin-1 receptor[3,24] has many common features, as well as differing features, with other GPCRs, such as the μ-opioid receptor,[140] the β_2-AR,[144,145] and the ox2r,[7] as shown in Figure 30.[152,169]

	1	Human Sequences																						
		See Key on last page With Absolute Sequence Numbers Below																						
1																								
Orexin-1																							M	E
Orexin-1																							1	2
Orexin-2																M	S	G	T	K	L	E	D	S	P
Orexin-2																1	2	3	4	5	6	7	8	9	10
Beta-2																								
Beta-2																								
MOR	M	D	S	S	A	A	P	T	N	A	S	N	C	T	D	A	L	A	Y	S	S	C	S	P	A	P
MOR	1	2	3	4	5	6	7	8	9	10	11	12	13	14	15	16	17	18	19	20	21	22	23	24	25	26
	N-Ter→																									
2																										
Orexin-1	P	S	A	T	P	G	A	Q	M	G	V	P	P	G	S	R	E	P	S	P	V	P	P	D	Y	E
Orexin-1	3	4	5	6	7	8	9	10	11	12	13	14	15	16	17	18	19	20	21	22	23	24	25	26	27	28
Orexin-2	P	C	R	N	W	S	S	A	S	E	L	N	E	T	Q	E	P	F	L	N	P	T	D	Y	D	D
Orexin-2	11	12	13	14	15	16	17	18	19	20	21	22	23	24	25	26	27	28	29	30	31	32	33	34	35	36
Beta-2												M	G	Q	P	G	N	G	S	A	F	L	L	A	P	N
Beta-2												1	2	3	4	5	6	7	8	9	10	11	12	13	14	15
MOR	S	P	G	S	W	V	N	L	S	H	L	D	G	N	L	S	D	P	C	G	P	N	R	T	D	L
MOR	27	28	29	30	31	32	33	34	35	36	37	38	39	40	41	42	43	44	45	46	47	48	49	50	51	52

Figure 30. Sequence Alignment[152,169] of the Ox1r,[3,24] Ox2r,[7] β_2-AR,[144,145] and the μ-opioid Receptor.[140]

																1	1	1	1	1	1	1	1	1	1	1
																2	3	3	3	3	3	3	3	3	3	3
3																9	0	1	2	3	4	5	6	7	8	9
Orexin-1	D	E	F		L	R	Y	L	W	R	D	Y	L	Y	P	K	Q	Y	E	W	V	L	I	A	A	Y
Orexin-1	29	30	31		32	33	34	35	36	37	38	39	40	41	42	43	44	45	46	47	48	49	50	51	52	53
Orexin-2	E	E	F		L	R	Y	L	W	R	E	Y	L	H	P	K	E	Y	E	W	V	L	I	A	G	Y
Orexin-2	37	38	39		40	41	42	43	44	45	46	47	48	49	50	51	52	53	54	55	56	57	58	59	60	61
Beta-2	R	S	H		A	P	D	H	D	V	T	Q	Q	R	D	E	V	W	V	V	G	M	G	I	V	M
Beta-2	16	17	18		19	20	21	22	23	24	25	26	27	28	29	30	31	32	33	34	35	36	37	38	39	40
MOR	G	G	R		D	S	L	C	P	P	T	G	S	P	S	M		I	T	A	I	T	I	M	A	L	Y
MOR	53	54	55		56	57	58	59	60	61	62	63	64	65	66	67		68	69	70	71	72	73	74	75	76	77
																TMH1→										
	1	1	1		1	1	1	1	1	1	1	1	1	1	1	1	1	1	1	1	1	1	1			
	3	4	4		4	4	4	4	4	4	4	5	5	5	5	5	5	5	5	5	6	6	6			
4	0	1	2		3	4	5	6	7	8	9	0	1	2	3	4	5	6	7	8	9	0	1	2			
Orexin-1	V	A	V		F	V	V	A	L	V	G	N	T	L	V	C	L	A	V	W	R	N			H	H	M
Orexin-1	54	55	56		57	58	59	60	61	62	63	64	65	66	67	68	69	70	71	72	73	74			75	76	77
Orexin-2	I	I	V		F	V	V	A	L	I	G	N	V	L	V	C	V	A	V	W	K	N			H	H	M
Orexin-2	62	63	64		65	66	67	68	69	70	71	72	73	74	75	76	77	78	79	80	81	82			83	84	85
Beta-2	S	L	I		V	L	A	I	V	F	G	N	V	L	V	I	T	A	I	A	K	F			E	R	L
Beta-2	41	42	43		44	45	46	47	48	49	50	51	52	53	54	55	56	57	58	59	60	61			62	63	64
MOR	S	I	V		C	V	V	G	L	F	G	N	F	L	V	M	Y	V	I	V	R	Y	T	K			M
MOR	78	79	80		81	82	83	84	85	86	87	88	89	90	91	92	93	94	95	96	97	98	99	100			101
																									IC1 Loop→		
			2		2	2	2	2	2	2	2	2	2	2	2	2	2	2	2	2	2	2	2	2	2	2	2
			3		3	4	4	4	4	4	4	4	4	4	4	5	5	5	5	5	5	5	5	5	5	6	6
5			8		9	0	1	2	3	4	5	6	7	8	9	0	1	2	3	4	5	6	7	8	9	0	1
Orexin-1	R	T	V		T	N	Y	F	I	V	N	L	S	L	A	D	V	L	V	T	A	I	C	L	P	A	S
Orexin-1	78	79	80		81	82	83	84	85	86	87	88	89	90	91	92	93	94	95	96	97	98	99	100	101	102	103
Orexin-2	R	T	V		T	N	Y	F	I	V	N	L	S	L	A	D	V	L	V	T	I	T	C	L	P	A	T
Orexin-2	86	87	88		89	90	91	92	93	94	95	96	97	98	99	100	101	102	103	104	105	106	107	108	109	110	111
Beta-2	Q	T	V		T	N	Y	F	I	T	S	L	A	C	A	D	L	V	M	G	L	A	V	V	P	F	G
Beta-2	65	66	67		68	69	70	71	72	73	74	75	76	77	78	79	80	81	82	83	84	85	86	87	88	89	90
MOR	K	T	A		T	N	I	Y	I	F	N	L	A	L	A	D	A	L	A	T	S	T	L	P	F	Q	S
MOR	102	103	104		105	106	107	108	109	110	111	112	113	114	115	116	117	118	119	120	121	122	123	124	125	126	127
				TMH2→																							

Figure 30. Cont.

	2	2	2	2	2	2							3	3	3	3	3	3	3	3	3	3	3	3	3
	6	6	6	6	6	6							2	2	2	2	2	2	2	3	3	3	3	3	3
6	2	3	4	5	6	7							2	3	4	5	6	7	8	9	0	1	2	3	4	5
Orexin-1	L	L	V	D	I	T	E	S	W	L	F	G	H	A	L	C	K	V	I	P	Y	L	Q	A	V	S
Orexin-1	104	105	106	107	108	109	110	111	112	113	114	115	116	117	118	119	120	121	122	123	124	125	126	127	128	129
Orexin-2	L	V	V	D	I	T	E	T	W	F	F	G	Q	S	L	C	K	V	I	P	Y	L	Q	T	V	S
Orexin-2	112	113	114	115	116	117	118	119	120	121	122	123	124	125	126	127	128	129	130	131	132	133	134	135	136	137
Beta-2	A	A	H	I	L	M	K	M	W	T	F	G	N	F	W	C	E	F	W	T	S	I	D	V	L	C
Beta-2	91	92	93	94	95	96	97	98	99	100	101	102	103	104	105	106	107	108	109	110	111	112	113	114	115	116
MOR	V	N	Y	L	M	G	T	W	P	F	G		T	I	L	C	K	I	V	I	S	I	D	Y	Y	N
MOR	128	129	130	131	132	133	134	135	136	137	138		139	140	141	142	143	144	145	146	147	148	149	150	151	152
							EC1 Loop→						TMH3→													
		3	3	3	3	3	3	3	3	3	3	3	3	3	3	3	3	3	3	3	3					
		3	3	3	4	4	4	4	4	4	4	4	4	4	5	5	5	5	5	5	5					
7		7	8	9	0	1	2	3	4	5	6	7	8	9	0	1	2	3	4	5	6					
Orexin-1	V	S	V	A	V	L	T	L	S	F	I	A	L	D	R	W	Y	A	I	C	H	P	L	L	F	K
Orexin-1	130	131	132	133	134	135	136	137	138	139	140	141	142	143	144	145	146	147	148	149	150	151	152	153	154	155
Orexin-2	V	S	V	S	V	L	T	L	S	C	I	A	L	D	R	W	Y	A	I	C	H	P	L	M	F	K
Orexin-2	138	139	140	141	142	143	144	145	146	147	148	149	150	151	152	153	154	155	156	157	158	159	160	161	162	163
Beta-2	V	T	A	S	I	E	T	L	C	V	I	A	V	D	R	Y	F	A	I	T	S	P	F	K	Y	Q
Beta-2	117	118	119	120	121	122	123	124	125	126	127	128	129	130	131	132	133	134	135	136	137	138	139	140	141	142
MOR	M	F	T	S	I	F	T	L	C	T	M	S	V	D	R	Y	I	A	V	C	H	P	V	K	A	L
MOR	153	154	155	156	157	158	159	160	161	162	163	164	165	166	167	168	169	170	171	172	173	174	175	176	177	178
														D/ERY/F/W Motif							IC2 Loop→				
				4	4	4	4	4	4	4	4	4	4	4	4	4	4	4	4	4	4	4	4	4	4	4
				3	3	4	4	4	4	4	4	4	4	4	4	5	5	5	5	5	5	5	5	5	5	6
8				8	9	0	1	2	3	4	5	6	7	8	9	0	1	2	3	4	5	6	7	8	9	0
Orexin-1	S			T	A	R	R	A	R	G	S	I	L	G	I	W	A	V	S	L	A	I	M	V	P	Q
Orexin-1	156			157	158	159	160	161	162	163	164	165	166	167	168	169	170	171	172	173	174	175	176	177	178	179
Orexin-2	S			T	A	K	R	A	R	N	S	I	V	I	I	W	I	V	S	C	I	I	M	I	P	Q
Orexin-2	164			165	166	167	168	169	170	171	172	173	174	175	176	177	178	179	180	181	182	183	184	185	186	187
Beta-2	S	L	L	T	K	N	K	A	R	V	I	I	L	M	V	W	I	V	S	G	L	T	S	F	L	P
Beta-2	143	144	145	146	147	148	149	150	151	152	153	154	155	156	157	158	159	160	161	162	163	164	165	166	167	168
MOR	D	F	R	T	P	R	N	A	K	I	I	N	V	C	N	W	I	L	S	S	A	I	G	L	P	V
MOR	179	180	181	182	183	184	185	186	187	188	189	190	191	192	193	194	195	196	197	198	199	200	201	202	203	204
					TMH4→																					

Figure 30. Cont.

	4	4	45	45	45	45	45	45	45	45	45	45	45	45	45	45	45	45	45	45	45	45	45	45	45	45
	6	6	3	3	3	3	3	3	3	3	3	3	4	4	4	4	4	4	4	4	4	5	5	5	5	
9	1	2	0	1	2	3	4	5	6	7	8	9	0	1	2	3	4	5	6	7	8	9	0	1	2	3
Orexin-1	A	A	V	M	E	C	S	S	V	L	P	E	L	A	N	R	T	R	L	F	S	V	C	D	E	R
Orexin-1	180	181	182	183	184	185	186	187	188	189	190	191	192	193	194	195	196	197	198	199	200	201	202	203	204	205
Orexin-2	A	I	V	M	E	C	S	T	V	F	P	G	L	A	N	K	T	T	L	F	T	V	C	D	E	R
Orexin-2	188	189	190	191	192	193	194	195	196	197	198	199	200	201	202	203	204	205	206	207	208	209	210	211	212	213
Beta-2	I	Q	M	H	W	Y	R	A	T	H	Q	E	A	I	N	C	Y	A	N	E	T	C	C	D	F	F
Beta-2	169	170	171	172	173	174	175	176	177	178	179	180	181	182	183	184	185	186	187	188	189	190	191	192	193	194
MOR	M	F									M	A	T	T	K	Y	R	Q	G	S	I	D	C	T	L	T
MOR	205	206									207	208	209	210	211	212	213	214	215	216	217	218	219	220	221	222
			EC2 Loop→													Internal loop							C3.25			
																disulfide							disulfide			
																bridge							bridge			
	45	45	45	5	5	5	5	5	5	5	5	5	5	5	5	5	5	5	5	5	5	5	5	5	5	5
	5	5	5	3	3	3	3	3	3	3	3	3	3	4	4	4	4	4	4	4	4	4	4	5	5	5
10	4	5	6	0	1	2	3	4	5	6	7	8	9	0	1	2	3	4	5	6	7	8	9	0	1	2
Orexin-1	W	A	D			D	L	Y	P	K	I	Y	H	S	C	F	F	I	V	T	Y	L	A	P	L	G
Orexin-1	206	207	208			209	210	211	212	213	214	215	216	217	218	219	220	221	222	223	224	225	226	227	228	229
Orexin-2	W	G	G			E	I	Y	P	K	M	Y	H	I	C	F	F	L	V	T	Y	M	A	P	L	C
Orexin-2	214	215	216			217	218	219	220	221	222	223	224	225	226	227	228	229	230	231	232	233	234	235	236	237
Beta-2	T	N								Q	A	Y	A	I	A	S	S	I	V	S	F	Y	V	P	L	V
Beta-2	195	196								197	198	199	200	201	202	203	204	205	206	207	208	209	210	211	212	213
MOR	F	S	H	P	T	W	Y	W	E	N	L	L	K	I	C	V	F	I	F	A	F	I	M	P	V	L
MOR	223	224	225	226	227	228	229	230	231	232	233	234	235	236	237	238	239	240	241	242	243	244	245	246	247	248
										TMH5→																
	5	5	5	5	5	5	5	5	5	5	5	5	5	5												
	5	5	5	5	5	5	5	6	6	6	6	6	6	6												
11	3	4	5	6	7	8	9	0	1	2	3	4	5	6												
Orexin-1	L	M	A	M	A	Y	F	Q	I	F	R	K	L	W	G	R	Q	I	P	G	T	T	S	A	L	V
Orexin-1	230	231	232	233	234	235	236	237	238	239	240	241	242	243	244	245	246	247	248	249	250	251	252	253	254	255
Orexin-2	L	M	V	L	A	Y	L	Q	I	F	R	K	L	W	C	R	Q	I	P	G	T	S	S	V	V	Q
Orexin-2	238	239	240	241	242	243	244	245	246	247	248	249	250	251	252	253	254	255	256	257	258	259	260	261	262	263
Beta-2	I	M	V	F	V	Y	S	R	V	F	Q	E	A	K	R	Q	L	Q	K	I	D	K	S	E	G	R
Beta-2	214	215	216	217	218	219	220	221	222	223	224	225	226	227	228	229	230	231	232	233	234	235	236	237	238	239
MOR	I	I	T	V	C	Y	G	L	M	I	L	R	L	K	S	V	R	M	L	S	G	S				
MOR	249	250	251	252	253	254	255	256	257	258	259	260	261	262	263	264	265	266	267	268	269	270				
															IC3 Loop→											

Figure 30. Cont.

12																										
Orexin-1	R	N	W	K	R	P	S	D	Q	L	G	D	L	E	Q	G	L	S	G	E	P	Q	P	R	A	R
Orexin-1	256	257	258	259	260	261	262	263	264	265	266	267	268	269	270	271	272	273	274	275	276	277	278	279	280	281
Orexin-2	R	K	W	K	P	L	Q	P	V	S	Q	P	R	G	P	G	Q	P	T	K	S	R	M	S	A	V
Orexin-2	264	265	266	267	268	269	270	271	272	273	274	275	276	277	278	279	280	281	282	283	284	285	286	287	288	289
Beta-2	F	H	V	Q	N	L	S	Q	V	E	Q	D	G	R	T	G	H	G	L	R	R	S				
Beta-2	240	241	242	243	244	245	246	247	248	249	250	251	252	253	254	255	256	257	258	259	260	261				
MOR																										
MOR																										
												6	6	6	6	6	6	6	6	6	6	6	6	6	6	6
												3	3	3	3	3	3	3	3	3	3	4	4	4	4	4
13												0	1	2	3	4	5	6	7	8	9	0	1	2	3	4
Orexin-1	A	F	L	A	E	V	K	Q	M	R	A	R	R	K	T	A	K	M	L	M	V	V	L	L	V	F
Orexin-1	282	283	284	285	286	287	288	289	290	291	292	293	294	295	296	297	298	299	300	301	302	303	304	305	306	307
Orexin-2	A	A	E			I	K	Q	I	R	A	R	R	K	T	A	R	M	L	M	I	V	L	L	V	F
Orexin-2	290	291	292			293	294	295	296	297	298	299	300	301	302	303	304	305	306	307	308	309	310	311	312	313
Beta-2						S	K	F	C	L	K	E	H	K	A	L	K	T	L	G	I	I	M	G	T	F
Beta-2						262	263	264	265	266	267	268	269	270	271	272	273	274	275	276	277	278	279	280	281	282
MOR						K	E	K	D	R	N	L	R	R	I	T	R	M	V	L	V	V	V	A	V	F
MOR						271	272	273	274	275	276	277	278	279	280	281	282	283	284	285	286	287	288	289	290	291
												TMH6→														
	6	6	6	6	6	6	6	6	6	6	6	6	6	6	6	6	6									
	4	4	4	4	4	5	5	5	5	5	5	5	5	5	5	6	6									
14	5	6	7	8	9	0	1	2	3	4	5	6	7	8	9	0	1									
Orexin-1	A	L	C	Y	L	P	I	S	V	L	N	V	L	K	R	V	F	G	M	F	R	Q	A	S	D	R
Orexin-1	308	309	310	311	312	313	314	315	316	317	318	319	320	321	322	323	324	325	326	327	328	329	330	331	332	333
Orexin-2	A	I	C	Y	L	P	I	S	I	L	N	V	L	K	R	V	F	G	M	F	A	H	T	E	D	R
Orexin-2	314	315	316	317	318	319	320	321	322	323	324	325	326	327	328	329	330	331	332	333	334	335	336	337	338	339
Beta-2	T	L	C	W	L	P	F	F	I	V	N	I	V	H	V	I	Q	D	N	L	I	R				
Beta-2	283	284	285	286	287	288	289	290	291	292	293	294	295	296	297	298	299	300	301	302	303	304				
MOR	I	V	C	W	T	P	I	H	I	Y	V	I	I	K	A	L	V	T	I	P	E	T				
MOR	292	293	294	295	296	297	298	299	300	301	302	303	304	305	306	307	308	309	310	311	312	313				
			CWXP Motif															EC3 Loop→								

Figure 30. Cont.

	7	7	7	7	7	7	7	7	7	7	7	7	7	7	7	7	7	7	7	7	7	7	7	7	7	7
	2	3	3	3	3	3	3	3	3	3	3	4	4	4	4	4	4	4	4	4	5	5	5	5	5	
15	9	0	1	2	3	4	5	6	7	8	9	0	1	2	3	4	5	6	7	8	9	0	1	2	3	4
Orexin-1	E	A	V	Y	A	C	F	T	F	S	H	W	L	V	Y	A	N	S	A	A	N	P	I	I	Y	N
Orexin-1	334	335	336	337	338	339	340	341	342	343	344	345	346	347	348	349	350	351	352	353	354	355	356	357	358	359
Orexin-2	E	T	V	Y	A	W	F	T	F	S	H	W	L	V	Y	A	N	S	A	A	N	P	I	I	Y	N
Orexin-2	340	341	342	343	344	345	346	347	348	349	350	351	352	353	354	355	356	357	358	359	360	361	362	363	364	365
Beta-2				K	E	V	Y	I	L	L	N	W	I	G	Y	V	N	S	G	F	N	P	L	I	Y	C
Beta-2				305	306	307	308	309	310	311	312	313	314	315	316	317	318	319	320	321	322	323	324	325	326	327
MOR	T	F	Q	T	V	S	W	H	F	C	I	A	L	G	Y	T	N	S	C	L	N	P	V	L	Y	A
MOR	314	315	316	317	318	319	320	321	322	323	324	325	326	327	328	329	330	331	332	333	334	335	336	337	338	339
	TMH7→																				NPXXY					
																					Motif					
	7	7	7	7	7	7	7	7	7	7	7	7	7	7	7											
	5	5	5	5	5	6	6	6	6	6	6	6	6	6	6											
16	5	6	7	8	9	0	1	2	3	4	5	6	7	8	9											
Orexin-1	F	L	S	G	K	F	R	E	Q	F	K	A	A	F	S	C	C	L	P	G	L	G	P	C	G	S
Orexin-1	360	361	362	363	364	365	366	367	368	369	370	371	372	373	374	375	376	377	378	379	380	381	382	383	384	385
Orexin-2	F	L	S	G	K	F	R	E	E	F	K	A	A	F	S	C	C	C	L	G	V	H	H	R	Q	E
Orexin-2	366	367	368	369	370	371	372	373	374	375	376	377	378	379	380	381	382	383	384	385	386	387	388	389	390	391
Beta-2	R		S	P	D	F	R	I	A	F	Q	E	L	L	C	L	R	R	S	S	L	K	A	Y	G	N
Beta-2	328		329	330	331	332	333	334	335	336	337	338	339	340	341	342	343	344	345	346	347	348	349	350	351	352
MOR	F	L	D	E	N	F	K	R	C	F	R	E	F	C	I	P	T	S	S	N	I	E	Q	Q	N	S
MOR	340	341	342	343	344	345	346	347	348	349	350	351	352	353	354	355	356	357	358	359	360	361	362	363	364	365
			Elbow				HX8→									C-Ter→										
17																										
Orexin-1	L	K	A	P	S	P	R	S	S	A	S	H	K	S	L	S	L	Q	S	R	C	S	I	S	K	I
Orexin-1	386	387	388	389	390	391	392	393	394	395	396	397	398	399	400	401	402	403	404	405	406	407	408	409	410	411
Orexin-2	D	R	L	T	R	G	R	T	S	T	E	S	R	K	S	L	T	T	Q	I	S	N	F	D	N	I
Orexin-2	392	393	394	395	396	397	398	399	400	401	402	403	404	405	406	407	408	409	410	411	412	413	414	415	416	417
Beta-2	G	Y	S	S	N	G	N	T	G	E	Q	S	G	Y	H	V	E	Q	E	K	E	N	K	L	L	C
Beta-2	353	354	355	356	357	358	359	360	361	362	363	364	365	366	367	368	369	370	371	372	373	374	375	376	377	378
MOR	T	R	I	R	Q	N	T	R	D	H	P	S	T	A	N	T	V	D	R	T	N	H	Q	L	E	N
MOR	366	367	368	369	370	371	372	373	374	375	376	377	378	379	380	381	382	383	384	385	386	387	388	389	390	391

Figure 30. Cont.

18																									
Orexin-1	S	E	H	V	V	L	T	S	V	T	T	V	L	P											
Orexin-1	412	413	414	415	416	417	418	419	420	421	422	423	424	425											
Orexin-2	S	K	L	S	E	Q	V	V	L	T	S	I	S	T	L	P	A	A	N	G	A	G	P	L	Q	N
Orexin-2	418	419	420	421	422	423	424	425	426	427	428	429	430	431	432	433	434	435	436	437	438	439	440	441	442	443
Beta-2	E	D	L	P	G	T	E	D	F	V	G	H	Q	G	T	V	P	S	D	N	I	D	S	Q	G	R
Beta-2	379	380	381	382	383	384	385	386	387	388	389	390	391	392	393	394	395	396	397	398	399	400	401	402	403	404
MOR	L	E	A	E	T	A	P	L	P																	
MOR	392	393	394	395	396	397	398	399	400																	
																						Sequence total			
19																						residues			
Orexin-1																						425	Orexin-1		
Orexin-1																						425	Orexin-1		
Orexin-2	W																					444	Orexin-2		
Orexin-2	444																					444	Orexin-2		
Beta-2	N	C	S	T	N	D	S	L	L													413	Beta-2		
Beta-2	405	406	407	408	409	410	411	412	413													413	Beta-2		
MOR																						400	MOR		
MOR																						400	MOR		
	Key																								
20	Sequence			Uniprot ID																					
	Orexin-1			O43613																					
	Orexin-2			O43614																					
	MOR			P35372																					
	Beta-2			P07550																					
Notes:				Nterm and the boxed residues (TMH1) are missing from the D3 crystal structure.																					
				If the gray TMH regions extend or don't seem to match up with the ends of other sequences																					
				it is because we can see in a crystal structure the change and we don't know for sure where the																					
				phospholipid bilayer headgroups would lie or the natural tilt of the TMH7 bundle.																					

Figure 30. Cont.

	Key	
20	Sequence	Uniprot ID
	Orexin-1	O43613
	Orexin-2	O43614
	MOR	P35372
	Beta-2	P07550
Notes:		Nterm and the boxed residues (TMH1) are missing from the D3 crystal structure.
		If the gray TMH regions extend or don't seem to match up with the ends of other sequences
		it is because we can see in a crystal structure the change and we don't know for sure where the
		phospholipid bilayer headgroups would lie or the natural tilt of the TMH7 bundle.

21		Color Key
		Prolines
		Highly conserved
		Reasonably conserved
		Loop gap warning (only used in TMH7 to HX8 elbow)
		TMH and helical regions: modified for crystal structures
		Assorted Motifs: N-ter glycosylation sites, GG motif, and GW motif
C		In a disulfide bridge
C		C3.25 disulfide bridge from EC2 Loop
C		Internal within the same loop or termini disulfide bridge
X		Loop w/helical secondary structure
X		Loop w/beta-sheet secondary structure
S		Known phosphorylation site
D		Alternate Beta-Arrestin site instead of phosphorylated S or T
T		Possible phosphorylation motif
C		Possible Palmitoylation site
K		Show sequence conflict.
		May have alternate listed nearby on the table as with S1PR1 KSL vs NV
		Glycosylation Motif is NXS or NXT, and X can't be a Proline
L		Underlined font=IC1 hydrophobic residue commonly pointing
		towards extracellular and not towards intracellular

Figure 30. Cont.

Absent from both the μ-opioid receptor[140] and the β_2-AR,[144,145] yet present in both orexin receptors,[3,7,24] is a proline at position 3.29, as this allows for a kink to occur in Helix 3 in both orexin receptors,[3,7,24] yet in neither the μ-opioid receptor[140] nor the β_2-AR.[144,145] Unlike the μ-opioid receptor (F1.51)[140] and the β_2-AR and the ox2r (V1.51),[7,144,145] the ox1r has T1.51[3,24] to allow for increased ability to kink the TMH1.[148] Both orexin receptors possess W3.51-Y5.32,[3,7,24] whereas the μ-opioid receptor and the β_2-AR both possess Y3.51-I3.52(μ)/F3.52(β_2).[140,144,145] In helices 2 and 4, among both orexin receptors,[3,7,24] the μ-opioid receptor,[140] and the β_2-AR,[144,145] one of these receptors has the proline in a different position than the other three. For instance, the μ-opioid receptor has the helix 2 proline at P2.58,[140] whereas the others have that proline at P2.59.[3,7,24,144,145] Another instance is the helix 4 proline, in which the β_2-AR has its own at P4.60,[144,145] whereas the others have it at P4.59.[3,7,24,140]

However, of the 4 GPCRs, only the β_2-AR has the conserved E6.30 for the R3.50-E6.30 salt bridge,[124,125,126,127,128,129,130,144,145] so the μ-opioid receptor must use T6.34 as a hydrogen bond acceptor,[124,125,126,127,128,129,130,140,141] with T6.33 performing a similar role, in addition to an arginine-arginine T-stack between R3.50 and R6.30, in both orexin receptors.[3,7,24,124,125,126,127,128,129,130,139,141] Within the TMH6 toggle switch, all 4 receptors have a phenylalanine at F6.44 and a cysteine at C6.47,[3,7,24,140,144,145] but the orexin receptors possess a tyrosine at Y6.48[3,7,24] instead of the conserved tryptophan at W6.48 in the other two,[140,144,145] and all three differ with respect to X6.52: the orexin receptors have S6.52,[3,7,24] the μ-opioid receptor has H6.52,[140] and the β_2-AR has F6.52.[144,145] In TMH7, the μ-opioid receptor has A7.40,[140] whereas the others have W7.40.[3,7,24,144,145] However,

the β_2-AR skips 7.56, and has a proline at P7.58 (-SP),[144,145] a feature that both orexin receptors (LSG) and the μ-opioid receptor lack (LDE).[3,7,24,140]

General Topology, Structure, and Interactions of the Orexin-1 Receptor

Following the above steps produced two orexin-1 receptor models: one R model and one R* model. The R model with SB-674042 bound is shown in Figure 31.[3,7,24] The R* model with orexin-A bound is shown in Figure 32.[3,4,7,22,24]

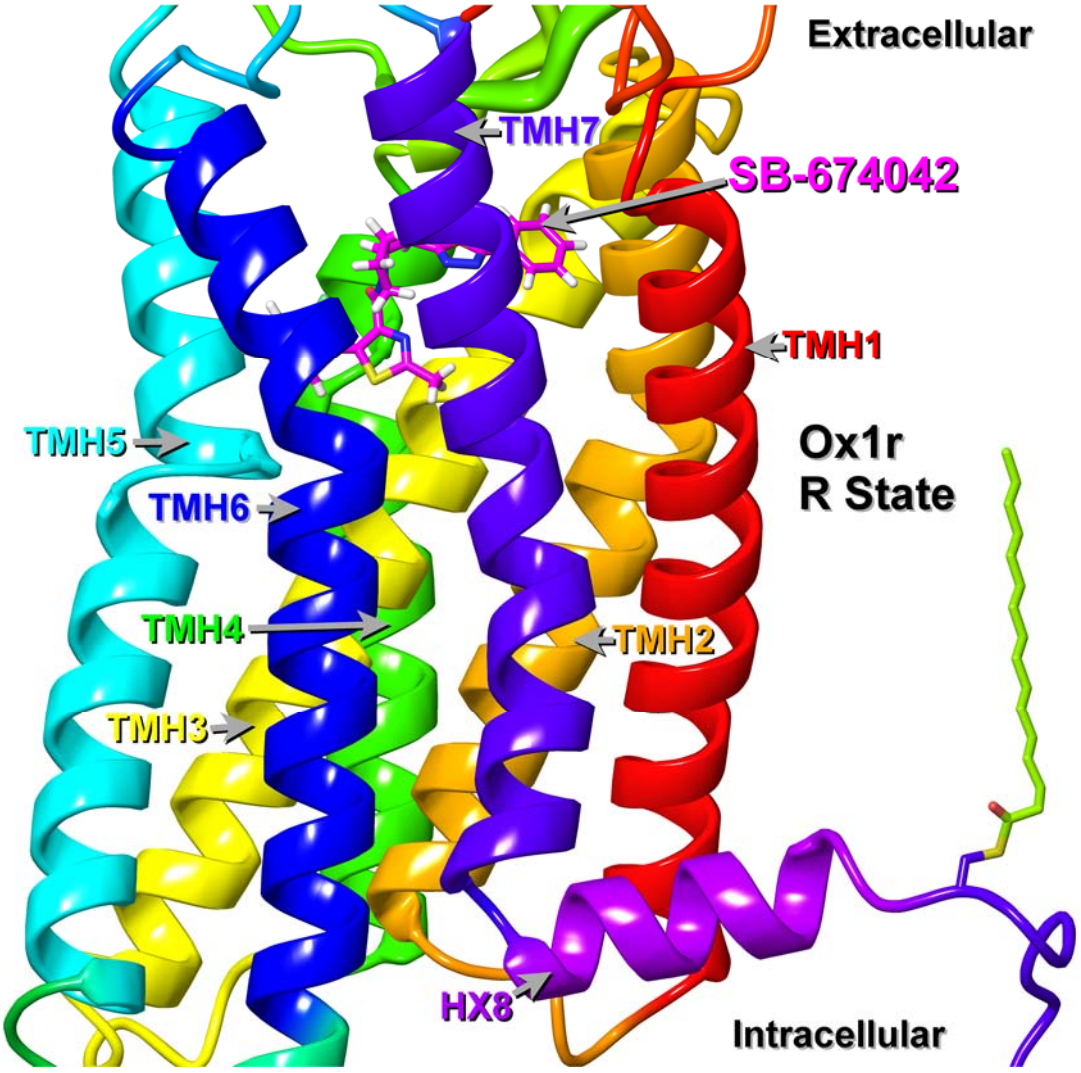

Figure 31. The Finished Ox1r R Model.[3,7,24]

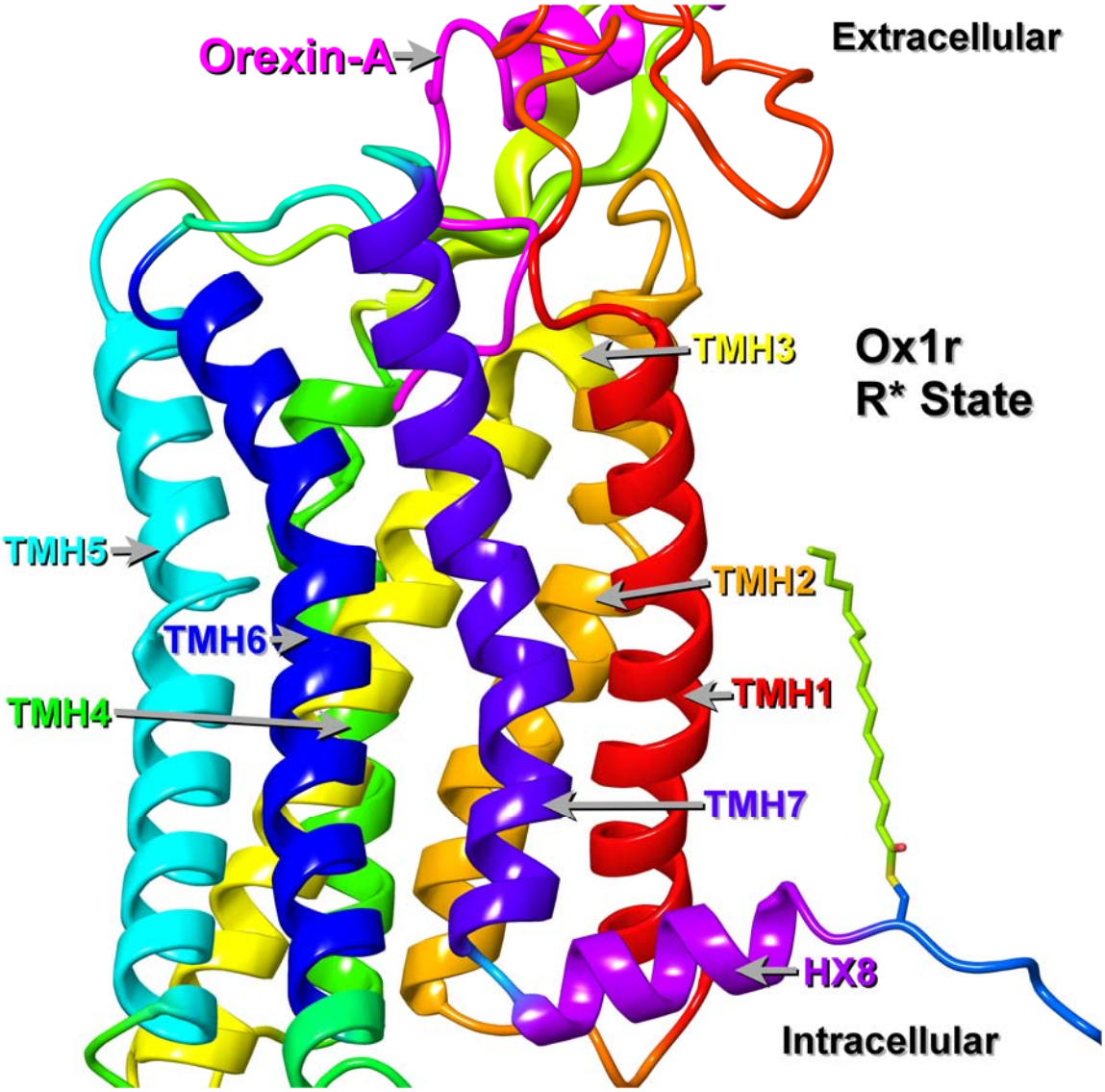

Figure 32. The Finished Ox1r R* Model.[3,4,7,22,24]

Each consists of seven transmembrane α-helices arranged in a bundle, counterclockwise from the EC side. The transmembrane helices I (red), III (yellow), V (light blue), and VII (blue-purple) have their N-terminal ends of these helices on the EC side and the C-terminal ends of these helices on the IC side.[3,7,24] The transmembrane helices II (orange), IV (green), and VI (royal blue) have their N-terminal ends of these

helices on the IC side and the C-terminal ends of these helices on the EC side.[3,7,24] At the C-terminal end of transmembrane helix VII, there is a 1-residue elbow (medium blue) that connects it to a helix parallel to the lipid bilayer.[3,7,24] This helix is horizontal helix VIII (purple).[3,7,24] These helices (I, II, III, IV, V, VI, and the VII-VIII complex) are connected with loops, as IC loops connect helices I and II (IC1, orange), III and IV (IC2, yellow), and V and VI (IC3, light green), and EC loops connect helices II and III (EC1, yellow orange), IV and V (EC2, yellow green), and VI and VII (EC3, sky blue).[3,7,24] The improved coloration is necessary to ease navigation of different GPCRs, as they differ in length yet have common motifs, leading to Maestro's (Schrödinger 2006) residue position color scheme changing from one GPCR to another.[3,7,24,144,145,146] The color codes are listed in Table 6.

Table 6

RGB Color Codes of the Carbons of Each TM Helix, Helix 8, the Ligand, and the Palmitoyl Group, with the Minimum at 0 and the Maximum at 255. All Other Carbons are Colored by Ox1r Residue Position, and All Other Elements are Colored by Element.[3,7,24]

RGB Color Codes for Ox1r Carbons and Ligand Carbons				
Part	***Residues or Chain***	***Red***	***Green***	***Blue***
TMH1	**Residues 43-74**	**255**	**0**	**0**
TMH2	**Residues 80-109**	**255**	**170**	**0**
TMH3	**Residues 116-150**	**255**	**255**	**0**
TMH4	**Residues 157-181**	**0**	**255**	**0**
TMH5	**Residues 209-243**	**0**	**255**	**255**
TMH6	**Residues 293-324**	**0**	**0**	**255**
TMH7	**Residues 334-361**	**85**	**0**	**255**
HX8	**Residues 363-374**	**170**	**0**	**255**
Palmitoyl	**Residue 426**	**170**	**255**	**0**
Ligand	**Chain B**	**255**	**0**	**255**

In a way similar to the β_2-AR[144,145] and the ox2r,[7] the EC1 loop is arranged so that W112 is pointed into lipid, holding the EC1 loop rigid. In the first working R bundle, also similar to the β_2-AR,[144,145] the EC2 loop is arranged so that the half N-terminal to C45.50 (202), the EC2a loop, forms an α-helix. In the working R* bundle and in the second working R bundle, the EC2a loop instead forms a pair of β-strands that form a β-sheet, as is common to many peptide-binding receptors.[3,7,140,146,180,181,182,183,184,185,186,187] Furthermore, as the ox2r[7] and β_2-AR[144,145] have, the part C-terminal to C45.50 (202), the EC2b loop, has D45.51 (203) pointed upward with a salt bridge interaction with R6.59 (322), E45.52 (204) pointed downward and accepting a hydrogen bond from H5.39, R45.53 (205) pointed upward, and W45.54 (206) pointed downward in an aromatic stack in the R model as shown in Figure 33.[3,7,24]

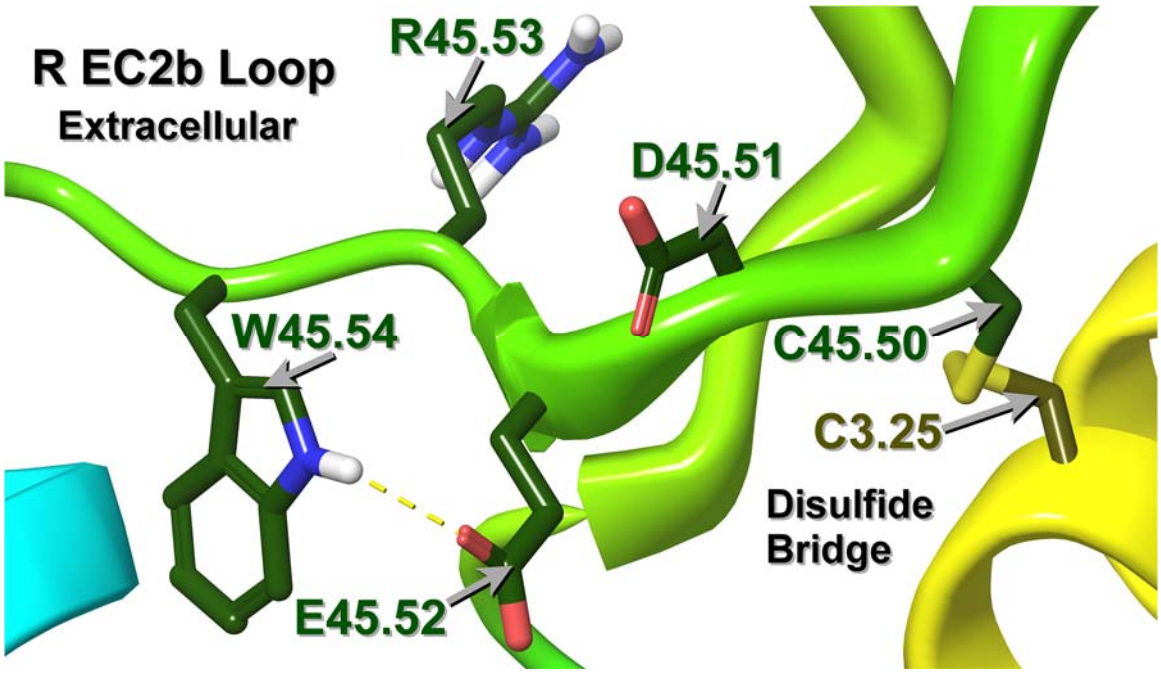

Figure 33. The EC2b Loop of the R Structure.[3,7,24]

The EC2b loop is shown for the R* model in a similar way in Figure 34.[3,7,24] This keeps the EC2b loop out of the binding pocket.[3,24] IC1 and IC2 are short connections that interact freely with cytosol, and IC3 extends in the form of α-helical extensions of transmembrane helices V and VI, similar to rhodopsin[2] and the $P2Y_{12}$ receptor.[141] The N-terminus is kept away from the top of each bundle, as is prevalent in the β_2-AR,[144,145] but unlike rhodopsin,[2] as orexin-A is a positively-charged (+1) signaling peptide that enters from the extracellular side.[3,4,22,24] The C-terminus is kept away from the bottom of the bundle so that a G protein[12] or β-arrestin[15] can bind, and both termini are kept away from the lipid bilayer[2,144,145,157] and in an aqueous environment.[2,144,145] In each model, there is a palmitoyl group bound to a thioester linkage to C375, helping anchor the ox1r in the lipid membrane regardless of activation state.[3,7,156]

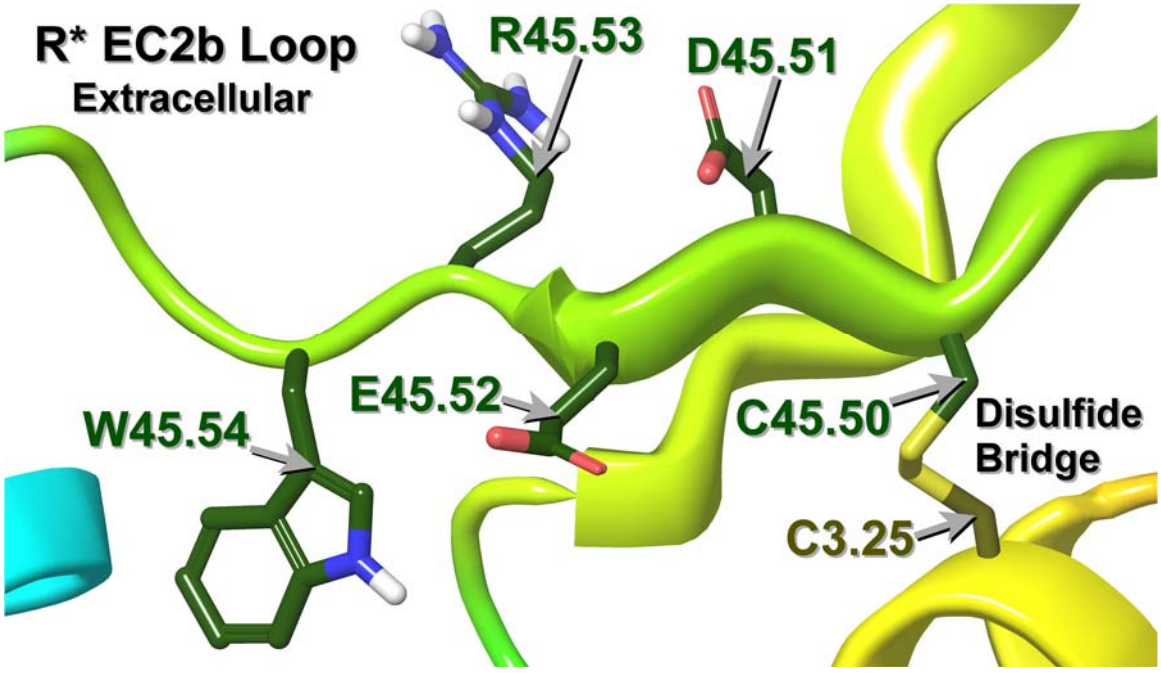

Figure 34. The EC2b Loop of the R* Structure.[3,7,24]

The helices of the ox1r interact with one another in numerous ways. Both the R and R* models have these interactions, beginning with N1.50 donating a hydrogen bond to S7.46's backbone oxygen, as shown in Figure 35 for the R structure.[3,7,24]

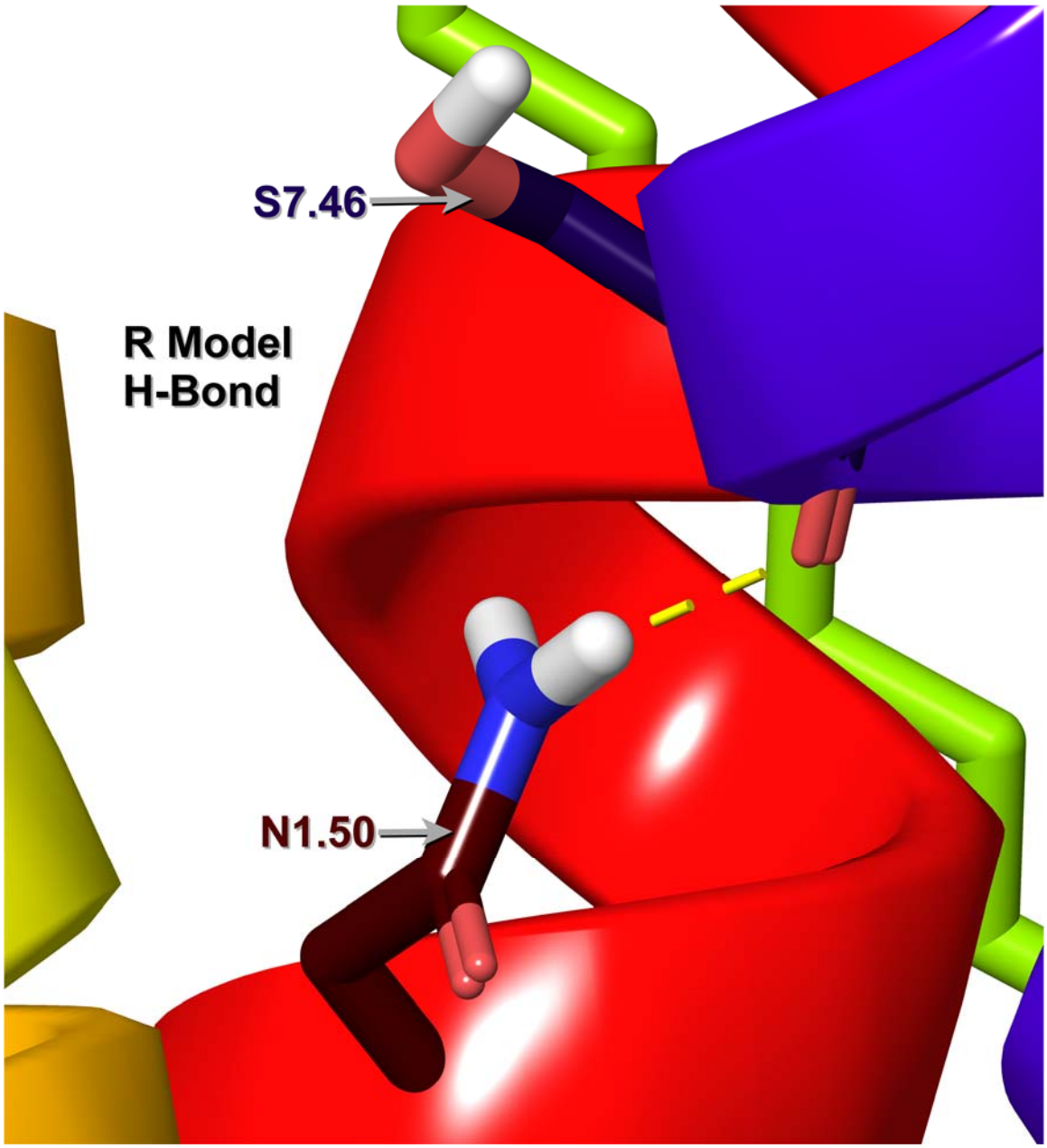

Figure 35. N1.50 Donates a Hydrogen Bond to S7.46's Backbone Oxygen in the R Model.[3,7,24]

The helices of the ox1r interact with one another in numerous ways. Both the R and R* models have these interactions, beginning with N1.50 donating a hydrogen bond to S7.46's backbone oxygen, as shown in Figure 36 for the R* structure.[3,7,24] The R model's TMH2, TMH3, and TMH4 also interact as well by N2.45 donating a hydrogen bond to T3.42 and additionally accepting one from W4.50, as shown in Figure 37.[3,7,24]

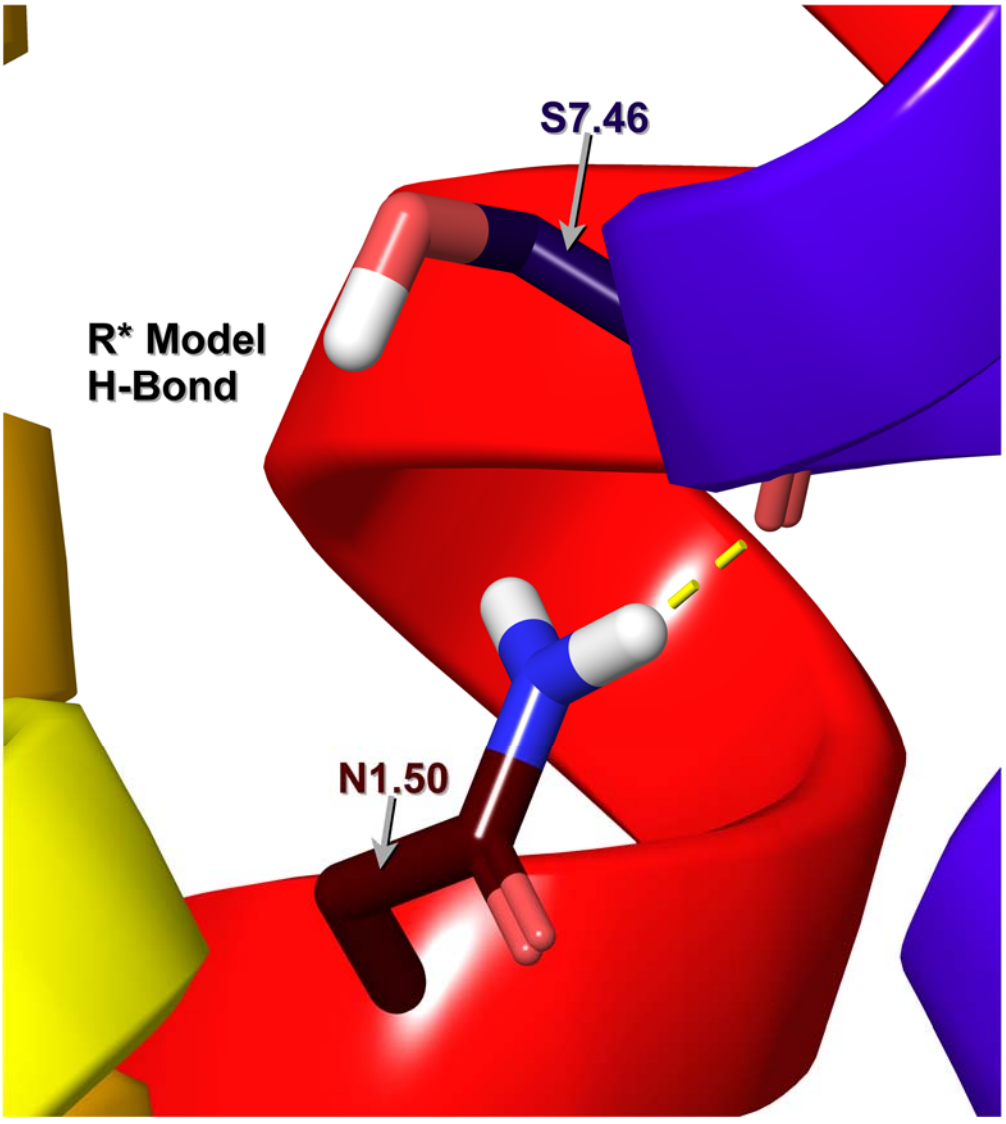

Figure 36. N1.50 Donates a Hydrogen Bond to S7.46's Backbone Oxygen in the R* Model.[3,7,24]

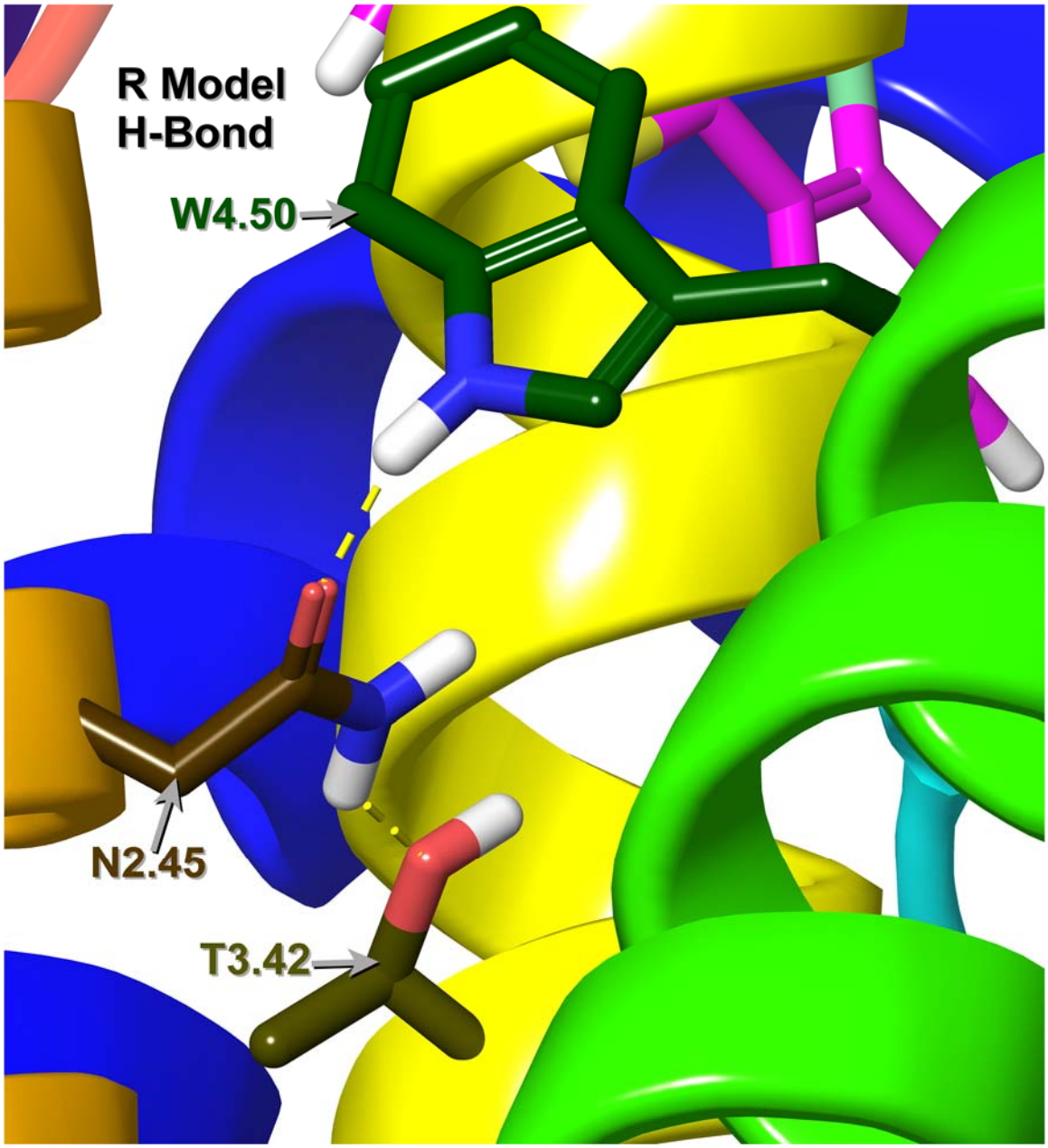

Figure 37. N2.45 Donates a Hydrogen Bond to T3.42 and Accepts One from W4.50, in the R Model.[3,7,24]

The R* model's TMH2, TMH3, and TMH4 also interact as well by N2.45 donating a hydrogen bond to T3.42 and additionally accepting one from W4.50, as shown in Figure 38.[3,7,24]

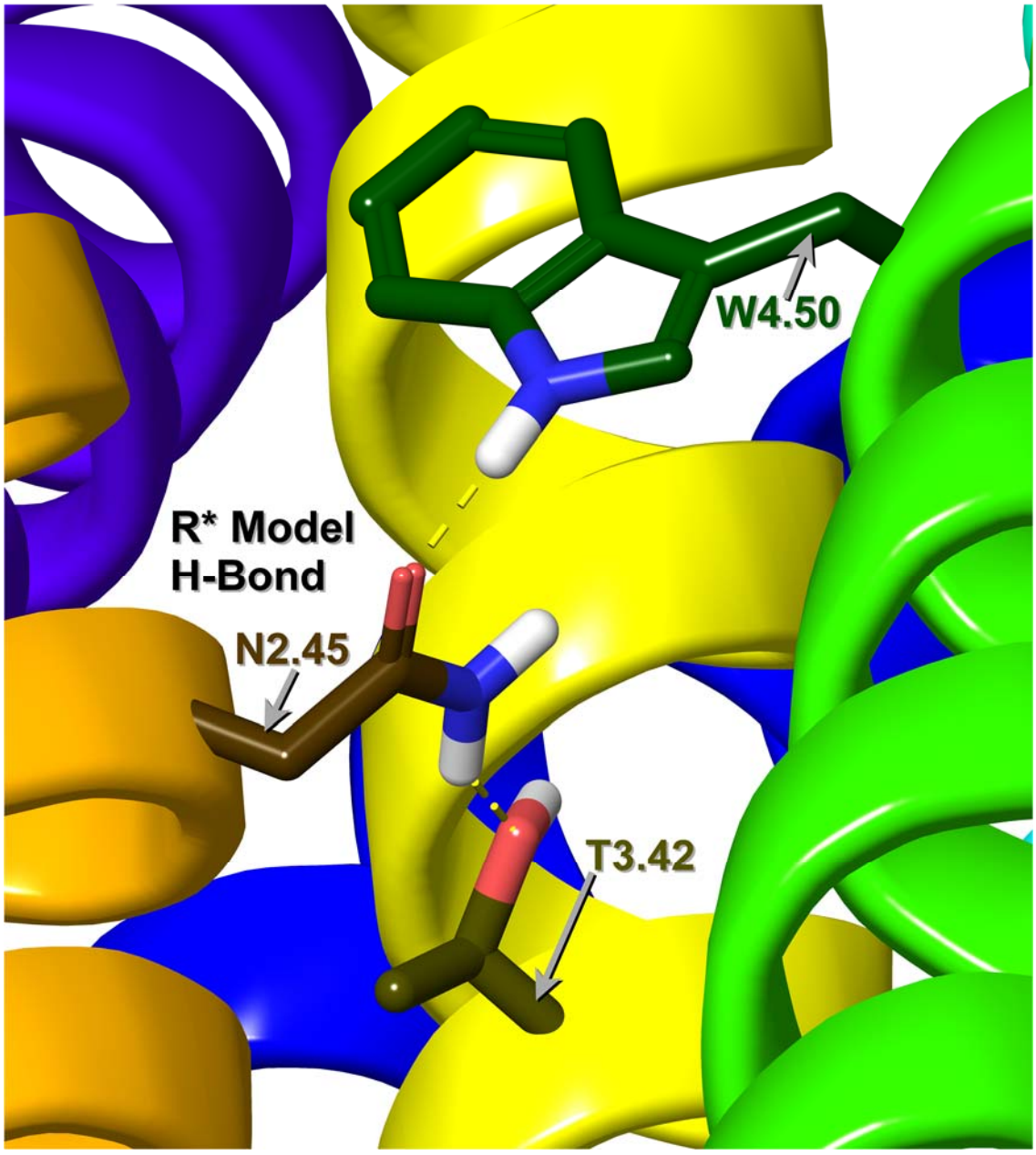

Figure 38. N2.45 Donates a Hydrogen Bond to T3.42 and Accepts One from W4.50, in the R* Model.[3,7,24]

D2.50 accepts a hydrogen bond from N7.49 in the ox1r R structure, as shown in Figure 39.[3,7,24]

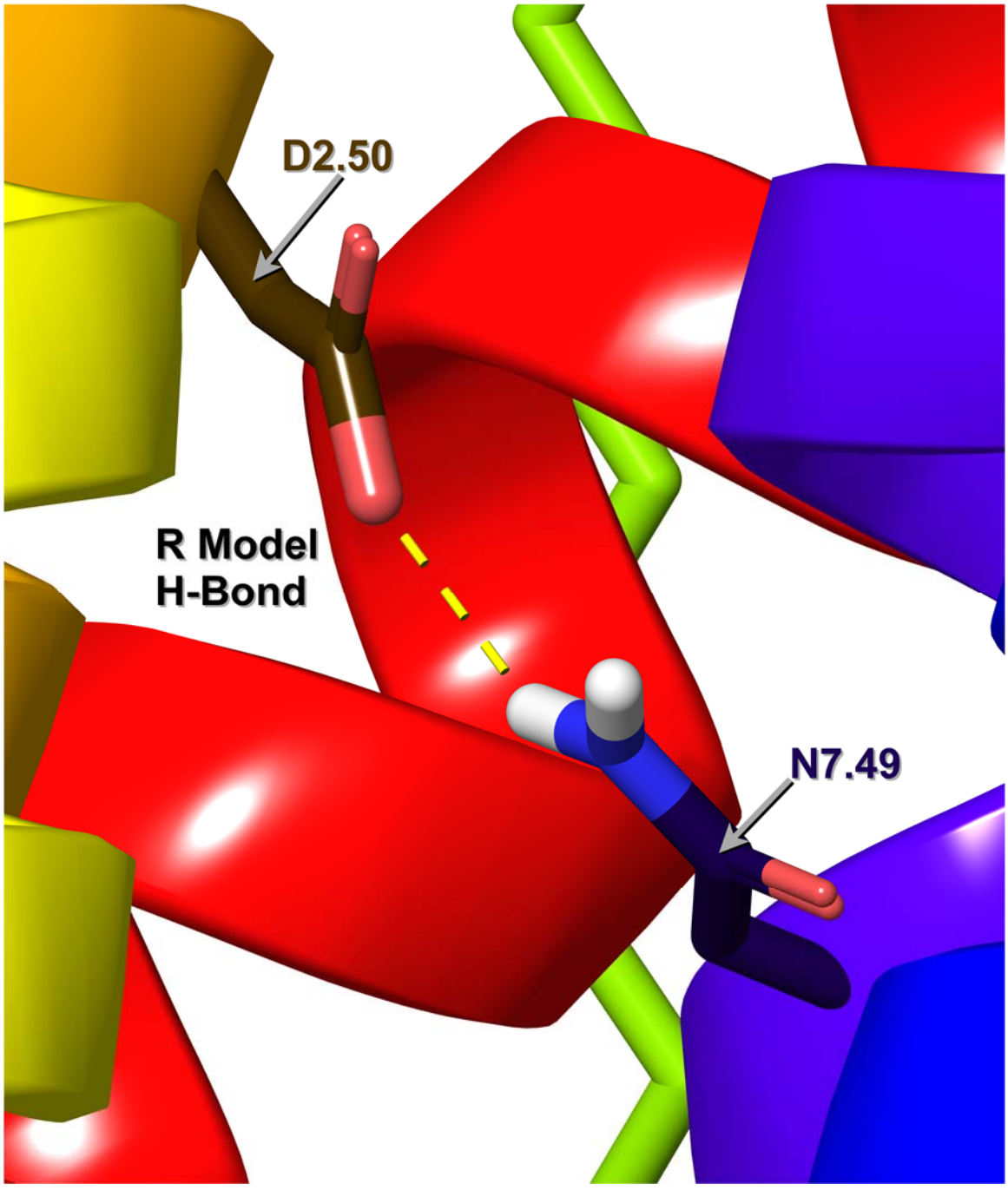

Figure 39. D2.50 Accepts a Hydrogen Bond from N7.49 in the R Model.[3,7,24]

D2.50 accepts a hydrogen bond from N7.49 in the ox1r R* structure, as shown in Figure 40.[3,7,24]

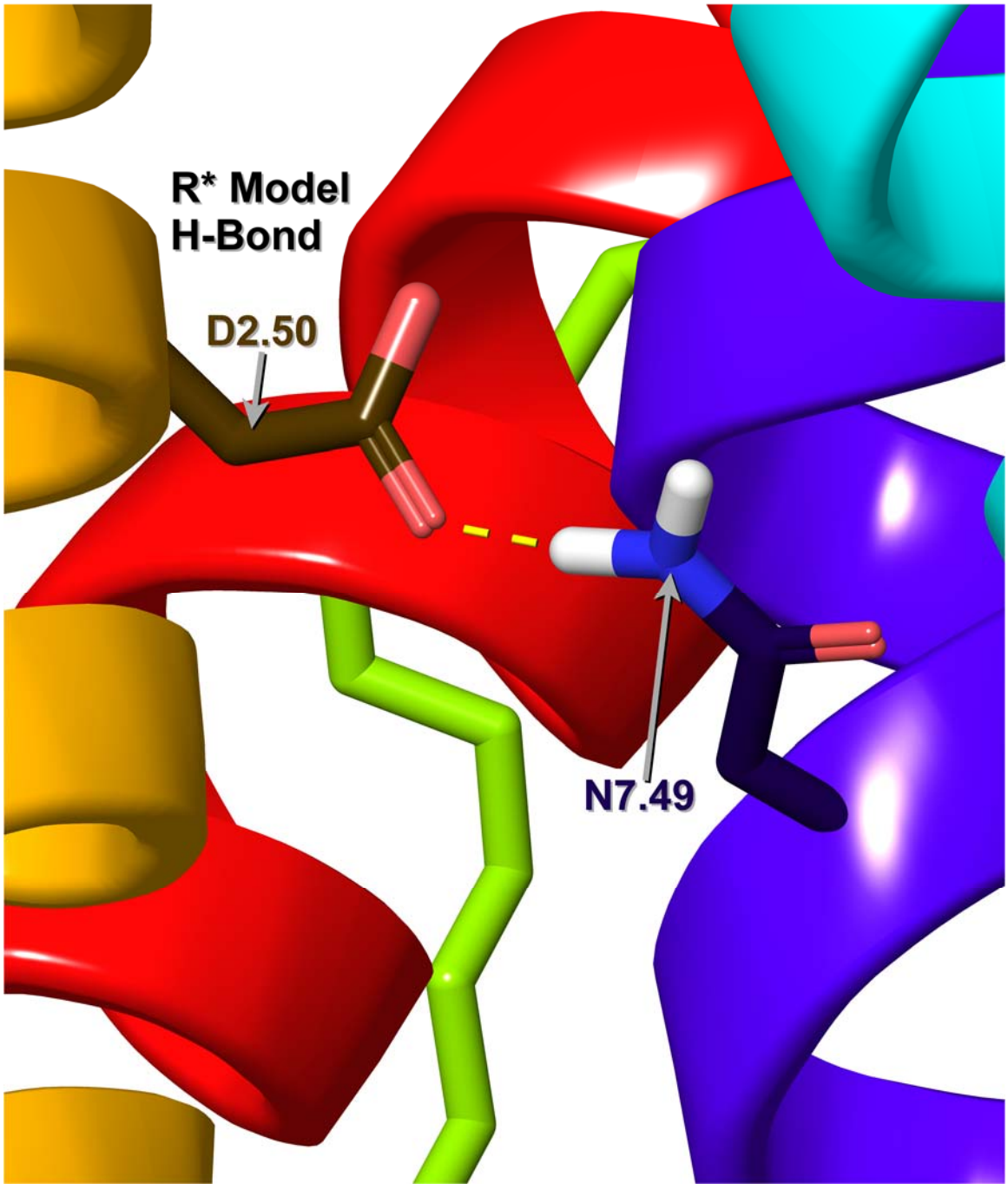

Figure 40. D2.50 Accepts a Hydrogen Bond from N7.49 in the R* Model.[3,7,24]

R6.59 has its role in keeping the EC2 loop and TMH6 together, as it donates salt bridge hydrogen bonds to E45.52, as shown in Figures 41 and 42.[3,7,24]

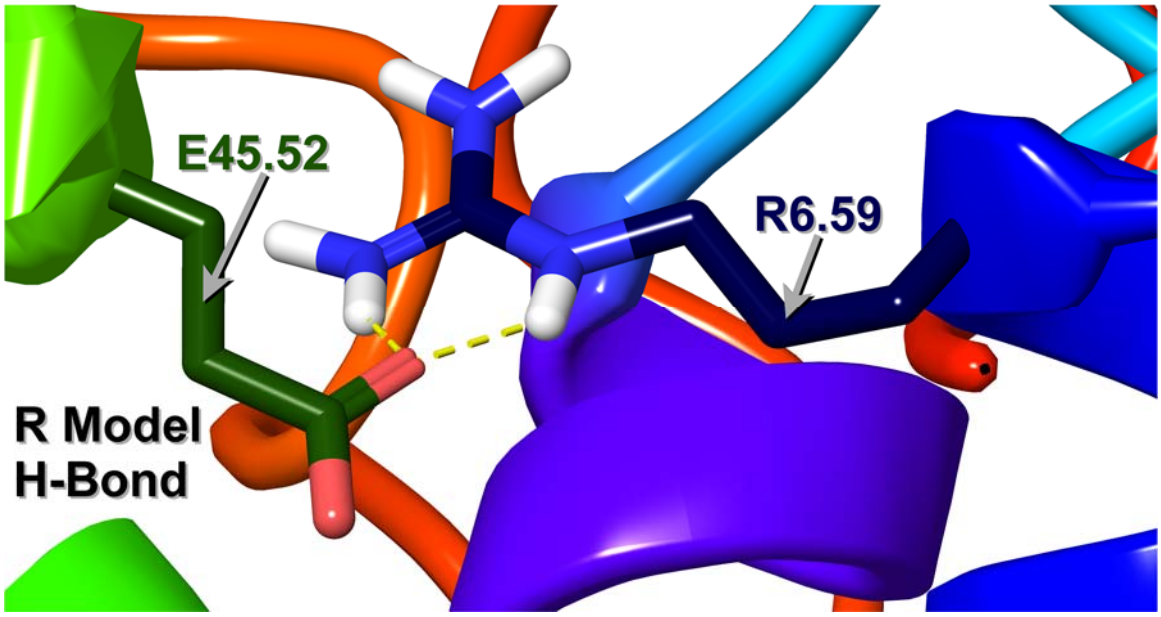

Figure 41. R6.59 Donates Salt Bridge Hydrogen Bonds to E45.52 in the R Model.[3,7,24]

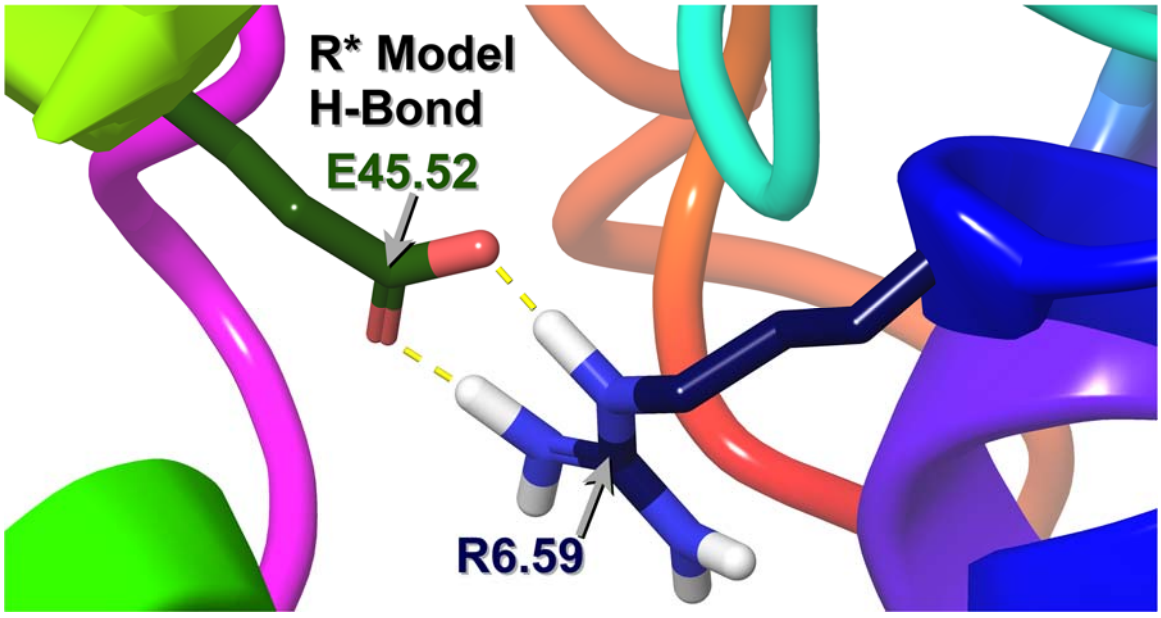

Figure 42. R6.59 Donates Salt Bridge Hydrogen Bonds to E45.52 in the R* Model.[3,7,24]

There are also cation-π and π-stack interactions common to both the R and R* models, with one being F114 donating a π-π T-stack to W112 in the EC1 loop, as shown in Figure 43 for the R bundle.[3,7,24]

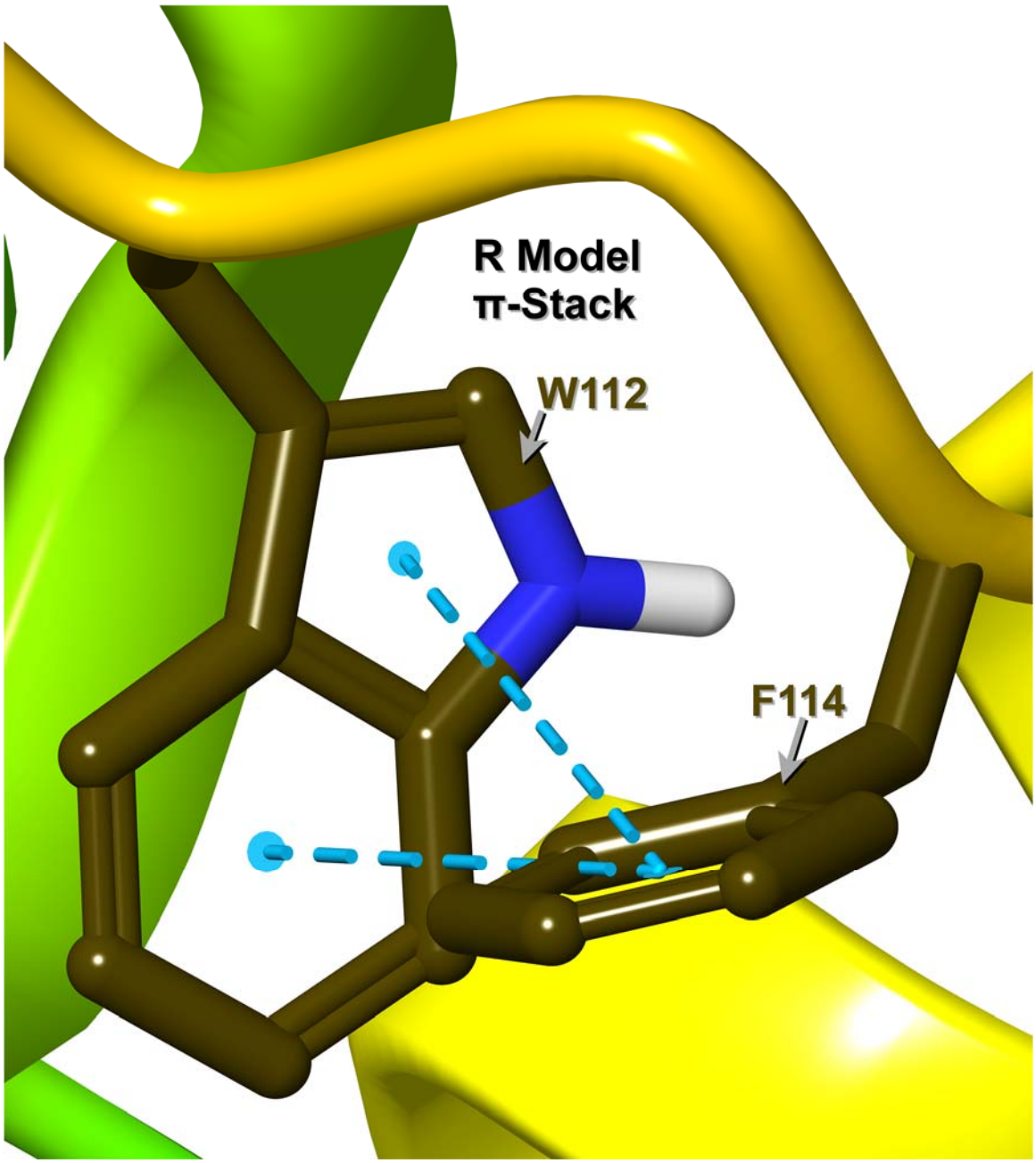

Figure 43. F114 Donates a π-π T-stack Interaction to W112 in the R Model.[3,7,24]

F114 donates a π-π T-stack to W112 in the EC1 loop in a similar way as it does for the ox1r R bundle's EC1 loop, and both in a similar way to the ox2r crystal structure, as is shown in Figure 44 for the R* bundle.[3,7,24]

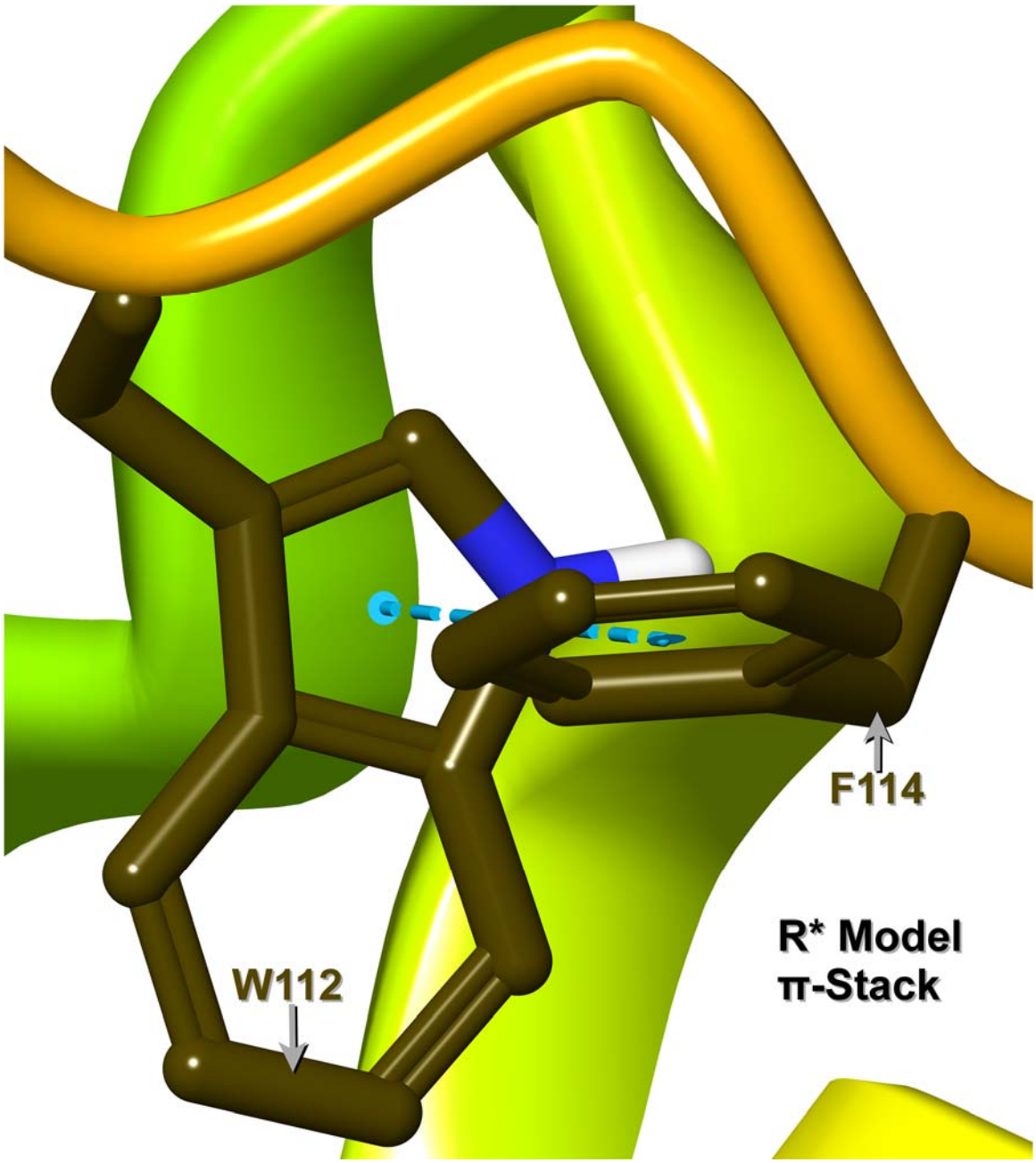

Figure 44. F114 Donates a π-π T-stack Interaction to W112 in the R* Model.[3,7,24]

Yet another common interaction is H3.56 donating a π-π T-stack to W3.51 in TMH3, which in turn donates another to Y3.52, as shown in Figure 45 for the R structure.[3,7,24]

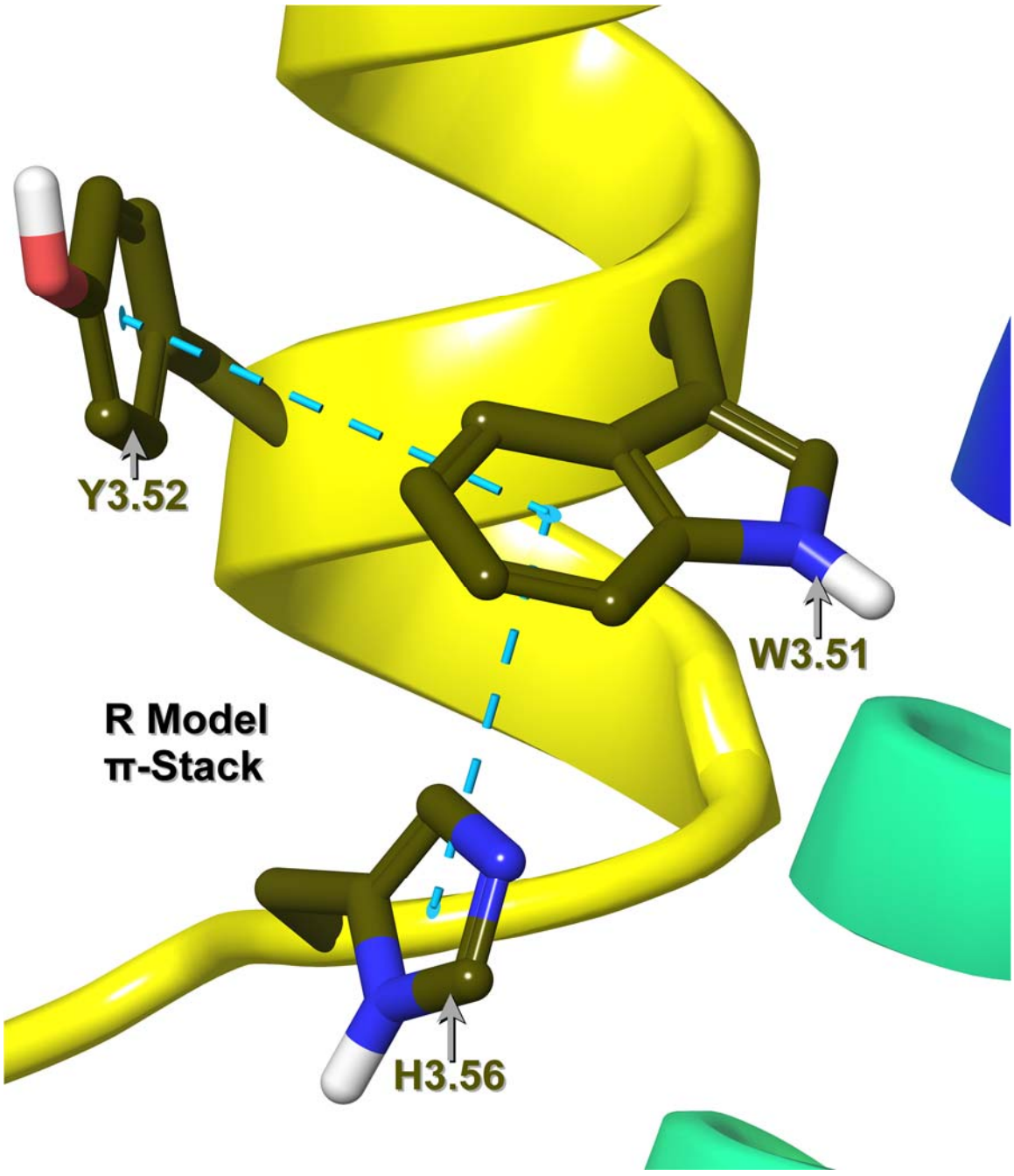

Figure 45. H3.56 Donates a π-π T-stack Interaction to W3.51, Which in Turn Donates Another to Y3.52, in the R Model.[3,7,24]

The interaction of H3.56 donating a π-π T-stack to W3.51 in TMH3, which in turn donates another to Y3.52, is also shown in Figure 46 for the R* structure.[3,7,24]

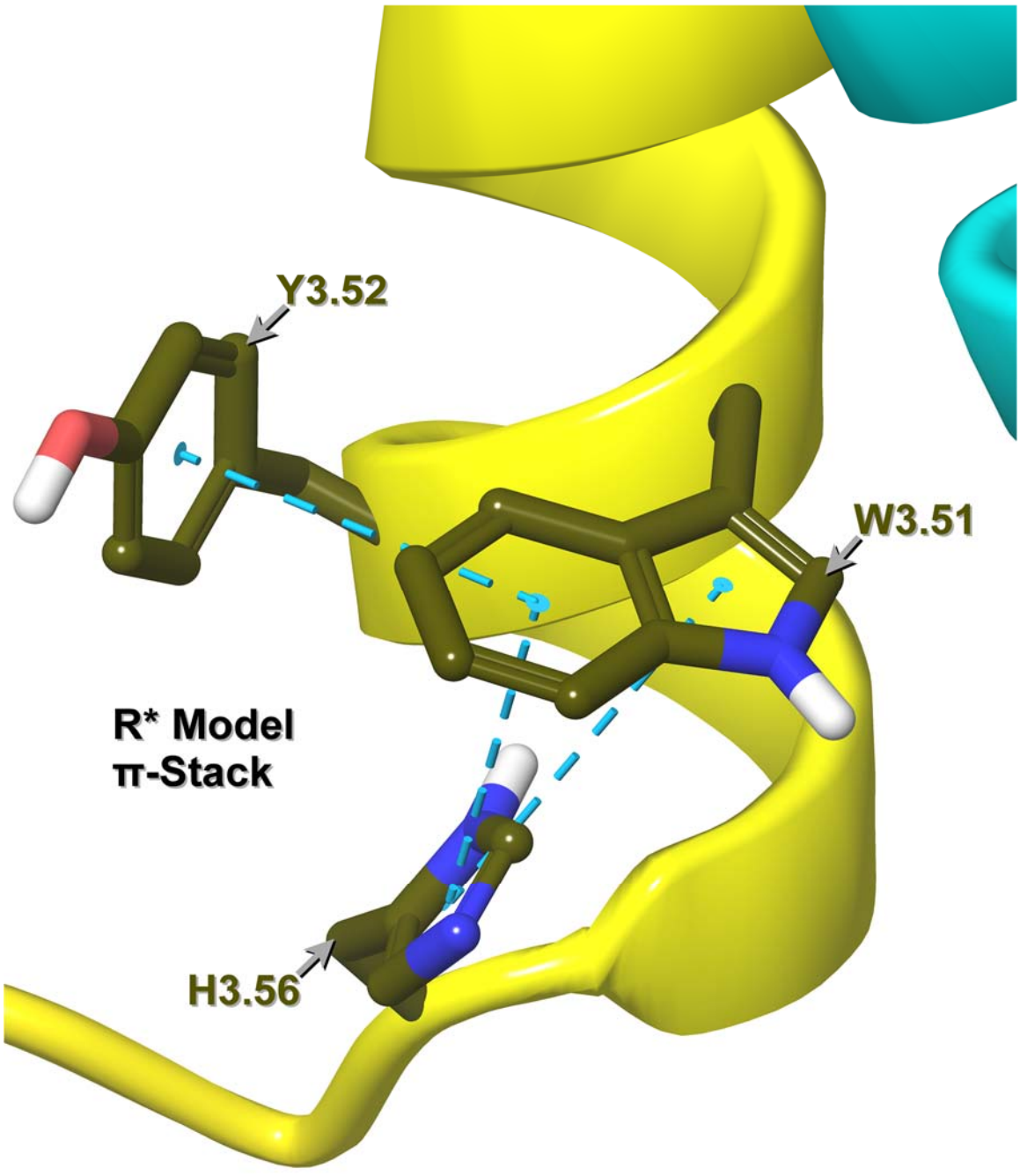

Figure 46. H3.56 Donates a π-π T-stack Interaction to W3.51, Which in Turn Donates Another to Y3.52, in the R* Model.[3,7,24]

The R model has some interactions that are absent from the R* model, as shown here. R3.50 donates salt bridge hydrogen bonds to D3.49[124,125,126,127,128,129,130] and donates an arginine-arginine T-stack[139] to R6.30,[3,7,24] as shown in Figure 47.

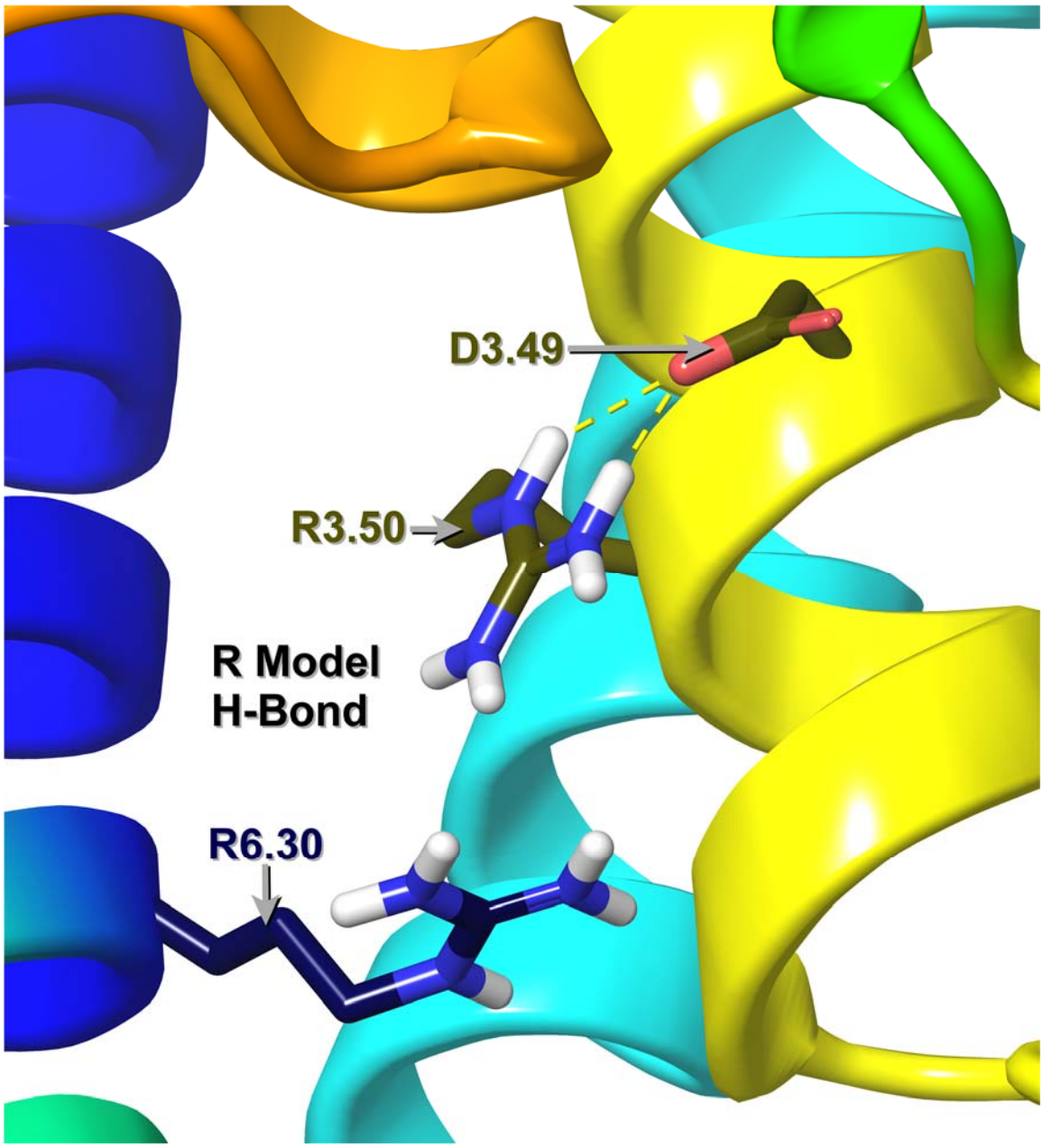

Figure 47. R3.50 Donates Salt Bridge Hydrogen Bonds to D3.49,[124,125,126,127,128,129,130] and an Arginine-Arginine T-stack[139] to R6.30,[3,7,24] in the R Model.

A cluster of interactions occurs in the IC1 region, as N2.40 and Y2.41 interact with M77, R78, and T79, as shown in Figure 48 for the R structure.[3,7,24]

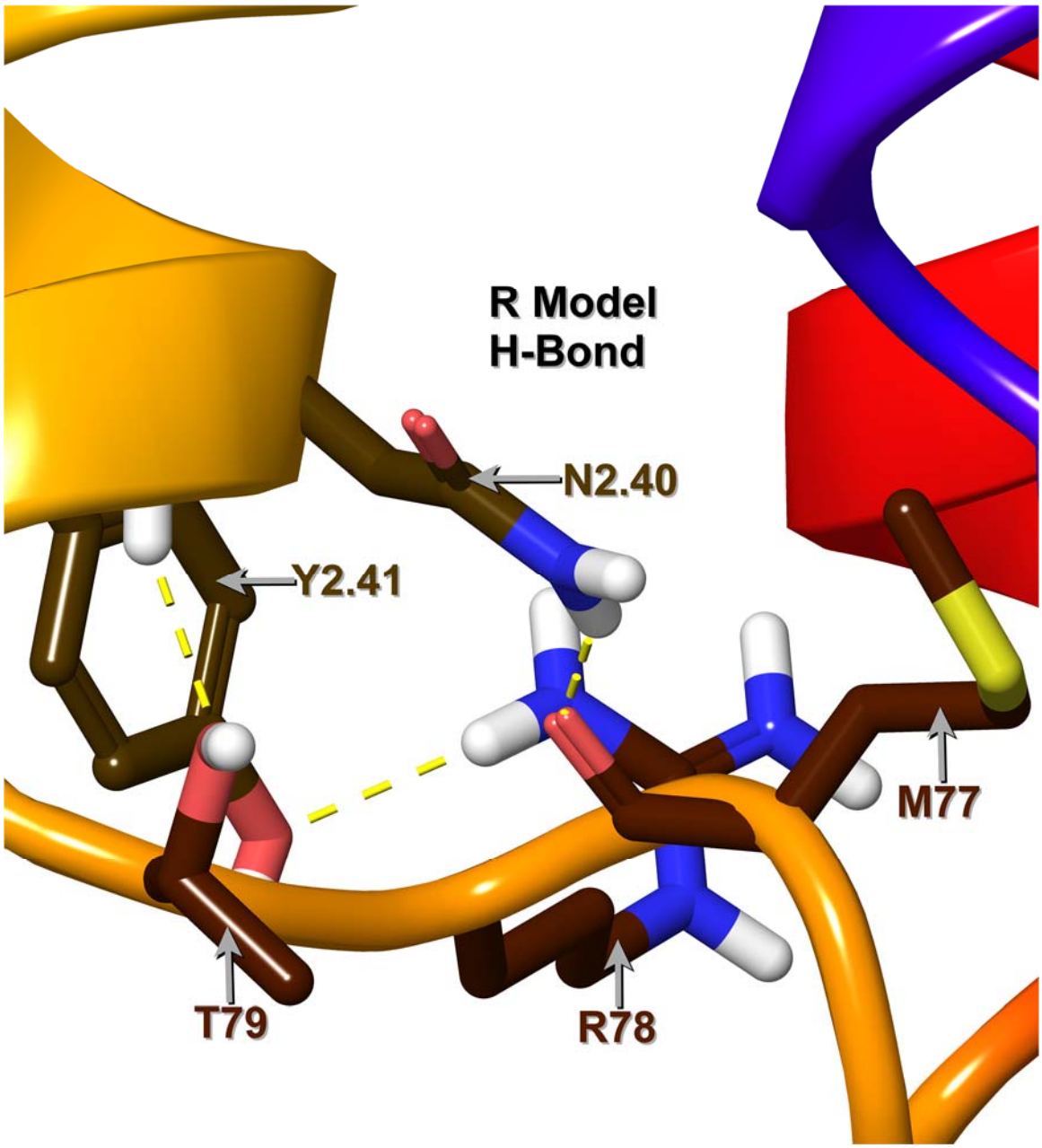

Figure 48. N2.40 Uses its Amide Side Chain to Donate a Hydrogen Bond to M77's Backbone Oxygen, and its Backbone Amide to Donate One to T79, While Y2.41 Accepts a Hydrogen Bond from R78, in the R Model.[3,7,24]

D2.65 in TMH2 is shown to accept two hydrogen bonds from Y7.32 and H7.39 in TMH7, as shown in Figure 49.[3,7,24]

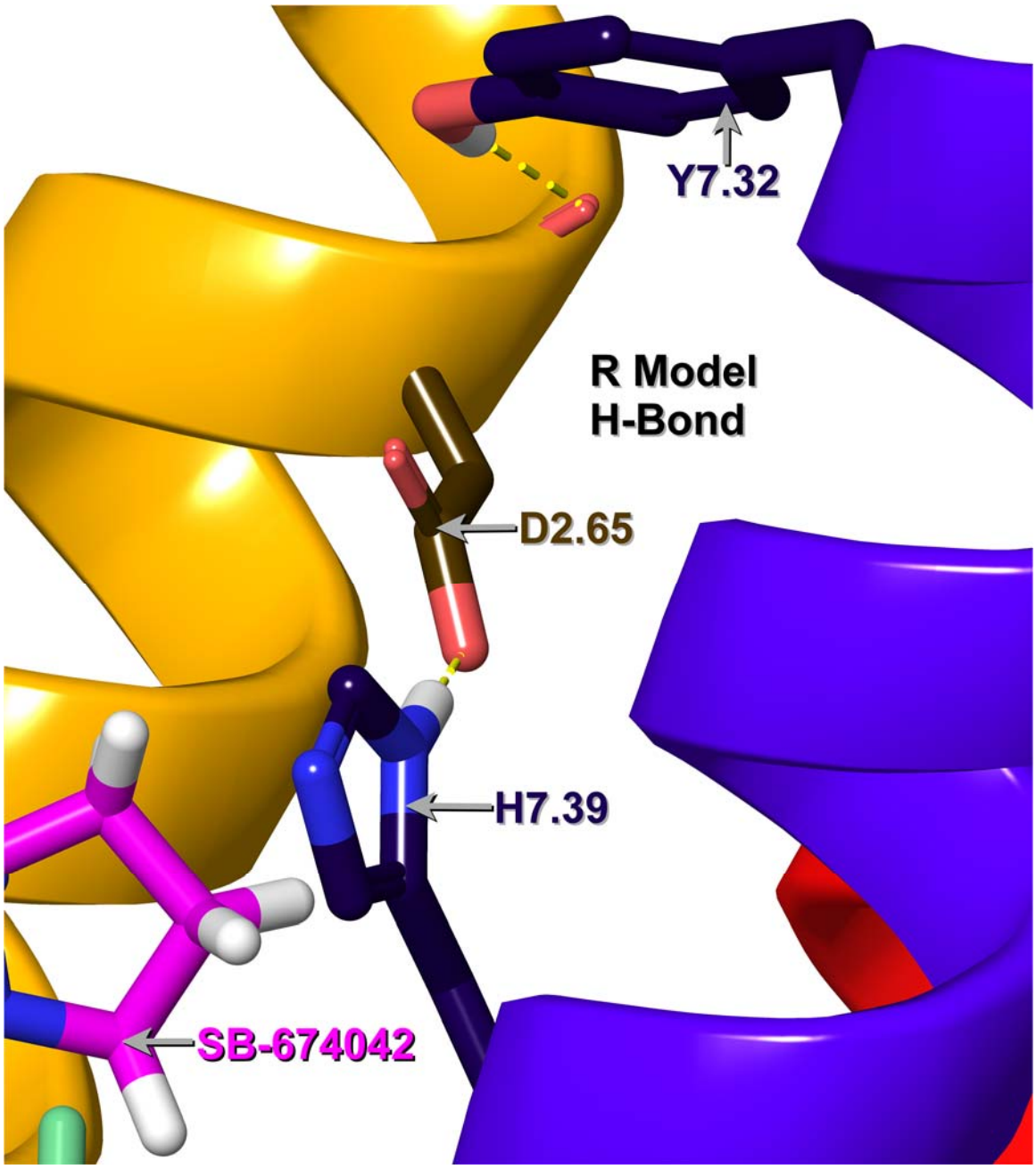

Figure 49. D2.65 Uses its Backbone Oxygen to Accept a Hydrogen Bond from Y7.32, and its Side Chain to Accept One from H7.39, in the R Model.[3,7,24]

Another interaction similar to one in the ox2r is the pair of hydrogen bonds that R6.31 donates to L5.65's backbone, as shown in Figure 50.[3,7,24]

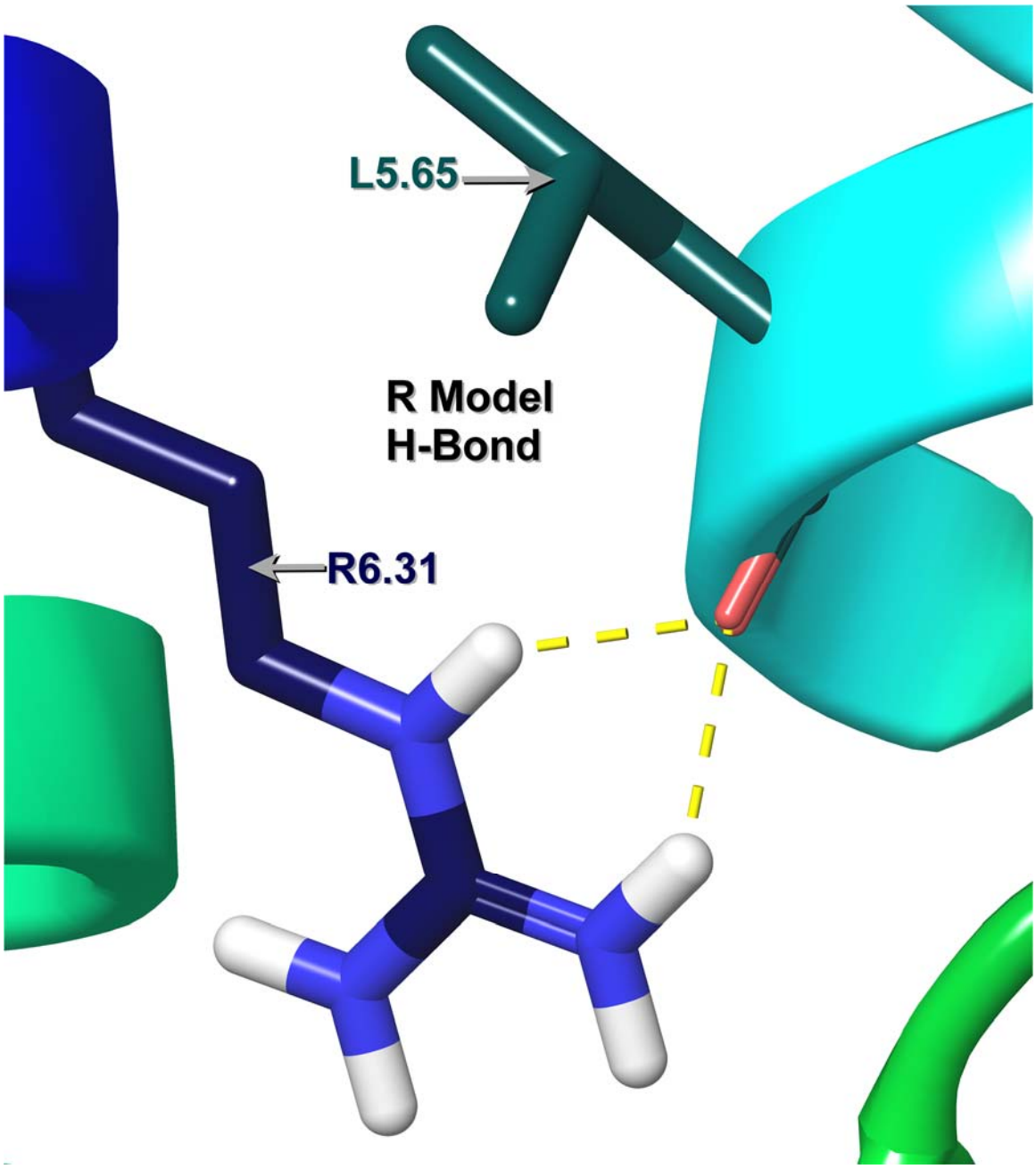

Figure 50. R6.31 Donates Two Hydrogen Bonds to L5.65's Backbone in the R Model.[3,7,24]

Q4.60 has its role in keeping the EC2 loop, TMH4, and TMH5 together in the R structure, as it donates a hydrogen bond to E45.52 and accepts one from Y5.38, as shown in Figure 51.[3,7,24]

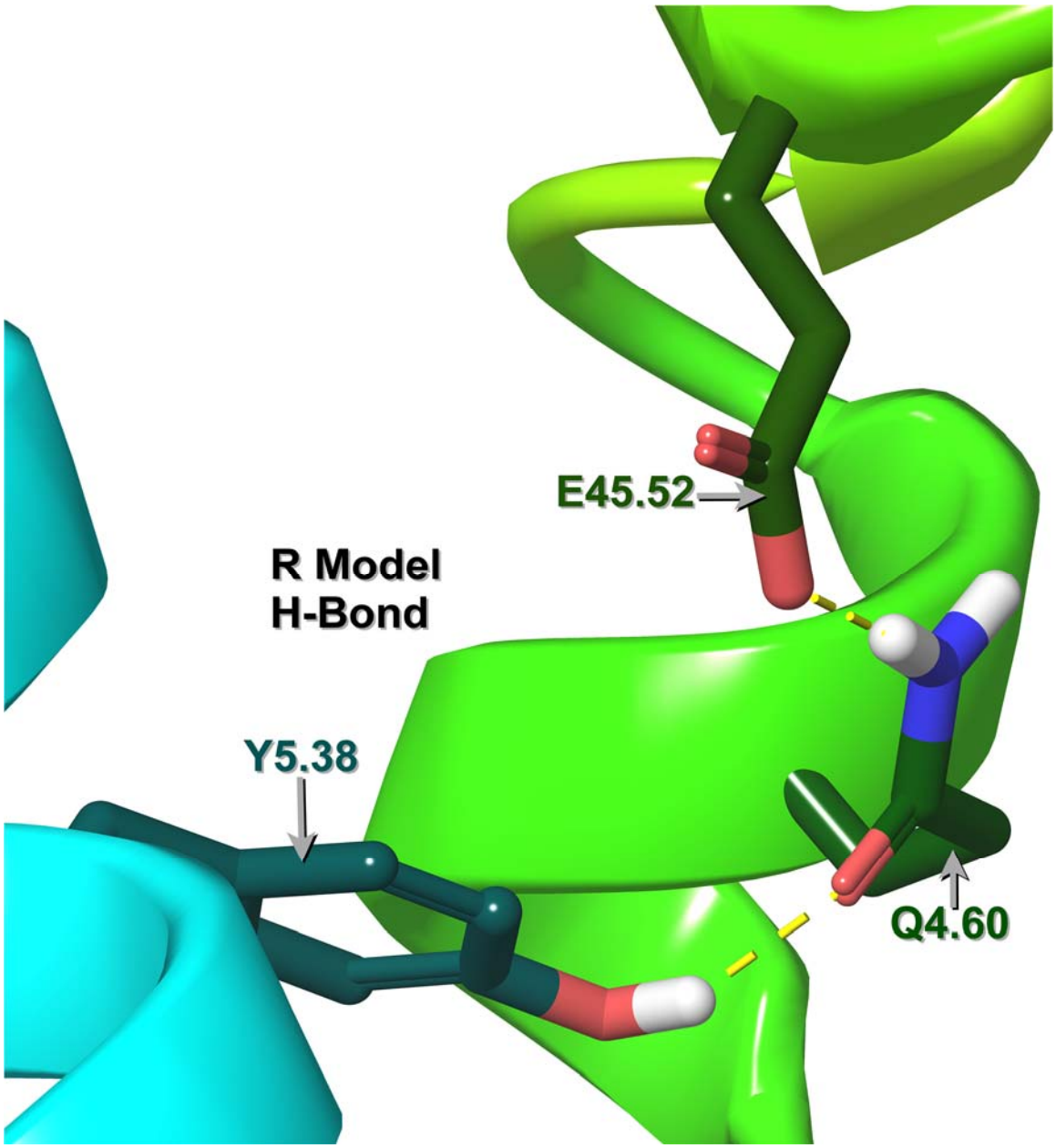

Figure 51. Q4.60 Donates a Hydrogen Bond to E45.52 and Accepts One from Y5.38 in the R Model.[3,7,24]

As originally present in the ox2r crystal structure, H5.39 donates a hydrogen bond to E45.52, as shown in Figure 52.[3,7,24]

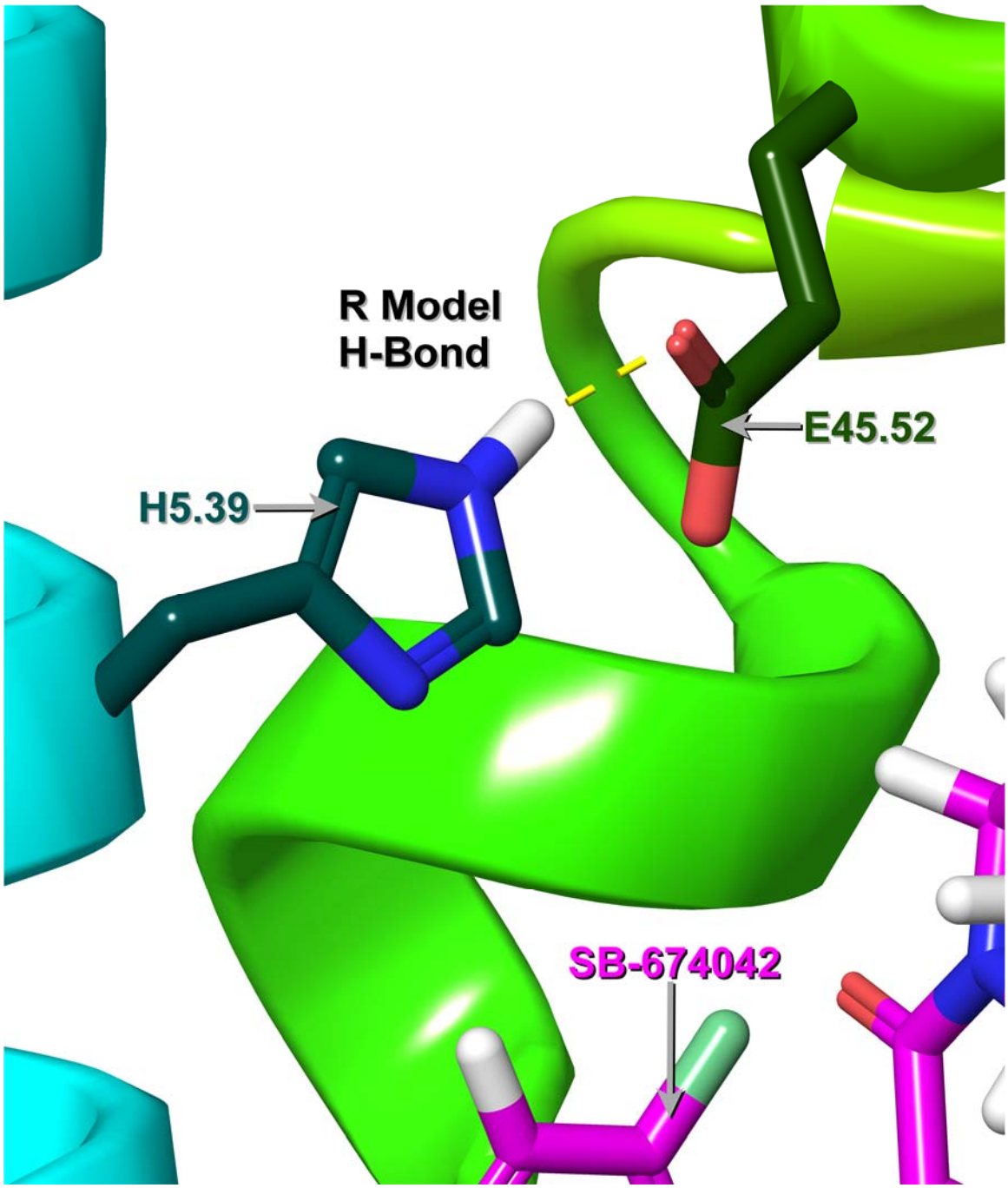

Figure 52. H5.39 Donates a Hydrogen Bond to E45.52 in the R Model.[3,7,24]

Another such interaction is R4.43 donating a cation-π interaction to Y2.41, as shown in Figure 53.[3,7,24]

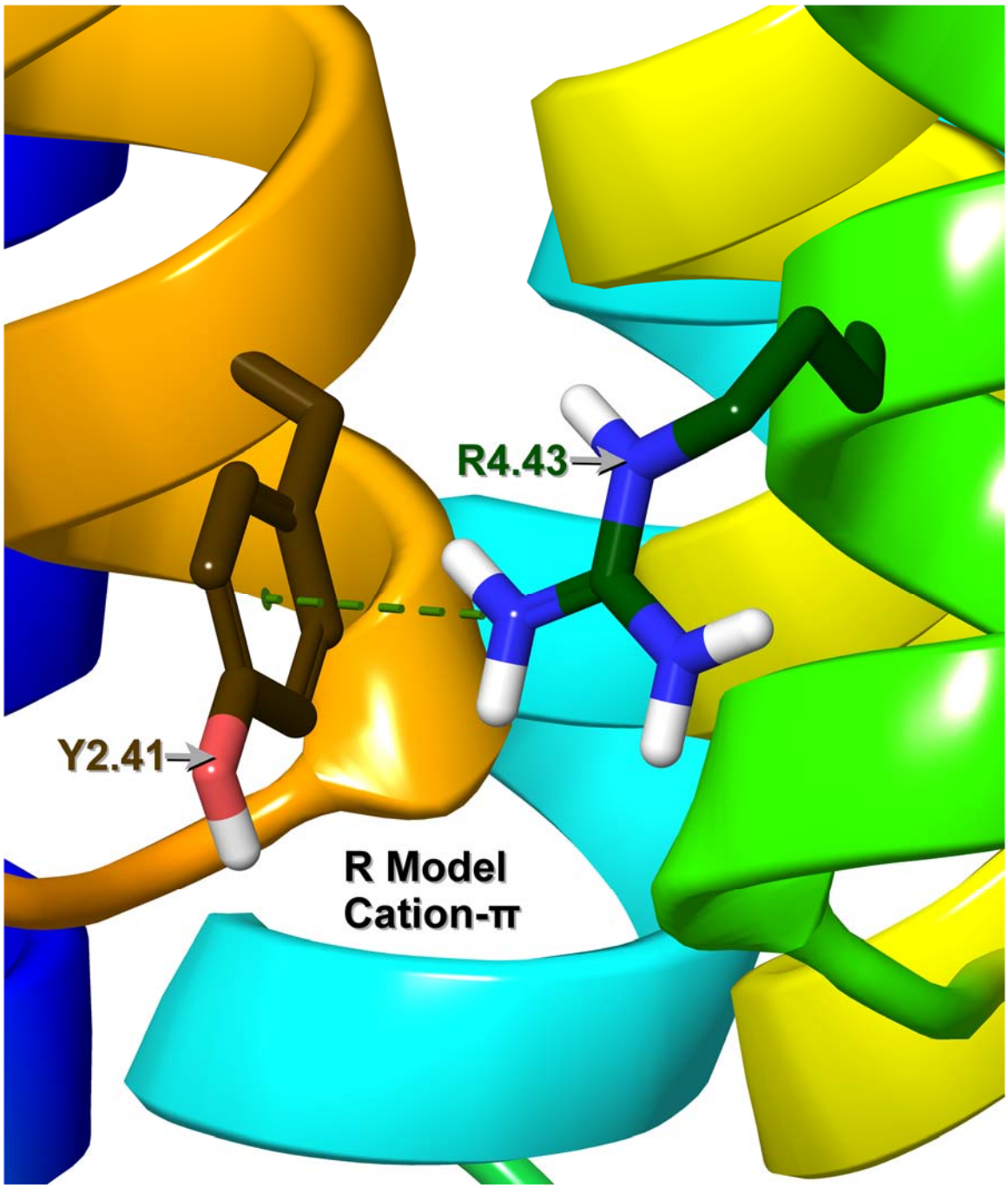

Figure 53. R4.43 Donates a cation-π Interaction to Y2.41 in the R Model.[3,7,24]

Another such interaction is Y5.38 donating a π-π T-stack to H5.39, with W45.54 nearby, as part of the aromatic cluster between the EC2b loop and TMH5, as shown in Figure 54 in the R structure.[3,7,24]

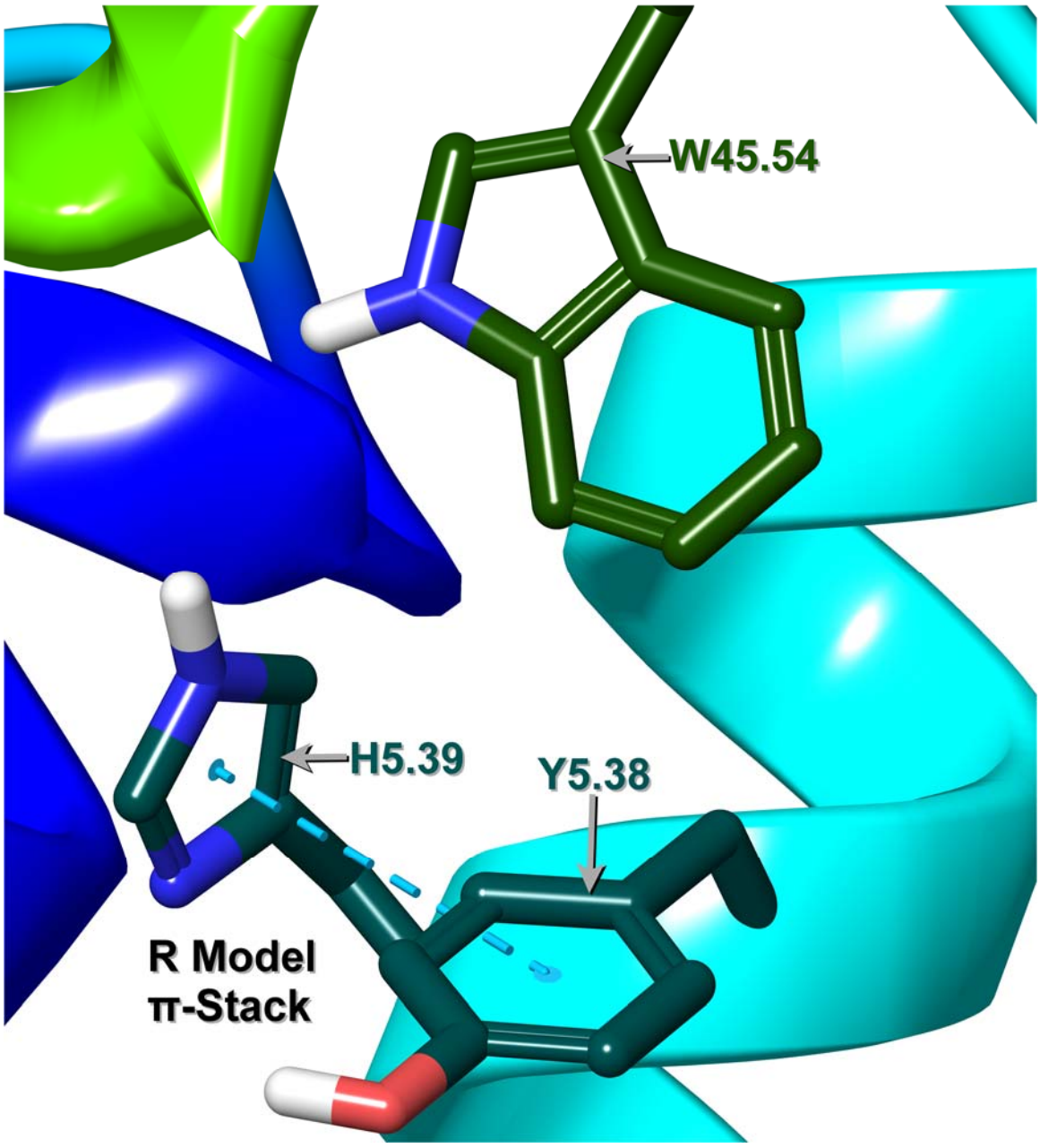

Figure 54. Y5.38 Donates a π-π T-stack Interaction to H5.39 in the R Model.[3,7,24]

The R* bundle has its own hydrogen bond interactions, as well. Y6.48 donates a hydrogen bond to T5.46's backbone oxygen, helping stabilize the R* state,[124,125,126,127,128,129,130] as shown in Figure 55.[3,7,24]

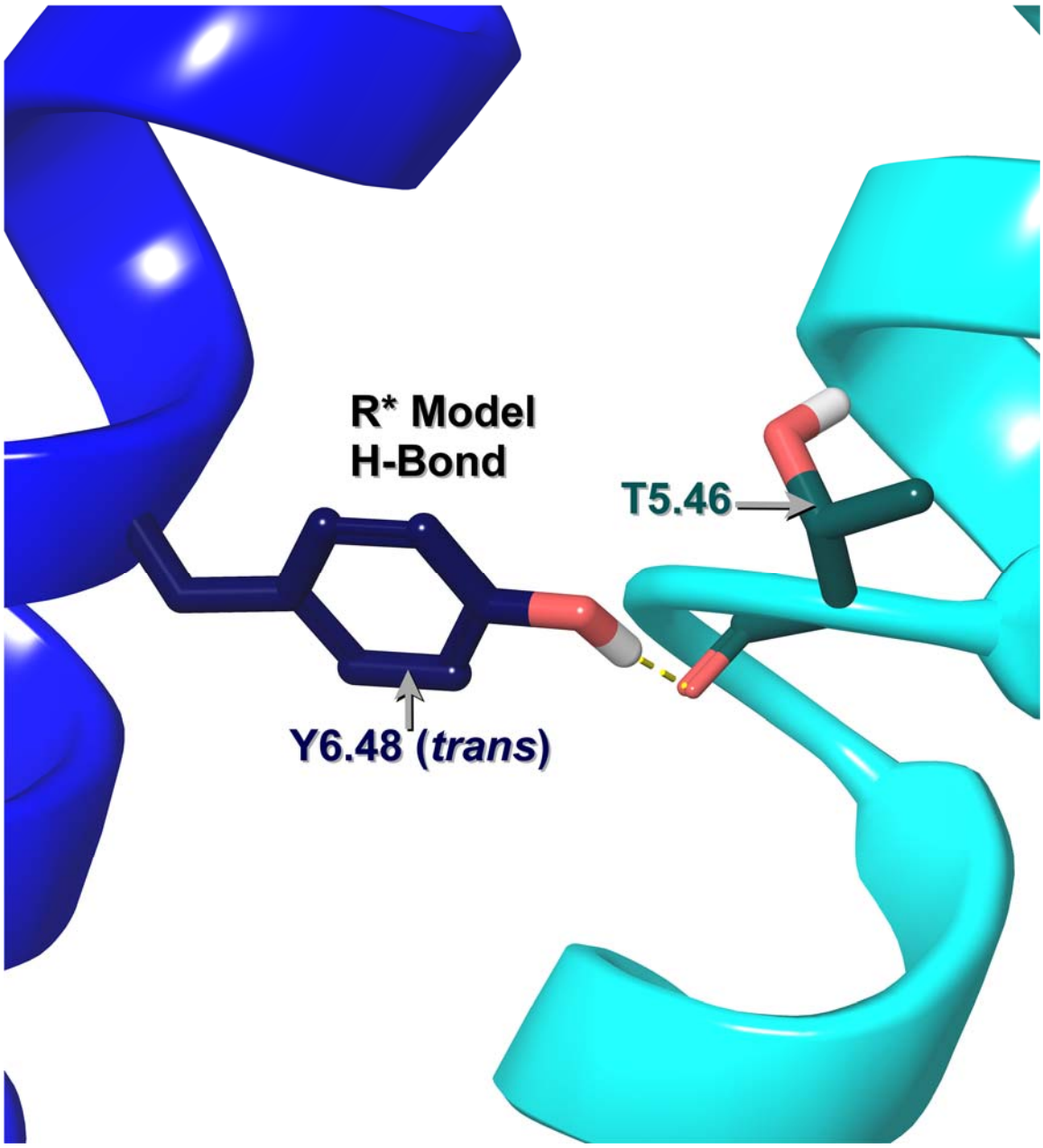

Figure 55. Y6.48 Donates a Hydrogen Bond to T5.46's Backbone Oxygen in the R* Model.[3,7,24,124,125,126,127,128,129,130]

Another set of interactions in the R* bundle involve Y39 in the ox1r N-terminus donating a hydrogen bond to E110 in the EC1 loop, as shown in Figure 56.[3,7,24]

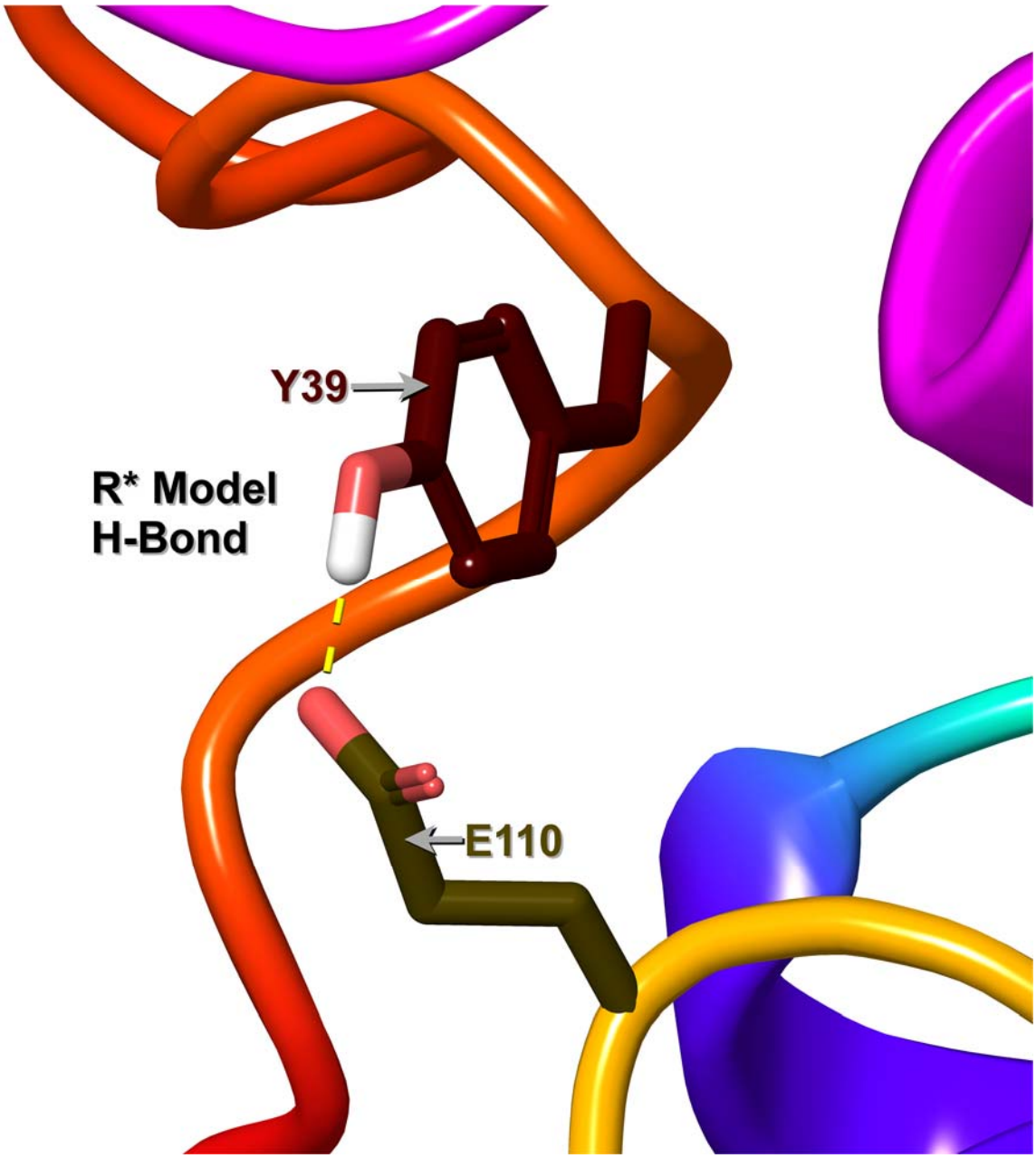

Figure 56. Y39 Donates a Hydrogen Bond to E110 in the EC1 Loop in the R* Model.[3,7,24]

Another set of interactions in the R* bundle involve Y41 in the ox1r N-terminus donating a hydrogen bond to the backbone oxygen of D332 in the EC3 loop, as shown in Figure 57.[3,7,24]

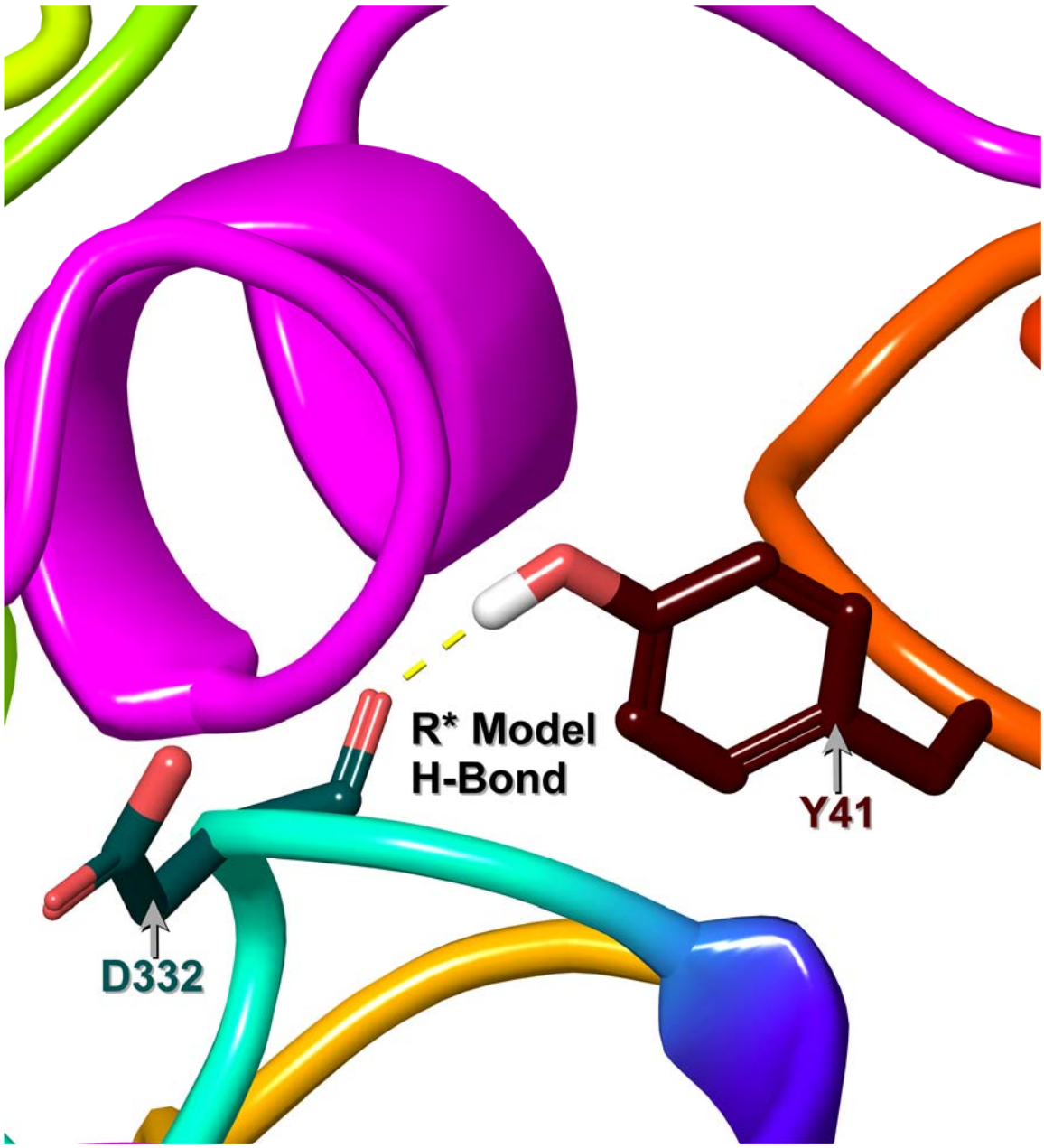

Figure 57. Y41 Donates a Hydrogen Bond to the Backbone Oxygen of D332 in the EC3 Loop in the R* Model.[3,7,24]

A cluster of interactions in the R* structure occurs in the IC1 region, as V1.57, W1.58, and N2.40 interact with M77 and R78, as shown in Figure 58.[3,7,24]

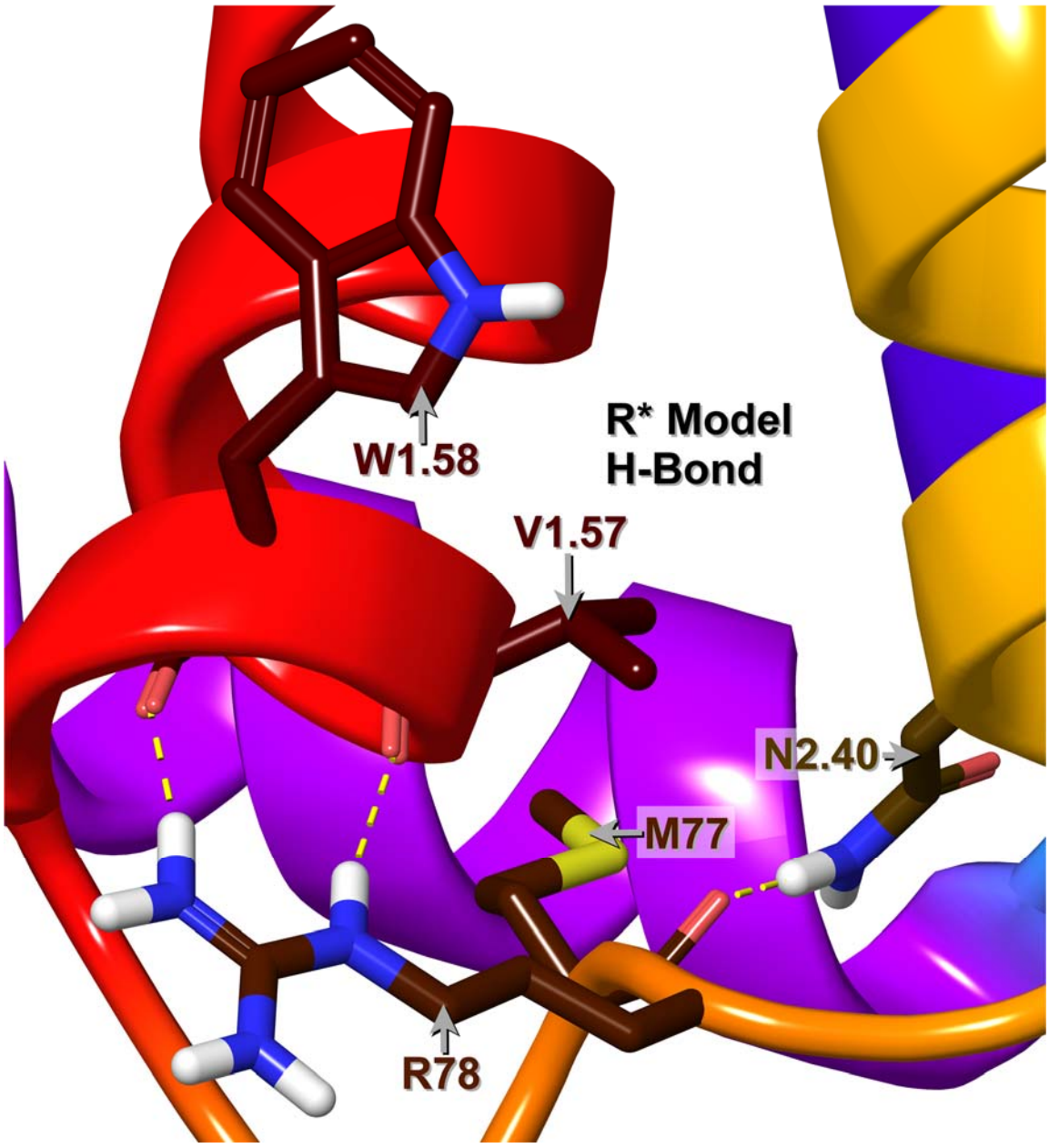

Figure 58. N2.40 Uses its Amide Side Chain to Donate a Hydrogen Bond to M77's Backbone Oxygen, While V1.57 and W1.58 Use Their Backbone Oxygens to Accept Two Hydrogen Bonds from R78, in the R* Model.[3,7,24]

D2.65 in the R* model's TMH2 is shown to accept two hydrogen bonds from K1.29 and one more from Y1.39, as Y1.39 accepts a hydrogen bond from S2.61, as shown in Figure 59.[3,7,24]

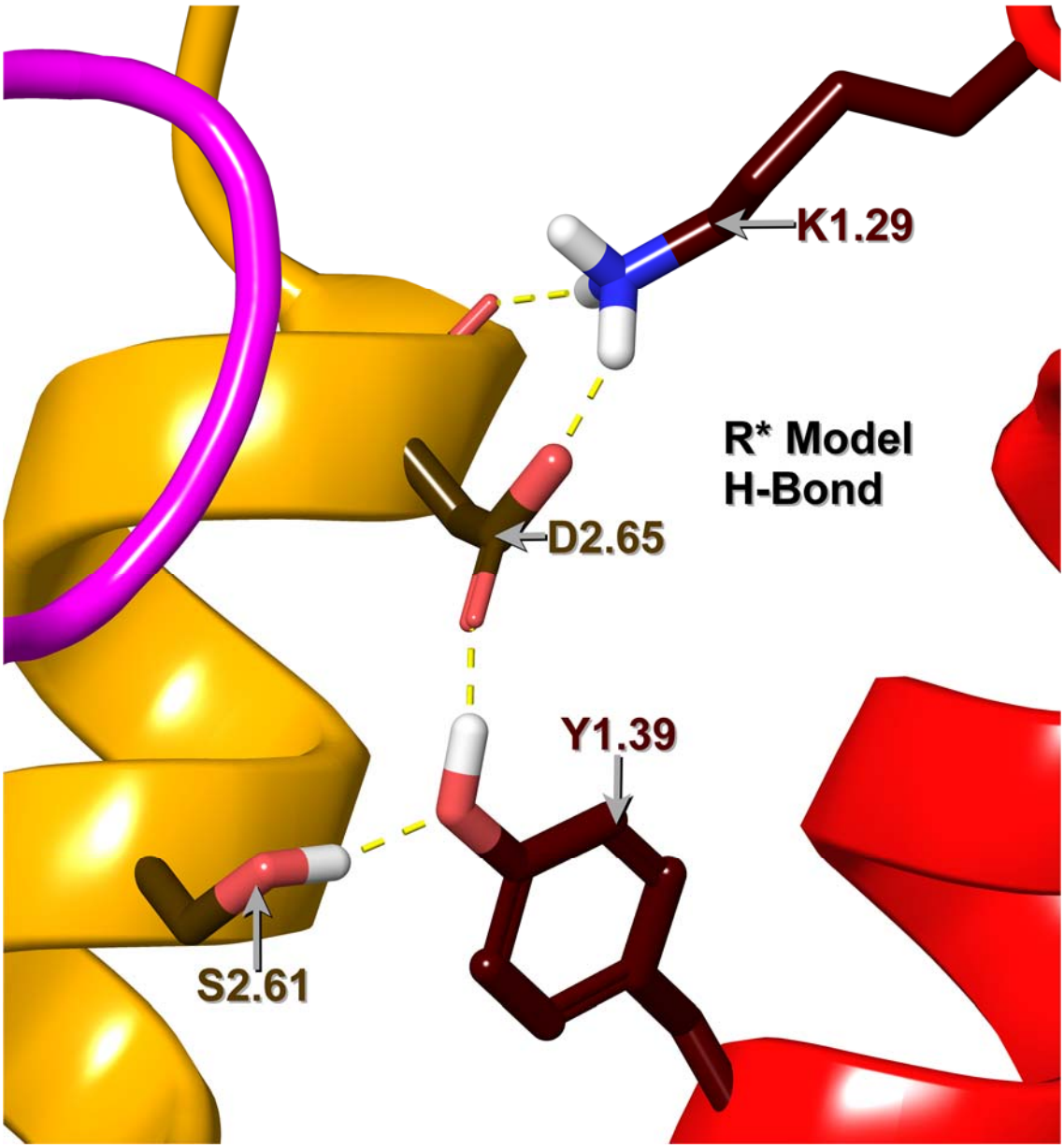

Figure 59. D2.65 Uses Its Backbone Oxygen and Side Chain to Accept Two Hydrogen Bonds from K1.29, and Also Uses its Side Chain to Accept Another Hydrogen Bond from Y1.39, While Y1.39 Accepts a Hydrogen Bond from S2.61, in the R* Model.[3,7,24]

Q4.60 and Y5.38 have their roles in keeping the EC2 loop, TMH4, and TMH5 together in the R* structure as Q4.60 accepts a hydrogen bond from W45.54, while Y5.38 donates a hydrogen bond to I4.56's backbone oxygen, as shown in Figure 60.[3,7,24]

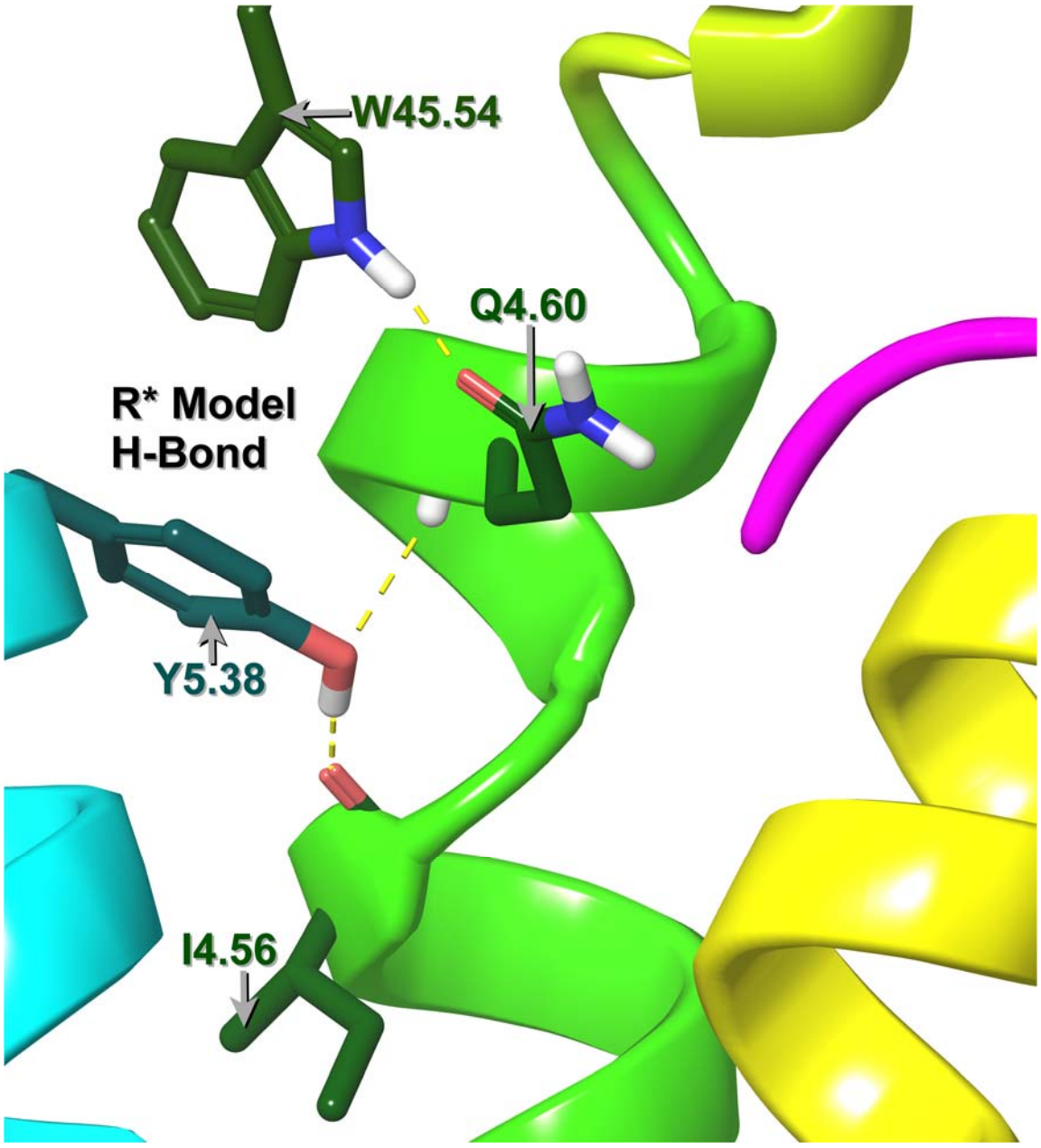

Figure 60. Q4.60 Accepts a Hydrogen Bond from W45.54, as Y5.38 Donates a Hydrogen Bond to I4.56's Backbone Oxygen, in the R* Model.[3,7,24]

In the R* model, H5.39 accepts a hydrogen bond from N6.55, which in turn accepts one from R6.59, as shown in Figure 61.[3,7,24]

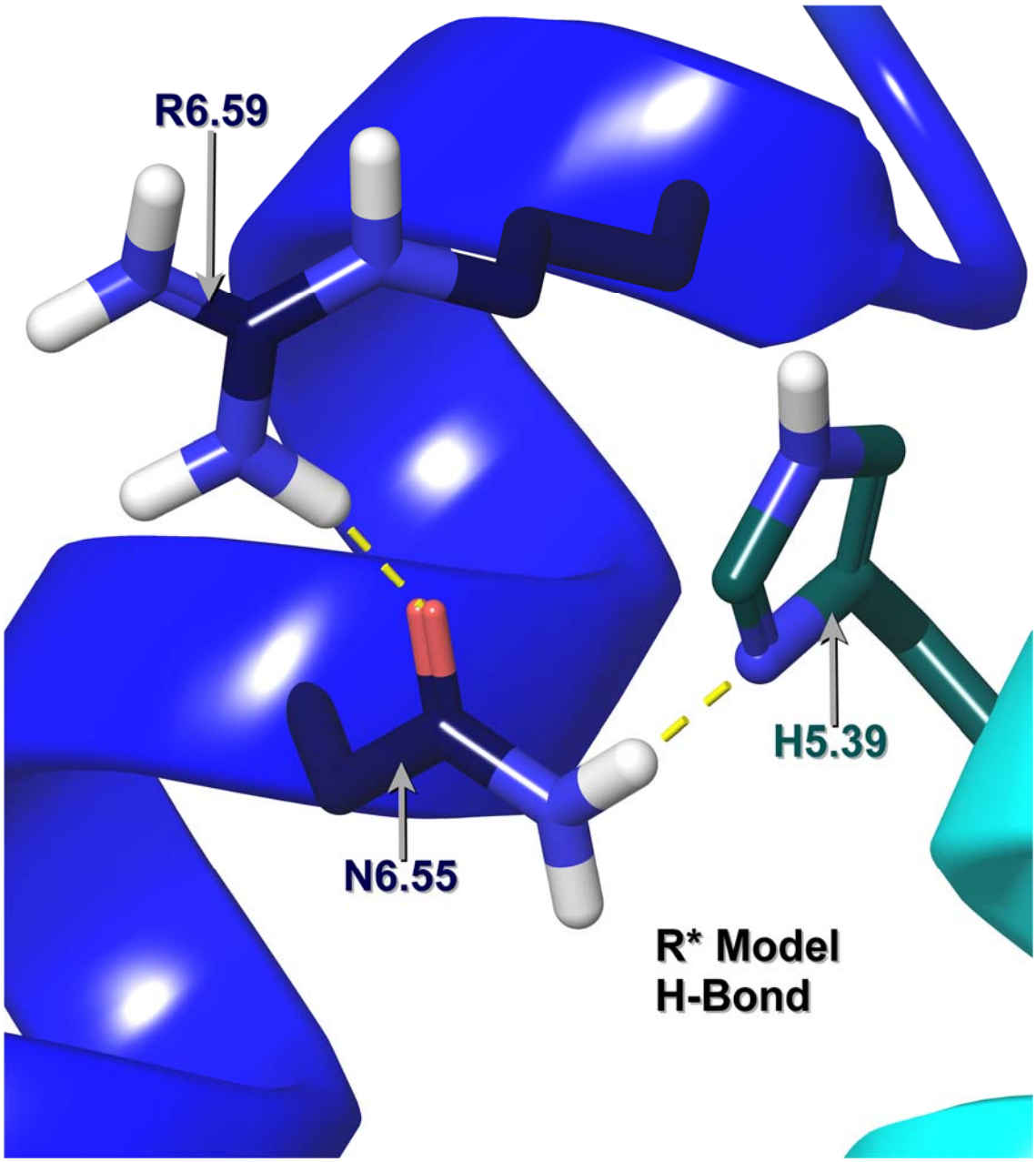

Figure 61. H5.39 Accepts a Hydrogen Bond from N6.55, as N6.55 Accepts Another Hydrogen Bond from R6.59, in the R* Model.[3,7,24]

Yet another set of interactions in the R* bundle involves R6.30, which donates a hydrogen bond each to Q6.26's backbone oxygen and side chain, while donating another to L5.65's backbone oxygen, as shown in Figure 62.[3,7,24]

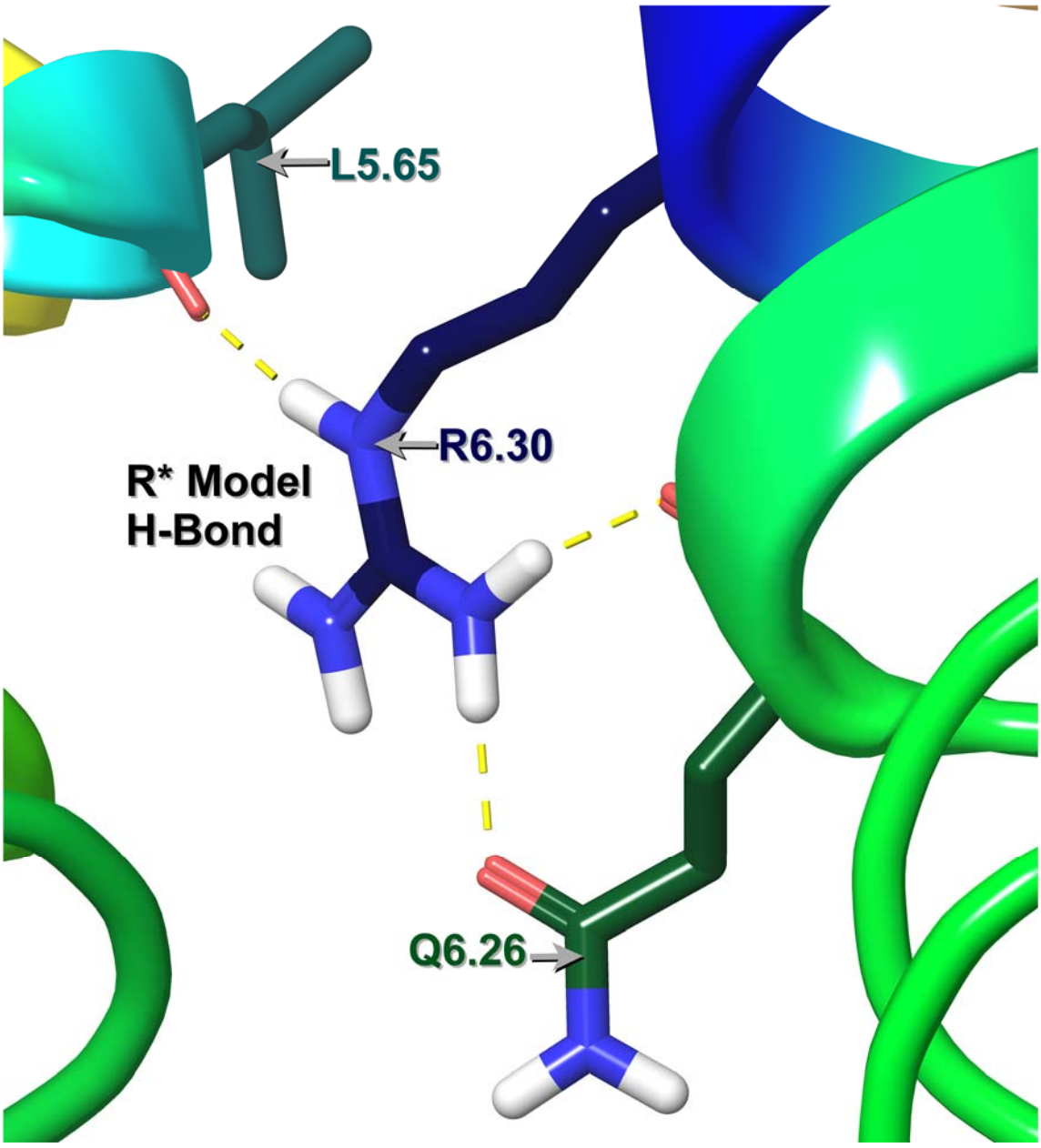

Figure 62. R6.30 Donates a Hydrogen Bond Each to Q6.26's Backbone Oxygen and Side Chain, While Donating Another to L5.65's Backbone Oxygen, in the R* Model.[3,7,24]

Yet another set of interactions in the R* bundle also involves K7.59 donating a hydrogen bond each to H76 and to E7.62, while N1.60 donates another hydrogen bond to Q7.63, as shown in Figure 63.[3,7,24]

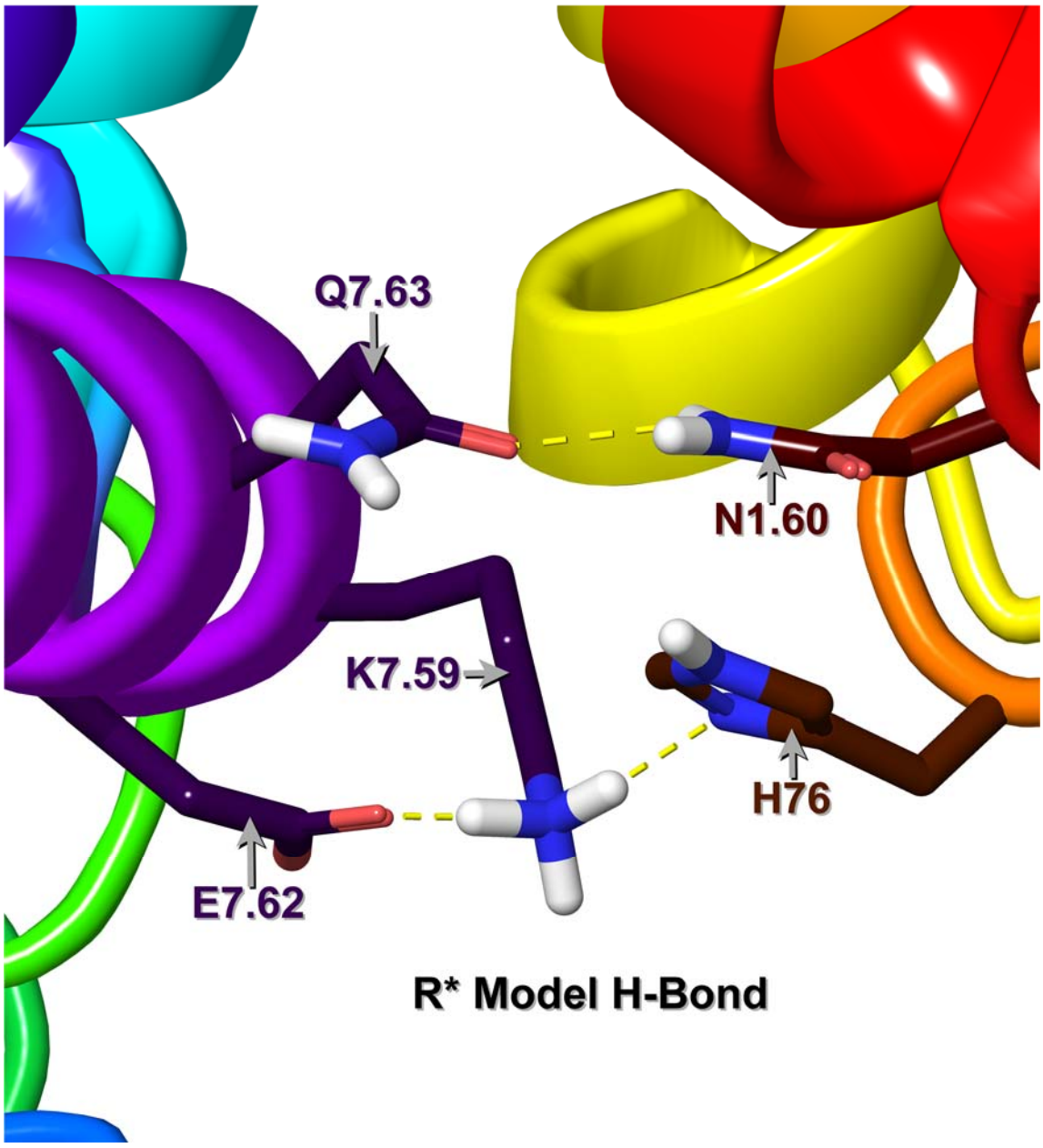

Figure 63. K7.59 Donates a Hydrogen Bond Each to H76 and to E7.62, While N1.60 Donates Another Hydrogen Bond to Q7.63, in the R* Model.[3,7,24]

Another hydrogen bond formed is K6.32 donating a hydrogen bond to F7.55's backbone oxygen, while R7.61 donates another hydrogen bond to N7.54's backbone oxygen, as shown in Figure 64.[3,7,24]

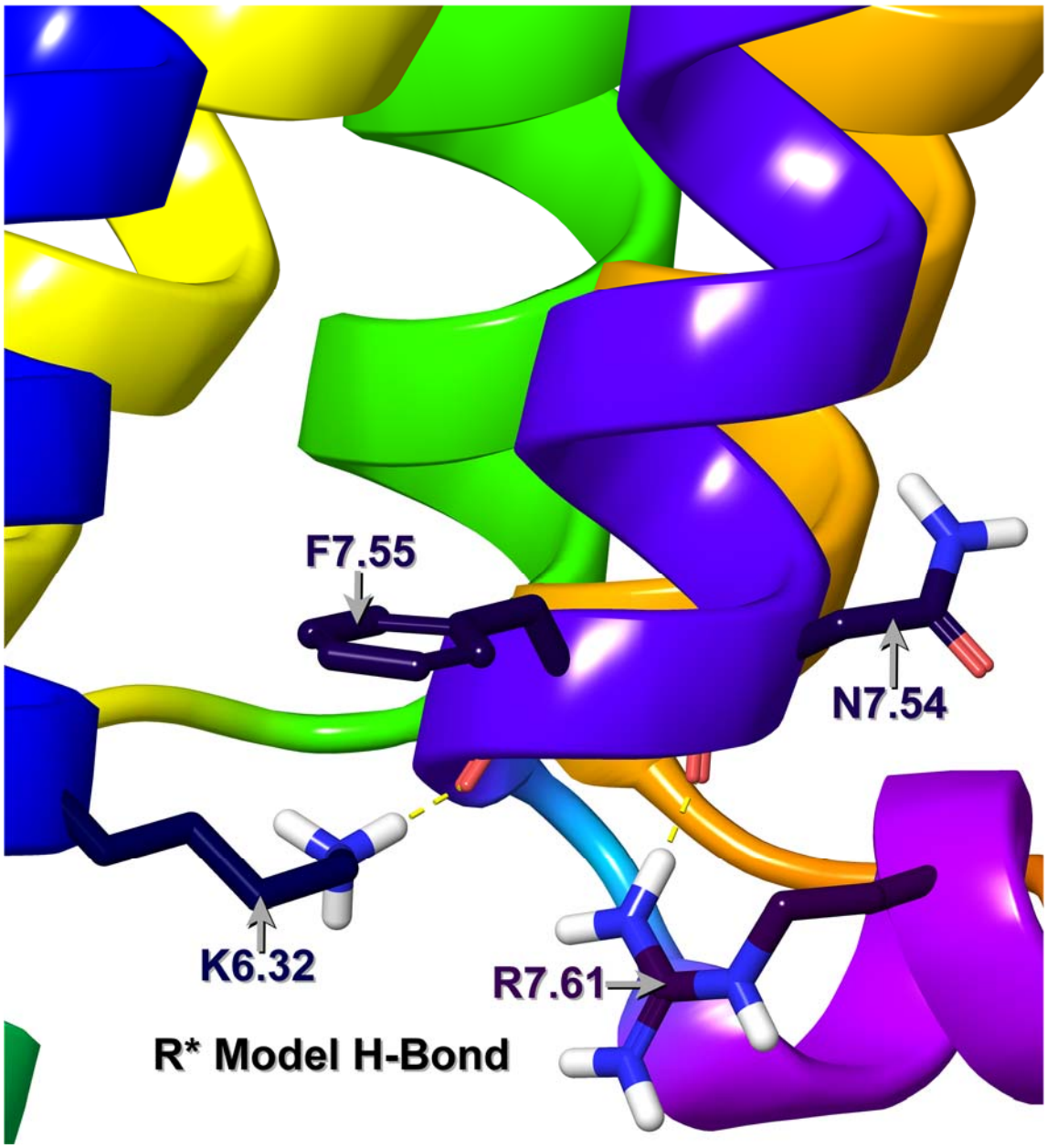

Figure 64. K6.32 Donates a Hydrogen Bond to F7.55's Backbone Oxygen, While R7.61 Donates Another Hydrogen Bond to N7.54's Backbone Oxygen, in the R* Model.[3,7,24]

Another new interaction formed in the R* structure is K6.32 donating a cation-π interaction to F7.55 in TMH7, as shown in Figure 65.[3,7,24]

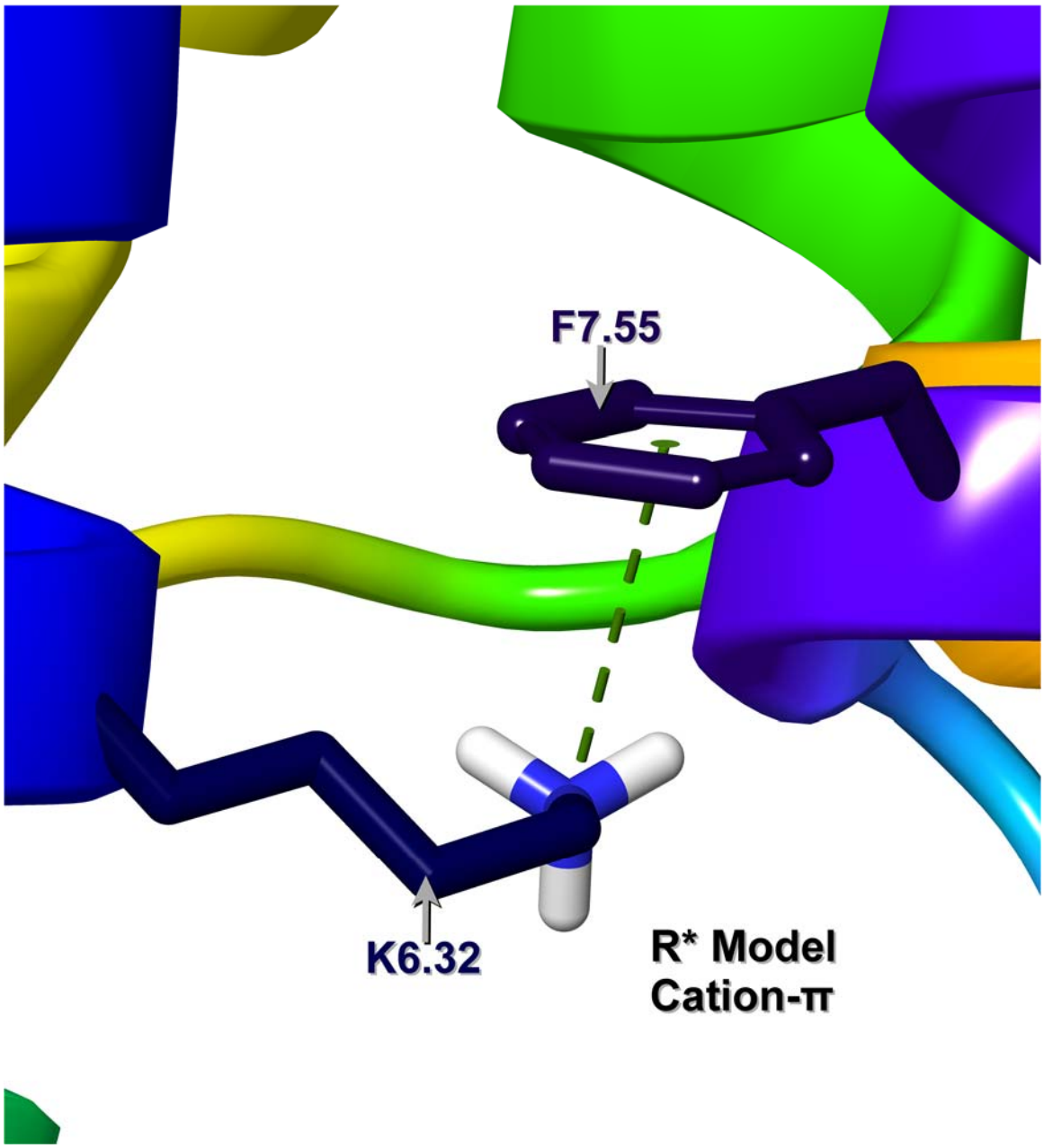

Figure 65. K6.32 Donates a Cation-π Interaction to F7.55 in the R* Model.[3,7,24]

Another such interaction in the R* structure is Y5.38 donating a π-π T-stack to H5.39, while the latter donates another to W45.54, as part of the aromatic cluster between the EC2b loop and TMH5, as shown in Figure 66.[3,7,24]

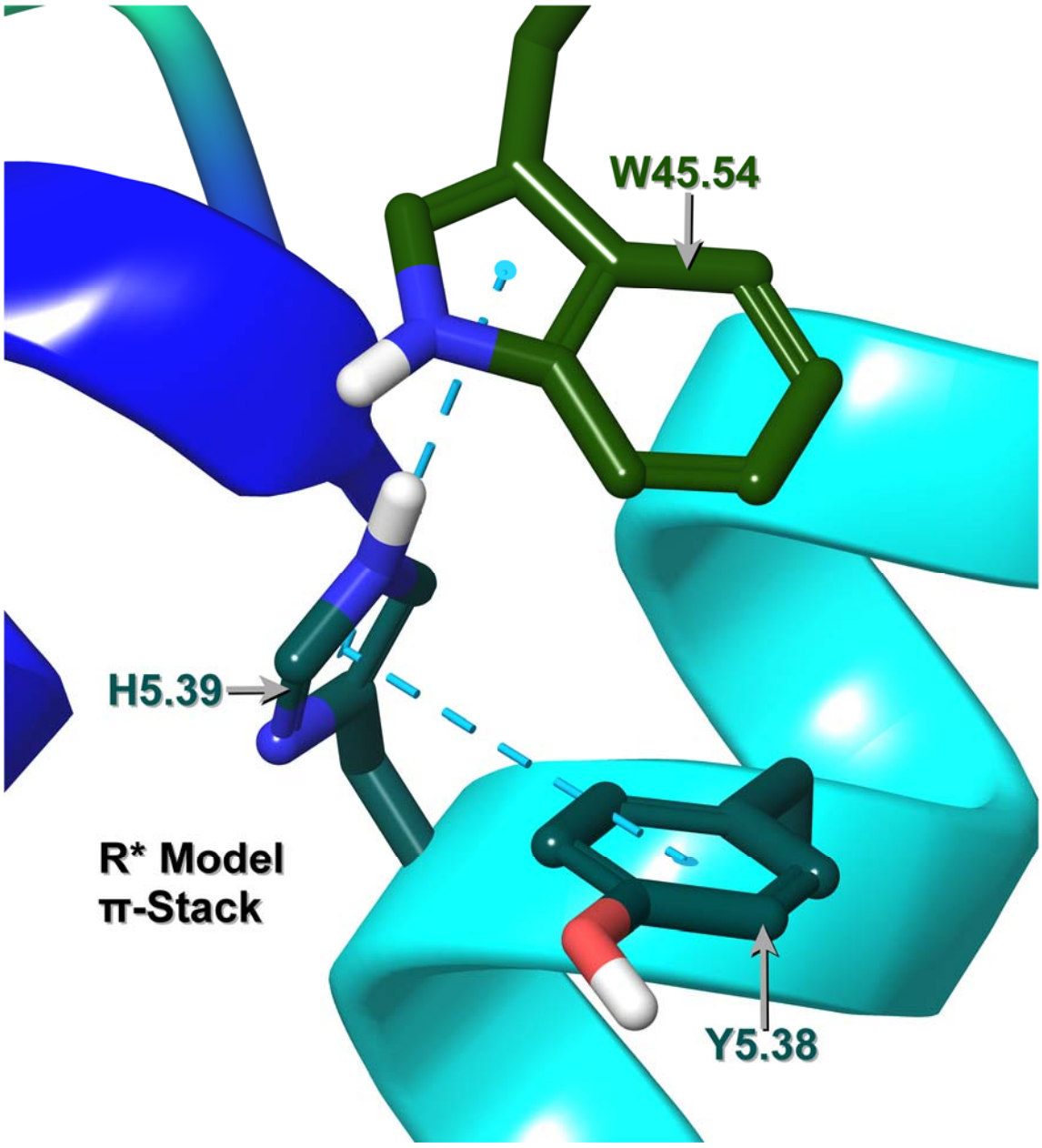

Figure 66. Y5.38 Donates a π-π T-stack Interaction to H5.39, as H5.39 Donates Another to W45.54, in the R* Model.[3,7,24]

Another new interaction formed in the R* structure is R45.45 in the EC2 loop donating a cation-π interaction to F45.47, as shown in Figure 67.[3,7,24]

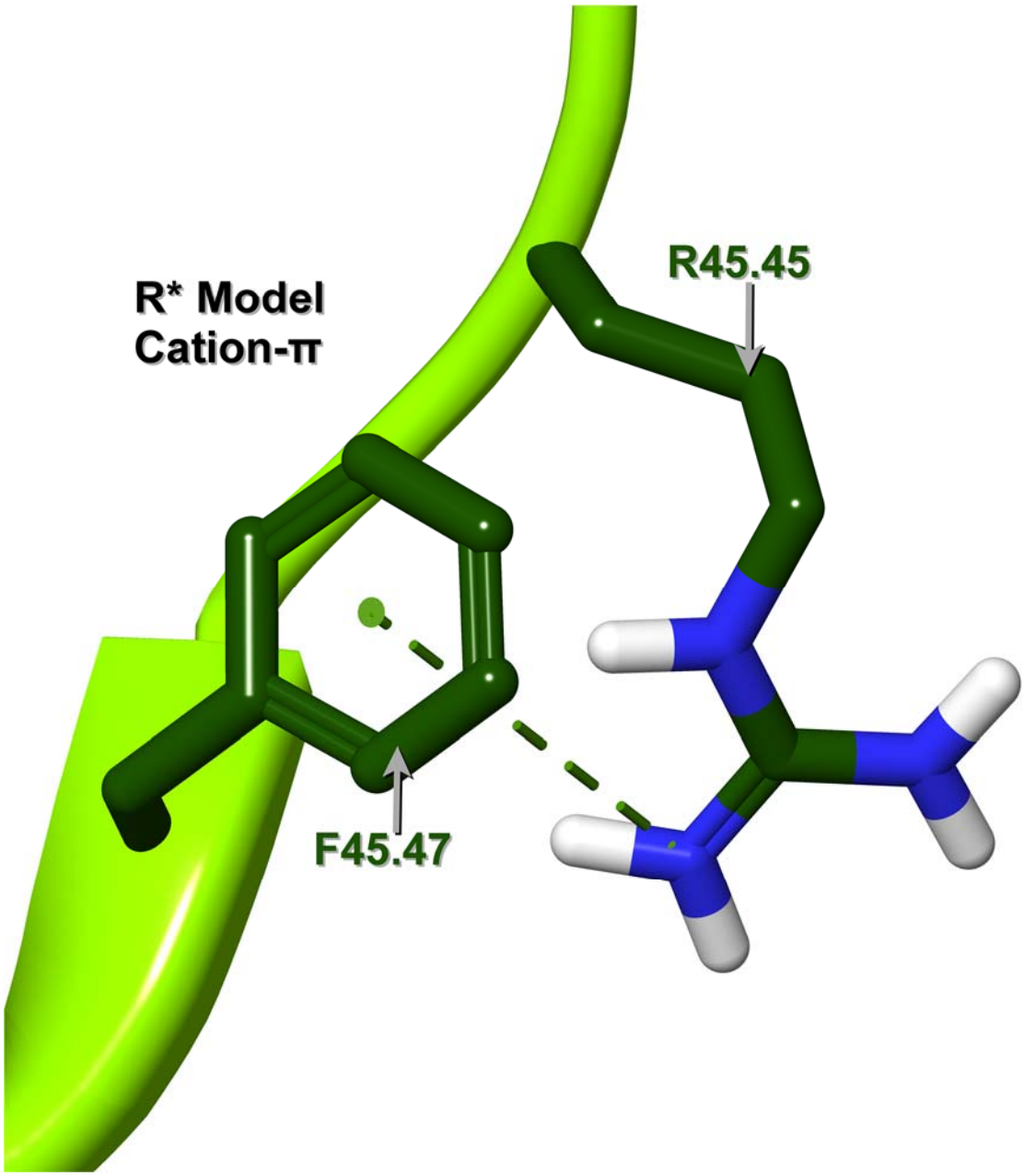

Figure 67. R45.45 in the EC2 Loop Donates a Cation-π Interaction to F45.47 in the R* Model.[3,7,24]

Another new interaction formed in the R* structure is K6.25 in the IC3 loop donating a cation-π interaction to F6.20, as shown in Figure 68.[3,7,24]

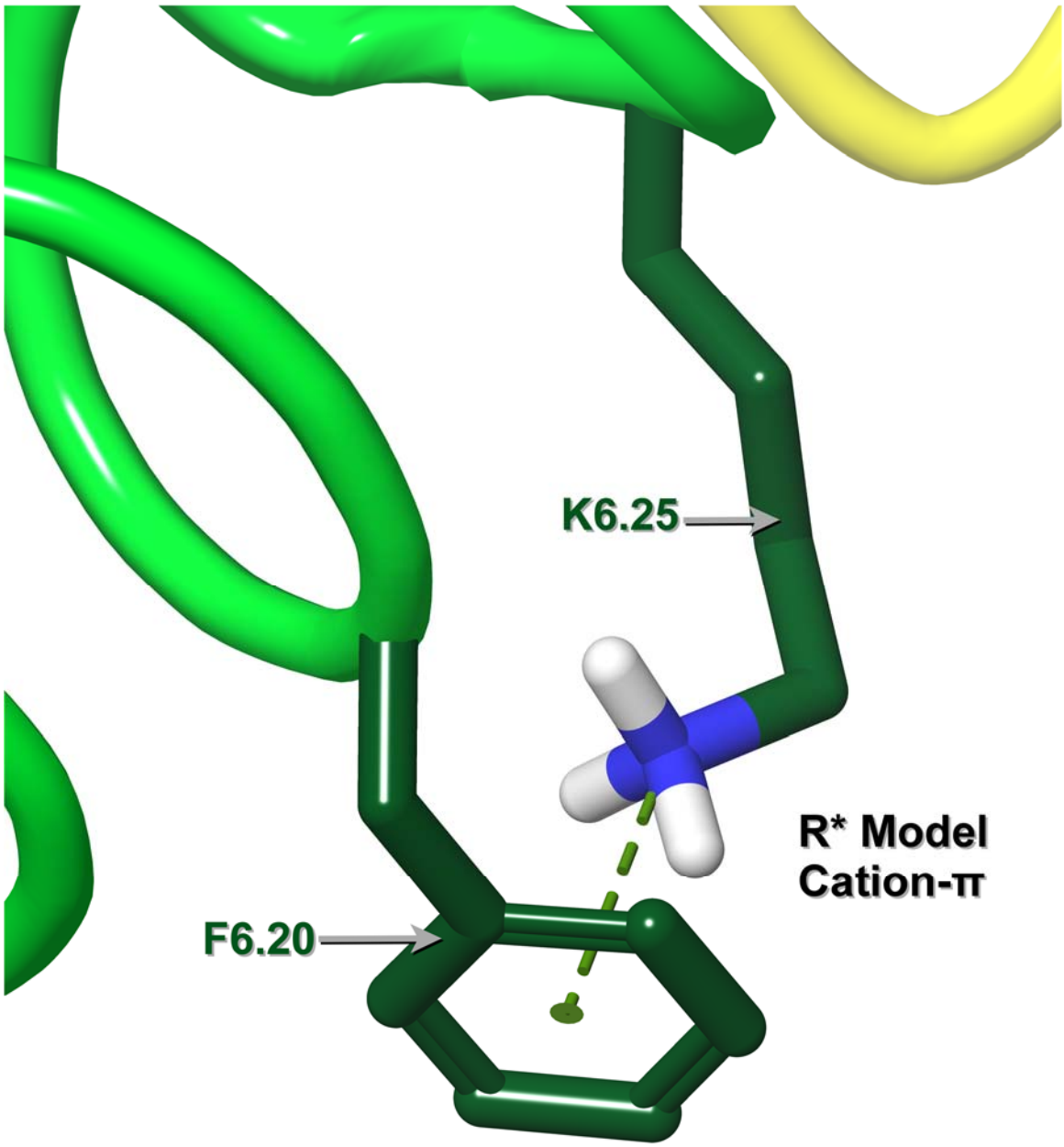

Figure 68. K6.25 in the IC3 Loop Donates a Cation-π Interaction to F6.20 in the R* Model.[3,7,24]

Interactions of the Orexin-1 Receptor R Structure with SB-674042

In the R bundle, SB-674042 chiefly interacts with the residue Q3.32 by using its N40 oxadiazole nitrogen to accept a hydrogen bond,[3,7,24] as shown in Figures 69 and 70.

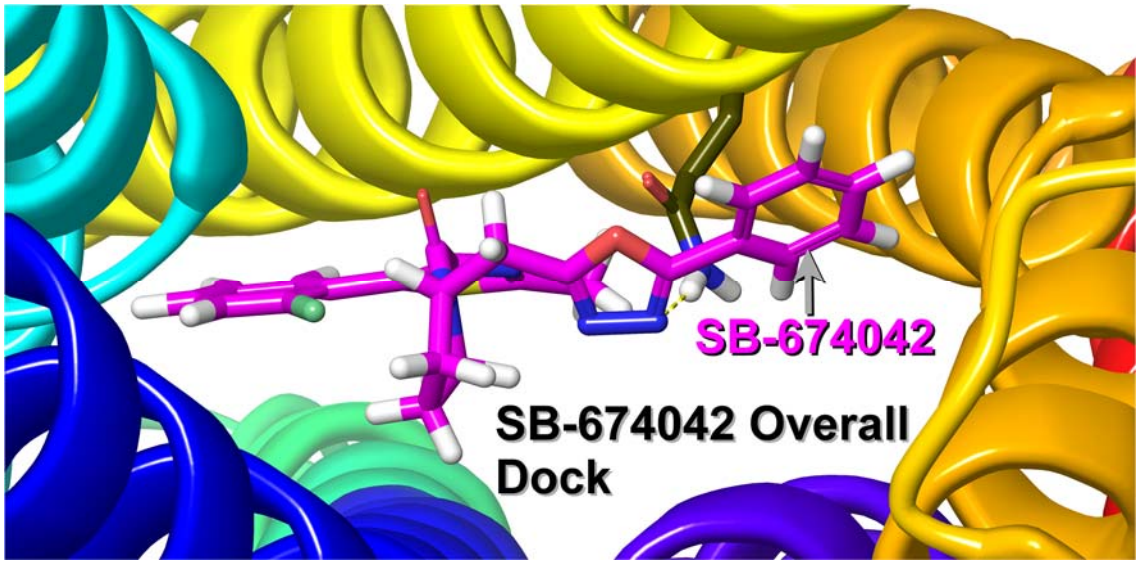

Figure 69. Overall Dock of SB-674042 in the R Model.[3,7,24]

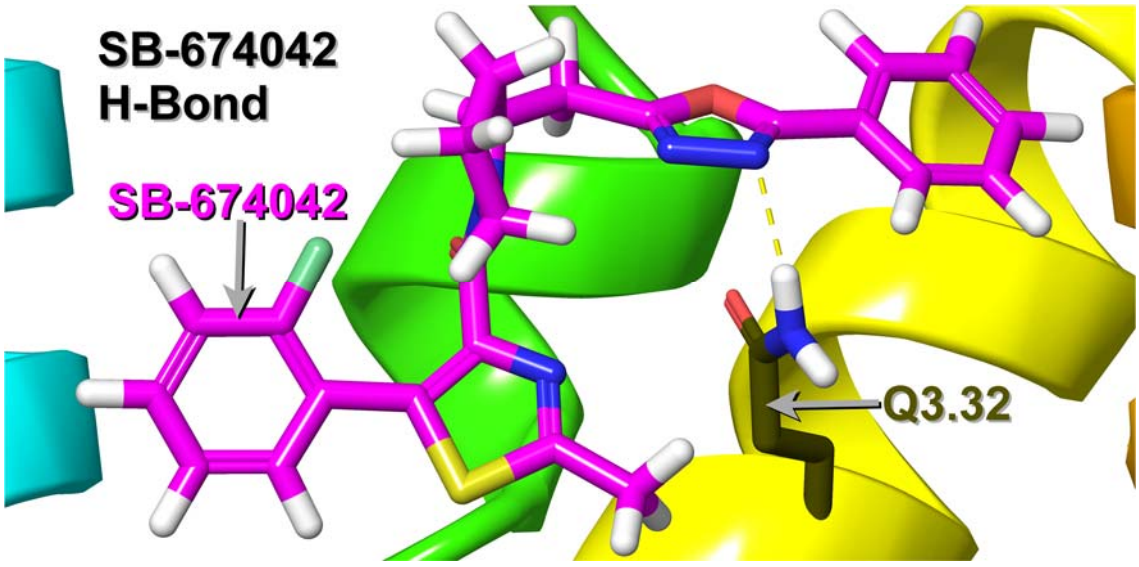

Figure 70. Main Interaction of SB-674042 Accepting a Hydrogen Bond from Q3.32 in the R Model.[3,7,24]

Part 1 of SB-674042 (the A-ring) interacts with the ox1r by means of light van der Waals contacts with V3.36 and Y5.47 and a wide range of heavy van der Waals contacts with F5.42, F5.43, T5.46, I6.51, S6.52, and N6.55, as shown in Figure 71, and accepts a π-π T-stack from F5.42, as shown in Figure 72.[3,7,24]

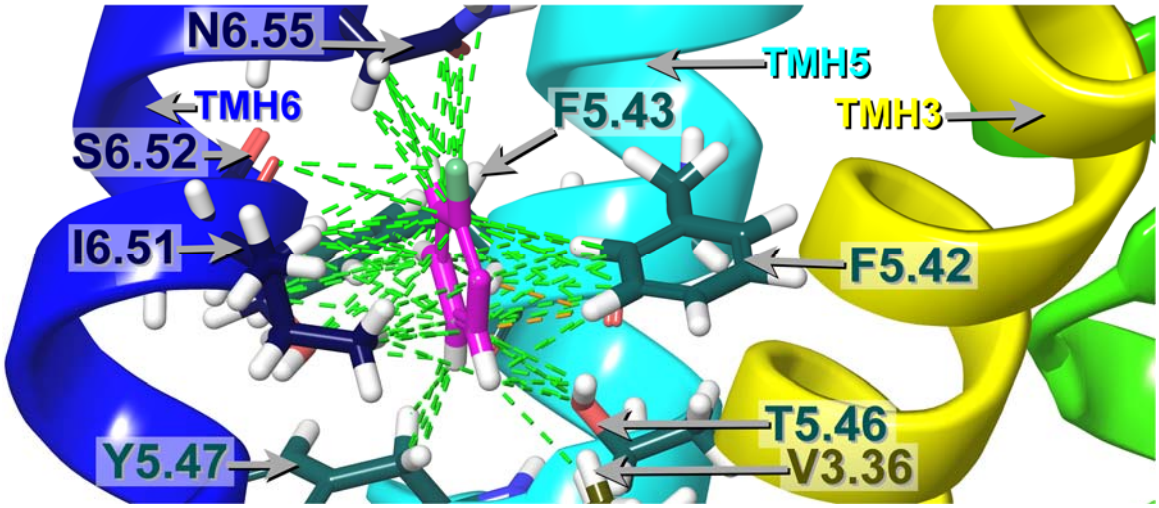

Figure 71. Part 1 of SB-674042 Interacts with V3.36, F5.42, F5.43, T5.46, Y5.47, I6.51, S6.52, and N6.55 by van der Waals in the R Model.[3,7,24]

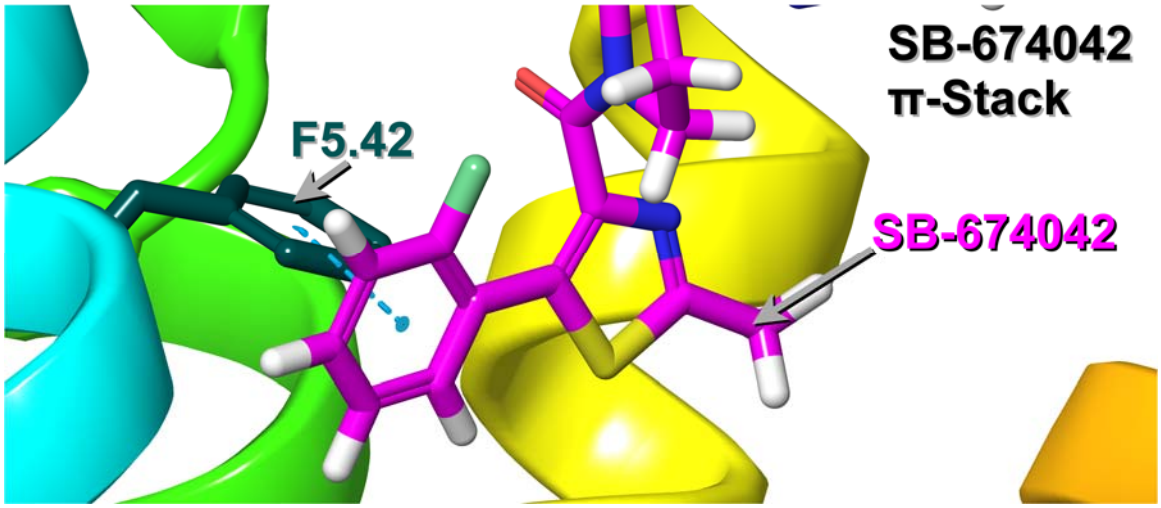

Figure 72. Part 1 of SB-674042 Interacts with F5.42 by Accepting a π-π T-stack in the R Model.[3,7,24]

Part 2 of SB-674042 (including the B ring) interacts with the ox1r by means of multiple heavy van der Waals contacts with Q3.32, V3.36, F5.42, Y6.48, I6.51, and V7.42, as shown in Figure 73, and by accepting a π-π T-stack from F5.42 in Figure 74.[3,7,24,124]

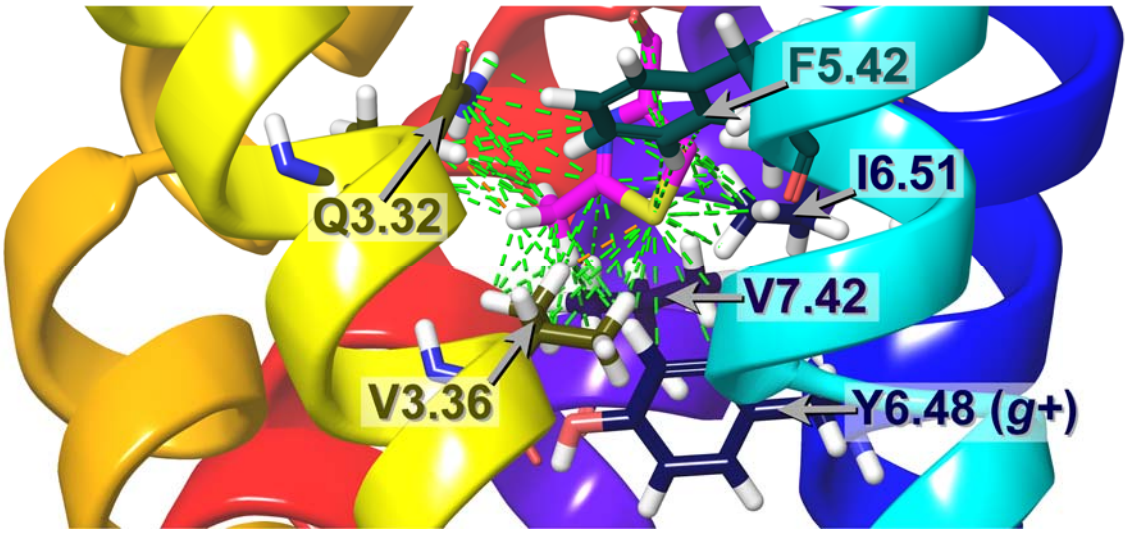

Figure 73. Part 2 of SB-674042 Interacts with Q3.32, V3.36, F5.42, Y6.48, I6.51, and V7.42 by van der Waals in the R Model.[3,7,24,124]

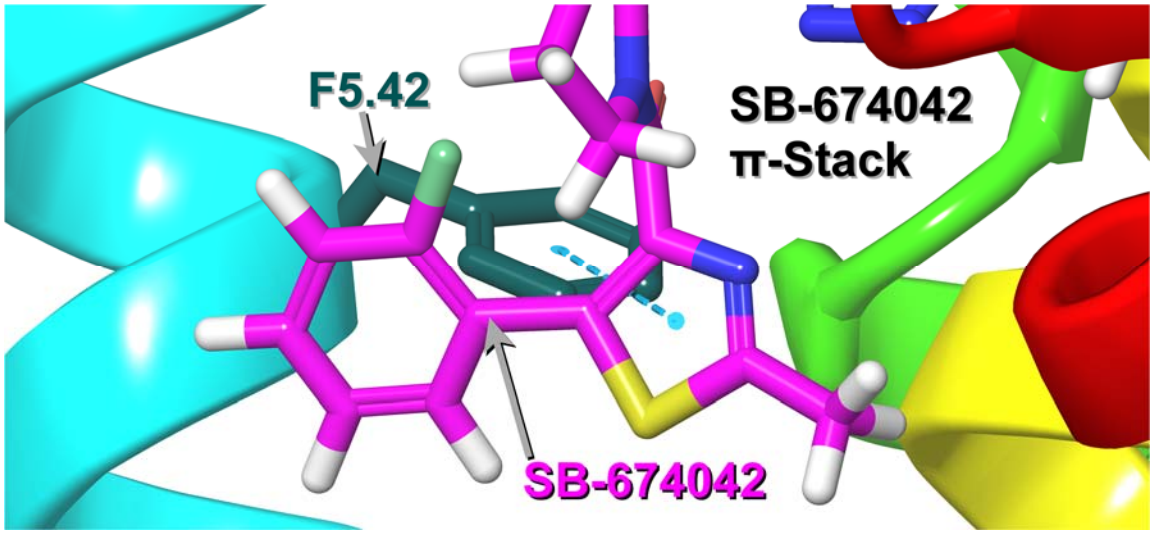

Figure 74. Part 2 of SB-674042 Interacts with F5.42 by Accepting a π-π T-stack in the R Model.[3,7,24]

Part 3 of SB-674042 (the C-ring) interacts with the ox1r by means of many heavy van der Waals contacts with I6.51, N6.55, F7.35 and H7.39, as shown in Figure 75.[3,7,24]

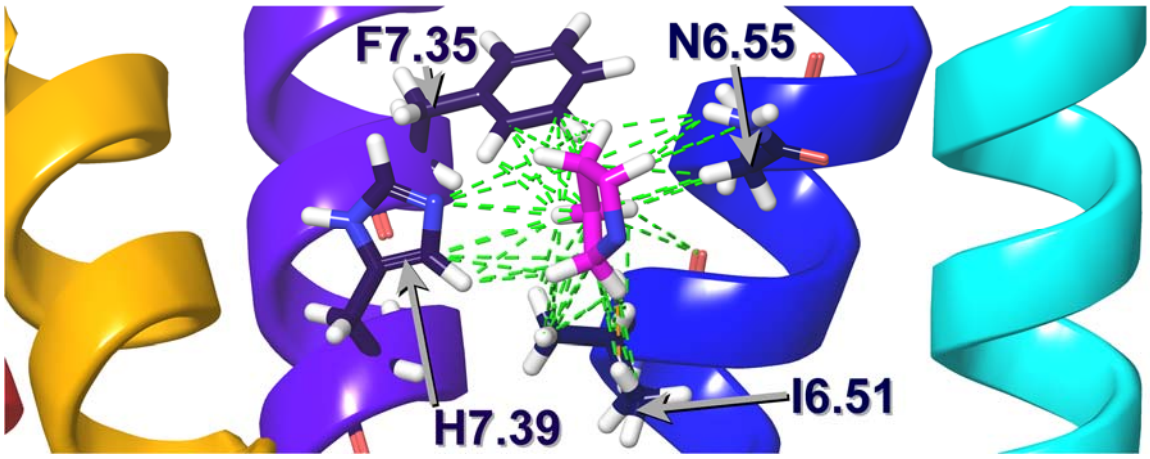

Figure 75. Part 3 of SB-674042 Interacts with I6.51, N6.55, F7.35, and H7.39 By van der Waals in the R Model.[3,7,24]

Part 4 of SB-674042 (the methylene bridge) was not close enough to interact with the ox1r by means of van der Waals contacts, as it was a small part of SB-674042, as shown in Figure 76.[3,7,24]

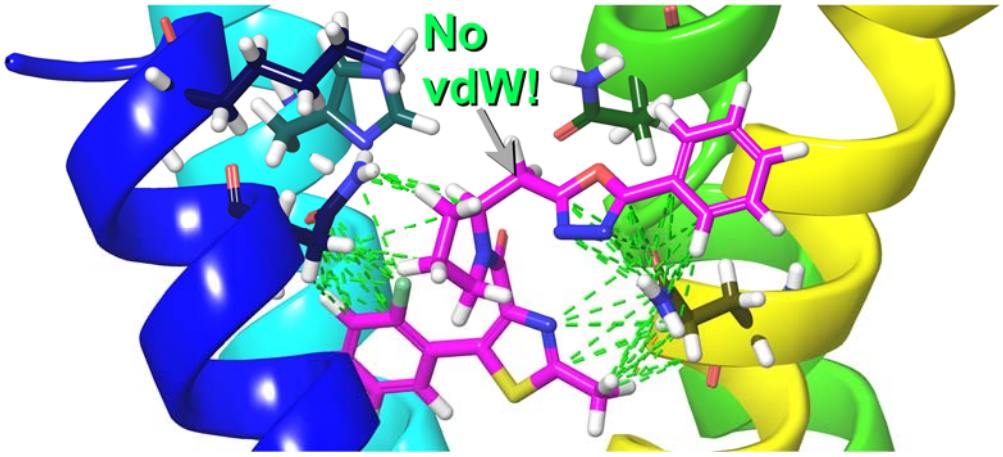

Figure 76. Part 4 of SB-674042 is Not Close Enough to Interact By van der Waals in the R Model.[3,7,24]

Part 5 of SB-674042 (the D-ring) interacts with the ox1r by means of light van der Waals contacts with H7.39 and heavy van der Waals contacts with Q3.32, as shown in Figure 77, and donates a π-π T-stack to H7.39, as shown in Figure 78.[3,7,24]

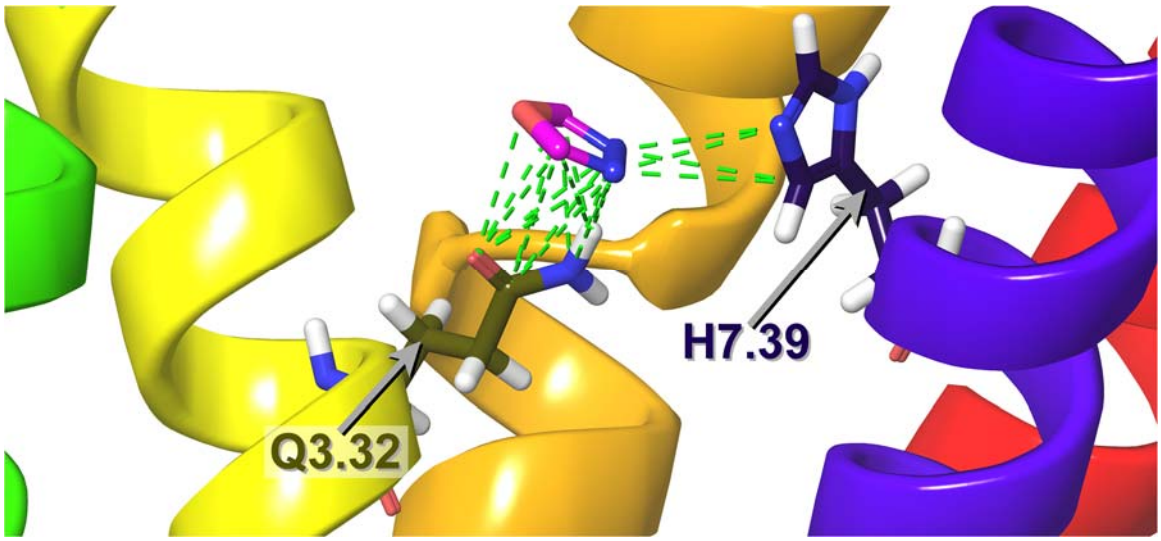

Figure 77. Part 5 of SB-674042 Interacts with Q3.32 and H7.39 By van der Waals in the R Model.[3,7,24]

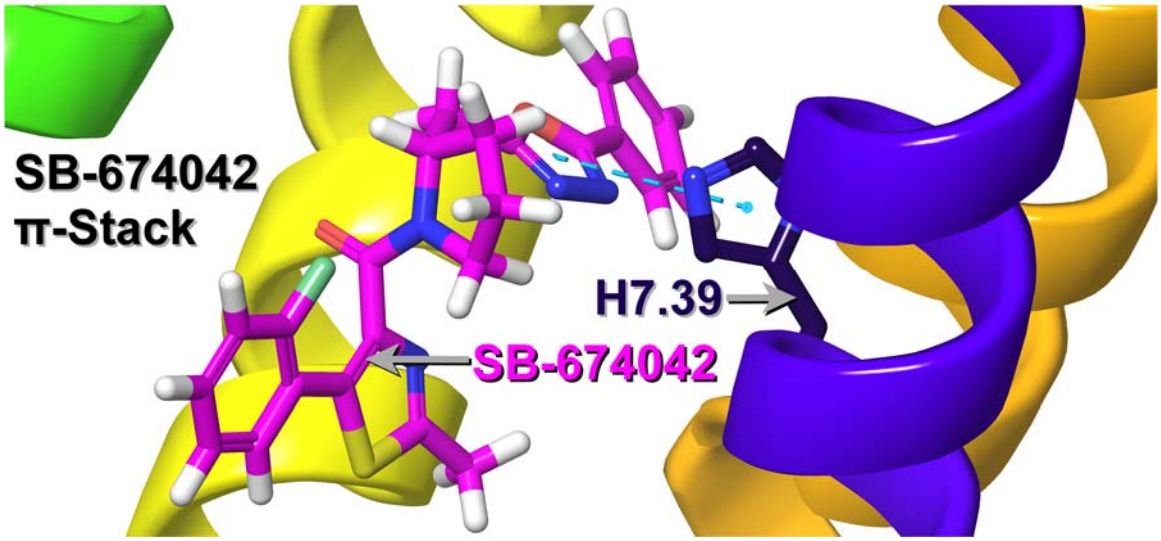

Figure 78. Part 5 of SB-674042 Interacts with H7.39 By Donating a π-π T-stack in the R Model.[3,7,24]

Part 6 of SB-674042 (the E ring) interacts with the ox1r by means of light van der Waals contacts with C2.57 and Y7.43, and numerous heavy van der Waals contacts with S2.61, W112 (EC1), I3.28, P3.29, and Q3.32, as shown in Figure 79.[3,7,24]

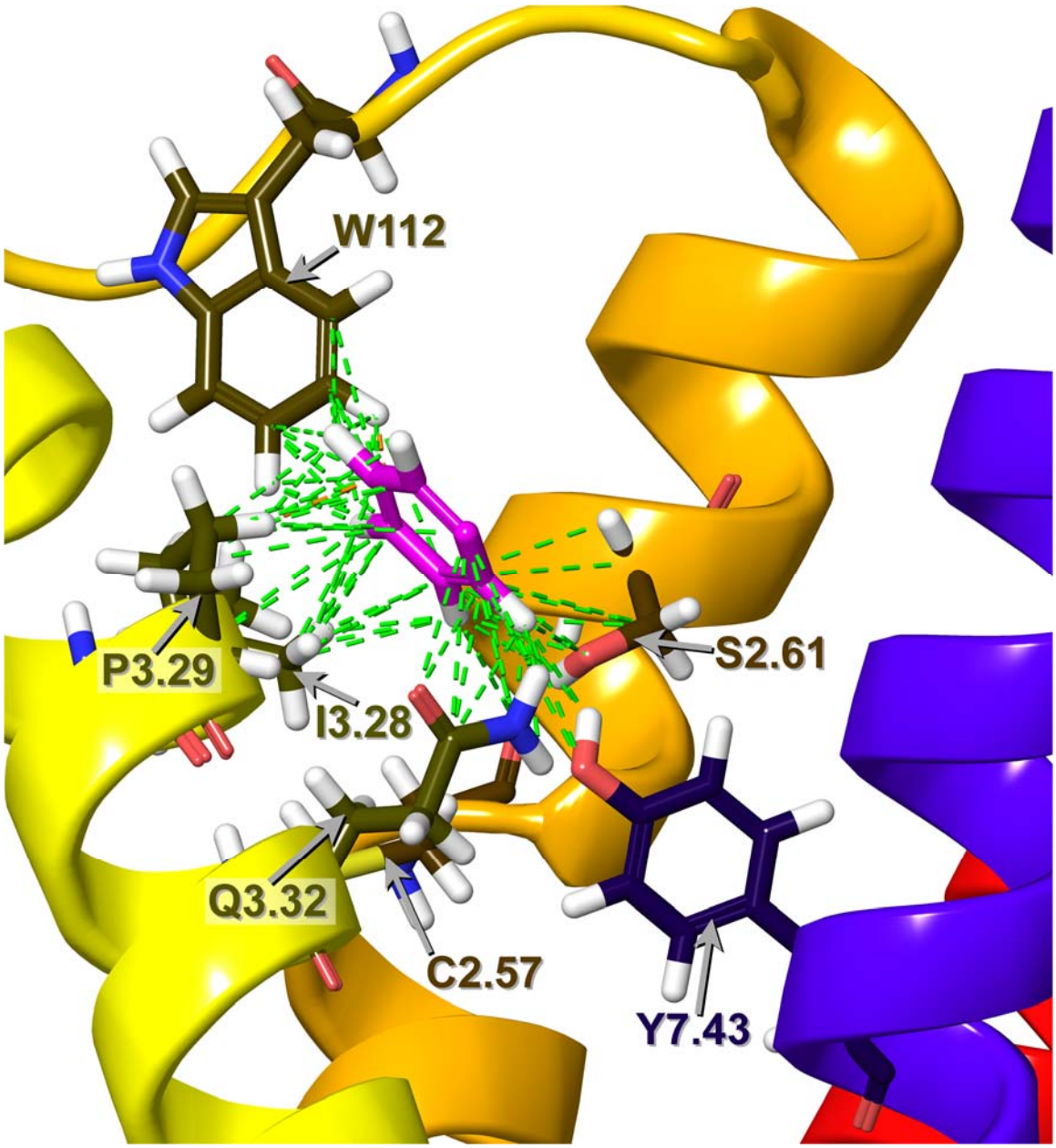

Figure 79. Part 6 of SB-674042 Interacts with C2.57, S2.61, W112 (EC1), I3.28, P3.29, Q3.32, and Y7.43 By van der Waals in the R Model.[3,7,24]

In the ox1r, a reason why D45.51A may not be an effective mutation is that D45.51 is a negatively charged residue, whereas SB-674042 has no hydrogen bond donors that can interact with the carboxylic acid side chain it has.[3,7,24] Furthermore, the reason that Q3.32A had as much effect as it did was that mutation to an alanine costs the ox1r the hydrogen bond and much of the contacts Q3.32 would cause.[3,7,24] The reason that A3.33T would have its effect is that it could cause TMH3 to bend and change the structure of the binding pocket.[3,7,24,148,149] W45.54A has its effect of abolishing binding because W45.54 is situated between TMH4 and TMH5 and stabilizes them, interacting very heavily with its surrounding residues, and mutation to an alanine would cause a large gap between TMH4 and TMH5 that would cause the ox1r to partially collapse on that side.[3,7,24] Y5.38A has its strong effect because Y5.38 helps hold TMH4 and TMH5 together, especially by donating a hydrogen bond to Q4.60 as found by Heifetz et al. and Yin et al., and donating a π-π T-stack to H5.39 as found by Yin et al., and a mutation to alanine would abolish all of those, possibly causing another partial collapse.[3,7,24] F5.42A was effective because it would cause a partial collapse of the ox1r there, while costing the ox1r the van der Waals contacts and flat π-π stack F5.42 would cause.[3,7,24] Y6.48A, H7.39A, and Y7.43A were all effective mutations because each of those mutations would cost the ox1r much of the contacts that Y6.48, H7.39, and Y7.43 would cause respectively.[3,7,24]

Interactions of the Orexin-1 Receptor R* Structure with Orexin-A

The R* structure admits orexin-A through a small opening in the extracellular side of the ox1r, similar to the structure of the ox2r.[3,4,7,22,24] The structure of orexin-A is

an α-helix comprised of its residues R15 to A23, with an N-terminal structure consisting of a short α-helix of its residues C6 to Q9 with two disulfide bonds (C6-C12 and C7-C14), keeping it close to that middle helix, while the C-terminal end of orexin-A, originally an α-helix from its N25 to its C-terminus, becomes a random coil that extends into the ox1r binding pocket to activate the ox1r.[3,4,7,22,24] The R* bundle featured many interactions with the ox1r, from the middle helix of orexin-A, especially L16, L19, and L20, interacting with the ox1r EC2 loop's β-sheets, to the C-terminus of orexin-A interacting with the ox1r transmembrane core, as shown in Figure 80.[3,4,7,22,24]

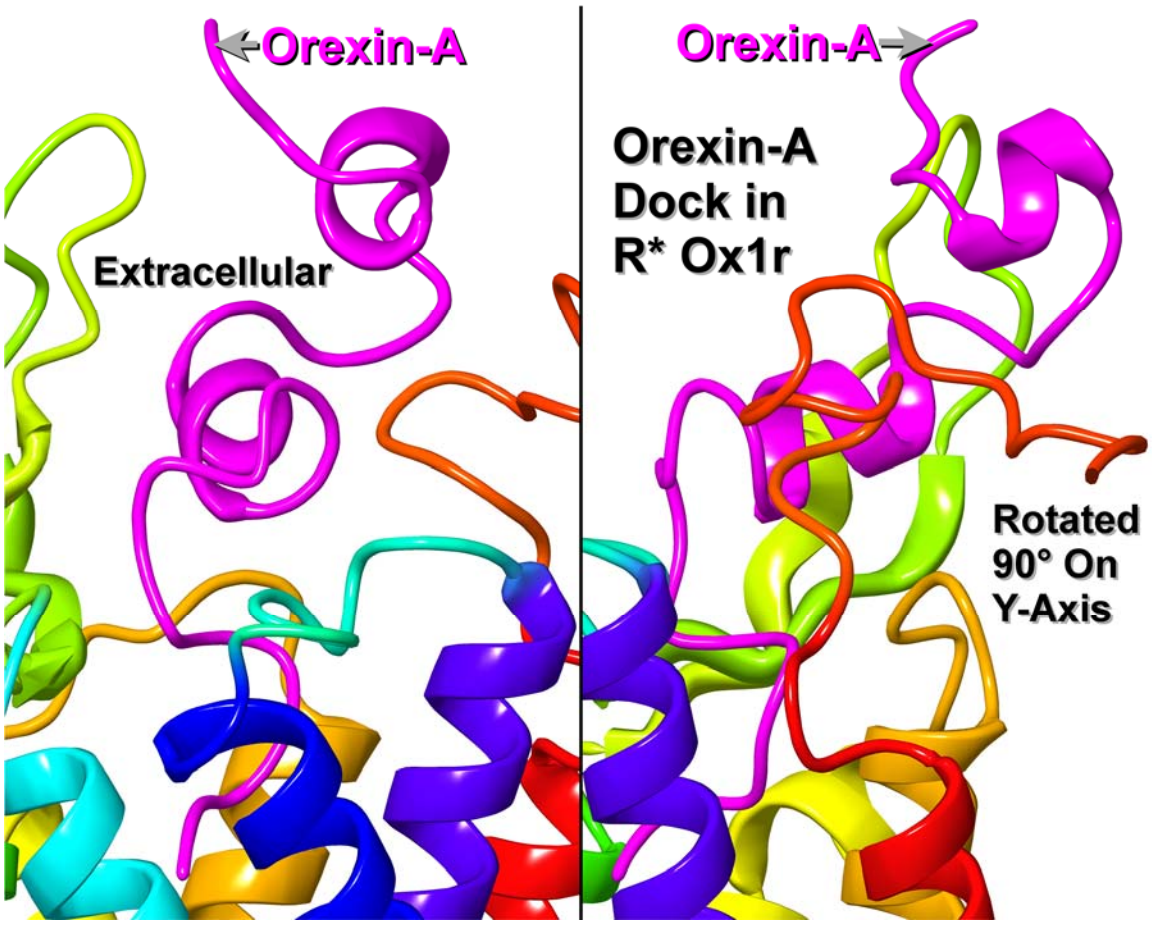

Figure 80. Overall Dock of Orexin-A in the R* Model.[3,4,7,22,24]

A closer view of orexin-A's interactions with the ox1r (showing the orexin-A N-terminus and hydrophilic region) is shown in Figures 81 and 82.[3,4,7,22,24]

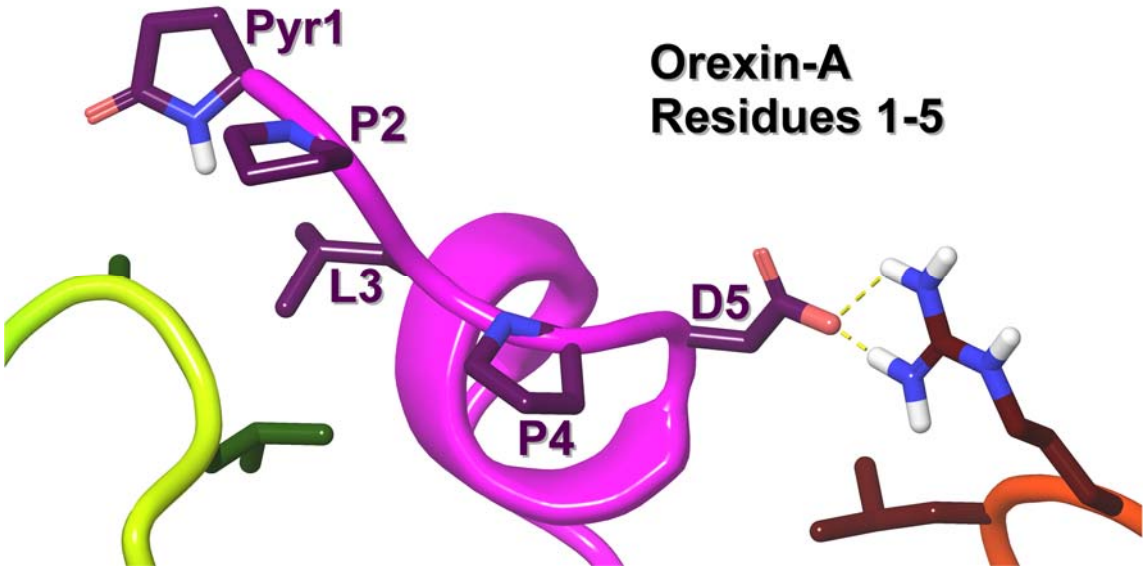

Figure 81. Dock of Orexin-A in the R* Model, as Seen from Orexin-A Residues 1-5 and the Ox1r N-terminus and Its EC2 Loop.[3,4,7,22,24]

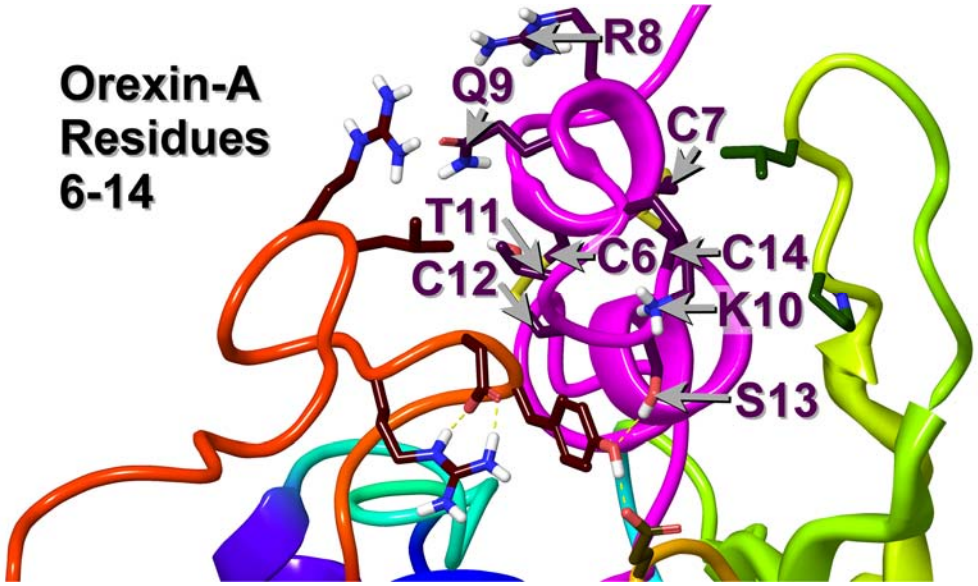

Figure 82. Dock of Orexin-A in the R* Model, as Seen from Orexin-A Residues 6-14 and the Ox1r N-terminus and EC1 and EC2 Loops.[3,4,7,22,24]

A closer view of orexin-A's interactions with the ox1r (showing the orexin-A central helix and first half of the orexin-A C-terminus) is shown in Figures 83 and 84.[3,4,7,22,24]

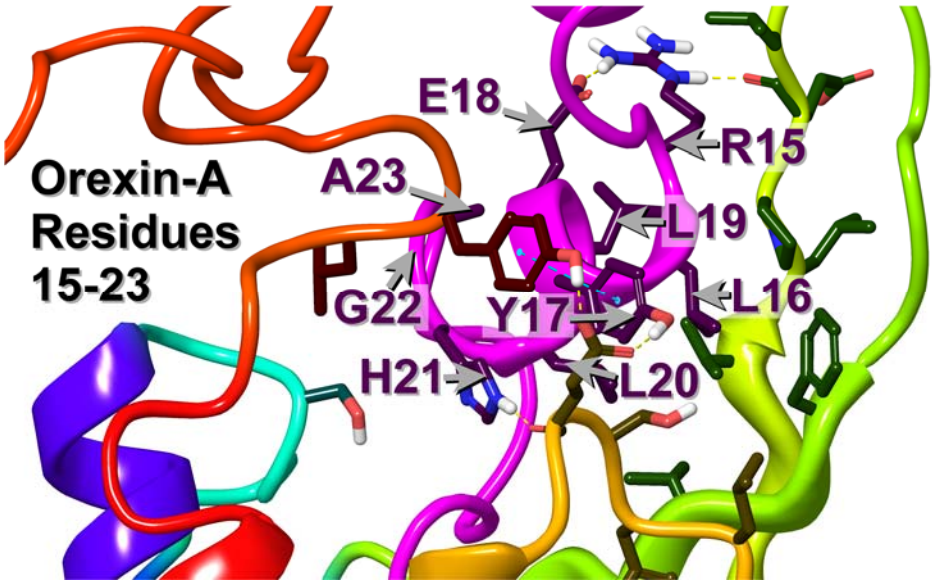

Figure 83. Dock of Orexin-A in the R* Model, as Seen from Orexin-A Residues 15-23 and the Ox1r EC2 Loop.[3,4,7,22,24]

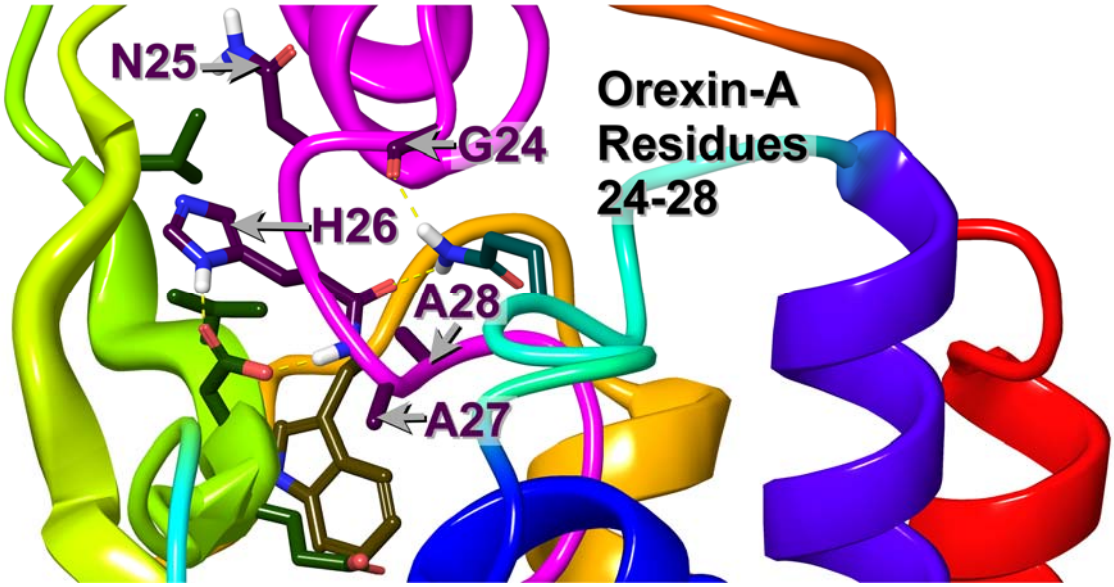

Figure 84. Dock of Orexin-A in the R* Model, as Seen from Orexin-A Residues 24-28 and the Ox1r Transmembrane Region Opening.[3,4,7,22,24]

A closer view of orexin-A's interactions with the ox1r (showing the second half of the orexin-A C-terminus, which is where the most important interactions with the ox1r would be) is shown in Figure 85.[3,4,7,22,24]

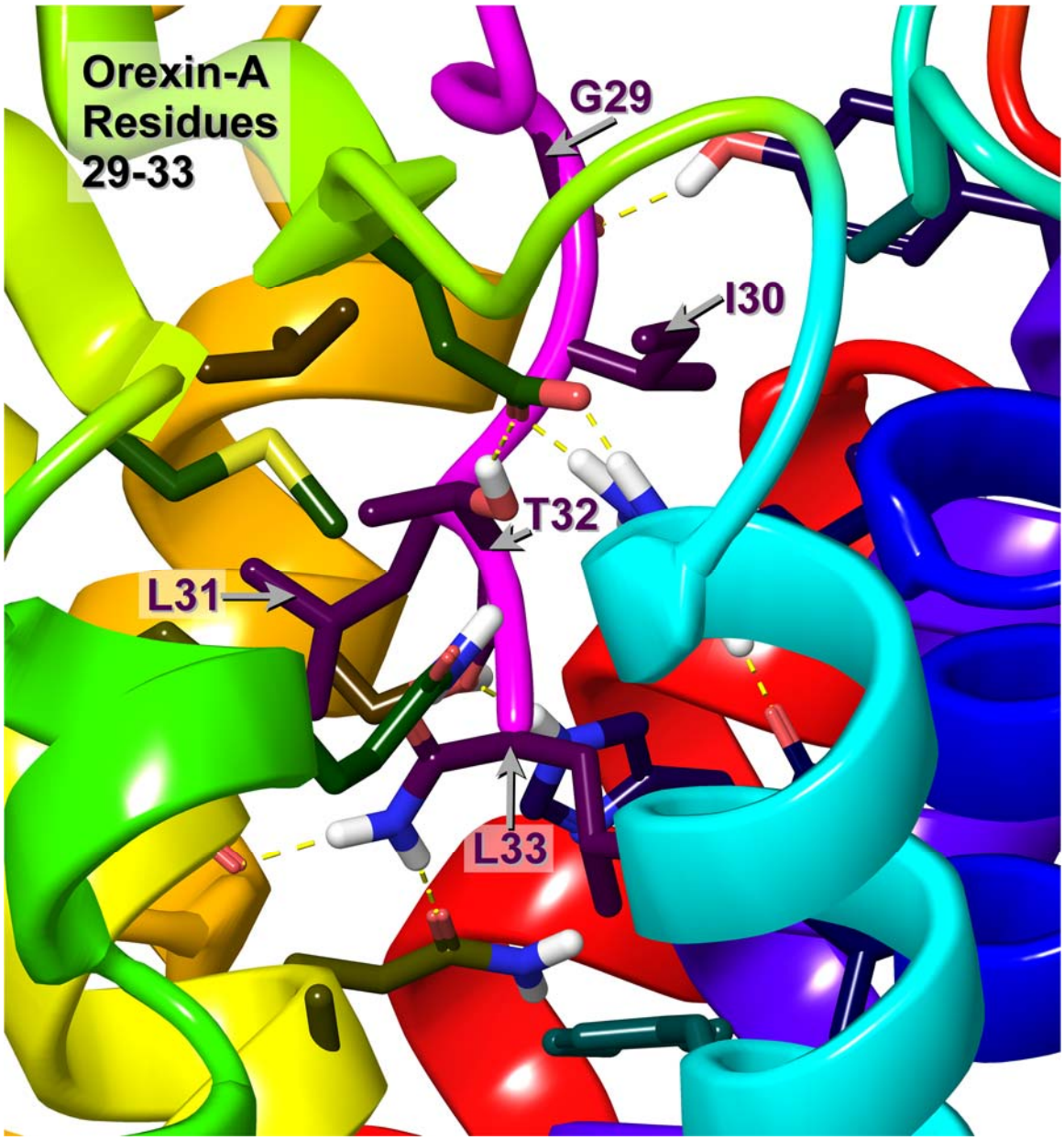

Figure 85. Dock of Orexin-A in the R* Model, as Seen from Orexin-A Residues 29-33 and the Ox1r Transmembrane Region.[3,4,7,22,24]

The first of these interactions between orexin-A and the ox1r is a small sampling of interactions between the N-termini of both orexin-A and the ox1r, with orexin-A's Y17 interacting by a π-π flat stack with ox1r's Y39 and donating a hydrogen bond to ox1r's E110 in the EC1 loop, while orexin-A's S13 donates a hydrogen bond to ox1r's Y39 and orexin-A's H21 donates another hydrogen bond to ox1r's E110's backbone oxygen, as shown in Figure 86.[3,4,7,22,24]

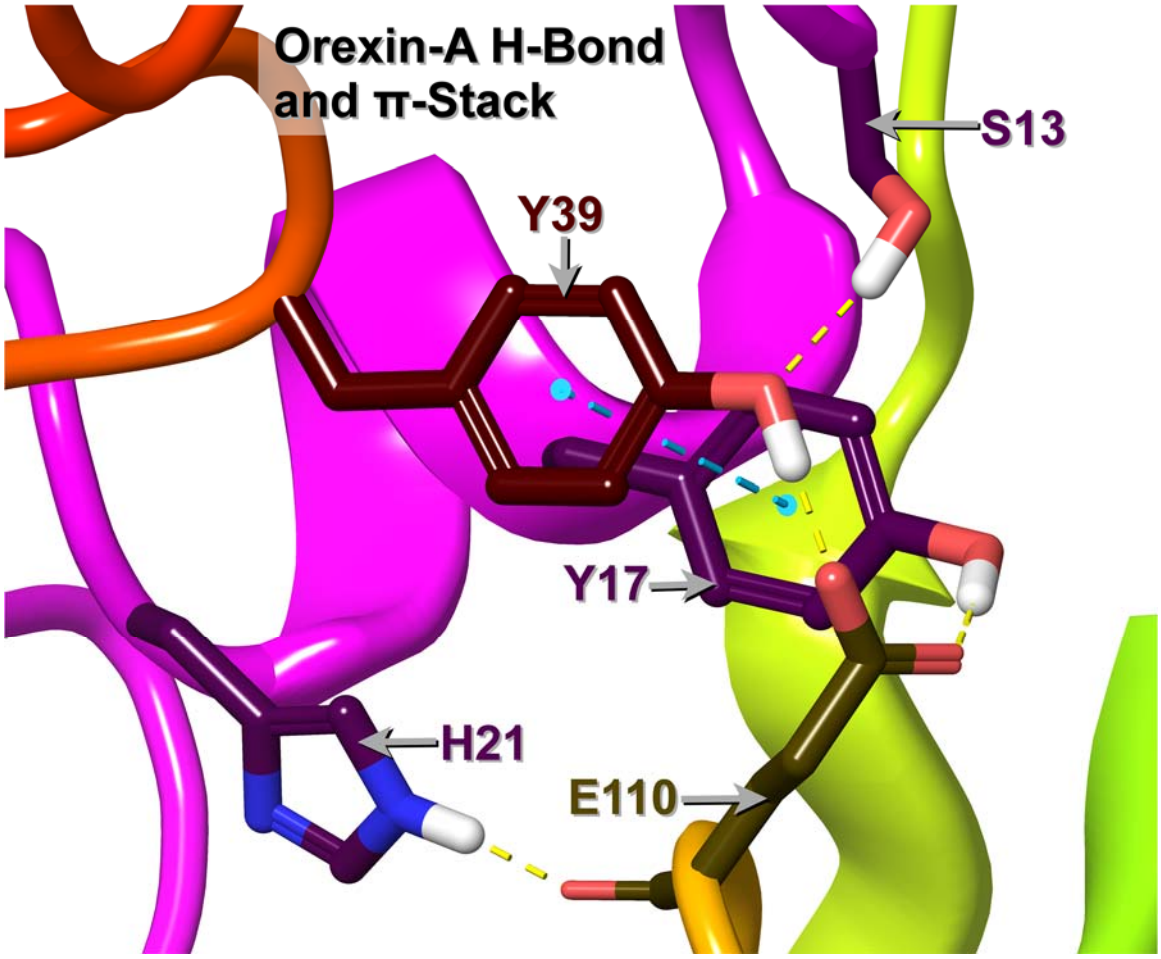

Figure 86. Orexin-A's Y17 Interacts by Means of a π-π Flat Stack with Ox1r's Y39 and Donating a Hydrogen Bond to E110 in the Ox1r's EC1 Loop, While Orexin-A's S13 Donates a Hydrogen Bond to Ox1r's Y39 and Orexin-A's H21 Donates Another Hydrogen Bond to Ox1r's E110's Backbone Oxygen.[3,4,7,22,24]

Another sampling is orexin-A's D5 interacting with the ox1r N-terminus by accepting a hydrogen bond from R33, as shown in Figure 87.[3,4,7,22,24]

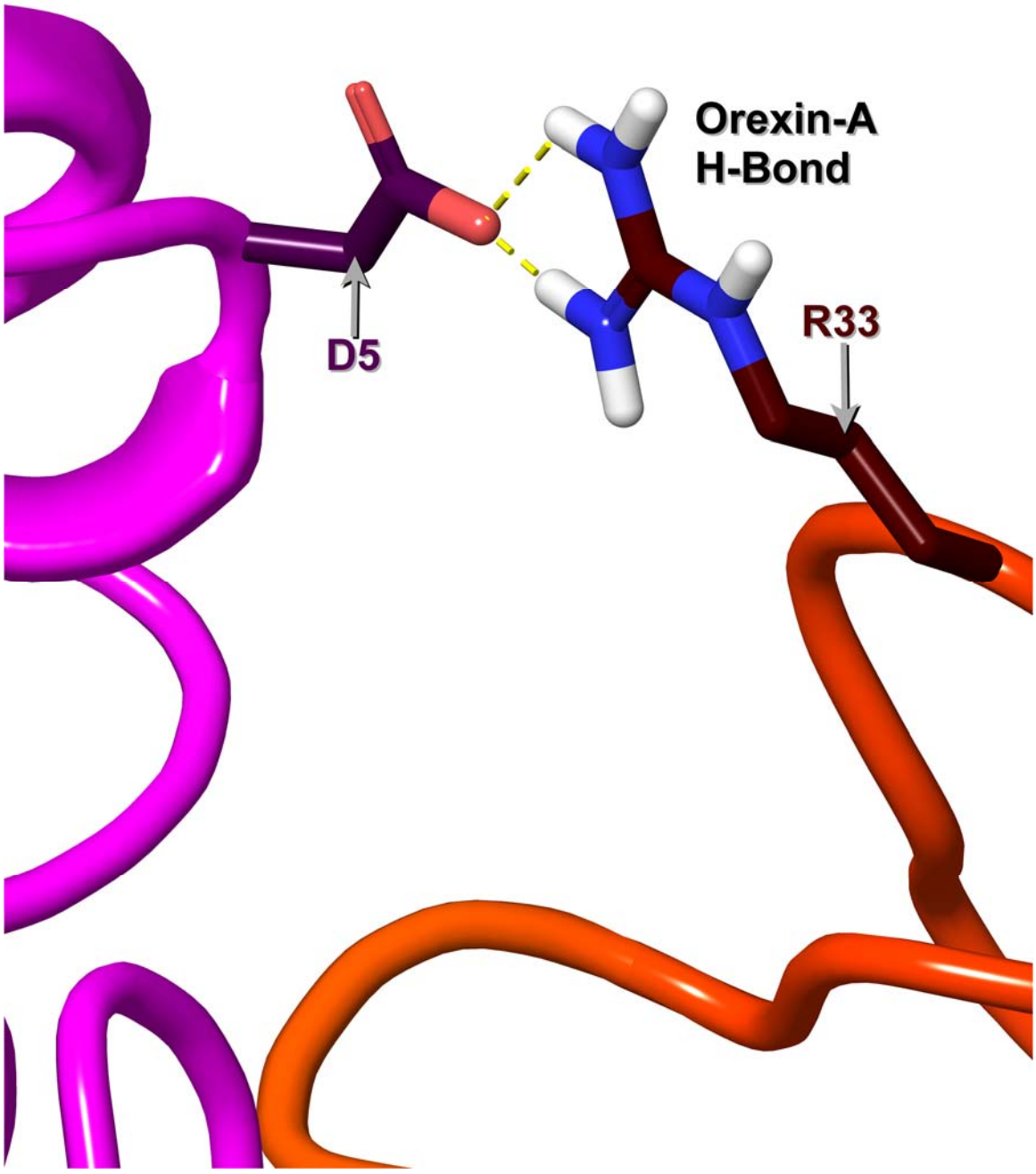

Figure 87. Orexin-A's D5 Interacts By Accepting a Hydrogen Bond from R33 of the Ox1r R* Model.[3,4,7,22,24]

Another sampling is orexin-A's R15 interacting with the ox1r EC2 loop by donating a hydrogen bond to E45.39's backbone oxygen, as shown in Figure 88.[3,4,7,22,24]

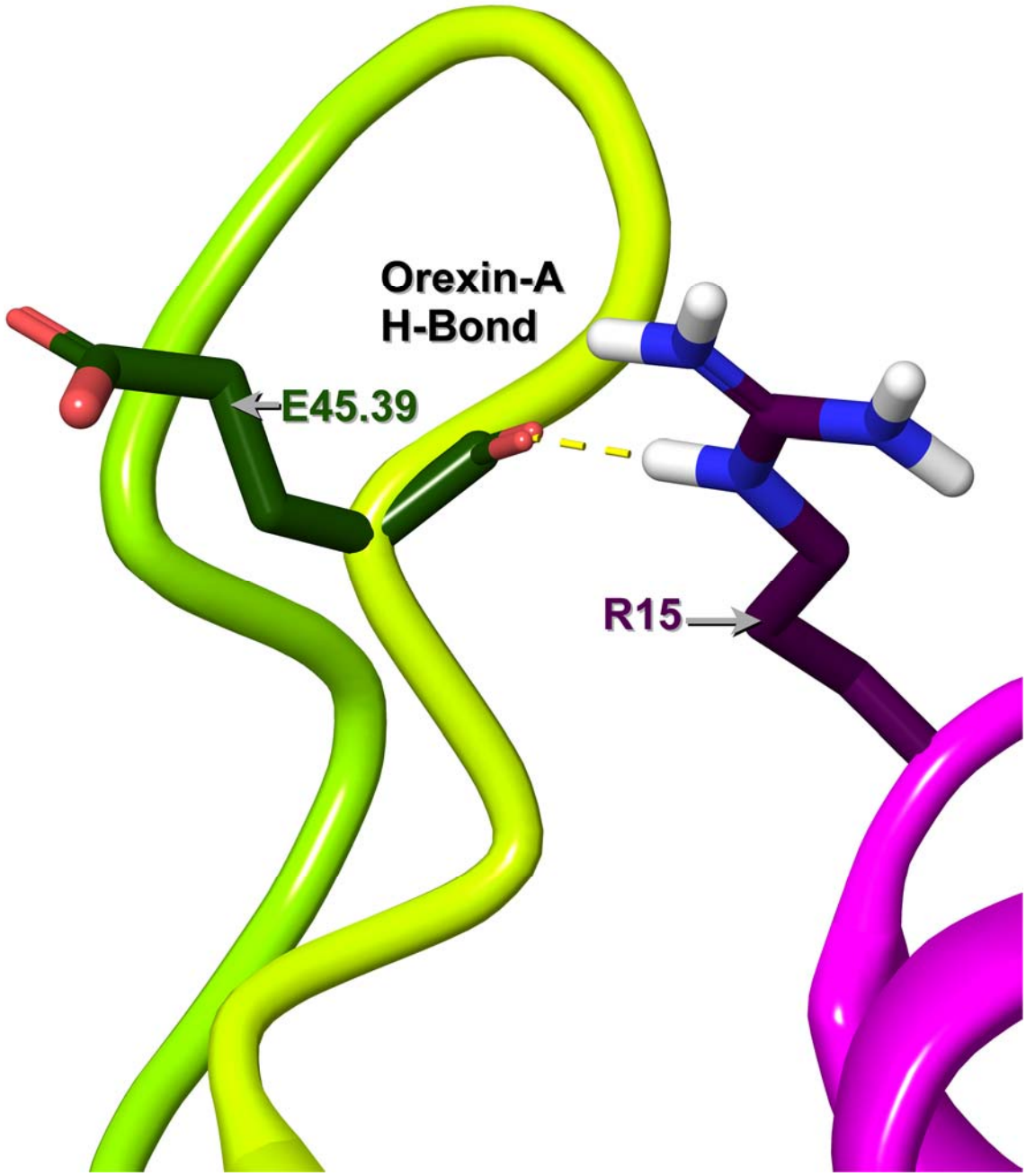

Figure 88. Orexin-A's R15 Interacts By Donating a Hydrogen Bond to E45.39's Backbone Oxygen of the Ox1r R* Model.[3,4,7,22,24]

Orexin-A's L16 interacts with the ox1r EC1 and EC2 loops by heavy van der Waals contacts with S111 in the EC1 loop, V45.36, P45.38, and F45.47, as shown in Figure 89.[3,4,7,22,24]

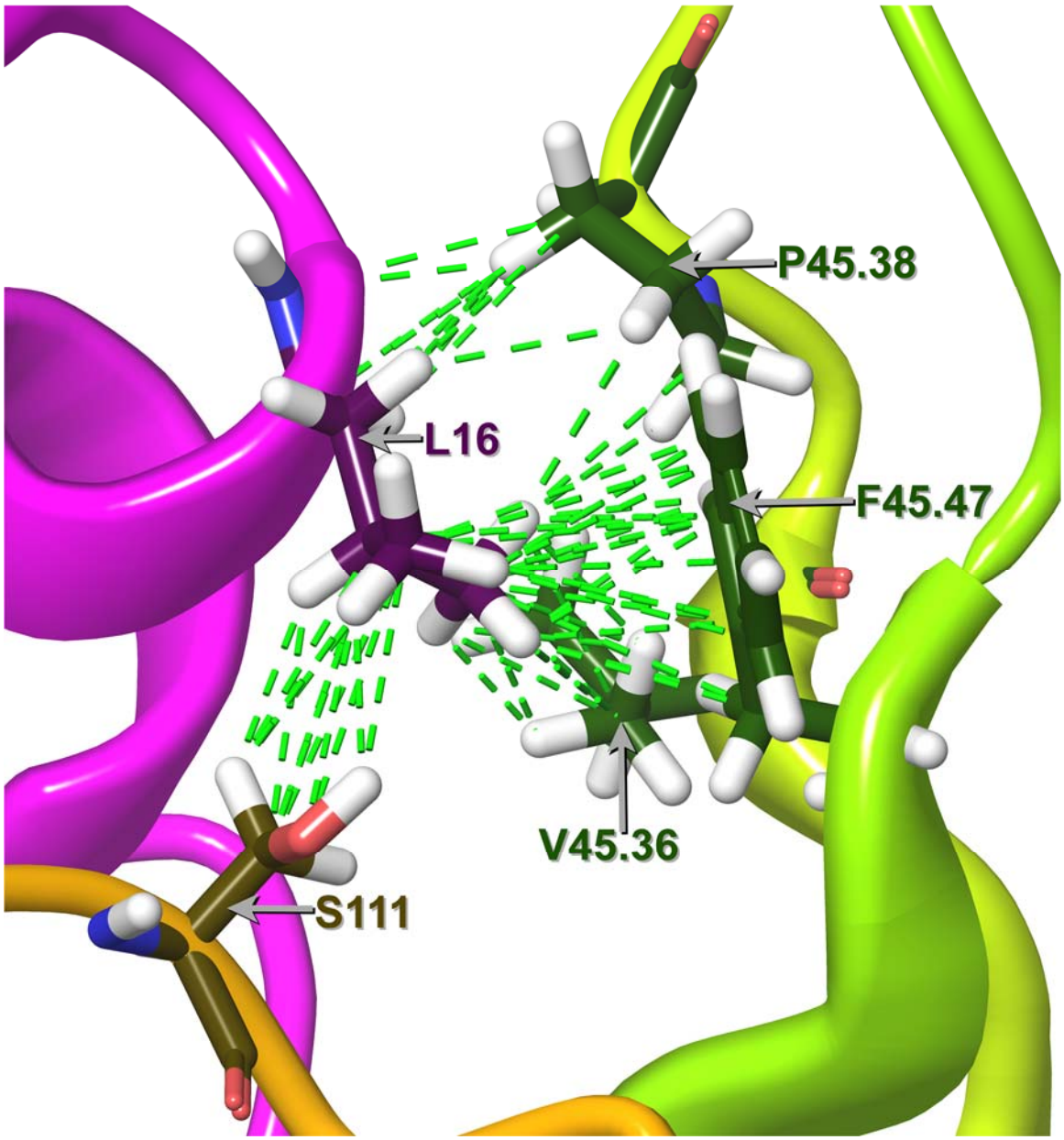

Figure 89. Orexin-A's L16 Interacts By van der Waals Contacts with S111 (EC1), V45.36, P45.38, and F45.47 of the Ox1r R* Model.[3,4,7,22,24]

Next is orexin-A's L19 interacting with the ox1r EC2 loop by light van der Waals contacts with P45.38, and by heavy van der Waals contacts with V45.36 and L45.37, as shown in Figure 90.[3,4,7,22,24]

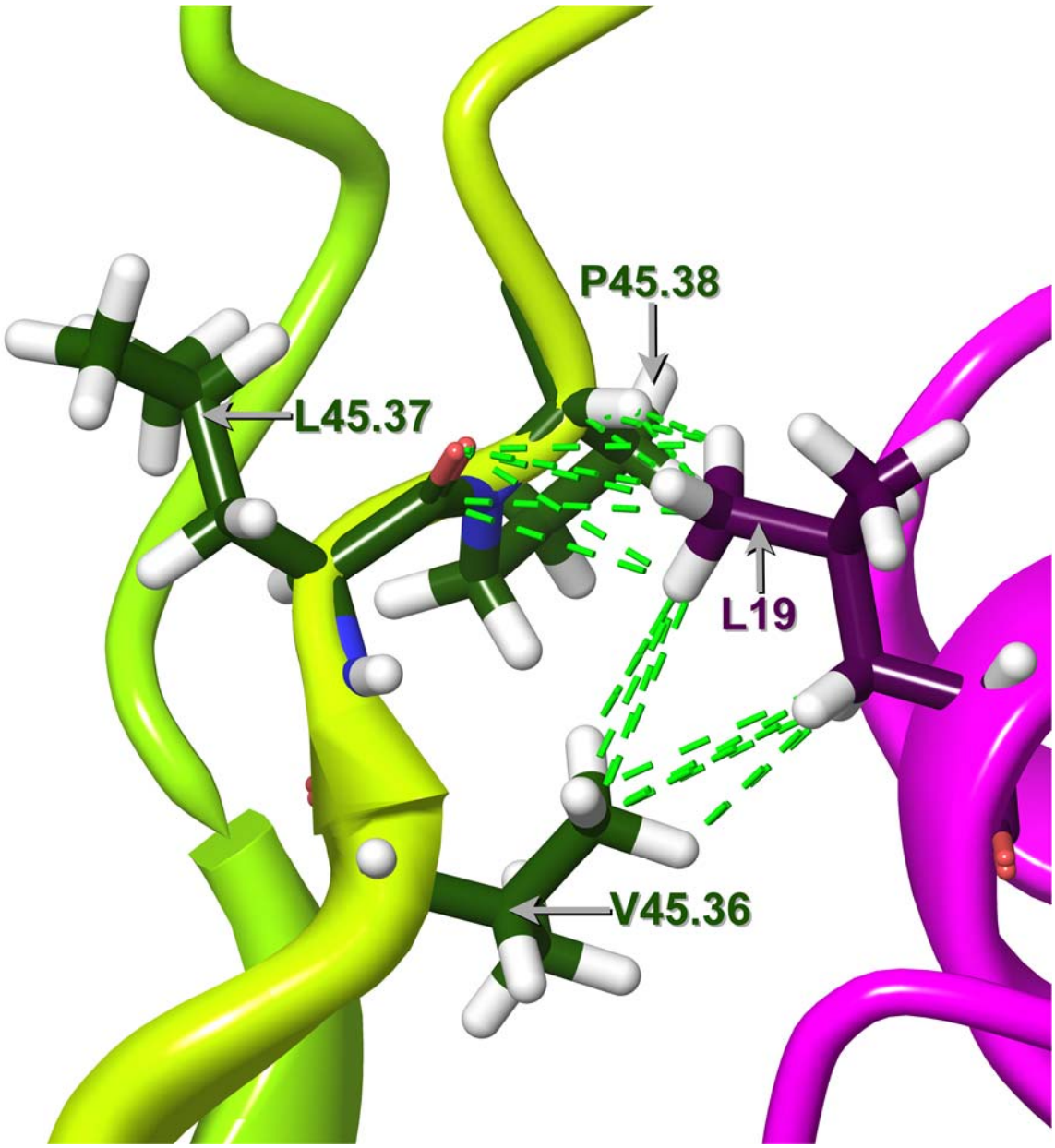

Figure 90. Orexin-A's L19 Interacts By van der Waals Contacts with V45.36, L45.37, and P45.38 of the Ox1r R* Model.[3,4,7,22,24]

Afterward is orexin-A's L20 interacting with the ox1r EC1 and EC2 loops by light van der Waals contacts with W112 in the EC1 loop, and by heavy van der Waals contacts with S111 in the EC1 loop, V45.36, and V45.49, as shown in Figure 91.[3,4,7,22,24]

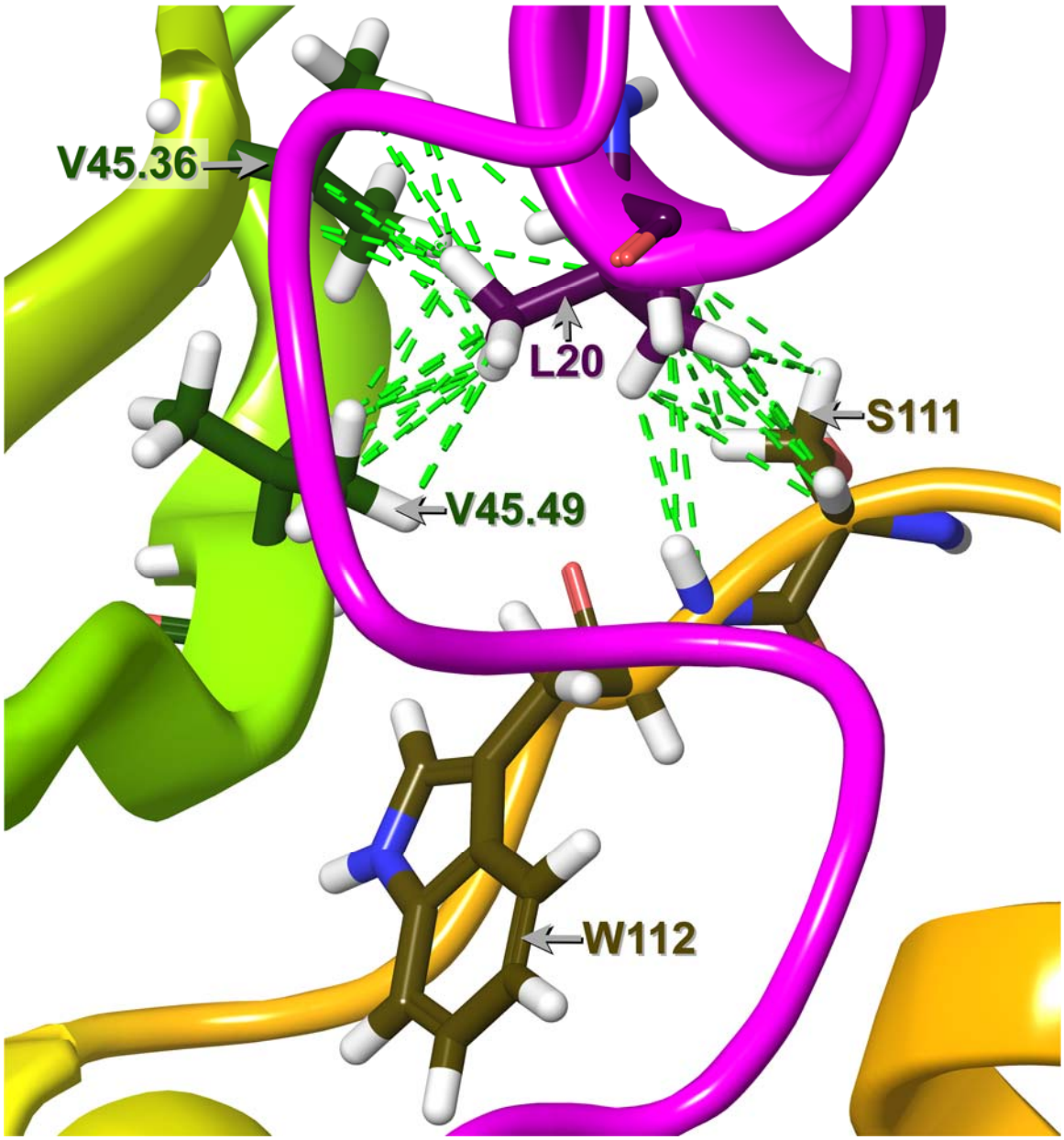

Figure 91. Orexin-A's L20 Interacts By van der Waals Contacts with S111 (EC1), W112 (EC1), V45.36, and V45.49 of the Ox1r R* Model.[3,4,7,22,24]

One major interaction is orexin-A's H26, which interacts with the ox1r EC2 and EC3 loops by donating a hydrogen bond to D45.51, as well as using its backbone to accept another from Q329 in the EC3 loop, as shown in Figure 92.[3,4,7,22,24]

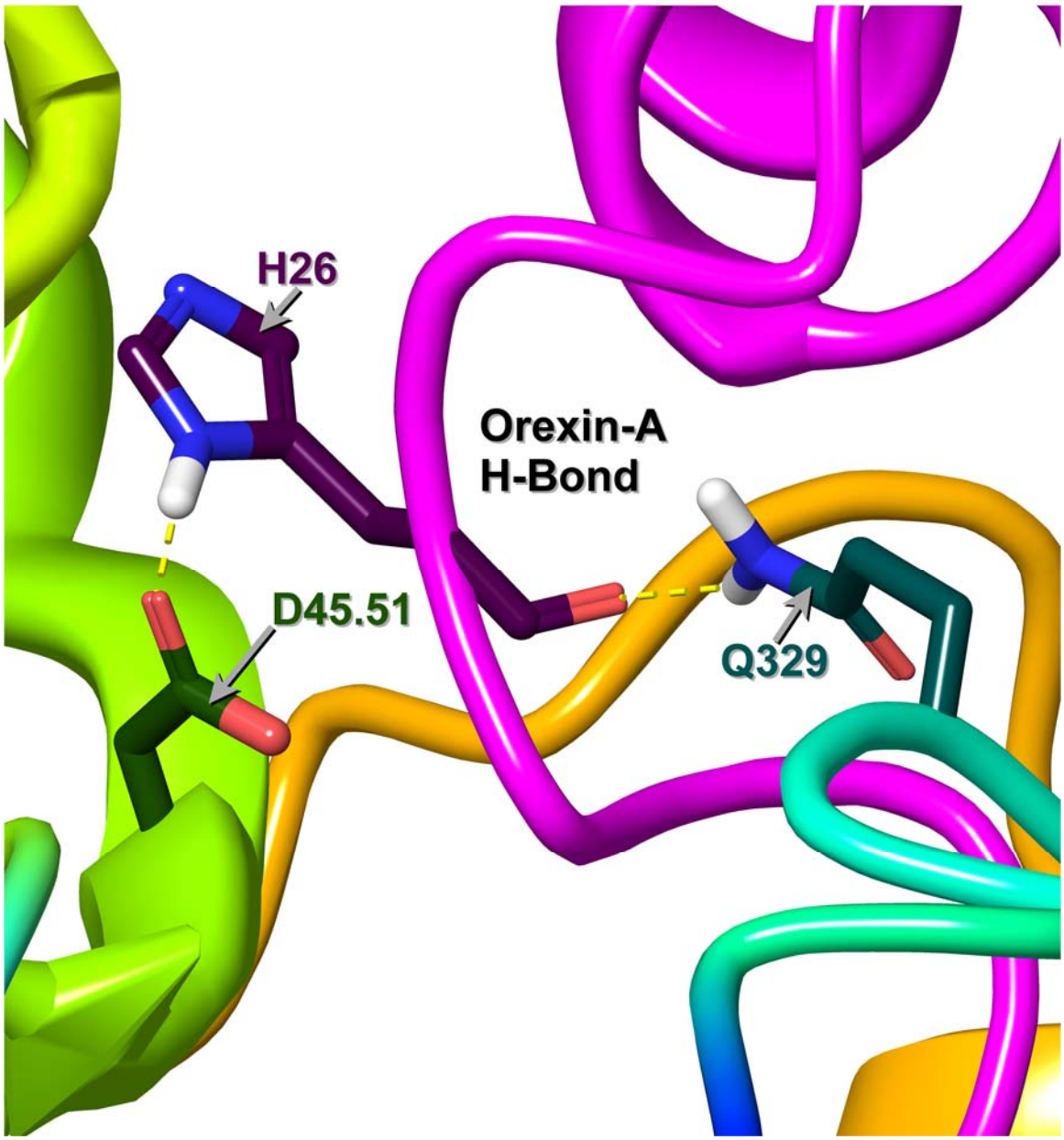

Figure 92. Orexin-A's H26 Interacts By Donating a Hydrogen Bond to D45.51, and Using Its Backbone to Accept Another from Q329 (EC3), of the Ox1r R* Model.[3,4,7,22,24]

Orexin-A's H26 also interacts with the ox1r EC2 and EC3 loops by light van der Waals contacts with V45.36, C45.50, and Q329 in the EC3 loop, and by heavy van der Waals contacts with V45.49 and D45.51, as shown in Figure 93.[3,4,7,22,24]

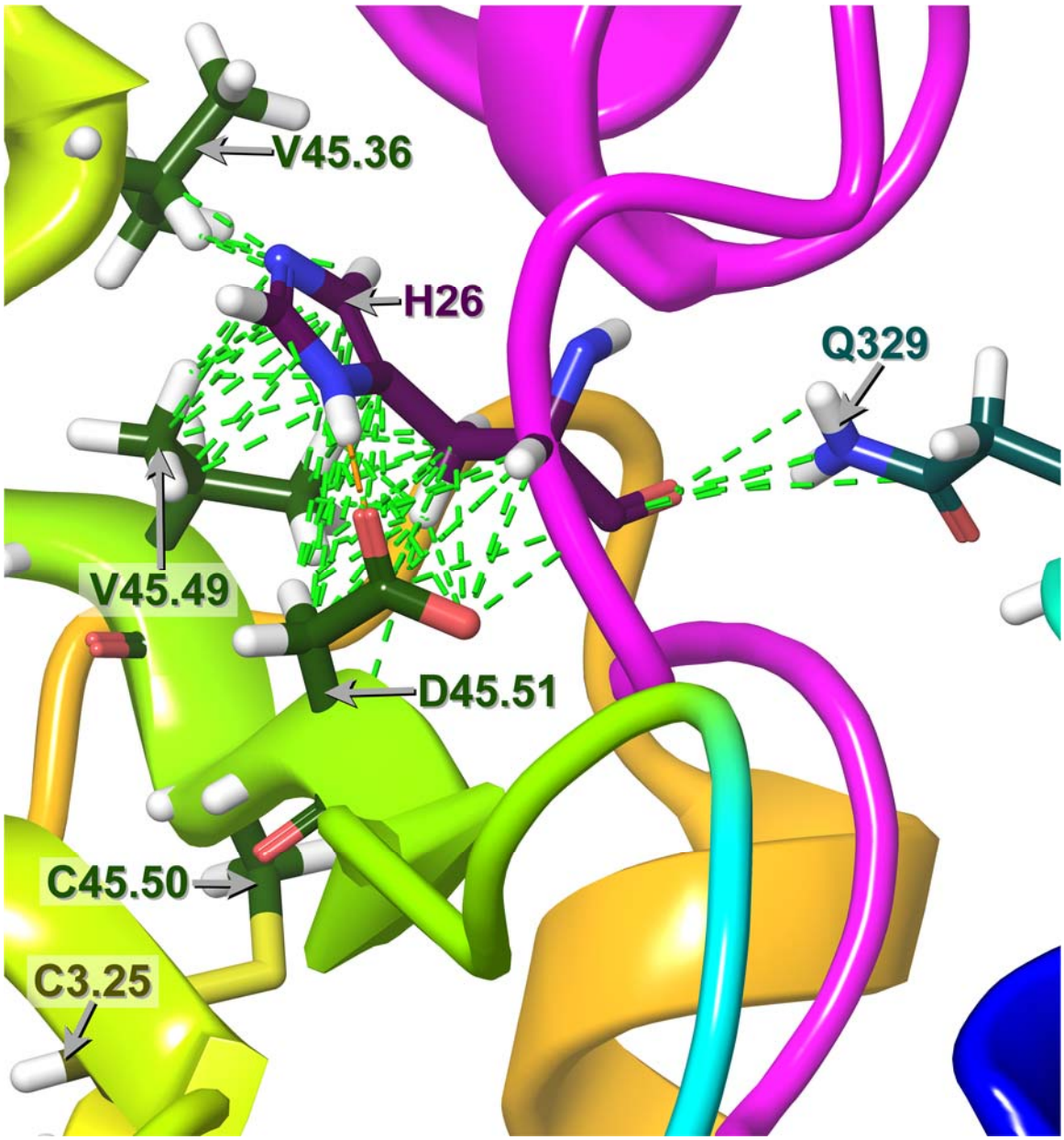

Figure 93. Orexin-A's H26 Interacts By van der Waals Contacts with V45.36, V45.49, C45.50, D45.51, and Q329 (EC3) of the Ox1r R* Model.[3,4,7,22,24]

Following H26 is orexin-A's A27, which interacts with the ox1r EC2 loop by using its backbone amide to donate a hydrogen bond to D45.51, as shown in Figure 94.[3,4,7,22,24]

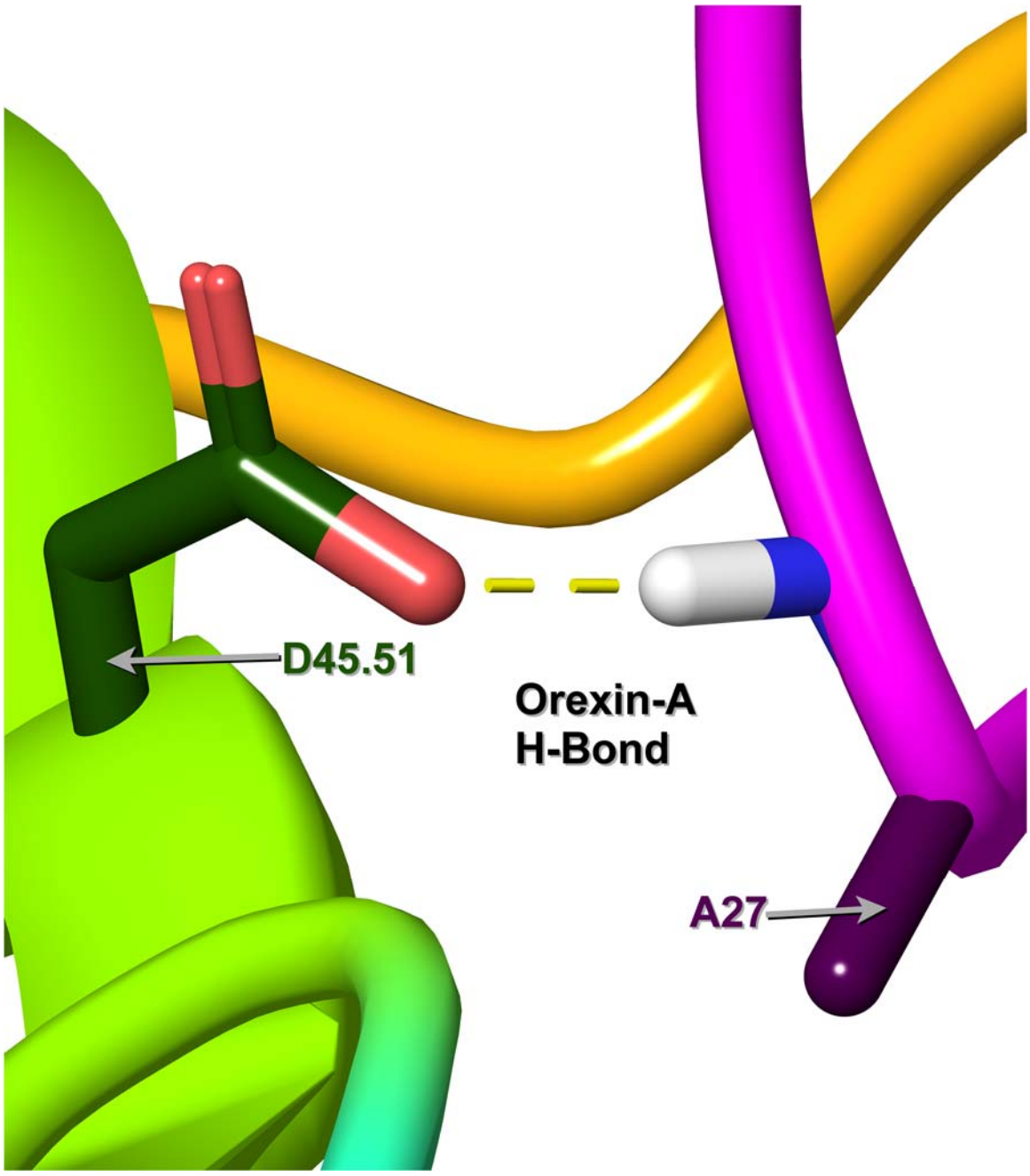

Figure 94. Orexin-A's A27 Interacts By Using Its Backbone Amide to Donate a Hydrogen Bond to D45.51 of the Ox1r R* Model.[3,4,7,22,24]

Following H26 is orexin-A's A27, which interacts with the ox1r EC2 loop by light van der Waals contacts with C45.50, and by heavy van der Waals contacts with D45.51 and E45.52, as shown in Figure 95.[3,4,7,22,24]

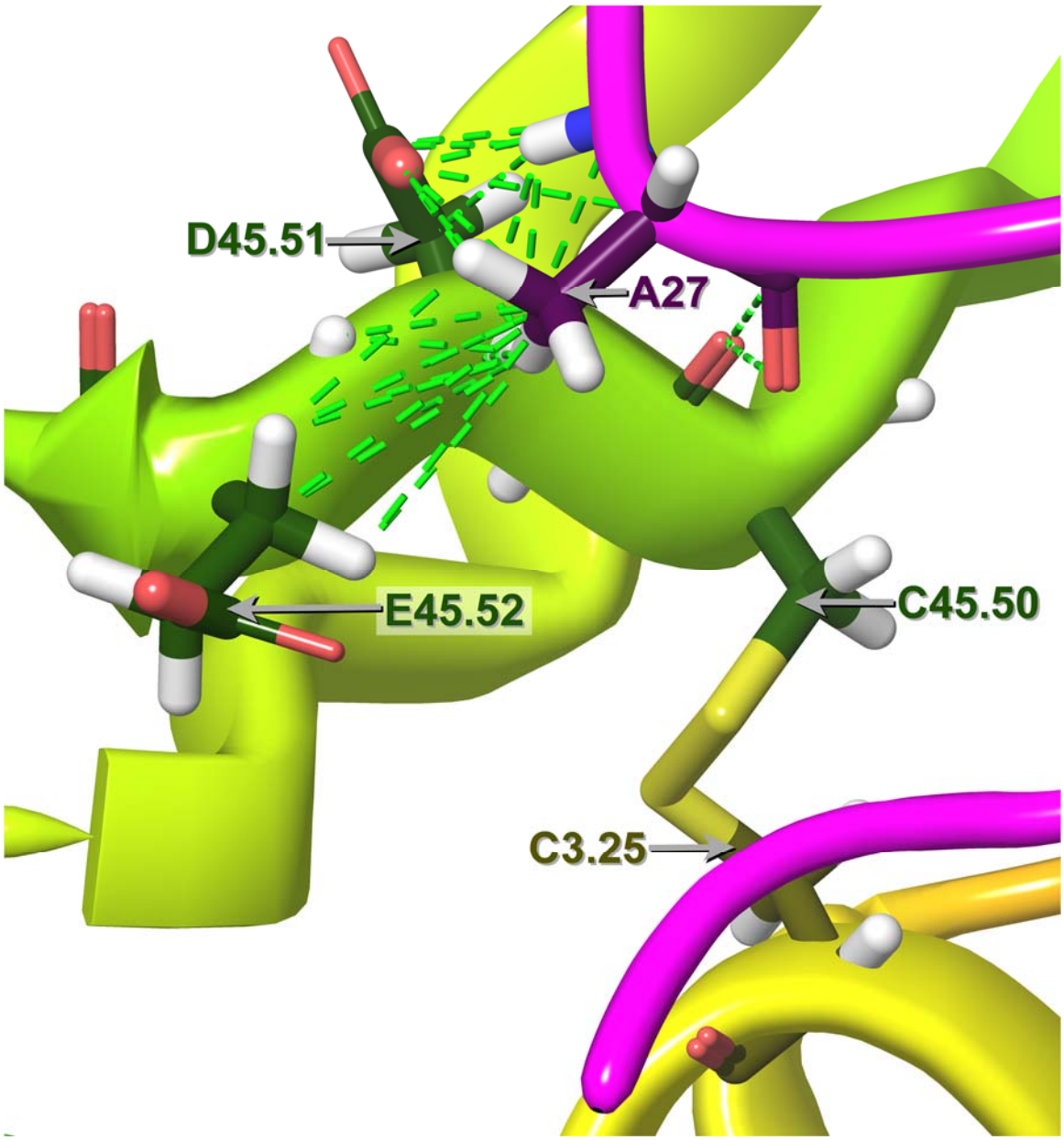

Figure 95. Orexin-A's A27 Interacts By van der Waals Contacts with C45.50, D45.51, and E45.52 of the Ox1r R* Model.[3,4,7,22,24]

Subsequent is orexin-A's A28 interacting with the ox1r EC1 and EC2 loops by light van der Waals contacts with W112 in the EC1 loop, V45.49, and C45.50, as shown in Figure 96.[3,4,7,22,24]

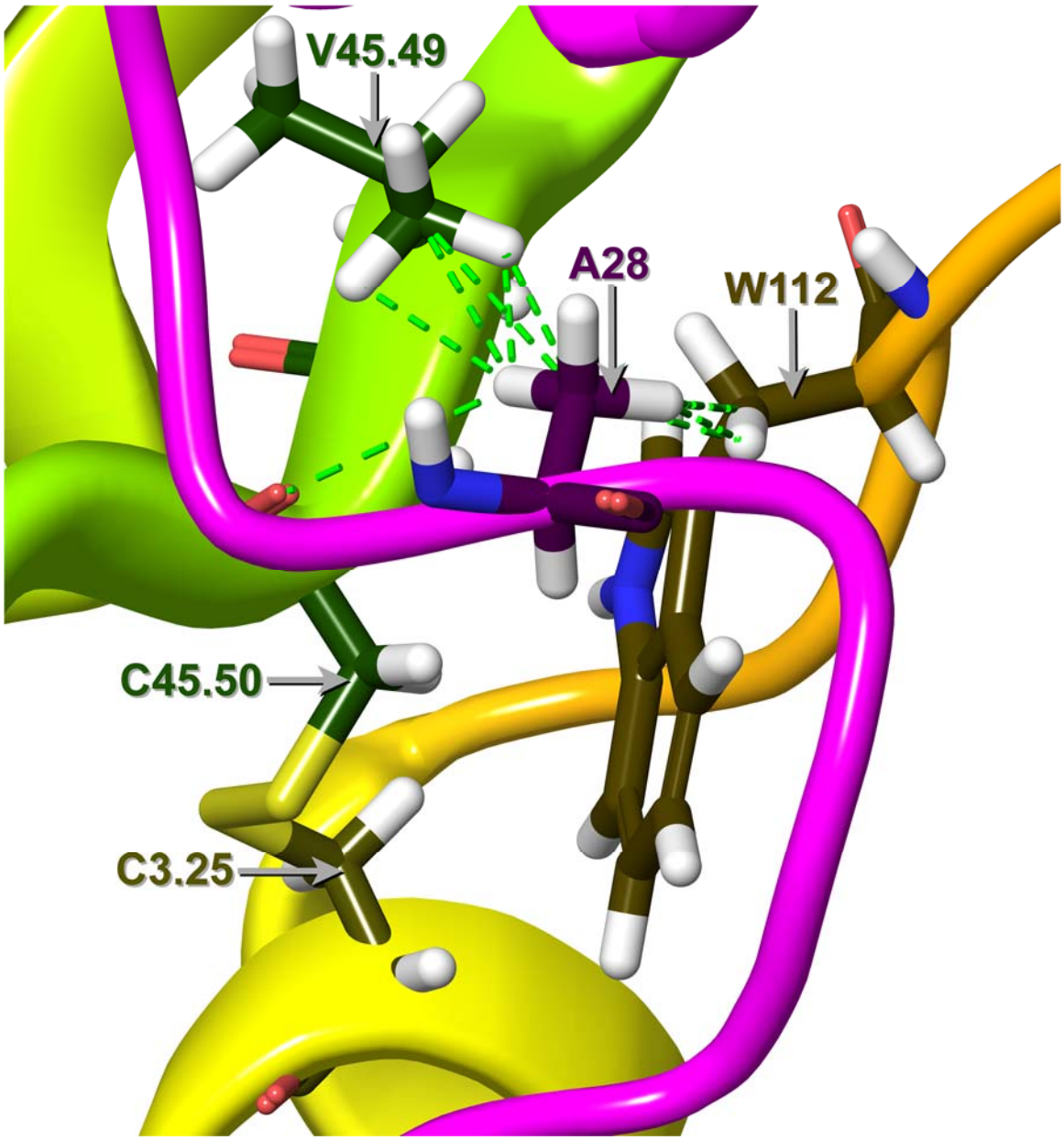

Figure 96. Orexin-A's A28 Interacts By van der Waals Contacts with W112 (EC1), V45.49, and C45.50 of the Ox1r R* Model.[3,4,7,22,24]

Subsequent is orexin-A's G29 interacting with the ox1r TMH7 by using its backbone to accept a hydrogen bond from Y7.32, as shown in Figure 97.[3,4,7,22,24]

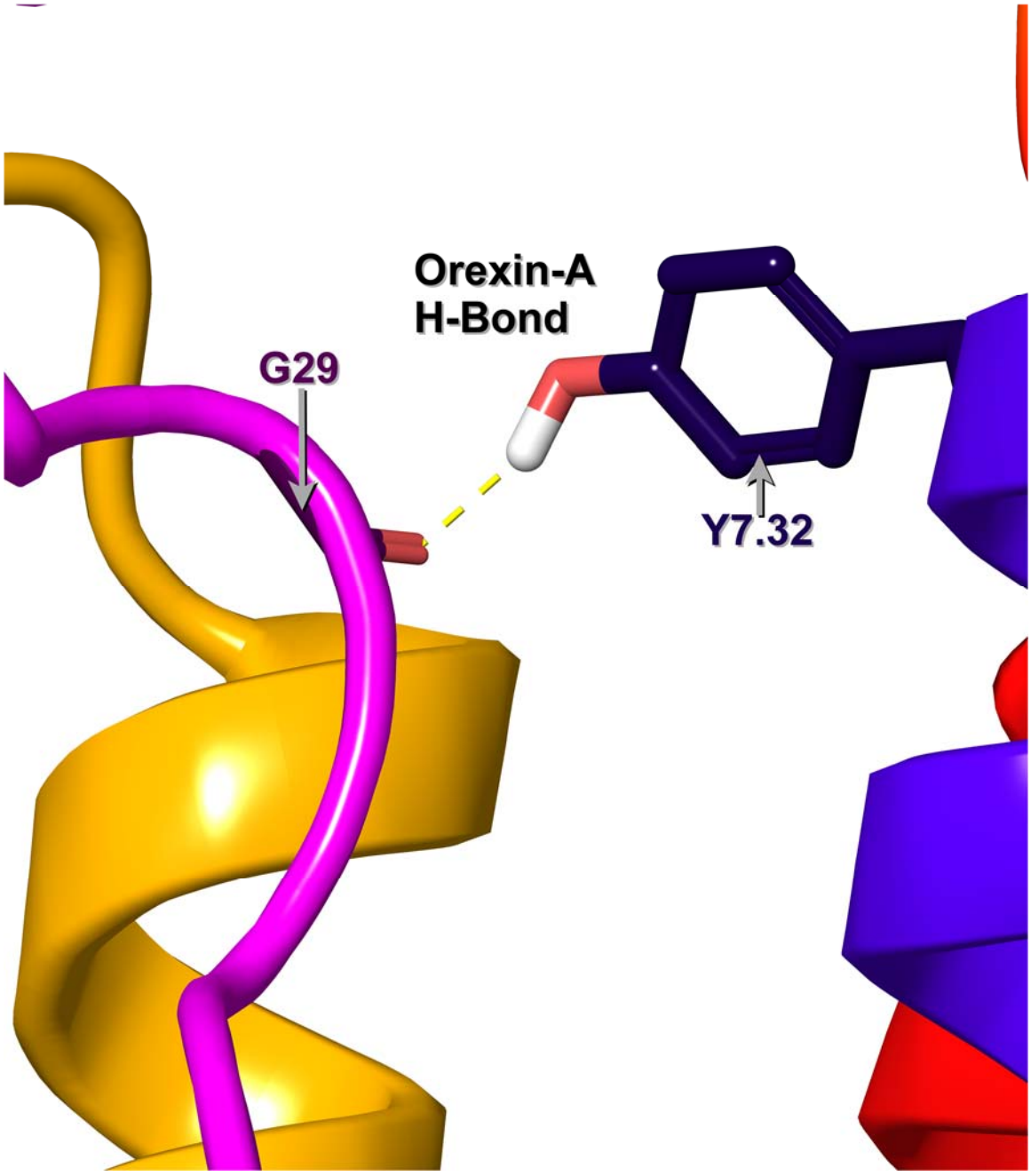

Figure 97. Orexin-A's G29 Interacts By Using Its Backbone to Accept a Hydrogen Bond from Y7.32 of the Ox1r R* Model.[3,4,7,22,24]

Afterward is orexin-A's G29 interacting with the ox1r TM region by light van der Waals contacts with V2.64 and D2.65, and by heavy van der Waals contacts with Y7.32, as shown in Figure 98.[3,4,7,22,24]

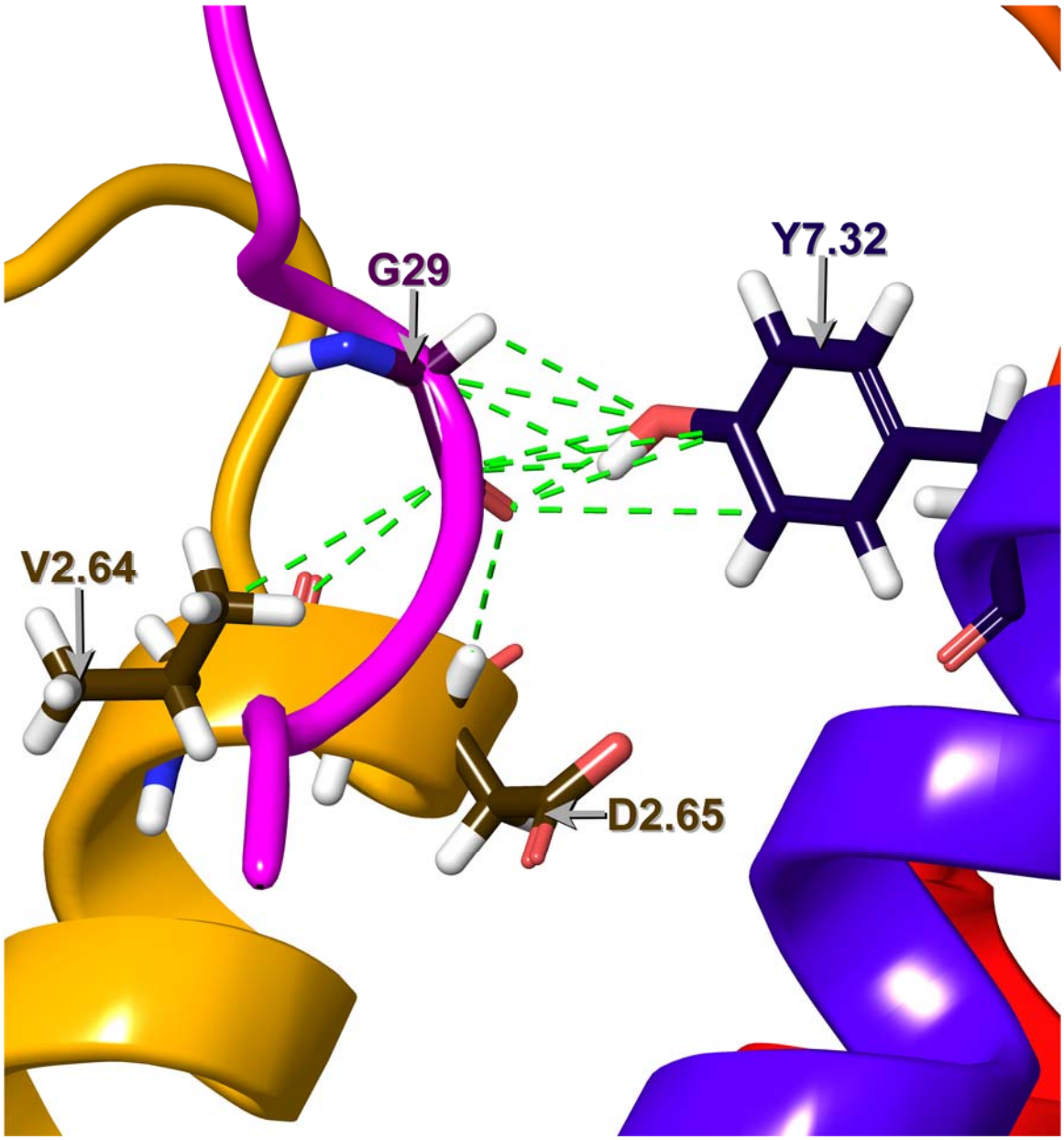

Figure 98. Orexin-A's G29 Interacts By van der Waals Contacts with V2.64, D2.65, and Y7.32 of the Ox1r R* Model.[3,4,7,22,24]

Next is orexin-A's I30 interacting with the ox1r TM region and EC3 loop by light van der Waals contacts with D2.65, and by heavy van der Waals contacts with V2.64, A330 of the EC3 loop, Y7.32, and T7.36, as shown in Figure 99.[3,4,7,22,24]

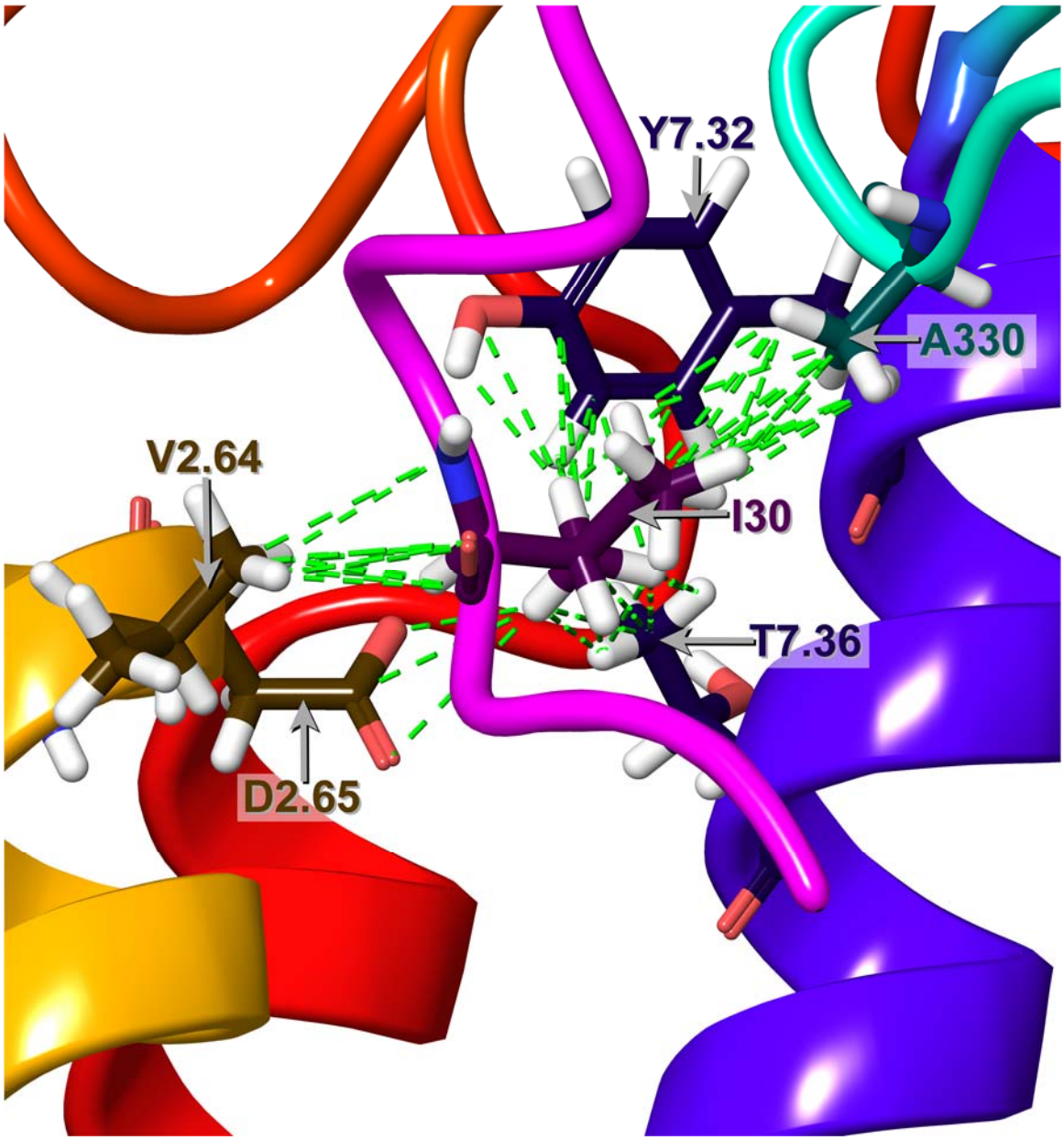

Figure 99. Orexin-A's I30 Interacts By van der Waals Contacts with V2.64, D2.65, A330 (EC3), Y7.32, and T7.36 of the Ox1r R* Model.[3,4,7,22,24]

Afterward is orexin-A's L31 interacting with the ox1r EC1 loop and transmembrane region by light van der Waals contacts with C2.57, V2.64, W112 of the EC1 loop, P3.29, and Y7.43, and by heavy van der Waals contacts with S2.61, I3.28, and H7.39, as shown in Figure 100.[3,4,7,22,24]

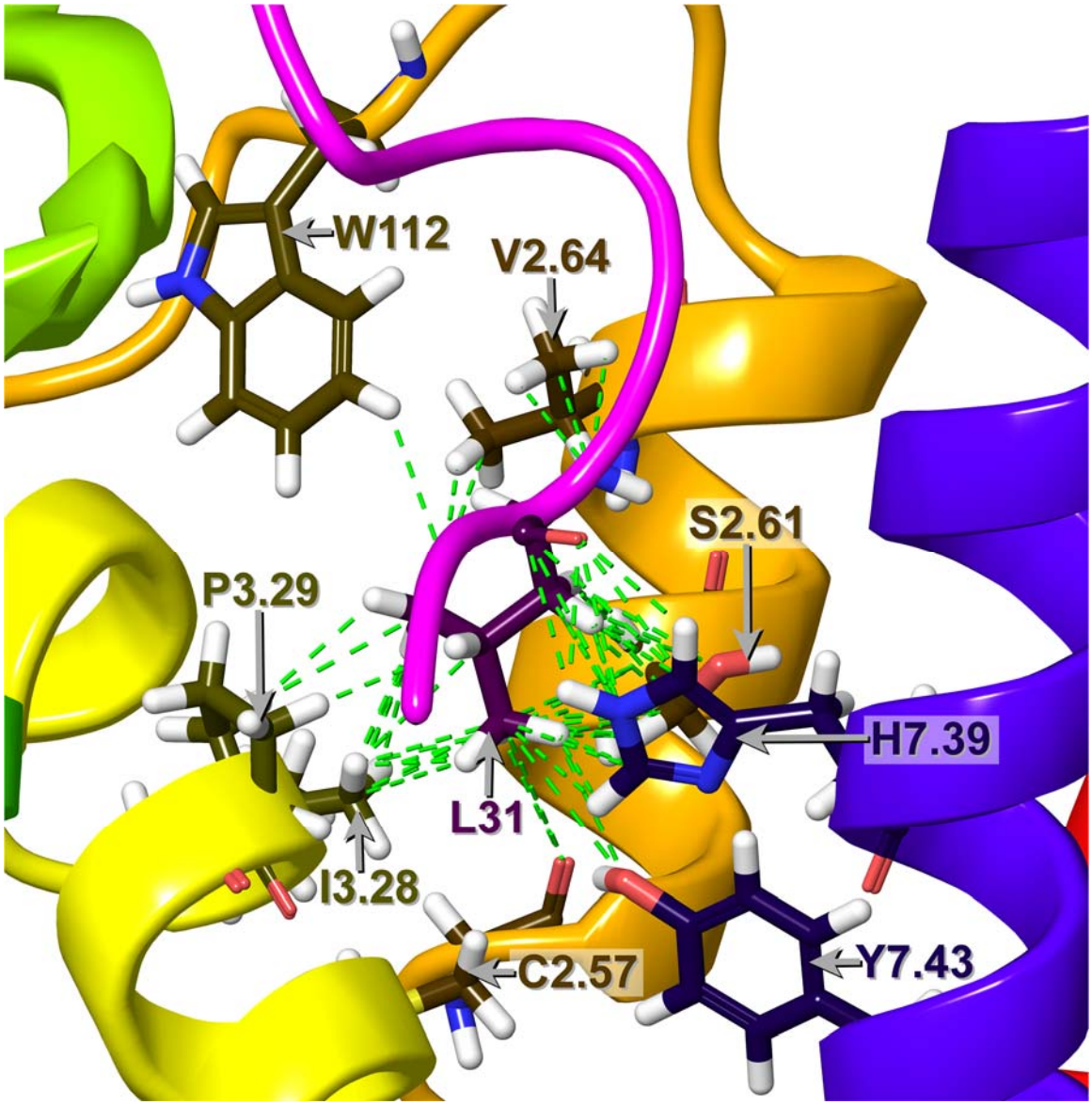

Figure 100. Orexin-A's L31 Interacts By van der Waals Contacts with C2.57, S2.61, V2.64, W112 (EC1), I3.28, P3.29, H7.39, and Y7.43 of the Ox1r R* Model.[3,4,7,22,24]

Following L31 is orexin-A's T32, which interacts with the ox1r transmembrane region by donating a hydrogen bond to E45.52, and using its backbone to accept another hydrogen bond from H7.39, as shown in Figure 101.[3,4,7,9,22,24]

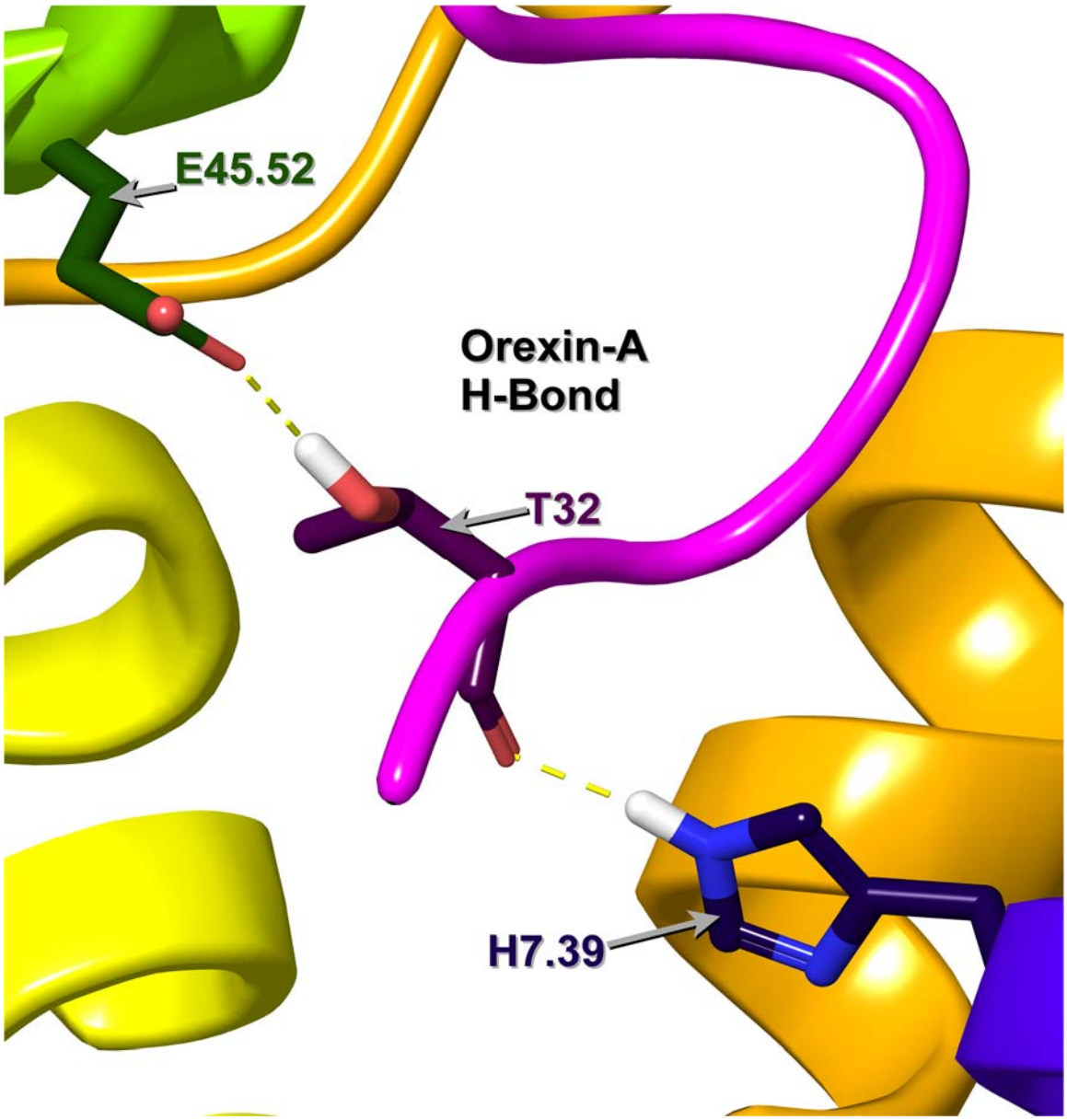

Figure 101. Orexin-A's T32 Interacts By Donating a Hydrogen Bond to E45.52, While Using Its Backbone Oxygen to Accept Another from H7.39, of the Ox1r R* Model.[3,4,7,9,22,24]

Orexin-A's T32 also interacts with the ox1r EC2 loop and TM region by light van der Waals contacts with E45.52 and H7.39, and by heavy van der Waals contacts with P3.29, M45.31, and R6.59, as shown in Figure 102.[3,4,7,9,22,24]

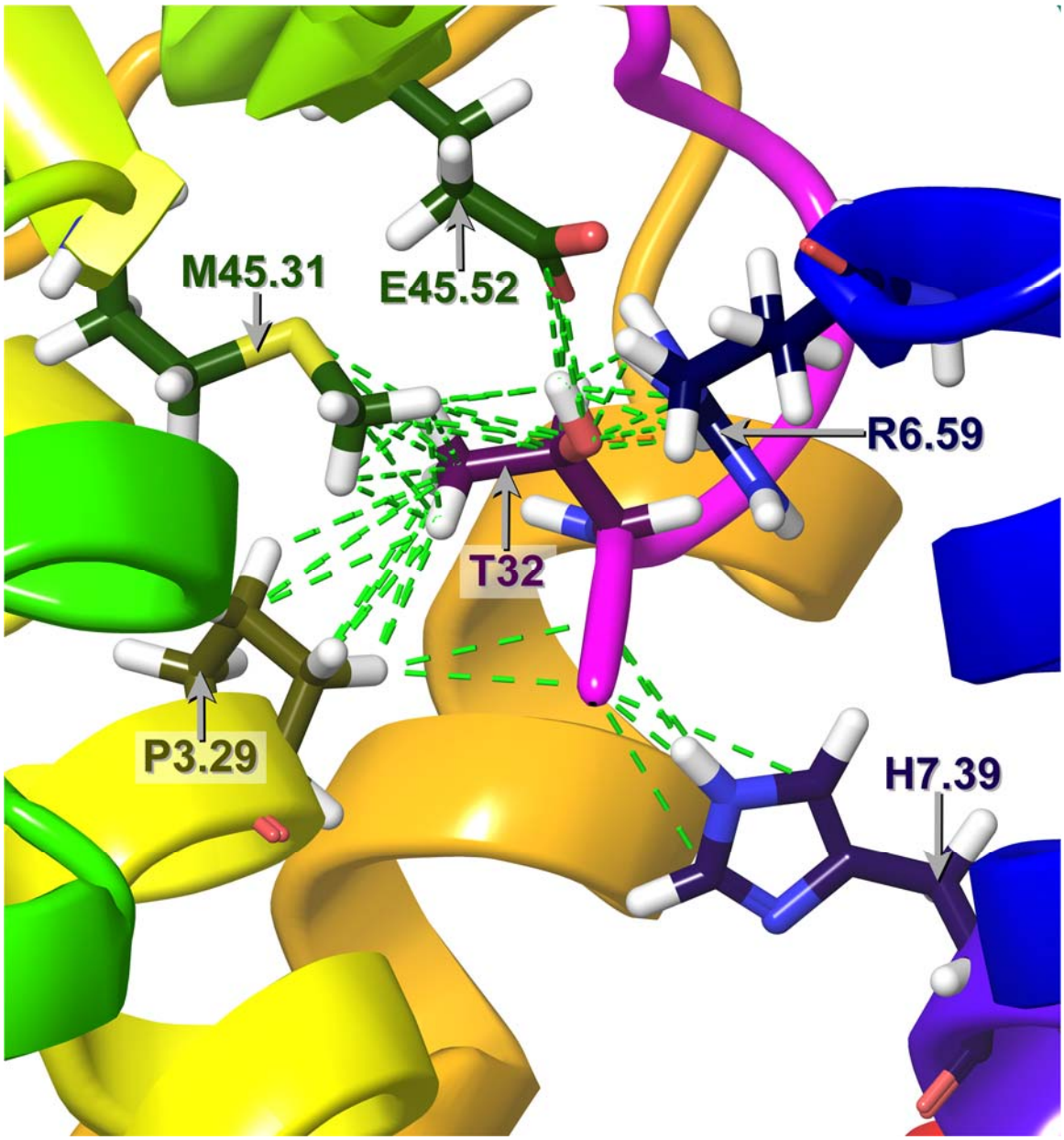

Figure 102. Orexin-A's T32 Interacts By van der Waals Contacts with P3.29, M45.31, E45.52, R6.59, and H7.39 of the Ox1r R* Model.[3,4,7,9,22,24]

Lastly is orexin-A's L33 and its amide cap, which interact with the ox1r transmembrane region by using its backbone oxygen to accept a hydrogen bond from Q4.60, while the amide cap donates a hydrogen bond each to the backbone oxygen of P3.29 and to Q3.32's side chain, as shown in Figure 103.[3,4,7,22,24]

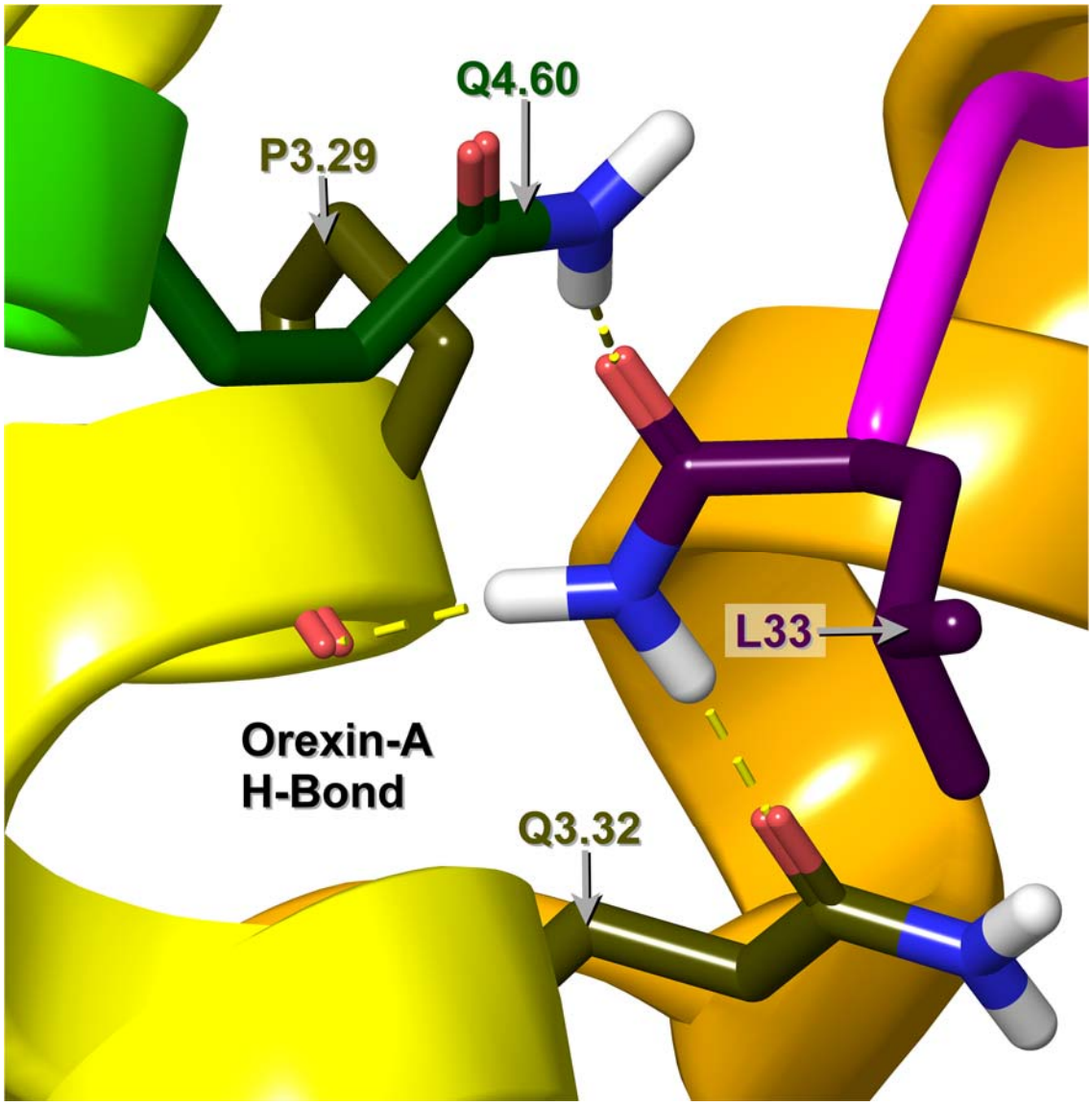

Figure 103. Orexin-A's L33 Interacts By Using Its Backbone Oxygen to Accept a Hydrogen Bond from Q4.60, While Using Its Amide Cap to Donate a Hydrogen Bond Each to the Backbone of P3.29 and to Q3.32's Side Chain of the Ox1r R* Model.[3,4,7,22,24]

Lastly is orexin-A's L33 and its amide cap, which interact with the ox1r EC2 loop and transmembrane region by light van der Waals contacts with M45.31, and by heavy van der Waals contacts with P3.29, Q3.32, A3.33, Q4.60, F5.42, I6.51, N6.55, and R6.59, as shown in Figure 104.[3,4,7,22,24,124]

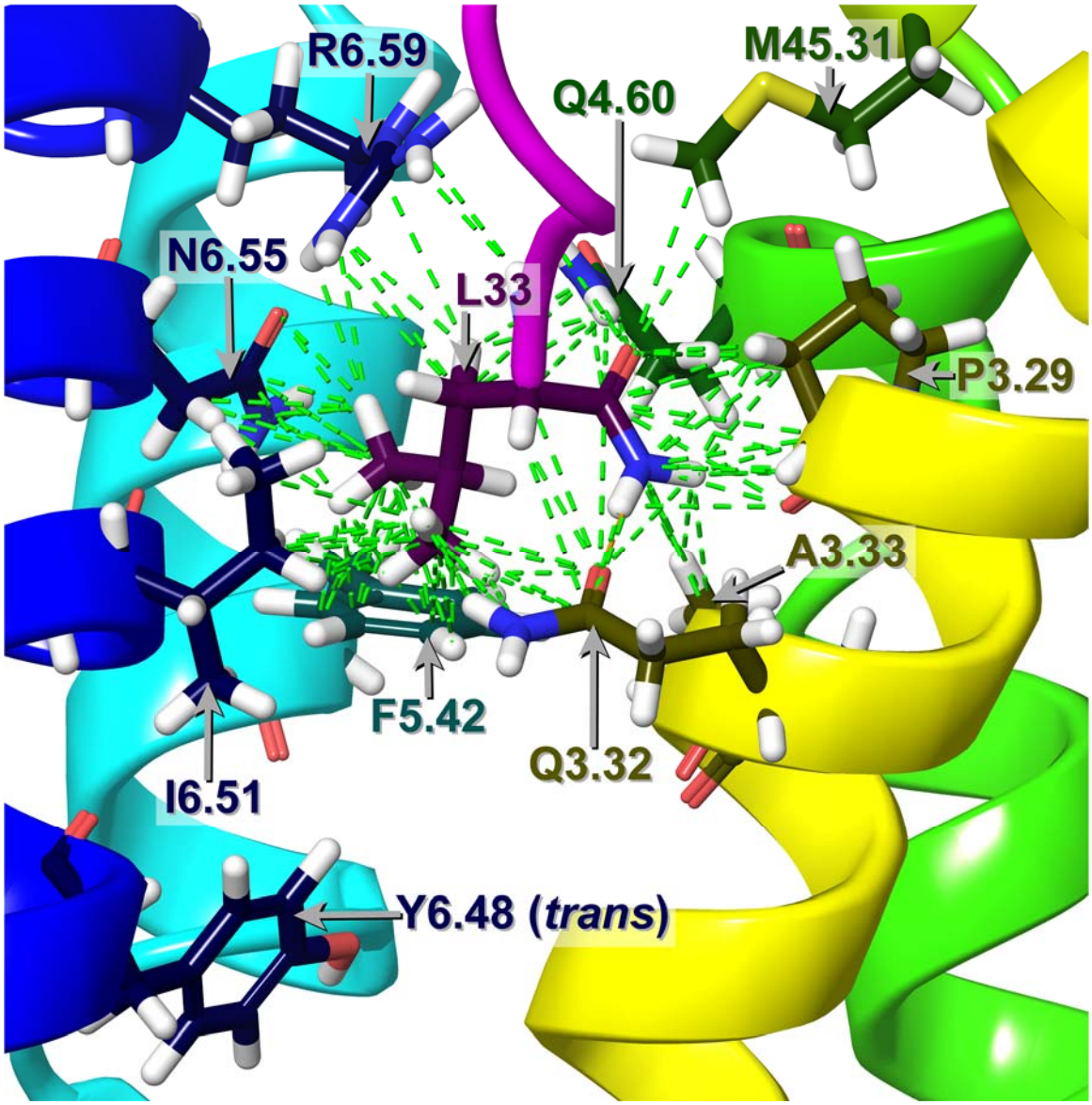

Figure 104. Orexin-A's L33 Interacts By van der Waals Contacts with P3.29, Q3.32, A3.33, Q4.60, M45.31, F5.42, I6.51, N6.55, and R6.59 of the Ox1r R* Model.[3,4,7,22,24,124]

The orexin-A mutation R15A was not effective because R15 was pointing into the extracellular fluid, and its interactions would easily be replaced by those of water.[3,4,7,22,24] L16A was effective because it would cost orexin-A many of the contacts L16 would cause, and less water would be displaced between orexin-A and the EC2 loop.[3,4,7,22,24] Y17A was not effective because it would cause the N-terminus of orexin-A to close the gap the mutation would cause, as Y17 contacts both the central helix and N-terminus of orexin-A, yet though its side chain has heavy van der Waals contacts with Y39, E110, and S111, and a hydrogen bond to E110, those interactions can be replaced with those from the orexin-A N-terminus and water.[3,4,7,22,24] E18A was not an effective mutation as it points into extracellular fluid, and its interactions would easily be replaced with those of water.[3,4,7,22,24] L19A and L20A were both effective because each would cost orexin-A many of the contacts that L19 and L20 would cause, respectively, and less water would be displaced between orexin-A and the EC2 loop for each of those two mutations.[3,4,7,22,24] H21A was not an effective mutation, as it could cause Y17 to switch to *trans* to replace the contacts lost, and in turn cause the N-terminus to close the gap caused by that mutation just as it would for Y17A, again with no significant loss of contact.[3,4,7,22,24] G22A and G24A were not effective mutations because they would not sterically crowd any nearby residue significantly, and they contribute little to no contact with the ox1r.[3,4,7,22,24] N25A was not an effective mutation because it points into extracellular fluid, and its interactions would easily be replaced with those of water.[3,4,7,22,24] H26A was a very effective mutation as it costs orexin-A much of the contacts H26 would cause, as well as the one hydrogen bond its side chain would donate and the cation-π interaction

it would accept.[3,4,7,22,24] A27G and A28G were effective mutations as they each cost orexin-A much of the contacts A27 and A28 would cause, respectively.[3,4,7,22,24,155] G29A was effective because it would lose conformational flexibility.[3,4,7,22,24,148,149] I30A and L31A were effective as they each cost orexin-A much of the contacts that I30 and L31 would cause, respectively, with less water displaced from the ox1r binding pocket for each.[3,4,7,22,24] T32A was effective because it would not only cost orexin-A much of the contacts T32 would cause, it would also lose the hydrogen bond T32 donates to E45.52 and the internal one it accepts from L33's backbone amide hydrogen.[3,4,7,9,22,24] Furthermore, chiral inversion of T32 would sterically crowd I30, likely cost T32 the hydrogen bond it would donate to E45.52, and likely force L33 to crowd the ox1r binding pocket to retain the hydrogen bond to L33, as shown in Figure 105.[3,4,7,9,22,24]

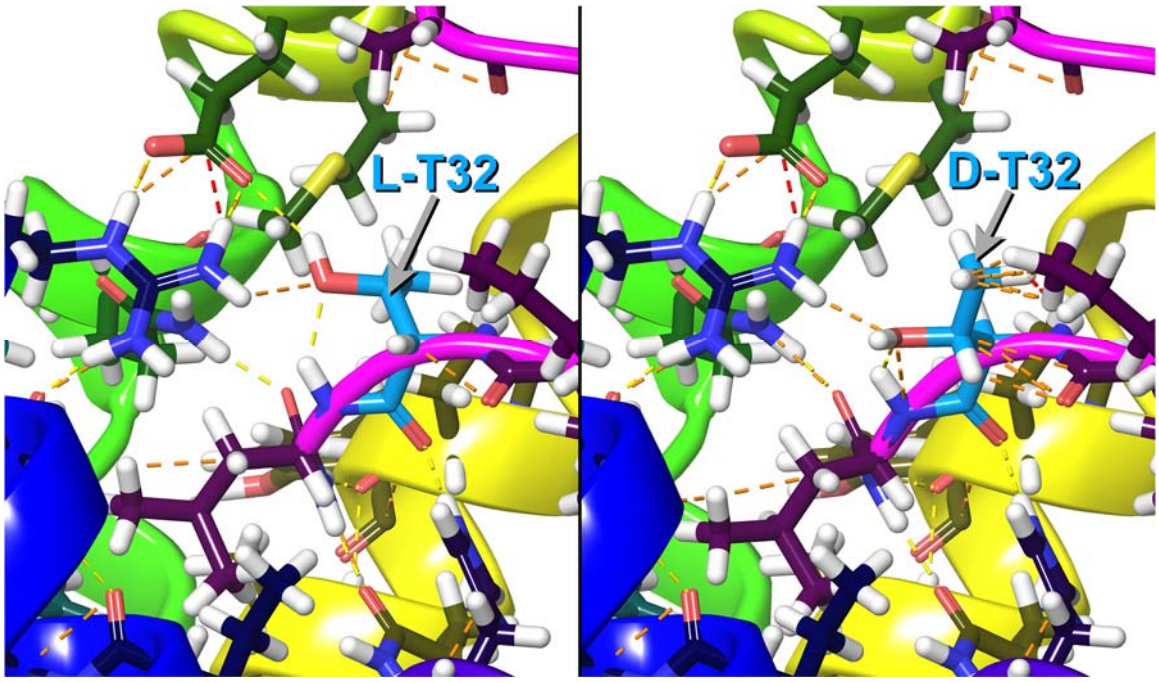

Figure 105. Chiral Inversion of Orexin-A's T32 and Its Effects.[3,4,7,9,22,24]

L33A was effective as it costs orexin-A much of the contacts that L33 would cause, and displace less water from the ox1r binding pocket as well.[3,4,7,22,24] Furthermore, chiral inversion of L33 would cost orexin-A some contacts and a hydrogen bond between L33's backbone oxygen and Q4.60, and another hydrogen bond between the C-terminal amide and P3.29's backbone oxygen, while the hydrogen bond donated to Q3.32 is substituted for one accepted from Q3.32 along with steric strain, as shown in Figure 106.[3,4,7,22,24]

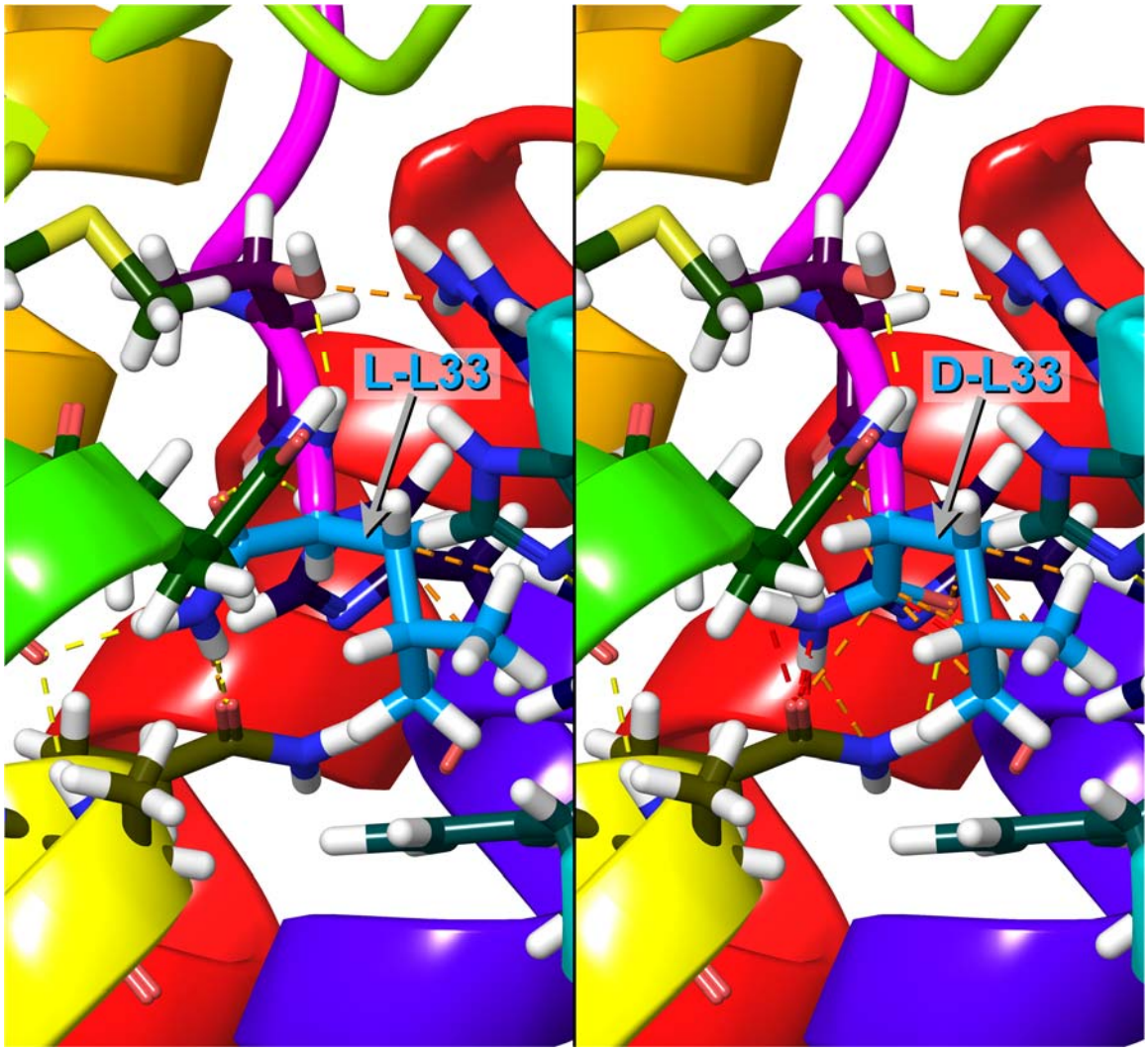

Figure 106. Chiral Inversion of Orexin-A's L33 and Its Effects.[3,4,7,22,24]

In the ox1r, a reason why Q3.32A may not be an effective mutation is that Q3.32 is a polar residue, which could have water molecules replace the contribution it has, since alanine would be small enough to admit them nearby.[3,4,7,22,24] Furthermore, the reason that A3.33T had no significant effect was that it would reduce the surface area of the ox1r binding pocket's hydrophobic patch, as threonine is partially hydrophobic.[3,4,7,22,24] The reason that V3.36A would have its effect is that it would also reduce the hydrophobic patch's surface area.[3,4,7,22,24] D45.51A has its effect because it would cost ox1r a residue that stabilizes the EC2b loop, as an alanine would be hydrophobic and change the EC2 loop's shape, and also cost it the van der Waals contacts and hydrogen bonds D45.51 would cause.[3,4,7,22,24] W45.54A has its effect of abolishing binding because W45.54 is situated between TMH4 and TMH5 and stabilizes them, interacting very heavily with its surrounding residues, and mutation to an alanine would cause a large gap between TMH4 and TMH5 that would cause the ox1r to partially collapse on that side, as well as costing the ox1r the contacts W45.54 would cause.[3,4,7,22,24] Y5.38A has its strong effect because Y5.38 helps hold TMH4 and TMH5 together, especially by donating a hydrogen bond to TMH4, whether to Q4.60 as found by Heifetz et al. and Yin et al. or to I4.56's backbone oxygen, and donating a π-π T-stack to H5.39 as found by Yin et al., and a mutation to alanine would abolish all of those, possibly causing another partial collapse.[3,4,7,22,24] F5.42A was effective because it would cause a partial collapse of the ox1r there, while costing the ox1r the van der Waals contacts F5.42 would cause.[3,4,7,22,24] Y5.47A has its effect because it would cost the ox1r the contacts with Y6.48 that Y5.47 would cause.[3,4,7,22,24] Y6.48A is an effective mutation because Y6.48's χ1 conformational

change would be necessary for activation,[124,125,126,127,128,129,130] and that mutation would also cost the ox1r the prospective contacts, and the hydrogen bond to T5.46, that Y6.48 would cause.[3,4,7,22,24] H7.39A was an effective mutation because it would cost the ox1r the contacts and the hydrogen bond that H7.39 would cause.[3,4,7,22,24] However, Y7.43A was not an effective mutation because it was not close enough to orexin-A to contact it very well.[3,4,7,22,24]

This showed a greater understanding of how SB-674042 and orexin-A interact with the ox1r.[3,4,7,22,24]

CHARMM Atom Types

New atom types were created for the optimization of the CHARMM parameters, with unique atom types made for each respective set of atoms depending on which part of the molecules they may occupy, and their subsequent use in MD simulation, and Lennard-Jones van der Waals nonbonded parameters were created for each, using the CGenFF database, as is shown in Tables 7, 8, and 9.[4,137,158,159,160,161,162,163,164]

Table 7

CHARMM Atom Types Required for SB-674042 and Pyroglutamate, Their Masses, and Their Corresponding Elements, with the "Present" Set of Atoms Already Present as CHARMM Atoms in the Atom Type List, and the "Added" Set of Atoms Added to the Atom Type List, as They Were Not Present.[4,137,158,159,160,161,162,163,164]

CHARMM Atomic Mass Table			
Present Mass Numbers	***CHARMM Atom Types***	***Element***	***Atomic Mass***
1	**H**	**H**	**1.00800**
20	**C**	**C**	**12.01100**
22	**CT1**	**C**	**12.01100**
29	**CP1**	**C**	**12.01100**
31	**CP3**	**C**	**12.01100**

Table 7

Cont.

CHARMM Atomic Mass Table			
Present Mass Numbers	***CHARMM Atom Types***	***Element***	***Atomic Mass***
50	**N**	**N**	**14.00700**
54	**NH1**	**N**	**14.00700**
70	**O**	**O**	**15.99900**
Added Mass Numbers	***CHARMM Atom Types***	***Element***	***Atomic Mass***
122	**C61**	**C**	**12.01100**
123	**H61**	**H**	**1.00800**
124	**C51**	**C**	**12.01100**
125	**C53**	**C**	**12.01100**
126	**N50**	**N**	**14.00700**
127	**O50**	**O**	**15.99900**
128	**C11**	**C**	**12.01100**
129	**C21**	**C**	**12.01100**
130	**C31**	**C**	**12.01100**
131	**HG1**	**H**	**1.00800**
132	**HG2**	**H**	**1.00800**
133	**HG3**	**H**	**1.00800**
134	**HP1**	**H**	**1.00800**
135	**N11**	**N**	**14.00700**
136	**HG52**	**H**	**1.00800**
137	**N50X**	**N**	**14.00700**
138	**O50X**	**O**	**15.99900**
139	**NG0**	**N**	**14.00700**
140	**CO1**	**C**	**12.01100**
141	**OD1**	**O**	**15.99940**
142	**C215**	**C**	**12.01100**
143	**S50**	**S**	**32.06000**
144	**S50Y**	**S**	**32.06000**
145	**N50Y**	**N**	**14.00700**
146	**FR1**	**F**	**18.99800**
147	**C66**	**C**	**12.01100**
148	**H62**	**H**	**1.00800**
149	**HAY**	**H**	**1.00800**
150	**HBY**	**H**	**1.00800**

Table 7

Cont.

CHARMM Atomic Mass Table			
Added Mass Numbers	***CHARMM Atom Types***	***Element***	***Atomic Mass***
151	**CTY1**	**C**	**12.01100**
152	**CTY2**	**C**	**12.01100**
153	**CTY3**	**C**	**12.01100**
154	**H5**	**H**	**1.00800**
155	**CCY**	**C**	**12.01100**
156	**NG2**	**N**	**14.00700**

Table 8

CHARMM Atom Types Required for SB-674042 and Pyroglutamate, and the Instructions for Use of Each, with the Words Sourced from the Original CGenFF Topology File Spelled Verbatim (e.g., "Flourine," "Uera," etc.).[4,137,158,159,160,161,162,163,164]

CHARMM Atom Type Information	
CHARMM Atom Types	***Notes (spelling is as present in topology file)***
H	**polar H**
C	**carbonyl C, peptide backbone**
CT1	**aliphatic sp3 C for CH**
CP1	**tetrahedral C (proline CA)**
CP3	**tetrahedral C (proline CD)**
N	**proline N**
NH1	**peptide nitrogen**
O	**carbonyl oxygen**
C61	**aromatic C**
H61	**aromatic H**
C51	**his CG and CD2 carbons**
C53	**his CE1 carbon**
N50	**neutral his unprotonated ring nitrogen**
O50	**furan oxygen**
C11	**aliphatic sp3 C for CH**
C21	**aliphatic sp3 C for CH2**
C31	**aliphatic sp3 C for CH3**

Table 8

Cont.

CHARMM Atom Type Information	
CHARMM Atom Types	***Notes (spelling is as present in topology file)***
HG1	**alkane, CH, new LJ params**
	(see toppar_all22_prot_aliphatic_c27.str)
HG2	**alkane, CH2, new LJ params**
	(see toppar_all22_prot_aliphatic_c27.str)
HG3	**alkane, CH3, new LJ params**
	(see toppar_all22_prot_aliphatic_c27.str)
HP1	**polar H**
N11	**primary amine nitrogen**
HG52	**oxadiazole aromatic H and formamide H (RCOH)**
N50X	**neutral his unprotonated ring nitrogen**
	for 1,3,4-oxadiazole
O50X	**furan oxygen for 1,3,4-oxadiazole**
NG0	**N,N-disubstituted amide, proline N (CO=NRR')**
CO1	**carbonyl C: amides**
OD1	**carbonyl O: amides, esters,**
	[neutral] carboxylic acids, aldehydes, uera
C215	**aliphatic sp3 C for CH2 for cyclopentane**
S50	**THIP, thiophene**
S50Y	**THIP, thiophene**
N50Y	**neutral his unprotonated ring nitrogen**
	for 1,3-thiazole
FR1	**aromatic flourine**
C66	**6-mem aromatic carbon bound to F**
H62	**nonpolar H, neutral 6-mem planar ring C**
	adjacent to heteroatom
HAY	**nonpolar H for pyroglutamate ring**
HBY	**backbone H for pyroglutamate ring**
CTY1	**aliphatic sp3 C for CH for pyroglutamate ring**
CTY2	**aliphatic sp3 C for CH2 for pyroglutamate ring**
CTY3	**aliphatic sp3 C for CH3 for pyroglutamate ring**
H5	**polar H**
CCY	**carbonyl C, asn,asp,gln,glu,cter,ct2,pca**
NG2	**amide nitrogen**

Table 9

CHARMM Atom Types Required for SB-674042 and Pyroglutamate, and Their Lennard-Jones van der Waals Parameters.[4,137,158,159,160,161,162,163,164]

CHARMM Lennard-Jones Nonbonded Parameters				
CHARMM Atom Types	***Epsilon***	***$R_{min}/2$***	***Epsilon, 1-4***	***$R_{min}/2$, 1-4***
H	**-0.046000**	**0.224500**	**x**	**x**
C	**-0.110000**	**2.000000**	**x**	**x**
CT1	**-0.020000**	**2.275000**	**-0.010000**	**1.900000**
CP1	**-0.020000**	**2.275000**	**-0.010000**	**1.900000**
CP3	**-0.055000**	**2.175000**	**-0.010000**	**1.900000**
N	**-0.200000**	**1.850000**	**-0.000100**	**1.850000**
NH1	**-0.200000**	**1.850000**	**-0.200000**	**1.550000**
O	**-0.120000**	**1.700000**	**-0.120000**	**1.400000**
C61	**-0.070000**	**1.992400**	**x**	**x**
H61	**-0.022000**	**1.320000**	**x**	**x**
C51	**-0.050000**	**1.800000**	**x**	**x**
C53	**-0.050000**	**1.800000**	**x**	**x**
N50	**-0.200000**	**1.850000**	**x**	**x**
O50	**-0.152100**	**1.770000**	**x**	**x**
C11	**-0.020000**	**2.275000**	**-0.010000**	**1.900000**
C21	**-0.055000**	**2.175000**	**-0.010000**	**1.900000**
C31	**-0.080000**	**2.060000**	**-0.010000**	**1.900000**
HG1	**-0.022000**	**1.320000**	**x**	**x**
HG2	**-0.028000**	**1.340000**	**x**	**x**
HG3	**-0.024000**	**1.340000**	**x**	**x**
HP1	**-0.046000**	**0.224500**	**x**	**x**
N11	**-0.200000**	**1.850000**	**x**	**x**
HG52	**-0.046000**	**0.900000**	**x**	**x**
N50X	**-0.200000**	**1.850000**	**x**	**x**
O50X	**-0.152100**	**1.770000**	**x**	**x**
NG0	**-0.200000**	**1.850000**	**-0.000100**	**1.850000**
CO1	**-0.110000**	**2.000000**	**x**	**x**
OD1	**-0.120000**	**1.700000**	**-0.120000**	**1.400000**
C215	**-0.055000**	**2.175000**	**-0.010000**	**1.900000**
S50	**-0.450000**	**2.000000**	**x**	**x**
S50Y	**-0.450000**	**2.000000**	**x**	**x**
N50Y	**-0.200000**	**1.850000**	**x**	**x**

Table 9

Cont.

CHARMM Lennard-Jones Nonbonded Parameters				
CHARMM Atom Types	***Epsilon***	***$R_{min}/2$***	***Epsilon, 1-4***	***$R_{min}/2$, 1-4***
FR1	**-0.120000**	**1.700000**	**x**	**x**
C66	**-0.070000**	**1.900000**	**x**	**x**
H62	**-0.046000**	**1.100000**	**x**	**x**
HAY	**-0.022000**	**1.320000**	**x**	**x**
HBY	**-0.022000**	**1.320000**	**x**	**x**
CTY1	**-0.020000**	**2.275000**	**-0.010000**	**1.900000**
CTY2	**-0.055000**	**2.175000**	**-0.010000**	**1.900000**
CTY3	**-0.080000**	**2.060000**	**-0.010000**	**1.900000**
H5	**-0.046000**	**0.224500**	**x**	**x**
CCY	**-0.070000**	**2.000000**	**x**	**x**
NG2	**-0.200000**	**1.850000**	**x**	**x**

These atom types, masses, usage instructions, and Lennard-Jones van der Waals nonbonded parameters were acquired, leading to the next step: obtaining charge parameters and building compound topologies.[4,137,158,159,160,161,162,163,164,165,166,167]

CHARMM Charge Parameters and Compound Topologies

The structure, atom names, atom types, and charges for the model compound 1,3,4-oxadiazole were determined, and shown in Table 10 and Figure 107.[137,158,159,160,161,162,163,164,165,166,167]

Table 10

Atom Names, Atom Types, and Charges of 1,3,4-oxadiazole.[137,158,159,160,161,162,163,164,165,166,167]

1,3,4-Oxadiazole Charges			
Atom Name	***Atom Type***	***Old Charges***	***New Charges***
		Group	***Group***
C1	**C53**	**0.335**	***0.630***
N2	**N50**	**-0.355**	***-0.490***
N3	**N50**	**-0.355**	***-0.490***
C4	**C53**	**0.335**	***0.630***
O5	**O50**	**-0.320**	***-0.440***
H6	**HG52**	**0.180**	***0.080***
H7	**HG52**	**0.180**	***0.080***

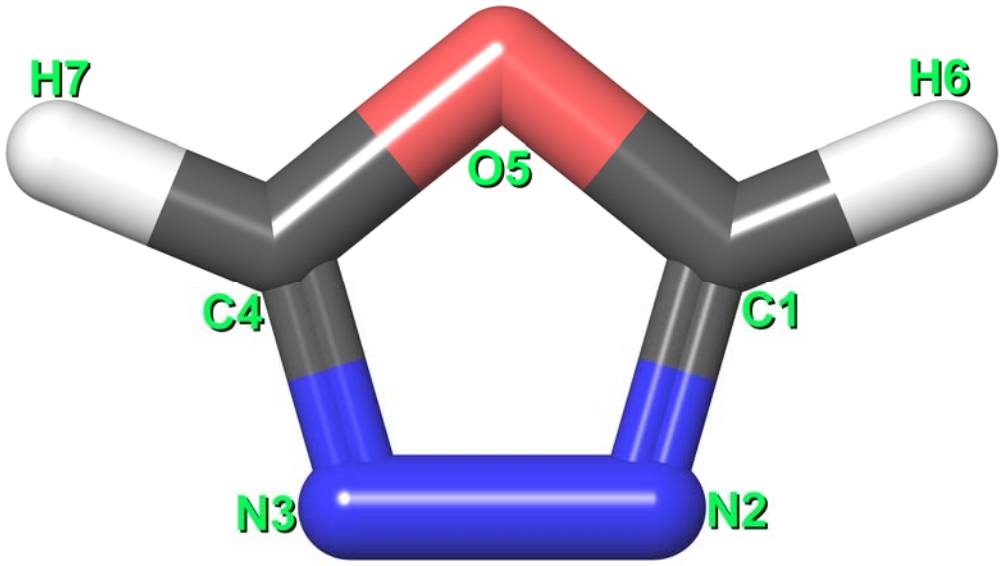

Figure 107. Structure and Atom Names of 1,3,4-oxadiazole.[137,158,159,160,161,162,163,164,165,166,167]

It was included among the remaining charge model compounds for both SB-674042 and pyroglutamate-NMA, all of which had their charges taken directly from CGenFF, then

assembled as previously stated to determine the charges of the BAT model compounds and the charges of SB-674042 and pyroglutamate-NMA, the first of which is SB-674042 BAT Model Compound 1 (made to connect rings D and E of SB-674042), whose structure, atom names, atom types, and charges are shown in Table 11 and Figure 108.[137,158,159,160,161,162,163,164,165,166,167]

Table 11

Atom Names, Atom Types, and Charges of SB-674042 BAT Model Compound 1.[137,158,159,160,161,162,163,164,165,166,167]

SB-674042 BAT Model Compound 1 Charges			
Atom Name	***Atom Type***	***Old Charges***	***New Charges***
		Group	***Group***
C1	**C61**	**0.169**	***0.000***
C2	**C61**	**-0.116**	***-0.115***
C3	**C61**	**-0.115**	**-0.115**
C4	**C61**	**-0.115**	**-0.115**
C5	**C61**	**-0.115**	**-0.115**
C6	**C61**	**-0.116**	***-0.115***
H7	**H61**	**0.115**	**0.115**
H8	**H61**	**0.115**	**0.115**
H9	**H61**	**0.115**	**0.115**
H10	**H61**	**0.115**	**0.115**
H11	**H61**	**0.115**	**0.115**
C12	**C53**	**0.453**	***0.710***
N13	**N50X**	**-0.458**	***-0.490***
N14	**N50X**	**-0.361**	***-0.490***
C15	**C53**	**0.344**	***0.630***
O16	**O50X**	**-0.325**	***-0.440***
H17	**HG52**	**0.180**	***0.080***

The structure and atom names of SB-674042 BAT Model Compound 1 are shown in Figure 108.[137,158,159,160,161,162,163,164,165,166,167]

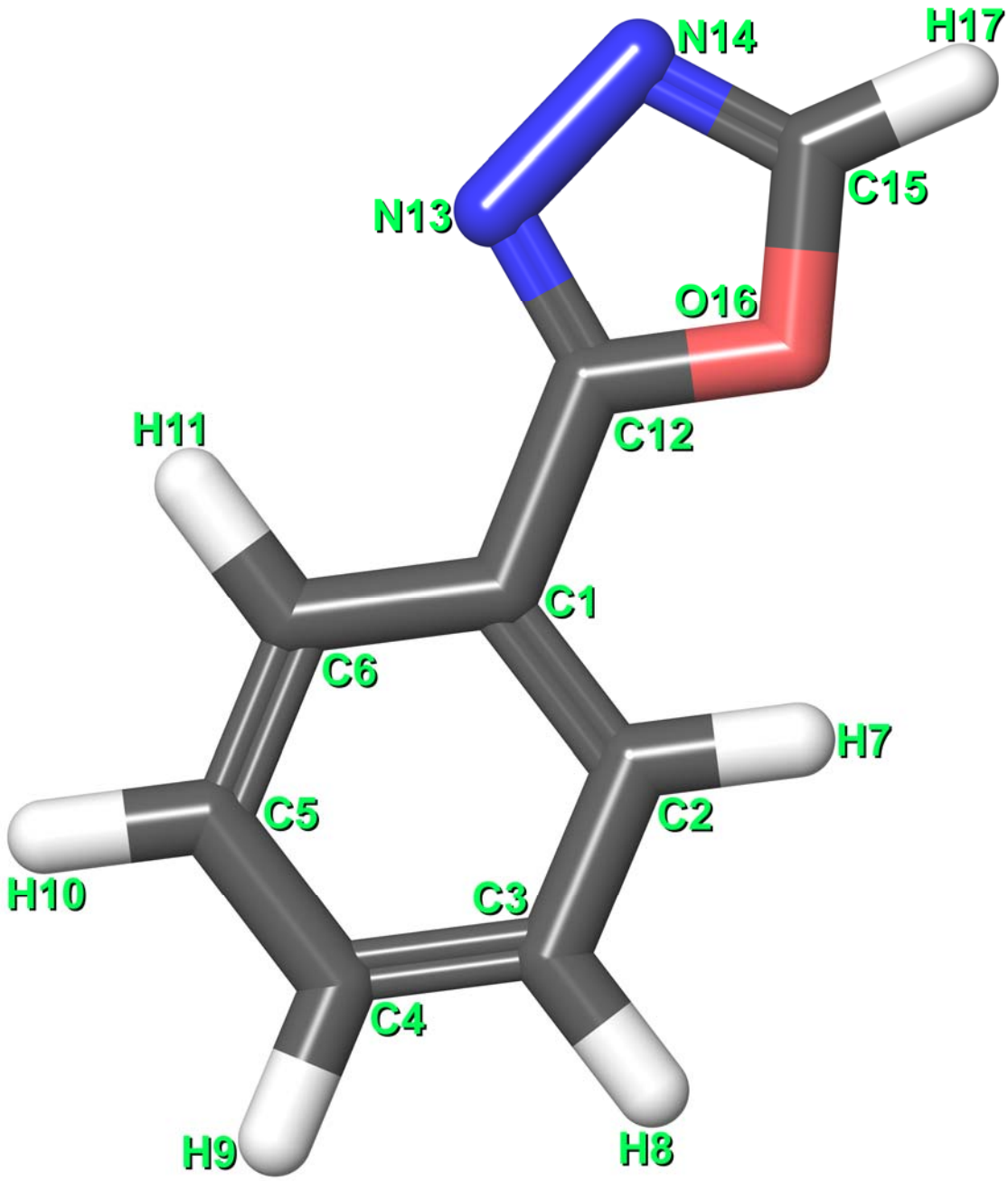

Figure 108. Structure and Atom Names of SB-674042 BAT Model Compound 1.[137,158,159,160,161,162,163,164,165,166,167]

Next is SB-674042 BAT Model Compound 2, whose structure, atom names, atom types, and charges are shown in Figure 109 and Table 12.[137,158,159,160,161,162,163,164,165,166,167]

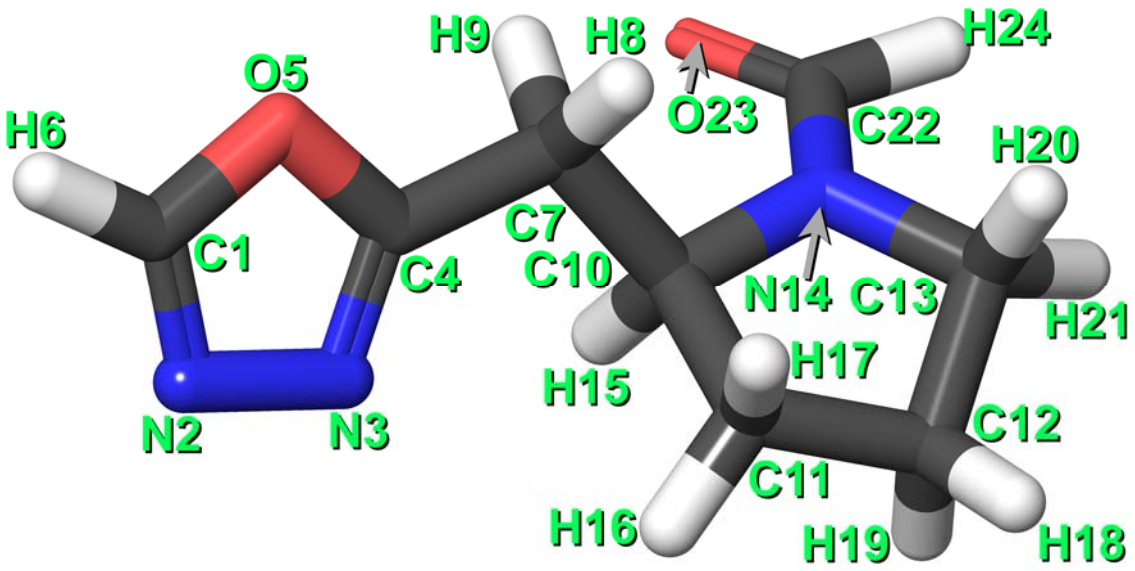

Figure 109. Structure and Atom Names of SB-674042 BAT Model Compound 2.[137,158,159,160,161,162,163,164,165,166,167]

Table 12

Atom Names, Atom Types, and Charges of SB-674042 BAT Model Compound 2.[137,158,159,160,161,162,163,164,165,166,167]

SB-674042 BAT Model Compound 2 Charges			
Atom Name	***Atom Type***	***Old Charges***	***New Charges***
		Group	***Group***
C1	**C53**	**0.344**	***0.630***
N2	**N50X**	**-0.361**	***-0.490***
N3	**N50X**	**-0.410**	***-0.490***
C4	**C53**	**0.408**	***0.710***
O5	**O50X**	**-0.283**	***-0.440***
H6	**HG52**	**0.180**	***0.080***
C7	**C21**	**-0.060**	***-0.180***
H8	**HG2**	**0.090**	**0.090**
H9	**HG2**	**0.090**	**0.090**

Table 12

Cont.

SB-674042 BAT Model Compound 2 Charges			
Atom Name	***Atom Type***	***Old Charges***	***New Charges***
C10	**C11**	**0.014**	***0.084***
C11	**C215**	**-0.183**	***-0.180***
C12	**C215**	**-0.178**	***-0.180***
C13	**C215**	**-0.006**	**-0.006**
N14	**NG0**	**-0.291**	***-0.332***
H15	**HG1**	**0.090**	**0.090**
H16	**HG2**	**0.090**	**0.090**
H17	**HG2**	**0.090**	**0.090**
H18	**HG2**	**0.090**	**0.090**
H19	**HG2**	**0.090**	**0.090**
H20	**HG2**	**0.090**	**0.090**
H21	**HG2**	**0.090**	**0.090**
C22	**CO1**	**0.441**	***0.427***
O23	**OD1**	**-0.501**	***-0.519***
H24	**HG52**	**0.076**	**0.076**

Afterward is SB-674042 BAT Model Compound 3, whose structure, atom names, atom types, and charges are shown in Table 13 and Figure 110.[137,158,159,160,161,162,163,164,165,166,167]

Table 13

Atom Names, Atom Types, and Charges of SB-674042 BAT Model Compound 3.[137,158,159,160,161,162,163,164,165,166,167]

SB-674042 BAT Model Compound 3 Charges			
Atom Name	***Atom Type***	***Old Charges***	***New Charges***
		Group	***Group***
C1	**C53**	**0.303**	***0.360***
N2	**N50Y**	**-0.676**	***-0.610***
C3	**C51**	**0.268**	***0.331***
C4	**C51**	**-0.311**	***-0.301***

Table 13

Cont.

SB-674042 BAT Model Compound 3 Charges			
Atom Name	***Atom Type***	***Old Charges***	***New Charges***
S5	**S50Y**	**0.017**	***0.010***
H6	**HG52**	**0.210**	**0.210**
C7	**C31**	**-0.145**	***-0.270***
H8	**HG3**	**0.090**	**0.090**
H9	**HG3**	**0.090**	**0.090**
H10	**HG3**	**0.090**	**0.090**
C11	**CO1**	**0.522**	***0.503***
O12	**OD1**	**-0.453**	***-0.519***
C13	**C11**	**0.031**	***0.084***
C14	**C215**	**-0.184**	***-0.180***
C15	**C215**	**-0.180**	**-0.180**
C16	**C215**	**0.018**	***-0.006***
H17	**HG1**	**0.090**	**0.090**
H18	**HG2**	**0.090**	**0.090**
H19	**HG2**	**0.090**	**0.090**
H20	**HG2**	**0.090**	**0.090**
H21	**HG2**	**0.090**	**0.090**
H22	**HG2**	**0.090**	**0.090**
H23	**HG2**	**0.090**	**0.090**
N24	**NG0**	**-0.328**	***-0.332***
C25	**C31**	**-0.262**	***-0.270***
H26	**HG3**	**0.090**	**0.090**
H27	**HG3**	**0.090**	**0.090**
H28	**HG3**	**0.090**	**0.090**

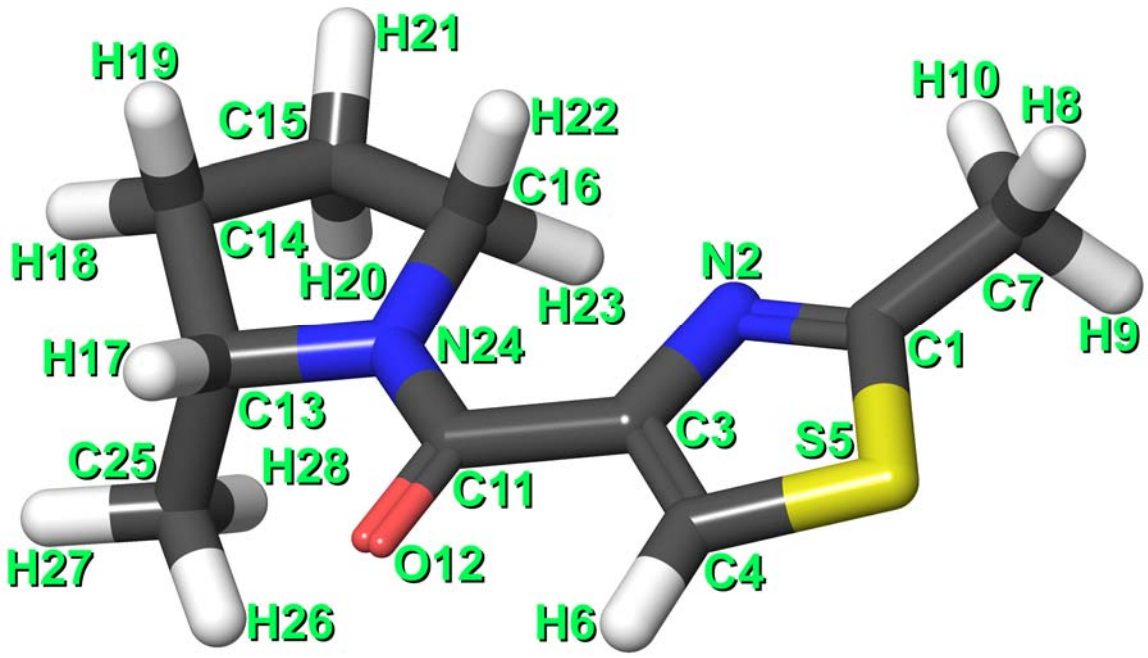

Figure 110. Structure and Atom Names of SB-674042 BAT Model Compound 3.[137,158,159,160,161,162,163,164,165,166,167]

Following SB-674042 BAT Model Compound 3 is SB-674042 BAT Model Compound 4, whose structure, atom names, atom types, and charges are shown in Figure 111 and Table 14.[137,158,159,160,161,162,163,164,165,166,167]

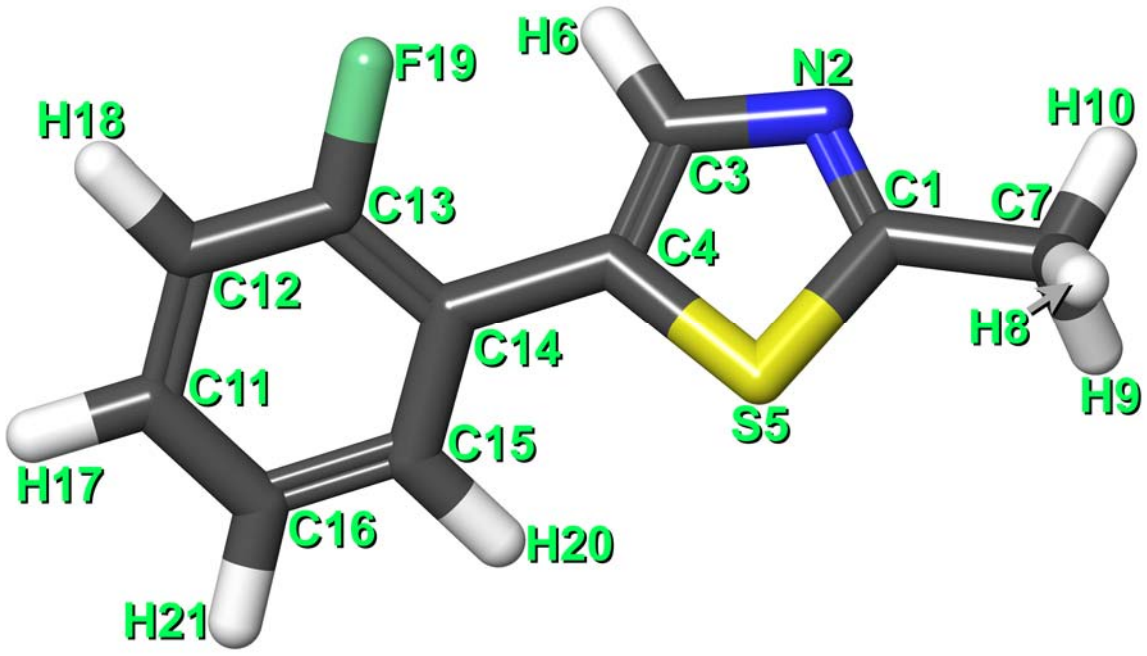

Figure 111. Structure and Atom Names of SB-674042 BAT Model Compound 4.[137,158,159,160,161,162,163,164,165,166,167]

Table 14

Atom Names, Atom Types, and Charges of SB-674042 BAT Model Compound 4.[137,158,159,160,161,162,163,164,165,166,167]

SB-674042 BAT Model Compound 4 Charges			
Atom Name	***Atom Type***	***Old Charges***	***New Charges***
		Group	***Group***
C1	**C53**	**0.301**	***0.360***
N2	**N50Y**	**-0.669**	***-0.610***
C3	**C51**	**0.150**	***0.201***
C4	**C51**	**-0.239**	***-0.091***
S5	**S50Y**	**0.011**	***0.010***
H6	**HG52**	**0.173**	***0.130***
C7	**C31**	**-0.145**	***-0.270***
H8	**HG3**	**0.090**	**0.090**
H9	**HG3**	**0.090**	**0.090**
H10	**HG3**	**0.090**	**0.090**

Table 14

Cont.

SB-674042 BAT Model Compound 4 Charges			
Atom Name	***Atom Type***	***Old Charges***	***New Charges***
C11	**C61**	**-0.175**	**-0.175**
C12	**C61**	**-0.050**	***-0.095***
C13	**C66**	**0.029**	***0.118***
C14	**C61**	**0.307**	***0.099***
C15	**C61**	**-0.179**	***-0.175***
C16	**C61**	**-0.104**	***-0.107***
H17	**H61**	**0.115**	**0.115**
H18	**H62**	**0.194**	**0.194**
F19	**FR1**	**-0.219**	***-0.204***
H20	**H61**	**0.115**	**0.115**
H21	**H61**	**0.115**	**0.115**

Subsequent is SB-674042 BAT Model Compound 5, whose structure, atom names, atom types, and charges are shown in Table 15 and Figure 112.[137,158,159,160,161,162,163,164,165,166,167]

Table 15

Atom Names, Atom Types, and Charges of SB-674042 BAT Model Compound 5.[137,158,159,160,161,162,163,164,165,166,167]

SB-674042 BAT Model Compound 5 Charges			
Atom Name	***Atom Type***	***Old Charges***	***New Charges***
		Group	***Group***
C1	**C61**	**0.325**	***0.099***
C2	**C66**	**0.029**	***0.118***
C3	**C61**	**-0.050**	***-0.095***
C4	**C61**	**-0.175**	**-0.175**
C5	**C61**	**-0.104**	***-0.107***
C6	**C61**	**-0.179**	***-0.175***
F7	**FR1**	**-0.219**	***-0.204***
H8	**H62**	**0.194**	**0.194**

Table 15

Cont.

SB-674042 BAT Model Compound 5 Charges			
Atom Name	***Atom Type***	***Old Charges***	***New Charges***
H9	**H61**	**0.115**	**0.115**
H10	**H61**	**0.115**	**0.115**
H11	**H61**	**0.115**	**0.115**
C12	**C51**	**-0.260**	***-0.091***
C13	**C51**	**0.293**	***0.331***
N14	**N50Y**	**-0.675**	***-0.610***
C15	**C53**	**0.303**	***0.360***
S16	**S50Y**	**0.017**	***0.010***
C17	**C31**	**-0.145**	***-0.270***
H18	**HG3**	**0.090**	**0.090**
H19	**HG3**	**0.090**	**0.090**
H20	**HG3**	**0.090**	**0.090**
C21	**CO1**	**0.704**	***0.548***
O22	**OD1**	**-0.482**	***-0.544***
H23	**HP1**	**0.374**	***0.309***
N24	**NG2**	**-0.939**	***-0.622***
H25	**HP1**	**0.374**	***0.309***

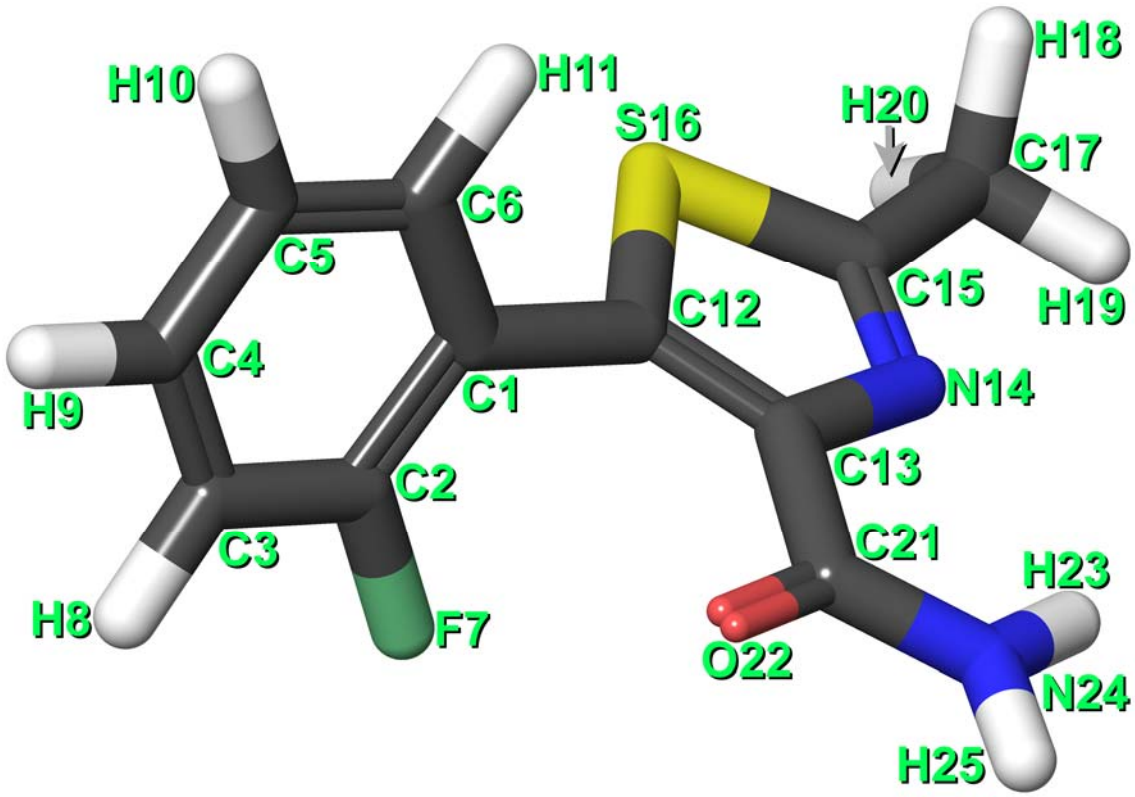

Figure 112. Structure and Atom Names of SB-674042 BAT Model Compound 5.[137,158,159,160,161,162,163,164,165,166,167]

Subsequent is the whole molecule of SB-674042, whose structure, atom names, atom types, and charges are shown in Figure 113 and Table 16.[137,158,159,160,161,162,163,164,165,166,167]

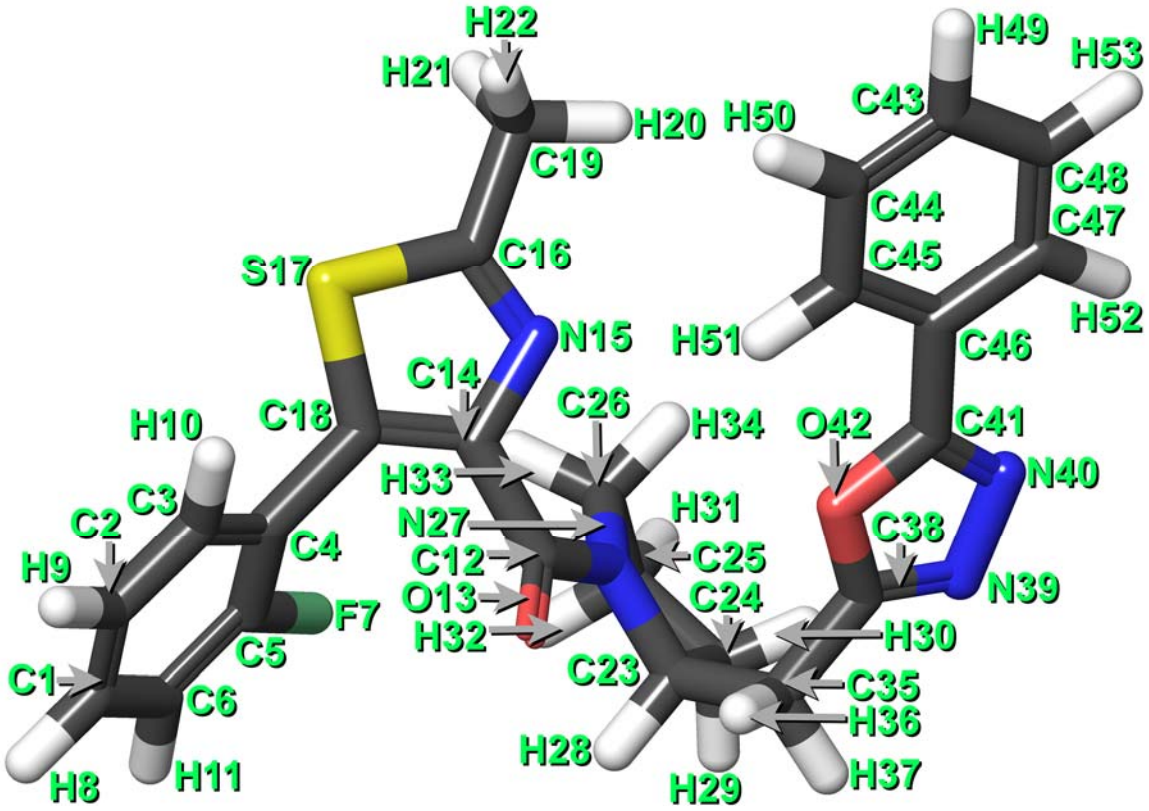

Figure 113. Structure and Atom Names of the Whole Molecule of SB-674042.[137,158,159,160,161,162,163,164,165,166,167]

Table 16

Atom Names, Atom Types, and Charges of the Whole Molecule of SB-674042.[137,158,159,160,161,162,163,164,165,166,167]

Whole Molecule of SB-674042 Charges			
Atom Name	***Atom Type***	***Old Charges***	***New Charges***
		Group	***Group***
C1	**C61**	**-0.175**	**-0.175**
C2	**C61**	**-0.104**	***-0.107***
C3	**C61**	**-0.179**	***-0.175***
C4	**C61**	**0.325**	***0.099***
C5	**C66**	**0.029**	***0.118***
C6	**C61**	**-0.050**	***-0.095***
F7	**FR1**	**-0.219**	***-0.204***

Table 16

Cont.

Whole Molecule of SB-674042 Charges			
Atom Name	***Atom Type***	***Old Charges***	***New Charges***
H8	**H61**	**0.115**	**0.115**
H9	**H61**	**0.115**	**0.115**
H10	**H61**	**0.115**	**0.115**
H11	**H62**	**0.194**	**0.194**
			Group
C12	**CO1**	**0.522**	***0.503***
O13	**OD1**	**-0.453**	***-0.519***
C14	**C51**	**0.260**	***0.331***
N15	**N50Y**	**-0.675**	***-0.610***
C16	**C53**	**0.303**	***0.360***
S17	**S50Y**	**0.017**	***0.010***
C18	**C51**	**-0.260**	***-0.091***
C19	**C31**	**-0.145**	***-0.270***
H20	**HG3**	**0.090**	**0.090**
H21	**HG3**	**0.090**	**0.090**
H22	**HG3**	**0.090**	**0.090**
C23	**C11**	**0.038**	***0.084***
C24	**C215**	**-0.183**	***-0.180***
C25	**C215**	**-0.178**	***-0.180***
C26	**C215**	**0.018**	***-0.006***
N27	**NG0**	**-0.328**	***-0.332***
H28	**HG1**	**0.090**	**0.090**
H29	**HG2**	**0.090**	**0.090**
H30	**HG2**	**0.090**	**0.090**
H31	**HG2**	**0.090**	**0.090**
H32	**HG2**	**0.090**	**0.090**
H33	**HG2**	**0.090**	**0.090**
H34	**HG2**	**0.090**	**0.090**
			Group
C35	**C21**	**-0.060**	***-0.180***
H36	**HG2**	**0.090**	**0.090**
H37	**HG2**	**0.090**	**0.090**

Table 16

Cont.

Whole Molecule of SB-674042 Charges			
Atom Name	***Atom Type***	***Old Charges***	***New Charges***
			Group
C38	**C53**	**0.417**	***0.710***
N39	**N50X**	**-0.416**	***-0.490***
N40	**N50X**	**-0.464**	***-0.490***
C41	**C53**	**0.462**	***0.710***
O42	**O50X**	**-0.288**	***-0.440***
			Group
C43	**C61**	**-0.115**	**-0.115**
C44	**C61**	**-0.115**	**-0.115**
C45	**C61**	**-0.116**	***-0.115***
C46	**C61**	**0.169**	***0.000***
C47	**C61**	**-0.116**	***-0.115***
C48	**C61**	**-0.115**	**-0.115**
H49	**H61**	**0.115**	**0.115**
H50	**H61**	**0.115**	**0.115**
H51	**H61**	**0.115**	**0.115**
H52	**H61**	**0.115**	**0.115**
H53	**H61**	**0.115**	**0.115**

Subsequent is the pyroglutamate-NMA, whose structure, atom names, atom types, and charges are shown in Figure 114 and Table 17.[4,158,159,160,161,162,163,164,165,166,167]

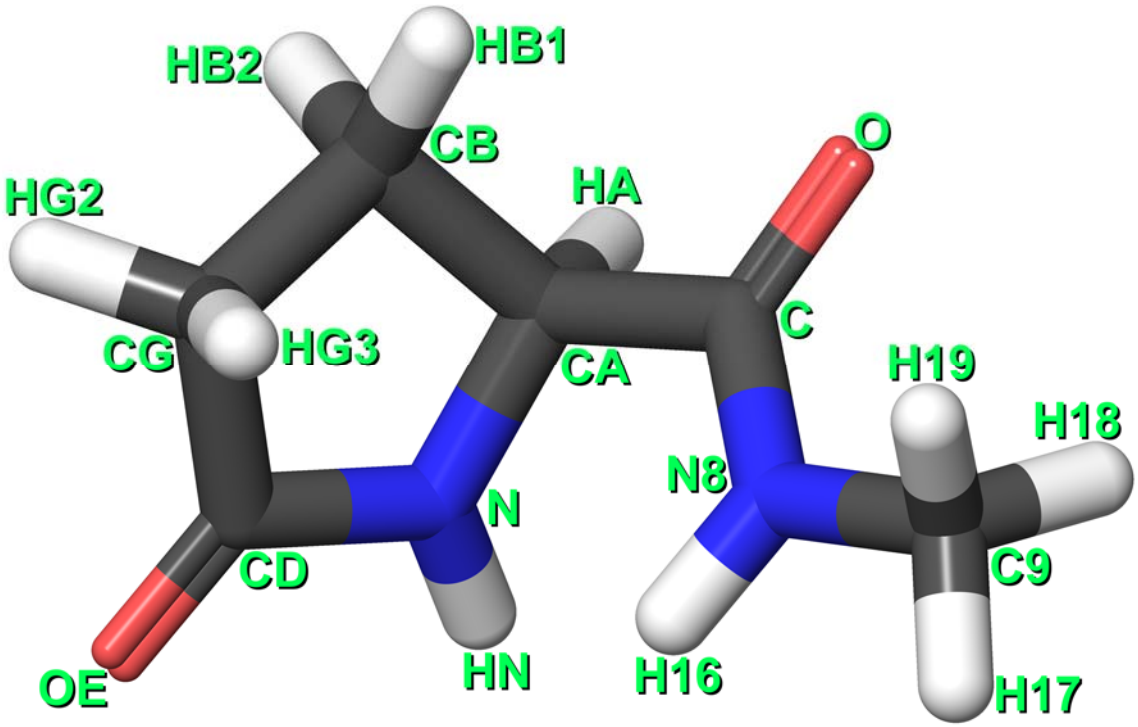

Figure 114. Structure and Atom Names of Pyroglutamate-NMA.[4,158,159,160,161,162,163,164,165,166,167]

Table 17

Atom Names, Atom Types, and Charges of Pyroglutamate-NMA.[4,158,159,160,161,162,163,164,165,166,167]

Pyroglutamate-NMA Charges			
Atom Name	***Atom Type***	***Old Charges***	***New Charges***
		Group	***Group***
N	**NH1**	**-0.596**	***-0.580***
HN	**H**	**0.371**	***0.360***
CA	**CTY1**	**0.163**	***0.160***
HA	**HBY**	**0.090**	**0.090**
CB	**CTY2**	**-0.192**	***-0.190***
HB2	**HAY**	**0.090**	**0.090**
HB1	**HAY**	**0.090**	**0.090**
CG	**CTY2**	**-0.011**	***-0.010***

Table 17

Cont.

Pyroglutamate-NMA Charges			
Atom Name	***Atom Type***	***Old Charges***	***New Charges***
HG3	**HAY**	**0.090**	**0.090**
HG2	**HAY**	**0.090**	**0.090**
CD	**CCY**	**0.299**	***0.300***
OE	**O**	**-0.490**	**-0.490**
			Group
C	**C**	**0.508**	***0.510***
O	**O**	**-0.500**	***-0.510***
			Group
N8	**NH1**	**-0.472**	***-0.470***
H16	**H5**	**0.310**	**0.310**
C9	**CTY3**	**-0.110**	**-0.110**
H17	**HG3**	**0.090**	**0.090**
H18	**HG3**	**0.090**	**0.090**
H19	**HG3**	**0.090**	**0.090**

These charge parameters allowed the bond length, bond angle, and dihedral torsion parameters to be determined.[4,137,158,159,160,161,162,163,164,165,166,167]

CHARMM Bond Length, Bond Angle, Urey-Bradley, Dihedral, and Improper Dihedral Parameters

The bond length, bond angle, Urey-Bradley, dihedral torsion, and improper torsion parameters were initially taken from the CGenFF force field and were the starting point for the purposes of recursively optimizing the bond length and bond angle parameters, with measurement comparisons for the bond lengths as done for SB-674042 before and after recursively optimizing bonds and angles together, then dihedrals, and listing the bond lengths outside the margin of error as highlighted olive, boxed, and

italicized, with the SB-674042 bond lengths before this optimization compiled in Table 18.[137,158,159,160,161,162,163,164,165,166,167]

Table 18

SB-674042 Bond Lengths Prior to Optimization[137,158,159,160,161,162,163,164,165,166,167]

SB-674042 Length Test Before CHARMM Optimization					
Bond	***QM Length***	***MM Length***	***Difference***	***Square***	***Check***
(atoms)	***(angstroms)***	***(angstroms)***	***(angstroms)***	***(sq. Å)***	***(angstroms^{-1})***
C1 -H8	**1.0744**	**1.0808**	**0.0064**	**0.0000**	**#DIV/0!**
C1 -C2	**1.3856**	**1.3999**	**0.0143**	**0.0002**	**#DIV/0!**
C2 -H9	**1.0745**	**1.0815**	**0.0070**	**0.0000**	**#DIV/0!**
C2 -C3	**1.3834**	**1.4001**	**0.0167**	**0.0003**	**#DIV/0!**
C3 -H10	**1.0747**	**1.0798**	**0.0051**	**0.0000**	**#DIV/0!**
C3 -C4	**1.3922**	**1.4042**	**0.0120**	**0.0001**	**#DIV/0!**
C1 -C6	**1.3838**	**1.4019**	**0.0181**	**0.0003**	**#DIV/0!**
C6 -H11	**1.0738**	**1.0790**	**0.0052**	**0.0000**	**#DIV/0!**
C6 -C5	**1.3762**	**1.3922**	**0.0159**	**0.0003**	**#DIV/0!**
C5 -F7	**1.3317**	**1.3608**	**0.0291**	**0.0008**	**#DIV/0!**
C5 -C4	**1.3855**	**1.4018**	**0.0163**	**0.0003**	**#DIV/0!**
C4 -C18	**1.4784**	**1.4847**	**0.0063**	**0.0000**	**#DIV/0!**
C18-S17	**1.7409**	**1.7136**	**-0.0273**	**0.0007**	**#DIV/0!**
C16-S17	***1.7371***	***1.6978***	***-0.0394***	***0.0015***	***100106.95187***
C18-C14	***1.3470***	***1.3829***	***0.0359***	***0.0013***	***100168.91892***
N15-C14	***1.3783***	***1.4231***	***0.0448***	***0.0020***	***100067.61325***
N15-C16	***1.2757***	***1.3171***	***0.0414***	***0.0017***	***100088.02817***
C16-C19	**1.4993**	**1.4942**	**-0.0051**	**0.0000**	**#DIV/0!**
C19-H20	***1.0809***	***1.1114***	***0.0305***	***0.0009***	***102222.22222***
C19-H21	**1.0843**	**1.1095**	**0.0252**	**0.0006**	**#DIV/0!**
C19-H22	**1.0838**	**1.1095**	**0.0257**	**0.0007**	**#DIV/0!**
C14-C12	**1.5029**	**1.5106**	**0.0077**	**0.0001**	**#DIV/0!**
C12-O13	**1.2045**	**1.2341**	**0.0296**	**0.0009**	**#DIV/0!**
C12-N27	**1.3477**	**1.3665**	**0.0188**	**0.0004**	**#DIV/0!**
C23-N27	**1.4655**	**1.4402**	**-0.0253**	**0.0006**	**#DIV/0!**

Table 18

Cont.

SB-674042 Length Test Before CHARMM Optimization					
Bond	***QM Length***	***MM Length***	***Difference***	***Square***	***Check***
(atoms)	***(angstroms)***	***(angstroms)***	***(angstroms)***	***(sq. Å)***	***(angstroms^{-1})***
C26-N27	**1.4646**	**1.4628**	**-0.0018**	**0.0000**	**#DIV/0!**
C26-H33	**1.0797**	**1.1019**	**0.0222**	**0.0005**	**#DIV/0!**
C26-H34	**1.0837**	**1.1033**	**0.0196**	**0.0004**	**#DIV/0!**
C26-C25	**1.5275**	**1.5230**	**-0.0045**	**0.0000**	**#DIV/0!**
C25-C24	**1.5289**	**1.5363**	**0.0074**	**0.0001**	**#DIV/0!**
C25-H31	**1.0834**	**1.0981**	**0.0147**	**0.0002**	**#DIV/0!**
C25-H32	**1.0859**	**1.1023**	**0.0164**	**0.0003**	**#DIV/0!**
C24-H29	**1.0828**	**1.0975**	**0.0147**	**0.0002**	**#DIV/0!**
C24-H30	**1.0835**	**1.1023**	**0.0188**	**0.0004**	**#DIV/0!**
C24-C23	**1.5357**	**1.5329**	**-0.0028**	**0.0000**	**#DIV/0!**
C23-H28	**1.0838**	**1.1067**	**0.0229**	**0.0005**	**#DIV/0!**
C23-C35	**1.5397**	**1.5360**	**-0.0037**	**0.0000**	**#DIV/0!**
C35-H36	**1.0806**	**1.1099**	**0.0293**	**0.0009**	**#DIV/0!**
C35-H37	**1.0837**	**1.1086**	**0.0249**	**0.0006**	**#DIV/0!**
C35-C38	**1.4913**	**1.4968**	**0.0054**	**0.0000**	**#DIV/0!**
C38-O42	**1.3421**	**1.3581**	**0.0160**	**0.0003**	**#DIV/0!**
C38-N39	***1.2679***	***1.3206***	***0.0527***	***0.0028***	***100044.05286***
N39-N40	***1.3794***	***1.3036***	***-0.0758***	***0.0057***	***100021.82453***
N40-C41	***1.2704***	***1.3366***	***0.0661***	***0.0044***	***100027.66252***
C41-O42	**1.3391**	**1.3669**	**0.0278**	**0.0008**	**#DIV/0!**
C41-C46	***1.4665***	***1.5040***	***0.0375***	***0.0014***	***100133.15579***
C46-C45	**1.3889**	**1.4124**	**0.0235**	**0.0006**	**#DIV/0!**
C46-C47	**1.3918**	**1.4127**	**0.0209**	**0.0004**	**#DIV/0!**
C45-H51	**1.0732**	**1.0813**	**0.0081**	**0.0001**	**#DIV/0!**
C47-H52	**1.0735**	**1.0816**	**0.0081**	**0.0001**	**#DIV/0!**
C45-C44	**1.3857**	**1.3993**	**0.0136**	**0.0002**	**#DIV/0!**
C47-C48	**1.3825**	**1.3993**	**0.0168**	**0.0003**	**#DIV/0!**
C44-H50	**1.0756**	**1.0807**	**0.0051**	**0.0000**	**#DIV/0!**
C48-H53	**1.0746**	**1.0808**	**0.0062**	**0.0000**	**#DIV/0!**
C43-C44	**1.3848**	**1.3993**	**0.0145**	**0.0002**	**#DIV/0!**

Table 18

Cont.

SB-674042 Length Test Before CHARMM Optimization					
Bond	***QM Length***	***MM Length***	***Difference***	***Square***	***Check***
(atoms)	***(angstroms)***	***(angstroms)***	***(angstroms)***	***(sq. Å)***	***(angstroms^{-1})***
C43-C48	**1.3873**	**1.3993**	**0.0120**	**0.0001**	**#DIV/0!**
C43-H49	**1.0756**	**1.0807**	**0.0051**	**0.0000**	**#DIV/0!**
	Largest absolute error		***0.0758***	**0.0057**	***100021.82453***
		RMS error		***0.0249***	***#DIV/0!***

The SB-674042 bond lengths after this optimization, with MM bond lengths that more closely mirror the QM bond lengths, were compiled in Table 19.[137,158,159,160,161,162,163,164,165,166,167]

Table 19

SB-674042 Bond Lengths After Optimization.[137,158,159,160,161,162,163,164,165,166,167]

SB-674042 Length Test After CHARMM Optimization					
Bond	***QM Length***	***MM Length***	***Difference***	***Square***	***Check***
(atoms)	***(angstroms)***	***(angstroms)***	***(angstroms)***	***(sq. Å)***	***(angstroms^{-1})***
C1 -H8	**1.0744**	**1.0809**	**0.0065**	**0.0000**	**#DIV/0!**
C1 -C2	**1.3856**	**1.3983**	**0.0127**	**0.0002**	**#DIV/0!**
C2 -H9	**1.0745**	**1.0816**	**0.0071**	**0.0001**	**#DIV/0!**
C2 -C3	**1.3834**	**1.3991**	**0.0156**	**0.0002**	**#DIV/0!**
C3 -H10	**1.0747**	**1.0801**	**0.0054**	**0.0000**	**#DIV/0!**
C3 -C4	**1.3922**	**1.4070**	**0.0148**	**0.0002**	**#DIV/0!**
C1 -C6	**1.3838**	**1.4005**	**0.0167**	**0.0003**	**#DIV/0!**
C6 -H11	**1.0738**	**1.0791**	**0.0053**	**0.0000**	**#DIV/0!**
C6 -C5	**1.3762**	**1.3915**	**0.0153**	**0.0002**	**#DIV/0!**
C5 -F7	**1.3317**	**1.3336**	**0.0019**	**0.0000**	**#DIV/0!**

Table 19

Cont.

SB-674042 Length Test After CHARMM Optimization					
Bond	***QM Length***	***MM Length***	***Difference***	***Square***	***Check***
(atoms)	***(angstroms)***	***(angstroms)***	***(angstroms)***	***(sq. Å)***	***(angstroms^{-1})***
C5 -C4	1.3855	1.4062	0.0207	0.0004	#DIV/0!
C4 -C18	1.4784	1.4753	-0.0031	0.0000	#DIV/0!
C18-S17	1.7409	1.7228	-0.0181	0.0003	#DIV/0!
C16-S17	1.7371	1.7310	-0.0061	0.0000	#DIV/0!
C18-C14	1.3470	1.3571	0.0101	0.0001	#DIV/0!
N15-C14	1.3783	1.3888	0.0105	0.0001	#DIV/0!
N15-C16	1.2757	1.2732	-0.0025	0.0000	#DIV/0!
C16-C19	1.4993	1.4971	-0.0022	0.0000	#DIV/0!
C19-H20	1.0809	1.0827	0.0018	0.0000	#DIV/0!
C19-H21	1.0843	1.0807	-0.0036	0.0000	#DIV/0!
C19-H22	1.0838	1.0807	-0.0031	0.0000	#DIV/0!
C14-C12	1.5029	1.4920	-0.0109	0.0001	#DIV/0!
C12-O13	1.2045	1.2115	0.0070	0.0000	#DIV/0!
C12-N27	1.3477	1.3677	0.0200	0.0004	#DIV/0!
C23-N27	1.4655	1.4729	0.0074	0.0001	#DIV/0!
C26-N27	1.4646	1.4644	-0.0002	0.0000	#DIV/0!
C26-H33	1.0797	1.1019	0.0222	0.0005	#DIV/0!
C26-H34	1.0837	1.1022	0.0185	0.0003	#DIV/0!
C26-C25	1.5275	1.5300	0.0025	0.0000	#DIV/0!
C25-C24	1.5289	1.5374	0.0085	0.0001	#DIV/0!
C25-H31	1.0834	1.0978	0.0144	0.0002	#DIV/0!
C25-H32	1.0859	1.1021	0.0162	0.0003	#DIV/0!
C24-H29	1.0828	1.0977	0.0149	0.0002	#DIV/0!
C24-H30	1.0835	1.1023	0.0188	0.0004	#DIV/0!
C24-C23	1.5357	1.5252	-0.0105	0.0001	#DIV/0!
C23-H28	1.0838	1.1068	0.0230	0.0005	#DIV/0!
C23-C35	1.5397	1.5370	-0.0027	0.0000	#DIV/0!
C35-H36	1.0806	1.1094	0.0288	0.0008	#DIV/0!
C35-H37	1.0837	1.1094	0.0257	0.0007	#DIV/0!
C35-C38	1.4913	1.4916	0.0003	0.0000	#DIV/0!

Table 19

Cont.

SB-674042 Length Test After CHARMM Optimization					
Bond	***QM Length***	***MM Length***	***Difference***	***Square***	***Check***
(atoms)	***(angstroms)***	***(angstroms)***	***(angstroms)***	***(sq. Å)***	***(angstroms^{-1})***
C38-O42	**1.3421**	**1.3274**	**-0.0147**	**0.0002**	**#DIV/0!**
C38-N39	**1.2679**	**1.2640**	**-0.0039**	**0.0000**	**#DIV/0!**
N39-N40	**1.3794**	**1.3857**	**0.0063**	**0.0000**	**#DIV/0!**
N40-C41	**1.2704**	**1.2704**	**0.0000**	**0.0000**	**#DIV/0!**
C41-O42	**1.3391**	**1.3333**	**-0.0058**	**0.0000**	**#DIV/0!**
C41-C46	**1.4665**	**1.4631**	**-0.0034**	**0.0000**	**#DIV/0!**
C46-C45	**1.3889**	**1.4127**	**0.0237**	**0.0006**	**#DIV/0!**
C46-C47	**1.3918**	**1.4108**	**0.0190**	**0.0004**	**#DIV/0!**
C45-H51	**1.0732**	**1.0808**	**0.0076**	**0.0001**	**#DIV/0!**
C47-H52	**1.0735**	**1.0811**	**0.0076**	**0.0001**	**#DIV/0!**
C45-C44	**1.3857**	**1.4003**	**0.0146**	**0.0002**	**#DIV/0!**
C47-C48	**1.3825**	**1.4005**	**0.0180**	**0.0003**	**#DIV/0!**
C44-H50	**1.0756**	**1.0806**	**0.0050**	**0.0000**	**#DIV/0!**
C48-H53	**1.0746**	**1.0808**	**0.0062**	**0.0000**	**#DIV/0!**
C43-C44	**1.3848**	**1.4011**	**0.0162**	**0.0003**	**#DIV/0!**
C43-C48	**1.3873**	**1.4013**	**0.0140**	**0.0002**	**#DIV/0!**
C43-H49	**1.0756**	**1.0806**	**0.0050**	**0.0000**	**#DIV/0!**
	Largest absolute error		***0.0288***	**0.0008**	***#DIV/0!***
		RMS error		***0.0129***	***#DIV/0!***

The same was done for pyroglutamate-NMA's bond lengths before and after recursively optimizing bonds and angles, then dihedrals, and listing the bond lengths outside the margin of error as highlighted olive, boxed, and italicized, with the pyroglutamate-NMA bond lengths before this optimization shown in Table 20.[4,158,159,160,161,162,163,164,165,166,167]

Table 20

Pyroglutamate-NMA Bond Lengths Prior to Optimization.[4,158,159,160,161,162,163,164,165,166,167]

Pyroglutamate-NMA Length Test Before CHARMM Optimization					
Bond	***QM Length***	***MM Length***	***Difference***	***Square***	***Check***
(atoms)	***(angstroms)***	***(angstroms)***	***(angstroms)***	***(sq. Å)***	***(angstroms^{-1})***
OE -CD	***1.1933***	***1.2251***	***0.0318***	***0.0010***	***100549.45055***
CD -N	**1.3636**	**1.3754**	**0.0118**	**0.0001**	**#DIV/0!**
N -HN	**0.9963**	**0.9957**	**-0.0006**	**0.0000**	**#DIV/0!**
N -CA	**1.4463**	**1.4692**	**0.0229**	**0.0005**	**#DIV/0!**
CD -CG	**1.5185**	**1.5253**	**0.0068**	**0.0000**	**#DIV/0!**
CG -HG2	**1.0811**	**1.0979**	**0.0168**	**0.0003**	**#DIV/0!**
CG -HG3	**1.0862**	**1.0985**	**0.0123**	**0.0002**	**#DIV/0!**
CG -CB	**1.5328**	**1.5252**	**-0.0076**	**0.0001**	**#DIV/0!**
CB -HB1	**1.0799**	**1.1001**	**0.0201**	**0.0004**	**#DIV/0!**
CB -HB2	**1.0835**	**1.1031**	**0.0196**	**0.0004**	**#DIV/0!**
CB -CA	**1.5493**	**1.5276**	**-0.0217**	**0.0005**	**#DIV/0!**
CA -HA	**1.0821**	**1.1015**	**0.0194**	**0.0004**	**#DIV/0!**
CA -C	**1.5294**	**1.5208**	**-0.0086**	**0.0001**	**#DIV/0!**
C -O	**1.2030**	**1.2279**	**0.0249**	**0.0006**	**#DIV/0!**
C -N8	**1.3415**	**1.3478**	**0.0063**	**0.0000**	**#DIV/0!**
N8 -H16	**0.9924**	**0.9966**	**0.0042**	**0.0000**	**#DIV/0!**
N8 -C9	**1.4475**	**1.4442**	**-0.0033**	**0.0000**	**#DIV/0!**
C9 -H17	***1.0815***	***1.1124***	***0.0309***	***0.0010***	***101111.11111***
C9 -H18	***1.0816***	***1.1141***	***0.0325***	***0.0011***	***100404.85830***
C9 -H19	***1.0833***	***1.1141***	***0.0308***	***0.0009***	***101282.05128***
	Largest absolute error		***0.0325***	**0.0011**	***100404.85830***
		RMS error		***0.0195***	***#DIV/0!***

The pyroglutamate-NMA bond lengths after this optimization, with MM bond lengths more closely approximating the QM bond lengths, were compiled in Table 21.[4,158,159,160,161,162,163,164,165,166,167]

Table 21

Pyroglutamate-NMA Bond Lengths After Optimization.[4,158,159,160,161,162,163,164,165,166,167]

Pyroglutamate-NMA Length Test After CHARMM Optimization					
Bond	***QM Length***	***MM Length***	***Difference***	***Square***	***Check***
(atoms)	***(angstroms)***	***(angstroms)***	***(angstroms)***	***(sq. Å)***	***(angstroms^{-1})***
OE -CD	**1.1933**	**1.1908**	**-0.0025**	**0.0000**	**#DIV/0!**
CD -N	**1.3636**	**1.3764**	**0.0128**	**0.0002**	**#DIV/0!**
N -HN	**0.9963**	**0.9960**	**-0.0003**	**0.0000**	**#DIV/0!**
N -CA	**1.4463**	**1.4678**	**0.0215**	**0.0005**	**#DIV/0!**
CD -CG	**1.5185**	**1.5282**	**0.0096**	**0.0001**	**#DIV/0!**
CG -HG2	**1.0811**	**1.0978**	**0.0167**	**0.0003**	**#DIV/0!**
CG -HG3	**1.0862**	**1.0984**	**0.0121**	**0.0001**	**#DIV/0!**
CG -CB	**1.5328**	**1.5276**	**-0.0052**	**0.0000**	**#DIV/0!**
CB -HB1	**1.0799**	**1.0999**	**0.0200**	**0.0004**	**#DIV/0!**
CB -HB2	**1.0835**	**1.1031**	**0.0196**	**0.0004**	**#DIV/0!**
CB -CA	**1.5493**	**1.5238**	**-0.0255**	**0.0006**	**#DIV/0!**
CA -HA	**1.0821**	**1.1002**	**0.0181**	**0.0003**	**#DIV/0!**
CA -C	**1.5294**	**1.5228**	**-0.0066**	**0.0000**	**#DIV/0!**
C -O	**1.2030**	**1.2280**	**0.0250**	**0.0006**	**#DIV/0!**
C -N8	**1.3415**	**1.3479**	**0.0064**	**0.0000**	**#DIV/0!**
N8 -H16	**0.9924**	**0.9976**	**0.0052**	**0.0000**	**#DIV/0!**
N8 -C9	**1.4475**	**1.4447**	**-0.0028**	**0.0000**	**#DIV/0!**
C9 -H17	**1.0815**	**1.0821**	**0.0006**	**0.0000**	**#DIV/0!**
C9 -H18	**1.0816**	**1.0833**	**0.0017**	**0.0000**	**#DIV/0!**
C9 -H19	**1.0833**	**1.0833**	**0.0000**	**0.0000**	**#DIV/0!**
	Largest absolute error		***0.0255***	**0.0006**	***#DIV/0!***
		RMS error		***0.0136***	***#DIV/0!***

Similar measurement comparisons for the bond angles before and after recursively optimizing bonds and angles, then dihedrals, were done for SB-674042, and listing the bond angles outside the margin of error as highlighted olive, boxed, and italicized, with its bond angles before this optimization listed in Table 22.[137,158,159,160,161,162,163,164,165,166,167]

Table 22

SB-674042 Bond Angles Before Optimization.[137,158,159,160,161,162,163,164,165,166,167]

SB-674042 Angle Test Before CHARMM Optimization					
Angle	***QM Angle***	***MM Angle***	***Difference***	***Square***	***Check***
(atoms)	***(degrees)***	***(degrees)***	***(degrees)***	***(sq. deg.)***	***(degrees^{-1})***
C2 -C1 -H8	120.31	119.95	-0.36	0.13	#DIV/0!
C6 -C1 -H8	119.69	120.19	0.50	0.25	#DIV/0!
C2 -C1 -C6	120.00	119.86	-0.14	0.02	#DIV/0!
C1 -C2 -H9	120.31	119.76	-0.56	0.31	#DIV/0!
C1 -C6 -H11	121.99	120.65	-1.34	1.79	#DIV/0!
C1 -C2 -C3	119.85	120.48	0.63	0.40	#DIV/0!
C1 -C6 -C5	118.97	119.13	0.16	0.03	#DIV/0!
H9 -C2 -C3	119.83	119.76	-0.07	0.00	#DIV/0!
H11-C6 -C5	119.04	120.22	1.17	1.38	#DIV/0!
C2 -C3 -C4	121.30	120.12	-1.18	1.39	#DIV/0!
C6 -C5 -C4	122.76	121.87	-0.89	0.79	#DIV/0!
C2 -C3 -H10	119.71	120.06	0.35	0.12	#DIV/0!
C6 -C5 -F7	118.08	117.91	-0.18	0.03	#DIV/0!
H10-C3 -C4	118.98	119.82	0.84	0.70	#DIV/0!
F7 -C5 -C4	119.16	120.22	1.06	1.13	#DIV/0!
C3 -C4 -C18	121.36	120.42	-0.95	0.89	#DIV/0!
C5 -C4 -C18	121.50	121.05	-0.46	0.21	#DIV/0!
C3 -C4 -C5	117.12	118.54	1.41	1.99	#DIV/0!
C4 -C18-C14	130.62	129.78	-0.83	0.69	#DIV/0!
C4 -C18-S17	121.03	120.04	-0.99	0.98	#DIV/0!
C14-C18-S17	108.34	109.92	1.58	2.48	#DIV/0!
C18-S17-C16	89.59	90.34	0.75	0.56	#DIV/0!
S17-C16-N15	113.87	116.44	2.57	6.58	#DIV/0!
S17-C16-C19	122.23	123.18	0.95	0.91	#DIV/0!
N15-C16-C19	*123.90*	*120.24*	*-3.66*	*13.42*	*100001.50830*
C16-N15-C14	111.99	109.00	-2.99	8.94	#DIV/0!
C16-C19-H20	108.63	109.90	1.26	1.60	#DIV/0!
C16-C19-H21	110.90	109.54	-1.36	1.86	#DIV/0!
C16-C19-H22	111.19	110.41	-0.78	0.61	#DIV/0!

Table 22

Cont.

SB-674042 Angle Test Before CHARMM Optimization					
Angle	***QM Angle***	***MM Angle***	***Difference***	***Square***	***Check***
(atoms)	***(degrees)***	***(degrees)***	***(degrees)***	***(sq. deg.)***	***(degrees^{-1})***
H20-C19-H21	109.04	108.82	-0.22	0.05	#DIV/0!
H20-C19-H22	109.07	108.74	-0.33	0.11	#DIV/0!
H21-C19-H22	107.96	109.41	1.45	2.09	#DIV/0!
N15-C14-C18	116.19	114.21	-1.98	3.91	#DIV/0!
C12-C14-C18	124.80	126.24	1.44	2.07	#DIV/0!
N15-C14-C12	118.90	119.40	0.50	0.25	#DIV/0!
C14-C12-O13	120.09	119.16	-0.93	0.86	#DIV/0!
N27-C12-O13	122.65	121.18	-1.47	2.17	#DIV/0!
C14-C12-N27	117.24	119.66	2.41	5.83	#DIV/0!
C12-N27-C23	119.33	121.99	2.66	7.07	#DIV/0!
C12-N27-C26	125.79	125.06	-0.73	0.54	#DIV/0!
C23-N27-C26	112.28	112.50	0.22	0.05	#DIV/0!
N27-C26-C25	102.82	103.23	0.41	0.17	#DIV/0!
N27-C26-H33	110.98	112.27	1.29	1.67	#DIV/0!
N27-C26-H34	110.60	108.11	-2.49	6.19	#DIV/0!
C25-C26-H33	112.68	113.14	0.46	0.21	#DIV/0!
C25-C26-H34	111.53	111.84	0.32	0.10	#DIV/0!
H33-C26-H34	108.20	108.14	-0.06	0.00	#DIV/0!
C26-C25-C24	102.89	102.71	-0.18	0.03	#DIV/0!
C26-C25-H31	112.49	113.40	0.91	0.83	#DIV/0!
C26-C25-H32	109.63	109.95	0.32	0.10	#DIV/0!
C24-C25-H31	113.15	113.34	0.20	0.04	#DIV/0!
C24-C25-H32	110.48	110.18	-0.30	0.09	#DIV/0!
H31-C25-H32	108.14	107.24	-0.90	0.81	#DIV/0!
C25-C24-C23	104.01	104.79	0.78	0.60	#DIV/0!
C25-C24-H29	113.30	113.10	-0.19	0.04	#DIV/0!
C25-C24-H30	110.10	109.37	-0.73	0.54	#DIV/0!
C23-C24-H29	111.39	112.95	1.56	2.44	#DIV/0!
C23-C24-H30	110.39	110.16	-0.23	0.05	#DIV/0!
H29-C24-H30	107.66	106.49	-1.18	1.38	#DIV/0!

Table 22

Cont.

SB-674042 Angle Test Before CHARMM Optimization					
Angle	***QM Angle***	***MM Angle***	***Difference***	***Square***	***Check***
(atoms)	***(degrees)***	***(degrees)***	***(degrees)***	***(sq. deg.)***	***(degrees^{-1})***
N27-C23-C24	**103.72**	**104.55**	**0.83**	**0.68**	**#DIV/0!**
N27-C23-C35	**113.26**	**111.82**	**-1.44**	**2.08**	**#DIV/0!**
N27-C23-H28	**108.58**	**110.38**	**1.80**	**3.25**	**#DIV/0!**
C24-C23-C35	**114.20**	**112.97**	**-1.23**	**1.52**	**#DIV/0!**
C24-C23-H28	**110.41**	**108.12**	**-2.29**	**5.27**	**#DIV/0!**
C35-C23-H28	**106.60**	**108.89**	**2.29**	**5.25**	**#DIV/0!**
C23-C35-C38	**114.23**	**112.56**	**-1.67**	**2.78**	**#DIV/0!**
C23-C35-H36	**109.09**	**108.79**	**-0.30**	**0.09**	**#DIV/0!**
C23-C35-H37	**108.53**	**110.27**	**1.75**	**3.05**	**#DIV/0!**
C38-C35-H36	**108.76**	**107.40**	**-1.36**	**1.85**	**#DIV/0!**
C38-C35-H37	**107.60**	**109.48**	**1.88**	**3.54**	**#DIV/0!**
H36-C35-H37	**108.49**	**108.20**	**-0.29**	**0.08**	**#DIV/0!**
C35-C38-O42	***119.36***	***124.57***	***5.21***	***27.17***	***100000.45196***
C35-C38-N39	***129.00***	***122.13***	***-6.87***	***47.18***	***100000.25850***
O42-C38-N39	**111.65**	**113.13**	**1.48**	**2.19**	**#DIV/0!**
C38-O42-C41	**103.39**	**100.83**	**-2.56**	**6.57**	**#DIV/0!**
C38-N39-N40	**106.72**	**106.77**	**0.05**	**0.00**	**#DIV/0!**
N39-N40-C41	**106.45**	**108.11**	**1.66**	**2.76**	**#DIV/0!**
N40-C41-O42	**111.79**	**111.15**	**-0.64**	**0.41**	**#DIV/0!**
N40-C41-C46	***128.58***	***125.09***	***-3.49***	***12.21***	***100002.02347***
O42-C41-C46	***119.62***	***123.75***	***4.13***	***17.07***	***100000.88355***
C41-C46-C45	**120.72**	**120.18**	**-0.54**	**0.29**	**#DIV/0!**
C41-C46-C47	**119.27**	**121.57**	**2.29**	**5.26**	**#DIV/0!**
C45-C46-C47	**120.01**	**118.25**	**-1.76**	**3.10**	**#DIV/0!**
C46-C45-H51	**119.95**	**119.78**	**-0.17**	**0.03**	**#DIV/0!**
C46-C45-C44	**119.78**	**120.88**	**1.10**	**1.20**	**#DIV/0!**
H51-C45-C44	**120.27**	**119.34**	**-0.93**	**0.86**	**#DIV/0!**
C46-C47-H52	**119.39**	**119.65**	**0.26**	**0.07**	**#DIV/0!**
C46-C47-C48	**119.90**	**120.85**	**0.94**	**0.89**	**#DIV/0!**
H52-C47-C48	**120.71**	**119.51**	**-1.20**	**1.45**	**#DIV/0!**

Table 22

Cont.

SB-674042 Angle Test Before CHARMM Optimization					
Angle	***QM Angle***	***MM Angle***	***Difference***	***Square***	***Check***
(atoms)	***(degrees)***	***(degrees)***	***(degrees)***	***(sq. deg.)***	***(degrees^{-1})***
C45-C44-C43	**120.19**	**119.99**	**-0.20**	**0.04**	**#DIV/0!**
C45-C44-H50	**119.66**	**120.00**	**0.34**	**0.12**	**#DIV/0!**
H50-C44-C43	**120.15**	**120.02**	**-0.13**	**0.02**	**#DIV/0!**
C47-C48-C43	**120.10**	**120.01**	**-0.09**	**0.01**	**#DIV/0!**
C47-C48-H53	**119.79**	**119.95**	**0.16**	**0.02**	**#DIV/0!**
H53-C48-C43	**120.11**	**120.05**	**-0.07**	**0.00**	**#DIV/0!**
C44-C43-C48	**120.02**	**120.03**	**0.01**	**0.00**	**#DIV/0!**
C44-C43-H49	**119.99**	**120.01**	**0.03**	**0.00**	**#DIV/0!**
C48-C43-H49	**119.99**	**119.96**	**-0.04**	**0.00**	**#DIV/0!**
	Largest absolute error		***6.87***	**47.18**	***100000.25850***
		RMS error		***1.59***	***#DIV/0!***

The SB-674042 bond angles after this optimization, with MM bond angles that more closely match the QM bond angles, were compiled as follows in Table 23.[137,158,159,160,161,162,163,164,165,166,167]

Table 23

SB-674042 Bond Angles After Optimization.[137,158,159,160,161,162,163,164,165,166,167]

SB-674042 Angle Test After CHARMM Optimization					
Angle	***QM Angle***	***MM Angle***	***Difference***	***Square***	***Check***
(atoms)	***(degrees)***	***(degrees)***	***(degrees)***	***(sq. deg.)***	***(degrees^{-1})***
C2 -C1 -H8	**120.31**	**120.00**	**-0.31**	**0.10**	**#DIV/0!**
C6 -C1 -H8	**119.69**	**120.25**	**0.56**	**0.31**	**#DIV/0!**
C2 -C1 -C6	**120.00**	**119.75**	**-0.25**	**0.06**	**#DIV/0!**

Table 23

Cont.

SB-674042 Angle Test After CHARMM Optimization					
Angle	***QM Angle***	***MM Angle***	***Difference***	***Square***	***Check***
(atoms)	***(degrees)***	***(degrees)***	***(degrees)***	***(sq. deg.)***	***(degrees^{-1})***
C1 -C2 -H9	120.31	119.79	-0.52	0.27	#DIV/0!
C1 -C6 -H11	121.99	120.61	-1.38	1.92	#DIV/0!
C1 -C2 -C3	119.85	120.42	0.57	0.32	#DIV/0!
C1 -C6 -C5	118.97	119.18	0.21	0.04	#DIV/0!
H9 -C2 -C3	119.83	119.79	-0.04	0.00	#DIV/0!
H11-C6 -C5	119.04	120.22	1.17	1.38	#DIV/0!
C2 -C3 -C4	121.30	120.78	-0.52	0.27	#DIV/0!
C6 -C5 -C4	122.76	122.36	-0.40	0.16	#DIV/0!
C2 -C3 -H10	119.71	119.71	0.00	0.00	#DIV/0!
C6 -C5 -F7	118.08	117.25	-0.84	0.70	#DIV/0!
H10-C3 -C4	118.98	119.51	0.53	0.28	#DIV/0!
F7 -C5 -C4	119.16	120.34	1.19	1.41	#DIV/0!
C3 -C4 -C18	121.36	120.45	-0.92	0.84	#DIV/0!
C5 -C4 -C18	121.50	121.91	0.41	0.17	#DIV/0!
C3 -C4 -C5	117.12	117.50	0.37	0.14	#DIV/0!
C4 -C18-C14	130.62	130.88	0.27	0.07	#DIV/0!
C4 -C18-S17	121.03	121.41	0.38	0.14	#DIV/0!
C14-C18-S17	108.34	107.49	-0.86	0.74	#DIV/0!
C18-S17-C16	89.59	90.89	1.29	1.67	#DIV/0!
S17-C16-N15	113.87	113.63	-0.24	0.06	#DIV/0!
S17-C16-C19	122.23	122.30	0.08	0.01	#DIV/0!
N15-C16-C19	123.90	124.07	0.17	0.03	#DIV/0!
C16-N15-C14	111.99	111.48	-0.51	0.26	#DIV/0!
C16-C19-H20	108.63	110.06	1.42	2.03	#DIV/0!
C16-C19-H21	110.90	109.68	-1.23	1.50	#DIV/0!
C16-C19-H22	111.19	109.71	-1.48	2.19	#DIV/0!
H20-C19-H21	109.04	109.00	-0.04	0.00	#DIV/0!
H20-C19-H22	109.07	108.85	-0.23	0.05	#DIV/0!
H21-C19-H22	107.96	109.54	1.57	2.47	#DIV/0!

Table 23

Cont.

SB-674042 Angle Test After CHARMM Optimization					
Angle	***QM Angle***	***MM Angle***	***Difference***	***Square***	***Check***
(atoms)	***(degrees)***	***(degrees)***	***(degrees)***	***(sq. deg.)***	***(degrees^{-1})***
N15-C14-C18	**116.19**	**116.51**	**0.32**	**0.10**	**#DIV/0!**
C12-C14-C18	**124.80**	**122.65**	**-2.15**	**4.64**	**#DIV/0!**
N15-C14-C12	**118.90**	**120.65**	**1.74**	**3.04**	**#DIV/0!**
C14-C12-O13	**120.09**	**119.02**	**-1.07**	**1.14**	**#DIV/0!**
N27-C12-O13	**122.65**	**121.40**	**-1.25**	**1.55**	**#DIV/0!**
C14-C12-N27	**117.24**	**119.56**	**2.32**	**5.36**	**#DIV/0!**
C12-N27-C23	**119.33**	**122.16**	**2.83**	**8.03**	**#DIV/0!**
C12-N27-C26	**125.79**	**124.01**	**-1.78**	**3.18**	**#DIV/0!**
C23-N27-C26	**112.28**	**111.89**	**-0.39**	**0.15**	**#DIV/0!**
N27-C26-C25	**102.82**	**103.35**	**0.53**	**0.28**	**#DIV/0!**
N27-C26-H33	**110.98**	**112.47**	**1.50**	**2.25**	**#DIV/0!**
N27-C26-H34	**110.60**	**108.07**	**-2.53**	**6.41**	**#DIV/0!**
C25-C26-H33	**112.68**	**112.96**	**0.28**	**0.08**	**#DIV/0!**
C25-C26-H34	**111.53**	**111.80**	**0.28**	**0.08**	**#DIV/0!**
H33-C26-H34	**108.20**	**108.09**	**-0.11**	**0.01**	**#DIV/0!**
C26-C25-C24	**102.89**	**102.64**	**-0.25**	**0.06**	**#DIV/0!**
C26-C25-H31	**112.49**	**113.26**	**0.77**	**0.59**	**#DIV/0!**
C26-C25-H32	**109.63**	**110.03**	**0.40**	**0.16**	**#DIV/0!**
C24-C25-H31	**113.15**	**113.34**	**0.20**	**0.04**	**#DIV/0!**
C24-C25-H32	**110.48**	**110.29**	**-0.19**	**0.04**	**#DIV/0!**
H31-C25-H32	**108.14**	**107.27**	**-0.87**	**0.75**	**#DIV/0!**
C25-C24-C23	**104.01**	**103.56**	**-0.45**	**0.20**	**#DIV/0!**
C25-C24-H29	**113.30**	**113.26**	**-0.04**	**0.00**	**#DIV/0!**
C25-C24-H30	**110.10**	**109.67**	**-0.43**	**0.18**	**#DIV/0!**
C23-C24-H29	**111.39**	**113.07**	**1.68**	**2.84**	**#DIV/0!**
C23-C24-H30	**110.39**	**110.52**	**0.13**	**0.02**	**#DIV/0!**
H29-C24-H30	**107.66**	**106.78**	**-0.88**	**0.77**	**#DIV/0!**
N27-C23-C24	**103.72**	**103.89**	**0.16**	**0.03**	**#DIV/0!**
N27-C23-C35	**113.26**	**114.39**	**1.12**	**1.26**	**#DIV/0!**

Table 23

Cont.

SB-674042 Angle Test After CHARMM Optimization					
Angle	***QM Angle***	***MM Angle***	***Difference***	***Square***	***Check***
(atoms)	***(degrees)***	***(degrees)***	***(degrees)***	***(sq. deg.)***	***(degrees^{-1})***
N27-C23-H28	**108.58**	**107.74**	**-0.85**	**0.72**	**#DIV/0!**
C24-C23-C35	**114.20**	**113.62**	**-0.58**	**0.34**	**#DIV/0!**
C24-C23-H28	**110.41**	**110.17**	**-0.25**	**0.06**	**#DIV/0!**
C35-C23-H28	**106.60**	**106.93**	**0.33**	**0.11**	**#DIV/0!**
C23-C35-C38	**114.23**	**112.84**	**-1.39**	**1.92**	**#DIV/0!**
C23-C35-H36	**109.09**	**109.66**	**0.56**	**0.32**	**#DIV/0!**
C23-C35-H37	**108.53**	**109.35**	**0.82**	**0.67**	**#DIV/0!**
C38-C35-H36	**108.76**	**108.48**	**-0.29**	**0.08**	**#DIV/0!**
C38-C35-H37	**107.60**	**108.53**	**0.94**	**0.87**	**#DIV/0!**
H36-C35-H37	**108.49**	**107.86**	**-0.63**	**0.39**	**#DIV/0!**
C35-C38-O42	**119.36**	**119.39**	**0.03**	**0.00**	**#DIV/0!**
C35-C38-N39	**129.00**	**127.32**	**-1.68**	**2.81**	**#DIV/0!**
O42-C38-N39	**111.65**	**113.29**	**1.64**	**2.70**	**#DIV/0!**
C38-O42-C41	**103.39**	**102.78**	**-0.61**	**0.38**	**#DIV/0!**
C38-N39-N40	**106.72**	**105.43**	**-1.28**	**1.65**	**#DIV/0!**
N39-N40-C41	**106.45**	**106.32**	**-0.13**	**0.02**	**#DIV/0!**
N40-C41-O42	**111.79**	**112.16**	**0.37**	**0.13**	**#DIV/0!**
N40-C41-C46	**128.58**	**128.57**	**-0.02**	**0.00**	**#DIV/0!**
O42-C41-C46	**119.62**	**119.27**	**-0.35**	**0.12**	**#DIV/0!**
C41-C46-C45	**120.72**	**120.72**	**0.00**	**0.00**	**#DIV/0!**
C41-C46-C47	**119.27**	**119.26**	**-0.01**	**0.00**	**#DIV/0!**
C45-C46-C47	**120.01**	**120.01**	**0.00**	**0.00**	**#DIV/0!**
C46-C45-H51	**119.95**	**120.79**	**0.84**	**0.70**	**#DIV/0!**
C46-C45-C44	**119.78**	**119.67**	**-0.12**	**0.01**	**#DIV/0!**
H51-C45-C44	**120.27**	**119.54**	**-0.73**	**0.53**	**#DIV/0!**
C46-C47-H52	**119.39**	**120.48**	**1.10**	**1.20**	**#DIV/0!**
C46-C47-C48	**119.90**	**119.68**	**-0.22**	**0.05**	**#DIV/0!**
H52-C47-C48	**120.71**	**119.83**	**-0.88**	**0.77**	**#DIV/0!**
C45-C44-C43	**120.19**	**120.19**	**0.00**	**0.00**	**#DIV/0!**

Table 23

Cont.

SB-674042 Angle Test After CHARMM Optimization					
Angle	***QM Angle***	***MM Angle***	***Difference***	***Square***	***Check***
(atoms)	***(degrees)***	***(degrees)***	***(degrees)***	***(sq. deg.)***	***(degrees^{-1})***
C45-C44-H50	**119.66**	**119.84**	**0.19**	**0.03**	**#DIV/0!**
H50-C44-C43	**120.15**	**119.97**	**-0.18**	**0.03**	**#DIV/0!**
C47-C48-C43	**120.10**	**120.20**	**0.10**	**0.01**	**#DIV/0!**
C47-C48-H53	**119.79**	**119.87**	**0.08**	**0.01**	**#DIV/0!**
H53-C48-C43	**120.11**	**119.93**	**-0.18**	**0.03**	**#DIV/0!**
C44-C43-C48	**120.02**	**120.25**	**0.23**	**0.05**	**#DIV/0!**
C44-C43-H49	**119.99**	**119.90**	**-0.08**	**0.01**	**#DIV/0!**
C48-C43-H49	**119.99**	**119.85**	**-0.14**	**0.02**	**#DIV/0!**
	Largest absolute error		***2.83***	**8.03**	***#DIV/0!***
		RMS error		***0.90***	***#DIV/0!***

The same was done for the angles of pyroglutamate-NMA before and after recursively optimizing bonds and angles, then dihedrals, and listing the bond angles outside the margin of error as highlighted olive, boxed, and italicized, with its bond angles prior to this optimization shown in Table 24.[4,158,159,160,161,162,163,164,165,166,167]

Table 24

Pyroglutamate-NMA Bond Angles Prior to Optimization.[4,158,159,160,161,162,163,164,165,166,167]

Pyroglutamate-NMA Angle Test Before CHARMM Optimization					
Angle	***QM Angle***	***MM Angle***	***Difference***	***Square***	***Check***
(atoms)	***(degrees)***	***(degrees)***	***(degrees)***	***(sq. deg.)***	***(degrees^{-1})***
CD -N -HN	**119.74**	**120.62**	**0.88**	**0.78**	**#DIV/0!**
CD -N -CA	**115.43**	**115.40**	**-0.04**	**0.00**	**#DIV/0!**

Table 24

Cont.

Pyroglutamate-NMA Angle Test Before CHARMM Optimization					
Angle	***QM Angle***	***MM Angle***	***Difference***	***Square***	***Check***
(atoms)	***(degrees)***	***(degrees)***	***(degrees)***	***(sq. deg.)***	***(degrees^{-1})***
CA -N -HN	123.42	123.95	0.53	0.28	#DIV/0!
N -CD -CG	106.82	106.13	-0.69	0.47	#DIV/0!
N -CD -OE	125.49	125.77	0.28	0.08	#DIV/0!
CG -CD -OE	127.68	128.03	0.35	0.13	#DIV/0!
CD -CG -CB	103.99	103.15	-0.85	0.71	#DIV/0!
CD -CG -HG2	110.30	111.40	1.11	1.23	#DIV/0!
CD -CG -HG3	108.19	109.55	1.36	1.85	#DIV/0!
CB -CG -HG2	114.25	113.16	-1.09	1.19	#DIV/0!
CB -CG -HG3	112.21	112.07	-0.13	0.02	#DIV/0!
HG2-CG -HG3	107.75	107.50	-0.25	0.06	#DIV/0!
CG -CB -CA	104.19	105.89	1.69	2.86	#DIV/0!
CG -CB -HB1	114.26	112.52	-1.74	3.04	#DIV/0!
CG -CB -HB2	109.87	109.84	-0.03	0.00	#DIV/0!
CA -CB -HB1	111.68	113.16	1.48	2.18	#DIV/0!
CA -CB -HB2	108.83	109.43	0.60	0.36	#DIV/0!
HB1-CB -HB2	107.89	106.01	-1.88	3.53	#DIV/0!
CB -CA -N	102.71	101.22	-1.48	2.20	#DIV/0!
CB -CA -C	*111.35*	*114.48*	*3.12*	*9.76*	*100008.02568*
CB -CA -HA	110.80	109.89	-0.91	0.83	#DIV/0!
N -CA -C	115.26	114.46	-0.80	0.64	#DIV/0!
N -CA -HA	111.33	109.43	-1.89	3.59	#DIV/0!
C -CA -HA	105.53	107.24	1.72	2.94	#DIV/0!
CA -C -O	119.14	119.21	0.07	0.01	#DIV/0!
CA -C -N8	117.45	118.36	0.91	0.83	#DIV/0!
N8 -C -O	123.42	122.43	-0.98	0.97	#DIV/0!
C -N8 -C9	121.37	122.13	0.77	0.59	#DIV/0!
C -N8 -H16	118.88	119.14	0.26	0.07	#DIV/0!
C9 -N8 -H16	119.71	118.61	-1.10	1.22	#DIV/0!
N8 -C9 -H17	108.63	110.59	1.96	3.84	#DIV/0!

Table 24

Cont.

Pyroglutamate-NMA Angle Test Before CHARMM Optimization					
Angle	***QM Angle***	***MM Angle***	***Difference***	***Square***	***Check***
(atoms)	***(degrees)***	***(degrees)***	***(degrees)***	***(sq. deg.)***	***(degrees^{-1})***
N8 -C9 -H18	**110.50**	**110.73**	**0.23**	**0.05**	**#DIV/0!**
N8 -C9 -H19	**111.26**	**110.72**	**-0.54**	**0.29**	**#DIV/0!**
H17-C9 -H18	**109.10**	**108.31**	**-0.80**	**0.63**	**#DIV/0!**
H17-C9 -H19	**109.01**	**108.30**	**-0.72**	**0.51**	**#DIV/0!**
H18-C9 -H19	**108.30**	**108.10**	**-0.19**	**0.04**	**#DIV/0!**
	Largest absolute error		***3.12***	**9.76**	***100008.02568***
		RMS error		***1.15***	***#DIV/0!***

The pyroglutamate-NMA bond angles, which have the MM angle measurements more closely approximate the QM angle measurements, after this optimization of bond lengths, bond angles, and dihedral torsion angles, were compiled in Table 25.[4,158,159,160,161,162,163,164,165,166,167]

Table 25

Pyroglutamate-NMA Bond Angles After Optimization.[4,158,159,160,161,162,163,164,165,166,167]

Pyroglutamate-NMA Angle Test After CHARMM Optimization					
Angle	***QM Angle***	***MM Angle***	***Difference***	***Square***	***Check***
(atoms)	***(degrees)***	***(degrees)***	***(degrees)***	***(sq. deg.)***	***(degrees^{-1})***
CD -N -HN	**119.74**	**120.15**	**0.41**	**0.17**	**#DIV/0!**
CD -N -CA	**115.43**	**114.43**	**-1.00**	**1.00**	**#DIV/0!**
CA -N -HN	**123.42**	**123.83**	**0.41**	**0.17**	**#DIV/0!**
N -CD -CG	**106.82**	**106.07**	**-0.75**	**0.57**	**#DIV/0!**
N -CD -OE	**125.49**	**125.83**	**0.34**	**0.12**	**#DIV/0!**

Table 25

Cont.

Pyroglutamate-NMA Angle Test After CHARMM Optimization					
Angle	***QM Angle***	***MM Angle***	***Difference***	***Square***	***Check***
(atoms)	***(degrees)***	***(degrees)***	***(degrees)***	***(sq. deg.)***	***(degrees^{-1})***
CG -CD -OE	127.68	128.05	0.37	0.14	#DIV/0!
CD -CG -CB	103.99	102.83	-1.16	1.35	#DIV/0!
CD -CG -HG2	110.30	111.42	1.13	1.27	#DIV/0!
CD -CG -HG3	108.19	109.68	1.50	2.24	#DIV/0!
CB -CG -HG2	114.25	113.15	-1.10	1.21	#DIV/0!
CB -CG -HG3	112.21	112.16	-0.05	0.00	#DIV/0!
HG2-CG -HG3	107.75	107.58	-0.17	0.03	#DIV/0!
CG -CB -CA	104.19	104.79	0.60	0.36	#DIV/0!
CG -CB -HB1	114.26	112.73	-1.53	2.34	#DIV/0!
CG -CB -HB2	109.87	109.91	0.04	0.00	#DIV/0!
CA -CB -HB1	111.68	113.78	2.10	4.41	#DIV/0!
CA -CB -HB2	108.83	109.55	0.72	0.52	#DIV/0!
HB1-CB -HB2	107.89	106.10	-1.80	3.23	#DIV/0!
CB -CA -N	102.71	102.24	-0.47	0.22	#DIV/0!
CB -CA -C	111.35	111.28	-0.07	0.00	#DIV/0!
CB -CA -HA	110.80	112.12	1.32	1.74	#DIV/0!
N -CA -C	115.26	112.90	-2.36	5.57	#DIV/0!
N -CA -HA	111.33	112.94	1.62	2.61	#DIV/0!
C -CA -HA	105.53	105.57	0.04	0.00	#DIV/0!
CA -C -O	119.14	119.21	0.08	0.01	#DIV/0!
CA -C -N8	117.45	118.30	0.85	0.72	#DIV/0!
N8 -C -O	123.42	122.49	-0.92	0.86	#DIV/0!
C -N8 -C9	121.37	122.46	1.09	1.19	#DIV/0!
C -N8 -H16	118.88	118.58	-0.30	0.09	#DIV/0!
C9 -N8 -H16	119.71	118.93	-0.78	0.61	#DIV/0!
N8 -C9 -H17	108.63	110.45	1.81	3.29	#DIV/0!
N8 -C9 -H18	110.50	110.64	0.14	0.02	#DIV/0!
N8 -C9 -H19	111.26	110.64	-0.62	0.38	#DIV/0!
H17-C9 -H18	109.10	108.40	-0.71	0.50	#DIV/0!

Table 25

Cont.

Pyroglutamate-NMA Angle Test After CHARMM Optimization					
Angle	***QM Angle***	***MM Angle***	***Difference***	***Square***	***Check***
(atoms)	***(degrees)***	***(degrees)***	***(degrees)***	***(sq. deg.)***	***(degrees^{-1})***
H17-C9 -H19	**109.01**	**108.39**	**-0.62**	**0.39**	**#DIV/0!**
H18-C9 -H19	**108.30**	**108.25**	**-0.05**	**0.00**	**#DIV/0!**
	Largest absolute error		***2.36***	**5.57**	***#DIV/0!***
		RMS error		***1.02***	***#DIV/0!***

The resulting bond length parameters, with the repaired force constants and equilibrium lengths highlighted for increased visibility, and the parameters for pyroglutamate and SB-674042 listed after the parameters to connect pyroglutamate to peptides, are listed in Table 26.[4,137,158,159,160,161,162,163,164,165,166,167]

Table 26

Bond Length Parameters, with Repaired Parameters Highlighted.[4,137,158,159,160,161,162,163,164,165,166,167]

Bond Length Parameters			
Atom Type 1	***Atom Type 2***	***K_b (kcal mol^{-1}Å^{-2})***	***b_0 length (Å)***
NH1	**C**	**370.00**	**1.3450**
NH1	**CT1**	**320.00**	**1.4300**
NH1	**H**	**440.00**	**0.9970**
O	**C**	**620.00**	**1.2300**
N	**C**	**260.00**	**1.3000**
N	**CP1**	**320.00**	**1.4340**
N	**CP3**	**320.00**	**1.4550**
C53	**C61**	***492.73***	***1.4366***
C53	**N50**	**400.00**	**1.3200**

Table 26

Cont.

Bond Length Parameters			
Atom Type 1	*Atom Type 2*	*K_b (kcal mol^{-1}Å^{-2})*	*b_0 length (Å)*
C53	N50X	*911.70*	*1.2644*
C53	O50	450.00	1.3710
C53	O50X	*643.62*	*1.3313*
C53	HG52	340.00	1.0900
C61	C61	305.00	1.3750
C61	H61	340.00	1.0800
N50	N50	340.00	1.2900
N50X	N50X	*497.43*	*1.3833*
CO1	NG0	430.00	1.3500
CO1	OD1	*1138.69*	*1.2091*
CO1	HG52	317.13	1.1000
C53	C21	*454.61*	*1.4935*
C21	C11	222.50	1.5280
C21	HG2	309.00	1.1110
C11	C215	195.00	1.5180
C11	NG0	*420.16*	*1.4710*
C11	HG1	307.00	1.1000
C215	C215	195.00	1.5300
C215	NG0	320.00	1.4550
C215	HG2	307.00	1.1000
CO1	C51	*488.45*	*1.4678*
C51	C51	*725.64*	*1.3275*
C51	N50Y	*565.70*	*1.3501*
C51	S50Y	300.00	1.7300
C51	HG52	375.00	1.0830
C53	C31	*499.48*	1.5000
C53	N50Y	*893.91*	*1.2808*
C53	S50Y	*313.19*	*1.7920*
C31	C11	222.50	1.5280
C31	HG3	322.00	*1.0810*
C51	C61	*478.71*	*1.4652*

Table 26

Cont.

Bond Length Parameters			
Atom Type 1	*Atom Type 2*	*K_b (kcal mol^{-1}Å^{-2})*	*b_0 length (Å)*
C61	C66	305.00	1.3700
C61	H62	340.00	1.0800
C66	FR1	*638.80*	*1.3319*
C	CTY1	250.00	1.4900
CCY	CTY2	300.00	1.5300
CCY	NH1	460.00	1.3800
CCY	O	*1400.00*	*1.1949*
CTY3	NH1	320.00	1.4300
CTY3	HG3	*480.00*	*1.0803*
CTY1	CTY2	195.00	1.5180
CTY1	NH1	370.00	1.4500
CTY1	HBY	307.00	1.1000
CTY2	CTY2	195.00	1.5300
CTY2	HAY	307.00	1.1000
NH1	H5	440.00	0.9970
CO1	NG2	430.00	1.3600
NG2	HP1	480.00	1.0000

The resulting bond angle parameters, are listed in Table 27, highlighting the force constants and equilibrium angles similarly.[4,137,158,159,160,161,162,163,164,165,166,167]

Table 27

Bond Angle Parameters, with Repaired Parameters Highlighted.[4,137,158,159,160,161,162,163,164,165,166,167]

Angle Parameters				
Atom Type 1	*Atom Type 2*	*Atom Type 3*	*K_θ (kcal mol^{-1}radian^{-2})*	*θ_0 angle (degrees)*
CP1	N	C	60.000	117.0000

Table 27

Cont.

Angle Parameters				
Atom Type 1	***Atom Type 2***	***Atom Type 3***	***K_θ (kcal mol^{-1}radian^{-2})***	***θ_0 angle (degrees)***
CP3	N	C	60.000	117.0000
CP3	N	CP1	100.000	114.2000
CT1	NH1	C	50.000	120.0000
H	NH1	C	34.000	123.0000
H	NH1	CT1	35.000	117.0000
O	C	N	80.000	122.5000
O	C	NH1	80.000	122.5000
C61	C53	N50	65.000	127.8000
C61	C53	N50X	*44.980*	*129.0600*
C61	C53	O50	65.000	127.8000
C61	C53	O50X	*59.030*	*118.6900*
N50	C53	O50	120.000	115.7000
N50X	C53	O50X	120.000	115.7000
N50	C53	HG52	39.000	124.8000
N50X	C53	HG52	*46.950*	*129.5600*
O50	C53	HG52	25.000	119.5000
O50X	C53	HG52	*32.210*	*118.6900*
C53	C61	C61	*47.240*	*109.8400*
C61	C61	C61	40.000	120.0000
C61	C61	H61	30.000	120.0000
C53	N50	N50	110.000	106.8000
C53	N50X	N50X	110.000	106.8000
C53	O50	C53	140.000	104.0000
C53	O50X	C53	140.000	104.0000
NG0	CO1	OD1	80.000	124.0000
NG0	CO1	HG52	43.000	115.0000
OD1	CO1	HG52	44.000	122.0000
C21	C53	N50X	*44.460*	*128.5100*
C21	C53	O50X	*68.770*	*119.6900*
C53	C21	C11	*82.720*	*113.4100*

Table 27

Cont.

Angle Parameters				
Atom Type 1	*Atom Type 2*	*Atom Type 3*	*K_θ (kcal mol^{-1}radian^{-2})*	*θ_0 angle (degrees)*
C53	C21	HG2	55.000	109.5000
C11	C21	HG2	34.600	110.1000
HG2	C21	HG2	35.500	109.0000
C21	C11	C215	58.000	115.0000
C21	C11	NG0	94.330	113.1100
C21	C11	HG1	34.600	106.6000
C215	C11	NG0	70.000	112.0000
C215	C11	HG1	48.720	111.7700
NG0	C11	HG1	88.230	108.5300
C11	C215	C215	58.000	109.5000
C11	C215	HG2	35.000	111.4000
C215	C215	C215	58.000	109.5000
C215	C215	NG0	70.000	110.5000
C215	C215	HG2	35.000	111.4000
NG0	C215	HG2	48.000	108.0000
HG2	C215	HG2	38.500	106.8000
CO1	NG0	C11	60.000	115.9000
CO1	NG0	C215	60.000	115.0000
C11	NG0	C215	100.000	114.2000
C51	CO1	NG0	80.000	116.5000
C51	CO1	OD1	30.000	121.0000
CO1	C51	C51	90.510	122.1700
CO1	C51	N50Y	35.280	119.9100
C51	C51	N50Y	132.060	104.5500
C51	C51	S50Y	141.280	99.7100
C51	C51	HG52	22.000	130.0000
S50Y	C51	HG52	45.000	121.0000
C31	C53	N50Y	63.360	125.3200
C31	C53	S50Y	49.780	121.8800
N50Y	C53	S50Y	110.000	117.2000

Table 27

Cont.

Angle Parameters				
Atom Type 1	*Atom Type 2*	*Atom Type 3*	*K_θ (kcal $mol^{-1} radian^{-2}$)*	*θ_0 angle (degrees)*
N50	C53	S50	110.000	117.2000
C53	C31	HG3	55.000	109.5000
C11	C31	HG3	34.600	110.1000
HG3	C31	HG3	35.500	108.4000
C31	C11	C215	58.000	115.0000
C31	C11	NG0	*94.330*	*111.1100*
C31	C11	HG1	34.600	110.1000
C51	N50Y	C53	*119.130*	*102.9500*
C51	S50Y	C53	110.000	97.0000
C51	C51	C61	*49.150*	*127.1700*
C61	C51	S50Y	*49.690*	*121.2800*
N50Y	C51	HG52	25.000	120.0000
N50	C51	HG52	25.000	120.0000
C51	C61	C61	*84.170*	*121.8300*
C51	C61	C66	*52.270*	*122.7800*
C61	C61	C66	40.000	119.0000
C61	C61	H62	30.000	120.0000
C66	C61	H62	30.000	121.5000
C61	C66	C61	40.000	122.5000
C61	C66	FR1	60.000	118.7500
CTY1	C	N	80.000	116.5000
CTY1	C	NH1	80.000	116.5000
CTY1	C	O	80.000	118.0000
CTY2	CCY	NH1	120.000	105.5000
CTY2	CCY	O	65.000	126.7000
NH1	CCY	O	65.000	127.8000
NH1	CTY3	HG3	51.500	109.5000
HG3	CTY3	HG3	35.500	108.4000
C	CTY1	CTY2	*48.750*	*103.9500*
C	CTY1	NH1	*47.920*	*105.9200*

Table 27

Cont.

Angle Parameters				
Atom Type 1	***Atom Type 2***	***Atom Type 3***	***K_θ (kcal mol^{-1}radian^{-2})***	***θ_0 angle (degrees)***
C	**CTY1**	**HBY**	***51.000***	***106.9500***
CTY2	**CTY1**	**NH1**	**90.000**	**104.5000**
CTY2	**CTY1**	**HBY**	**35.000**	**111.4000**
NH1	**CTY1**	**HBY**	**59.000**	**111.0000**
CCY	**CTY2**	**CTY2**	**70.000**	**106.5000**
CCY	**CTY2**	**HAY**	**58.000**	**111.0000**
CTY1	**CTY2**	**CTY2**	**58.000**	**109.5000**
CTY1	**CTY2**	**HAY**	**35.000**	**111.4000**
CTY2	**CTY2**	**HAY**	**35.000**	**111.4000**
HAY	**CTY2**	**HAY**	**38.500**	**106.8000**
CCY	**NH1**	**CTY1**	**75.000**	**111.0000**
CCY	**NH1**	**H**	**38.000**	**119.5000**
CTY1	**NH1**	**H**	**38.000**	**116.0000**
C	**NH1**	**CTY3**	**50.000**	**120.0000**
C	**NH1**	**H5**	**34.000**	**123.0000**
CTY3	**NH1**	**H5**	**35.000**	**117.0000**
C51	**CO1**	**NG2**	**50.000**	**110.2300**
NG2	**CO1**	**OD1**	**75.000**	**122.5000**
CO1	**NG2**	**HP1**	**50.000**	**120.0000**
HP1	**NG2**	**HP1**	**23.000**	**120.0000**

The resulting Urey-Bradley parameters, with no necessary repairs determined or required to be made, are listed in Table 28.[4,137,158,159,160,161,162,163,164,165,166,167]

Table 28

Urey-Bradley Parameters.[4,137,158,159,160,161,162,163,164,165,166,167]

Urey-Bradley Parameters				
Atom Type 1	***Atom Type 2***	***Atom Type 3***	K_{UB}***(kcal mol^{-1}Å^{-2})***	s_0***length (Å)***
O50	C53	HG52	20.00	2.14000
O50X	C53	HG52	20.00	2.14000
C61	C61	C61	35.00	2.41620
C61	C61	H61	22.00	2.15250
C11	C21	HG2	22.53	2.17900
HG2	C21	HG2	5.40	1.80200
C21	C11	C215	8.00	2.56100
C21	C11	HG1	22.53	2.17900
C215	C11	HG1	22.53	2.17900
C11	C215	C215	11.16	2.56100
C11	C215	HG2	22.53	2.17900
C215	C215	C215	11.16	2.56100
C215	C215	HG2	22.53	2.17900
HG2	C215	HG2	5.40	1.80200
C51	C51	HG52	15.00	2.21500
C11	C31	HG3	22.53	2.17900
HG3	C31	HG3	5.40	1.80200
C31	C11	C215	8.00	2.56100
C31	C11	HG1	22.53	2.17900
N50Y	C51	HG52	20.00	2.14000
N50	C51	HG52	20.00	2.14000
C61	C61	C66	35.00	2.41620
C61	C61	H62	22.00	2.15250
C66	C61	H62	22.00	2.15250
C61	C66	C61	35.00	2.41620
HG3	CTY3	HG3	5.40	1.80200
CTY2	CTY1	HBY	22.53	2.17900
CTY1	CTY2	CTY2	11.16	2.56100
CTY1	CTY2	HAY	22.53	2.17900
CTY2	CTY2	HAY	22.53	2.17900
HAY	CTY2	HAY	5.40	1.80200
NG2	CO1	OD1	50.00	2.37000

Measurement comparisons for the dihedral angles, in a similar fashion as was done for the bond lengths and bond angles, were made for SB-674042 before and after recursively optimizing bonds and angles, then dihedrals, with the dihedral check formula modified to add only 10000 for the purposes of space, and the SB-674042 dihedral angles prior to this optimization listed in Table 29.[137,158,159,160,161,162,163,164,165,166,167]

Table 29

SB-674042 Dihedral Angles Prior to Optimization.[137,158,159,160,161,162,163,164,165,166,167]

SB-674042 Dihedral Test Before CHARMM Optimization					
Dihedral	***QM Twist***	***MM Twist***	***Difference***	***Square***	***Check***
(atoms)	***(degrees)***	***(degrees)***	***(degrees)***	***(sq. deg.)***	***(degrees^{-1})***
H8 -C1 -C2 -H9	**0.24**	**0.09**	**-0.15**	**0.02**	**#DIV/0!**
H8 -C1 -C2 -C3	**179.80**	**179.81**	**0.01**	**0.00**	**#DIV/0!**
C6 -C1 -C2 -H9	**-179.71**	**-179.75**	**-0.04**	**0.00**	**#DIV/0!**
C6 -C1 -C2 -C3	**-0.15**	**-0.02**	**0.12**	**0.02**	**#DIV/0!**
H8 -C1 -C6 -H11	**0.17**	**0.04**	**-0.14**	**0.02**	**#DIV/0!**
H8 -C1 -C6 -C5	**-179.88**	**-179.79**	**0.09**	**0.01**	**#DIV/0!**
C2 -C1 -C6 -H11	**-179.88**	**179.87**	**-0.26**	**0.07**	**#DIV/0!**
C2 -C1 -C6 -C5	**0.07**	**0.04**	**-0.03**	**0.00**	**#DIV/0!**
C1 -C2 -C3 -C4	**0.01**	**-0.01**	**-0.02**	**0.00**	**#DIV/0!**
C1 -C2 -C3 -H10	**-179.09**	**-179.48**	**-0.39**	**0.15**	**#DIV/0!**
H9 -C2 -C3 -C4	**179.58**	**179.71**	**0.13**	**0.02**	**#DIV/0!**
H9 -C2 -C3 -H10	**0.48**	**0.24**	**-0.24**	**0.06**	**#DIV/0!**
C1 -C6 -C5 -C4	**0.15**	**-0.02**	**-0.17**	**0.03**	**#DIV/0!**
C1 -C6 -C5 -F7	**-179.26**	**-179.14**	**0.12**	**0.01**	**#DIV/0!**
H11-C6 -C5 -C4	**-179.90**	**-179.85**	**0.05**	**0.00**	**#DIV/0!**
H11-C6 -C5 -F7	**0.68**	**1.03**	**0.34**	**0.12**	**#DIV/0!**
C2 -C3 -C4 -C5	**0.20**	**0.03**	**-0.17**	**0.03**	**#DIV/0!**
C2 -C3 -C4 -C18	**178.91**	**-179.54**	**1.56**	**2.42**	**#DIV/0!**
H10-C3 -C4 -C5	**179.30**	**179.50**	**0.20**	**0.04**	**#DIV/0!**
H10-C3 -C4 -C18	**-1.99**	**-0.07**	**1.92**	**3.69**	**#DIV/0!**

Table 29

Cont.

SB-674042 Dihedral Test Before CHARMM Optimization					
Dihedral	***QM Twist***	***MM Twist***	***Difference***	***Square***	***Check***
(atoms)	***(degrees)***	***(degrees)***	***(degrees)***	***(sq. deg.)***	***(degrees^{-1})***
C6 -C5 -C4 -C3	-0.28	-0.02	0.27	0.07	#DIV/0!
C6 -C5 -C4 -C18	-178.99	179.55	-1.46	2.13	#DIV/0!
F7 -C5 -C4 -C3	179.13	179.09	-0.04	0.00	#DIV/0!
F7 -C5 -C4 -C18	0.42	-1.35	-1.77	3.12	#DIV/0!
C3 -C4 -C18-C14	*132.30*	*123.56*	*-8.74*	*76.35*	*10001.35520*
C5 -C4 -C18-C14	-49.04	-55.99	-6.95	48.29	#DIV/0!
C3 -C4 -C18-S17	*-48.96*	*-62.87*	*-13.92*	*193.64*	*10000.16904*
C5 -C4 -C18-S17	*129.70*	*117.57*	*-12.13*	*147.06*	*10000.24232*
C4 -C18-S17-C16	-179.66	-177.56	2.09	4.38	#DIV/0!
C14-C18-S17-C16	-0.66	-2.82	-2.16	4.66	#DIV/0!
C18-S17-C16-N15	1.00	2.18	1.18	1.39	#DIV/0!
C18-S17-C16-C19	-179.50	177.80	-2.70	7.30	#DIV/0!
S17-C16-C19-H20	*174.15*	*148.38*	*-25.77*	*664.04*	*10000.05628*
S17-C16-C19-H21	*-66.03*	*-92.12*	*-26.09*	*680.76*	*10000.05527*
S17-C16-C19-H22	*54.11*	*28.43*	*-25.68*	*659.56*	*10000.05656*
N15-C16-C19-H20	*-6.40*	*-36.16*	*-29.76*	*885.70*	*10000.04595*
N15-C16-C19-H21	*113.42*	*83.34*	*-30.08*	*904.99*	*10000.04528*
N15-C16-C19-H22	*-126.44*	*-156.11*	*-29.67*	*880.52*	*10000.04614*
S17-C16-N15-C14	-1.03	-0.83	0.19	0.04	#DIV/0!
C19-C16-N15-C14	179.48	-176.59	3.93	15.45	#DIV/0!
C16-N15-C14-C12	-175.94	-177.35	-1.42	2.00	#DIV/0!
C16-N15-C14-C18	0.50	-1.45	-1.95	3.79	#DIV/0!
C4 -C18-C14-N15	179.12	177.07	-2.05	4.20	#DIV/0!
C4 -C18-C14-C12	-4.68	-7.35	-2.67	7.15	#DIV/0!
S17-C18-C14-N15	0.26	3.00	2.74	7.51	#DIV/0!
S17-C18-C14-C12	176.45	178.57	2.11	4.47	#DIV/0!
C18-C14-C12-O13	-44.92	-42.00	2.93	8.58	#DIV/0!
C18-C14-C12-N27	136.72	137.25	0.53	0.28	#DIV/0!
N15-C14-C12-O13	131.18	133.37	2.19	4.80	#DIV/0!

Table 29

Cont.

SB-674042 Dihedral Test Before CHARMM Optimization					
Dihedral	***QM Twist***	***MM Twist***	***Difference***	***Square***	***Check***
(atoms)	***(degrees)***	***(degrees)***	***(degrees)***	***(sq. deg.)***	***(degrees^{-1})***
N15-C14-C12-N27	**-47.18**	**-47.39**	**-0.21**	**0.05**	**#DIV/0!**
C14-C12-N27-C26	**-20.09**	**-18.68**	**1.41**	**2.00**	**#DIV/0!**
C14-C12-N27-C23	***179.66***	***169.67***	***-9.99***	***99.77***	***10000.50294***
O13-C12-N27-C26	**161.60**	**160.55**	**-1.05**	**1.10**	**#DIV/0!**
O13-C12-N27-C23	***1.35***	***-11.10***	***-12.45***	***155.07***	***10000.22459***
C12-N27-C26-C25	***-141.22***	***-149.60***	***-8.38***	***70.26***	***10002.61780***
C12-N27-C26-H33	**-20.50**	**-27.43**	**-6.92**	**47.95**	**#DIV/0!**
C12-N27-C26-H34	**99.60**	**91.78**	**-7.82**	**61.18**	**#DIV/0!**
C23-N27-C26-C25	**20.22**	**22.74**	**2.52**	**6.37**	**#DIV/0!**
C23-N27-C26-H33	**140.93**	**144.91**	**3.98**	**15.84**	**#DIV/0!**
C23-N27-C26-H34	**-98.97**	**-95.88**	**3.08**	**9.51**	**#DIV/0!**
N27-C26-C25-C24	**-34.73**	**-33.44**	**1.29**	**1.67**	**#DIV/0!**
N27-C26-C25-H31	**-156.82**	**-156.14**	**0.68**	**0.46**	**#DIV/0!**
N27-C26-C25-H32	**82.82**	**83.82**	**1.00**	**1.00**	**#DIV/0!**
H33-C26-C25-C24	**-154.27**	**-155.03**	**-0.75**	**0.57**	**#DIV/0!**
H33-C26-C25-H31	**83.64**	**82.28**	**-1.36**	**1.86**	**#DIV/0!**
H33-C26-C25-H32	**-36.72**	**-37.76**	**-1.05**	**1.09**	**#DIV/0!**
H34-C26-C25-C24	**83.80**	**82.56**	**-1.25**	**1.55**	**#DIV/0!**
H34-C26-C25-H31	**-38.28**	**-40.14**	**-1.86**	**3.45**	**#DIV/0!**
H34-C26-C25-H32	**-158.64**	**-160.18**	**-1.54**	**2.37**	**#DIV/0!**
C26-C25-C24-C23	**37.07**	**32.94**	**-4.12**	**17.01**	**#DIV/0!**
C26-C25-C24-H29	**158.17**	**156.38**	**-1.79**	**3.21**	**#DIV/0!**
C26-C25-C24-H30	**-81.21**	**-85.13**	**-3.92**	**15.39**	**#DIV/0!**
H31-C25-C24-C23	**158.71**	**155.68**	**-3.03**	**9.17**	**#DIV/0!**
H31-C25-C24-H29	**-80.18**	**-80.88**	**-0.70**	**0.49**	**#DIV/0!**
H31-C25-C24-H30	**40.44**	**37.61**	**-2.83**	**8.00**	**#DIV/0!**
H32-C25-C24-C23	**-79.89**	**-84.15**	**-4.27**	**18.20**	**#DIV/0!**
H32-C25-C24-H29	**41.22**	**39.29**	**-1.93**	**3.74**	**#DIV/0!**
H32-C25-C24-H30	**161.84**	**157.78**	**-4.07**	**16.53**	**#DIV/0!**

Table 29

Cont.

SB-674042 Dihedral Test Before CHARMM Optimization					
Dihedral	***QM Twist***	***MM Twist***	***Difference***	***Square***	***Check***
(atoms)	***(degrees)***	***(degrees)***	***(degrees)***	***(sq. deg.)***	***(degrees^{-1})***
C25-C24-C23-N27	**-24.80**	**-19.67**	**5.13**	**26.32**	**#DIV/0!**
C25-C24-C23-C35	**-148.54**	**-141.48**	**7.06**	**49.91**	**#DIV/0!**
C25-C24-C23-H28	**91.37**	**97.95**	**6.59**	**43.38**	**#DIV/0!**
H29-C24-C23-N27	**-147.17**	**-143.20**	**3.97**	**15.74**	**#DIV/0!**
H29-C24-C23-C35	**89.08**	**94.98**	**5.90**	**34.82**	**#DIV/0!**
H29-C24-C23-H28	**-31.01**	**-25.59**	**5.42**	**29.41**	**#DIV/0!**
H30-C24-C23-N27	**93.28**	**97.87**	**4.59**	**21.05**	**#DIV/0!**
H30-C24-C23-C35	**-30.47**	**-23.94**	**6.52**	**42.53**	**#DIV/0!**
H30-C24-C23-H28	**-150.56**	**-144.51**	**6.04**	**36.54**	**#DIV/0!**
C12-N27-C23-C35	**-70.06**	**-66.73**	**3.33**	**11.06**	**#DIV/0!**
C12-N27-C23-C24	**165.59**	**170.71**	**5.12**	**26.23**	**#DIV/0!**
C12-N27-C23-H28	**48.14**	**54.65**	**6.51**	**42.41**	**#DIV/0!**
C26-N27-C23-C35	**127.17**	**120.66**	**-6.51**	**42.44**	**#DIV/0!**
C26-N27-C23-C24	**2.82**	**-1.90**	**-4.72**	**22.26**	**#DIV/0!**
C26-N27-C23-H28	**-114.63**	**-117.96**	**-3.33**	**11.07**	**#DIV/0!**
N27-C23-C35-C38	***-53.31***	***-36.48***	***16.83***	***283.24***	***10000.11326***
N27-C23-C35-H36	***68.62***	***82.43***	***13.80***	***190.46***	***10000.17239***
N27-C23-C35-H37	***-173.34***	***-159.06***	***14.28***	***204.02***	***10000.15915***
C24-C23-C35-C38	***65.13***	***81.14***	***16.00***	***256.15***	***10000.12493***
C24-C23-C35-H36	***-172.93***	***-159.95***	***12.98***	***168.37***	***10000.20098***
C24-C23-C35-H37	***-54.90***	***-41.44***	***13.46***	***181.13***	***10000.18320***
H28-C23-C35-C38	***-172.66***	***-158.73***	***13.93***	***194.00***	***10000.16868***
H28-C23-C35-H36	***-50.72***	***-39.82***	***10.90***	***118.80***	***10000.34489***
H28-C23-C35-H37	***67.31***	***78.69***	***11.38***	***129.56***	***10000.29565***
C23-C35-C38-N39	***-94.43***	***-84.07***	***10.36***	***107.34***	***10000.42362***
C23-C35-C38-O42	**85.55**	**90.79**	**5.24**	**27.43**	**#DIV/0!**
H36-C35-C38-N39	***143.45***	***156.21***	***12.76***	***162.91***	***10000.20993***
H36-C35-C38-O42	**-36.57**	**-28.93**	**7.64**	**58.38**	**#DIV/0!**
H37-C35-C38-N39	***26.12***	***38.95***	***12.83***	***164.70***	***10000.20689***

Table 29

Cont.

SB-674042 Dihedral Test Before CHARMM Optimization					
Dihedral	***QM Twist***	***MM Twist***	***Difference***	***Square***	***Check***
(atoms)	***(degrees)***	***(degrees)***	***(degrees)***	***(sq. deg.)***	***(degrees^{-1})***
H37-C35-C38-O42	**-153.90**	**-146.19**	**7.71**	**59.44**	**#DIV/0!**
C35-C38-O42-C41	**-179.67**	**-174.13**	**5.54**	**30.66**	**#DIV/0!**
N39-C38-O42-C41	**0.32**	**1.14**	**0.82**	**0.67**	**#DIV/0!**
C35-C38-N39-N40	**179.66**	**174.66**	**-5.00**	**25.00**	**#DIV/0!**
O42-C38-N39-N40	**-0.33**	**-0.75**	**-0.41**	**0.17**	**#DIV/0!**
C38-N39-N40-C41	**0.20**	**-0.03**	**-0.23**	**0.05**	**#DIV/0!**
N39-N40-C41-C46	**179.80**	**-178.70**	**1.49**	**2.23**	**#DIV/0!**
N39-N40-C41-O42	**0.00**	**0.77**	**0.77**	**0.60**	**#DIV/0!**
C38-O42-C41-C46	**179.99**	**178.35**	**-1.64**	**2.68**	**#DIV/0!**
C38-O42-C41-N40	**-0.19**	**-1.13**	**-0.94**	**0.89**	**#DIV/0!**
N40-C41-C46-C45	**174.40**	**177.17**	**2.77**	**7.69**	**#DIV/0!**
N40-C41-C46-C47	**-5.54**	**-1.77**	**3.77**	**14.20**	**#DIV/0!**
O42-C41-C46-C45	**-5.81**	**-2.24**	**3.57**	**12.75**	**#DIV/0!**
O42-C41-C46-C47	**174.25**	**178.82**	**4.57**	**20.85**	**#DIV/0!**
C41-C46-C45-C44	**179.91**	**-179.04**	**1.06**	**1.11**	**#DIV/0!**
C41-C46-C45-H51	**-0.57**	**0.24**	**0.80**	**0.65**	**#DIV/0!**
C47-C46-C45-C44	**-0.16**	**-0.06**	**0.09**	**0.01**	**#DIV/0!**
C47-C46-C45-H51	**179.37**	**179.21**	**-0.16**	**0.02**	**#DIV/0!**
C41-C46-C47-C48	**-179.95**	**179.07**	**-0.98**	**0.96**	**#DIV/0!**
C41-C46-C47-H52	**-0.11**	**-0.78**	**-0.67**	**0.45**	**#DIV/0!**
C45-C46-C47-C48	**0.11**	**0.11**	**0.00**	**0.00**	**#DIV/0!**
C45-C46-C47-H52	**179.96**	**-179.74**	**0.31**	**0.09**	**#DIV/0!**
C46-C45-C44-C43	**0.04**	**-0.03**	**-0.07**	**0.00**	**#DIV/0!**
C46-C45-C44-H50	**-179.73**	**179.96**	**-0.32**	**0.10**	**#DIV/0!**
H51-C45-C44-C43	**-179.48**	**-179.31**	**0.18**	**0.03**	**#DIV/0!**
H51-C45-C44-H50	**0.75**	**0.68**	**-0.07**	**0.00**	**#DIV/0!**
C46-C47-C48-C43	**0.05**	**-0.07**	**-0.12**	**0.01**	**#DIV/0!**
C46-C47-C48-H53	**179.91**	**179.94**	**0.02**	**0.00**	**#DIV/0!**
H52-C47-C48-C43	**-179.80**	**179.78**	**-0.43**	**0.18**	**#DIV/0!**

Table 29

Cont.

SB-674042 Dihedral Test Before CHARMM Optimization					
Dihedral	***QM Twist***	***MM Twist***	***Difference***	***Square***	***Check***
(atoms)	***(degrees)***	***(degrees)***	***(degrees)***	***(sq. deg.)***	***(degrees^{-1})***
H52-C47-C48-H53	**0.07**	**-0.22**	**-0.29**	**0.08**	**#DIV/0!**
C47-C48-C43-C44	**-0.17**	**-0.03**	**0.14**	**0.02**	**#DIV/0!**
C47-C48-C43-H49	**179.83**	**179.95**	**0.12**	**0.01**	**#DIV/0!**
H53-C48-C43-C44	**179.97**	**179.97**	**0.00**	**0.00**	**#DIV/0!**
H53-C48-C43-H49	**-0.03**	**-0.06**	**-0.02**	**0.00**	**#DIV/0!**
C45-C44-C43-C48	**0.12**	**0.08**	**-0.04**	**0.00**	**#DIV/0!**
C45-C44-C43-H49	**-179.88**	**-179.90**	**-0.02**	**0.00**	**#DIV/0!**
H50-C44-C43-C48	**179.88**	**-179.91**	**0.20**	**0.04**	**#DIV/0!**
H50-C44-C43-H49	**-0.11**	**0.11**	**0.22**	**0.05**	**#DIV/0!**
	Largest absolute error		***30.08310***	***904.99291***	***10000.04528***
		RMS error		***7.76708***	***#DIV/0!***

The SB-674042 dihedral angles, after optimizing bond lengths, bond angles, and dihedral angles, were listed in Table 30.[137,158,159,160,161,162,163,164,165,166,167]

Table 30

SB-674042 Dihedrals After Optimization.[137,158,159,160,161,162,163,164,165,166,167]

SB-674042 Dihedral Test After CHARMM Optimization					
Dihedral	***QM Twist***	***MM Twist***	***Difference***	***Square***	***Check***
(atoms)	***(degrees)***	***(degrees)***	***(degrees)***	***(sq. deg.)***	***(degrees^{-1})***
H8 -C1 -C2 -H9	**0.24**	**-0.02**	**-0.26**	**0.07**	**#DIV/0!**
H8 -C1 -C2 -C3	**179.80**	**-179.93**	**0.26**	**0.07**	**#DIV/0!**
C6 -C1 -C2 -H9	**-179.71**	**179.70**	**-0.59**	**0.35**	**#DIV/0!**
C6 -C1 -C2 -C3	**-0.15**	**-0.21**	**-0.06**	**0.00**	**#DIV/0!**
H8 -C1 -C6 -H11	**0.17**	**0.37**	**0.20**	**0.04**	**#DIV/0!**

Table 30

Cont.

SB-674042 Dihedral Test After CHARMM Optimization					
Dihedral	***QM Twist***	***MM Twist***	***Difference***	***Square***	***Check***
(atoms)	***(degrees)***	***(degrees)***	***(degrees)***	***(sq. deg.)***	***(degrees^{-1})***
H8 -C1 -C6 -C5	-179.88	-179.79	0.09	0.01	#DIV/0!
C2 -C1 -C6 -H11	-179.88	-179.35	0.52	0.28	#DIV/0!
C2 -C1 -C6 -C5	0.07	0.48	0.42	0.17	#DIV/0!
C1 -C2 -C3 -C4	0.01	-0.80	-0.81	0.66	#DIV/0!
C1 -C2 -C3 -H10	-179.09	179.83	-1.08	1.17	#DIV/0!
H9 -C2 -C3 -C4	179.58	179.29	-0.29	0.08	#DIV/0!
H9 -C2 -C3 -H10	0.48	-0.08	-0.56	0.31	#DIV/0!
C1 -C6 -C5 -C4	0.15	0.25	0.10	0.01	#DIV/0!
C1 -C6 -C5 -F7	-179.26	-177.16	2.11	4.44	#DIV/0!
H11-C6 -C5 -C4	-179.90	-179.91	-0.01	0.00	#DIV/0!
H11-C6 -C5 -F7	0.68	2.68	2.00	3.99	#DIV/0!
C2 -C3 -C4 -C5	0.20	1.48	1.28	1.65	#DIV/0!
C2 -C3 -C4 -C18	178.91	177.19	-1.72	2.96	#DIV/0!
H10-C3 -C4 -C5	179.30	-179.15	1.55	2.40	#DIV/0!
H10-C3 -C4 -C18	-1.99	-3.44	-1.45	2.12	#DIV/0!
C6 -C5 -C4 -C3	-0.28	-1.22	-0.94	0.88	#DIV/0!
C6 -C5 -C4 -C18	-178.99	-176.86	2.13	4.54	#DIV/0!
F7 -C5 -C4 -C3	179.13	176.11	-3.02	9.12	#DIV/0!
F7 -C5 -C4 -C18	0.42	0.47	0.05	0.00	#DIV/0!
C3 -C4 -C18-C14	132.30	132.59	0.29	0.08	#DIV/0!
C5 -C4 -C18-C14	-49.04	-51.90	-2.86	8.15	#DIV/0!
C3 -C4 -C18-S17	-48.96	-53.56	-4.60	21.19	#DIV/0!
C5 -C4 -C18-S17	129.70	121.95	-7.75	60.00	#DIV/0!
C4 -C18-S17-C16	-179.66	-175.93	3.73	13.90	#DIV/0!
C14-C18-S17-C16	-0.66	-0.80	-0.14	0.02	#DIV/0!
C18-S17-C16-N15	1.00	0.51	-0.50	0.25	#DIV/0!
C18-S17-C16-C19	-179.50	-179.51	-0.01	0.00	#DIV/0!
S17-C16-C19-H20	174.15	177.11	2.96	8.78	#DIV/0!
S17-C16-C19-H21	-66.03	-62.98	3.05	9.30	#DIV/0!

Table 30

Cont.

SB-674042 Dihedral Test After CHARMM Optimization					
Dihedral	***QM Twist***	***MM Twist***	***Difference***	***Square***	***Check***
(atoms)	***(degrees)***	***(degrees)***	***(degrees)***	***(sq. deg.)***	***(degrees^{-1})***
S17-C16-C19-H22	54.11	57.37	3.26	10.63	#DIV/0!
N15-C16-C19-H20	-6.40	-2.91	3.50	12.22	#DIV/0!
N15-C16-C19-H21	113.42	117.00	3.58	12.84	#DIV/0!
N15-C16-C19-H22	-126.44	-122.65	3.79	14.39	#DIV/0!
S17-C16-N15-C14	-1.03	-0.04	0.98	0.97	#DIV/0!
C19-C16-N15-C14	179.48	179.97	0.49	0.24	#DIV/0!
C16-N15-C14-C12	-175.94	-175.68	0.26	0.07	#DIV/0!
C16-N15-C14-C18	0.50	-0.64	-1.13	1.28	#DIV/0!
C4 -C18-C14-N15	179.12	175.48	-3.65	13.30	#DIV/0!
C4 -C18-C14-C12	-4.68	-9.59	-4.91	24.13	#DIV/0!
S17-C18-C14-N15	0.26	0.97	0.72	0.51	#DIV/0!
S17-C18-C14-C12	176.45	175.91	-0.55	0.30	#DIV/0!
C18-C14-C12-O13	-44.92	-43.20	1.72	2.97	#DIV/0!
C18-C14-C12-N27	136.72	135.29	-1.43	2.05	#DIV/0!
N15-C14-C12-O13	131.18	131.53	0.35	0.12	#DIV/0!
N15-C14-C12-N27	-47.18	-49.98	-2.80	7.86	#DIV/0!
C14-C12-N27-C26	-20.09	-18.63	1.47	2.15	#DIV/0!
C14-C12-N27-C23	179.66	178.53	-1.13	1.27	#DIV/0!
O13-C12-N27-C26	161.60	159.83	-1.77	3.13	#DIV/0!
O13-C12-N27-C23	1.35	-3.02	-4.36	19.04	#DIV/0!
C12-N27-C26-C25	-141.22	-147.62	-6.40	41.01	#DIV/0!
C12-N27-C26-H33	-20.50	-25.48	-4.98	24.77	#DIV/0!
C12-N27-C26-H34	99.60	93.76	-5.84	34.10	#DIV/0!
C23-N27-C26-C25	20.22	16.77	-3.45	11.91	#DIV/0!
C23-N27-C26-H33	140.93	138.91	-2.02	4.10	#DIV/0!
C23-N27-C26-H34	-98.97	-101.85	-2.89	8.34	#DIV/0!
N27-C26-C25-C24	-34.73	-33.46	1.27	1.63	#DIV/0!
N27-C26-C25-H31	-156.82	-156.03	0.78	0.61	#DIV/0!
N27-C26-C25-H32	82.82	83.92	1.10	1.21	#DIV/0!

Table 30

Cont.

SB-674042 Dihedral Test After CHARMM Optimization					
Dihedral	***QM Twist***	***MM Twist***	***Difference***	***Square***	***Check***
(atoms)	***(degrees)***	***(degrees)***	***(degrees)***	***(sq. deg.)***	***(degrees^{-1})***
H33-C26-C25-C24	**-154.27**	**-155.28**	**-1.00**	**1.01**	**#DIV/0!**
H33-C26-C25-H31	**83.64**	**82.15**	**-1.50**	**2.24**	**#DIV/0!**
H33-C26-C25-H32	**-36.72**	**-37.90**	**-1.18**	**1.39**	**#DIV/0!**
H34-C26-C25-C24	**83.80**	**82.54**	**-1.27**	**1.60**	**#DIV/0!**
H34-C26-C25-H31	**-38.28**	**-40.04**	**-1.76**	**3.09**	**#DIV/0!**
H34-C26-C25-H32	**-158.64**	**-160.08**	**-1.44**	**2.07**	**#DIV/0!**
C26-C25-C24-C23	**37.07**	**38.24**	**1.18**	**1.38**	**#DIV/0!**
C26-C25-C24-H29	**158.17**	**161.09**	**2.92**	**8.50**	**#DIV/0!**
C26-C25-C24-H30	**-81.21**	**-79.74**	**1.47**	**2.15**	**#DIV/0!**
H31-C25-C24-C23	**158.71**	**160.76**	**2.06**	**4.22**	**#DIV/0!**
H31-C25-C24-H29	**-80.18**	**-76.39**	**3.80**	**14.41**	**#DIV/0!**
H31-C25-C24-H30	**40.44**	**42.78**	**2.35**	**5.50**	**#DIV/0!**
H32-C25-C24-C23	**-79.89**	**-78.95**	**0.93**	**0.87**	**#DIV/0!**
H32-C25-C24-H29	**41.22**	**43.90**	**2.68**	**7.16**	**#DIV/0!**
H32-C25-C24-H30	**161.84**	**163.07**	**1.22**	**1.50**	**#DIV/0!**
C25-C24-C23-N27	**-24.80**	**-28.05**	**-3.25**	**10.59**	**#DIV/0!**
C25-C24-C23-C35	**-148.54**	**-152.96**	**-4.42**	**19.51**	**#DIV/0!**
C25-C24-C23-H28	**91.37**	**87.10**	**-4.26**	**18.16**	**#DIV/0!**
H29-C24-C23-N27	**-147.17**	**-151.02**	**-3.85**	**14.81**	**#DIV/0!**
H29-C24-C23-C35	**89.08**	**84.07**	**-5.01**	**25.12**	**#DIV/0!**
H29-C24-C23-H28	**-31.01**	**-35.87**	**-4.86**	**23.58**	**#DIV/0!**
H30-C24-C23-N27	**93.28**	**89.34**	**-3.94**	**15.51**	**#DIV/0!**
H30-C24-C23-C35	**-30.47**	**-35.57**	**-5.10**	**26.03**	**#DIV/0!**
H30-C24-C23-H28	**-150.56**	**-155.51**	**-4.95**	**24.47**	**#DIV/0!**
C12-N27-C23-C35	**-70.06**	**-63.70**	**6.36**	**40.45**	**#DIV/0!**
C12-N27-C23-C24	**165.59**	**171.89**	**6.30**	**39.72**	**#DIV/0!**
C12-N27-C23-H28	**48.14**	**55.02**	**6.88**	**47.38**	**#DIV/0!**
C26-N27-C23-C35	**127.17**	**131.58**	**4.41**	**19.43**	**#DIV/0!**
C26-N27-C23-C24	**2.82**	**7.17**	**4.35**	**18.93**	**#DIV/0!**

Table 30

Cont.

SB-674042 Dihedral Test After CHARMM Optimization					
Dihedral	***QM Twist***	***MM Twist***	***Difference***	***Square***	***Check***
(atoms)	***(degrees)***	***(degrees)***	***(degrees)***	***(sq. deg.)***	***(degrees^{-1})***
C26-N27-C23-H28	-114.63	-109.70	4.93	24.32	#DIV/0!
N27-C23-C35-C38	-53.31	-49.37	3.95	15.58	#DIV/0!
N27-C23-C35-H36	68.62	71.67	3.04	9.27	#DIV/0!
N27-C23-C35-H37	-173.34	-170.26	3.09	9.53	#DIV/0!
C24-C23-C35-C38	65.13	69.70	4.56	20.83	#DIV/0!
C24-C23-C35-H36	-172.93	-169.27	3.66	13.41	#DIV/0!
C24-C23-C35-H37	-54.90	-51.19	3.70	13.72	#DIV/0!
H28-C23-C35-C38	-172.66	-168.55	4.11	16.92	#DIV/0!
H28-C23-C35-H36	-50.72	-47.51	3.21	10.31	#DIV/0!
H28-C23-C35-H37	67.31	70.57	3.25	10.59	#DIV/0!
C23-C35-C38-N39	-94.43	-99.66	-5.22	27.26	#DIV/0!
C23-C35-C38-O42	85.55	81.08	-4.47	20.02	#DIV/0!
H36-C35-C38-N39	143.45	138.64	-4.81	23.11	#DIV/0!
H36-C35-C38-O42	-36.57	-40.63	-4.06	16.49	#DIV/0!
H37-C35-C38-N39	26.12	21.70	-4.42	19.53	#DIV/0!
H37-C35-C38-O42	-153.90	-157.57	-3.67	13.49	#DIV/0!
C35-C38-O42-C41	-179.67	-179.20	0.47	0.22	#DIV/0!
N39-C38-O42-C41	0.32	1.44	1.11	1.24	#DIV/0!
C35-C38-N39-N40	179.66	179.62	-0.04	0.00	#DIV/0!
O42-C38-N39-N40	-0.33	-1.08	-0.75	0.56	#DIV/0!
C38-N39-N40-C41	0.20	0.24	0.04	0.00	#DIV/0!
N39-N40-C41-C46	179.80	-178.94	1.25	1.57	#DIV/0!
N39-N40-C41-O42	0.00	0.66	0.67	0.44	#DIV/0!
C38-O42-C41-C46	179.99	178.40	-1.59	2.54	#DIV/0!
C38-O42-C41-N40	-0.19	-1.25	-1.07	1.14	#DIV/0!
N40-C41-C46-C45	174.40	173.31	-1.08	1.17	#DIV/0!
N40-C41-C46-C47	-5.54	-5.87	-0.33	0.11	#DIV/0!
O42-C41-C46-C45	-5.81	-6.27	-0.46	0.21	#DIV/0!
O42-C41-C46-C47	174.25	174.55	0.30	0.09	#DIV/0!

Table 30

Cont.

SB-674042 Dihedral Test After CHARMM Optimization					
Dihedral	***QM Twist***	***MM Twist***	***Difference***	***Square***	***Check***
(atoms)	***(degrees)***	***(degrees)***	***(degrees)***	***(sq. deg.)***	***(degrees^{-1})***
C41-C46-C45-C44	**179.91**	**-179.40**	**0.69**	**0.47**	**#DIV/0!**
C41-C46-C45-H51	**-0.57**	**0.02**	**0.58**	**0.34**	**#DIV/0!**
C47-C46-C45-C44	**-0.16**	**-0.23**	**-0.07**	**0.01**	**#DIV/0!**
C47-C46-C45-H51	**179.37**	**179.19**	**-0.18**	**0.03**	**#DIV/0!**
C41-C46-C47-C48	**-179.95**	**179.52**	**-0.53**	**0.28**	**#DIV/0!**
C41-C46-C47-H52	**-0.11**	**-0.49**	**-0.39**	**0.15**	**#DIV/0!**
C45-C46-C47-C48	**0.11**	**0.33**	**0.22**	**0.05**	**#DIV/0!**
C45-C46-C47-H52	**179.96**	**-179.68**	**0.36**	**0.13**	**#DIV/0!**
C46-C45-C44-C43	**0.04**	**-0.01**	**-0.05**	**0.00**	**#DIV/0!**
C46-C45-C44-H50	**-179.73**	**179.95**	**-0.32**	**0.10**	**#DIV/0!**
H51-C45-C44-C43	**-179.48**	**-179.43**	**0.05**	**0.00**	**#DIV/0!**
H51-C45-C44-H50	**0.75**	**0.52**	**-0.23**	**0.05**	**#DIV/0!**
C46-C47-C48-C43	**0.05**	**-0.20**	**-0.26**	**0.07**	**#DIV/0!**
C46-C47-C48-H53	**179.91**	**179.88**	**-0.03**	**0.00**	**#DIV/0!**
H52-C47-C48-C43	**-179.80**	**179.81**	**-0.40**	**0.16**	**#DIV/0!**
H52-C47-C48-H53	**0.07**	**-0.11**	**-0.17**	**0.03**	**#DIV/0!**
C47-C48-C43-C44	**-0.17**	**-0.03**	**0.14**	**0.02**	**#DIV/0!**
C47-C48-C43-H49	**179.83**	**-179.97**	**0.20**	**0.04**	**#DIV/0!**
H53-C48-C43-C44	**179.97**	**179.88**	**-0.09**	**0.01**	**#DIV/0!**
H53-C48-C43-H49	**-0.03**	**-0.06**	**-0.02**	**0.00**	**#DIV/0!**
C45-C44-C43-C48	**0.12**	**0.14**	**0.02**	**0.00**	**#DIV/0!**
C45-C44-C43-H49	**-179.88**	**-179.93**	**-0.05**	**0.00**	**#DIV/0!**
H50-C44-C43-C48	**179.88**	**-179.82**	**0.29**	**0.09**	**#DIV/0!**
H50-C44-C43-H49	**-0.11**	**0.12**	**0.23**	**0.05**	**#DIV/0!**
	Largest absolute error		***7.74580***	**59.99742**	***#DIV/0!***
		RMS error		***2.75208***	***#DIV/0!***

Measurement comparisons for the dihedral angles were made for pyroglutamate-NMA with dihedral angles before optimization listed in Table 31.[4,158,159,160,161,162,163,164,165,166,167]

Table 31

Pyroglutamate-NMA Dihedral Angles Prior to Optimization.[4,158,159,160,161,162,163,164,165,166,167]

Pyroglutamate-NMA Dihedral Test Before CHARMM Optimization					
Dihedral	***QM Twist***	***MM Twist***	***Difference***	***Square***	***Check***
(atoms)	***(degrees)***	***(degrees)***	***(degrees)***	***(sq. deg.)***	***(degrees^{-1})***
C9 -N8 -C -CA	-178.90	-179.55	-0.65	0.42	#DIV/0!
C9 -N8 -C -O	0.64	0.28	-0.35	0.12	#DIV/0!
H16-N8 -C -CA	-1.20	-3.48	-2.28	5.19	#DIV/0!
H16-N8 -C -O	178.34	176.35	-1.99	3.94	#DIV/0!
N8 -C -CA -N	-5.64	-2.59	3.05	9.31	#DIV/0!
N8 -C -CA -CB	110.82	112.89	2.07	4.27	#DIV/0!
N8 -C -CA -HA	-128.89	-124.97	3.92	15.40	#DIV/0!
O -C -CA -N	174.81	177.58	2.77	7.68	#DIV/0!
O -C -CA -CB	-68.73	-66.95	1.79	3.19	#DIV/0!
O -C -CA -HA	51.55	55.19	3.65	13.29	#DIV/0!
C -CA -CB -CG	-101.17	-98.56	2.61	6.83	#DIV/0!
C -CA -CB -HB1	22.65	25.29	2.64	6.98	#DIV/0!
C -CA -CB -HB2	141.66	143.26	1.61	2.58	#DIV/0!
N -CA -CB -CG	22.73	24.48	1.75	3.07	#DIV/0!
N -CA -CB -HB1	146.55	148.33	1.78	3.16	#DIV/0!
N -CA -CB -HB2	-94.44	-93.70	0.74	0.55	#DIV/0!
HA -CA -CB -CG	141.71	140.79	-0.92	0.84	#DIV/0!
HA -CA -CB -HB1	-94.47	-95.36	-0.89	0.79	#DIV/0!
HA -CA -CB -HB2	24.53	22.61	-1.92	3.70	#DIV/0!
C -CA -N -CD	109.92	110.01	0.08	0.01	#DIV/0!
C -CA -N -HN	*-83.69*	*-72.58*	*11.11*	*123.48*	*10000.32131*
CB -CA -N -CD	-11.35	-11.94	-0.59	0.35	#DIV/0!
CB -CA -N -HN	*155.04*	*165.47*	*10.43*	*108.88*	*10000.41076*
HA -CA -N -CD	-129.95	-128.71	1.25	1.55	#DIV/0!

Table 31

Cont.

Pyroglutamate-NMA Dihedral Test Before CHARMM Optimization					
Dihedral	***QM Twist***	***MM Twist***	***Difference***	***Square***	***Check***
(atoms)	***(degrees)***	***(degrees)***	***(degrees)***	***(sq. deg.)***	***(degrees^{-1})***
HA -CA -N -HN	***36.44***	***48.71***	***12.27***	***150.67***	***10000.23393***
CA -CB -CG -CD	**-25.96**	**-28.21**	**-2.25**	**5.06**	**#DIV/0!**
CA -CB -CG -HG3	**90.72**	**89.55**	**-1.17**	**1.37**	**#DIV/0!**
CA -CB -CG -HG2	**-146.25**	**-148.76**	**-2.50**	**6.27**	**#DIV/0!**
HB1-CB -CG -CD	**-148.10**	**-152.63**	**-4.53**	**20.51**	**#DIV/0!**
HB1-CB -CG -HG3	**-31.41**	**-34.86**	**-3.45**	**11.91**	**#DIV/0!**
HB1-CB -CG -HG2	**91.61**	**86.83**	**-4.78**	**22.88**	**#DIV/0!**
HB2-CB -CG -CD	**90.49**	**89.69**	**-0.80**	**0.64**	**#DIV/0!**
HB2-CB -CG -HG3	**-152.83**	**-152.55**	**0.28**	**0.08**	**#DIV/0!**
HB2-CB -CG -HG2	**-29.80**	**-30.86**	**-1.05**	**1.11**	**#DIV/0!**
CA -N -CD -CG	**-5.30**	**-5.71**	**-0.41**	**0.17**	**#DIV/0!**
CA -N -CD -OE	**175.90**	**177.25**	**1.35**	**1.81**	**#DIV/0!**
HN -N -CD -CG	***-172.22***	***176.78***	***-11.00***	***120.93***	***10000.33369***
HN -N -CD -OE	***8.97***	***-0.26***	***-9.24***	***85.36***	***10000.80723***
N -CD -CG -CB	**19.80**	**20.91**	**1.11**	**1.22**	**#DIV/0!**
N -CD -CG -HG3	**-99.66**	**-98.61**	**1.05**	**1.10**	**#DIV/0!**
N -CD -CG -HG2	**142.72**	**142.64**	**-0.08**	**0.01**	**#DIV/0!**
OE -CD -CG -CB	**-161.43**	**-162.13**	**-0.71**	**0.50**	**#DIV/0!**
OE -CD -CG -HG3	**79.11**	**78.35**	**-0.76**	**0.58**	**#DIV/0!**
OE -CD -CG -HG2	**-38.51**	**-40.41**	**-1.90**	**3.59**	**#DIV/0!**
	Largest absolute error		***12.27***	**150.67**	***10000.23393***
		RMS error		***4.16***	***#DIV/0!***

The pyroglutamate-NMA dihedral angles, after optimizing its bond lengths, bond angles, and dihedral torsion angles as had been done for SB-674042, were compiled in Table 32.[4,158,159,160,161,162,163,164,165,166,167]

Table 32

Pyroglutamate-NMA Dihedral Angles After Optimization.[4,158,159,160,161,162,163,164,165,166,167]

Pyroglutamate-NMA Dihedral Test After CHARMM Optimization					
Dihedral	***QM Twist***	***MM Twist***	***Difference***	***Square***	***Check***
(atoms)	***(degrees)***	***(degrees)***	***(degrees)***	***(sq. deg.)***	***(degrees^{-1})***
C9 -N8 -C -CA	-178.90	-179.49	-0.59	0.35	#DIV/0!
C9 -N8 -C -O	0.64	0.05	-0.59	0.35	#DIV/0!
H16-N8 -C -CA	-1.20	-1.45	-0.25	0.06	#DIV/0!
H16-N8 -C -O	178.34	178.09	-0.25	0.06	#DIV/0!
N8 -C -CA -N	-5.64	-6.37	-0.73	0.54	#DIV/0!
N8 -C -CA -CB	110.82	107.92	-2.90	8.41	#DIV/0!
N8 -C -CA -HA	-128.89	-130.21	-1.32	1.73	#DIV/0!
O -C -CA -N	174.81	174.07	-0.73	0.54	#DIV/0!
O -C -CA -CB	-68.73	-71.63	-2.90	8.40	#DIV/0!
O -C -CA -HA	51.55	50.24	-1.31	1.73	#DIV/0!
C -CA -CB -CG	-101.17	-94.39	6.78	46.02	#DIV/0!
C -CA -CB -HB1	22.65	29.19	6.54	42.76	#DIV/0!
C -CA -CB -HB2	141.66	147.74	6.09	37.03	#DIV/0!
N -CA -CB -CG	22.73	26.39	3.66	13.40	#DIV/0!
N -CA -CB -HB1	146.55	149.97	3.42	11.66	#DIV/0!
N -CA -CB -HB2	-94.44	-91.48	2.96	8.78	#DIV/0!
HA -CA -CB -CG	141.71	147.63	5.93	35.14	#DIV/0!
HA -CA -CB -HB1	-94.47	-88.79	5.68	32.29	#DIV/0!
HA -CA -CB -HB2	24.53	29.76	5.23	27.35	#DIV/0!
C -CA -N -CD	109.92	107.75	-2.17	4.71	#DIV/0!
C -CA -N -HN	-83.69	-86.63	-2.94	8.64	#DIV/0!
CB -CA -N -CD	-11.35	-11.90	-0.55	0.31	#DIV/0!
CB -CA -N -HN	155.04	153.72	-1.32	1.75	#DIV/0!
HA -CA -N -CD	-129.95	-132.57	-2.62	6.88	#DIV/0!
HA -CA -N -HN	36.44	33.04	-3.39	11.50	#DIV/0!
CA -CB -CG -CD	-25.96	-31.07	-5.11	26.07	#DIV/0!
CA -CB -CG -HG3	90.72	86.69	-4.04	16.29	#DIV/0!
CA -CB -CG -HG2	-146.25	-151.39	-5.14	26.40	#DIV/0!
HB1-CB -CG -CD	-148.10	-155.32	-7.22	52.06	#DIV/0!

Table 32

Cont.

Pyroglutamate-NMA Dihedral Test After CHARMM Optimization					
Dihedral	***QM Twist***	***MM Twist***	***Difference***	***Square***	***Check***
(atoms)	***(degrees)***	***(degrees)***	***(degrees)***	***(sq. deg.)***	***(degrees^{-1})***
HB1-CB -CG -HG3	**-31.41**	**-37.56**	**-6.15**	**37.77**	**#DIV/0!**
HB1-CB -CG -HG2	**91.61**	**84.37**	**-7.25**	**52.54**	**#DIV/0!**
HB2-CB -CG -CD	**90.49**	**86.56**	**-3.93**	**15.41**	**#DIV/0!**
HB2-CB -CG -HG3	**-152.83**	**-155.68**	**-2.86**	**8.16**	**#DIV/0!**
HB2-CB -CG -HG2	**-29.80**	**-33.76**	**-3.96**	**15.66**	**#DIV/0!**
CA -N -CD -CG	**-5.30**	**-7.78**	**-2.49**	**6.18**	**#DIV/0!**
CA -N -CD -OE	**175.90**	**174.60**	**-1.30**	**1.69**	**#DIV/0!**
HN -N -CD -CG	**-172.22**	**-173.98**	**-1.76**	**3.09**	**#DIV/0!**
HN -N -CD -OE	**8.97**	**8.41**	**-0.57**	**0.32**	**#DIV/0!**
N -CD -CG -CB	**19.80**	**24.04**	**4.24**	**17.96**	**#DIV/0!**
N -CD -CG -HG3	**-99.66**	**-95.46**	**4.21**	**17.70**	**#DIV/0!**
N -CD -CG -HG2	**142.72**	**145.54**	**2.82**	**7.94**	**#DIV/0!**
OE -CD -CG -CB	**-161.43**	**-158.42**	**3.01**	**9.08**	**#DIV/0!**
OE -CD -CG -HG3	**79.11**	**82.09**	**2.98**	**8.89**	**#DIV/0!**
OE -CD -CG -HG2	**-38.51**	**-36.92**	**1.59**	**2.54**	**#DIV/0!**
	Largest absolute error		***7.25***	**52.54**	***#DIV/0!***
		RMS error		***3.80***	***#DIV/0!***

The resulting dihedral parameters, with repaired force constants (listed as K_χ in the parameter file), multiplicities (n), and offset constants (δ) highlighted for increased visibility, some extra parameters added with newer multiplicities for better optimization of these compounds, and the parameters for pyroglutamate and SB-674042 listed after the parameters used to connect pyroglutamate to peptides, are listed in Table 33.[4,137,158,159,160,161,162,163,164,165,166,167]

Table 33

Dihedral Parameters, with Repaired Parameters Highlighted.[4,137,158,159,160,161,162,163,164,165,166,167]

Dihedral Parameters as listed in the parameter file						
Atom Type 1	*Atom Type 2*	*Atom Type 3*	*Atom Type 4*	K_χ*(kcal mol^{-1})*	*n (multiplicity)*	*δ (degrees)*
CTY1	C	N	CP1	2.7500	2	180.00
CTY1	C	N	CP1	0.3000	4	0.00
CTY1	C	N	CP3	2.7500	2	180.00
CTY1	C	N	CP3	0.3000	4	0.00
CTY1	C	NH1	CT1	1.6000	1	0.00
CTY1	C	NH1	CT1	2.5000	2	180.00
H	NH1	C	CTY1	2.5000	2	180.00
NH1	C	CTY1	NH1	0.6000	1	0.00
NH1	CTY1	C	N	0.4000	1	0.00
O	C	CTY1	NH1	0.0000	1	0.00
O	C	N	CP1	2.7500	2	180.00
O	C	N	CP1	0.3000	4	0.00
O	C	N	CP3	2.7500	2	180.00
O	C	N	CP3	0.3000	4	0.00
O	C	NH1	CT1	2.5000	2	180.00
O	C	NH1	H	2.5000	2	180.00
N50	C53	C61	C61	1.0000	2	180.00
N50X	C53	C61	C61	*1.1156*	2	180.00
O50	C53	C61	C61	1.0000	2	180.00
O50X	C53	C61	C61	*1.1156*	2	180.00
C61	C53	N50	N50	8.5000	2	180.00
C61	C53	N50X	N50X	*6.5616*	2	180.00
O50	C53	N50	N50	14.0000	2	180.00
O50X	C53	N50X	N50X	*13.9271*	2	180.00
HG52	C53	N50	N50	3.3000	2	180.00
HG52	C53	N50X	N50X	3.3000	2	180.00
C61	C53	O50	C53	8.5000	2	180.00
C61	C53	O50X	C53	*6.5280*	2	180.00
N50	C53	O50	C53	8.5000	2	180.00

Table 33

Cont.

Dihedral Parameters as listed in the parameter file						
Atom Type 1	*Atom Type 2*	*Atom Type 3*	*Atom Type 4*	*K_χ(kcal mol^{-1})*	*n (multiplicity)*	*δ (degrees)*
N50X	C53	O50X	C53	8.5000	2	180.00
HG52	C53	O50	C53	3.8000	2	180.00
HG52	C53	O50X	C53	3.8000	2	180.00
C53	C61	C61	C61	*5.2810*	2	180.00
C53	C61	C61	H61	*3.9265*	2	180.00
C61	C61	C61	C61	3.1000	2	180.00
C61	C61	C61	H61	4.2000	2	180.00
H61	C61	C61	H61	2.4000	2	180.00
C53	N50	N50	C53	14.0000	2	180.00
C53	N50X	N50X	C53	*12.9127*	2	180.00
OD1	CO1	NG0	C11	2.7500	2	180.00
OD1	CO1	NG0	C11	0.3000	4	0.00
OD1	CO1	NG0	C215	2.7500	2	180.00
OD1	CO1	NG0	C215	0.3000	4	0.00
HG52	CO1	NG0	C11	2.6000	2	180.00
HG52	CO1	NG0	C215	2.6000	2	180.00
N50X	*C53*	*C21*	*C11*	*0.3000*	*2*	*0.00*
N50X	*C53*	*C21*	*C11*	*-0.7000*	*4*	*0.00*
N50X	C53	C21	C11	*1.5000*	3	*180.00*
N50X	*C53*	*C21*	*C11*	*-1.3000*	*1*	*0.00*
N50X	C53	C21	HG2	*0.0000*	3	0.00
O50X	C53	C21	C11	*0.0000*	*1*	*180.00*
O50X	C53	C21	HG2	*0.0000*	3	0.00
C21	C53	N50X	N50X	*4.4143*	2	180.00
C21	C53	O50X	C53	*11.2830*	2	180.00
C53	C21	C11	C215	*0.7000*	*3*	*0.00*
C53	C21	C11	NG0	*0.3000*	*1*	0.00
C53	C21	C11	HG1	*0.0000*	3	0.00
HG2	C21	C11	C215	*0.0000*	3	0.00
HG2	C21	C11	NG0	*0.0000*	3	0.00

Table 33

Cont.

Dihedral Parameters as listed in the parameter file						
Atom Type 1	*Atom Type 2*	*Atom Type 3*	*Atom Type 4*	*K_χ(kcal mol^{-1})*	*n (multiplicity)*	*δ (degrees)*
HG2	C21	C11	HG1	*0.0000*	3	0.00
C21	C11	C215	C215	*1.7900*	3	0.00
C21	C11	C215	HG2	0.1900	3	0.00
NG0	C11	C215	C215	0.1400	3	0.00
NG0	C11	C215	HG2	0.1400	3	0.00
HG1	C11	C215	C215	0.1900	3	0.00
HG1	C11	C215	HG2	0.1900	3	0.00
C21	C11	NG0	CO1	0.8000	3	0.00
C21	*C11*	*NG0*	*CO1*	*0.0800*	*6*	*0.00*
C21	C11	NG0	C215	0.1000	3	0.00
C21	*C11*	*NG0*	*C215*	*0.0100*	*6*	*0.00*
C215	C11	NG0	CO1	0.8000	3	0.00
C215	*C11*	*NG0*	*CO1*	*0.0800*	*6*	*0.00*
C215	C11	NG0	C215	0.1000	3	0.00
C215	*C11*	*NG0*	*C215*	*0.0100*	*6*	*0.00*
HG1	C11	NG0	CO1	0.8000	3	0.00
HG1	*C11*	*NG0*	*CO1*	*0.0800*	*6*	*0.00*
HG1	C11	NG0	C215	0.1000	3	0.00
HG1	*C11*	*NG0*	*C215*	*0.0100*	*6*	*0.00*
C11	C215	C215	C215	0.4100	3	180.00
C11	C215	C215	HG2	0.1900	3	0.00
C215	C215	C215	NG0	0.1400	3	0.00
C215	C215	C215	HG2	0.1900	3	0.00
NG0	C215	C215	HG2	0.1400	3	0.00
HG2	C215	C215	HG2	0.1900	3	0.00
C215	C215	NG0	CO1	0.0000	3	180.00
C215	*C215*	*NG0*	*CO1*	*0.1000*	*6*	*180.00*
C215	C215	NG0	C11	0.1000	3	0.00
HG2	*C215*	*NG0*	*CO1*	*0.1000*	*6*	*180.00*
HG2	C215	NG0	CO1	0.0000	3	180.00

Table 33

Cont.

Dihedral Parameters as listed in the parameter file						
Atom Type 1	*Atom Type 2*	*Atom Type 3*	*Atom Type 4*	*K_χ(kcal mol^{-1})*	*n (multiplicity)*	*δ (degrees)*
HG2	C215	NG0	C11	0.1000	3	0.00
NG0	CO1	C51	C51	1.0000	2	180.00
NG0	CO1	C51	N50Y	1.0000	2	180.00
OD1	CO1	C51	C51	1.0000	2	180.00
OD1	CO1	C51	N50Y	1.0000	2	180.00
C51	CO1	NG0	C11	1.6000	1	0.00
C51	CO1	NG0	C11	4.0000	2	180.00
C51	CO1	NG0	C215	-6.3000	2	0.00
C51	CO1	NG0	C215	0.8000	4	0.00
C51	CO1	NG0	C215	0.4000	6	180.00
CO1	C51	C51	S50Y	4.7453	2	180.00
CO1	C51	C51	HG52	1.5000	2	180.00
N50Y	C51	C51	S50Y	27.9668	2	180.00
N50Y	C51	C51	HG52	3.0000	2	180.00
CO1	C51	N50Y	C53	5.7385	2	180.00
C51	C51	N50Y	C53	23.3184	2	180.00
C51	C51	S50Y	C53	31.8457	2	180.00
HG52	C51	S50Y	C53	5.5000	2	180.00
N50Y	C53	C31	HG3	0.0000	3	0.00
S50Y	C53	C31	HG3	0.0837	3	0.00
C31	C53	N50Y	C51	4.8178	2	180.00
S50Y	C53	N50Y	C51	6.0000	2	180.00
C31	C53	S50Y	C51	10.4678	2	180.00
N50Y	C53	S50Y	C51	8.5000	2	180.00
HG3	C31	C11	C215	0.1600	3	0.00
HG3	C31	C11	NG0	0.1950	3	0.00
HG3	C31	C11	HG1	0.1600	3	0.00
C31	C11	C215	C215	0.1900	3	0.00
C31	C11	C215	HG2	0.1900	3	0.00
C31	C11	NG0	CO1	0.8000	3	0.00

Table 33

Cont.

Dihedral Parameters as listed in the parameter file						
Atom Type 1	*Atom Type 2*	*Atom Type 3*	*Atom Type 4*	*K_χ(kcal mol^{-1})*	*n (multiplicity)*	*δ (degrees)*
C31	C11	NG0	C215	0.1000	3	0.00
C61	C51	C51	N50Y	*6.2321*	2	180.00
C61	C51	C51	HG52	2.8000	2	180.00
S50Y	C51	C51	HG52	5.5000	2	180.00
C51	C51	C61	C61	*-4.6000*	2	*0.00*
C51	*C51*	*C61*	*C61*	*0.1000*	*4*	*0.00*
C51	*C51*	*C61*	*C61*	*0.3000*	*6*	*180.00*
C51	*C51*	*C61*	*C61*	*0.5000*	*1*	*180.00*
C51	*C51*	*C61*	*C61*	*0.0000*	*3*	*0.00*
C51	C51	C61	C66	*0.0000*	2	180.00
S50Y	C51	C61	C61	0.0000	2	180.00
S50Y	C51	C61	C66	0.0000	2	180.00
HG52	C51	N50Y	C53	3.0000	2	180.00
C61	C51	S50Y	C53	*7.9685*	2	180.00
C51	C61	C61	C61	*4.7027*	2	180.00
C51	C61	C61	H61	*3.0813*	2	180.00
C61	C61	C61	C66	*10.5440*	2	180.00
C61	C61	C61	H62	4.2000	2	180.00
C66	C61	C61	H61	4.2000	2	180.00
H61	C61	C61	H62	2.4000	2	180.00
C51	C61	C66	C61	*4.2284*	2	180.00
C51	C61	C66	FR1	*5.9321*	2	180.00
C61	C61	C66	C61	*13.6398*	2	180.00
C61	C61	C66	FR1	4.5000	2	180.00
H62	C61	C66	C61	4.2000	2	180.00
H62	C61	C66	FR1	2.4000	2	180.00
NH1	C	CTY1	CTY2	*0.0000*	1	0.00
NH1	C	CTY1	CTY2	*0.0000*	2	0.00
NH1	C	CTY1	HBY	*0.0000*	1	180.00
NH1	C	CTY1	HBY	*0.0000*	2	0.00

Table 33

Cont.

Dihedral Parameters as listed in the parameter file						
Atom Type 1	*Atom Type 2*	*Atom Type 3*	*Atom Type 4*	*K_χ(kcal mol^{-1})*	*n (multiplicity)*	*δ (degrees)*
N	C	CTY1	CTY2	*0.0000*	1	0.00
N	C	CTY1	CTY2	*0.0000*	2	0.00
N	C	CTY1	HBY	*0.0000*	1	180.00
N	C	CTY1	HBY	*0.0000*	2	0.00
O	C	CTY1	CTY2	*0.0000*	1	180.00
O	C	CTY1	CTY2	*0.0000*	2	0.00
O	*C*	*CTY1*	*CTY2*	*0.2000*	*6*	*180.00*
O	C	CTY1	HBY	*0.0000*	1	0.00
O	C	CTY1	HBY	*0.0000*	2	0.00
CTY1	C	NH1	CTY3	1.6000	1	0.00
CTY1	C	NH1	CTY3	2.5000	2	180.00
CTY1	C	NH1	H5	2.5000	2	180.00
O	C	NH1	CTY3	2.5000	2	180.00
O	C	NH1	H5	2.5000	2	180.00
NH1	CCY	CTY2	CTY2	1.0500	3	180.00
NH1	CCY	CTY2	HAY	0.0000	3	180.00
O	CCY	CTY2	CTY2	0.0800	3	0.00
O	CCY	CTY2	HAY	0.0000	3	0.00
CTY2	CCY	NH1	CTY1	0.4000	2	180.00
CTY2	CCY	NH1	H	*7.2700*	2	180.00
O	CCY	NH1	CTY1	2.5900	2	180.00
O	CCY	NH1	H	0.8600	2	180.00
HG3	CTY3	NH1	C	0.0000	3	0.00
HG3	CTY3	NH1	H5	0.0000	3	0.00
C	CTY1	CTY2	CTY2	0.1400	3	0.00
C	CTY1	CTY2	HAY	0.1400	3	0.00
NH1	CTY1	CTY2	CTY2	2.1300	3	0.00
NH1	CTY1	CTY2	HAY	0.0000	3	180.00
HBY	CTY1	CTY2	CTY2	0.1900	3	0.00
HBY	CTY1	CTY2	HAY	0.1900	3	0.00

Table 33

Cont.

Dihedral Parameters as listed in the parameter file						
Atom Type 1	*Atom Type 2*	*Atom Type 3*	*Atom Type 4*	K_χ*(kcal mol^{-1})*	*n (multiplicity)*	*δ (degrees)*
C	CTY1	NH1	CCY	*1.3478*	3	180.00
C	CTY1	NH1	H	0.7600	3	0.00
CTY2	CTY1	NH1	CCY	*1.8314*	3	180.00
CTY2	CTY1	NH1	H	0.7600	3	*180.00*
HBY	CTY1	NH1	CCY	0.0000	3	0.00
HBY	CTY1	NH1	H	0.0000	3	180.00
CCY	CTY2	CTY2	CTY1	0.3400	3	180.00
CCY	CTY2	CTY2	HAY	0.0000	3	0.00
CTY1	CTY2	CTY2	HAY	0.1900	3	0.00
HAY	CTY2	CTY2	HAY	0.1900	3	0.00
CO1	C51	C51	C61	*4.2491*	2	180.00
NG2	CO1	C51	C51	1.0000	2	180.00
NG2	CO1	C51	N50Y	1.0000	2	180.00
C51	CO1	NG2	HP1	1.0000	2	180.00
OD1	CO1	NG2	HP1	1.4000	2	180.00

The resulting improper dihedral parameters, with no necessary repairs determined or required to be made, are listed in Table 34.[4,137,158,159,160,161,162,163,164,165,166,167]

Table 34

Improper Dihedral Parameters.[4,137,158,159,160,161,162,163,164,165,166,167]

Improper Parameters					
Atom Type 1	*Atom Type 2*	*Atom Type 3*	*Atom Type 4*	K_ψ*(kcal mol^{-1}rad^{-2})*	ψ_0*(degrees)*
N	C	CP1	CP3	0.0000	0.0000
CO1	NG0	OD1	HG52	50.0000	0.0000

Table 34

Cont.

Improper Parameters					
Atom Type 1	***Atom Type 2***	***Atom Type 3***	***Atom Type 4***	K_ψ***(kcal mol^{-1}rad^{-2})***	ψ_0***(degrees)***
CO1	**C51**	**NG0**	**OD1**	**120.0000**	**0.0000**
C	**CTY1**	**NH1**	**O**	**120.0000**	**0.0000**
CCY	**CTY2**	**NH1**	**O**	**90.0000**	**0.0000**
CO1	**C51**	**NG2**	**OD1**	**120.0000**	**0.0000**

In the process of optimizing these bond, angle, and dihedral parameters, potential energy surfaces of these bonds, angles, and dihedrals were made, with the C1-C12 bond in SB-674042 BAT Model Compound 1 illustrated in Figure 115, and the CD-OE bond in pyroglutamate illustrated as examples in Figure 116.[4,137,158,159,160,161,162,163,164,165,166,167]

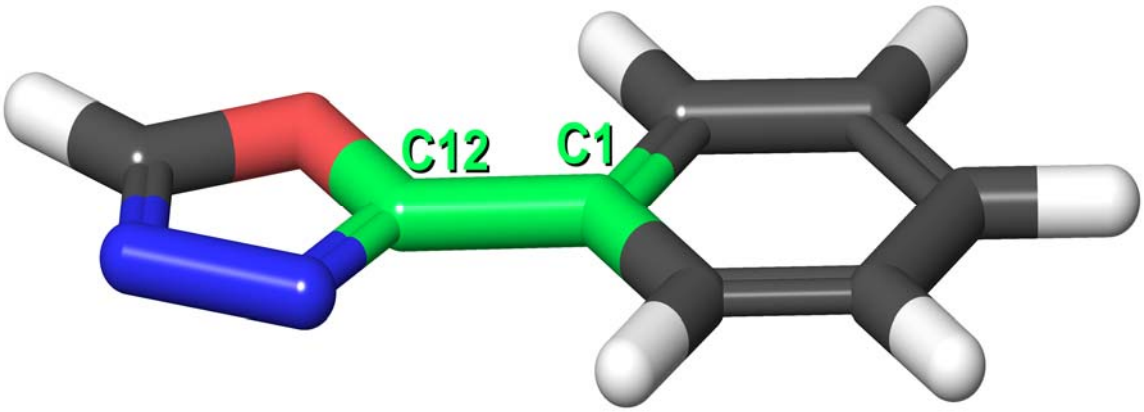

Figure 115. SB-674042 BAT Model Compound 1, with Bond C1-C12 Highlighted Green.[137,158,159,160,161,162,163,164,165,166,167]

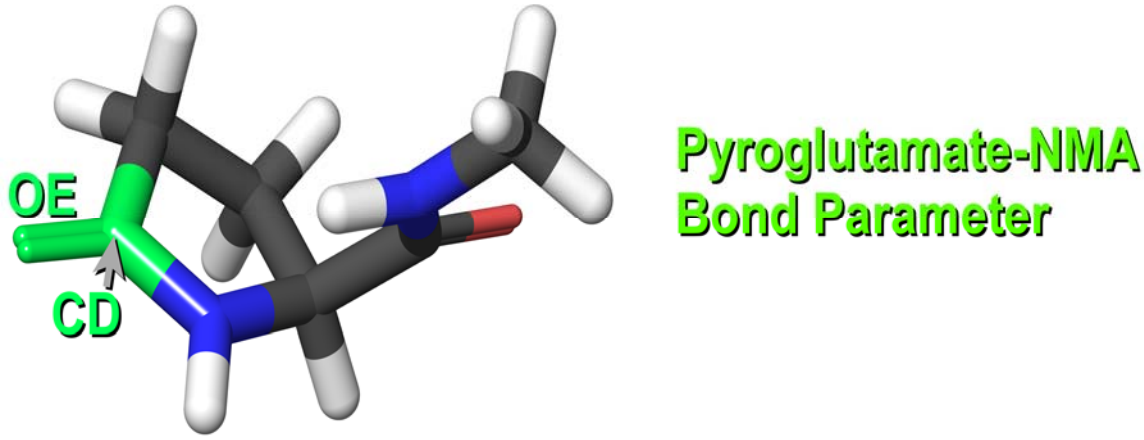

Figure 116. Pyroglutamate-NMA, with Bond CD-OE Highlighted Green.[4,158,159,160,161,162,163,164,165,166,167]

Since that bond connects the two rings of a compound that is absent from the CGenFF force field, and said bond was in need of repair, the potential energy surface of that same bond in SB-674042 BAT Model Compound 1 prior to parameter repair (namely the C51-C61 bond stretch parameter which atoms C12 and C1 represent, respectively) is shown in Figure 117, with a wide mismatch between the QM and MM energetic curves and minima.[137,158,159,160,161,162,163,164,165,166,167]

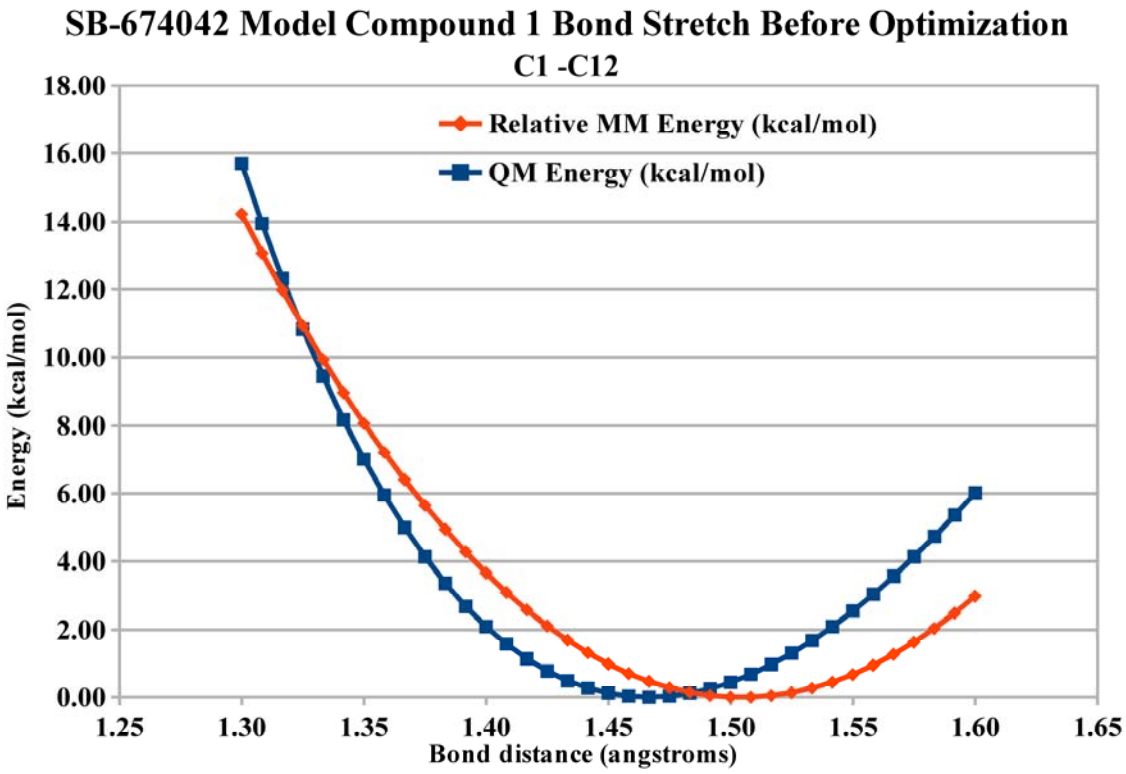

Figure 117. SB-674042 BAT Model Compound 1 Energy Profile for Bond C1-C12 Before Parameter Optimization, with a Notably Differing Mismatch Between the QM and MM Energetic Minima.[137,158,159,160,161,162,163,164,165,166,167]

The energy profile for the same C1-C12 bond in SB-674042 BAT Model Compound 1, but after bond length, bond angle, and dihedral angle optimization, with an improved energetic match between the QM minimum and the MM minimum, as well as the energetic curves of each, allowing both to line up almost perfectly, is shown in Figure 118.[137,158,159,160,161,162,163,164,165,166,167]

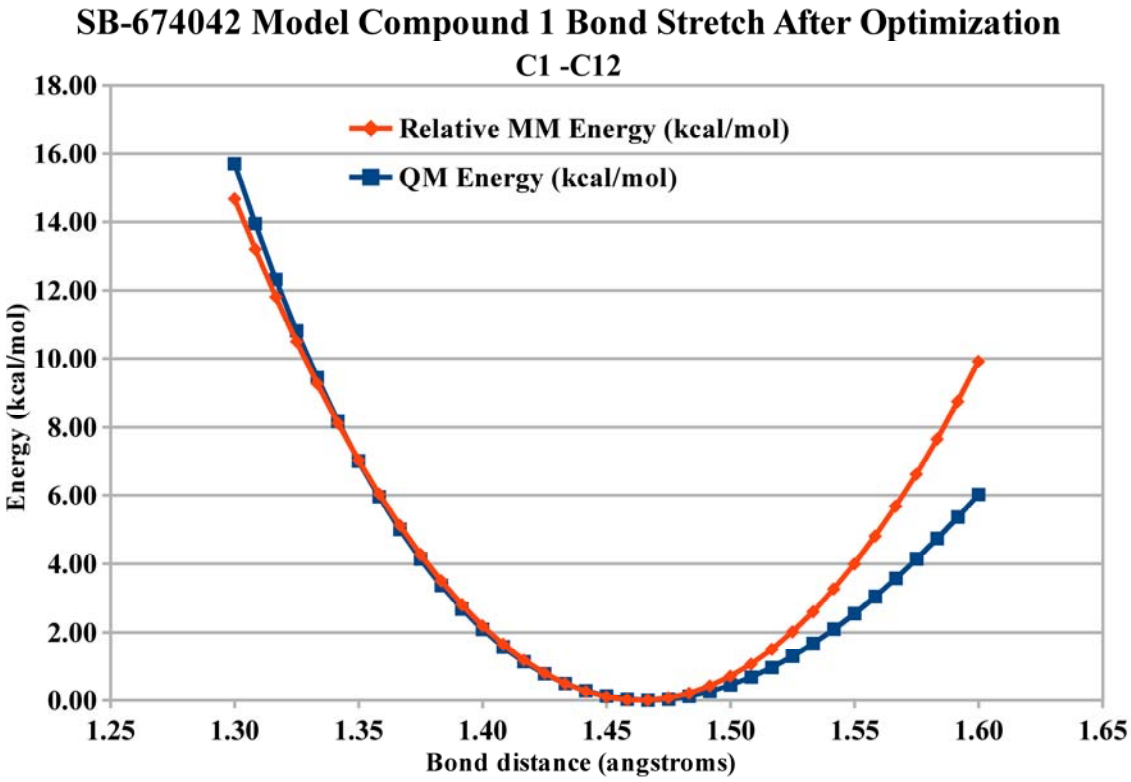

Figure 118. SB-674042 BAT Model Compound 1 Energy Profile for Bond C1-C12 After Parameter Optimization.[137,158,159,160,161,162,163,164,165,166,167]

More energy profiles were created for pyroglutamate-NMA's CD-OE bond representing the CCY-O bond stretch parameter, showing the mismatch of QM and MM energetic minima before, and a good lineup of QM and MM energetic minima after, bond length, bond angle, and dihedral angle parameter optimization.[4,158,159,160,161,162,163,164,165,166,167] The pyroglutamate-NMA bond CD-OE from before parameter optimization was performed shown in Figure 119.[4,158,159,160,161,162,163,164,165,166,167]

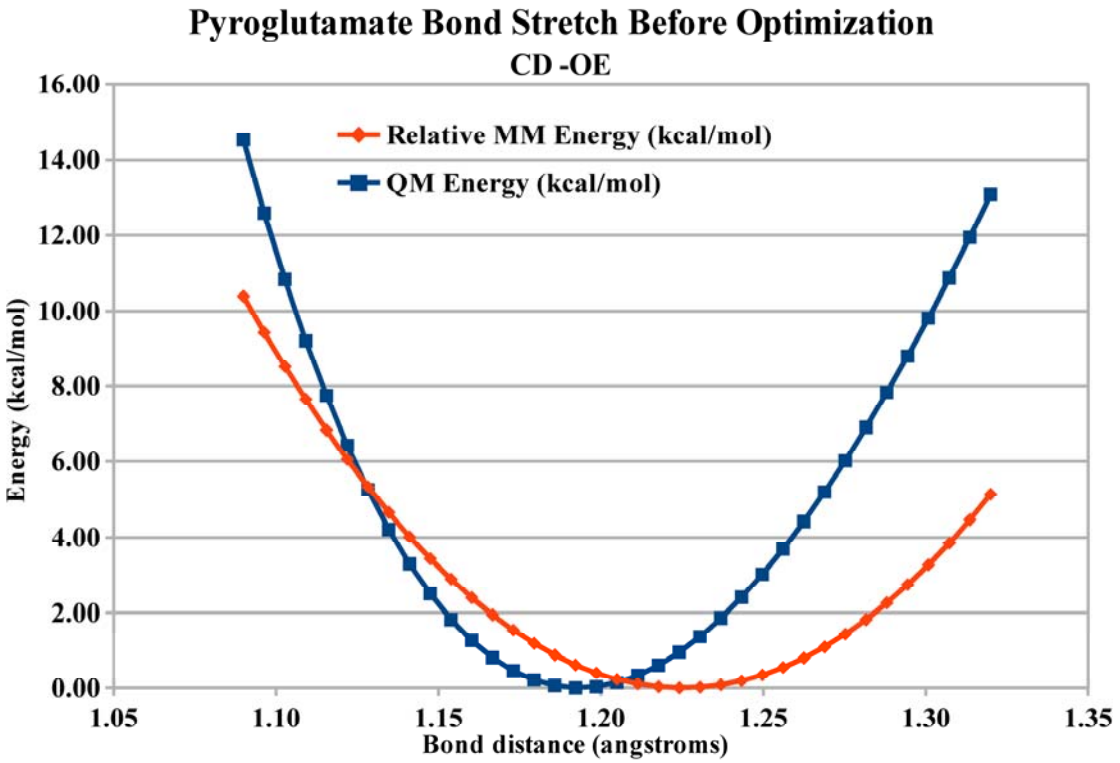

Figure 119. Pyroglutamate-NMA Energy Profile for Bond CD-OE Before Parameter Optimization, with a Notable Mismatch Between the QM and MM Energetic Minima.[4,158,159,160,161,162,163,164,165,166,167]

As was shown in Figure 117 for SB-674042 BAT Model Compound 1's C1-C12 bond and in Figure 119 for the pyroglutamate-NMA bond CD-OE, in both cases, the MM bond length was longer than the QM bond length, long enough to be outside the margin of QM-MM error, and the potential energy well to each side of the MM minimum was far shallower than that of the QM minimum, which allowed the MM compound to be more capable of deviating from its minimum, with these repaired bond parameters remedying that problem, and the potential energy surface for the pyroglutamate bond CD-OE after parameter optimization is shown in Figure 120.[4,158,159,160,161,162,163,164,165,166,167]

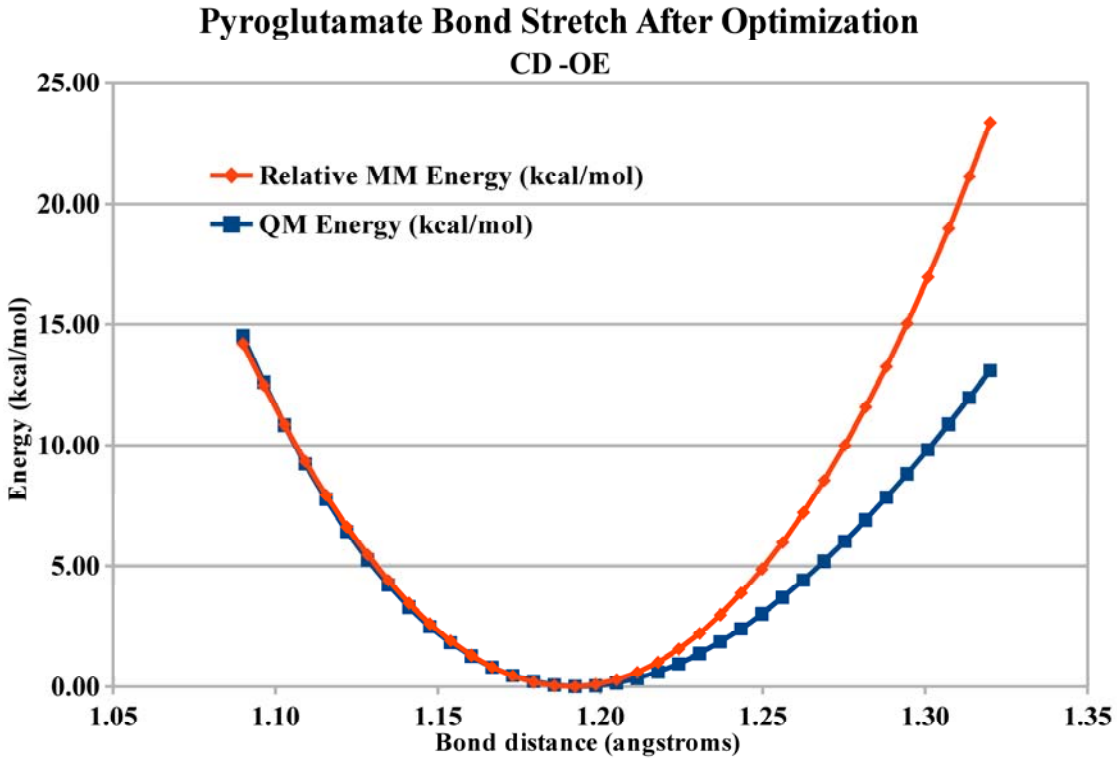

Figure 120. Pyroglutamate-NMA Energy Profile for Bond CD-OE After Parameter Optimization, with an Excellent Match Between the QM and MM Energetic Minima.[4,158,159,160,161,162,163,164,165,166,167]

As was seen in Figures 118 and 120, the implications of parameter repair are quite important, as not only does parameter optimization improve how well the QM and MM minima match up, it also improves the energetic wells' depth, allowing the MM compounds to be kept closer to their energetic minima, which already match up with the QM minima.[4,137,158,159,160,161,162,163,164,165,166,167] With that point made very clear, the example angles' potential energy surfaces will be shown, with SB-674042 BAT Model Compound 1's Bond Angle C1-C12-N13 and its energy profile prior to optimization illustrated in Figures 121 and 122.[137,158,159,160,161,162,163,164,165,166,167]

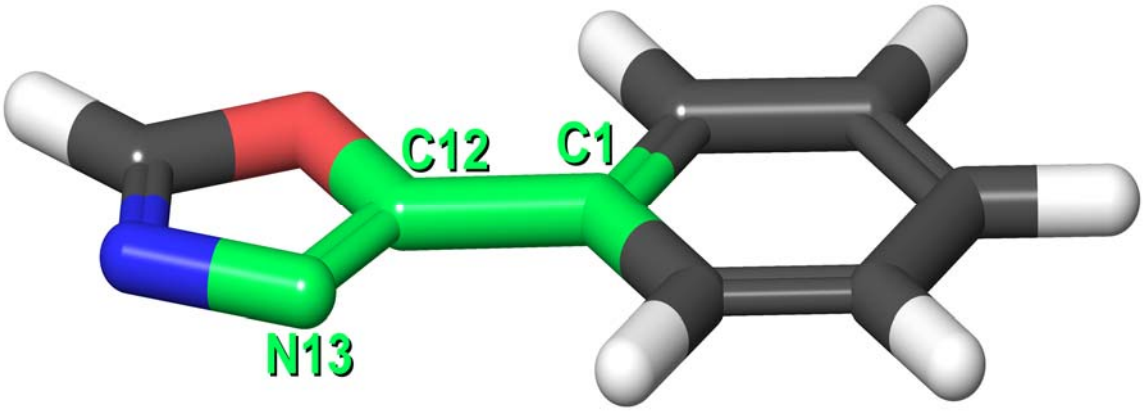

Figure 121. SB-674042 BAT Model Compound 1, with Angle C1-C12-N13 Highlighted Green.[137,158,159,160,161,162,163,164,165,166,167]

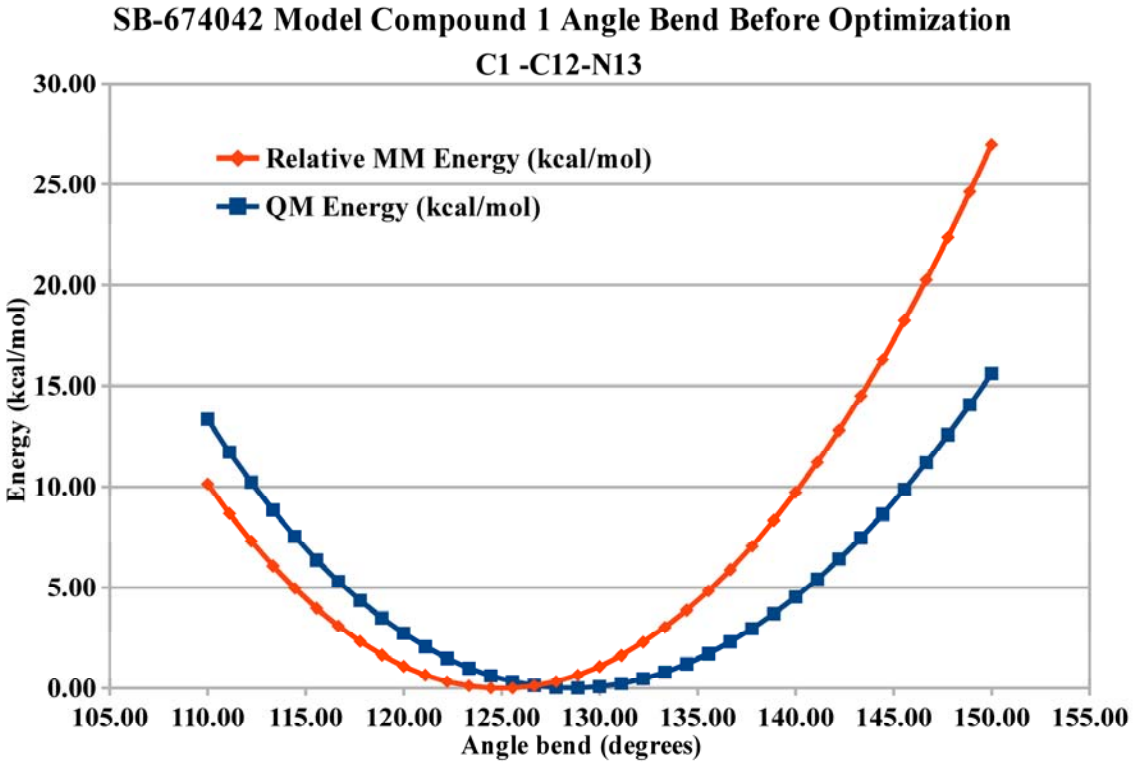

Figure 122. SB-674042 BAT Model Compound 1 Energy Profile for Angle C1-C12-N13 Before Parameter Optimization.[137,158,159,160,161,162,163,164,165,166,167]

The minima prior to parameter optimization did not line up well, but such is not the case after optimization, as shown in Figure 123 for that same angle, which did line up both the QM and MM minima and energetic wells quite well.[137,158,159,160,161,162,163,164,165,166,167]

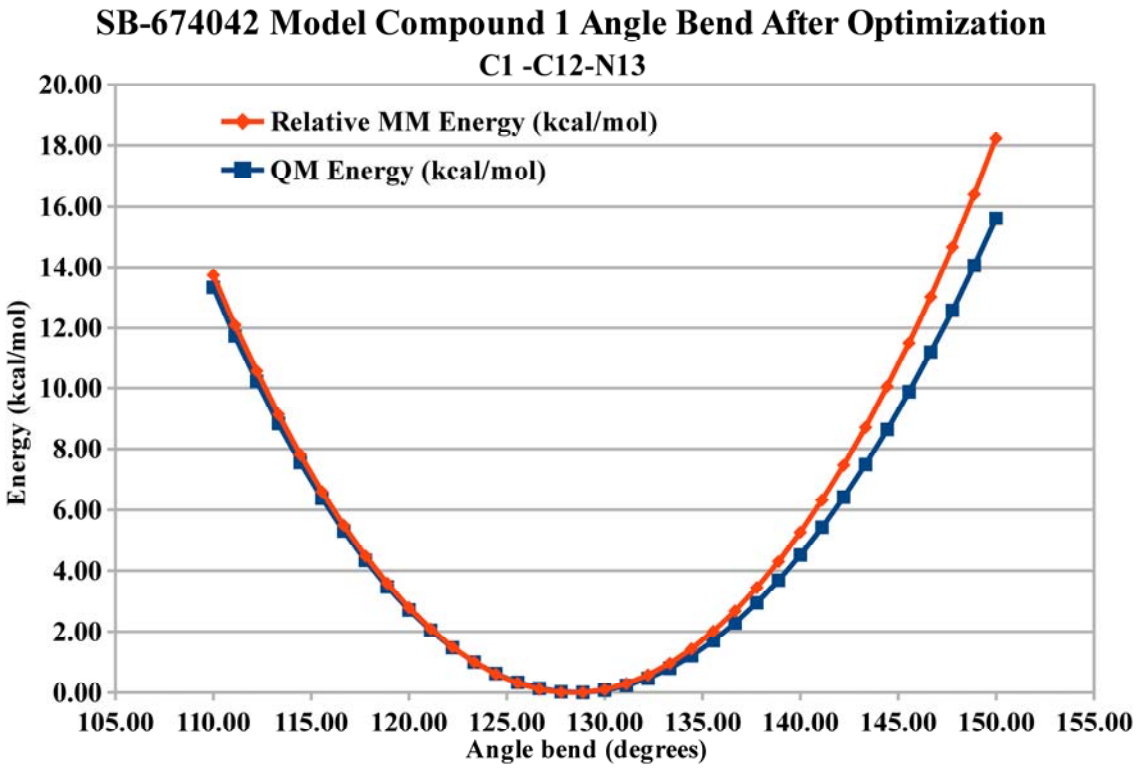

Figure 123. SB-674042 BAT Model Compound 1 Energy Profile for Angle C1-C12-N13 After Parameter Optimization.[137,158,159,160,161,162,163,164,165,166,167]

This angle optimization was also important in the pyroglutamate-NMA compound, as it would also be important to optimize any angle that connects atoms within a ring, unlike SB-674042 BAT Model Compound 1's C1-C12 bond or C1-C12-N13 angle, which each connect the two rings of that compound, or the CD-OE bond in pyroglutamate-NMA, which connects a ring carbon (CD) with its carbonyl oxygen (OE), with pyroglutamate-

NMA's Bond Angle C-CA-CB and its energy profile prior to optimization illustrated in Figures 124 and 125.[4,158,159,160,161,162,163,164,165,166,167]

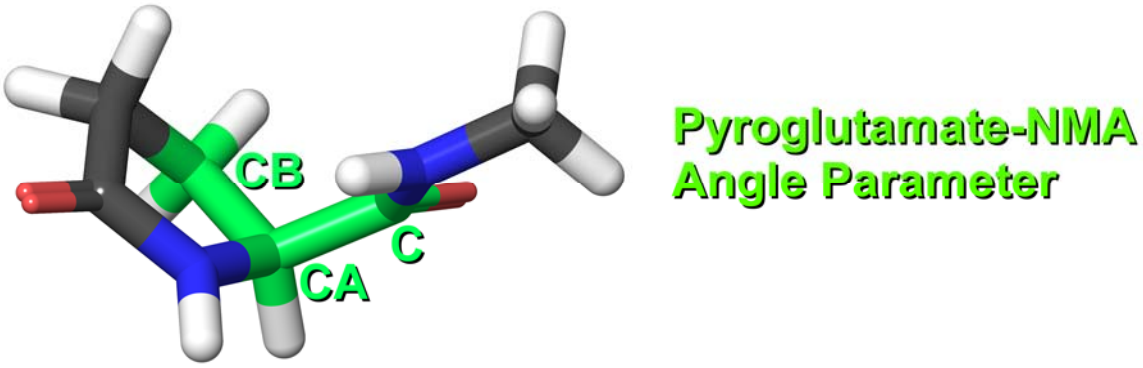

Figure 124. Pyroglutamate-NMA, with Angle C-CA-CB Highlighted Green.[4,158,159,160,161,162,163,164,165,166,167]

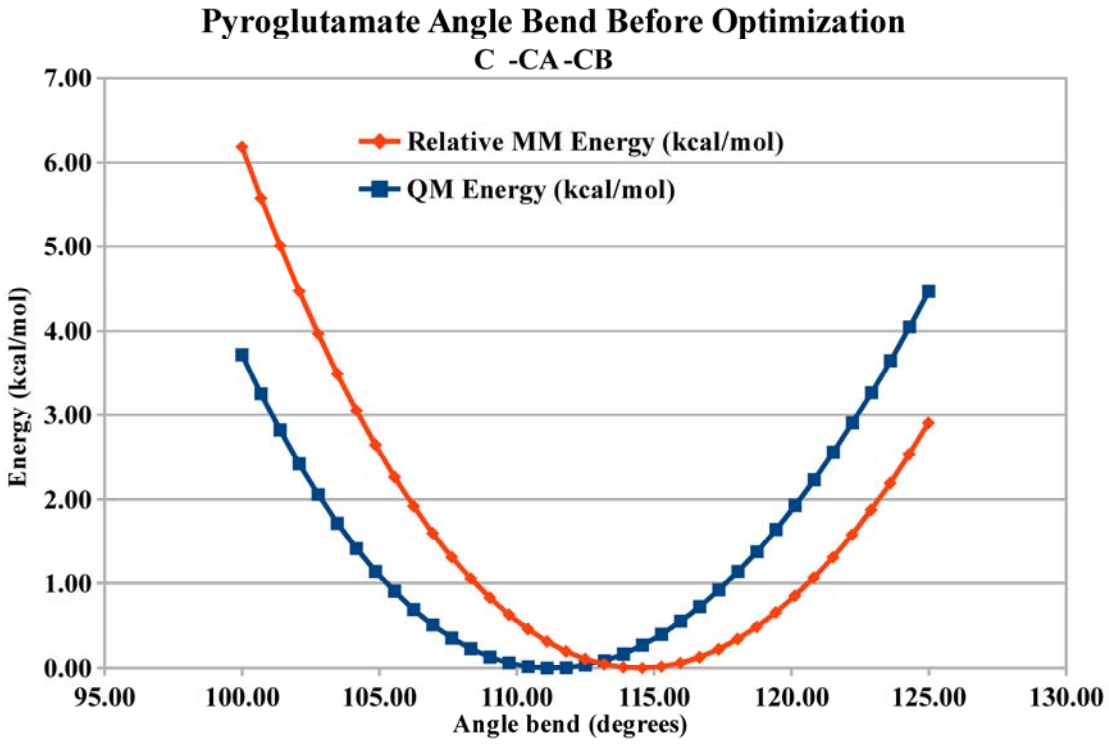

Figure 125. Pyroglutamate-NMA Energy Profile for Angle C-CA-CB Before Parameter Optimization.[4,158,159,160,161,162,163,164,165,166,167]

That MM bond angle energy profile was very different from the corresponding QM profile, as would be expected, but after parameter optimization, the energy profiles match extremely well, as seen in Figure 126.[4,158,159,160,161,162,163,164,165,166,167]

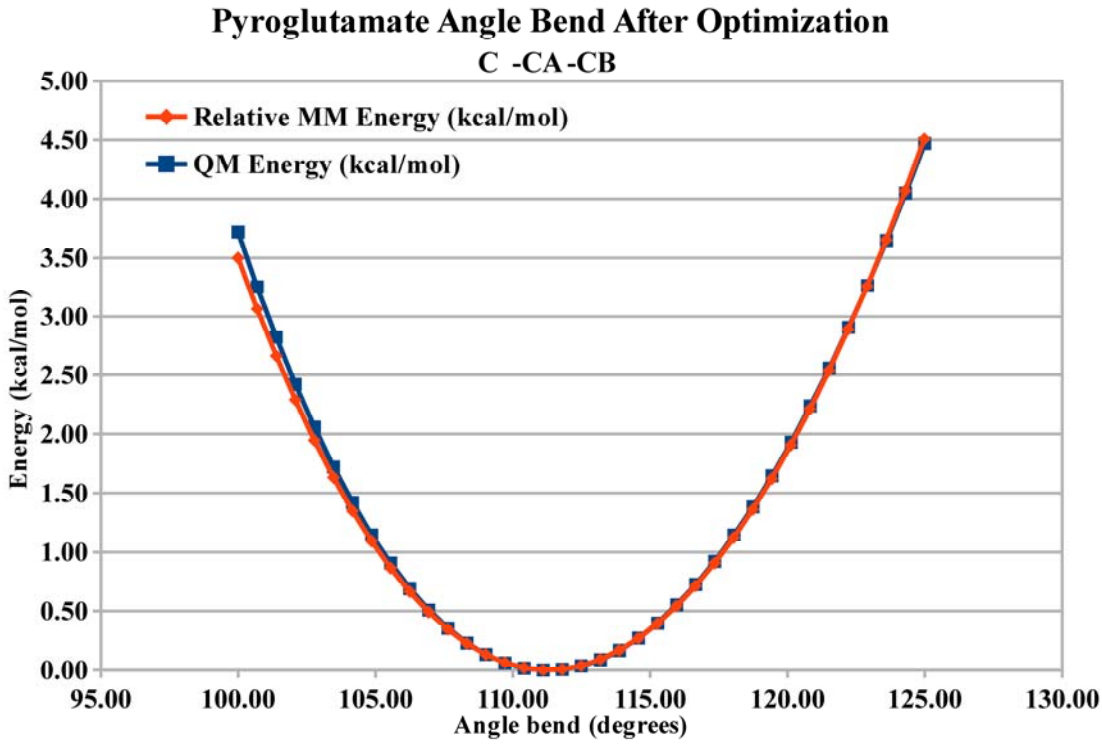

Figure 126. Pyroglutamate-NMA Energy Profile for Angle C-CA-CB After Parameter Optimization.[4,158,159,160,161,162,163,164,165,166,167]

Lastly, it is important that the dihedral minima match up, with less regard to the energetic peaks, as the minima would be the most populated areas on an energy profile, especially if the dihedral in question is an amide bond.[137,158,159,160,161,162,163,164,165,166,167] This would be the case, especially due to its high (at least 18 kcal/mol) energy barriers, for SB-674042 BAT Model Compound 3's amide bond C3-C11-N24-C16 (with intent to

resemble that of a proline)[3,137] and its corresponding energy profile prior to parameter optimization, as shown in Figures 127 and 128.[137,158,159,160,161,162,163,164,165,166,167]

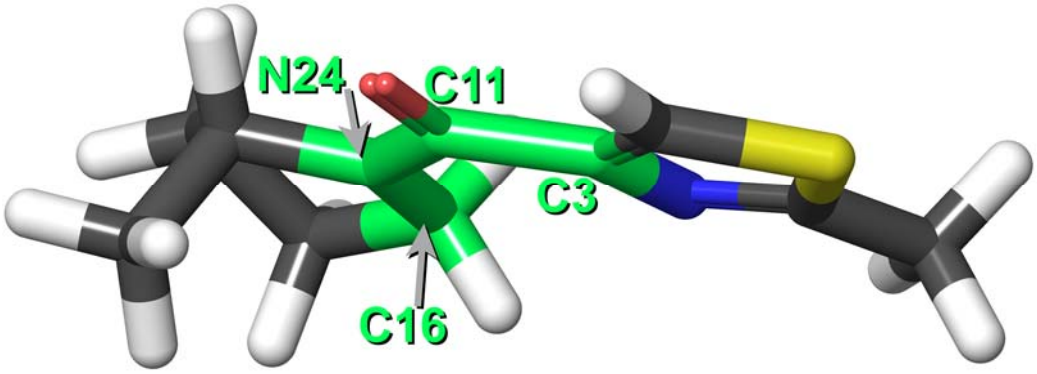

Figure 127. SB-674042 BAT Model Compound 3, with Dihedral C3-C11-N24-C16 Highlighted Green.[137,158,159,160,161,162,163,164,165,166,167]

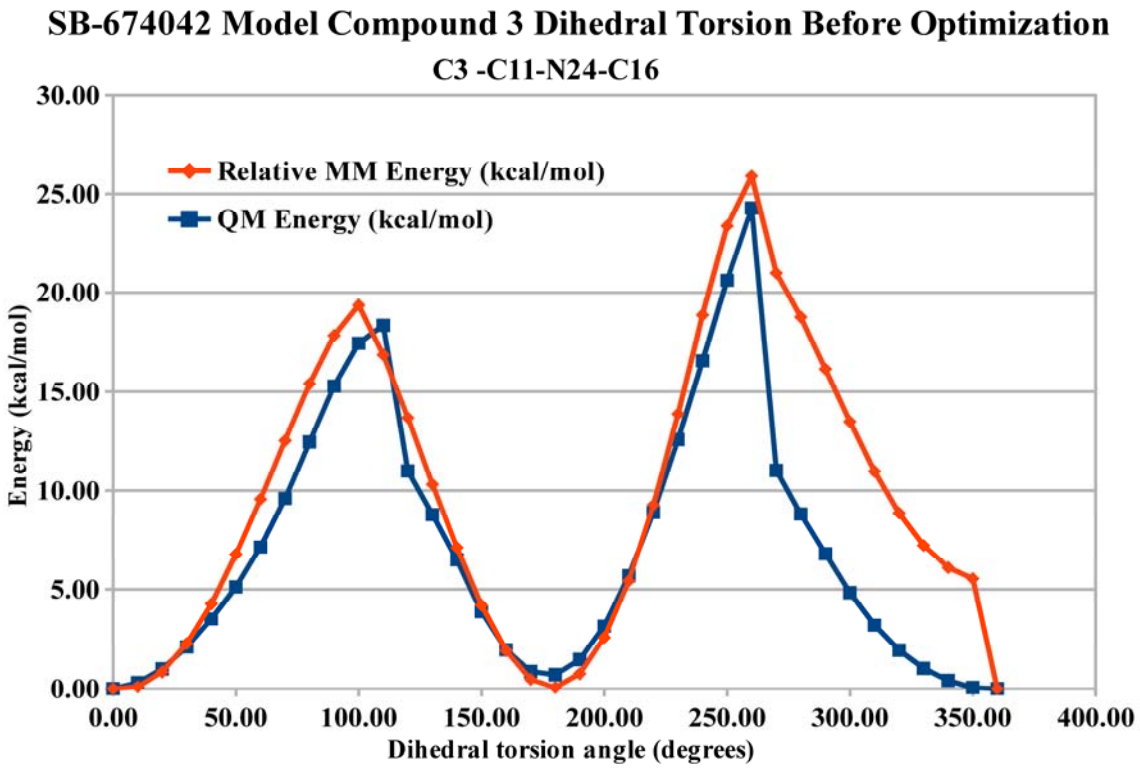

Figure 128. SB-674042 BAT Model Compound 3 Energy Profile for Dihedral C3-C11-N24-C16 Before Parameter Optimization.[137,158,159,160,161,162,163,164,165,166,167]

With 10-degree increments between each dihedral measurement, the minimum at a certain dihedral measurement would have to be between the two lowest energy values, thus showing that the global minimum has to be moved closer to 0°, as opposed to ~+5° as seen in Figure 128.[137,158,159,160,161,162,163,164,165,166,167] Figure 129 illustrates the tradeoff of raising the energy barriers to *cis*/*trans* conversion for this dihedral in exchange for centering the minima at 0° and 180°, after optimization.[137,158,159,160,161,162,163,164,165,166,167]

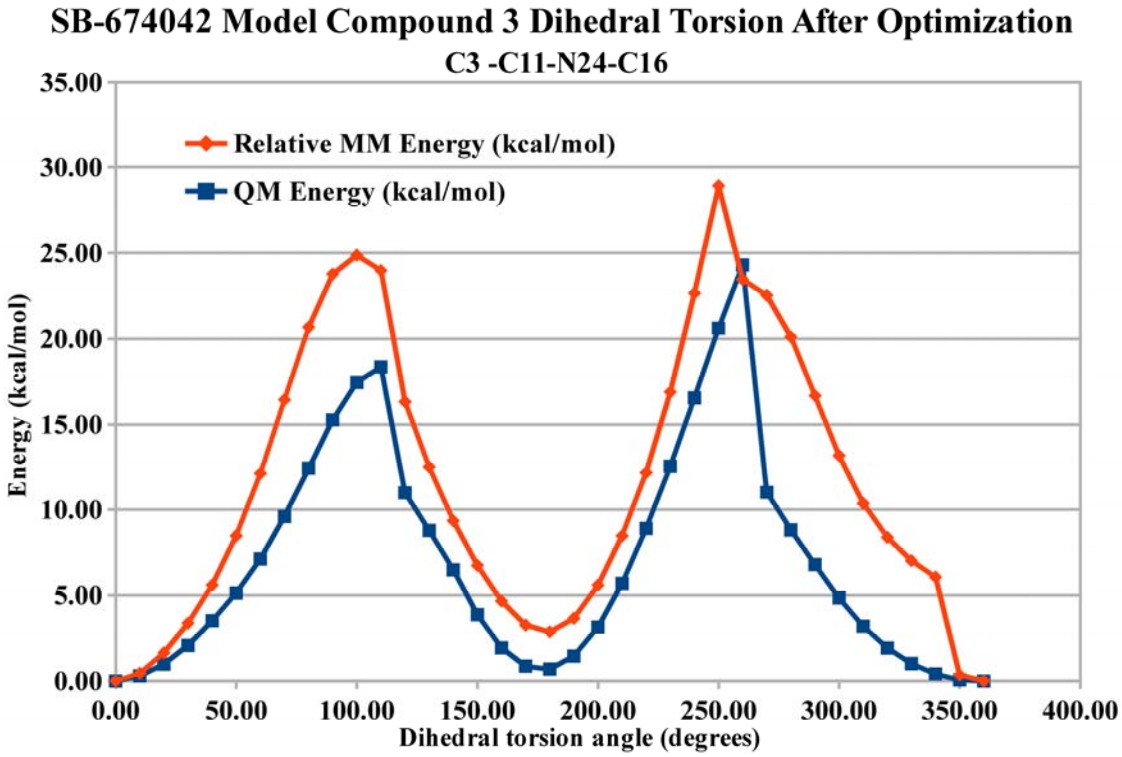

Figure 129. SB-674042 BAT Model Compound 3 Energy Profile for Dihedral C3-C11-N24-C16 After Parameter Optimization.[137,158,159,160,161,162,163,164,165,166,167]

That repair allowed all of the amide-centered dihedrals of SB-674042 BAT Model Compound 3, and by extension SB-674042, to fall within the margin of error for a

dihedral measurement.[137,158,159,160,161,162,163,164,165,166,167] Another example of a dihedral potential energy surface is Figures 130 and 131.[4,158,159,160,161,162,163,164,165,166,167]

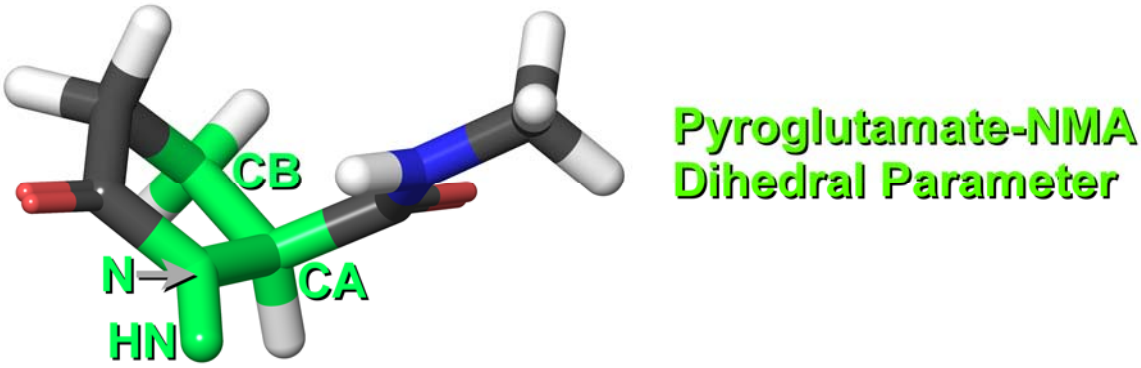

Figure 130. Pyroglutamate-NMA, with Dihedral CB-CA-N-HN Highlighted Green.[4,158,159,160,161,162,163,164,165,166,167]

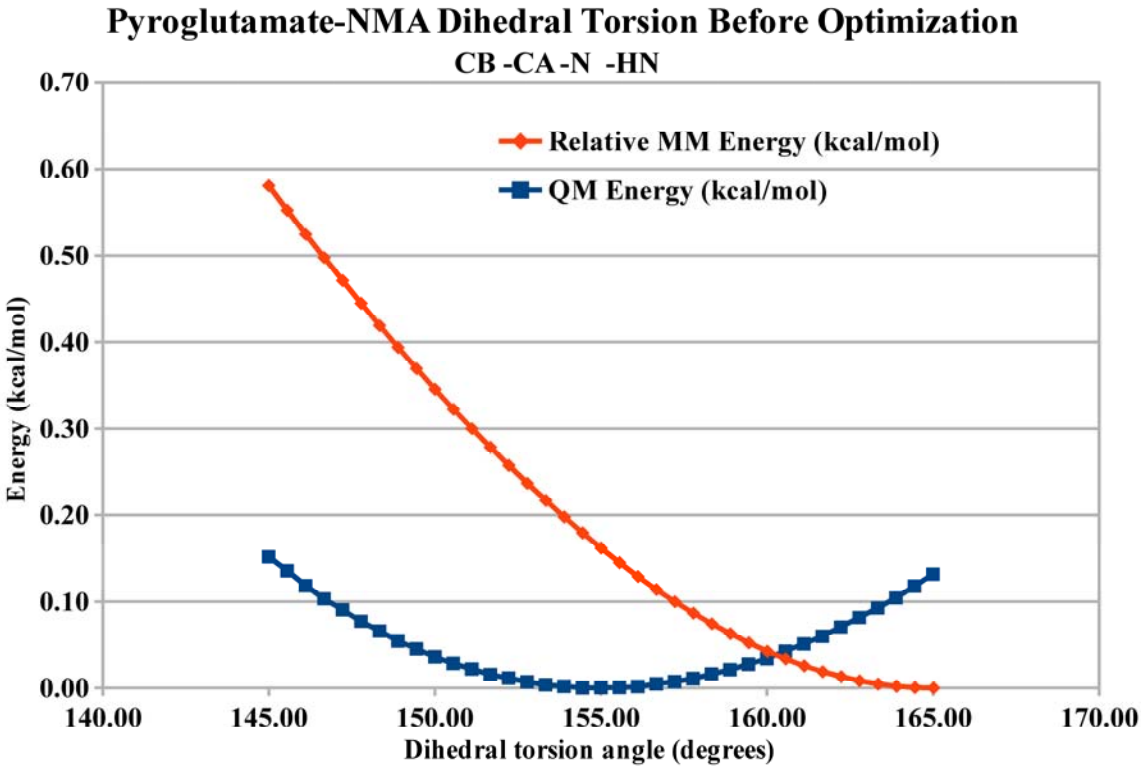

Figure 131. Pyroglutamate-NMA Energy Profile for Dihedral CB-CA-N-HN Before Parameter Optimization.[4,158,159,160,161,162,163,164,165,166,167]

The resulting MM energy profile had a minimum that was very far from the QM minimum, and the misplacement of HN was responsible for all of the MM dihedral measurements that were outside the margin of error, but repair of the adjacent CTY2-CCY-NH1-H dihedral parameter (representing the CG-CD-N-HN dihedral) beneficially impacted this dihedral and the other four that needed repair, as shown in Figure 132.[4,158,159,160,161,162,163,164,165,166,167]

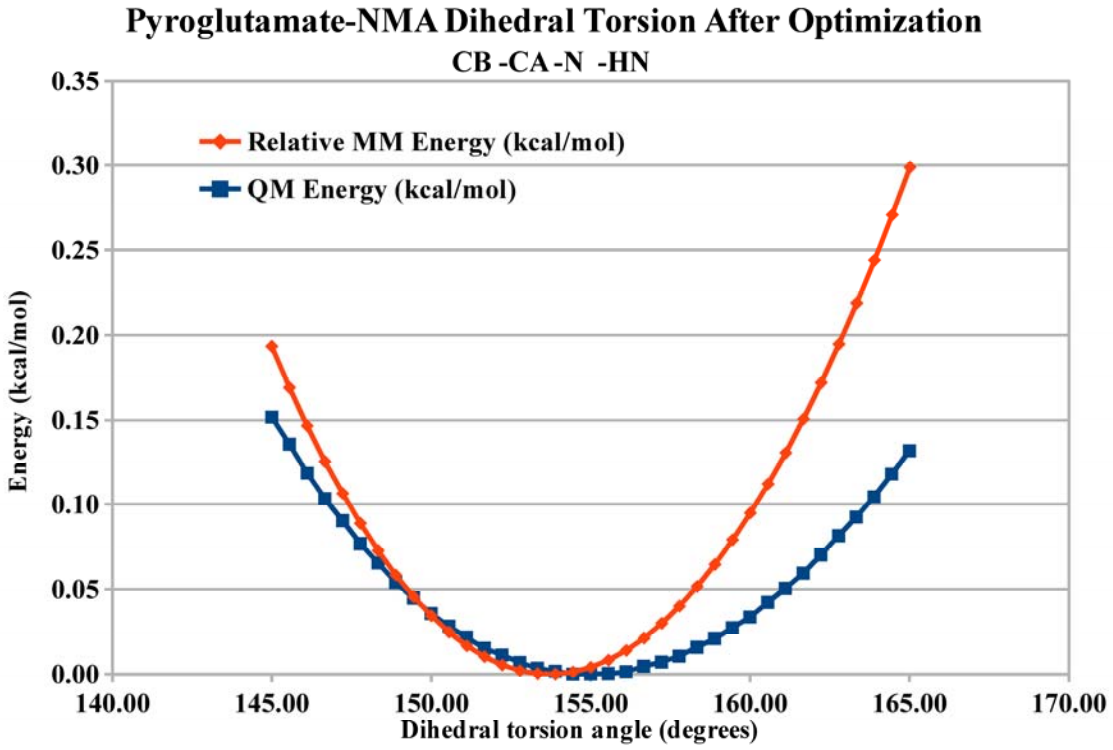

Figure 132. Pyroglutamate-NMA Energy Profile for Dihedral CB-CA-N-HN After Parameter Optimization.[4,158,159,160,161,162,163,164,165,166,167]

The difference between the QM and MM energetic minima was reduced to well within the acceptable margin of error, and both of the energetic wells were deep enough to allow the *cis*-amide to maintain its planarity in any situation.[4,158,159,160,161,162,163,164,165,166,167] As

a result, the parameters were created, and were ready to test on the global and local minima of SB-674042, and the global minimum of pyroglutamate-NMA using the "eye test."[4,137,158,159,160,161,162,163,164,165,166,167]

Eye Test of Parameters Using Local and Global Minima of SB-674042

Two local minima of SB-674042 were used alongside the global minimum of SB-674042 as part of an eye test to determine the overall appearance of SB-674042 once minimized with the new CHARMM parameters, with the QM global minimum and its pre-optimized MM counterpart shown in Figure 133.[137,158,159,160,161,162,163,164,165,166,167]

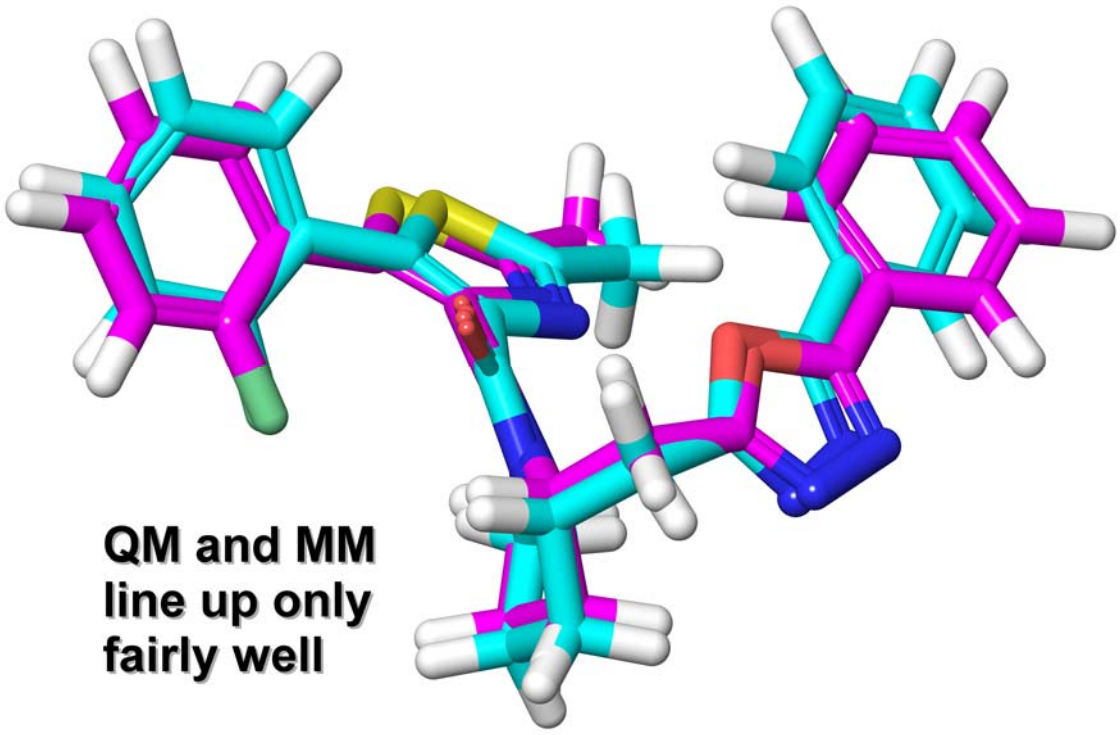

Figure 133. SB-674042 QM Global Minimum (Magenta Carbons) and the MM Global Minimum (Teal Carbons), the Latter Using the Bond Length, Bond Angle, and Dihedral Torsion Angle Parameters Prior to Their Optimization.[137,158,159,160,161,162,163,164,165,166,167]

A notable improvement in MM parameters became apparent with the newer optimized MM global minimum of SB-674042 being closer all-around to the QM global minimum than the pre-optimized MM global minimum was, especially within the tail phenyl and 1,3,4-oxadiazole end of SB-674042, with the QM global minimum and its optimized MM counterpart shown in Figure 134.[137,158,159,160,161,162,163,164,165,166,167]

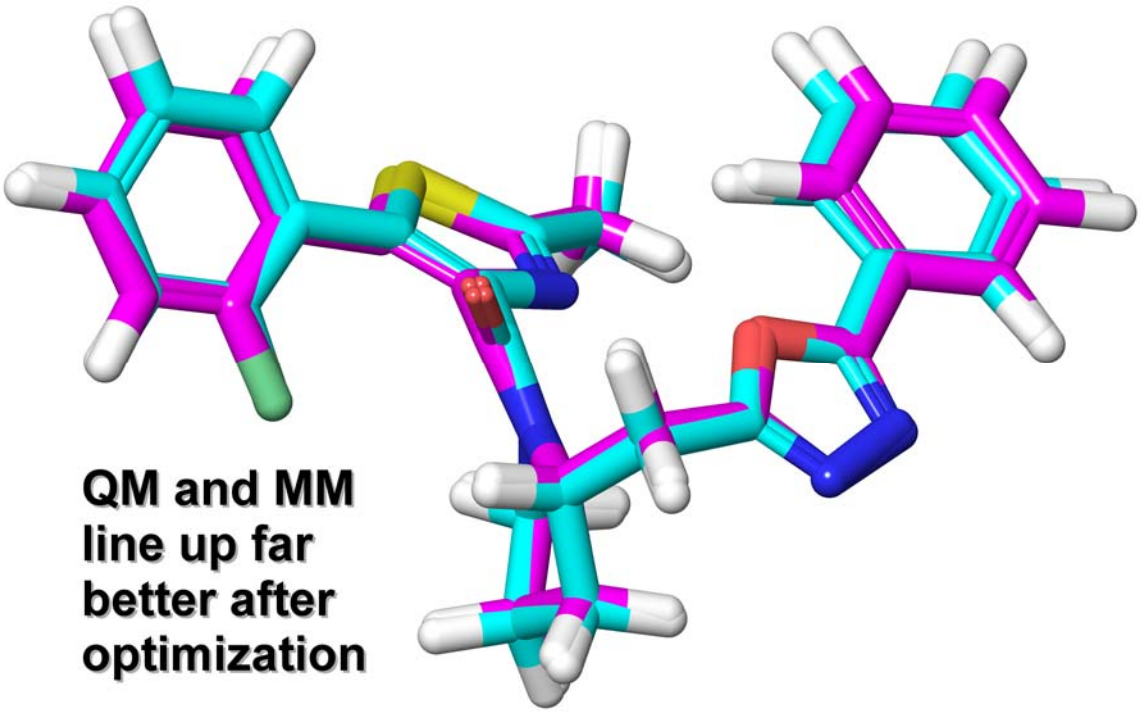

Figure 134. SB-674042 QM Global Minimum (Magenta Carbons) and the MM Global Minimum (Teal Carbons), the Latter Using the Bond Length, Bond Angle, and Dihedral Torsion Angle Parameters After Their Optimization.[137,158,159,160,161,162,163,164,165,166,167]

With a large improvement of parameters apparent in the global minimum, the local minima had to be consulted as well to show how the parameters improved their structures, with the two local minima being the “unpopped” global minimum of SB-674042 (the global minimum of the “unpopped” conformational search that still had a

higher energy than the true global minimum) and a local minimum of the conformational search of the "popped" SB-674042, and the first of these is the QM "unpopped" global minimum and its MM-pre-optimized counterpart, as is shown in Figure 135.[137,158,159,160,161,162,163,164,165,166,167]

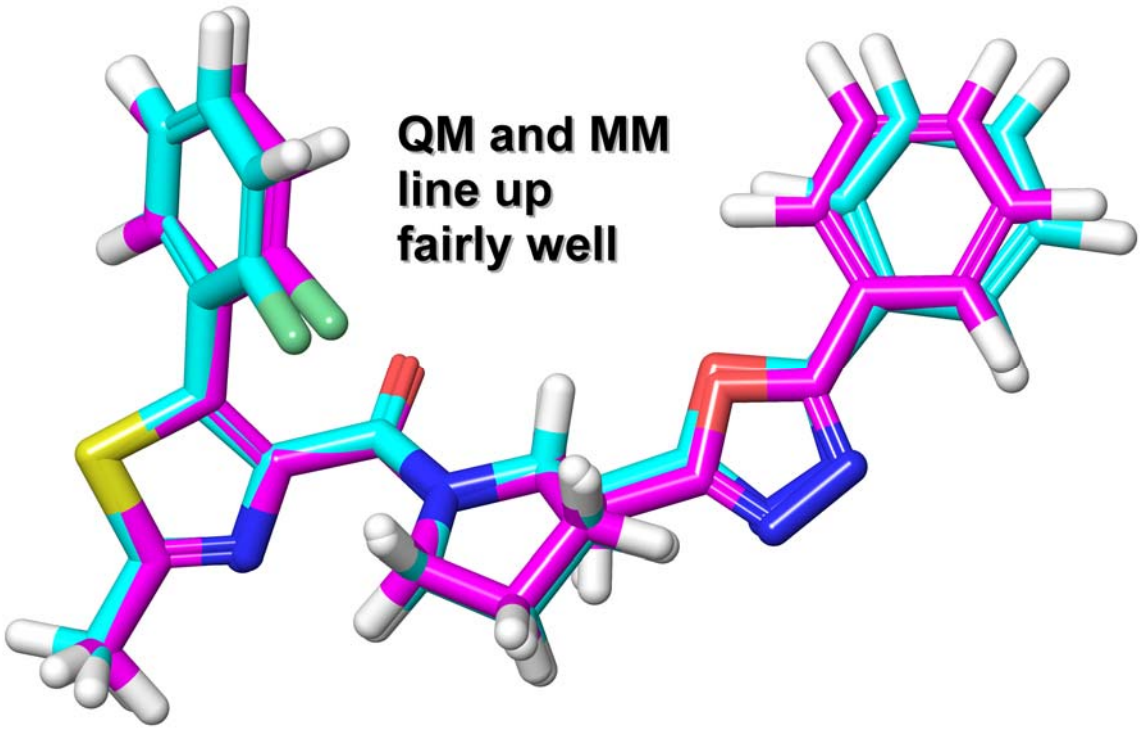

Figure 135. SB-674042 QM "Unpopped" Global Minimum (Magenta Carbons) and the MM "Unpopped" Global Minimum (Teal Carbons), the Latter Using the Bond Length, Bond Angle, and Dihedral Torsion Angle Parameters Prior to Their Optimization.[137,158,159,160,161,162,163,164,165,166,167]

The overall structure SB-674042 showed an on-average improvement, and individual parts improved as well, especially the head fluorophenyl and 1,3-thiazole end of SB-674042, when the newer optimized bond length, bond angle, and dihedral torsion angle parameters were used in place of the older pre-optimized parameters to minimize the MM

"unpopped" global minimum and superimpose it on the QM "unpopped" global minimum, with those two structures shown in Figure 136.[137,158,159,160,161,162,163,164,165,166,167]

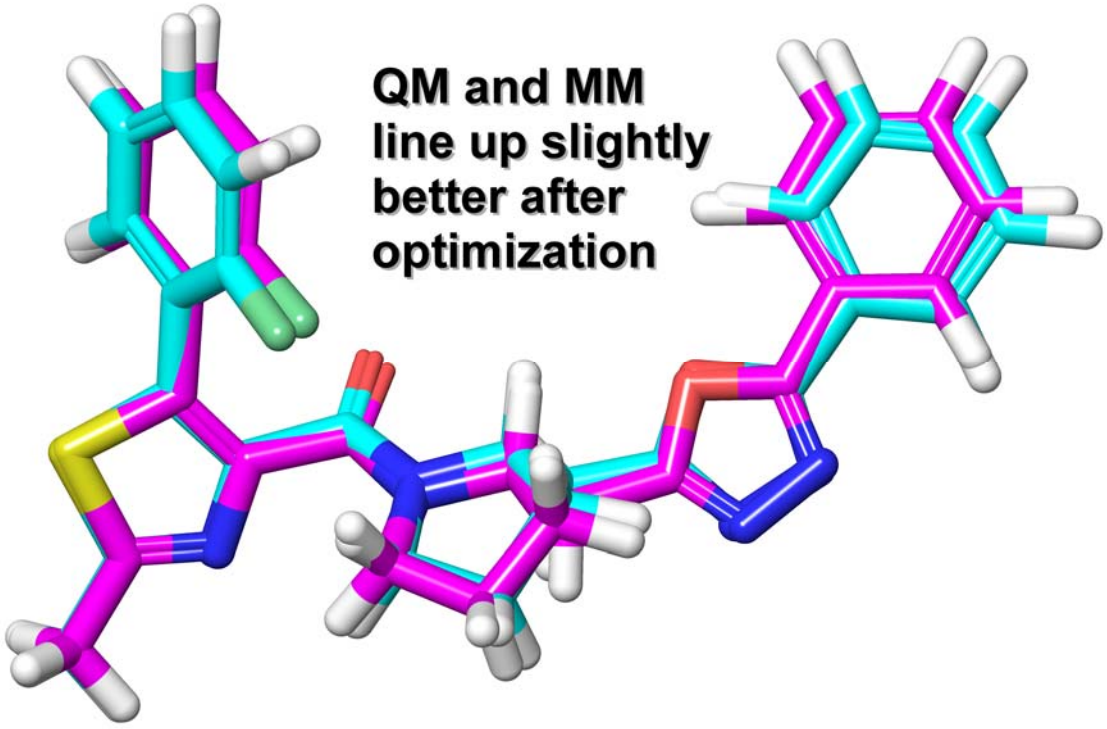

Figure 136. SB-674042 QM "Unpopped" Global Minimum (Magenta Carbons) and the MM "Unpopped" Global Minimum (Teal Carbons), the Latter Using the Bond Length, Bond Angle, and Dihedral Torsion Angle Parameters After Their Optimization.[137,158,159,160,161,162,163,164,165,166,167]

The last local minimum that had to be consulted was a local minimum of the "popped" SB-674042 conformational search, and the QM structure and its pre-optimized MM counterpart were superimposed, with a notable difference in structure between the QM and MM structures.[137,158,159,160,161,162,163,164,165,166,167] The MM structure especially had a greatly errant tail phenyl and 1,3,4-oxadiazole end of SB-674042, with the MM structure

having a C23-C35-C38-O42 dihedral angle that was ~50° less than that of the QM structure, as both structures are shown in Figure 137.[137,158,159,160,161,162,163,164,165,166,167]

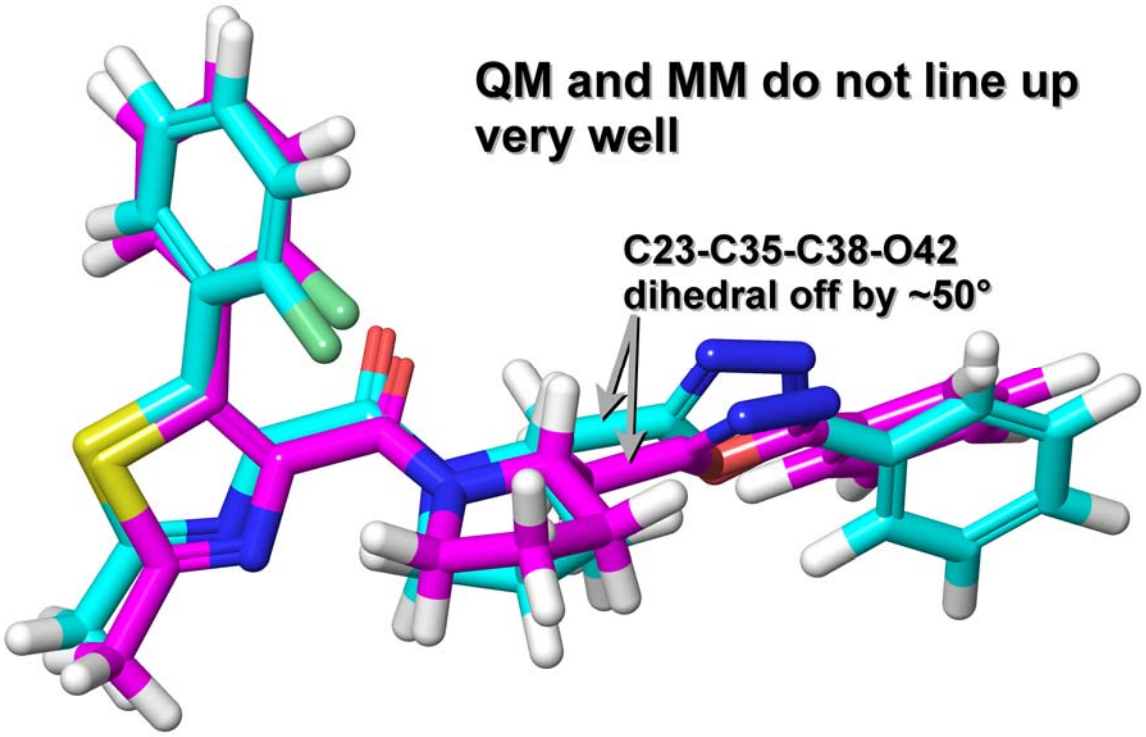

Figure 137. SB-674042 QM "Popped" Local Minimum (Magenta Carbons) and the MM "Popped" Local Minimum (Teal Carbons), the Latter Using the Bond Length, Bond Angle, and Dihedral Torsion Angle Parameters Before Optimization.[137,158,159,160,161,162,163,164,165,166,167]

When the optimized bond length, bond angle, and dihedral torsion angle parameters were used to minimize the "popped" local minimum, virtually everything in the MM structure improved, as the C23-C35-C38-O42 dihedral angle error between the MM and QM structures was reduced to as little as ~3°, and the optimized MM head fluorophenyl and 1,3-thiazole end fit much more closely together with their QM counterparts than the corresponding pre-optimized MM parts did.[137,158,159,160,161,162,163,164,165,166,167] This is

shown by superimposing the MM "popped" local minimum with optimized parameters on its QM counterpart, as is shown in Figure 138.[137,158,159,160,161,162,163,164,165,166,167]

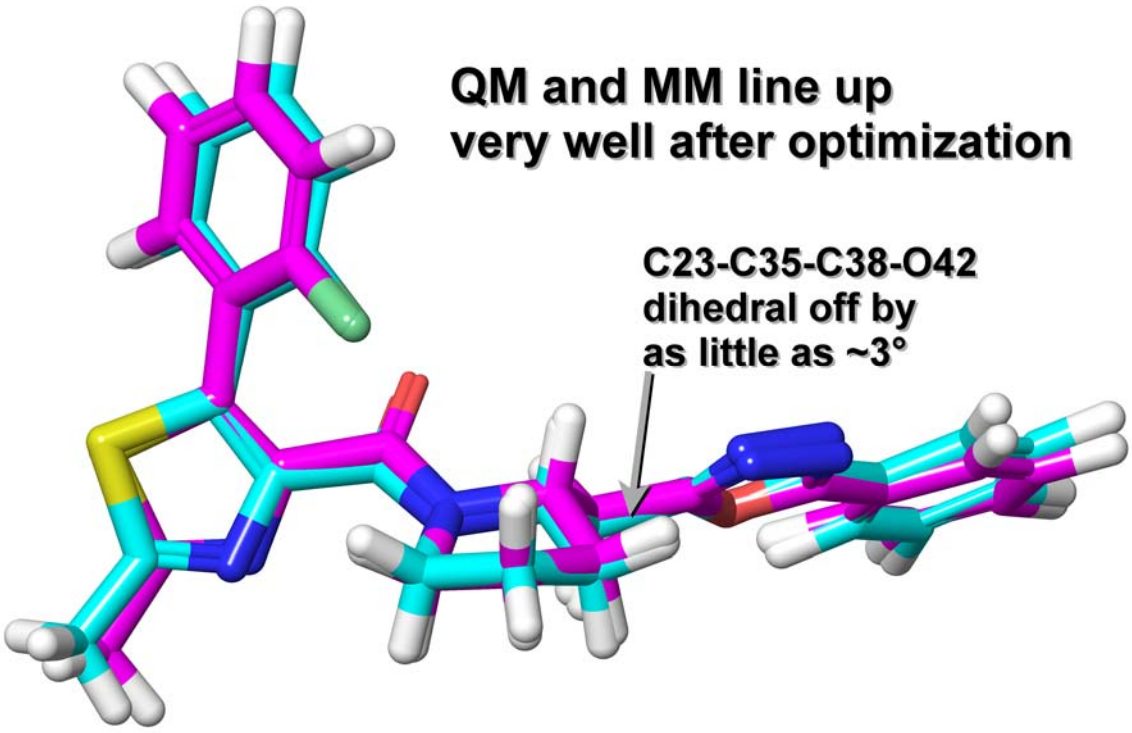

Figure 138. SB-674042 QM "Popped" Local Minimum (Magenta Carbons) and the MM "Popped" Local Minimum (Teal Carbons), the Latter Using the Bond Length, Bond Angle, and Dihedral Torsion Angle Parameters After Their Optimization.[137,158,159,160,161,162,163,164,165,166,167]

Eye Test of Parameters Using the Global Minimum of Pyroglutamate-NMA

A similar eye test to that of SB-674042 was performed on pyroglutamate-NMA using the global minimum of pyroglutamate-NMA, and since it was a far smaller molecule than SB-674042, pyroglutamate-NMA's global minimum was used for this experiment.[4,158,159,160,161,162,163,164,165,166,167] This global minimum was minimized first with the pre-optimized bond length, bond angle, and dihedral torsion angle parameters,

then with the optimized parameters, and the pre-optimized MM global minimum of pyroglutamate-NMA was superimposed on its QM counterpart, as shown in Figure 139.[4,158,159,160,161,162,163,164,165,166,167]

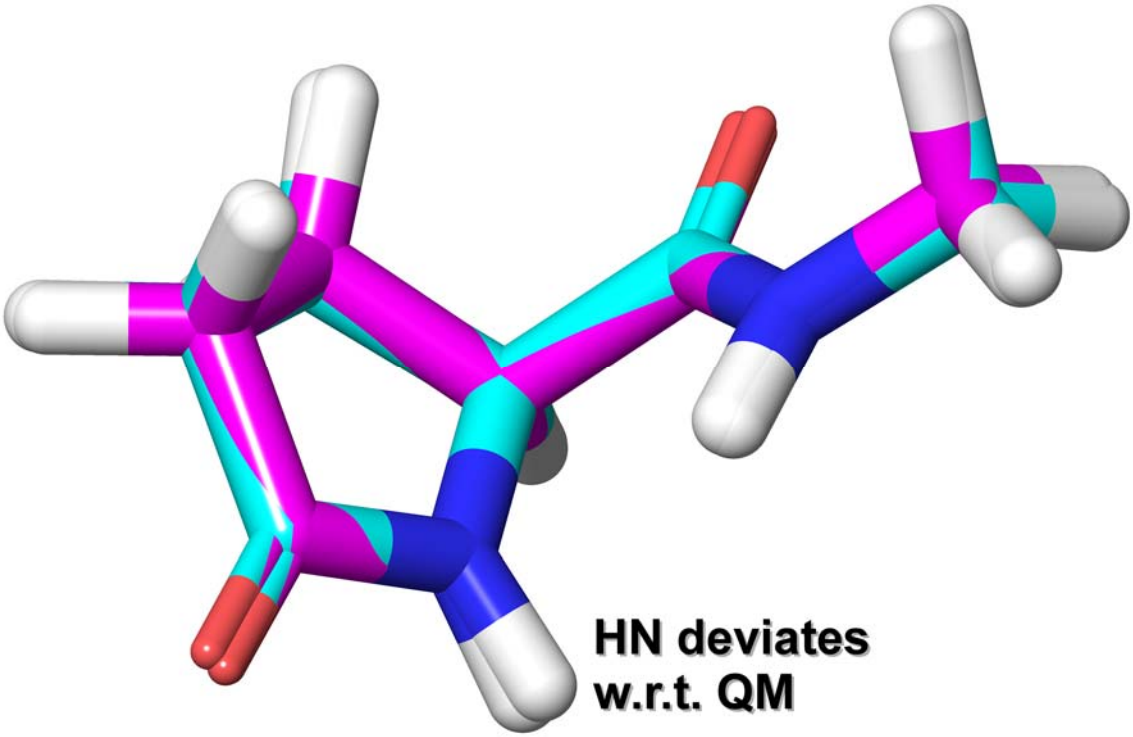

Figure 139. Pyroglutamate-NMA QM Global Minimum (Magenta Carbons) and the MM Global Minimum (Teal Carbons), the Latter Using the Bond Length, Bond Angle, and Dihedral Torsion Angle Parameters Prior to Their Optimization.[4,158,159,160,161,162,163,164,165,166,167]

Very little was required to be fixed, namely the HN that was pointed slightly differently in the pre-optimized MM structure, as well as CD-OE being too long and C-CA-CB being spread too wide, and using the optimized bond length, bond angle, and dihedral torsion angle parameters allowed all of those issues to be properly addressed for the MM structure.[4,158,159,160,161,162,163,164,165,166,167] The MM global minimum was minimized using

these newer optimized parameters and superimposed onto the QM global minimum, as is shown in Figure 140.[4,158,159,160,161,162,163,164,165,166,167]

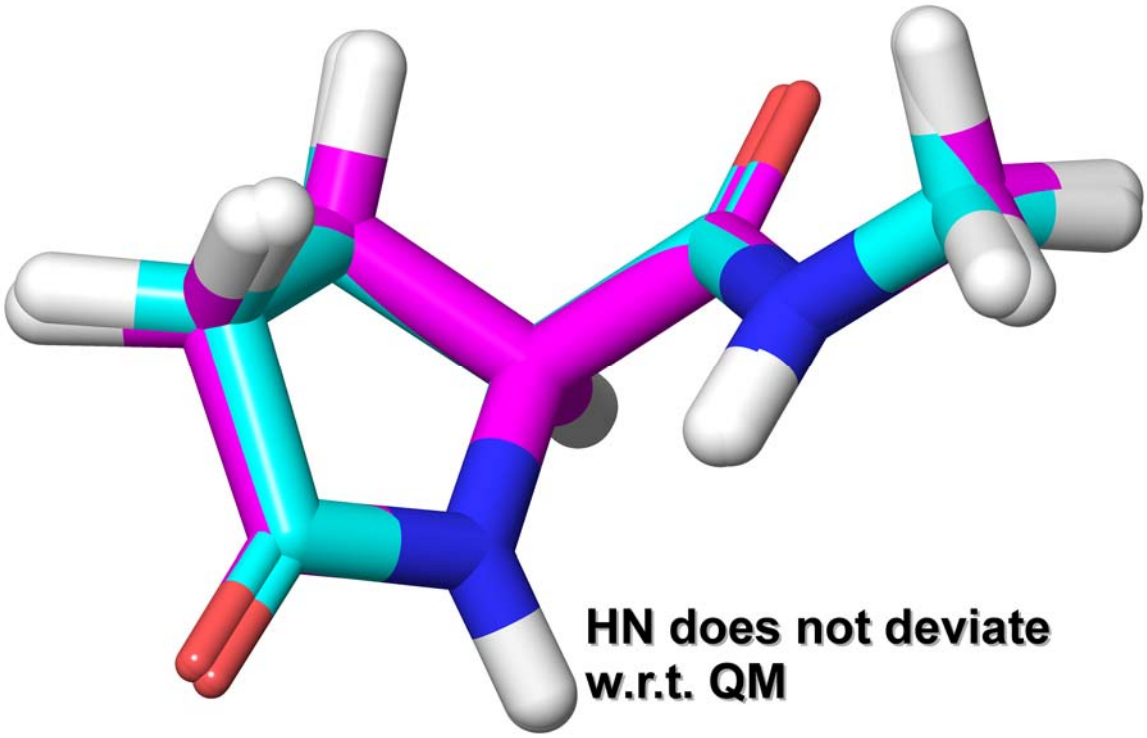

Figure 140. Pyroglutamate-NMA QM Global Minimum (Magenta Carbons) and the MM Global Minimum (Teal Carbons), the Latter Using the Bond Length, Bond Angle, and Dihedral Torsion Angle Parameters After Their Optimization.[4,158,159,160,161,162,163,164,165,166,167]

The newly optimized parameters were then ready to use in MD simulations.[4,137,158,159,160,161,162,163,164,165,166,167]

Molecular Dynamics RMSD, Dihedral, and Distance Measurements Results

The MD experiments produced two successful orexin-1 receptor models, with one of them an R model with SB-674042 bound,[3,7,24,175,176] and the other an R* model with orexin-A bound.[3,4,7,22,24,175,176] These bundles had RMSD measurement graphs of the

protein backbone and of the TMH Cαs, distance measurement graphs, dihedral measurement graphs, and component interaction energy comparison tables taken, along with pictures and videos of the structures.

The RMSD of the R state ox1r backbone was ~3.2, showing the bundle's overall stability as it settled at this number very early on as seen in Figure 141.[3,7,24,175,176]

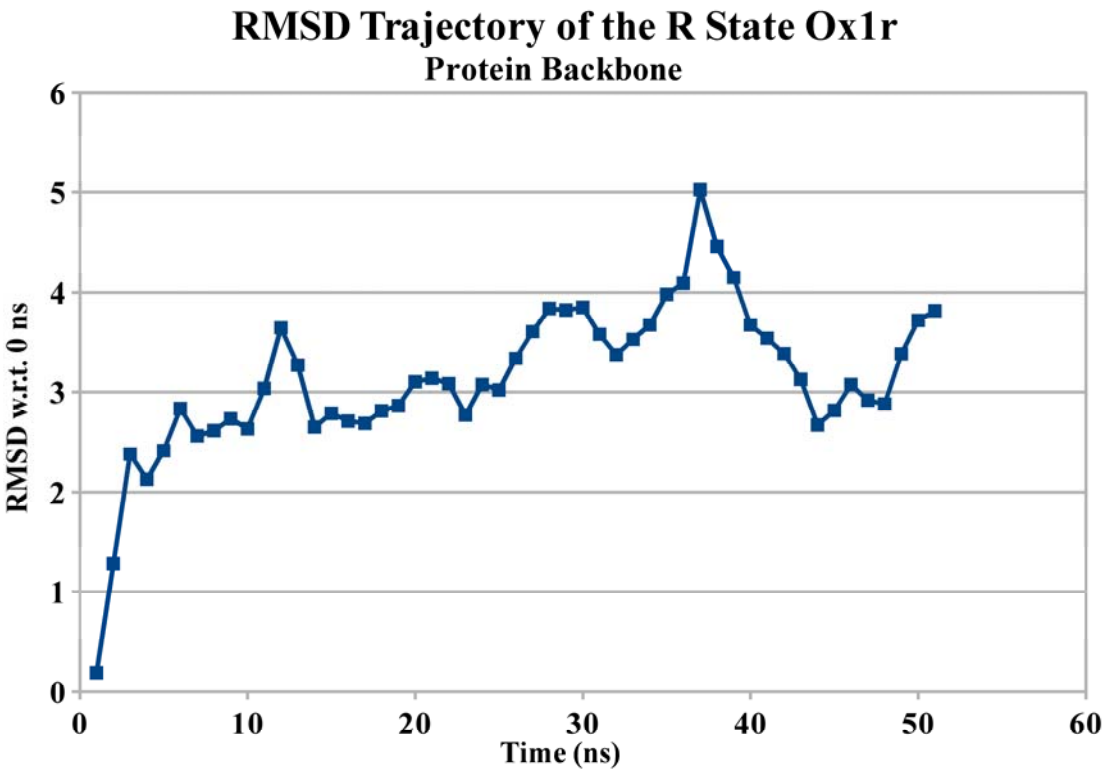

Figure 141. Graph of the RMSD for the Ox1r R Simulation Protein Backbone.[3,7,24,175,176]

This is due to the ox2r crystal structure being used as a basis for the R structure, allowing for a vast improvement in structural stability as the ox2r crystal structure was already a stable structure.[3,7,24] It also would not be as likely to rip apart as a "pull-apart-and-minimize" ox1r model, as the higher identity and homology of the ox2r crystal structure

made it a better basis for the ox1r models than the CM output and the corresponding superposition templates did.[3,7,24,133,147,188]

The RMSD of the R state's transmembrane Cαs was ~1.4, showing its stability in the transmembrane core as it settled at this number early in the trajectory.[3,7,24,175,176] This is also due to the use of the ox2r crystal structure as the ox1r R model's structural basis, and is visible in Figure 142.[3,7,24,175,176]

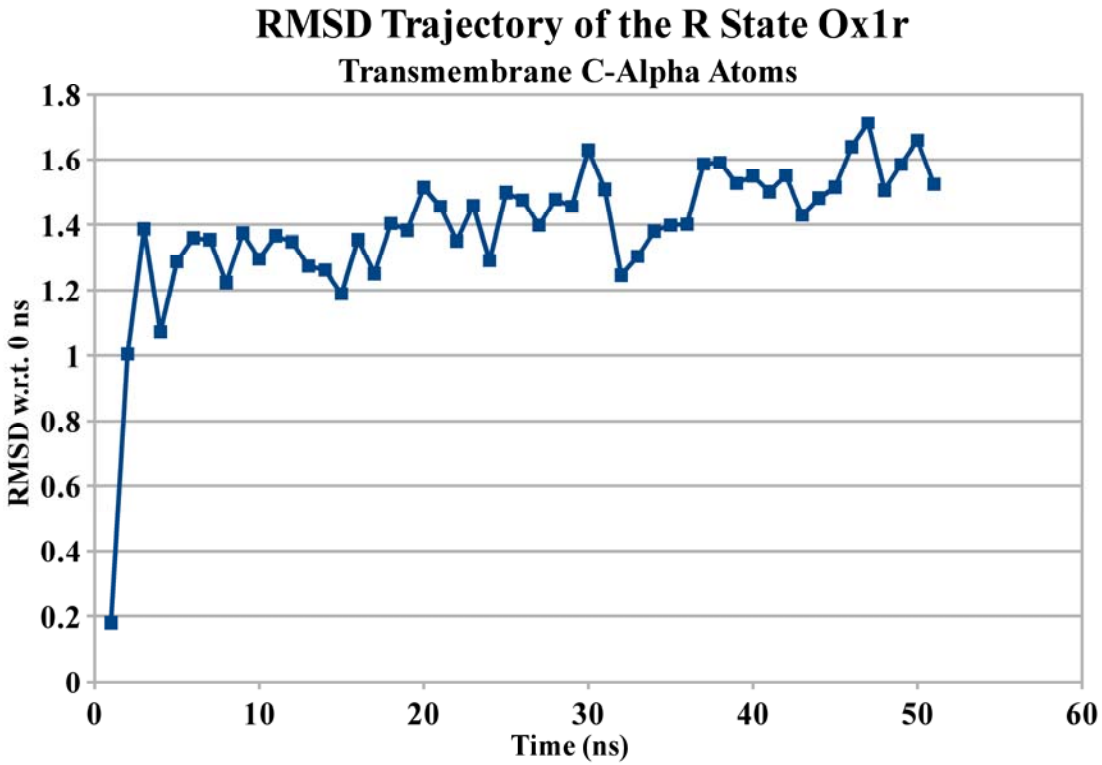

Figure 142. Graph of the RMSD for the Ox1r R Simulation Transmembrane Helix Cα Atoms.[3,7,24,175,176]

These RMSD measurements were as predicted, thus leading to the next phase of analysis: dihedral and distance measurement, with the hypothesis that the measurements would correspond to experimental data.[3,7,24,124,125,126,127,128,129,130,175,176]

The ox1r R structure had the Y6.48 χ1 dihedral measured, with the measurement and graph as shown in Figures 143 and 144.[3,7,24,124,125,126,127,128,129,130,175,176]

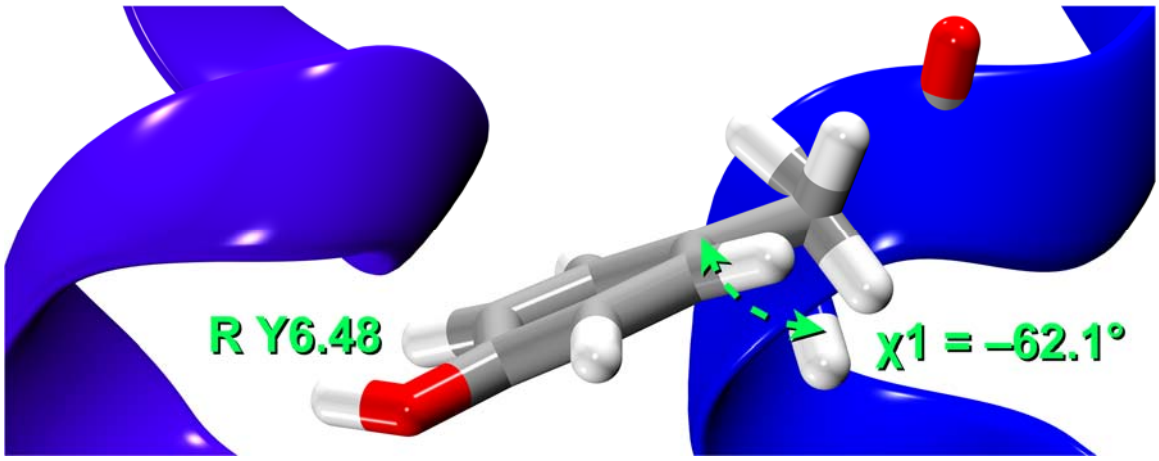

Figure 143. The Y6.48 χ1 Dihedral from the R Simulation.[3,7,24,124,125,126,127,128,129,130,175,176]

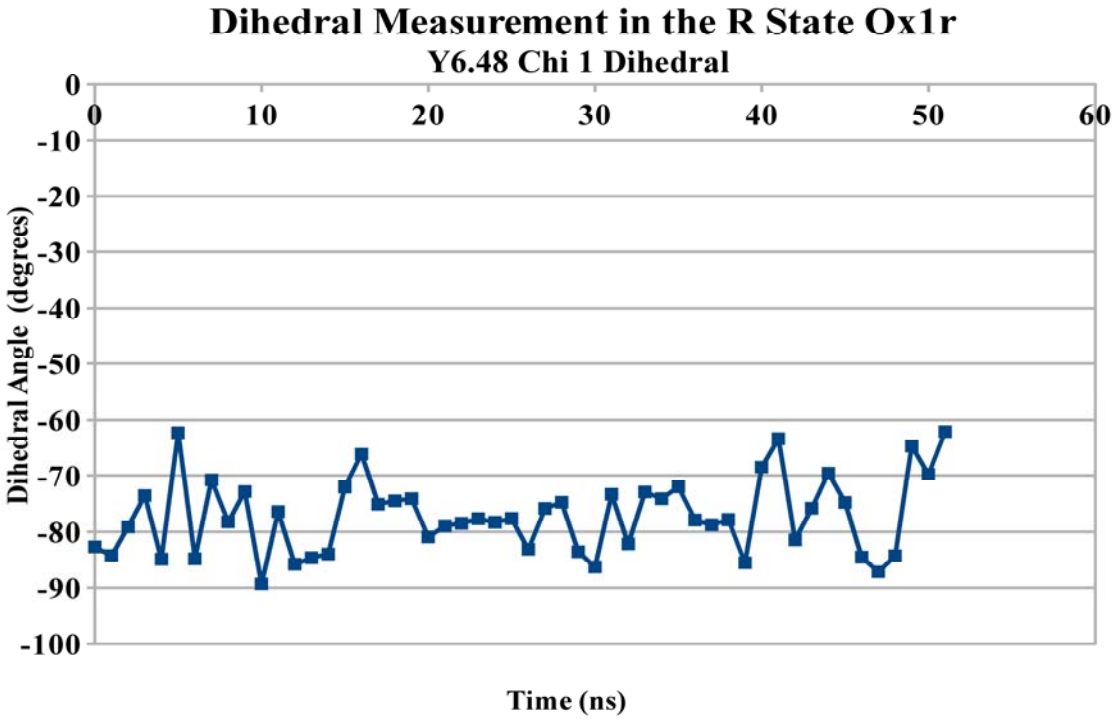

Figure 144. Graph of the Y6.48 χ1 Dihedral for the R Simulation.[3,7,24,124,125,126,127,128,129,130,175,176]

Y6.48 never deviated from its g^+ conformation throughout the simulation, consistent with an inactive GPCR's X6.48 χ1 dihedral.[3,7,24,124,125,126,127,128,129,130,175,176]

The ox1r R3.50-R6.30 Cα-Cα distance in the R simulation is shown in Figure 145.[3,7,24,124,125,126,127,128,129,130,175,176]

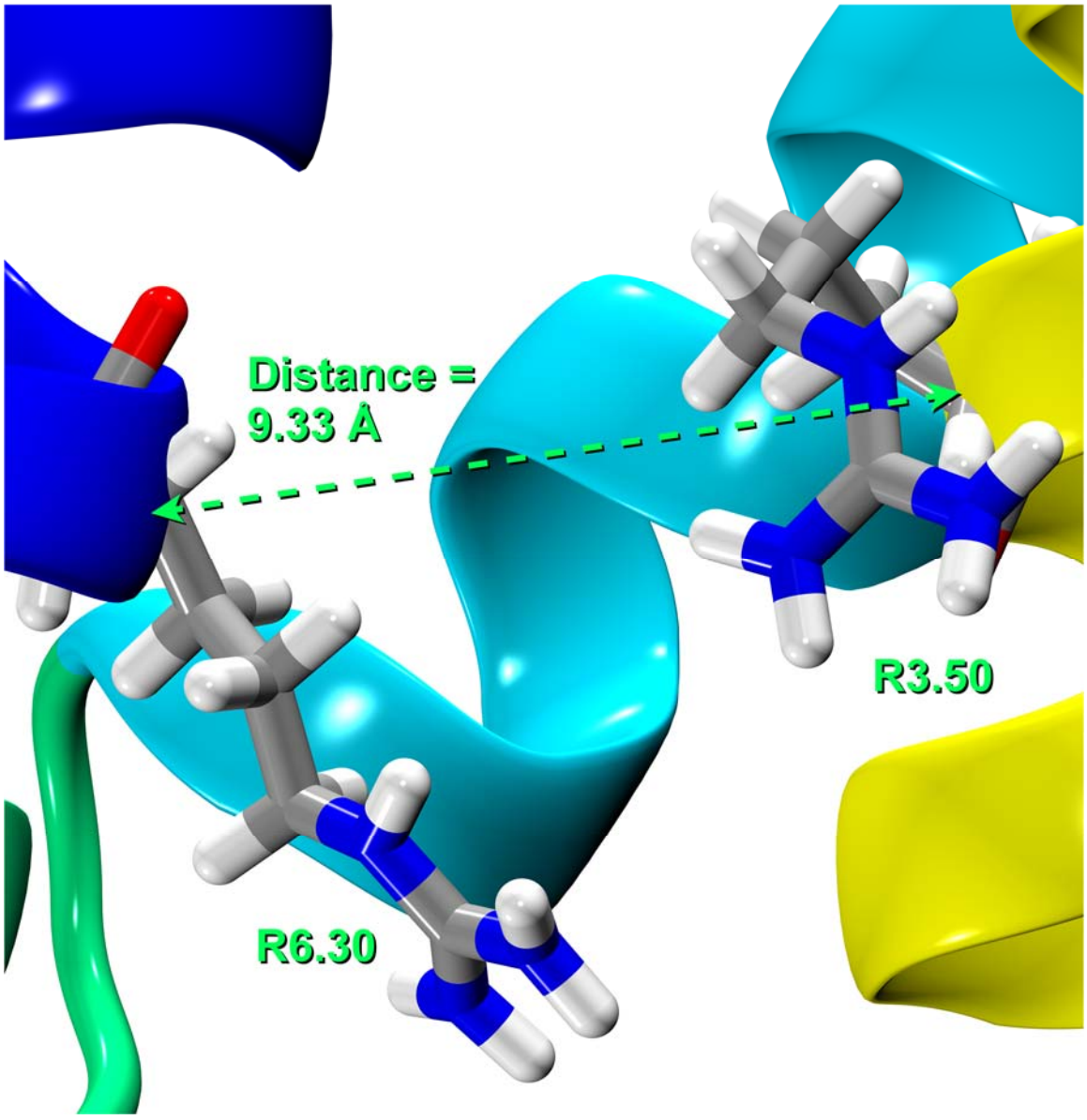

Figure 145. Picture of the R3.50-R6.30 Cα-Cα Distance from the R Simulation.[3,7,24,124,125,126,127,128,129,130,175,176]

The ox1r R3.50-R6.30 Cα-Cα distance in the R simulation is graphed in Figure 146.[3,7,24,124,125,126,127,128,129,130,175,176]

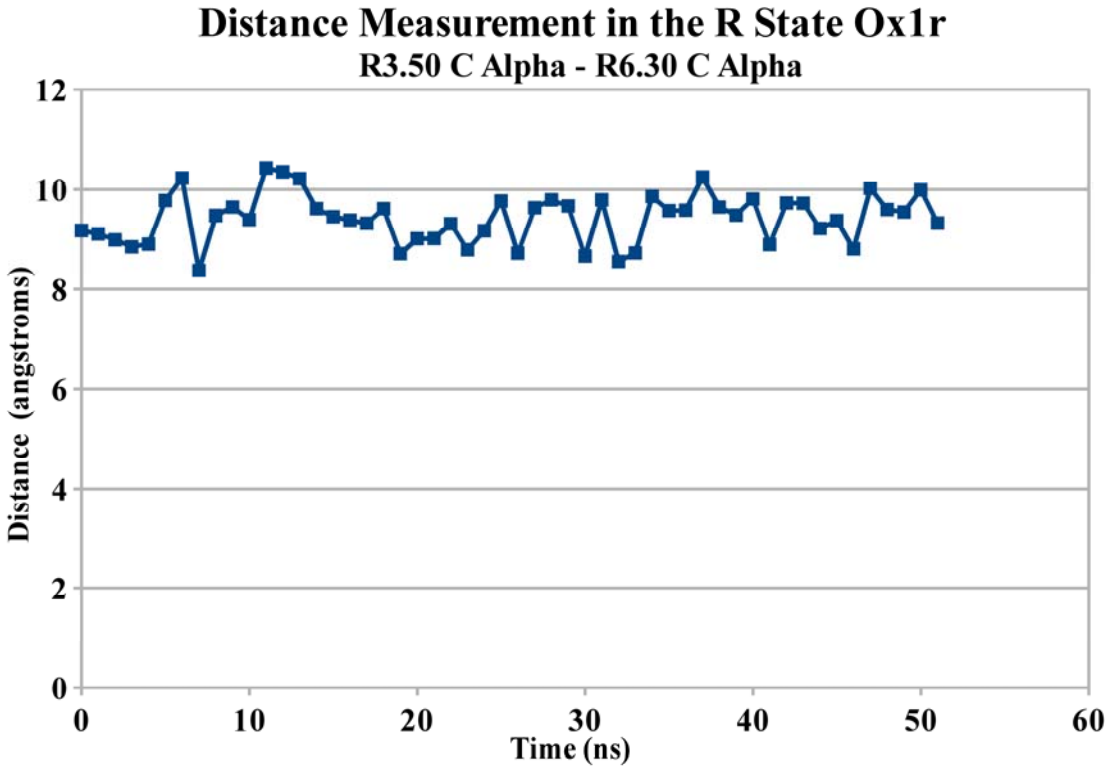

Figure 146. Graph of the R3.50-R6.30 Cα-Cα Distance for the R Simulation.[3,7,24,124,125,126,127,128,129,130,175,176]

The R3.50-R6.30 Cα-Cα distance was ~9.2 Å for much of the trajectory, consistent with an inactive GPCR's R3.50-X6.30 Cα-Cα distance.[3,7,24,124,125,126,127,128,129,130,175,176]

Three of the R simulation's newest interactions formed between F5.42 and the head fluorophenyl of SB-674042, between F5.42 and the thiazole group, and between H7.39 and SB-674042's 1,3,4-oxadiazole group, since at the start of the simulation F5.42 interacted by van der Waals and by π-π T-stacks with both groups, and Y6.48 only by van der Waals with the thiazole group.[3,7,24,175,176] Hence, new measurements must be

collected from this trajectory.[3,7,24,175,176] The ox1r I3.28-SB-674042 Cβ-C43 distance in the R simulation is shown and graphed in Figures 147 and 148.[3,7,24,175,176]

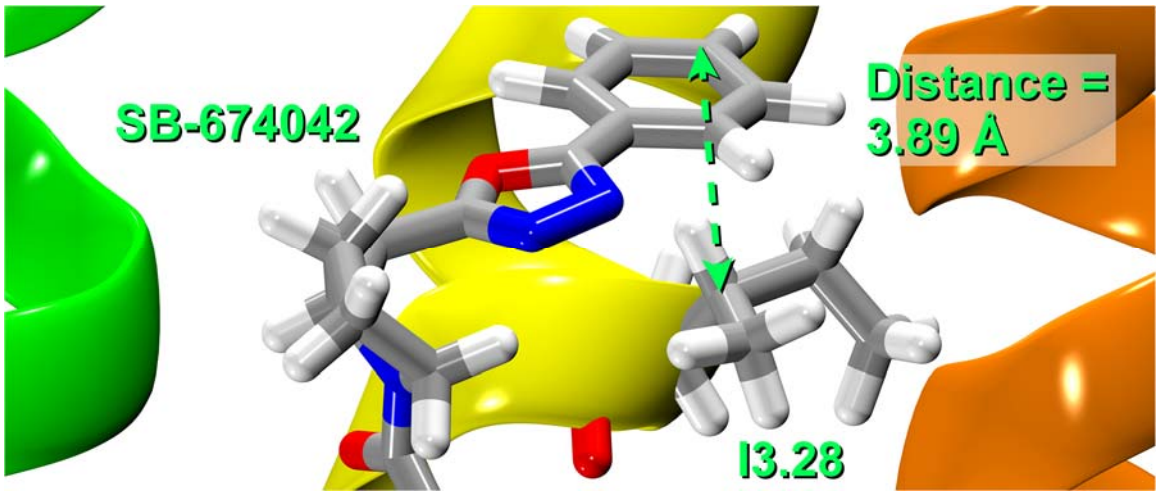

Figure 147. The R Simulation's I3.28-SB-674042 Cβ-C43 Distance.[3,7,24,175,176]

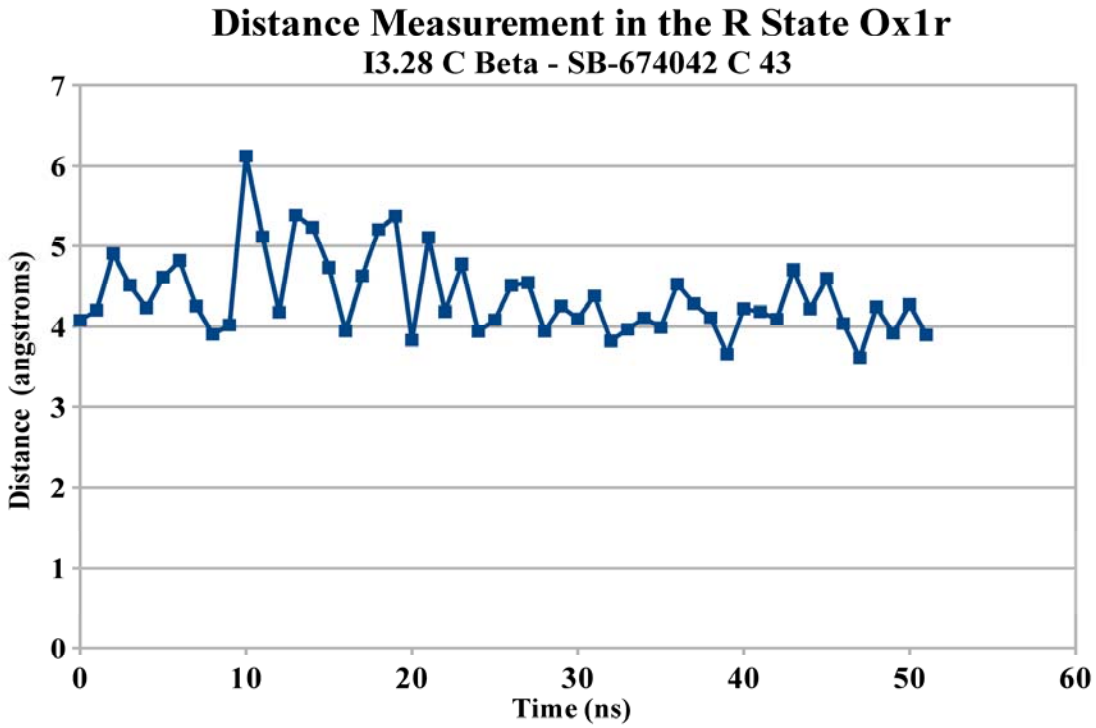

Figure 148. Graph of the R Simulation's I3.28-SB-674042 Cβ-C43 Distance.[3,7,24,175,176]

The ox1r F5.42-SB-674042 Cγ-C1 distance in the R simulation is shown and graphed in Figures 149 and 150.[3,7,24,175,176]

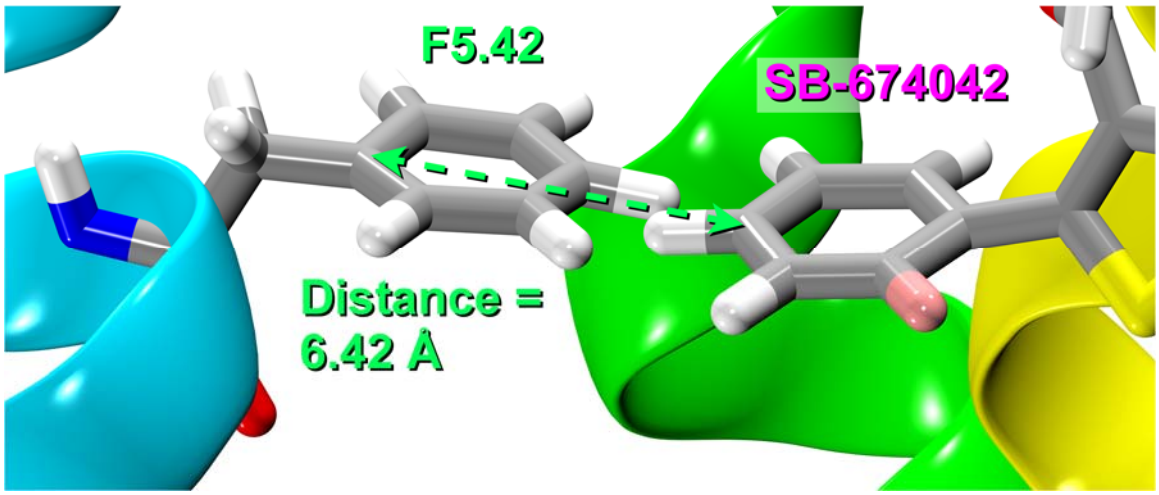

Figure 149. The R Simulation's F5.42-SB-674042 Cγ-C1 Distance.[3,7,24,175,176]

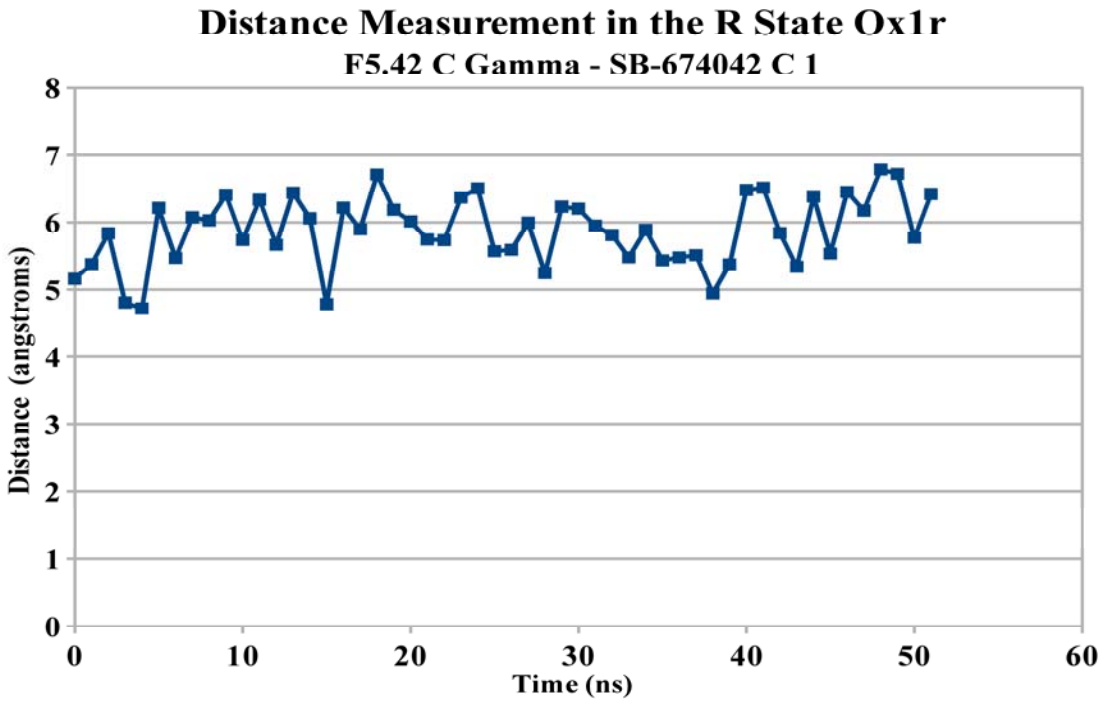

Figure 150. Graph of the R Simulation's F5.42-SB-674042 Cγ-C1 Distance.[3,7,24,175,176]

The ox1r H7.39-SB-674042 Cδ2-C25 distance in the R simulation is shown and graphed in Figures 151 and 152.[3,7,24,175,176]

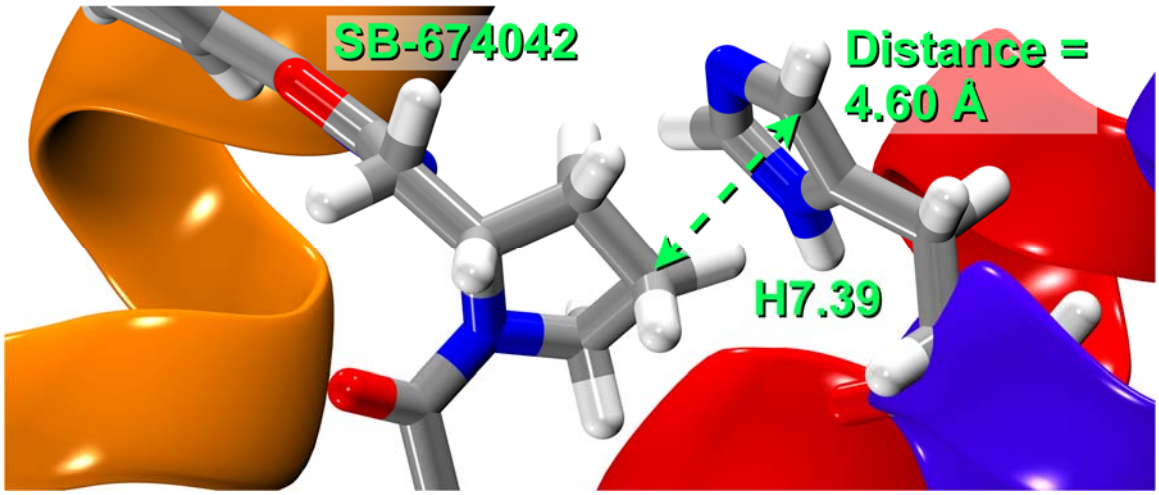

Figure 151. The R Simulation's H7.39-SB-674042 Cδ2-C25 Distance.[3,7,24,175,176]

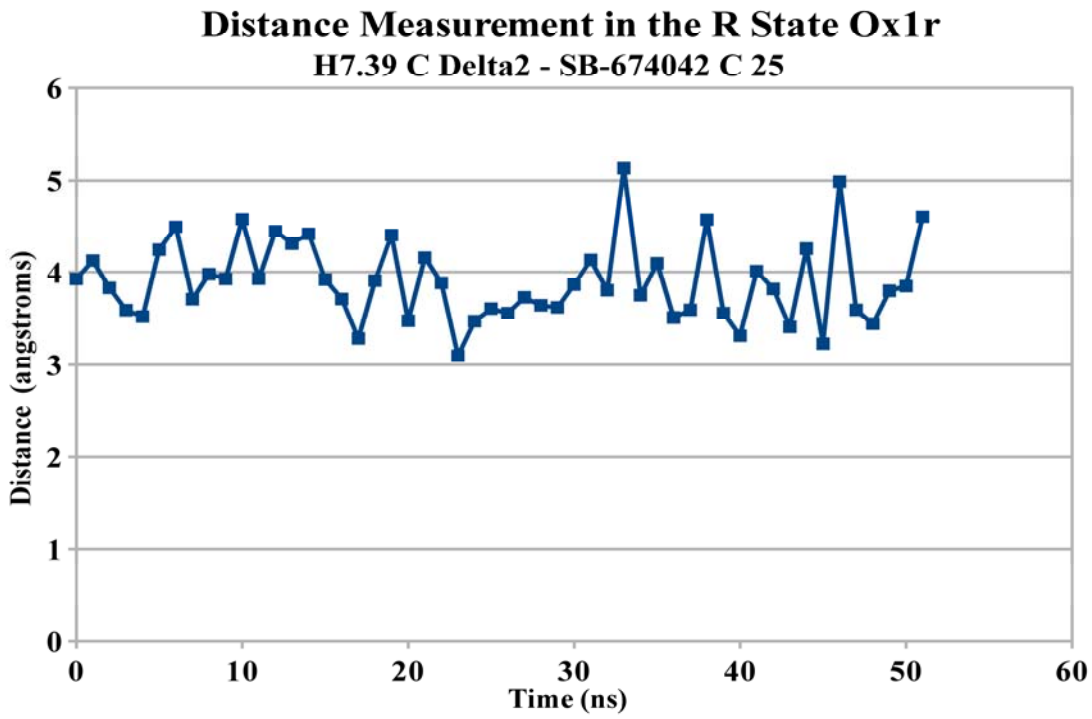

Figure 152. Graph of the R Simulation's H7.39-SB-674042 Cδ2-C25 Distance.[3,7,24,175,176]

The I3.28-SB-674042 Cβ-C43 distance in the R simulation was ~4.3 Å, consistent with SB-674042's ability to use its phenyl ring to interact by van der Waals from the nearby I3.28.[3,7,24,175,176] The F5.42-SB-674042 Cγ-C1 distance in the R simulation was ~5.7 Å, consistent with SB-674042's ability to use its fluorophenyl ring to interact by van der Waals with the nearby F5.42.[3,7,24,175,176] The H7.39-SB-674042 Cδ2-C25 distance in the R simulation was ~3.9 Å, consistent with SB-674042's ability to use its proline-like ring to interact by van der Waals with the nearby H7.39.[3,7,24,137,175,176]

The ox1r Y6.48-SB-674042 Cζ-S17 distance in the R simulation is graphed in Figure 153.[3,7,24,175,176]

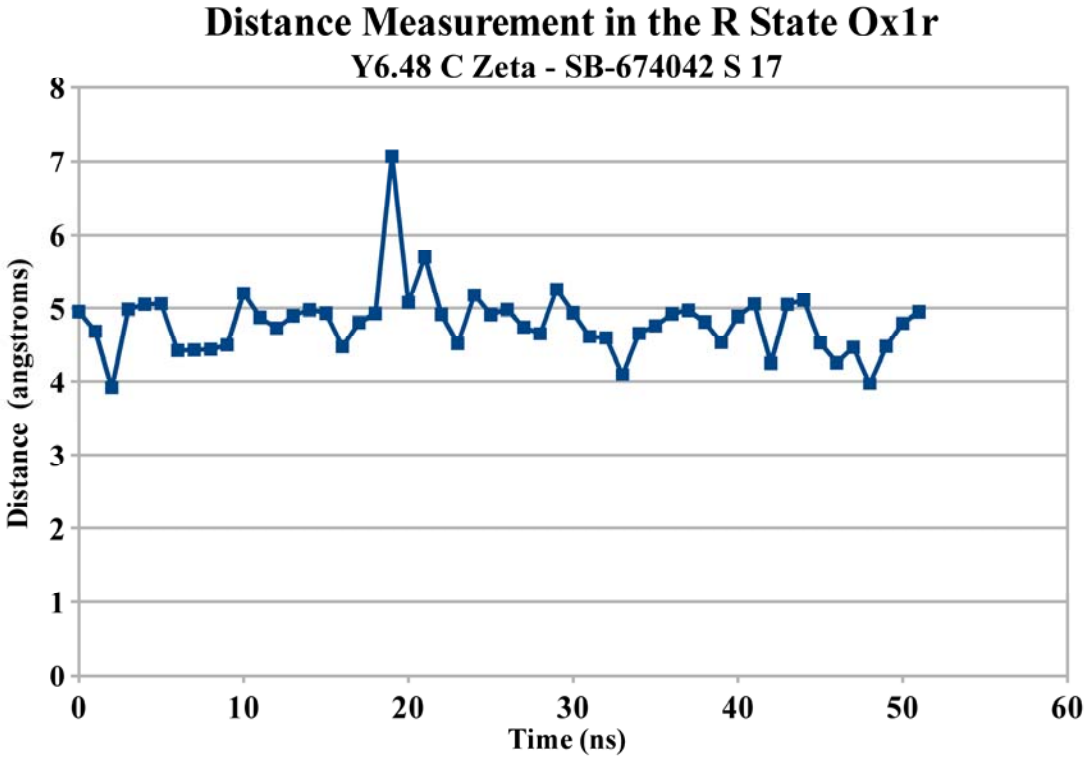

Figure 153. Graph of the Y6.48-SB-674042 Cζ-S17 Distance for the R Simulation.[3,7,24,175,176]

The ox1r Y6.48-SB-674042 Cζ-S17 distance in the R simulation is shown in Figure 154.[3,7,24,175,176]

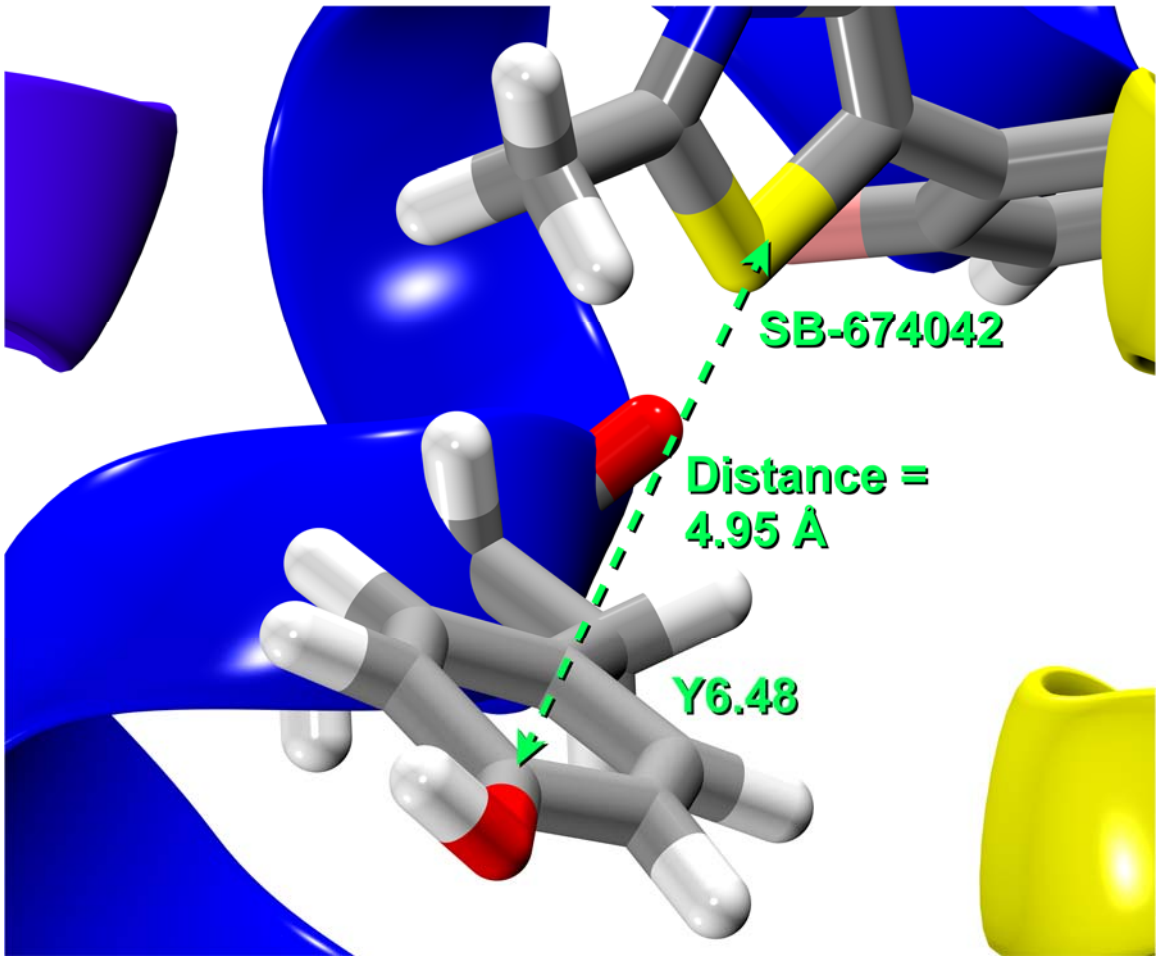

Figure 154. The Y6.48-SB-674042 Cζ-S17 Distance from the R Simulation.[3,7,24,175,176]

The Y6.48-SB-674042 Cζ-S17 distance in the R simulation was ~4.8 Å, consistent with SB-674042's ability to use its thiazole ring to interact by numerous van der Waals contacts with the nearby Y6.48, as well as the ability of that part of SB-674042 to hold Y6.48 in g^+.[3,7,24,124,125,126,127,128,129,130,175,176]

The interaction between Q3.32 and SB-674042 at the start and end of the R simulation are shown in Figures 155 and 156.[3,7,24,175,176]

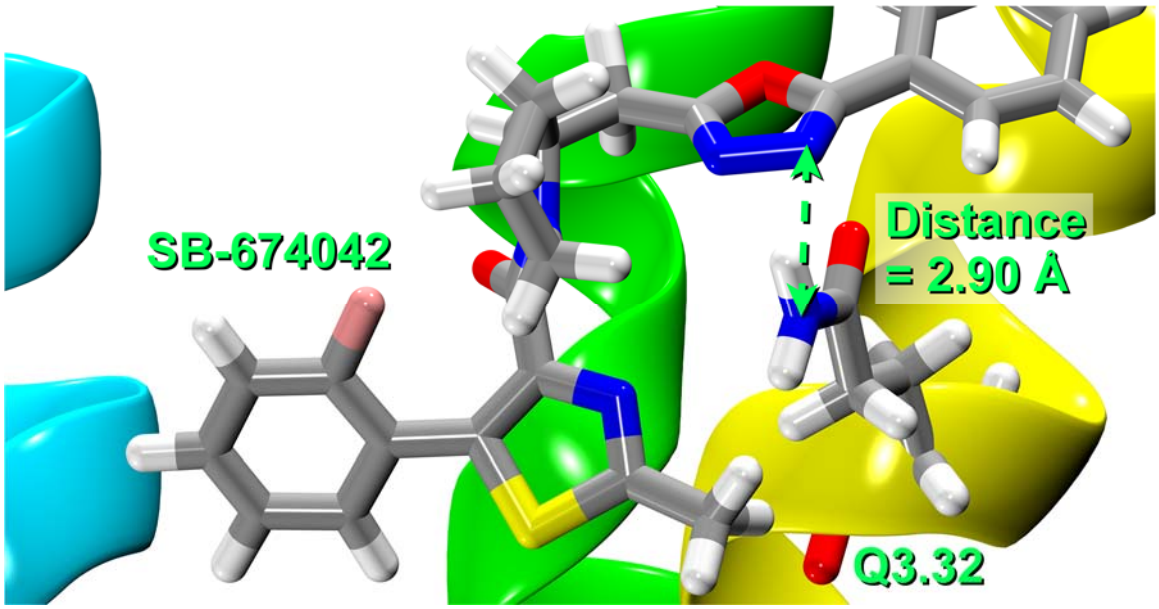

Figure 155. The Q3.32-SB-674042 Interaction at the Start of the R Simulation.[3,7,24,175,176]

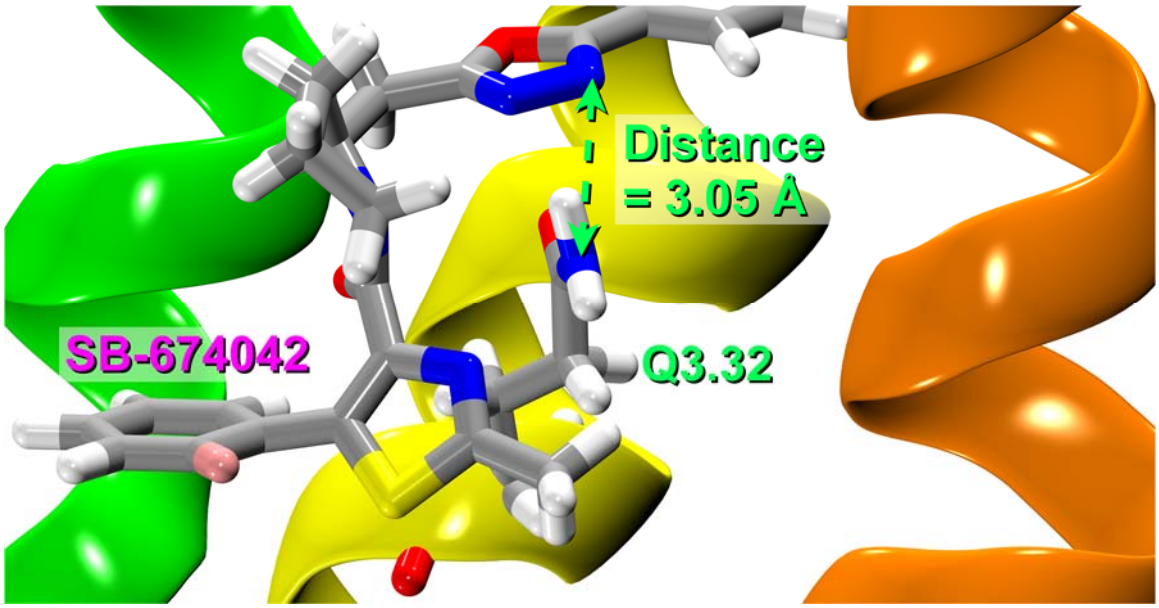

Figure 156. The Q3.32-SB-674042 Interaction at the End of the R Simulation.[3,7,24,175,176]

The distance in the R simulation between Q3.32's Nε2 and SB-674042's oxadiazole ring nitrogen N40 was steady at ~3.2 Å, and SB-674042 got no farther away from Q3.32.[3,7,24] The interaction between the two was excellent, as the original interaction was a hydrogen bond between the two, as well as having SB-674042 additionally draped around Q3.32 at the end, interacting heavily by van der Waals contacts over a large surface area, with the distance illustrated in Figure 157.[3,7,24,175,176]

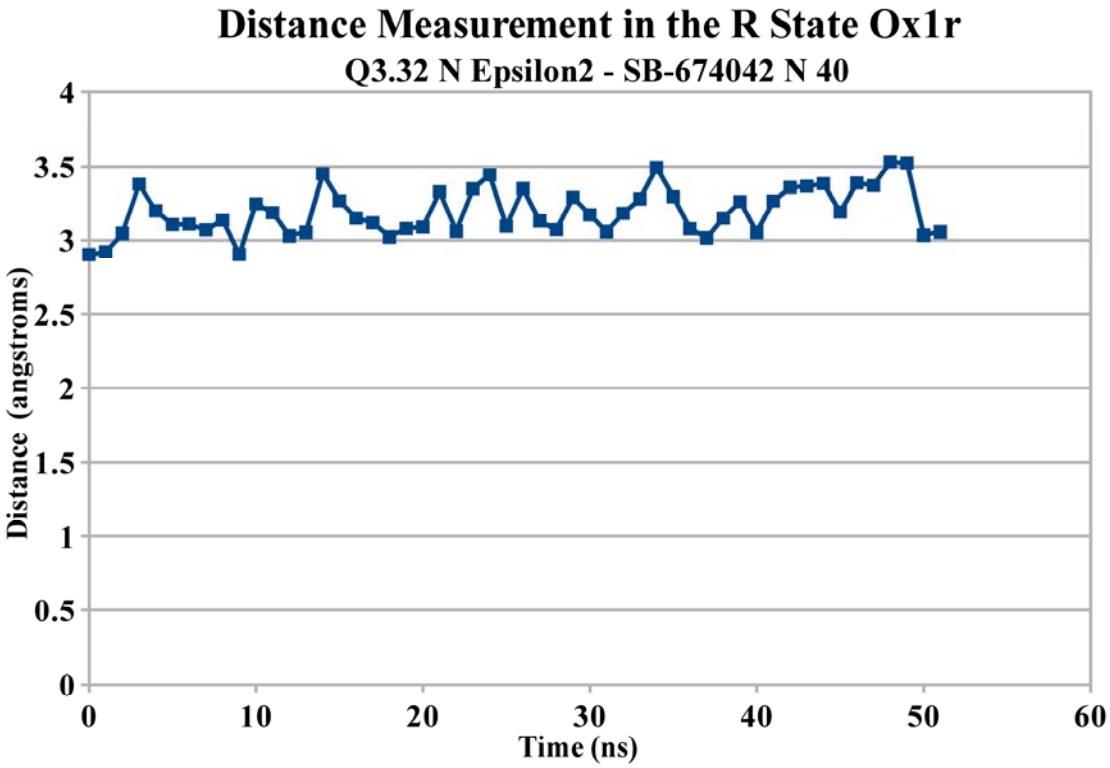

Figure 157. Graph of the Q3.32-SB-674042 Nε2-N40 Distance for the R Simulation.[3,7,24,175,176]

The R model's Q3.32 had a good binding energy with SB-674042, which had several π-stacking interactions with F5.42 and with H7.39, as the former (especially via the thiazole) kept Y6.48 in g^+.[3,7,24,124,125,126,127,128,129,130,175,176]

The RMSD of the R* state ox1r backbone was ~4.5, showing the bundle's overall stability during its run as it settled at this number very early on as seen in Figure 158.[3,4,7,22,24,175,176]

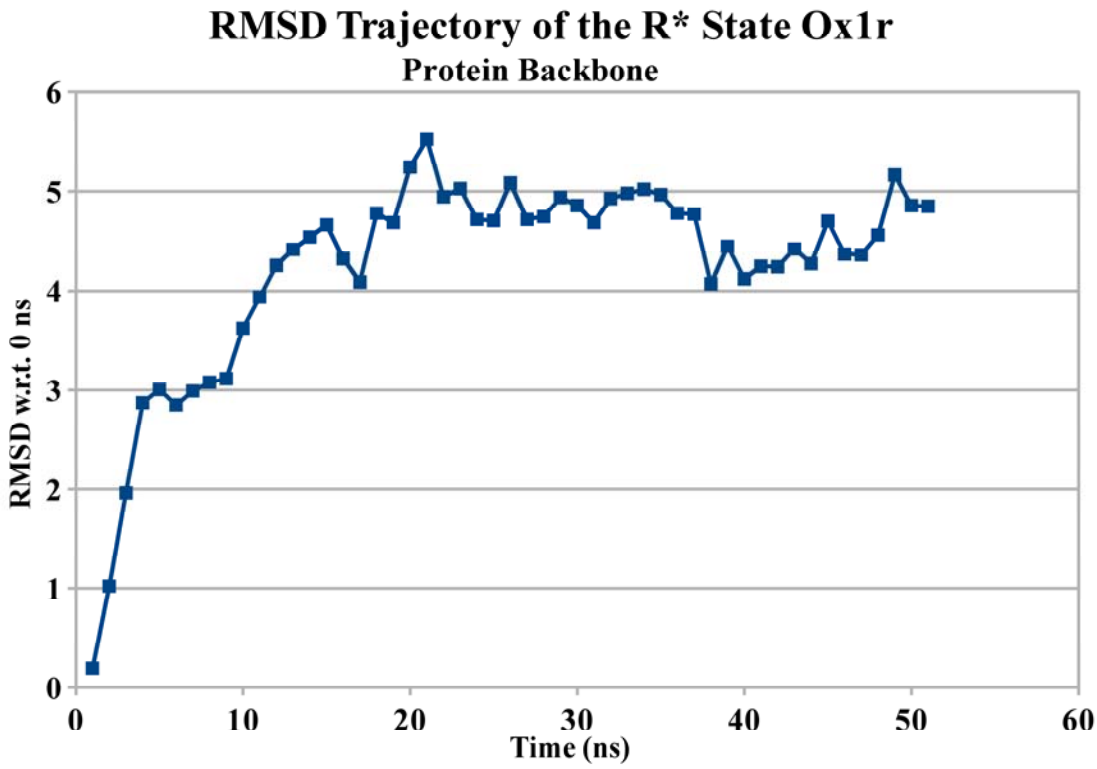

Figure 158. Graph of the RMSD for the Ox1r R* Simulation Protein Backbone.[3,4,7,22,24,175,176]

This is due to the ox2r crystal structure being used as a basis for the R* structure, allowing for a vast improvement in structural stability as the ox2r crystal structure was already a stable structure.[3,4,7,22,24] It also would not be as likely to rip apart as a "pull-apart-and-minimize" ox1r model, as the higher identity and homology of the ox2r crystal structure made it a better basis for the ox1r models than the CM output and the corresponding superposition templates did, even if the R* model of ox1r requires a partial

replacement of TMH6 with CM output as part of its structure.[3,4,7,22,24,124,125,126,127,128,129,130,133,143,147,188]

The RMSD of the R* state's transmembrane Cαs was ~1.4, showing its stability in the transmembrane core as it settled at this number early in the trajectory.[3,4,7,22,24,175,176] This is also due to the use of the ox2r crystal structure as the ox1r R* model's structural basis, and is visible in Figure 159.[3,4,7,22,24,175,176]

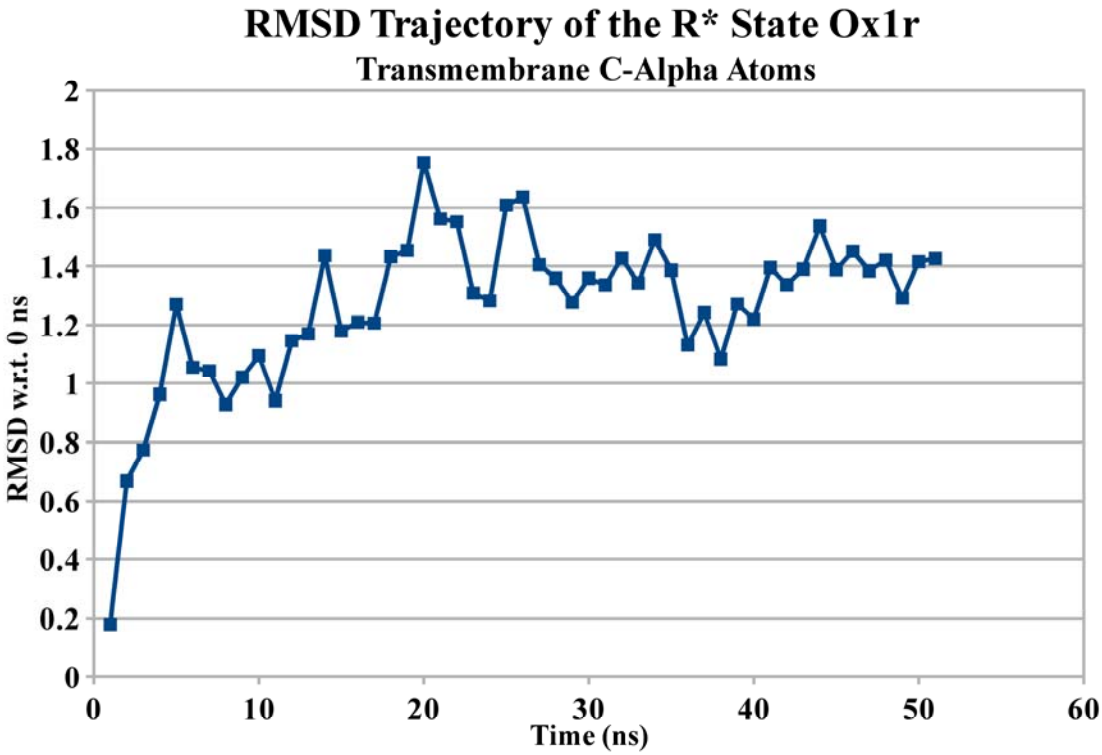

Figure 159. Graph of the RMSD for the Ox1r R* Simulation Transmembrane Helix Cα Atoms.[3,4,7,22,24,175,176]

These RMSD measurements were as predicted, thus leading to the next phase of analysis: dihedral and distance measurement, with the hypothesis that the measurements would correspond to experimental data.[3,4,7,22,24,124,125,126,127,128,129,130,175,176]

The R* structure had its Y6.48 χ1 dihedral measured, as shown in Figures 160 and 161.[3,4,7,22,24,124,125,126,127,128,129,130,175,176]

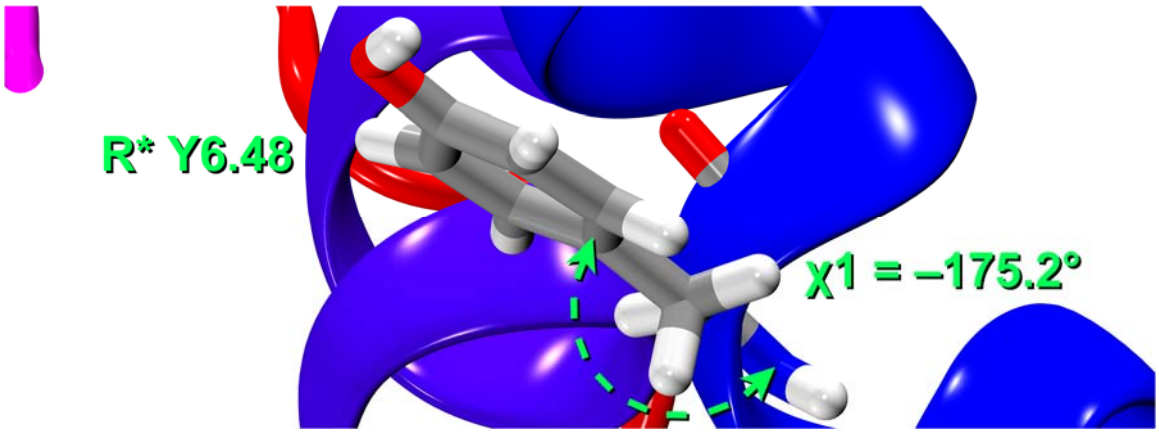

Figure 160. The Y6.48 χ1 Dihedral from the R* Simulation.[3,4,7,22,24,124,125,126,127,128,129,130,175,176]

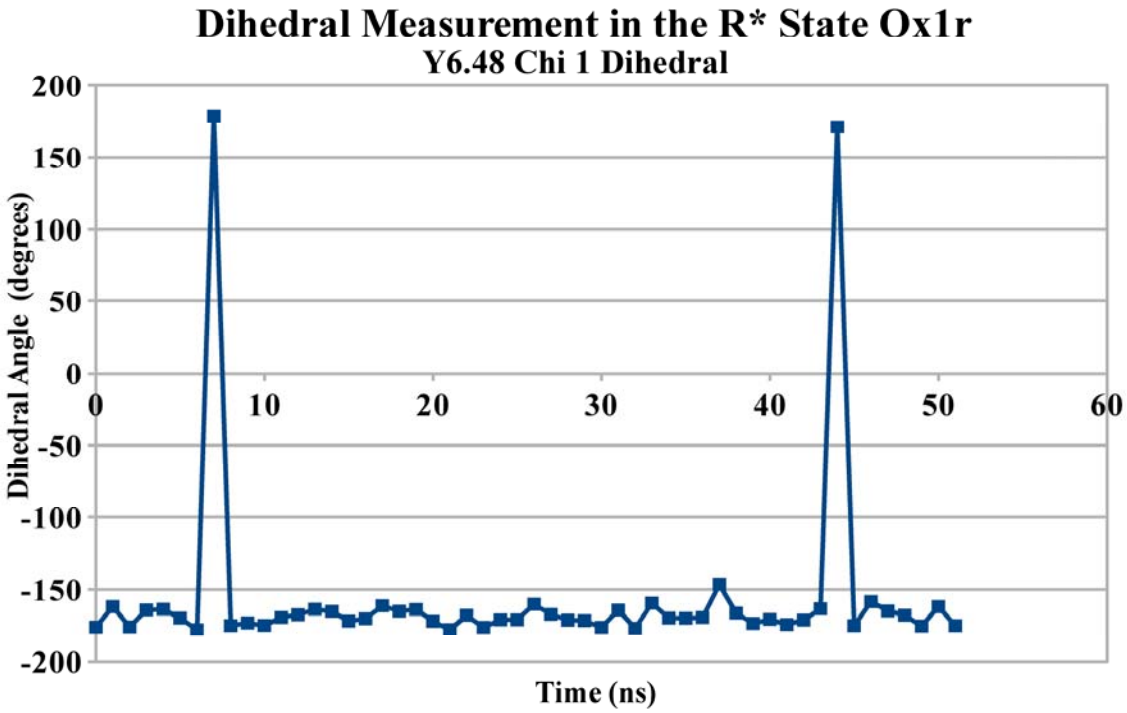

Figure 161. Graph of the Y6.48 χ1 Dihedral for the R* Simulation.[3,4,7,22,24,124,125,126,127,128,129,130,175,176]

The R* structure's Y6.48 χ1 dihedral was in a *trans* conformation throughout the simulation, consistent with an active GPCR's X6.48 χ1 dihedral.[3,4,7,22,24,124,125,126,127,128,129,130,175,176]

The R3.50-R6.30 Cα-Cα distance in the R* simulation was ~13.6 Å, as shown in Figure 162.[3,4,7,22,24,124,125,126,127,128,129,130,139,141,143,175,176]

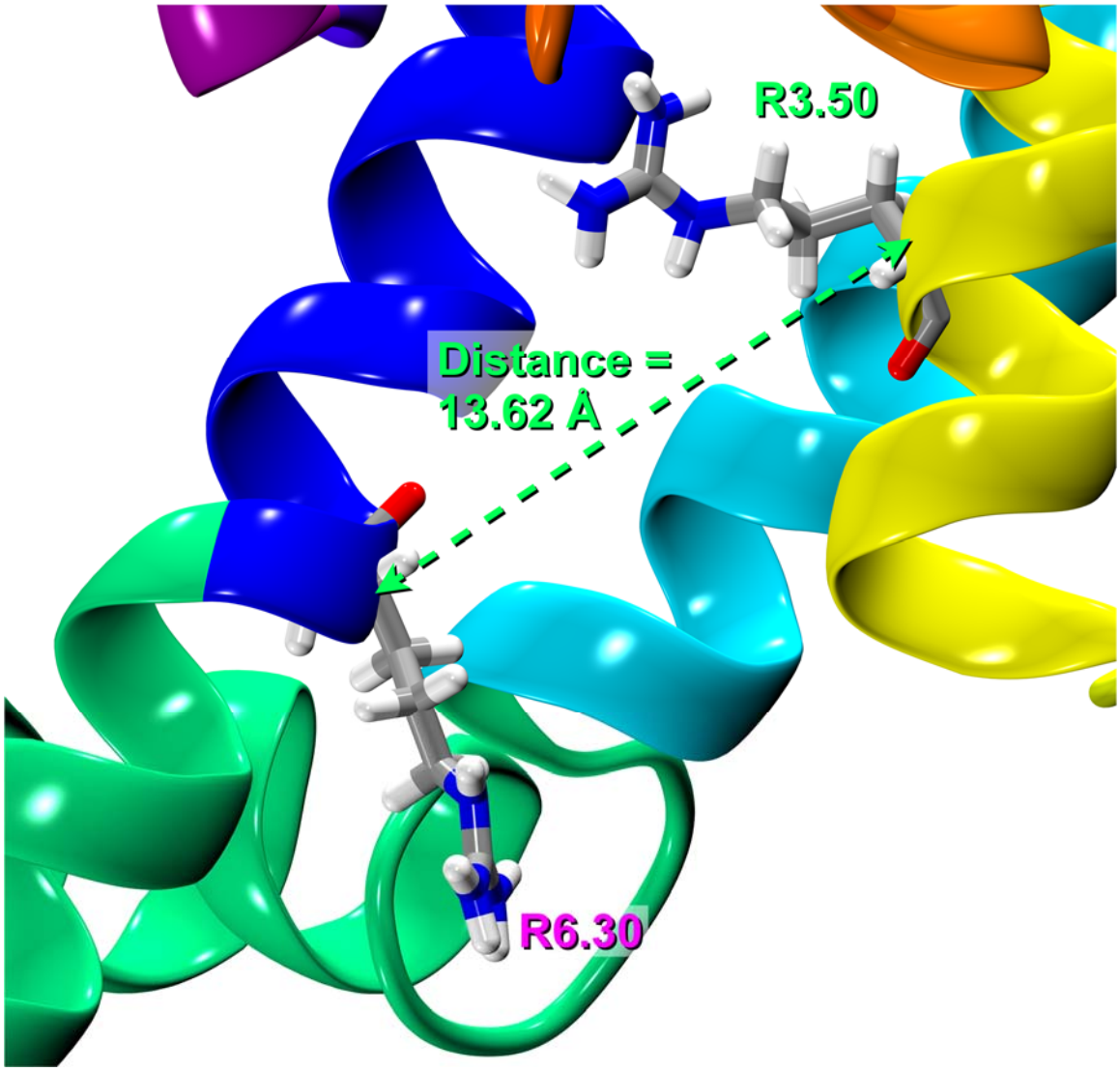

Figure 162. The R3.50-R6.30 Cα-Cα Distance from the R* Simulation.[3,4,7,22,24,124,125,126,127,128,129,130,139,141,143,175,176]

The ox1r R3.50-R6.30 Cα-Cα distance in the R* simulation is graphed in Figure 163.[3,4,7,22,24,124,125,126,127,128,129,130,139,141,143,175,176]

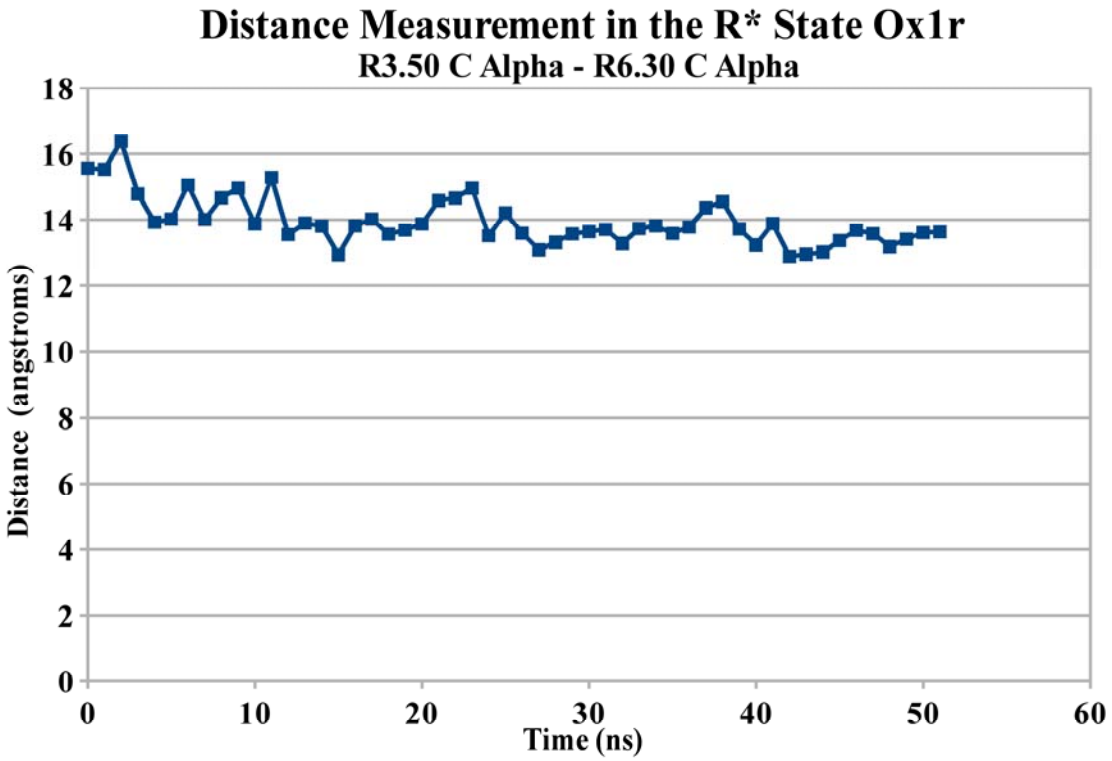

Figure 163. Graph of the R3.50-R6.30 Cα-Cα Distance for the R* Simulation.[3,4,7,22,24,124,125,126,127,128,129,130,139,141,143,175,176]

This R3.50-R6.30 distance measurement was consistent with an active GPCR's R3.50-X6.30 Cα-Cα distance, as it would be far enough apart to neither permit T6.33 to accept a hydrogen bond from R3.50, nor permit R6.30 to accept an arginine-arginine T-stack from R3.50.[3,4,7,22,24,124,125,126,127,128,129,130,139,141,143,175,176]

Two unique interactions are the van der Waals interactions between F5.42 and orexin-A's L33, along with Y6.48 and orexin-A's L33, with measurements of the distances between F5.42's Cζ and L33's Cγ, and between Y6.48's Cζ and L33's Cγ,

respectively. The ox1r F5.42-orexin-A L33 Cζ-Cγ distance in the R* simulation is shown and graphed in Figures 164 and 165.[3,4,7,22,24,175,176]

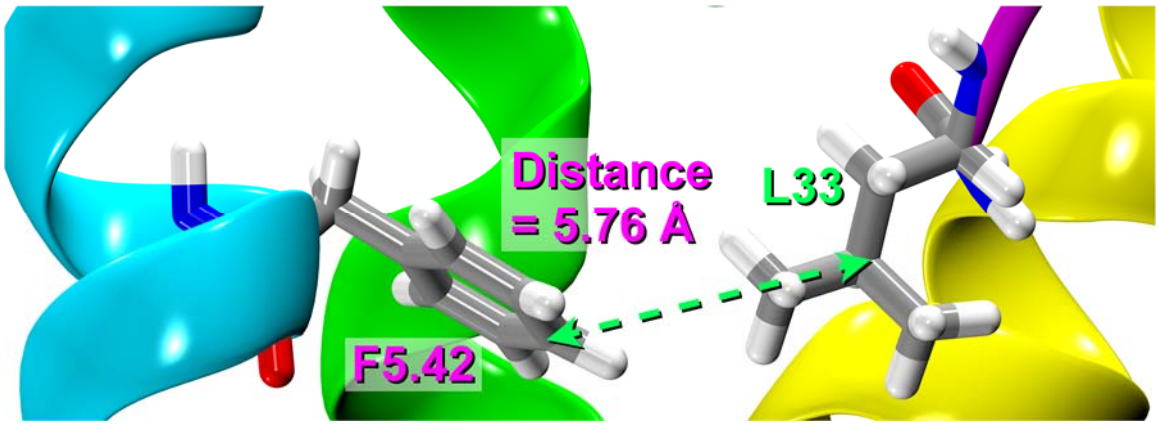

Figure 164. The R* Simulation's F5.42-orexin-A L33 Cζ-Cγ Distance.[3,4,7,22,24,175,176]

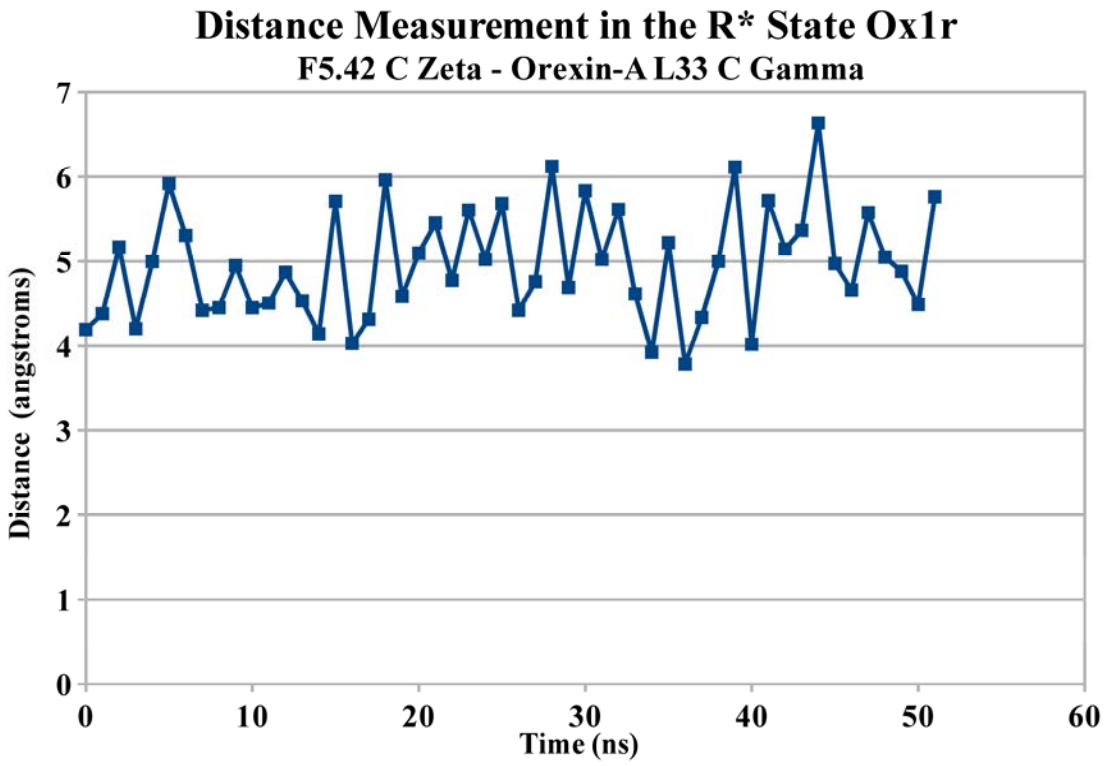

Figure 165. Graph of the R* Simulation's F5.42-orexin-A L33 Cζ-Cγ Distance.[3,4,7,22,24,175,176]

The F5.42-orexin-A L33 Cζ-Cγ distance was ~5.0 Å, consistent with orexin-A L33's ability to interact by a van der Waals interaction with the nearby F5.42, but though that interaction breaks, L33 can find other residues with which it can interact, and F5.42 remains an important residue for other reasons, such as maintaining ox1r stability.[3,4,7,22,24,175,176]

The ox1r Y6.48-orexin-A L33 Cζ-Cγ distance in the R* simulation is shown in Figure 166.[3,4,7,22,24,175,176]

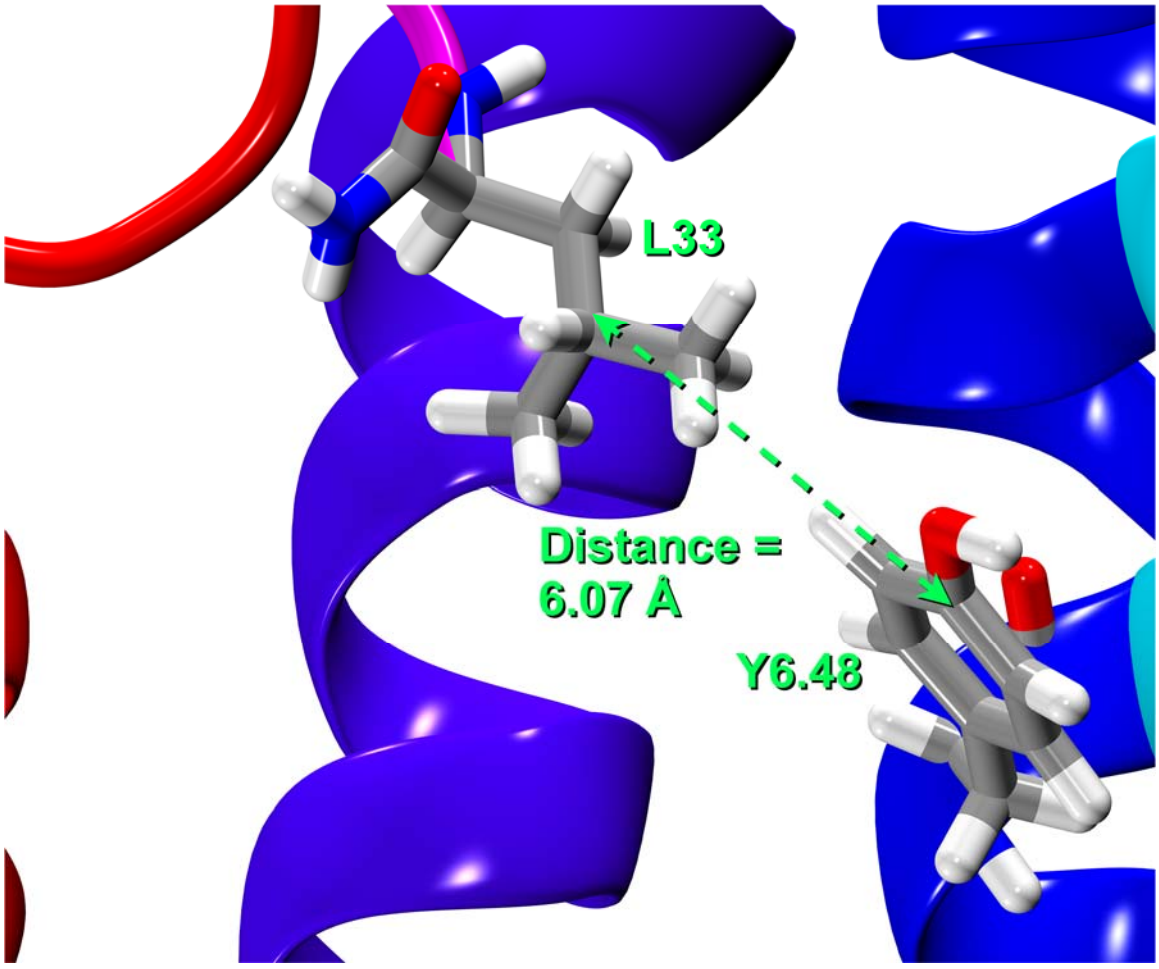

Figure 166. The R* Simulation's Y6.48-orexin-A L33 Cζ-Cγ Distance.[3,4,7,22,24,175,176]

The ox1r Y6.48-orexin-A L33 Cζ-Cγ distance in the R* simulation is graphed in Figure 167.[3,4,7,22,24,175,176]

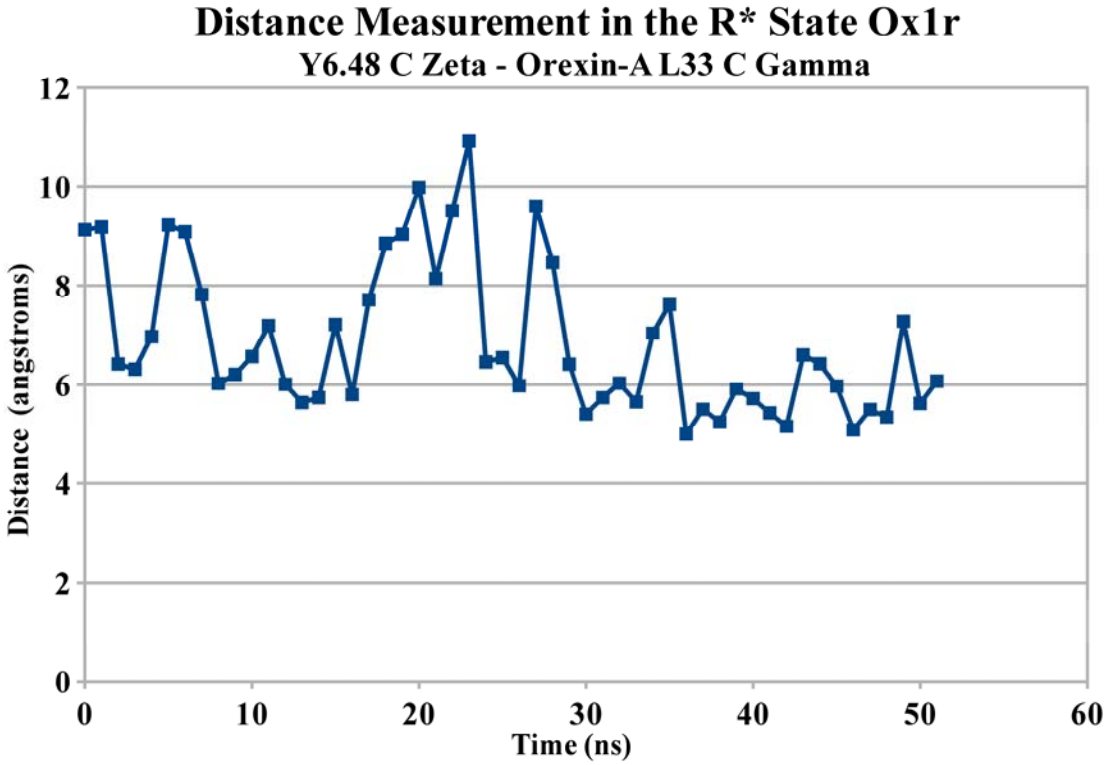

Figure 167. Graph of the R* Simulation's Y6.48-orexin-A L33 Cζ-Cγ Distance.[3,4,7,22,24,175,176]

The Y6.48-orexin-A L33 Cζ-Cγ distance in the R* simulation was ~6 Å, consistent with orexin-A's ability to use its L33 to interact by van der Waals contacts with the nearby Y6.48, as well as its ability to hold Y6.48 in *trans*.[3,4,7,22,24,124,125,126,127,128,129,130,133,142,143,175,176]

Nine more distances in the R* simulation were measured: H7.39-orexin-A L31 Nε2-O, orexin-A L33-orexin-A T32 N-Oγ1, D45.51-orexin-A H26 Cγ-Nδ1, C45.50-orexin-A H26 O-Nδ1, I3.28-orexin-A L31 Cβ-Cγ, C45.50-orexin-A L31 Sγ-Cγ, P3.29-

orexin-A L33 O-NT, R6.59-orexin-A L33 Cζ-O, and V45.49-orexin-A L20 Cβ-Cγ.[3,4,7,22,24,175,176] The first of these distances measures an interaction that is hypothesized to be the reason for H7.39's role in orexin-A binding in the ox1r, and the atoms involved in the R* simulation's H7.39-orexin-A L31 Nε2-O distance are shown in Figure 168.[3,4,7,22,24,175,176]

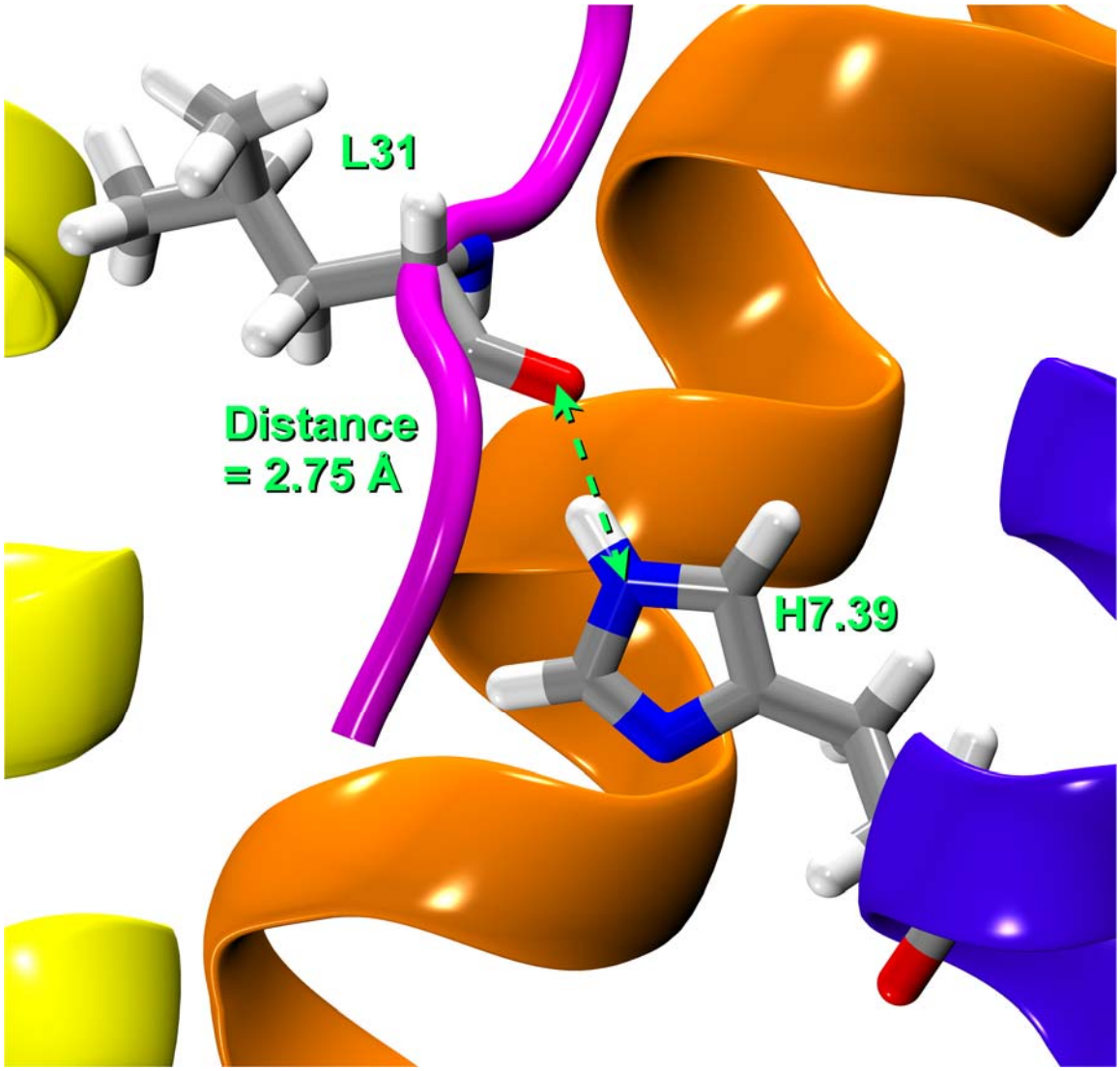

Figure 168. The R* Simulation's H7.39-orexin-A L31 Nε2-O Distance.[3,4,7,22,24,175,176]

The measurement, which was ~3.5 Å, of the R* simulation's H7.39-orexin-A L31 Nε2-O distance is shown in Figure 169.[3,4,7,22,24,175,176]

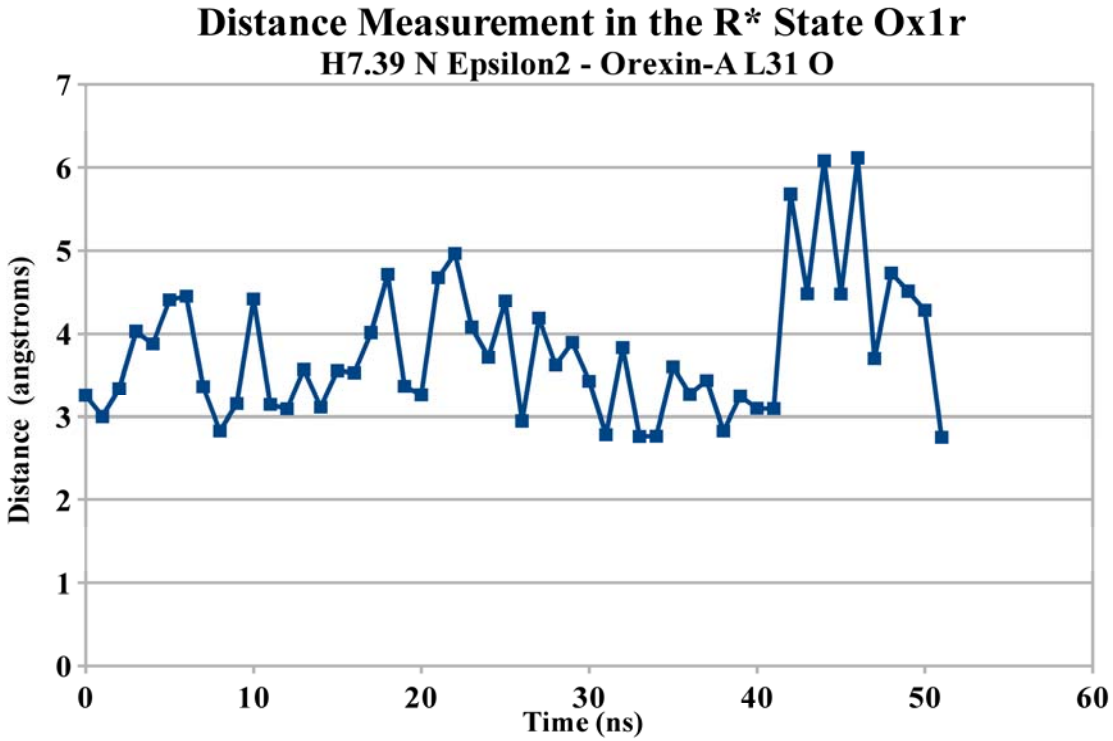

Figure 169. Graph of the R* Simulation's H7.39-orexin-A L31 Nε2-O Distance.[3,4,7,22,24,175,176]

This measurement shows that H7.39 changes its hydrogen bond acceptor partner from the backbone oxygen of oxA's T32 to that of oxA's L31 amidst competition from water and from S2.61.[3,4,7,22,24,175,176]

The orexin-A residue T32 faced competition from water and R6.59 for E45.52's carboxylate side chain, and the interaction broke as a result, but it was nevertheless important.[3,4,7,22,24,175,176] This is because T32 accepts an internal hydrogen bond from L33's amide hydrogen that stabilized orexin-A's C-terminus so that it could interact by

three hydrogen bonds: one with R6.59's guanidinium side chain, one with P3.29's amide oxygen, and one with Q3.32's amide side chain.[3,4,7,22,24,175,176] If T32 is mutated to an alanine, this internal hydrogen bond is lost completely, and the C-terminal orexin-A backbone has no energetic reason to attain this conformation.[3,4,7,22,24,175,176] If T32 is chirally inverted, this internal hydrogen bond flipped around, and the C-terminal orexin-A backbone attains a different conformation that is not amenable to binding in the ox1r.[3,4,7,22,24,175,176] The measurements in the orexin-A L33-orexin-A T32 N-Oγ1 measurement in the R* simulation are shown in Figure 170, with the measurement being ~3.0 Å.[3,4,7,22,24,175,176]

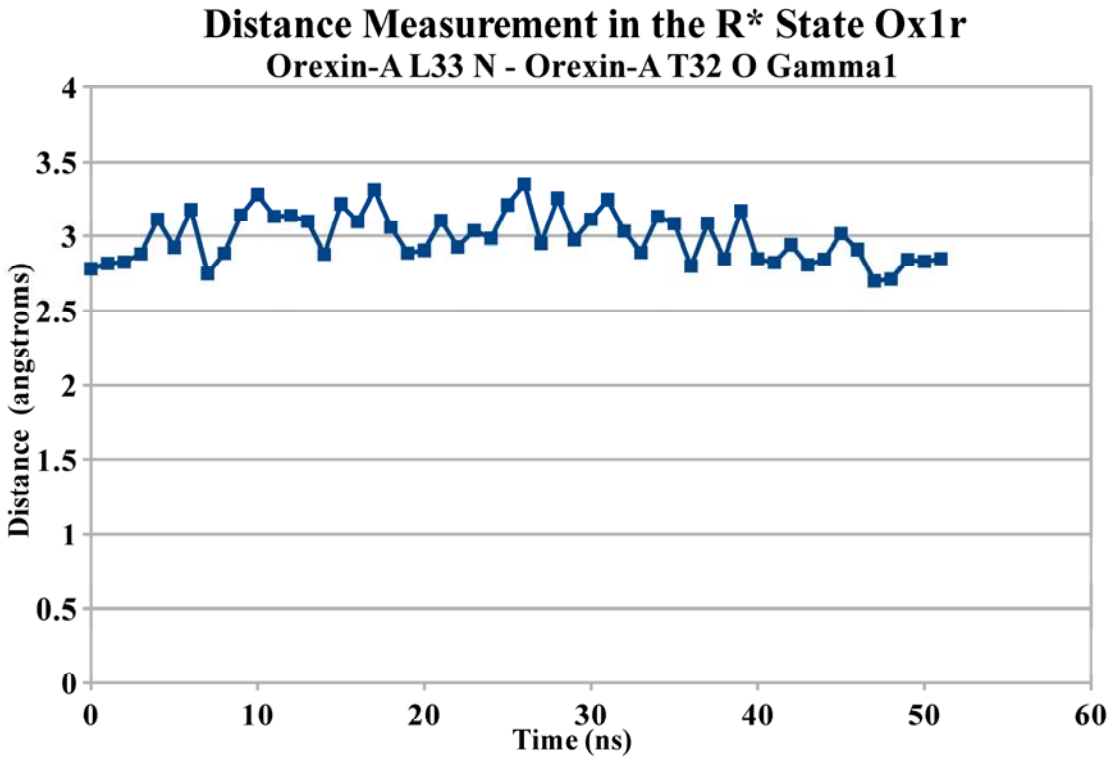

Figure 170. Graph of the R* Simulation's orexin-A L33-orexin-A T32 N-Oγ1 Distance.[3,4,7,22,24,175,176]

The atoms in the orexin-A L33-orexin-A T32 N-Oγ1 measurement in the R* simulation are shown in Figure 171.[3,4,7,22,24,175,176]

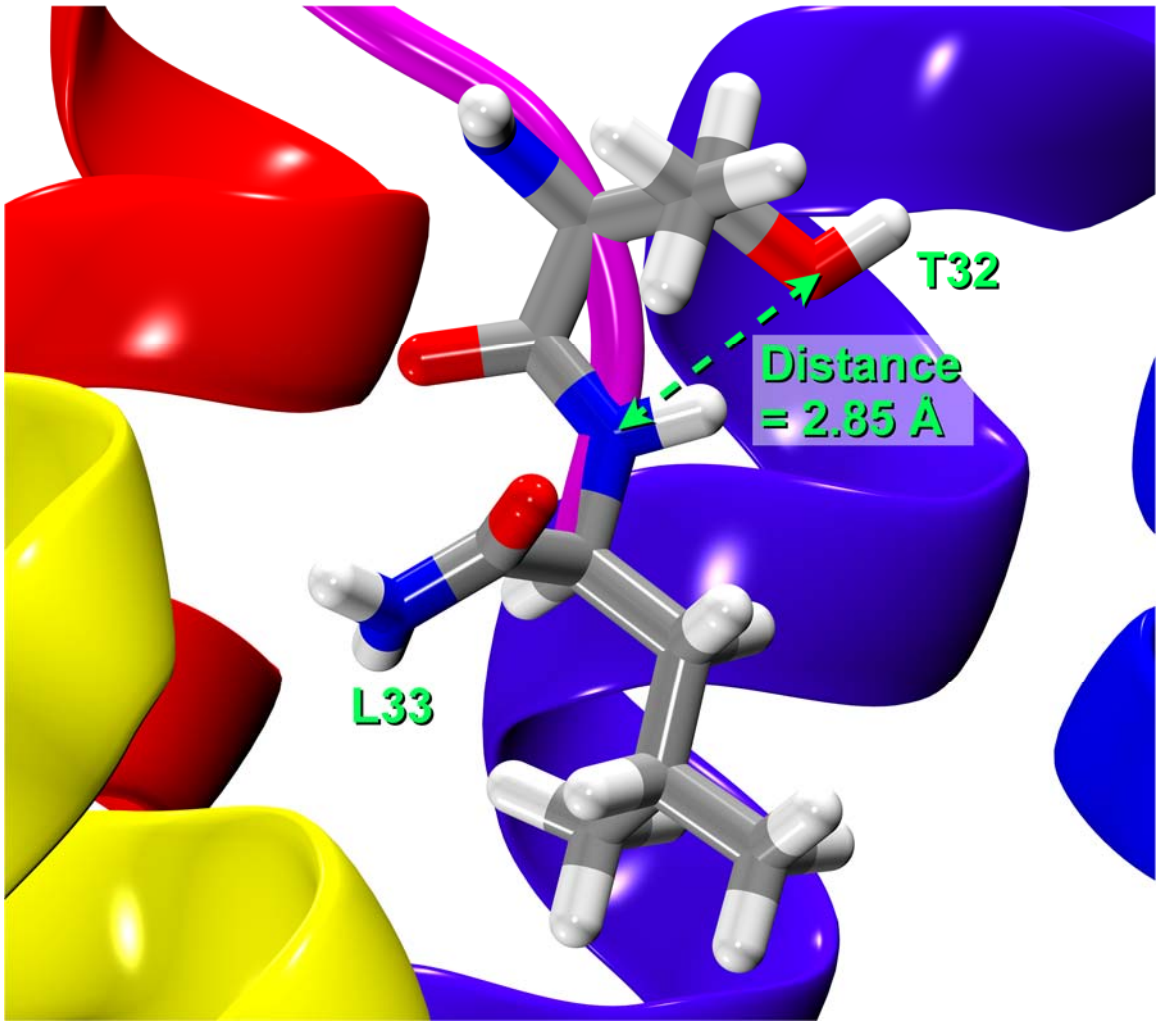

Figure 171. The R* Simulation's Orexin-A L33-orexin-A T32 N-Oγ1 Distance.[3,4,7,22,24,175,176]

The next two distances concern the residue H26, which is hypothesized to donate a hydrogen bond to D45.51, as that bond could be a reason for D45.51's and H26's respective roles in oxA binding in the ox1r, yet H26 transitions to donate a hydrogen

bond to C45.50's backbone oxygen at the end, keeping it involved.[3,4,7,22,24,175,176] The atoms in the D45.51-orexin-A H26 Cγ-Nδ1 measurement in the R* simulation are shown in Figure 172, with the measurements in Figure 173.[3,4,7,22,24,175,176]

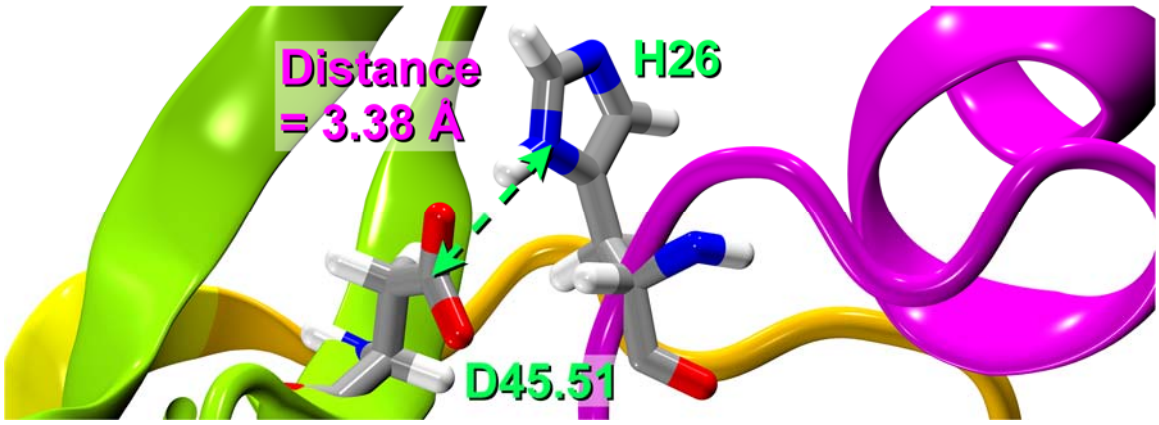

Figure 172. The R* Simulation's D45.51-oxA H26 Cγ-Nδ1 Distance.[3,4,7,22,24,175,176]

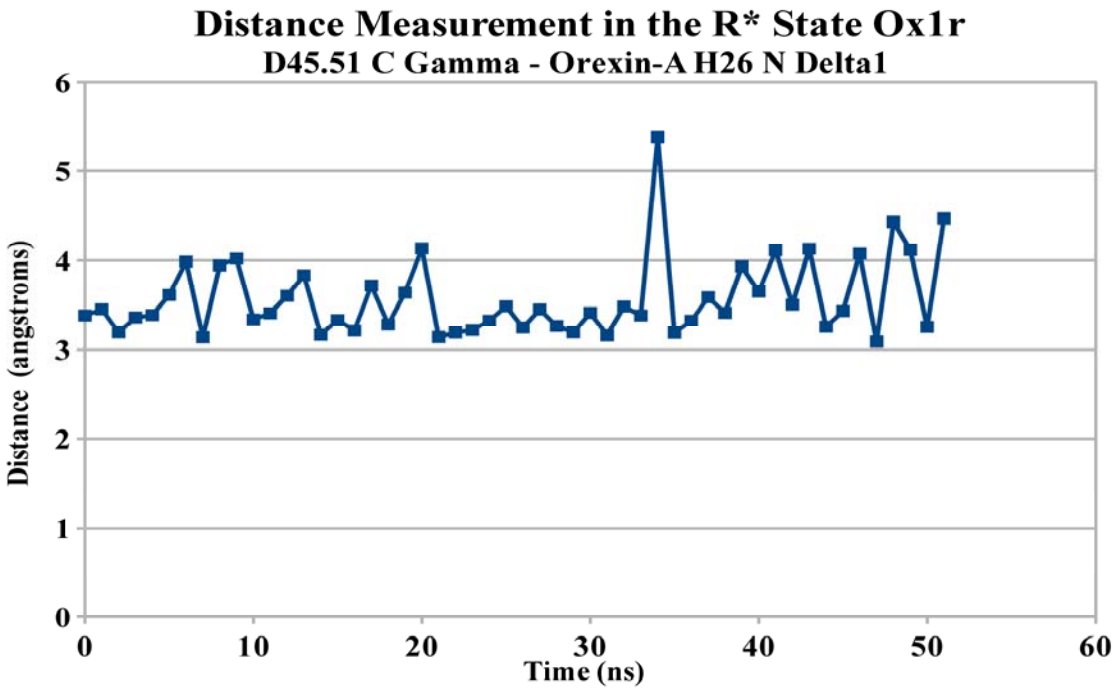

Figure 173. Graph of the R* Simulation's D45.51-oxA H26 Cγ-Nδ1 Distance.[3,4,7,22,24,175,176]

The atoms in the C45.50-orexin-A H26 O-Nδ1 measurement in the R* simulation are shown in Figure 174, with the measurements in Figure 175.[3,4,7,22,24,175,176]

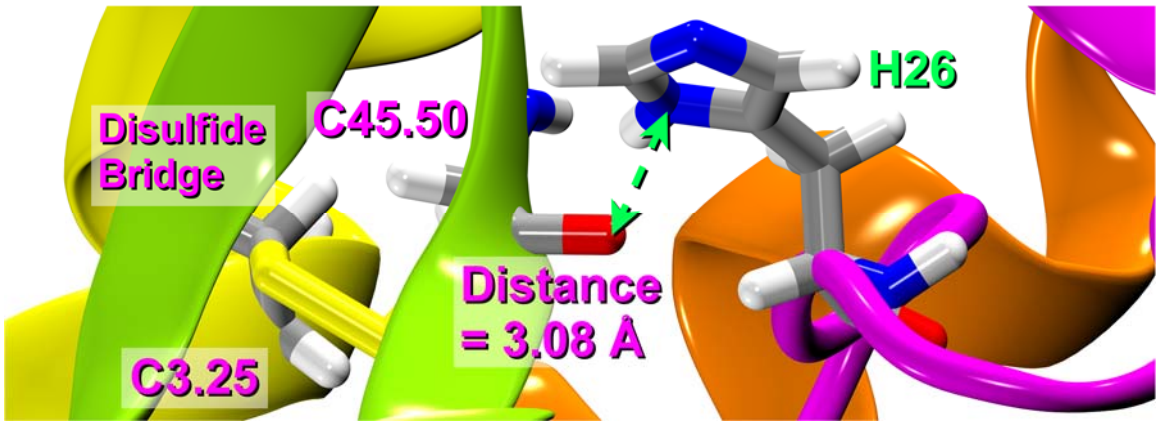

Figure 174. The R* Simulation's C45.50-oxA H26 O-Nδ1 Distance.[3,4,7,22,24,175,176]

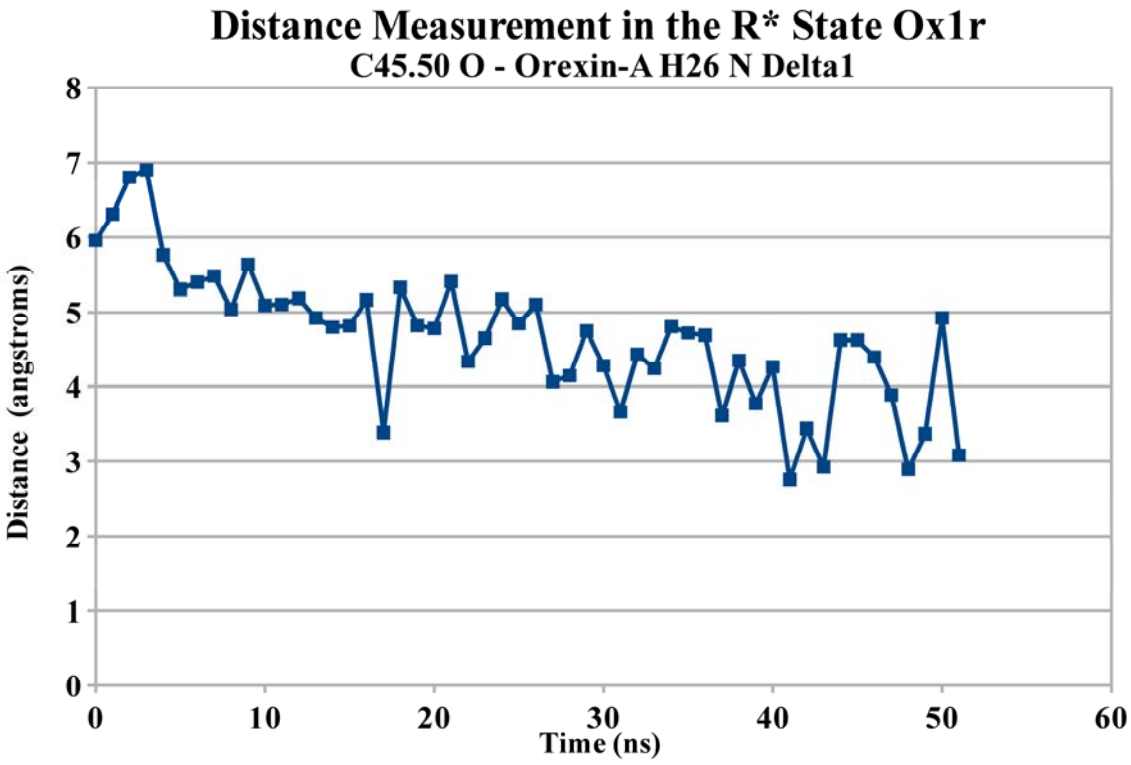

Figure 175. Graph of the R* Simulation's C45.50-oxA H26 O-Nδ1 Distance.[3,4,7,22,24,175,176]

The measurement of D45.51-orexin-A H26 Cγ-Nδ1 was ~3.5 Å, while the measurement of C45.50-orexin-A H26 O-Nδ1 was ~3.8 Å at the end, showing that H26 faced competition from water and from R45.53, and therefore shifted its hydrogen bond acceptor to the far less mobile C45.50 amide oxygen.[3,4,7,22,24,175,176]

The next two distances concern the residue L31, which is hypothesized to seat itself into the hydrophobic pocket formed between TMH2 and TMH3 and also involving residues in the EC1 loop, especially W112.[3,4,7,22,24,175,176] The measurement of the I3.28-orexin-A L31 Cβ-Cγ distance in the R* simulation is shown in Figure 176, as I3.28 is central to this binding pocket.[3,4,7,22,24,175,176]

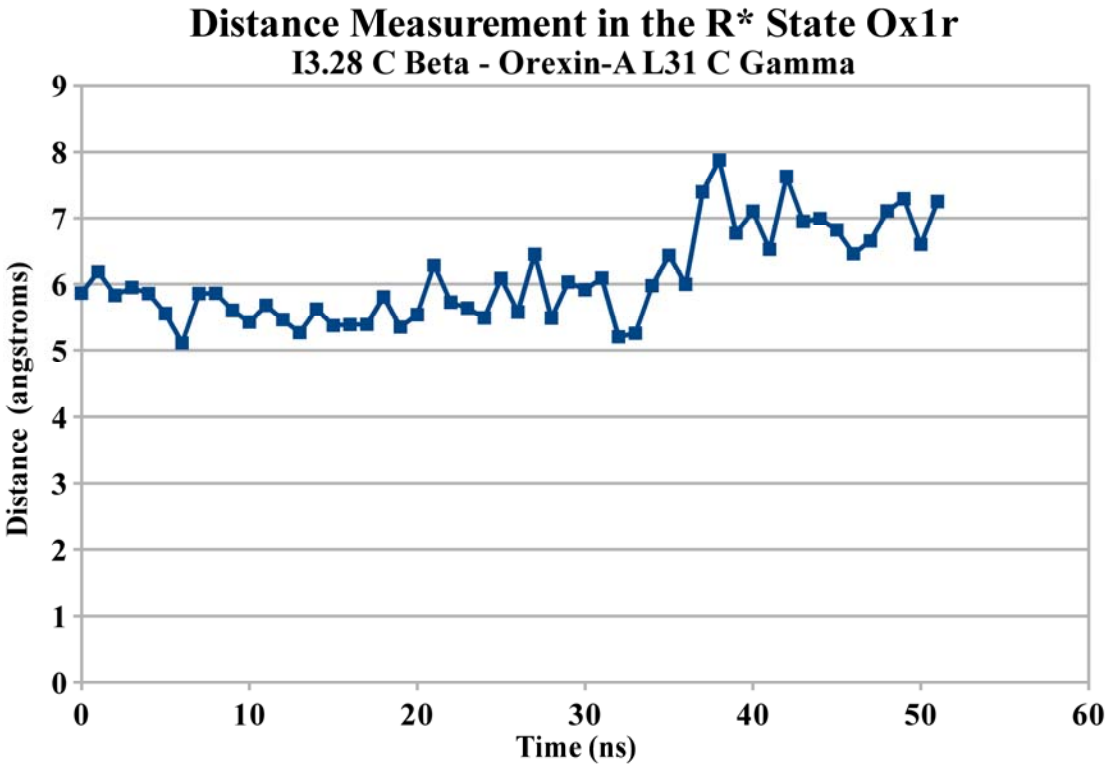

Figure 176. Graph of the R* Simulation's I3.28-orexin-A L31 Cβ-Cγ Distance.[3,4,7,22,24,175,176]

The atoms in the I3.28-orexin-A L31 Cβ-Cγ measurement in the R* simulation are shown in Figure 177.[3,4,7,22,24,175,176]

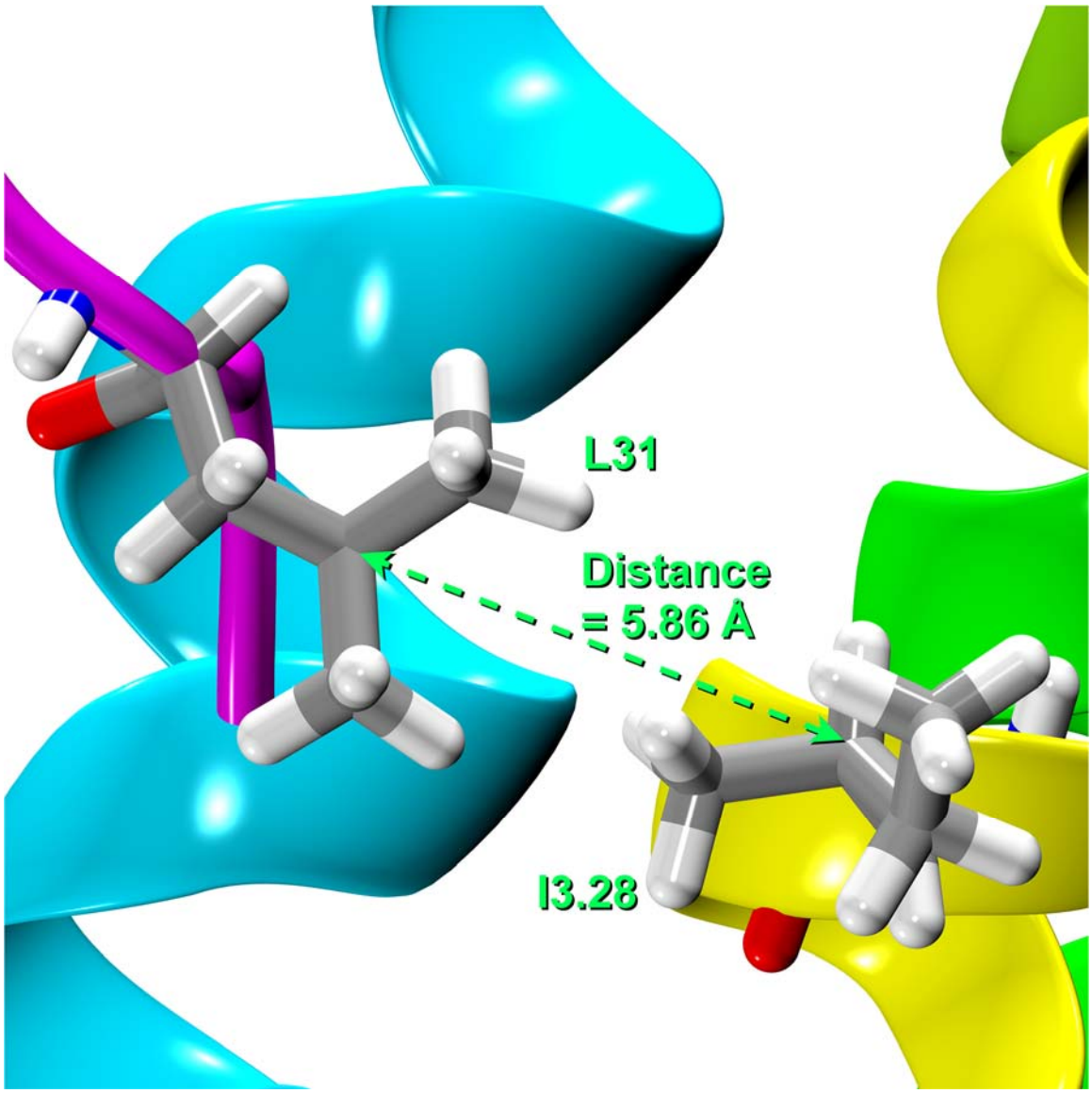

Figure 177. The R* Simulation's I3.28-orexin-A L31 Cβ-Cγ Distance.[3,4,7,22,24,175,176]

Over the course of the simulation, at about 36 ns in, the distance jumps from ~6.0 Å to ~7.0 Å, signifying the residue L31 shifting to a new hydrophobic pocket formed with the

EC2 loop and TMH3, with M45.31 and C45.50 key to this binding pocket.[3,4,7,22,24,175,176]

As C45.50 is central to this new binding pocket, the atoms in the C45.50-orexin-A L31 Sγ-Cγ measurement in the R* simulation are shown in Figure 178.[3,4,7,22,24,175,176]

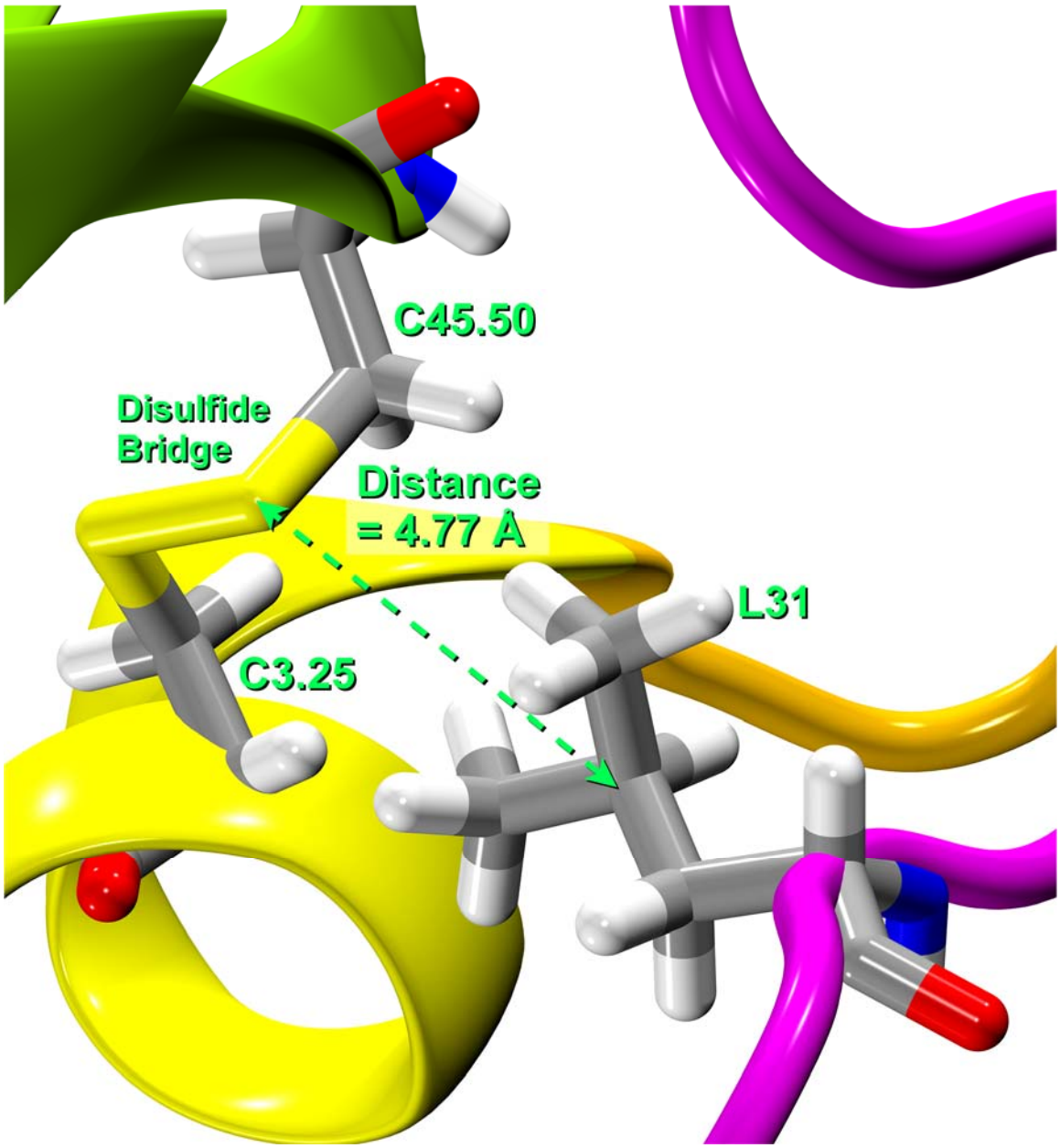

Figure 178. Picture of the R* Simulation's C45.50-orexin-A L31 Sγ-Cγ Distance.[3,4,7,22,24,175,176]

The measurement of the C45.50-orexin-A L31 Sγ-Cγ atoms in the R* simulation are shown in Figure 179.[3,4,7,22,24,175,176]

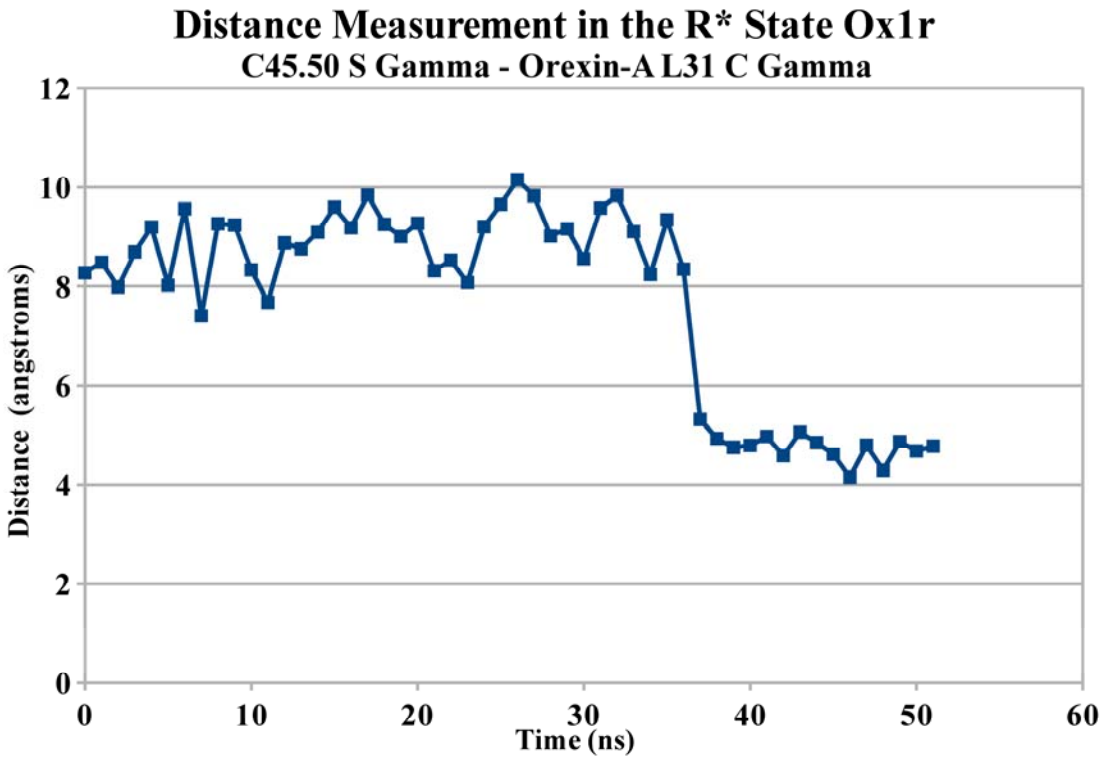

Figure 179. Graph of the R* Simulation's C45.50-orexin-A L31 Sγ-Cγ Distance.[3,4,7,22,24,175,176]

The measurement of C45.50-orexin-A L31 Sγ-Cγ falls from ~9.0 Å to ~5.0 Å at the end, showing that L31 not only found a new binding pocket, it actually stayed there, showing its importance as a key residue on orexin-A.[3,4,7,22,24,175,176]

The next two measurements concern the L33 amide cap and its ability to find specific hydrogen binding partners, one the almost immobile P3.29 backbone oxygen, and another the R6.59 guanidium, which interact with the amide cap's HT1 hydrogen and backbone oxygen, respectively.[3,4,7,22,24,175,176] Even though this does not involve L33's

side chain, these remain important.[3,4,7,22,24,175,176] The measurement of P3.29-orexin-A L33 O-NT and the atoms involved are shown in Figures 180 and 181.[3,4,7,22,24,175,176]

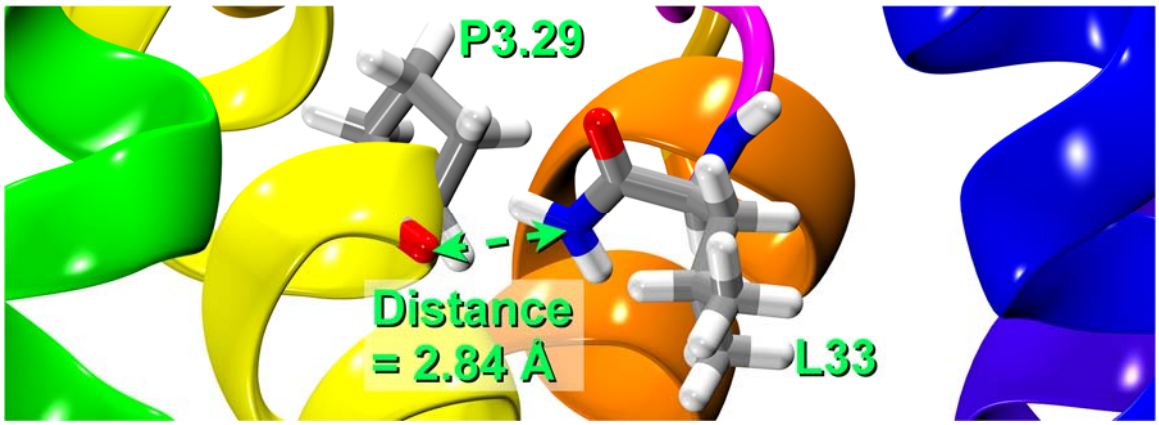

Figure 180. The R* Simulation's P3.29-orexin-A L33 O-NT Distance.[3,4,7,22,24,175,176]

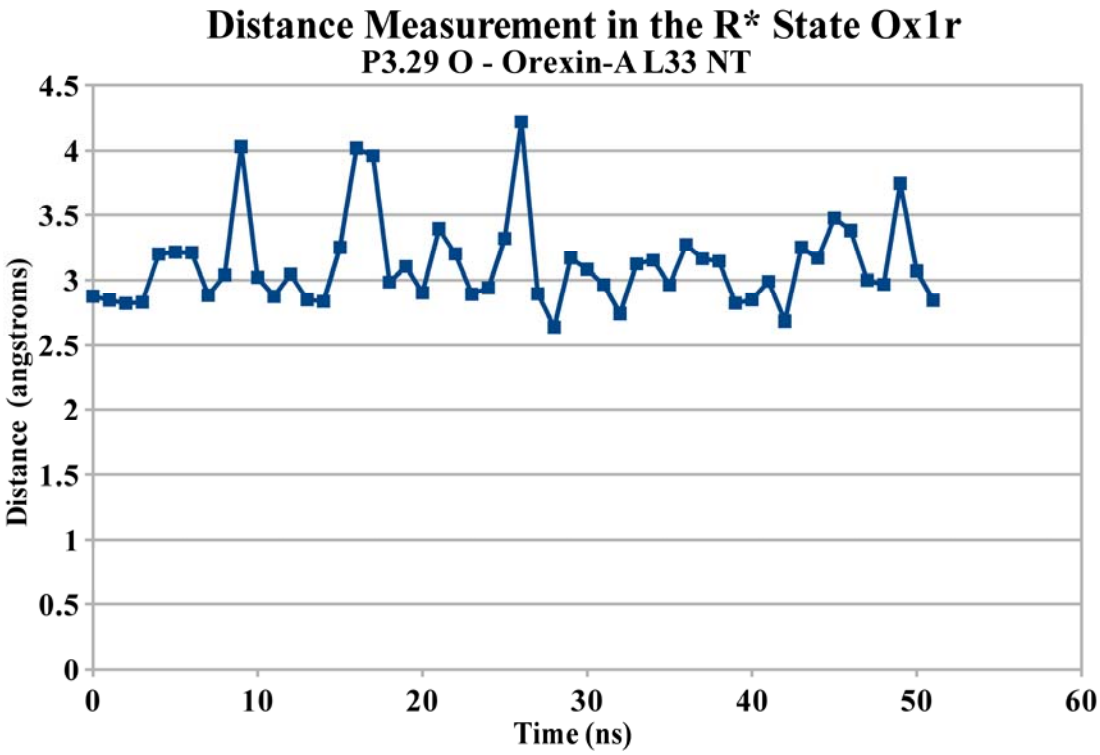

Figure 181. Graph of the R* Simulation's P3.29-orexin-A L33 O-NT Distance.[3,4,7,22,24,175,176]

The atoms in the R6.59-orexin-A L33 Cζ-O measurement in the R* simulation are shown in Figure 182, with the measurements in Figure 183.[3,4,7,22,24,175,176]

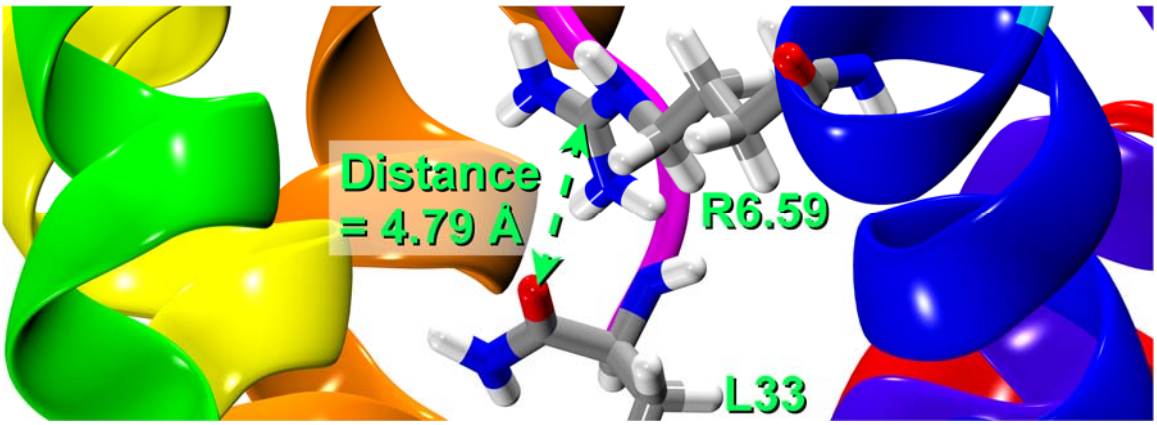

Figure 182. The R* Simulation's R6.59-orexin-A L33 Cζ-O Distance.[3,4,7,22,24,175,176]

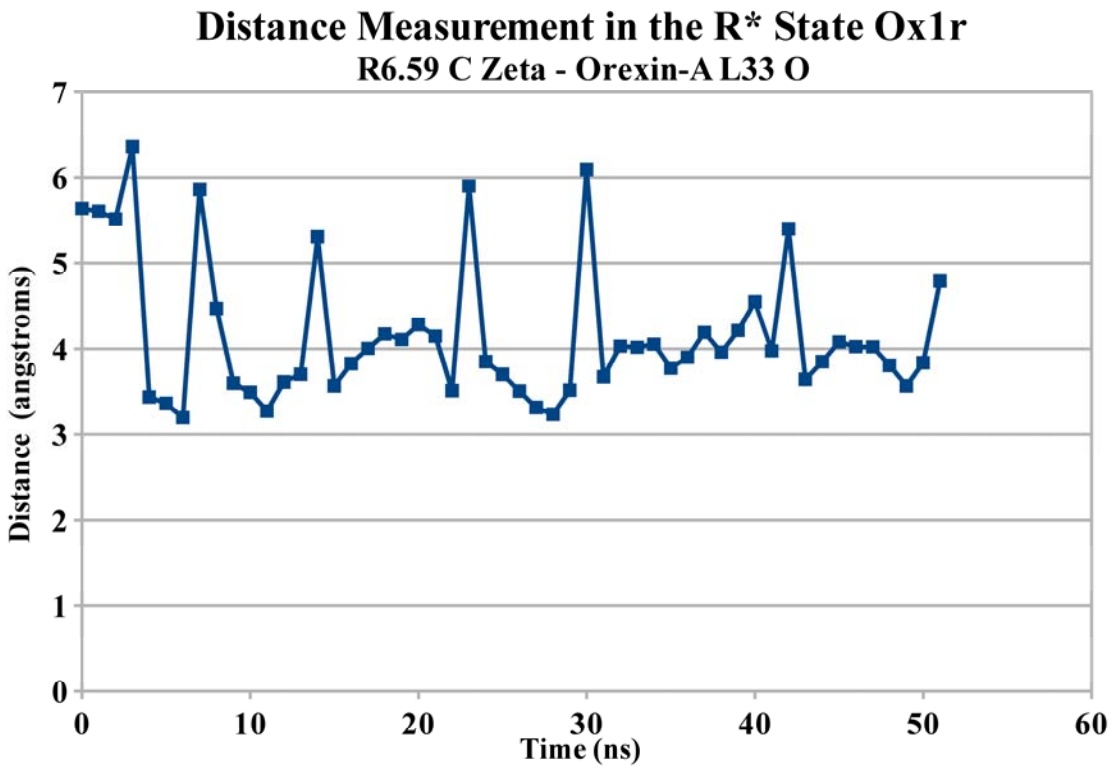

Figure 183. Graph of the R* Simulation's R6.59-orexin-A L33 Cζ-O Distance.[3,4,7,22,24,175,176]

The distances for P3.29-orexin-A L33 O-NT and R6.59-orexin-A L33 Cζ-O were ~3.0 Å and ~4.0 Å, consistent with strong hydrogen bonds between oxA and the ox1r, especially when it came to oxA binding to ox1r residues that were either immobile or charged, and also due to R6.59 supplanting Q4.60 as a hydrogen bond donor.[3,4,7,22,24,175,176] In fact, L33's bulky side chain immobilizes these interactions further still, and prevents water molecules from interfering with these hydrogen bonds.[3,4,7,22,24,175,176]

The last of these distances is V45.49-orexin-A L20 Cβ-Cγ, and the atoms involved are shown in Figure 184.[3,4,7,22,24,175,176]

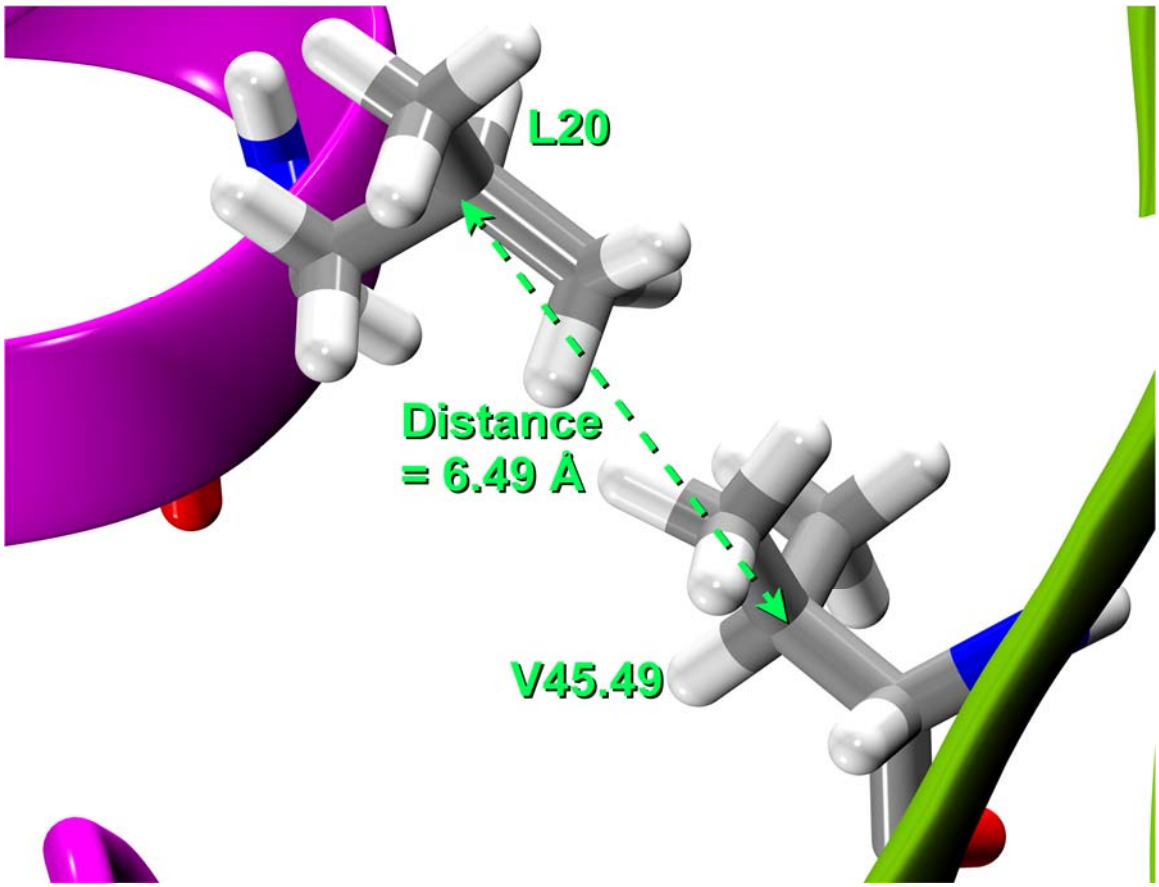

Figure 184. The R* Simulation's V45.49-orexin-A L20 Cβ-Cγ Distance.[3,4,7,22,24,175,176]

The measurement of the V45.49-orexin-A L20 Cβ-Cγ distance is shown in Figure 185.[3,4,7,22,24,175,176]

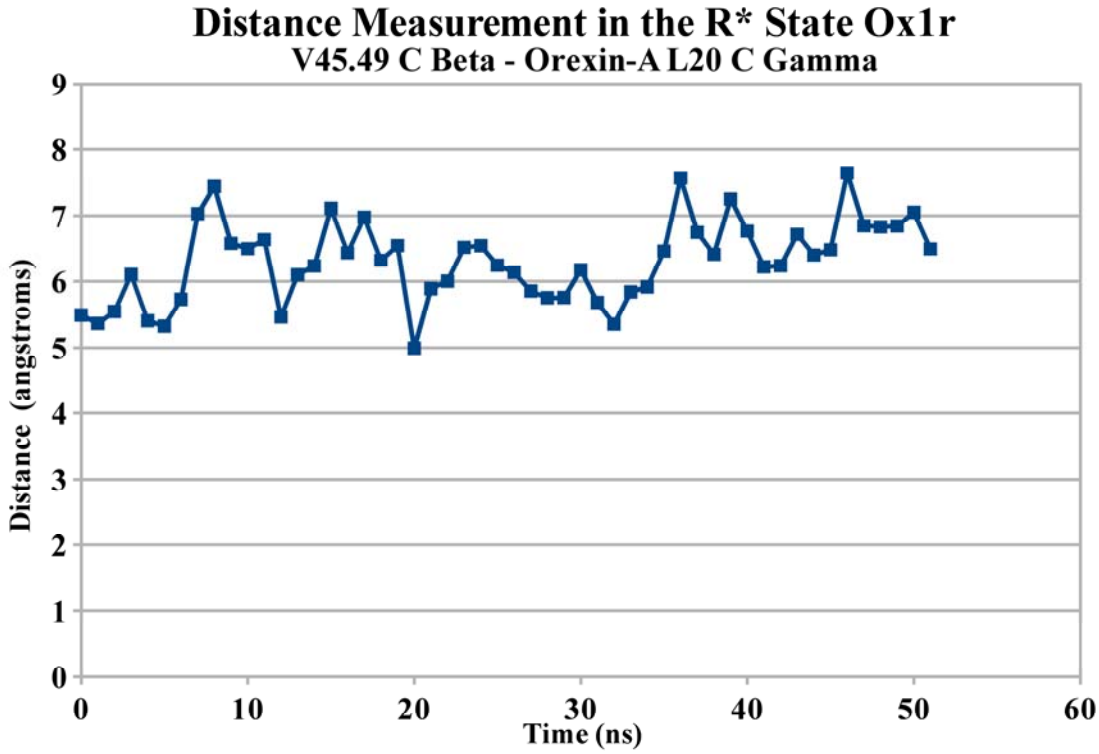

Figure 185. Graph of the R* Simulation's V45.49-orexin-A L20 Cβ-Cγ Distance.[3,4,7,22,24,175,176]

The distance between V45.49's Cβ and orexin-A's L20 Cγ is ~6.5 Å, showing a consistent interaction between L20 and a hydrophobic binding pocket formed by the ox1r EC1 and EC2 loops that also interacts with L16 and with L19.[3,4,7,22,24,175,176]

Molecular Dynamics Component Interaction Energy Measurements Results

Two energy comparison tables were created, each using the R model's interactions with SB-674042 in the first and last frames of its MD simulation so that each of those two structures' component interaction energies between the six parts of SB-

674042 and the residues of ox1r within 7 Å of each of those parts are calculated with the OPLS_2005 force field (as OPLS3 was unavailable for this calculation script), no solvent, extended cutoff, and force field charges were used for both "wet" and "dry" dielectric conditions, with "wet" as a constant dielectric of 80, and "dry" as a distance-dependent dielectric of 3.[3,7,24,175,176] Four different energy sets were made: "before dry," "before wet," "after dry," and "after wet." One of these tables was created to display the interaction energies between ox1r and each of the six parts of SB-674042, including a total energy for each, as shown in Table 35.[3,7,24,137,175,176]

Table 35

Interaction Energies between Ox1r and the Six Component Parts of SB-674042.[3,7,24,137,175,176]

Before Energy (kcal/mol)		***Part of SB-674042 (with description)***	***After Energy (kcal/mol)***	
Dry	***Wet***		***Dry***	***Wet***
-45.86	**-43.93**	**Part 1 (fluorophenyl)**	**-26.41**	**-24.55**
-37.30	**-38.81**	**Part 2 (1,3-thiazole with methyl and C=O)**	**-59.64**	**-56.93**
-25.29	**-25.68**	**Part 3 (proline-like part)**	**-19.55**	**-19.59**
-3.04	**-3.12**	**Part 4 (methylene)**	**-3.86**	**-3.88**
-13.59	**-5.93**	**Part 5 (1,3,4-oxadiazole)**	**-23.49**	**-15.82**
-45.77	**-46.81**	**Part 6 (phenyl)**	**-55.53**	**-55.86**
-170.86	***-164.28***	***Whole SB-674042***	***-188.49***	***-176.64***

The energies in Table 35 show which parts of SB-674042 had the most vital interaction energies with ox1r, namely the 1,3-thiazole part, which was one of the principal parts holding Y6.48 in g^+, and the 1,3,4-oxadiazole, which was the part that accepted the hydrogen bond from Q3.32.[3,7,24,175,176] Furthermore, the phenyl group tucked itself into

the TMH2-3 hydrophobic pocket quite well.[3,7,24,175,176] The other table was created to display the interaction energies between SB-674042 and selected individual residues of ox1r, along with binding data, as shown in Table 36.[3,7,24,175,176]

Table 36

Interaction Energies between SB-674042 and Key Individual Residues of Ox1r.[3,7,24,175,176]

Before Energy (kcal/mol)		***Residue of Ox1r*** K_d ***(Mutant) /*** K_d ***(WT)***	***After Energy (kcal/mol)***	
Dry	***Wet***		***Dry***	***Wet***
-23.44	**-14.08**	**Q3.32 → A 50.9*****	**-44.77**	**-34.58**
-2.02	**-1.86**	**A3.33 → T 20.2****	**-5.46**	**-5.53**
0.11	**-0.10**	**V3.36 → A 2.1**	**-8.91**	**-8.83**
-2.73	**-3.04**	**Y5.47 → A 1.8**	**-0.32**	**-0.33**
-9.51	**-9.25**	**Y6.48 → A 10.8****	**-8.52**	**-8.53**
-11.26	**-11.60**	**H7.39 → A 22.7*****	**-6.84**	**-7.45**
-4.13	**-4.80**	**Y7.43 → A 9.3*****	**-10.77**	**-9.03**

Note. $^{*}p < 0.05$, $^{**}p < 0.01$, $^{***}p < 0.001$, N.D.B. means no detectable binding because of high nonspecific binding.[3]

The energies in Table 36 show a consistency with the main important residues of interaction in ox1r interacting with SB-674042, with Q3.32 and Y6.48 each with strong energetic interactions, the latter being necessary to keep the ox1r in the R state.[3,7,24,124,125,126,127,128,129,130,175,176] Q3.32 gained a more significant role by having SB-674042 wrap around it, in addition to its strong electrostatic role.[3,7,24,175,176]

Two more energy comparison tables were created, each with the R* model's interactions with orexin-A in the first and last frames of the MD simulation, with the component interaction energy calculated between oxA and ox1r the same way as between SB-674042 and ox1r, for the same total of four different energy sets for each table:

"before wet," "before dry," "after wet," and "after dry."[3,4,7,22,24,155,175,176] One of these tables was created to display the interaction energies between ox1r and each individual residue of orexin-A, along with the sums of the energies for residues 16, 19, 20, and 26-33 of orexin-A (listed as "Majors") and for all of orexin-A's residues, as well as the total interaction energies and normalized efficacy for orexin-A, as shown in Table 37.[3,4,7,22,24,155,175,176]

Table 37

Interaction Energies between Ox1r and Each Residue of Orexin-A.[3,4,7,22,24,155,175,176]

Before Energy (kcal/mol)		***Whole Orexin-A Residue WT oxA (15-33) (pEC_{50} 6.45 ± 0.06, =)***	***After Energy (kcal/mol)***	
Dry	***Wet***		***Dry***	***Wet***
-6.34	**-5.88**	**Pyr1 (n/a, n/a)**	**-17.03**	**-15.51**
-14.93	**-15.20**	**P2 (n/a, n/a)**	**-14.51**	**-15.15**
-6.82	**-7.06**	**L3 (n/a, n/a)**	**-1.22**	**-1.54**
-2.67	**-3.31**	**P4 (n/a, n/a)**	**-23.41**	**-20.77**
-48.67	**-9.02**	**D5 (n/a, n/a)**	**9.95**	**0.09**
-10.28	**-10.46**	**C6 (n/a, n/a)**	**-3.00**	**-3.33**
-3.52	**-3.55**	**C7 (n/a, n/a)**	**-1.21**	**-1.21**
6.54	**0.92**	**R8 (n/a, n/a)**	**-7.18**	**-1.31**
-1.83	**-2.57**	**Q9 (n/a, n/a)**	**0.78**	**0.13**
-5.40	**-1.86**	**K10 (n/a, n/a)**	**-0.41**	**-0.11**
-1.15	**-1.37**	**T11 (n/a, n/a)**	**-0.18**	**-0.15**
-17.48	**-13.35**	**C12 (n/a, n/a)**	**-0.97**	**-1.23**
-12.76	**-10.22**	**S13 (n/a, n/a)**	**-17.06**	**-10.80**
-5.43	**-5.94**	**C14 (n/a, n/a)**	**-8.24**	**-6.72**
-46.02	**-30.39**	**R15 (→A 6.46 ± 0.03, =)**	**-15.67**	**-10.51**
-20.95	**-20.63**	**L16 (→A 71% of 10 µM oxA, ↓)**	**-23.71**	**-22.88**
-38.42	**-16.31**	**Y17 (→A 6.11 ± 0.03, =)**	**-39.64**	**-32.48**
2.02	**-1.18**	**E18 (→A 6.71 ± 0.04, =)**	**-6.48**	**-8.85**
-11.77	**-12.19**	**L19 (→A 60% of 10 µM oxA, ↓↓)**	**-20.86**	**-21.24**

Table 37

Cont.

Before Energy (kcal/mol)		*Whole Orexin-A Residue WT oxA (15-33) (pEC_{50} 6.45 ± 0.06, =)*	*After Energy (kcal/mol)*	
Dry	***Wet***		***Dry***	***Wet***
-17.81	**-17.60**	**L20 (→A 37% of 10 µM oxA, ↓↓)**	**-16.56**	**-16.14**
-39.30	**-30.00**	**H21 (→A 5.89 ± 0.02, =)**	**-29.55**	**-24.40**
-7.04	**-6.56**	**G22 (→A 6.19 ± 0.09, =)**	**-15.56**	**-15.39**
-1.84	**-1.77**	**A23 (n/a, =)**	**-13.03**	**-12.85**
-12.68	**-8.16**	**G24 (→A 6.08 ± 0.03, =)**	**-28.38**	**-23.13**
-3.25	**-5.34**	**N25 (→A 6.00 ± 0.09, =)**	**-18.52**	**-9.84**
-67.77	**-30.25**	**H26 (→A 61% of 10 µM oxA, ↓↓)**	**-49.07**	**-38.64**
-35.30	**-29.01**	**A27 (→G n/a, ↓↓)**	**-26.11**	**-20.80**
-15.26	**-16.64**	**A28 (→G n/a, ↓↓)**	**-10.56**	**-8.85**
-16.43	**-15.60**	**G29 (→A 15% of 10 µM oxA, ↓↓↓)**	**-15.61**	**-12.49**
-34.72	**-33.79**	**I30 (→A inactive at 10 µM, ↓↓↓)**	**-28.22**	**-28.29**
-49.80	**-47.30**	**L31 (→A 12% of 10 µM oxA, ↓↓↓)**	**-45.17**	**-34.87**
-42.47	**-19.50**	**T32 (→A 39% of 10 µM oxA, ↓↓↓) (→D-T inactive at 10 µM oxA, n/a)**	**-28.60**	**-29.38**
-79.99	**-53.80**	**L33 (→A 15% of 10 µM oxA, ↓↓↓) (→D-L 18% of 10 µM oxA, n/a)**	**-82.14**	**-67.46**
-392.26	***-296.32***	***Majors***	***-346.61***	***-301.04***
-669.51	***-484.88***	***Totals***	***-597.12***	***-516.09***

The energies in Table 37 show which parts of orexin-A had the most vital interaction energies with ox1r, showing a consistency with the most important residues of interaction oxA has with ox1r.[3,4,7,22,24,155,175,176] The other table was created to display the interaction

energies between oxA and the individual residues of ox1r, as well as normalized EC_{50}s for orexin-A, as shown in Table 38.[3,4,7,22,24,155,175,176]

Table 38

Interaction Energies between Orexin-A and the Important Residues of Ox1r.[3,4,7,22,24,155,175,176]

Before Energy (kcal/mol)		*Orexin-1 Receptor*	*After Energy (kcal/mol)*	
Dry	*Wet*	*EC_{50}(Mutant) / EC_{50}(WT)*	*Dry*	*Wet*
-18.75	**-10.44**	**Q3.32 → A 2.4-fold**	**-19.28**	**-16.57**
-3.86	**-4.61**	**A3.33 → T 1.8-fold**	**-7.89**	**-7.73**
-0.08	**-0.24**	**V3.36 → A 30.6-fold**	**-2.52**	**-2.67**
0.00	**0.00**	**Y5.47 → A 84.4-fold**	**0.00**	**-0.01**
-0.25	**-0.19**	**Y6.48 → A 163.9-fold**	**-3.78**	**-3.71**
-22.45	**-11.01**	**H7.39 → A 241.1-fold**	**-17.79**	**-6.38**
-2.43	**-2.29**	**Y7.43 → A 8.7-fold**	**-0.64**	**-0.43**

The energies in Table 38 show a consistency with the important residues of interaction in ox1r interacting with orexin-A.[3,4,7,22,24,155,175,176]

Orexin-B Dock in Ox1r Component Interaction Energy Measurements Results

Two more energy comparison tables were created, using the dock of orexin-A within the ox1r R* structure taken from the final frame of the MD simulation, and the dock of orexin-B in that same structure, with energies calculated as in Tables 37 and 38.[3,4,7,22,24,131,132,155,157,158,159,160,175,176] However, since the dock of orexin-B was minimized to clean it up, the orexin-A dock was minimized to the same energetic gradient of ~0.21 kJ/mol to improve dock-to-dock comparison, and the resulting data are shown in Table 39.[3,4,7,22,24,131,132,155,157,158,159,160,175,176]

Table 39

Interaction Energies between the Entire Ox1r and Each Residue of Orexin-A (Right) and Orexin-B (Left).[3,4,7,22,24,131,132,155,157,158,159,160,175,176]

OxB Energy (kcal/mol)		*Orexin Residues Orexin-B vs. Orexin-A*	*OxA Energy (kcal/mol)*	
Dry	*Wet*		*Dry*	*Wet*
0.00	0.00	N/a vs. Pyr1	-24.92	-22.95
0.00	0.00	N/a vs. P2	-15.13	-17.97
0.00	0.00	N/a vs. L3	-1.50	-1.85
0.00	0.00	N/a vs. P4	-23.68	-21.43
0.00	0.00	N/a vs. D5	9.43	1.02
-13.36	-5.83	R1 vs. C6	-3.71	-3.75
-0.75	-0.14	S2 vs. C7	-1.37	-1.20
0.01	0.00	G3 vs. R8	-6.62	-1.19
0.16	-0.24	P4 vs. Q9	-0.56	-0.14
0.61	-0.15	P5 vs. K10	-4.04	-1.68
-0.43	-0.99	G6 vs. T11	0.31	-0.09
-23.79	-24.34	L7 vs. C12	-1.11	-1.16
-3.17	-4.23	Q8 vs. S13	-18.28	-7.31
-5.31	-4.03	G9 vs. C14	-10.03	-9.95
-26.06	-18.04	R10 vs. R15	-16.93	-11.32
-29.91	-29.87	L11 vs. L16	-26.77	-25.59
-23.47	-19.01	Q12 vs. Y17	-38.21	-26.78
-12.85	-12.36	R13 vs. E18	-5.63	-8.54
-20.99	-21.33	L14 vs. L19	-21.27	-21.65
-32.36	-31.98	L15 vs. L20	-31.80	-31.32
-31.79	-26.95	Q16 vs. H21	-28.84	-24.29
-14.42	-13.74	A17 vs. G22	-7.02	-6.30
-5.33	-5.65	S18 vs. A23	-15.07	-15.43
-23.32	-18.99	G19 vs. G24	-34.11	-26.13
-27.41	-18.83	N20 vs. N25	-30.56	-18.06
-62.01	-45.62	H21 vs. H26	-54.47	-30.37
-29.06	-19.84	A22 vs. A27	-26.80	-20.05
-12.57	-11.67	A23 vs. A28	-11.80	-10.97
-18.18	-16.00	G24 vs. G29	-16.63	-14.61
-20.03	-20.44	I25 vs. I30	-20.25	-20.53
-52.09	-43.90	L26 vs. L31	-52.79	-45.54

Table 39

Cont.

OxB Energy (kcal/mol)		*Orexin Residues Orexin-B vs. Orexin-A*	*OxA Energy (kcal/mol)*	
Dry	*Wet*		*Dry*	*Wet*
-38.83	**-38.59**	**T27 vs. T32**	**-38.84**	**-38.53**
-97.36	**-79.83**	**M28 vs. L33**	**-91.23**	**-72.54**
-413.41	***-359.07***	***Majors***	***-392.66***	***-331.71***
-624.11	***-532.60***	***Total***	***-670.24***	***-558.19***

The energies in Table 39 show a consistency with how orexin-A interacts better with ox1r than orexin-B does with ox1r, especially using the first four and last four residues of orexin-A in the process.[3,4,7,22,24,131,132,155,157,158,159,160,175,176] The last four residues of both orexin-A and orexin-B both interact extremely well with the ox1r, but the first four residues of orexin-A combined have an interaction with the ox1r that is much stronger than that of orexin-B's L7, as orexin-B lacks the first five residues and the two stabilizing disulfide bridges of orexin-A.[3,4,7,22,24,131,132,155,157,158,159,160,175,176] Interaction energies between oxA and the individual residues of ox1r, as well as normalized EC_{50}s for orexin-A, are displayed in Table 40.[3,4,7,22,24,131,132,155,157,158,159,160,175,176]

Table 40

Interaction Energies between Orexin-A (Right) and Orexin-B (Left) and the Important Residues of Ox1r.[3,4,7,22,24,131,132,155,157,158,159,160,175,176]

OxB Energy (kcal/mol)		*Orexin-1 Receptor EC_{50}(Mutant) / EC_{50}(WT)*	*OxA Energy (kcal/mol)*	
Dry	*Wet*		*Dry*	*Wet*
-25.36	**-20.45**	**Q3.32 → A 2.4-fold**	**-20.17**	**-15.71**
-7.75	**-7.89**	**A3.33 → T 1.8-fold**	**-5.84**	**-5.92**
-4.40	**-4.86**	**V3.36 → A 30.6-fold**	**-1.25**	**-1.35**

Table 40

Cont.

OxB Energy (kcal/mol)		*Orexin-1 Receptor* EC_{50}*(Mutant) /* EC_{50}*(WT)*	*OxA Energy (kcal/mol)*	
Dry	*Wet*		*Dry*	*Wet*
0.00	**0.00**	**Y5.47 → A 84.4-fold**	**0.00**	**-0.01**
-3.61	**-3.44**	**Y6.48 → A 163.9-fold**	**-3.43**	**-3.40**
-25.42	**-16.18**	**H7.39 → A 241.1-fold**	**-25.38**	**-17.05**
-0.76	**-0.48**	**Y7.43 → A 8.7-fold**	**-0.56**	**-0.31**

The data for Table 40 are consistent with experimental data that show that oxB activates the ox1r as well as oxA does at high enough concentrations, as the N-terminus of the oxB dock in the ox1r shown in Figure 186.[3,4,7,22,24,131,132,155,157,158,159,160,175,176]

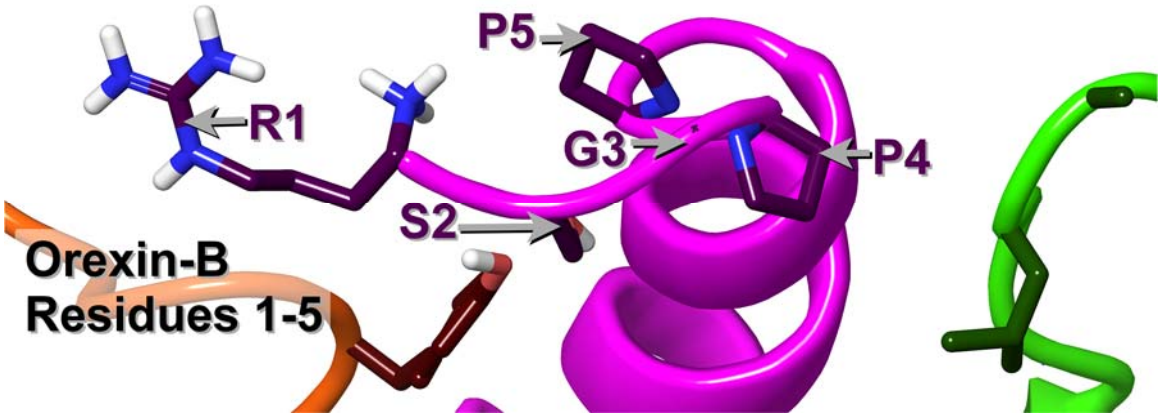

Figure 186. The OxB N-terminus Interacting with the Ox1r R* Structure.[3,4,7,22,24,131,132,155,157,158,159,160,175,176]

The central helix of orexin-B (residues G6 to Q16) is shown in Figure 187.[3,4,7,22,24,131,132,155,157,158,159,160,175,176]

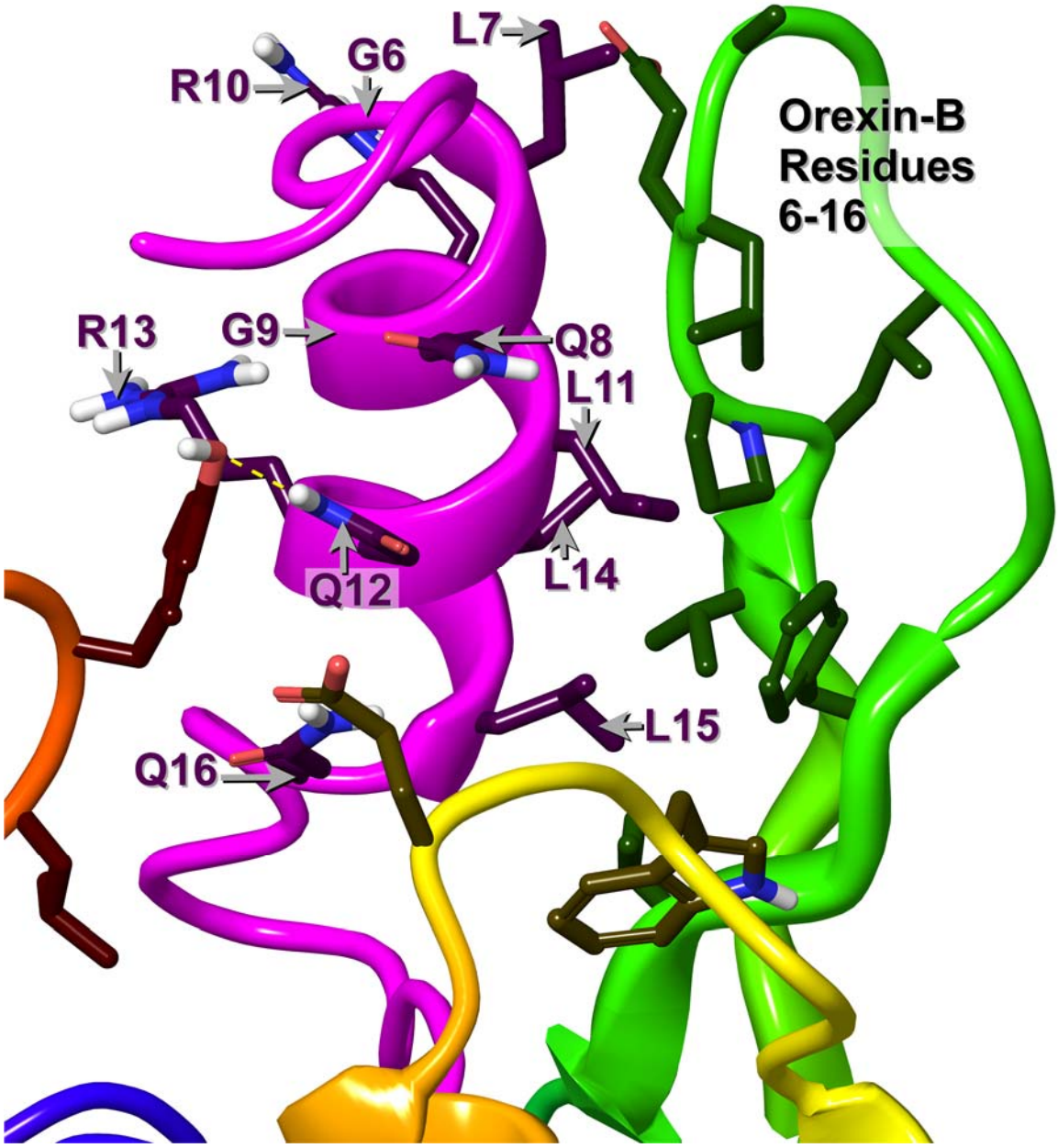

Figure 187. The Oxb Central Helix Interacting with the Ox1r R* Structure.[3,4,7,22,24,131,132,155,157,158,159,160,175,176]

The C-terminus of orexin-B (residues A17 to M28) is shown in Figure 188.[3,4,7,22,24,131,132,155,157,158,159,160,175,176]

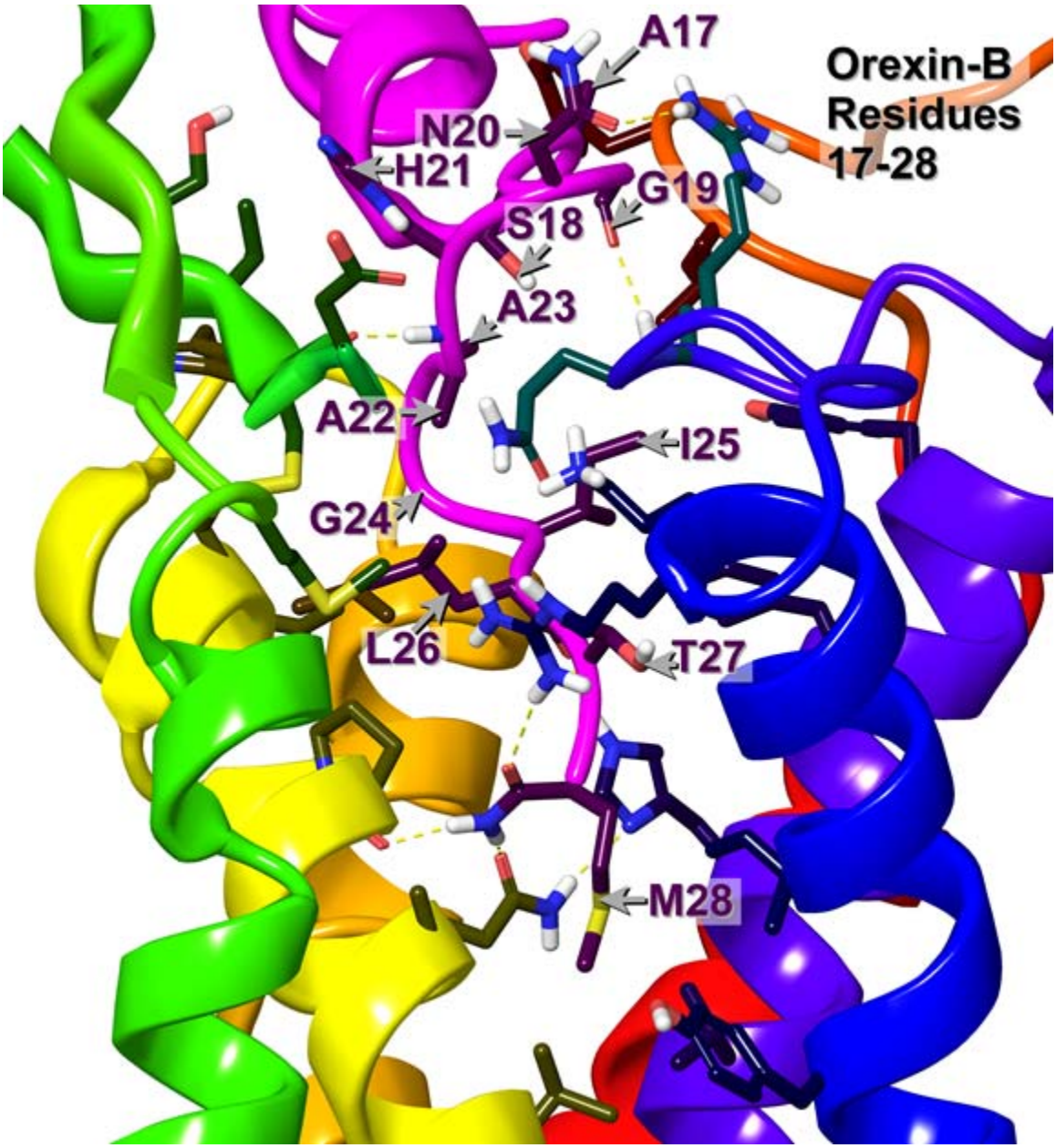

Figure 188. OxB C-terminus Interacting with the Ox1r R* Structure.[3,4,7,22,24,131,132,155,157,158,159,160,175,176]

These previous three images further bolster the data that shows oxB activates the ox1r as well as oxA does at high enough concentrations.[3,4,7,22,24,131,132,155,157,158,159,160,175,176]

Ox1r Crystal Structure Comparisons with the R and R* Structures

The recently released ox1r crystal structures, 4zj8 (with suvorexant bound) and 4zjc (with SB-674042 bound),[192] were compared with the orexin-1 receptor models before and after the MD simulations[3,4,7,22,24,157,158,159,160,175,176] to see the various structural similarities and differences between them.[3,4,7,22,24,192] First, the ox1r R* structure from the final frame of its MD experiment and the crystal structure 4zjc were superimposed, with the EC2 loops of both shown in Figure 189.[3,4,7,22,24,157,158,159,160,175,176,192]

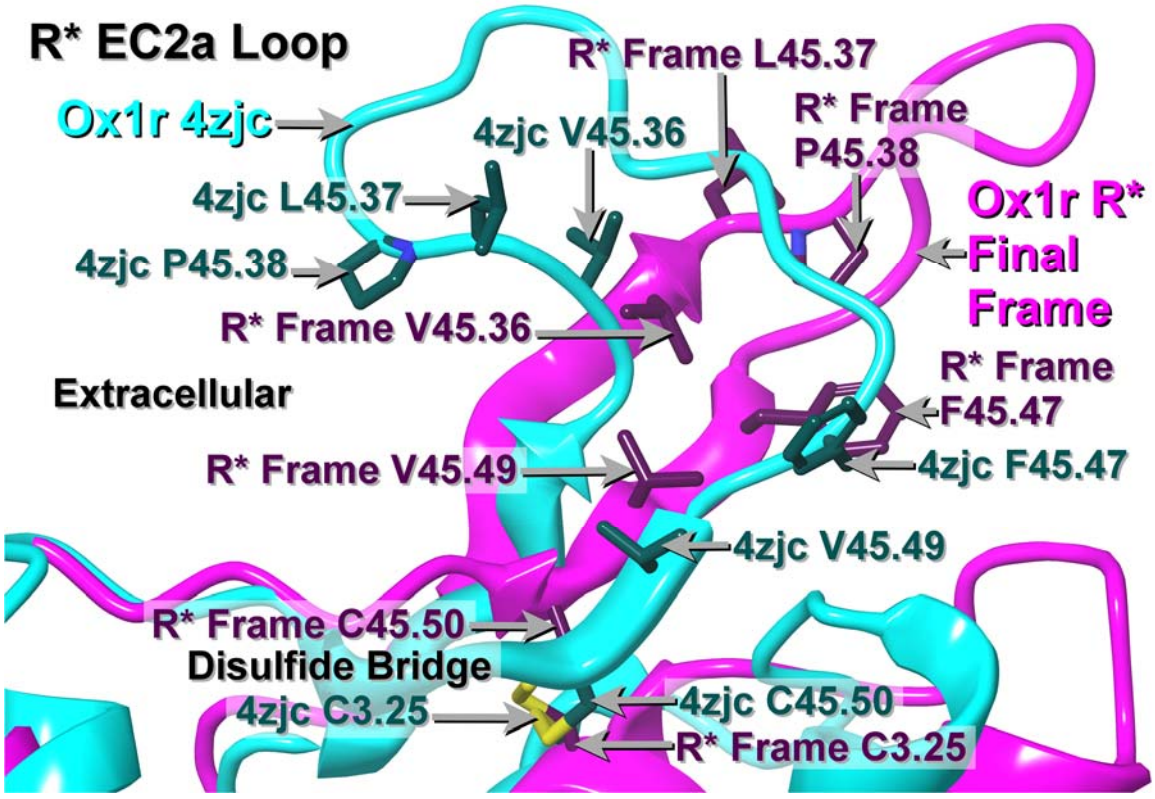

Figure 189. The EC2 Loops of the Ox1r R* Final Frame (Magenta) Superimposed on the Ox1r Crystal Structure 4zjc (Teal).[3,4,7,22,24,157,158,159,160,175,176,192]

Figure 189 shows that the residues on the ox1r R* final frame EC2 loop that bind L16, L19, and L20 on orexin-A were identical to those on 4zjc, and faced the same direction, into the orexin-A-binding hydrophobic pocket.[3,4,7,22,24,157,158,159,160,175,176,192]

Second, the crystal structure 4zjc and the ox1r R structure that was used as the input structure for the R model's MD experiment were compared, as shown in Figure 190.[3,4,7,22,24,192]

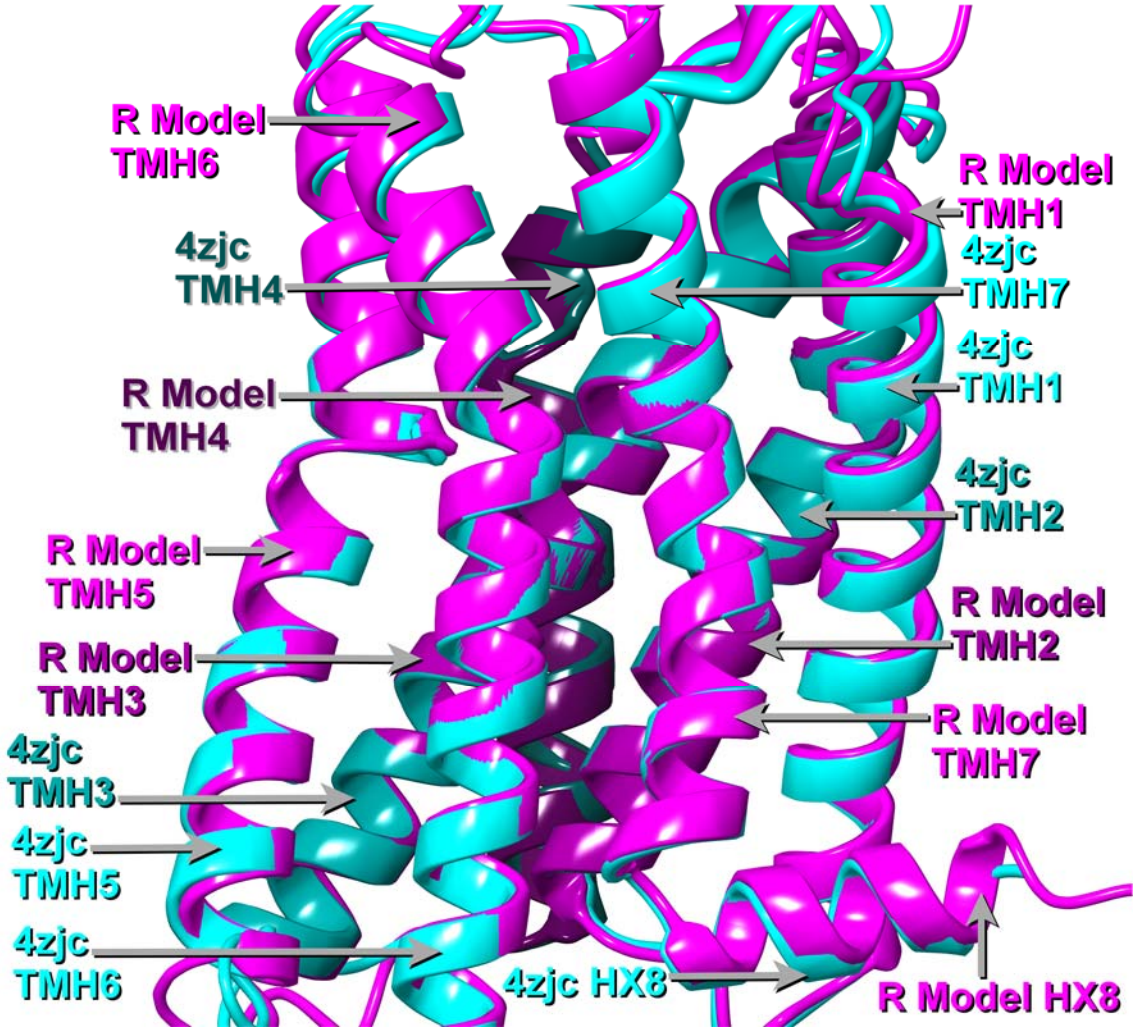

Figure 190. The Ox1r R Model (Magenta) Superimposed on the Ox1r Crystal Structure 4zjc (Teal).[3,4,7,22,24,192]

Third, the RMSD of the transmembrane helices of the crystal structure 4zjc and of the ox1r R structure that was used as the input structure for the R model's MD experiment was taken, and this was listed in Table 41.[3,4,7,22,24,192]

Table 41

RMSD between the Cαs of the Respective Transmembrane Helices of the Ox1r R Structure and of the Ox1r Crystal Structure 4zjc.[3,4,7,22,24,192]

TMH#	*1*	*2*	*3*	*4*	*5*	*6*	*7*	*8*
RMSD	**0.5383**	**0.2374**	**0.3416**	**0.3731**	**0.3839**	**0.2851**	**0.3074**	**0.5060**

The data suggest that both ox1r models, as the R* model was based on the R model before equilibration via MD, line up well with the ox1r crystal structures in both the transmembrane and loop regions, especially due to their high homology and high identity, rendering the models to be valid for these experiments.[3,4,7,22,24,157,158,159,160,175,176,188,192]

It is further hypothesized that the α-helix in the ox1r crystal structure N-terminus binds to the EC2 loop to hold it, but it is a weak van der Waals interaction.[3,4,7,22,24,192] This allows the ox1r N-terminal α-helix to clear the way when orexin-A or orexin-B binds to the EC2 loop and "discharges" its C-terminus into the ox1r.[3,4,7,22,24,140,146,180,181,182,183,184,185,186,187,192]

Ox1r Crystal Structure vs. R Model Component Interaction Energy Measurements

The last of these experiments involves the ox1r R model and the ox1r crystal structure 4zjc, both of which bind the ox1r antagonist SB-674042.[3,7,24,137,192] First, the hydrogens on both of these structures, 4zjc and the ox1r R model's final frame, were minimized to roughly the same gradient.[3,7,24,137,157,158,159,160,175,176,192] This experiment is a

component interaction calculation that compares the "wet" and "dry" interaction energies of the six parts of SB-674042 with individual residues of the ox1r crystal structure.[3,7,24,137,192] The resultant energies are added in a manner similar to Table 35, for ox1r's interaction with SB-674042 and parts thereof, and Table 36, for SB-674042's interaction with individual residues of the ox1r.[3,7,24,137,192] Interaction energies between ox1r and each of the six parts of SB-674042, including a total energy for each, are shown in Table 42.[3,7,24,137,157,158,159,160,175,176,192]

Table 42

Interaction Energies between Ox1r's Crystal Structure 4zjc, as Well as the Ox1r R Model's Final Frame, and the Six Component Parts of SB-674042.[3,7,24,137,157,158,159,160,175,176,192]

4zjc Energy (kcal/mol)		*Part of SB-674042 (with description)*	*R MD Energy (kcal/mol)*	
Dry	*Wet*		*Dry*	*Wet*
-41.43	**-40.87**	**Part 1 (fluorophenyl)**	**-29.81**	**-28.27**
-50.18	**-50.10**	**Part 2 (1,3-thiazole with methyl and C=O)**	**-59.77**	**-56.37**
-23.91	**-25.75**	**Part 3 (proline-like part)**	**-18.46**	**-18.59**
-11.82	**-11.45**	**Part 4 (methylene)**	**-3.87**	**-3.88**
-21.18	**-22.01**	**Part 5 (1,3,4-oxadiazole)**	**-24.48**	**-15.93**
-52.17	**-51.03**	**Part 6 (phenyl)**	**-56.58**	**-56.76**
-200.68	***-201.20***	***Whole SB-674042***	***-192.97***	***-179.80***

The energies in Table 42 show that SB-674042 interacts with the ox1r crystal structure almost entirely by means of van der Waals interactions between its six parts and the ox1r.[3,7,24,137,192] SB-674042's interactions with the ox1r R model are mostly by van der Waals forces, with the exception of Q3.32's electrostatic interactions with the 1,3-thiazole and the 1,3,4-oxadiazole, which helped the SB-674042 interaction energy with

the ox1r R model grow even more favorable.[3,7,24,137,192] However, the energies were, by and large, more favorable in the ox1r crystal structure than they were in the ox1r R model, with the exceptions of the thiazole and phenyl parts, because 4zjc's SB-674042 was able to achieve better hydrophobic contacts at the expense of those electrostatic interactions.[3,7,24,137,192] The two structures used in this experiment are shown in Figure 191, to show the position of SB-674042 in both.[3,7,24,137,157,158,159,160,175,176,192]

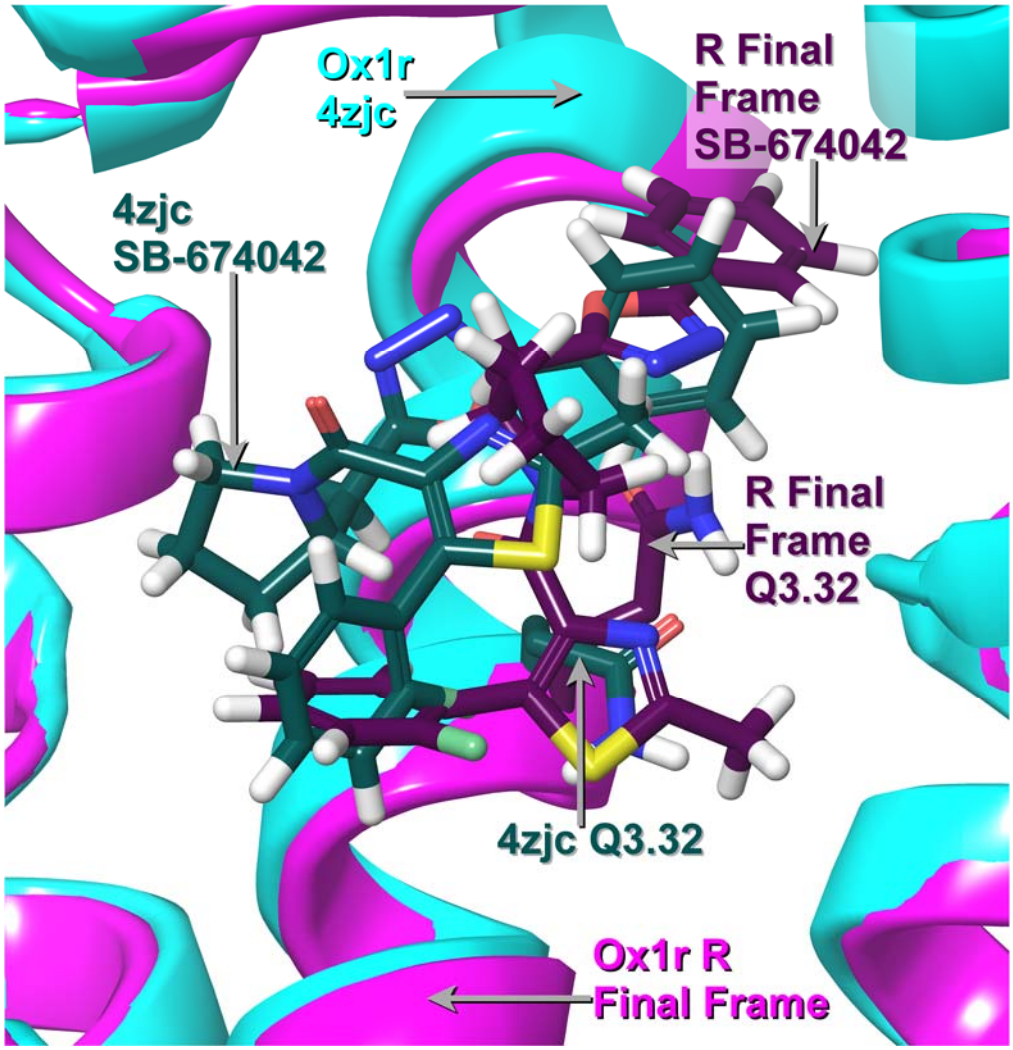

Figure 191. The Ox1r R Final Frame (Magenta) Superimposed on the Ox1r Crystal Structure 4zjc (Teal).[3,7,24,137,157,158,159,160,175,176,192]

Another table was created to display the interaction energies between SB-674042 and selected individual residues of ox1r, along with binding data, as shown in Table 43.[3,7,24,157,158,159,160,175,176,192]

Table 43

Interaction Energies between SB-674042 and Key Individual Residues of Ox1r.[3,7,24,157,158,159,160,175,176,192]

4zjc Energy (kcal/mol)		*Residue of Ox1r* K_d *(Mutant) /* K_d *(WT)*	*R MD Energy (kcal/mol)*	
Dry	*Wet*		*Dry*	*Wet*
-33.21	**-31.80**	**Q3.32 → A 50.9*****	**-46.12**	**-35.21**
-6.79	**-7.36**	**A3.33 → T 20.2****	**-5.30**	**-5.37**
-2.91	**-3.09**	**V3.36 → A 2.1**	**-9.78**	**-9.68**
-0.18	**-0.21**	**Y5.47 → A 1.8**	**-0.32**	**-0.33**
-5.94	**-5.89**	**Y6.48 → A 10.8****	**-8.66**	**-8.59**
-12.72	**-13.68**	**H7.39 → A 22.7*****	**-7.01**	**-7.60**
-7.59	**-8.41**	**Y7.43 → A 9.3*****	**-9.71**	**-7.91**

Note. $^{*}p < 0.05$, $^{**}p < 0.01$, $^{***}p < 0.001$, N.D.B. means no detectable binding because of high nonspecific binding.[3,192]

The results of Table 43 show overall consistency with the crystal structure and with experimental data, with Q3.32 having the most favorable binding energy.[3,7,24,192] However, Q3.32 is able to have an extremely favorable energy of interaction with SB-674042 in the crystal structure even without the aid of multiple electrostatic interactions as present in the R model.[3,7,24,192] Despite having lower binding energy in 4zjc than in the ox1r R model, Y6.48 still interacts well with SB-674042 in the crystal structure.[3,7,24,192]

In summary, the above figure and two tables comparing the interaction energy of SB-674042 with both the ox1r R model and the ox1r crystal structure 4zjc bolster its role in keeping the ox1r in its R state.[3,7,24,124,125,126,127,128,129,130,157,158,159,160,175,176,192]

CHAPTER IV

CONCLUSION

Implications of GPCR Modeling Technique

The conclusion of these experiments reveals several facts. These state that homology modeling of GPCRs works well, but the pull-apart homology modeling method that requires replacement of each transmembrane helix with its CM counterpart,[133,147] pulling the helices apart, then minimizing, works best when no high-homology crystal structures are available.[144,145] Furthermore, since the release of the ox2r crystal structure[7] and those of many peptide-bound GPCRs,[46,180,181,182,183,184,185,186,187] improved homology modeling methods can be created. This is because MD experiments[157,158,159,160,175,176] in a simulated lipid bilayer cause homology models created using the pull-apart-and-minimize method to be ripped apart, especially when no information about peptide docking in GPCRs was known prior.[146,180,181,182,183,184,185,186,187]

Due to improved crystal structures,[7,146,180,181,182,183,184,185,186,187] a GPCR crystal structure with closer homology—especially much higher identity[7,188]—with the GPCR sequence in question, would be used by direct mutation, with Modeller[134,135,136] only used to create the IC3 loop that the co-crystallizing protein replaced,[7] as well as the protein termini,[7] and CM only used to replace the inactive TMH6 with an active one.[124,125,126,127,128,129,130,133,142,143,144,145,147,148,149] Furthermore, this works best for the job as higher identity leads to an increased ability to predict overall structure,[7,144,145,188] and crystallizing peptide-bound GPCRs allows the proper way to dock peptide ligands to

become apparent,[146,180,181,182,183,184,185,186,187] e.g., using CM to create the docked part of a peptide ligand (in this case, orexin-A),[4,22,133,147] then using the original NMR or crystal structure to fill in the rest of the ligand (here, orexin-A's NMR structure).[4,22] Furthermore, Glide can be used to speed up ligand docking.[3,7,24,189,190,191]

Additionally, this method is easier to use as it starts by retaining as much of the crystal structure as possible,[7] and this increased structural fidelity[7,144,145,188] allows the creation of the EC1, EC2, EC3, IC1, or IC2 loops with Modeller,[134,135,136] as well as the creation of any transmembrane helix (except for the R* TMH6) using CM[124,125,126,127,128,129,130,133,143,144,145,147,148,149] to be obviated.

In fact, the extracellular half of TMH6 did not need to be replaced, as the top turn in the ox2r crystal structure TMH6 was wound less tightly than that of the CM TMH6, allowing for better interhelical packing, and only using residues 6.51-6.56 for superposition allowed improved alignment and also allowed the retention of the ox2r crystal structure TMH6 residues 6.51-6.61.[7,133,144,145,147]

To summarize modeling technique, as the ox1r crystal structures were released, they were shown to have a high enough identity with the ox2r that the residues in the EC2 loop that are pointed into the hypothesized orexin-A binding pocket, as well as all of the transmembrane helices, were lined up well enough with the respective R and R* models of the orexin-1 receptor that they were considered valid models for these experiments.[3,4,7,22,24,157,158,159,160,175,176,188,192] The new crystal structures even give insight into how the EC2 loop and N-terminus would be predicted to interact in the absence of orexin-A.[3,4,7,22,24,157,158,159,160,175,176,188,192]

Implications of Ligand Parametrization Technique

Improved ligand parametrization techniques[158,159,160,161,162,163,164,165,166,167,168] allowed SB-674042 and pyroglutamate to have new CHARMM parameters made for them with far greater speed,[158,159,160,161,162,163,164,165,166,167,168] by combining CHARMM scripts and spreadsheets in such a way as to immediately reveal problem parameters, determine how the parameter should act, and quickly repair that same parameter, at a much faster speed than the original scripts would have been able to do so.[158,159,160,161,162,163,164,165,166,167,168] This leads to the limiting factor in ligand parametrization speed becoming the QM conformational searches and QM energy profiles, as performed in these experiments in Spartan (Wavefunction Inc., Irvine, CA),[158,159,160,161,162,163,164,165,166,167,168] with parameters repaired quickly, and in many cases, a spreadsheet could be used to perfect one after one or two uses of a CHARMM script.[158,159,160,161,162,163,164,165,166,167,168] This in turn means that ligand parameters can be quickly made, thus speeding up research.[158,159,160,161,162,163,164,165,166,167,168]

Implications of R and R* Ox1r Model Results in a Ligand Binding Context

As for the ox1r models themselves, each one lends an improved insight as to how the orexin-1 receptor operates, since the R ox1r model has SB-674042 keep the ox1r in the R state,[3,7,24] while the R* ox1r model has oxA keep the ox1r in the R* state.[3,4,7,22,24]

First of all, the ox1r R model binds one end of SB-674042 using Q3.32 and H7.39, and subsequently the other end of SB-674042, which binds to both F5.42 and Y6.48 by π-π interactions, holds Y6.48 in g^+ and this holds TMH6 in an inactive conformation.[3,7,24,124,125,126,127,128,129,130,139,141]

Secondly, the ox1r R* model binds the peptide orexin-A using the EC2 β-sheet to bind the hydrophobic side of oxA Helix I,[3,4,7,22,24] then "discharges" the C-terminus into the receptor binding pocket,[146,180,181,182,183,184,185,186,187] with H26 pulled down so it could initially interact with D45.51, then pursue the less mobile C45.50 amide oxygen,[3,4,7,22,24] where the final C-terminal residues reach deep enough for L33 can contact F5.42 and Y6.48 and hold the latter in *trans*.[3,4,7,22,24,124,125,126,127,128,129,130,139,141,143] As L33 was forced deeper into the bundle, T32 (the C-terminal residue with the strongest available hydrogen bond donor) could bind to E45.52 and permit its backbone and L31's to bind to H7.39, holding TMH6 in an active conformation long enough for a G_q protein to bind.[3,4,7,10,11,12,,22,24,124,125,126,127,128,129,130,139,141,143,158,159,160,161,162,163,164,165,166,167,168]

Thirdly, experiments were performed by comparing the binding of orexin-B to the ox1r to orexin-A's binding to the ox1r, and the results show that orexin-A has superior binding energy to the ox1r with respect to orexin-B's binding energy, yet orexin-B interacts with Y6.48 as well as orexin-A does, consistent with experimental results that show orexin-A to have better ability to bind to the ox1r at lower concentrations, as oxB binds just as well as oxA does at high concentrations.[3,4,7,22,24,131,132,155,157,158,159,160,175,176]

Fourthly, another experiment was performed that compared the binding energy of SB-674042 in the R model's final frame to that of the 4zjc crystal structure, and the crystal structure had a superior binding energy with SB-674042 compared to the R model, despite depending almost entirely on van der Waals energy to acquire such interactions, as opposed to the R model, which still interacts well as it is aided by electrostatic interactions between Q3.32 and the 1,3-thiazole and 1,3,4-oxadiazole parts

of SB-674042, yet SB-674042 in both the R model and 4zjc keep the ox1r in its R state.[3,7,24,124,125,126,127,128,129,130,137,157,158,159,160,175,176,192]

Implications of R and R* Ox1r Model Results in a Pharmaceutical Context

The pharmaceutical implications of this series of experiments is staggering, as not only can improved homology modeling tactics[7,133,134,135,136,147,146,180,181,182,183,184,185,186,187] and improved parametrization methods[158,159,160,161,162,163,164,165,166,167,168] improve ligand and receptor construction and simulation (cite) and subsequently, improve drug design,[3,4,5,6,10,13,18] the ox1r itself is an impressive target for drugs, as new agonists[10,27,28,29,30,31,32,33,34,53,54,55,65,81,86,87,88,89,92,93,100,101,108,109,112,116] and antagonists[28,36,39,46,47,48,49,50,51,52,53,54,55,59,62,67,69,78,79,90,107] could be designed based on these experiments, and side effects of other drugs can be avoided using the results of these experiments.[60,83,102,120,121,122] In final conclusion, the results of this experiment will benefit the orexin drug design field, benefit other drug fields by removing side effects, and unlock knowledge about how to design drugs in many other drug fields in the same way.

REFERENCES

1. Nitkiewicz, A.; Smolinska, N.; Przala, J.; Kaminski, T., Expression of orexin receptors 1 (OX1R) and 2 (OX2R) in the porcine ovary during the oestrous cycle. *Regul Pept* **2010,** *165* (2-3), 186-90.

2. Palczewski, K.; Kumasaka, T.; Hori, T.; Behnke, C. A.; Motoshima, H.; Fox, B. A.; Le Trong, I.; Teller, D. C.; Okada, T.; Stenkamp, R. E.; Yamamoto, M.; Miyano, M., Crystal structure of rhodopsin: A G protein-coupled receptor. *Science* **2000,** *289* (5480), 739-45.

3. Malherbe, P.; Roche, O.; Marcuz, A.; Kratzeisen, C.; Wettstein, J. G.; Bissantz, C., Mapping the binding pocket of dual antagonist almorexant to human orexin 1 and orexin 2 receptors: comparison with the selective OX1 antagonist SB-674042 and the selective OX2 antagonist N-ethyl-2-[(6-methoxy-pyridin-3-yl)-(toluene-2-sulfonyl)-amino]-N-pyridin-3-ylmethyl-acetamide (EMPA). *Mol Pharmacol* **2010,** *78* (1), 81-93.

4. Takai, T.; Takaya, T.; Nakano, M.; Akutsu, H.; Nakagawa, A.; Aimoto, S.; Nagai, K.; Ikegami, T., Orexin-A is composed of a highly conserved C-terminal and a specific, hydrophilic N-terminal region, revealing the structural basis of specific recognition by the orexin-1 receptor. *J Pept Sci* **2006,** *12* (7), 443-54.

5. Winrow, C. J.; Gotter, A. L.; Cox, C. D.; Tannenbaum, P. L.; Garson, S. L.; Doran, S. M.; Breslin, M. J.; Schreier, J. D.; Fox, S. V.; Harrell, C. M.; Stevens, J.; Reiss, D. R.; Cui, D.; Coleman, P. J.; Renger, J. J., Pharmacological characterization of MK-6096 - a dual orexin receptor antagonist for insomnia. *Neuropharmacology* **2012,** *62* (2), 978-87.

6. Tran, D. T.; Bonaventure, P.; Hack, M.; Mirzadegan, T.; Dvorak, C.; Letavic, M.; Carruthers, N.; Lovenberg, T.; Sutton, S. W., Chimeric, mutant orexin receptors show key interactions between orexin receptors, peptides and antagonists. *Eur J Pharmacol* **2011,** *667* (1-3), 120-8.

7. Yin, J.; Mobarec, J. C.; Kolb, P.; Rosenbaum, D. M., Crystal structure of the human OX2 orexin receptor bound to the insomnia drug suvorexant. *Nature* **2014**.

8. Sakurai, T.; Amemiya, A.; Ishii, M.; Matsuzaki, I.; Chemelli, R. M.; Tanaka, H.; Williams, S. C.; Richardson, J. A.; Kozlowski, G. P.; Wilson, S.; Arch, J. R.; Buckingham, R. E.; Haynes, A. C.; Carr, S. A.; Annan, R. S.; McNulty, D. E.; Liu, W. S.; Terrett, J. A.; Elshourbagy, N. A.; Bergsma, D. J.; Yanagisawa, M., Orexins

and orexin receptors: a family of hypothalamic neuropeptides and G protein-coupled receptors that regulate feeding behavior. *Cell* **1998,** *92* (4), 573-85.

9. Karhu, L.; Turku, A.; Xhaard, H., Modeling of the OX1R-orexin-A complex suggests two alternative binding modes. *BMC Struct Biol* **2015,** *15*, 9.

10. Scammell, T. E.; Winrow, C. J., Orexin receptors: pharmacology and therapeutic opportunities. *Annu Rev Pharmacol Toxicol* **2011,** *51*, 243-66.11. Peltonen, H. M.; Akerman, K. E.; Bart, G., A role for PKD1 and PKD3 activation in modulation of calcium oscillations induced by orexin receptor 1 stimulation. *Biochim Biophys Acta* **2010,** *1803* (10), 1206-12.

12. Wettschureck, N.; Offermanns, S., Mammalian G proteins and their cell type specific functions. *Physiol Rev* **2005,** *85* (4), 1159-204.

13. Jäntti, M. H.; Putula, J.; Somerharju, P.; Frohman, M. A.; Kukkonen, J. P., OX1 orexin/hypocretin receptor activation of phospholipase D. *Br J Pharmacol* **2012,** *165* (4b), 1109-23.

14. Magga, J.; Bart, G.; Oker-Blom, C.; Kukkonen, J. P.; Akerman, K. E.; Näsman, J., Agonist potency differentiates G protein activation and Ca2+ signalling by the orexin receptor type 1. *Biochem Pharmacol* **2006,** *71* (6), 827-36.

15. Milasta, S.; Evans, N. A.; Ormiston, L.; Wilson, S.; Lefkowitz, R. J.; Milligan, G., The sustainability of interactions between the orexin-1 receptor and beta-arrestin-2 is defined by a single C-terminal cluster of hydroxy amino acids and modulates the kinetics of ERK MAPK regulation. *Biochem J* **2005,** *387* (Pt 3), 573-84.

16. Dalrymple, M. B.; Jaeger, W. C.; Eidne, K. A.; Pfleger, K. D., Temporal profiling of orexin receptor-arrestin-ubiquitin complexes reveals differences between receptor subtypes. *J Biol Chem* **2011,** *286* (19), 16726-33.

17. Luttrell, L. M.; Lefkowitz, R. J., The role of beta-arrestins in the termination and transduction of G-protein-coupled receptor signals. *Journal of cell science* **2002,** *115* (Pt 3), 455-65.

18. Putula, J.; Turunen, P. M.; Jäntti, M. H.; Ekholm, M. E.; Kukkonen, J. P., Agonist ligand discrimination by the two orexin receptors depends on the expression system. *Neurosci Lett* **2011,** *494* (1), 57-60.

19. Xu, T. R.; Ward, R. J.; Pediani, J. D.; Milligan, G., The orexin OX(1) receptor exists predominantly as a homodimer in the basal state: potential regulation of receptor organization by both agonist and antagonist ligands. *Biochem J* **2011,** *439* (1), 171-83.

20. Ellis, J.; Pediani, J. D.; Canals, M.; Milasta, S.; Milligan, G., Orexin-1 receptor-cannabinoid CB1 receptor heterodimerization results in both ligand-dependent and -independent coordinated alterations of receptor localization and function. *J Biol Chem* **2006,** *281* (50), 38812-24.

21. Ward, R. J.; Pediani, J. D.; Milligan, G., Heteromultimerization of cannabinoid CB(1) receptor and orexin OX(1) receptor generates a unique complex in which both protomers are regulated by orexin A. *J Biol Chem* **2011,** *286* (43), 37414-28.

22. Darker, J. G.; Porter, R. A.; Eggleston, D. S.; Smart, D.; Brough, S. J.; Sabido-David, C.; Jerman, J. C., Structure-activity analysis of truncated orexin-A analogues at the orexin-1 receptor. *Bioorg Med Chem Lett* **2001,** *11* (5), 737-40.

23. Lang, M.; Söll, R. M.; Dürrenberger, F.; Dautzenberg, F. M.; Beck-Sickinger, A. G., Structure-activity studies of orexin a and orexin B at the human orexin 1 and orexin 2 receptors led to orexin 2 receptor selective and orexin 1 receptor preferring ligands. *J Med Chem* **2004,** *47* (5), 1153-60.

24. Heifetz, A.; Morris, G. B.; Biggin, P. C.; Barker, O.; Fryatt, T.; Bentley, J.; Hallett, D.; Manikowski, D.; Pal, S.; Reifegerste, R.; Slack, M.; Law, R., Study of human Orexin-1 and -2 G-protein-coupled receptors with novel and published antagonists by modeling, molecular dynamics simulations, and site-directed mutagenesis. *Biochemistry* **2012,** *51* (15), 3178-97.

25. Machaalani, R.; Hunt, N. J.; Waters, K. A., Effects of changes in energy homeostasis and exposure of noxious insults on the expression of orexin (hypocretin) and its receptors in the brain. *Brain Res* **2013,** *1526*, 102-22.

26. Dillingham, C. M.; Frizzati, A.; Nelson, A. J.; Vann, S. D., How do mammillary body inputs contribute to anterior thalamic function? *Neurosci Biobehav Rev* **2015,** *54*, 108-19.

27. Piccoli, L.; Micioni Di Bonaventura, M. V.; Cifani, C.; Costantini, V. J.; Massagrande, M.; Montanari, D.; Martinelli, P.; Antolini, M.; Ciccocioppo, R.; Massi, M.; Merlo-Pich, E.; Di Fabio, R.; Corsi, M., Role of orexin-1 receptor mechanisms on compulsive food consumption in a model of binge eating in female rats. *Neuropsychopharmacology* **2012,** *37* (9), 1999-2011.

28. Sharf, R.; Sarhan, M.; Brayton, C. E.; Guarnieri, D. J.; Taylor, J. R.; DiLeone, R. J., Orexin signaling via the orexin 1 receptor mediates operant responding for food reinforcement. *Biol Psychiatry* **2010,** *67* (8), 753-60.

29. Haynes, A. C.; Jackson, B.; Chapman, H.; Tadayyon, M.; Johns, A.; Porter, R. A.; Arch, J. R., A selective orexin-1 receptor antagonist reduces food consumption in male and female rats. *Regul Pept* **2000,** *96* (1-2), 45-51.

30. Paranjape, S.; Vavaiya, K.; Kale, A.; Briski, K., Role of dorsal vagal motor nucleus orexin-receptor-1 in glycemic responses to acute versus repeated insulin administration. *Neuropeptides* **2007,** *41* (2), 111-6.

31. Bülbül, M.; Babygirija, R.; Zheng, J.; Ludwig, K. A.; Takahashi, T., Central orexin-A changes the gastrointestinal motor pattern from interdigestive to postprandial in rats. *Auton Neurosci* **2010,** *158* (1-2), 24-30.

32. Mavanji, V.; Teske, J. A.; Billington, C. J.; Kotz, C. M., Elevated sleep quality and orexin receptor mRNA in obesity-resistant rats. *Int J Obes (Lond)* **2010,** *34* (11), 1576-88.

33. Liu, Z. B.; Song, N. N.; Geng, W. Y.; Jin, W. Z.; Li, L.; Cao, Y. X.; Qian, Y.; Zhu, D. N.; Shen, L. L., Orexin-A and respiration in a rat model of smoke-induced chronic obstructive pulmonary disease. *Clin Exp Pharmacol Physiol* **2010,** *37* (10), 963-8.

34. Kotz, C. M.; Wang, C.; Teske, J. A.; Thorpe, A. J.; Novak, C. M.; Kiwaki, K.; Levine, J. A., Orexin A mediation of time spent moving in rats: neural mechanisms. *Neuroscience* **2006,** *142* (1), 29-36.

35. Shin, Y. O.; Lee, J. B.; Min, Y. K.; Yang, H. M., Heat acclimation affects circulating levels of prostaglandin E2, COX-2 and orexin in humans. *Neurosci Lett* **2013,** *542*, 17-20.

36. Sikder, D.; Kodadek, T., The neurohormone orexin stimulates hypoxia-inducible factor-1 activity. *Genes Dev* **2007,** *21* (22), 2995-3005.

37. Abbott, M.; Volkoff, H., Thyrotropin Releasing Hormone (TRH) in goldfish (Carassius auratus): role in the regulation of feeding and locomotor behaviors and interactions with the orexin system and cocaine- and amphetamine regulated transcript (CART). *Horm Behav* **2011,** *59* (2), 236-45.

38. I'anson, H.; Jethwa, P. H.; Warner, A.; Ebling, F. J., Histaminergic regulation of seasonal metabolic rhythms in Siberian hamsters. *Physiol Behav* **2011,** *103* (3-4), 268-78.

39. Girault, E. M.; Foppen, E.; Ackermans, M. T.; Fliers, E.; Kalsbeek, A., Central administration of an orexin receptor 1 antagonist prevents the stimulatory effect of Olanzapine on endogenous glucose production. *Brain Res* **2013,** *1527*, 238-45.

40. Yamada, H.; Takahashi, N.; Tanno, S.; Nagamine, M.; Takakusaki, K.; Okumura, T., A selective orexin-1 receptor antagonist, SB334867, blocks 2-DG-induced gastric acid secretion in rats. *Neurosci Lett* **2005,** *376* (2), 137-42.

41. Matsuo, K.; Kaibara, M.; Uezono, Y.; Hayashi, H.; Taniyama, K.; Nakane, Y., Involvement of cholinergic neurons in orexin-induced contraction of guinea pig ileum. *Eur J Pharmacol* **2002,** *452* (1), 105-9.

42. Lu, X. Y.; Bagnol, D.; Burke, S.; Akil, H.; Watson, S. J., Differential distribution and regulation of OX1 and OX2 orexin/hypocretin receptor messenger RNA in the brain upon fasting. *Horm Behav* **2000,** *37* (4), 335-44.

43. Dall'aglio, C.; Zannoni, A.; Forni, M.; Bacci, M. L.; Ceccarelli, P.; Boiti, C., Orexin system expression in the gastrointestinal tract of pigs. *Res Vet Sci* **2013,** *95* (1), 8-14.

44. Samson, W. K.; Resch, Z. T., The hypocretin/orexin story. *Trends Endocrinol Metab* **2000,** *11* (7), 257-62.

45. Kermani, M.; Eliassi, A., Gastric acid secretion induced by paraventricular nucleus microinjection of orexin A is mediated through activation of neuropeptide Yergic system. *Neuroscience* **2012,** *226*, 81-8.

46. Liu, F.; Xu, G. Z.; Wang, L.; Jiang, S. X.; Yang, X. L.; Zhong, Y. M., Gene expression and protein distribution of orexins and orexin receptors in rat retina. *Neuroscience* **2011,** *189*, 146-55.

47. Malherbe, P.; Borroni, E.; Pinard, E.; Wettstein, J. G.; Knoflach, F., Biochemical and electrophysiological characterization of almorexant, a dual orexin 1 receptor (OX1)/orexin 2 receptor (OX2) antagonist: comparison with selective OX1 and OX2 antagonists. *Mol Pharmacol* **2009,** *76* (3), 618-31.

48. Cox, C. D.; Breslin, M. J.; Whitman, D. B.; Schreier, J. D.; McGaughey, G. B.; Bogusky, M. J.; Roecker, A. J.; Mercer, S. P.; Bednar, R. A.; Lemaire, W.; Bruno, J. G.; Reiss, D. R.; Harrell, C. M.; Murphy, K. L.; Garson, S. L.; Doran, S. M.; Prueksaritanont, T.; Anderson, W. B.; Tang, C.; Roller, S.; Cabalu, T. D.; Cui, D.; Hartman, G. D.; Young, S. D.; Koblan, K. S.; Winrow, C. J.; Renger, J. J.; Coleman, P. J., Discovery of the dual orexin receptor antagonist [(7R)-4-(5-chloro-1,3-benzoxazol-2-yl)-7-methyl-1,4-diazepan-1-yl][5-methyl-2-(2H-1,2,3-triazol-2-yl)phenyl]methanone (MK-4305) for the treatment of insomnia. *J Med Chem* **2010,** *53* (14), 5320-32.

49. Passarella, S.; Duong, M. T., Diagnosis and treatment of insomnia. *Am J Health Syst Pharm* **2008,** *65* (10), 927-34.

50. Daley, M.; Morin, C. M.; LeBlanc, M.; Grégoire, J. P.; Savard, J.; Baillargeon, L., Insomnia and its relationship to health-care utilization, work absenteeism, productivity and accidents. *Sleep Med* **2009,** *10* (4), 427-38.

51. Sullivan, S. S.; Guilleminault, C., Emerging drugs for insomnia: new frontiers for old and novel targets. *Expert Opin Emerg Drugs* **2009,** *14* (3), 411-22.

52. Renger, J. J., Overview of experimental and conventional pharmacological approaches in the treatment of sleep and wake disorders. *Curr Top Med Chem* **2008,** *8* (11), 937-53.

53. Kalogiannis, M.; Grupke, S. L.; Potter, P. E.; Edwards, J. G.; Chemelli, R. M.; Kisanuki, Y. Y.; Yanagisawa, M.; Leonard, C. S., Narcoleptic orexin receptor knockout mice express enhanced cholinergic properties in laterodorsal tegmental neurons. *Eur J Neurosci* **2010,** *32* (1), 130-42.

54. Kalogiannis, M.; Hsu, E.; Willie, J. T.; Chemelli, R. M.; Kisanuki, Y. Y.; Yanagisawa, M.; Leonard, C. S., Cholinergic modulation of narcoleptic attacks in double orexin receptor knockout mice. *PLoS One* **2011,** *6* (4), e18697.

55. Sakurai, T., Orexin deficiency and narcolepsy. *Curr Opin Neurobiol* **2013,** *23* (5), 760-6.

56. Smith, M. I.; Piper, D. C.; Duxon, M. S.; Upton, N., Evidence implicating a role for orexin-1 receptor modulation of paradoxical sleep in the rat. *Neurosci Lett* **2003,** *341* (3), 256-8.

57. Dong, X. S.; Ma, S. F.; Cao, C. W.; Li, J.; An, P.; Zhao, L.; Liu, N. Y.; Yan, H.; Hu, Q. T.; Mignot, E.; Strohl, K. P.; Gao, Z. C.; Zeng, C.; Han, F., Hypocretin (orexin) neuropeptide precursor gene, HCRT, polymorphisms in early-onset narcolepsy with cataplexy. *Sleep Med* **2013,** *14* (6), 482-7.

58. Wang, W.; Pan, Y.; Li, Q.; Wang, L., Orexin: a potential role in the process of obstructive sleep apnea. *Peptides* **2013,** *42*, 48-54.

59. Di Fabio, R.; Pellacani, A.; Faedo, S.; Roth, A.; Piccoli, L.; Gerrard, P.; Porter, R. A.; Johnson, C. N.; Thewlis, K.; Donati, D.; Stasi, L.; Spada, S.; Stemp, G.; Nash, D.; Branch, C.; Kindon, L.; Massagrande, M.; Poffe, A.; Braggio, S.; Chiarparin, E.; Marchioro, C.; Ratti, E.; Corsi, M., Discovery process and pharmacological characterization of a novel dual orexin 1 and orexin 2 receptor antagonist useful for treatment of sleep disorders. *Bioorg Med Chem Lett* **2011,** *21* (18), 5562-7.

60. Hoch, M.; Hay, J. L.; Hoever, P.; de Kam, M. L.; te Beek, E. T.; van Gerven, J. M.; Dingemanse, J., Dual orexin receptor antagonism by almorexant does not potentiate impairing effects of alcohol in humans. *Eur Neuropsychopharmacol* **2013,** *23* (2), 107-17.

61. Dietrich, H.; Jenck, F., Intact learning and memory in rats following treatment with the dual orexin receptor antagonist almorexant. *Psychopharmacology (Berl)* **2010,** *212* (2), 145-54.

62. Winrow, C. J.; Tanis, K. Q.; Reiss, D. R.; Rigby, A. M.; Uslaner, J. M.; Uebele, V. N.; Doran, S. M.; Fox, S. V.; Garson, S. L.; Gotter, A. L.; Levine, D. M.; Roecker, A. J.; Coleman, P. J.; Koblan, K. S.; Renger, J. J., Orexin receptor antagonism prevents transcriptional and behavioral plasticity resulting from stimulant exposure. *Neuropharmacology* **2010,** *58* (1), 185-94.

63. Akbari, E.; Motamedi, F.; Naghdi, N.; Noorbakhshnia, M., The effect of antagonization of orexin 1 receptors in CA1 and dentate gyrus regions on memory processing in passive avoidance task. *Behav Brain Res* **2008,** *187* (1), 172-7.

64. Dhaher, R.; Hauser, S. R.; Getachew, B.; Bell, R. L.; McBride, W. J.; McKinzie, D. L.; Rodd, Z. A., The Orexin-1 Receptor Antagonist SB-334867 Reduces Alcohol Relapse Drinking, but not Alcohol-Seeking, in Alcohol-Preferring (P) Rats. *J Addict Med* **2010,** *4* (3), 153-9.

65. Adidharma, W.; Leach, G.; Yan, L., Orexinergic signaling mediates light-induced neuronal activation in the dorsal raphe nucleus. *Neuroscience* **2012,** *220*, 201-7.

66. Morgan, A. J.; Harrod, S. B.; Lacy, R. T.; Stanley, E. M.; Fadel, J. R., Intravenous prenatal nicotine exposure increases orexin expression in the lateral hypothalamus and orexin innervation of the ventral tegmental area in adult male rats. *Drug Alcohol Depend* **2013,** *132* (3), 562-70.

67. Jupp, B.; Krstew, E.; Dezsi, G.; Lawrence, A. J., Discrete cue-conditioned alcohol-seeking after protracted abstinence: pattern of neural activation and involvement of orexin$_1$ receptors. *Br J Pharmacol* **2011,** *162* (4), 880-9.

68. Moorman, D. E.; Aston-Jones, G., Orexin-1 receptor antagonism decreases ethanol consumption and preference selectively in high-ethanol--preferring Sprague--Dawley rats. *Alcohol* **2009,** *43* (5), 379-86.

69. Azizi, H.; Mirnajafi-Zadeh, J.; Rohampour, K.; Semnanian, S., Antagonism of orexin type 1 receptors in the locus coeruleus attenuates signs of naloxone-precipitated morphine withdrawal in rats. *Neurosci Lett* **2010,** *482* (3), 255-9.

70. Jäntti, M. H.; Putula, J.; Turunen, P. M.; Näsman, J.; Reijonen, S.; Lindqvist, C.; Kukkonen, J. P., Autocrine endocannabinoid signaling through CB1 receptors potentiates OX1 orexin receptor signaling. *Mol Pharmacol* **2013,** *83* (3), 621-32.

71. Roberts, D. C.; Gabriele, A.; Zimmer, B. A., Conflation of cocaine seeking and cocaine taking responses in IV self-administration experiments in rats:

methodological and interpretational considerations. *Neurosci Biobehav Rev* **2013,** *37* (9 Pt A), 2026-36.

72. Aston-Jones, G.; Smith, R. J.; Moorman, D. E.; Richardson, K. A., Role of lateral hypothalamic orexin neurons in reward processing and addiction. *Neuropharmacology* **2009,** *56 Suppl 1*, 112-21.

73. Aston-Jones, G.; Smith, R. J.; Sartor, G. C.; Moorman, D. E.; Massi, L.; Tahsili-Fahadan, P.; Richardson, K. A., Lateral hypothalamic orexin/hypocretin neurons: A role in reward-seeking and addiction. *Brain Res* **2010,** *1314*, 74-90.

74. Akbari, E.; Motamedi, F.; Davoodi, F. G.; Noorbakhshnia, M.; Ghanbarian, E., Orexin-1 receptor mediates long-term potentiation in the dentate gyrus area of freely moving rats. *Behav Brain Res* **2011,** *216* (1), 375-80.

75. Quarta, D.; Valerio, E.; Hutcheson, D. M.; Hedou, G.; Heidbreder, C., The orexin-1 receptor antagonist SB-334867 reduces amphetamine-evoked dopamine outflow in the shell of the nucleus accumbens and decreases the expression of amphetamine sensitization. *Neurochem Int* **2010,** *56* (1), 11-5.

76. Scott, M. M.; Marcus, J. N.; Pettersen, A.; Birnbaum, S. G.; Mochizuki, T.; Scammell, T. E.; Nestler, E. J.; Elmquist, J. K.; Lutter, M., Hcrtr1 and 2 signaling differentially regulates depression-like behaviors. *Behav Brain Res* **2011,** *222* (2), 289-94.

77. Zhou, L.; Smith, R. J.; Do, P. H.; Aston-Jones, G.; See, R. E., Repeated orexin 1 receptor antagonism effects on cocaine seeking in rats. *Neuropharmacology* **2012,** *63* (7), 1201-7.

78. Erami, E.; Azhdari-Zarmehri, H.; Rahmani, A.; Ghasemi-Dashkhasan, E.; Semnanian, S.; Haghparast, A., Blockade of orexin receptor 1 attenuates the development of morphine tolerance and physical dependence in rats. *Pharmacol Biochem Behav* **2012,** *103* (2), 212-9.

79. Rusyniak, D. E.; Zaretsky, D. V.; Zaretskaia, M. V.; Durant, P. J.; DiMicco, J. A., The orexin-1 receptor antagonist SB-334867 decreases sympathetic responses to a moderate dose of methamphetamine and stress. *Physiol Behav* **2012,** *107* (5), 743-50.

80. Johnson, P. L.; Samuels, B. C.; Fitz, S. D.; Federici, L. M.; Hammes, N.; Early, M. C.; Truitt, W.; Lowry, C. A.; Shekhar, A., Orexin 1 receptors are a novel target to modulate panic responses and the panic brain network. *Physiol Behav* **2012,** *107* (5), 733-42.

81. Zhang, W.; Shimoyama, M.; Fukuda, Y.; Kuwaki, T., Multiple components of the defense response depend on orexin: evidence from orexin knockout mice and orexin neuron-ablated mice. *Auton Neurosci* **2006,** *126-127*, 139-45.

82. Frederick-Duus, D.; Guyton, M. F.; Fadel, J., Food-elicited increases in cortical acetylcholine release require orexin transmission. *Neuroscience* **2007,** *149* (3), 499-507.

83. Kawada, Y.; Ueno, S.; Asayama, K.; Tsutsui, M.; Utsunomiya, K.; Toyohira, Y.; Morisada, N.; Tanaka, K.; Shirahata, A.; Yanagihara, N., Stimulation of catecholamine synthesis by orexin-A in bovine adrenal medullary cells through orexin receptor 1. *Biochem Pharmacol* **2003,** *66* (1), 141-7.

84. Johnson, P. L.; Truitt, W.; Fitz, S. D.; Minick, P. E.; Dietrich, A.; Sanghani, S.; Träskman-Bendz, L.; Goddard, A. W.; Brundin, L.; Shekhar, A., A key role for orexin in panic anxiety. *Nat Med* **2010,** *16* (1), 111-5.

85. McCorry, L. K., Physiology of the autonomic nervous system. *American journal of pharmaceutical education* **2007,** *71* (4), 78.

86. Tafuri, S.; Pavone, L. M.; Lo Muto, R.; Basile, M.; Langella, E.; Fiorillo, E.; Avallone, L.; Staiano, N.; Vittoria, A., Expression of orexin A and its receptor 1 in the rat epididymis. *Regul Pept* **2009,** *155* (1-3), 1-5.

87. Russo, F.; Maruccio, L.; Calamo, A.; de Girolamo, P.; Varricchio, E., Orexin 1 receptor in the seminiferous tubules of boar testis: An immunohistochemical study. *Acta Histochem* **2013**.

88. Liguori, G.; Assisi, L.; Squillacioti, C.; Paino, S.; Mirabella, N.; Vittoria, A., Presence, distribution and steroidogenic effect of the peptides orexin A and receptor 1 for orexins in the testis of the South American camelid alpaca (Vicugna pacos). *Gen Comp Endocrinol* **2012,** *179* (1), 137-42.

89. Argiolas, A.; Melis, M. R., Neuropeptides and central control of sexual behaviour from the past to the present: a review. *Prog Neurobiol* **2013,** *108*, 80-107.

90. Di Sebastiano, A. R.; Yong-Yow, S.; Wagner, L.; Lehman, M. N.; Coolen, L. M., Orexin mediates initiation of sexual behavior in sexually naive male rats, but is not critical for sexual performance. *Horm Behav* **2010,** *58* (3), 397-404.

91. Turunen, P. M.; Ekholm, M. E.; Somerharju, P.; Kukkonen, J. P., Arachidonic acid release mediated by OX1 orexin receptors. *Br J Pharmacol* **2010,** *159*, 212-21.

92. Fronczek, R.; Overeem, S.; Lee, S. Y.; Hegeman, I. M.; van Pelt, J.; van Duinen, S. G.; Lammers, G. J.; Swaab, D. F., Hypocretin (orexin) loss in Parkinson's disease. *Brain* **2007,** *130* (Pt 6), 1577-85.

93. Fronczek, R.; Overeem, S.; Lee, S. Y.; Hegeman, I. M.; van Pelt, J.; van Duinen, S. G.; Lammers, G. J.; Swaab, D. F., Hypocretin (orexin) loss and sleep disturbances in Parkinson's Disease. *Brain* **2008,** *131* (Pt 1), e88.

94. Tafuri, S.; Pavone, L. M.; Mastellone, V.; Spina, A.; Avallone, L.; Vittoria, A.; Staiano, N.; Scala, G., Expression of orexin A and its receptor 1 in the choroid plexuses from buffalo brain. *Neuropeptides* **2009,** *43* (2), 73-80.

95. Dohi, K.; Nishino, S.; Nakamachi, T.; Ohtaki, H.; Morikawa, K.; Takeda, T.; Shioda, S.; Aruga, T., CSF orexin A concentrations and expressions of the orexin-1 receptor in rat hippocampus after cardiac arrest. *Neuropeptides* **2006,** *40* (4), 245-50.

96. Nakamachi, T.; Endo, S.; Ohtaki, H.; Yin, L.; Kenji, D.; Kudo, Y.; Funahashi, H.; Matsuda, K.; Shioda, S., Orexin-1 receptor expression after global ischemia in mice. *Regul Pept* **2005,** *126* (1-2), 49-54.

97. Mihara, Y.; Dohi, K.; Yofu, S.; Nakamachi, T.; Ohtaki, H.; Shioda, S.; Aruga, T., Expression and localization of the orexin-1 receptor (OX1R) after traumatic brain injury in mice. *J Mol Neurosci* **2011,** *43* (2), 162-8.

98. Rodgers, R. J.; Wright, F. L.; Snow, N. F.; Taylor, L. J., Orexin-1 receptor antagonism fails to reduce anxiety-like behaviour in either plus-maze-naïve or plus-maze-experienced mice. *Behav Brain Res* **2013,** *243*, 213-9.

99. Chen, H.; Yang, L.; Chen, F.; Yan, J.; Yang, N.; Wang, Y. J.; Zhu, Z. R.; Hu, Z. A.; Sui, J. F.; Hu, B., Functional inactivation of orexin 1 receptors in the cerebellum disrupts trace eyeblink conditioning and local theta oscillations in guinea pigs. *Behav Brain Res* **2013,** *250*, 114-22.

100. Akbari, E.; Naghdi, N.; Motamedi, F., Functional inactivation of orexin 1 receptors in CA1 region impairs acquisition, consolidation and retrieval in Morris water maze task. *Behav Brain Res* **2006,** *173* (1), 47-52.

101. Akbari, E.; Naghdi, N.; Motamedi, F., The selective orexin 1 receptor antagonist SB-334867-A impairs acquisition and consolidation but not retrieval of spatial memory in Morris water maze. *Peptides* **2007,** *28* (3), 650-6.

102. Steiner, M. A.; Sciarretta, C.; Brisbare-Roch, C.; Strasser, D. S.; Studer, R.; Jenck, F., Examining the role of endogenous orexins in hypothalamus-pituitary-adrenal

axis endocrine function using transient dual orexin receptor antagonism in the rat. *Psychoneuroendocrinology* **2013,** *38* (4), 560-71.

103. Huang, S. C.; Dai, Y. W.; Lee, Y. H.; Chiou, L. C.; Hwang, L. L., Orexins depolarize rostral ventrolateral medulla neurons and increase arterial pressure and heart rate in rats mainly via orexin 2 receptors. *J Pharmacol Exp Ther* **2010,** *334* (2), 522-9.

104. Shahid, I. Z.; Rahman, A. A.; Pilowsky, P. M., Intrathecal orexin A increases sympathetic outflow and respiratory drive, enhances baroreflex sensitivity and blocks the somato-sympathetic reflex. *Br J Pharmacol* **2011,** *162* (4), 961-73.

105. Zhan, S.; Cai, G. Q.; Zheng, A.; Wang, Y.; Jia, J.; Fang, H.; Yang, Y.; Hu, M.; Ding, Q., Tumor necrosis factor-alpha regulates the Hypocretin system via mRNA degradation and ubiquitination. *Biochim Biophys Acta* **2011,** *1812* (4), 565-71.

106. Mendoza, J.; Lopez-Lopez, C.; Revel, F. G.; Jeanneau, K.; Delerue, F.; Prinssen, E.; Challet, E.; Moreau, J. L.; Grundschober, C., Dimorphic effects of leptin on the circadian and hypocretinergic systems of mice. *J Neuroendocrinol* **2011,** *23* (1), 28-38.

107. Xiao, F.; Jiang, M.; Du, D.; Xia, C.; Wang, J.; Cao, Y.; Shen, L.; Zhu, D., Orexin A regulates cardiovascular responses in stress-induced hypertensive rats. *Neuropharmacology* **2013,** *67*, 16-24.

108. Kuwaki, T.; Li, A.; Nattie, E., State-dependent central chemoreception: a role of orexin. *Respir Physiol Neurobiol* **2010,** *173* (3), 223-9.

109. Li, A.; Nattie, E., Antagonism of rat orexin receptors by almorexant attenuates central chemoreception in wakefulness in the active period of the diurnal cycle. *J Physiol* **2010,** *588* (Pt 15), 2935-44.

110. Dias, M. B.; Li, A.; Nattie, E., The orexin receptor 1 (OX1R) in the rostral medullary raphe contributes to the hypercapnic chemoreflex in wakefulness, during the active period of the diurnal cycle. *Respir Physiol Neurobiol* **2010,** *170* (1), 96-102.

111. Butterick, T. A.; Nixon, J. P.; Billington, C. J.; Kotz, C. M., Orexin A decreases lipid peroxidation and apoptosis in a novel hypothalamic cell model. *Neurosci Lett* **2012,** *524* (1), 30-4.

112. Azhdari Zarmehri, H.; Semnanian, S.; Fathollahi, Y.; Erami, E.; Khakpay, R.; Azizi, H.; Rohampour, K., Intra-periaqueductal gray matter microinjection of orexin-A decreases formalin-induced nociceptive behaviors in adult male rats. *J Pain* **2011,** *12* (2), 280-7.

113. Watson, S. L.; Watson, C. J.; Baghdoyan, H. A.; Lydic, R., Thermal nociception is decreased by hypocretin-1 and an adenosine A1 receptor agonist microinjected into the pontine reticular formation of Sprague Dawley rat. *J Pain* **2010,** *11* (6), 535-44.

114. Yamamoto, T.; Saito, O.; Shono, K.; Hirasawa, S., Activation of spinal orexin-1 receptor produces anti-allodynic effect in the rat carrageenan test. *Eur J Pharmacol* **2003,** *481* (2-3), 175-80.

115. Jeong, Y.; Holden, J. E., The role of spinal orexin-1 receptors in posterior hypothalamic modulation of neuropathic pain. *Neuroscience* **2009,** *159* (4), 1414-21.

116. Kajiyama, S.; Kawamoto, M.; Shiraishi, S.; Gaus, S.; Matsunaga, A.; Suyama, H.; Yuge, O., Spinal orexin-1 receptors mediate anti-hyperalgesic effects of intrathecally-administered orexins in diabetic neuropathic pain model rats. *Brain Res* **2005,** *1044* (1), 76-86.

117. Ranjbar-Slamloo, Y.; Azizi, H.; Fathollahi, Y.; Semnanian, S., Orexin receptor type-1 antagonist SB-334867 inhibits the development of morphine analgesic tolerance in rats. *Peptides* **2012,** *35* (1), 56-9.

118. Heidari-Oranjaghi, N.; Azhdari-Zarmehri, H.; Erami, E.; Haghparast, A., Antagonism of orexin-1 receptors attenuates swim- and restraint stress-induced antinociceptive behaviors in formalin test. *Pharmacol Biochem Behav* **2012,** *103* (2), 299-307.

119. Sadeghi, S.; Reisi, Z.; Azhdari-Zarmehri, H.; Haghparast, A., Involvement of orexin-1 receptors in the ventral tegmental area and the nucleus accumbens in antinociception induced by lateral hypothalamus stimulation in rats. *Pharmacol Biochem Behav* **2013,** *105*, 193-8.

120. Dugovic, C.; Shelton, J. E.; Aluisio, L. E.; Fraser, I. C.; Jiang, X.; Sutton, S. W.; Bonaventure, P.; Yun, S.; Li, X.; Lord, B.; Dvorak, C. A.; Carruthers, N. I.; Lovenberg, T. W., Blockade of orexin-1 receptors attenuates orexin-2 receptor antagonism-induced sleep promotion in the rat. *J Pharmacol Exp Ther* **2009,** *330* (1), 142-51.

121. Mochizuki, T.; Arrigoni, E.; Marcus, J. N.; Clark, E. L.; Yamamoto, M.; Honer, M.; Borroni, E.; Lowell, B. B.; Elmquist, J. K.; Scammell, T. E., Orexin receptor 2 expression in the posterior hypothalamus rescues sleepiness in narcoleptic mice. *Proc Natl Acad Sci U S A* **2011,** *108* (11), 4471-6.

122. Yu, L.; Zhang, X. Y.; Zhang, J.; Zhu, J. N.; Wang, J. J., Orexins excite neurons of the rat cerebellar nucleus interpositus via orexin 2 receptors in vitro. *Cerebellum* **2010,** *9* (1), 88-95.

123. Ballesteros, J. A.; Weinstein, H., Integrated methods for the construction of three-dimensional models and computational probing of structure-function relations in G protein-coupled receptors. In *Methods in Neurosciences*, 1995; Vol. 25, pp 366-428.

124. Shi, L.; Liapakis, G.; Xu, R.; Guarnieri, F.; Ballesteros, J. A.; Javitch, J. A., Beta2 adrenergic receptor activation. Modulation of the proline kink in transmembrane 6 by a rotamer toggle switch. *J Biol Chem* **2002,** *277* (43), 40989-96.

125. Farrens, D. L.; Altenbach, C.; Yang, K.; Hubbell, W. L.; Khorana, H. G., Requirement of rigid-body motion of transmembrane helices for light activation of rhodopsin. *Science* **1996,** *274* (5288), 768-70.

126. Ghanouni, P.; Steenhuis, J. J.; Farrens, D. L.; Kobilka, B. K., Agonist-induced conformational changes in the G-protein-coupling domain of the beta 2 adrenergic receptor. *Proc Natl Acad Sci U S A* **2001,** *98* (11), 5997-6002.

127. Javitch, J. A.; Fu, D.; Liapakis, G.; Chen, J., Constitutive activation of the beta2 adrenergic receptor alters the orientation of its sixth membrane-spanning segment. *J Biol Chem* **1997,** *272* (30), 18546-9.

128. Jensen, A. D.; Guarnieri, F.; Rasmussen, S. G.; Asmar, F.; Ballesteros, J. A.; Gether, U., Agonist-induced conformational changes at the cytoplasmic side of transmembrane segment 6 in the beta 2 adrenergic receptor mapped by site-selective fluorescent labeling. *J Biol Chem* **2001,** *276* (12), 9279-90.

129. Lin, S. W.; Sakmar, T. P., Specific tryptophan UV-absorbance changes are probes of the transition of rhodopsin to its active state. *Biochemistry* **1996,** *35* (34), 11149-59.

130. Nakanishi, J.; Takarada, T.; Yunoki, S.; Kikuchi, Y.; Maeda, M., FRET-based monitoring of conformational change of the beta2 adrenergic receptor in living cells. *Biochem Biophys Res Commun* **2006,** *343* (4), 1191-6.

131. Putula, J.; Turunen, P. M.; Johansson, L.; Näsman, J.; Ra, R.; Korhonen, L.; Kukkonen, J. P., Orexin/hypocretin receptor chimaeras reveal structural features important for orexin peptide distinction. *FEBS Lett* **2011,** *585* (9), 1368-74.

132. Putula, J.; Kukkonen, J. P., Mapping of the binding sites for the OX1 orexin receptor antagonist, SB-334867, using orexin/hypocretin receptor chimaeras. *Neurosci Lett* **2012,** *506* (1), 111-5.

133. Whitnell, R. M.; Hurst, D. P.; Reggio, P. H.; Guarnieri, F., Conformational memories with variable bond angles. *J Comput Chem* **2008,** *29* (5), 741-52.

134. Fiser, A.; Do, R. K.; Sali, A., Modeling of loops in protein structures. *Protein Sci* **2000,** *9* (9), 1753-73.

135. Martí-Renom, M. A.; Stuart, A. C.; Fiser, A.; Sánchez, R.; Melo, F.; Sali, A., Comparative protein structure modeling of genes and genomes. *Annu Rev Biophys Biomol Struct* **2000,** *29*, 291-325.

136. Sali, A.; Blundell, T. L., Comparative protein modelling by satisfaction of spatial restraints. *J Mol Biol* **1993,** *234* (3), 779-815.

137. Langmead, C. J.; Jerman, J. C.; Brough, S. J.; Scott, C.; Porter, R. A.; Herdon, H. J., Characterisation of the binding of [3H]-SB-674042, a novel nonpeptide antagonist, to the human orexin-1 receptor. *Br J Pharmacol* **2004,** *141* (2), 340-6.

138. Goncalves, J. A.; South, K.; Ahuja, S.; Zaitseva, E.; Opefi, C. A.; Eilers, M.; Vogel, R.; Reeves, P. J.; Smith, S. O., Highly conserved tyrosine stabilizes the active state of rhodopsin. *Proc Natl Acad Sci U S A* **2010,** *107*, 19861-6.

139. Vondrásek, J.; Mason, P. E.; Heyda, J.; Collins, K. D.; Jungwirth, P., The molecular origin of like-charge arginine-arginine pairing in water. *J Phys Chem B* **2009,** *113* (27), 9041-5.

140. Manglik, A.; Kruse, A. C.; Kobilka, T. S.; Thian, F. S.; Mathiesen, J. M.; Sunahara, R. K.; Pardo, L.; Weis, W. I.; Kobilka, B. K.; Granier, S., Crystal structure of the μ-opioid receptor bound to a morphinan antagonist. *Nature* **2012,** *485* (7398), 321-6.

141. Zhang, K.; Zhang, J.; Gao, Z. G.; Zhang, D.; Zhu, L.; Han, G. W.; Moss, S. M.; Paoletta, S.; Kiselev, E.; Lu, W.; Fenalti, G.; Zhang, W.; Muller, C. E.; Yang, H.; Jiang, H.; Cherezov, V.; Katritch, V.; Jacobson, K. A.; Stevens, R. C.; Wu, B.; Zhao, Q., Structure of the human P2Y12 receptor in complex with an antithrombotic drug. *Nature* **2014,** *509* (7498), 115-8.

142. Lee, S.; Bhattacharya, S.; Tate, C. G.; Grisshammer, R.; Vaidehi, N., Structural dynamics and thermostabilization of neurotensin receptor 1. *J Phys Chem B* **2015,** *119* (15), 4917-28.

143. Ballesteros, J. A.; Jensen, A. D.; Liapakis, G.; Rasmussen, S. G.; Shi, L.; Gether, U.; Javitch, J. A., Activation of the beta 2-adrenergic receptor involves disruption of an ionic lock between the cytoplasmic ends of transmembrane segments 3 and 6. *J Biol Chem* **2001,** *276* (31), 29171-7.

144. Rasmussen, S. G.; Choi, H. J.; Rosenbaum, D. M.; Kobilka, T. S.; Thian, F. S.; Edwards, P. C.; Burghammer, M.; Ratnala, V. R.; Sanishvili, R.; Fischetti, R. F.; Schertler, G. F.; Weis, W. I.; Kobilka, B. K., Crystal structure of the human beta2 adrenergic G-protein-coupled receptor. *Nature* **2007,** *450* (7168), 383-7.

145. Cherezov, V.; Rosenbaum, D. M.; Hanson, M. A.; Rasmussen, S. G.; Thian, F. S.; Kobilka, T. S.; Choi, H. J.; Kuhn, P.; Weis, W. I.; Kobilka, B. K.; Stevens, R. C., High-resolution crystal structure of an engineered human beta2-adrenergic G protein-coupled receptor. *Science* **2007,** *318* (5854), 1258-65.

146. Jaakola, V. P.; Griffith, M. T.; Hanson, M. A.; Cherezov, V.; Chien, E. Y.; Lane, J. R.; Ijzerman, A. P.; Stevens, R. C., The 2.6 angstrom crystal structure of a human A2A adenosine receptor bound to an antagonist. *Science* **2008,** *322* (5905), 1211-7.

147. Konvicka, K.; Guarnieri, F.; Ballesteros, J. A.; Weinstein, H., A proposed structure for transmembrane segment 7 of G protein-coupled receptors incorporating an asn-Pro/Asp-Pro motif. *Biophys J* **1998,** *75* (2), 601-11.

148. Ballesteros, J. A.; Deupi, X.; Olivella, M.; Haaksma, E. E.; Pardo, L., Serine and threonine residues bend alpha-helices in the chi(1) = g(-) conformation. *Biophys J* **2000,** *79* (5), 2754-60.

149. Visiers, I.; Braunheim, B. B.; Weinstein, H., Prokink: a protocol for numerical evaluation of helix distortions by proline. *Protein Eng* **2000,** *13* (9), 603-6.

150. Warne, T.; Serrano-Vega, M. J.; Baker, J. G.; Moukhametzianov, R.; Edwards, P. C.; Henderson, R.; Leslie, A. G.; Tate, C. G.; Schertler, G. F., Structure of a beta1-adrenergic G-protein-coupled receptor. *Nature* **2008,** *454* (7203), 486-91.

151. Wu, B.; Chien, E. Y.; Mol, C. D.; Fenalti, G.; Liu, W.; Katritch, V.; Abagyan, R.; Brooun, A.; Wells, P.; Bi, F. C.; Hamel, D. J.; Kuhn, P.; Handel, T. M.; Cherezov, V.; Stevens, R. C., Structures of the CXCR4 chemokine GPCR with small-molecule and cyclic peptide antagonists. *Science* **2010,** *330* (6007), 1066-71.

152. Chien, E. Y.; Liu, W.; Zhao, Q.; Katritch, V.; Han, G. W.; Hanson, M. A.; Shi, L.; Newman, A. H.; Javitch, J. A.; Cherezov, V.; Stevens, R. C., Structure of the human dopamine D3 receptor in complex with a D2/D3 selective antagonist. *Science* **2010,** *330* (6007), 1091-5.

153. Li, J.; Edwards, P. C.; Burghammer, M.; Villa, C.; Schertler, G. F., Structure of bovine rhodopsin in a trigonal crystal form. *J Mol Biol* **2004,** *343* (5), 1409-38.

154. Okada, T.; Fujiyoshi, Y.; Silow, M.; Navarro, J.; Landau, E. M.; Shichida, Y., Functional role of internal water molecules in rhodopsin revealed by X-ray crystallography. *Proc Natl Acad Sci U S A* **2002,** *99* (9), 5982-7.

155. Heifetz, A.; Barker, O.; Morris, G. B.; Law, R. J.; Slack, M.; Biggin, P. C., Toward an understanding of agonist binding to human Orexin-1 and Orexin-2 receptors with G-protein-coupled receptor modeling and site-directed mutagenesis. *Biochemistry* **2013,** *52* (46), 8246-60.

156. Oku, S.; Takahashi, N.; Fukata, Y.; Fukata, M., In silico screening for palmitoyl substrates reveals a role for DHHC1/3/10 (zDHHC1/3/11)-mediated neurochondrin palmitoylation in its targeting to Rab5-positive endosomes. *J Biol Chem* **2013,** *288* (27), 19816-29.

157. Lomize, M. A.; Lomize, A. L.; Pogozheva, I. D.; Mosberg, H. I., OPM: orientations of proteins in membranes database. *Bioinformatics* **2006,** *22* (5), 623-5.

158. Iliff, H. A.; Lynch, D. L.; Kotsikorou, E.; Reggio, P. H., Parameterization of Org27569: An Allosteric Modulator of the Cannabinoid CB1 G-Protein Coupled Receptor. *J Comput Chem* **2011,** *32* (10), 2119-2126.

159. MacKerell, A. D. J.; Bashford, D.; Bellot, M.; Dunbrack, R. L. J.; Evanseck, J. D.; Field, M. J.; Fischer, S.; Gao, J.; Guo, H.; Ha, S.; Joseph-McCarthy, D.; Kuchnir, L.; Kuczera, K.; Lau, F. T. K.; Mattos, C.; Michnick, S.; Ngo, T.; Nguyen, D. T.; Prodhom, B.; Reiher, W. E. I.; Roux, B.; Schlenkrich, M.; Smith, J. C.; Stote, R.; Straub, J.; Watanabe, M.; Wiorkiewicz-Kuczera, J.; Yin, D.; Karplus, M., All-Atom Empirical Potential for Molecular Modeling and Dynamics Studies of Proteins. *J Phys Chem B* **1998,** *102*, 3586-3616.

160. MacKerell, A. D. J., *Computational Biochemistry and Biophysics*. Marcel Dekker: New York, 2001.

161. Vanommeslaeghe, K.; Hatcher, E.; Acharya, C.; Kundu, S.; Zhong, S.; Shim, J.; Darian, E.; Guvench, O.; Lopes, P.; Vorobyov, I.; MacKerell, A. D. J., CHARMM general force field: A force field for drug-like molecules compatible with the CHARMM all-atom additive biological force fields. *J Comput Chem* **2010,** *31*, 671-90.

162. Yu, W.; He, X.; Vanommeslaeghe, K.; MacKerell, A. D., Jr., Extension of the CHARMM General Force Field to sulfonyl-containing compounds and its utility in biomolecular simulations. *J Comput Chem* **2012,** *33* (31), 2451-68.

163. Vanommeslaeghe, K.; MacKerell, A. D., Jr., Automation of the CHARMM General Force Field (CGenFF) I: bond perception and atom typing. *Journal of chemical information and modeling* **2012,** *52* (12), 3144-54.

164. Vanommeslaeghe, K.; Raman, E. P.; MacKerell, A. D., Jr., Automation of the CHARMM General Force Field (CGenFF) II: assignment of bonded parameters and partial atomic charges. *Journal of chemical information and modeling* **2012,** *52* (12), 3155-68.

165. Amaro, R.; Dhaliwal, B.; Luthey-Schulten, Z., Parameterizing a Novel Residue. In *http://www.ks.uiuc.edu/Training/Tutorials/science/forcefield-tutorial/forcefield.pdf*,

University of Illinois at Urbana-Champaign Luthey-Schulten Group, D. o. C. T. a. C. B. G., Ed. 2007; pp 1-37.

166. MacKerell, A. D. J., CHARMM force fields, parameterization strategies and future/ongoing force field developments. In *https://mmtsb.org/workshops/mmtsb-ctbp_2006/Lecture_pdf/params_alex_jul06a.pdf*, University of Maryland, B. S. o. P. M. C., Ed. 2006; pp 1-70.

167. MacKerell, A. D. J., The CHARMM Force FIeld. In *http://www.cecam.org/upload/files/file_1187.pdf*, University of Maryland, B. S. o. P., Ed. University College Dublin, Ireland, 2012; pp 1-124.

168. Guvench, O.; MacKerell, A. D. J., Automated conformational energy fitting for force-field development. *J Mol Model* **2008,** *14*, 667-79.

169. Hanson, M. A.; Roth, C. B.; Jo, E.; Griffith, M. T.; Scott, F. L.; Reinhart, G.; Desale, H.; Clemons, B.; Cahalan, S. M.; Schuerer, S. C.; Sanna, M. G.; Han, G. W.; Kuhn, P.; Rosen, H.; Stevens, R. C., Crystal structure of a lipid G protein-coupled receptor. *Science* **2012,** *335* (6070), 851-5.

170. Grossfield, A.; Feller, S. E.; Pitman, M. C., A role for direct interactions in the modulation of rhodopsin by omega-3 polyunsaturated lipids. *Proc Natl Acad Sci U S A* **2006,** *103* (13), 4888-93.

171. Klauda, J. B.; Venable, R. M.; Freites, J. A.; O'Connor, J. W.; Tobias, D. J.; Mondragon-Ramirez, C.; Vorobyov, I.; MacKerell, A. D., Jr.; Pastor, R. W., Update of the CHARMM all-atom additive force field for lipids: validation on six lipid types. *J Phys Chem B* **2010,** *114* (23), 7830-43.

172. Hurst, D. P.; Grossfield, A.; Lynch, D. L.; Feller, S.; Romo, T. D.; Gawrisch, K.; Pitman, M. C.; Reggio, P. H., A lipid pathway for ligand binding is necessary for a cannabinoid G protein-coupled receptor. *J Biol Chem* **2010,** *285* (23), 17954-64.

173. Brooks, B. R.; Brooks, C. L., 3rd; Mackerell, A. D., Jr.; Nilsson, L.; Petrella, R. J.; Roux, B.; Won, Y.; Archontis, G.; Bartels, C.; Boresch, S.; Caflisch, A.; Caves, L.; Cui, Q.; Dinner, A. R.; Feig, M.; Fischer, S.; Gao, J.; Hodoscek, M.; Im, W.; Kuczera, K.; Lazaridis, T.; Ma, J.; Ovchinnikov, V.; Paci, E.; Pastor, R. W.; Post, C. B.; Pu, J. Z.; Schaefer, M.; Tidor, B.; Venable, R. M.; Woodcock, H. L.; Wu, X.; Yang, W.; York, D. M.; Karplus, M., CHARMM: the biomolecular simulation program. *J Comput Chem* **2009,** *30* (10), 1545-614.

174. Phillips, J. C.; Braun, R.; Wang, W.; Gumbart, J.; Tajkhorshid, E.; Villa, E.; Chipot, C.; Skeel, R. D.; Kale, L.; Schulten, K., Scalable molecular dynamics with NAMD. *J Comput Chem* **2005,** *26* (16), 1781-802.

175. Case, D. A.; Darden, T. A.; Cheatham, I., T. E.; Simmerling, C. L.; Wang, J.; Duke, R. E.; Luo, R.; Walker, R. C.; Zhang, W.; Merz, K. M.; Roberts, B.; Hayik, S.; Roitberg, A.; Seabra, G.; Swails, J.; Götz, A. W.; Kolossváry, I.; Wong, K. F.; Paesani, F.; Vanicek, J.; Wolf, R. M.; Liu, J.; Wu, X.; Brozell, S. R.; Steinbrecher, T.; Gohlke, H.; Cai, Q.; Ye, X.; Wang, J.; Hsieh, M.-J.; Cui, G.; Roe, D. R.; Mathews, D. H.; Seetin, M. G.; Salomon-Ferrer, R.; Sagui, C.; Babin, V.; Luchko, T.; Gusarov, S.; Kovalenko, A.; Kollman, P. A., AMBER 12, Version 12.3. *University of California, San Francisco.* **2012**.

176. Case, D. A.; Darden, T. A.; Cheatham, I., T. E.; Simmerling, C. L.; Wang, J.; Duke, R. E.; Luo, R.; Walker, R. C.; Zhang, W.; Merz, K. M.; Roberts, B.; Hayik, S.; Roitberg, A.; Seabra, G.; Swails, J.; Götz, A. W.; Kolossváry, I.; Wong, K. F.; Paesani, F.; Vanicek, J.; Wolf, R. M.; Liu, J.; Wu, X.; Brozell, S. R.; Steinbrecher, T.; Gohlke, H.; Cai, Q.; Ye, X.; Wang, J.; Hsieh, M.-J.; Cui, G.; Roe, D. R.; Mathews, D. H.; Seetin, M. G.; Salomon-Ferrer, R.; Sagui, C.; Babin, V.; Luchko, T.; Gusarov, S.; Kovalenko, A.; Kollman, P. A., AMBER 12 Reference Manual, http://ambermd.org/doc12/Amber12.pdf. *University of California, San Francisco.* **2012**.

177. Salomon-Ferrer, R.; Gotz, A. W.; Poole, D.; Le Grand, S.; Walker, R. C., Routine Microsecond Molecular Dynamics Simulations with AMBER on GPUs. 2. Explicit Solvent Particle Mesh Ewald. *Journal of chemical theory and computation* **2013,** *9* (9), 3878-88.

178. Berendsen, H. J. C.; Postma, J. P. M.; van Gunsteren, W. F.; DiNola, A.; Haak, J. R., Molecular dynamics with coupling to an external bath. *The Journal of Chemical Physics* **1984,** *81*, 3684-3690.

179. Humphrey, W.; Dalke, A.; Schulten, K., VMD: visual molecular dynamics. *Journal of molecular graphics* **1996,** *14* (1), 33-8, 27-8.

180. Qin, L.; Kufareva, I.; Holden, L. G.; Wang, C.; Zheng, Y.; Zhao, C.; Fenalti, G.; Wu, H.; Han, G. W.; Cherezov, V.; Abagyan, R.; Stevens, R. C.; Handel, T. M., Structural biology. Crystal structure of the chemokine receptor CXCR4 in complex with a viral chemokine. *Science* **2015,** *347* (6226), 1117-22.

181. Egloff, P.; Hillenbrand, M.; Klenk, C.; Batyuk, A.; Heine, P.; Balada, S.; Schlinkmann, K. M.; Scott, D. J.; Schutz, M.; Pluckthun, A., Structure of signaling-competent neurotensin receptor 1 obtained by directed evolution in Escherichia coli. *Proc Natl Acad Sci U S A* **2014,** *111* (6), E655-62.

182. Krumm, B. E.; White, J. F.; Shah, P.; Grisshammer, R., Structural prerequisites for G-protein activation by the neurotensin receptor. *Nature communications* **2015,** *6*, 7895.

183. White, J. F.; Noinaj, N.; Shibata, Y.; Love, J.; Kloss, B.; Xu, F.; Gvozdenovic-Jeremic, J.; Shah, P.; Shiloach, J.; Tate, C. G.; Grisshammer, R., Structure of the agonist-bound neurotensin receptor. *Nature* **2012,** *490* (7421), 508-13.

184. Fenalti, G.; Zatsepin, N. A.; Betti, C.; Giguere, P.; Han, G. W.; Ishchenko, A.; Liu, W.; Guillemyn, K.; Zhang, H.; James, D.; Wang, D.; Weierstall, U.; Spence, J. C.; Boutet, S.; Messerschmidt, M.; Williams, G. J.; Gati, C.; Yefanov, O. M.; White, T. A.; Oberthuer, D.; Metz, M.; Yoon, C. H.; Barty, A.; Chapman, H. N.; Basu, S.; Coe, J.; Conrad, C. E.; Fromme, R.; Fromme, P.; Tourwe, D.; Schiller, P. W.; Roth, B. L.; Ballet, S.; Katritch, V.; Stevens, R. C.; Cherezov, V., Structural basis for bifunctional peptide recognition at human delta-opioid receptor. *Nature structural & molecular biology* **2015,** *22* (3), 265-8.

185. Burg, J. S.; Ingram, J. R.; Venkatakrishnan, A. J.; Jude, K. M.; Dukkipati, A.; Feinberg, E. N.; Angelini, A.; Waghray, D.; Dror, R. O.; Ploegh, H. L.; Garcia, K. C., Structural biology. Structural basis for chemokine recognition and activation of a viral G protein-coupled receptor. *Science* **2015,** *347* (6226), 1113-7.

186. Krumm, B. E.; Grisshammer, R., Peptide ligand recognition by G protein-coupled receptors. *Frontiers in pharmacology* **2015,** *6*, 48.

187. Wolf, S.; Grunewald, S., Sequence, structure and ligand binding evolution of rhodopsin-like G protein-coupled receptors: a crystal structure-based phylogenetic analysis. *PLoS One* **2015,** *10* (4), e0123533.

188. Nicole, P.; Couvineau, P.; Jamin, N.; Voisin, T.; Couvineau, A., Crucial role of the orexin-B C-terminus in the induction of OX1 receptor-mediated apoptosis: analysis by alanine scanning, molecular modelling and site-directed mutagenesis. *Br J Pharmacol* **2015,** *172* (21), 5211-23.

189. Friesner, R. A.; Banks, J. L.; Murphy, R. B.; Halgren, T. A.; Klicic, J. J.; Mainz, D. T.; Repasky, M. P.; Knoll, E. H.; Shelley, M.; Perry, J. K.; Shaw, D. E.; Francis, P.; Shenkin, P. S., Glide: a new approach for rapid, accurate docking and scoring. 1. Method and assessment of docking accuracy. *J Med Chem* **2004,** *47*, 1739-49.

190. Halgren, T. A.; Murphy, R. B.; Friesner, R. A.; Beard, H. S.; Frye, L. L.; Pollard, W. T.; Banks, J. L., Glide: a new approach for rapid, accurate docking and scoring. 2. Enrichment factors in database screening. *J Med Chem* **2004,** *47*, 1750-9.

191. Friesner, R. A.; Murphy, R. B.; Repasky, M. P.; Frye, L. L.; Greenwood, J. R.; Halgren, T. A.; Sanschagrin, P. C.; Mainz, D. T., Extra precision glide: docking and scoring incorporating a model of hydrophobic enclosure for protein-ligand complexes. *J Med Chem* **2006,** *49*, 6177-96.

192. Yin, J.; Babaoglu, K.; Brautigam, C. A.; Clark, L.; Shao, Z.; Scheuermann, T. H.; Harrell, C. M.; Gotter, A. L.; Roecker, A. J.; Winrow, C. J.; Renger, J. J.; Coleman, P. J.; Rosenbaum, D. M., Structure and ligand-binding mechanism of the human OX1 and OX2 orexin receptors. *Nature structural & molecular biology* **2016,** *23* (4), 293-9.